



**DELHI COLLEGE OF ENGINEERING**  
**LIBRARY**

CLASS NO.....621.1.2.....

BOOK NO.....411.....

ACCESSION NO.....51111.....







# ALTERNATING-CURRENT MACHINES

By

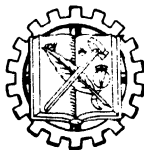
MICHAEL LIWSCHITZ-GARIK, Dr-Ing.

*Late Professor at the Polytechnic Institute of Brooklyn*

AND

CLYDE C. WHIPPLE, E.E.

*Professor Emeritus at the Polytechnic Institute of Brooklyn.*



SECOND EDITION

D. VAN NOSTRAND COMPANY, INC.

PRINCETON, NEW JERSEY

TORONTO

NEW YORK

LONDON

D. VAN NOSTRAND COMPANY, INC  
120 Alexander St., Princeton, New Jersey (*Principal office*)  
24 West 40 Street, New York 18, New York

D. VAN NOSTRAND COMPANY, LTD.  
358, Kensington High Street, London, W.14, England

D. VAN NOSTRAND COMPANY (Canada), LTD.  
25 Hollinger Road, Toronto 16, Canada

Copyright, ©, 1946, 1961 by  
D. VAN NOSTRAND COMPANY, INC.

---

Published simultaneously in Canada by  
D. VAN NOSTRAND COMPANY (Canada), LTD.

---

*No reproduction in any form of this book, in whole or in  
part (except for brief quotation in critical articles or reviews),  
may be made without written authorization from the publishers.*

---

***First Edition, September 1946***

*Eight Reprintings*

***Second Edition, April 1961***

*Reprinted September 1964, December 1966*

To The Late  
OLGA LIWSCHITZ-GARIK



## PREFACE

This new edition of *Alternating-Current Machines* is designed primarily as an undergraduate text, for use by Junior and Senior students in Electrical Engineering. The second part of the text is written to give the more advanced student as well as the practicing engineer and designer certain useful information of specific value not ordinarily available. It is based on a wide experience of Dr. Liwshitz-Garik in the theory and design of electric machinery.

The principal aim of the text is to provide an understanding between the basic laws of electrodynamics and the performance characteristics of the transformer and rotating electric machines. The basic laws on which the material is developed are: 1) Faraday's Law of Induction, 2) Kirchhoff's Mesh Law of Electric Circuits, 3) Circuital Law of the Magnetic Field (Ampere's Law), 4) Forces on Conductors in a Magnetic Field (Biot-Savart's Law).

The consistent application of these laws leads, in the opinion of the authors, to a basic understanding of the machines discussed. At the end of Part 2 will be found a discussion of power flow in electric machines.

In comparison with the First Edition (1946) of the book, much of the material has been entirely rewritten, leaving out material which did not seem, in the light of experience, to be helpful. The text has been subdivided into many more chapters, as experience seems to dictate. New material has been added, together with worked examples and a more complete set of appropriate problems.

Some of the more advanced and detailed work originally in the main part as well as in the Appendix of the first edition has been carefully selected and revised and is included in Part 2.

It is felt that Part 1, consisting of 49 Chapters provides the basis for a two-semester undergraduate course in *Alternating-Current Machines*. By a suitable choice of chapters, the material will serve for a one-semester course.

The material of the text in manuscript form was completed before the death of Dr. Liwshitz-Garik, on February 9th, 1958. Subsequently some revision and additions were made by Professor Whipple who also provided the chapters on Transformers, the chapters on Application and Control of Motors, as well as many of the problems. Professor Whipple completed the review of the galley and page proofs.

## ACKNOWLEDGMENTS

This volume is essentially the work of Dr. Liwshitz-Garik, who was assisted by his colleague Professor Clyde C. Whipple. The manuscript had been prepared and practically completed before the death of Dr. Liwshitz-Garik on February 9, 1959.

We wish to acknowledge the assistance given by our colleagues at Polytechnic—especially to Dr. E. Levi and R. Honigsbaum, who made helpful contributions, carefully read and checked much of the material, and provided many of the examples and problems in Part 2. Professor R. T. Weil, Jr., of Manhattan College, was helpful in suggestions and with the problems, as well as for the use of some material from the text *D-C and A-C Machines* by Liwshitz-Garik and Weil.

We are indebted to Dr. E. Weber, President of the Polytechnic Institute of Brooklyn, and to Professor Truxal, Head of the Department of Electrical Engineering, for their kind assistance in offering the facilities of the Institute necessary for the production of this work. We are especially indebted to our secretary, Miss Josephine McCoy, who has patiently worked so long and effectively in the typing of the entire work.

We are grateful to the following companies for their contribution of cuts, data, and photographs: General Electric Company, National Electric Coil Company, Westinghouse Electric Corporation, the Allis Chalmers Corporation, the Century Electric Company, Robbins and Meyers, Inc., Wagner Electric Corporation and the Cutler-Hammer Company.

C. C. W.

## TABLE OF CONTENTS

### CHAPTER 1 ELECTRIC MACHINES. POWER CONVERTERS. FUNDAMENTAL LAWS TO WHICH THE OPERATION OF THE ELECTRIC MACHINES ARE SUBJECT. METHOD OF APPROACH

	PAGE
1-1 Electric Machines as Power Converters .....	1
1-2 Fundamental Laws .....	1
(a) Faraday's Law of Induction .....	1
(b) Kirchhoff's Mesh Law .....	8
(c) Circuital Law of the Magnetic Field (Ampere's Law) .....	11
(d) Law of Force on a Conductor in a Magnetic Field (Biot-Savart's Law) .....	13
1-3 Method of Approach .....	16
Problems .....	16

### CHAPTER 2 TRANSFORMER CONSTRUCTION

2-1 Transformer Types .....	20
2-2 Windings .....	23
2-3 Cooling .....	26

### CHAPTER 3 THE TRANSFORMER AT NO-LOAD

3-1 The Transformer Primary .....	28
Problems .....	32

### CHAPTER 4 THE TRANSFORMER UNDER LOAD

4-1 The Behavior of the Transformer Under Load .....	34
4-2 Reduction of the Secondary Voltage, Current, and Parameters to the Primary .....	35
4-3 Kirchhoff's Mesh Law for the Secondary .....	36
4-4 The EMF $E_1 - E_2'$ Induced by the Main Flux Under Load .....	36
4-5 The Mutual Inductance of the Transformer .....	38
4-6 Application of the Fundamental Equations .....	39

### CHAPTER 5 THE PHASOR DIAGRAM AND EQUIVALENT CIRCUIT OF THE TRANSFORMER UNDER LOAD

5-1 The Phasor Diagram of the Transformer Under Load .....	41
5-2 The Equivalent Circuit of the Transformer .....	42
Example .....	45
Problems .....	46



CHAPTER 6 THE 3-PHASE TRANSFORMER		PAGE
6-1	Advantages, Disadvantages, Construction .....	47
6-2	Magnetic Circuit .....	49
CHAPTER 7 VOLTAGE REGULATION: THE KAPP DIAGRAM		
7-1	Voltage Regulation: The Kapp Diagram .....	50
CHAPTER 8 DETERMINATION OF PARAMETERS FROM A NO-LOAD AND A SHORT-CIRCUIT TEST		
8-1	The No-Load Test .....	54
8-2	The Short-Circuit Test .....	55
8-3	Transformer Efficiency .....	56
8-4	Per-Unit Calculation .....	56
	Example .....	57
	Problems .....	59
CHAPTER 9 SHAPE OF THE NO-LOAD AND LOAD-CURRENT WAVE		
9-1	Shape of the No-Load and Load-Current Wave .....	61
CHAPTER 10 TRANSFORMER POLARITY—POLYPHASE CONNECTION		
10-1	Transformer Polarity .....	64
10-2	Polyphase Connection: 3-phase to 3-phase .....	66
10-3	Polyphase Connection: 2-phase to 3-phase, or Vice Versa .....	70
10-4	Polyphase Connection: 3-phase to 6-phase .....	71
	Problems .....	74
CHAPTER 11 PARALLEL OPERATION OF TRANSFORMER		
11-1	Parallel Operation of Transformers .....	77
	Example .....	80
	Problems .....	82
CHAPTER 12 THE AUTO-TRANSFORMER. INSTRUMENT TRANSFORMERS. CONSTANT-CURRENT TRANSFORMER		
12-1	The Auto-Transformer .....	84
12-2	Instrument Transformers .....	85
12-3	Constant-Current Transformer .....	88
	Example .....	89
	Problems .....	90
CHAPTER 13 A-C WINDINGS		
13-1	A-C Windings .....	92
	Problems .....	99

## CHAPTER 14 EMF OF AN A-C WINDING

	PAGE
14-1 Distribution Factor .....	101
14-2 Pitch-Factor .....	103
14-3 Nonsinusoidal Flux (B-) Distribution Along the Armature Surface .....	104
Problems .....	105

CHAPTER 15 THE MMF OF AN A-C WINDING ALTERNATING MMF.  
ROTATING MMF

15-1 Alternating MMF .....	106
15-2 Rotating MMF .....	108
Example .....	112
Problems .....	113

CHAPTER 16 MECHANICAL ELEMENTS OF THE POLYPHASE INDUCTION  
MOTOR AND ITS MAGNETIC CIRCUIT

16-1 Mechanical Elements of the Polyphase Induction Motor and Its Magnetic Circuit .....	114
--	-----

## CHAPTER 17 THE POLYPHASE INDUCTION MOTOR AS A TRANSFORMER

17-1 The Induction Motor at Standstill .....	123
17-2 The Induction Motor When Running. The Slip .....	130
17-3 The Squirrel-Cage Rotor. Its Number of Poles and Phases .....	132
Problems .....	133

CHAPTER 18 APPLICATION OF THE FUNDAMENTAL EQUATION. PHASOR  
DIAGRAM AND EQUIVALENT CIRCUIT OF THE POLYPHASE INDUCTION  
MOTOR

18-1 Application of the Fundamental Equations .....	135
18-2 Phasor Diagram of the Polyphase Induction Motor .....	136
18-3 Equivalent Circuit of the Polyphase Induction Motor .....	137

## CHAPTER 19 POWER AND TORQUE RELATION. POWER BALANCE

19-1 Developed Mechanical Power and Torque .....	141
19-2 The Pull-Out Torque .....	143
19-3 Power Balance .....	144
Example 19-1 .....	145
Problems .....	148

CHAPTER 20 OPERATION OF THE INDUCTION MACHINE AS A BRAKE  
AND GENERATOR

20-1 Operation as a Brake .....	150
20-2 Operation as a Generator .....	151

CHAPTER 21 CIRCLE DIAGRAM OF THE POLYPHASE INDUCTION MOTOR

	PAGE
21-1 Determination of the Circle Diagram .....	155
21-2 Developed-Mechanical-Power Line and Delivered-Mechanical-Power Line .....	156
21-3 The Torque-Line and the Slip-Line .....	158
21-4 Determination of the Scales for the Power and Torque Lines .....	161
Problems .....	162

CHAPTER 22 DETERMINATION OF PARAMETERS FROM A NO-LOAD AND A LOCKED-ROTOR TEST. INFLUENCE OF PARAMETERS ON PERFORMANCE.  
INFLUENCE OF SKIN-EFFECT AND SATURATION ON THE PARAMETERS

22-1 The No-Load Test .....	163
22-2 The Short-Circuit (Locked-Rotor) Test .....	164
22-3 Per-Unit Values of the Parameters .....	166
22-4 Influence of the Parameters on the Performance of the Motor .....	167
22-5 Skin-Effect Motors .....	169
22-6 Influence of Saturation on the Parameters $x_1$ and $x_2'$ .....	170
22-7 Summary on Variation of Parameters with the Slip .....	172
Example 22-1 .....	174
Example 22-2 .....	177
Problems .....	179

CHAPTER 23 STARTING AND SPEED-CONTROL OF THE POLYPHASE  
INDUCTION MOTOR

23-1 Starting a Squirrel-Cage Motor .....	183
23-2 Starting a Wound-Rotor (Slip-Ring) Motor .....	186
23-3 Speed Control of the Polyphase Induction Motor .....	187
Problems .....	193

CHAPTER 24 INFLUENCE OF HARMONIC FLUXES ON THE TORQUE-SPEED  
CHARACTERISTICS

24-1 Order and Speed of the Harmonic MMF's and Fluxes .....	195
24-2 Influence of the Harmonic Fluxes on the Torque-Speed Characteristics ...	198
24-3 Means to Reduce or to Avoid the Parasitic Torques .....	199

CHAPTER 25 SOME SPECIAL INDUCTION MACHINES

25-1 The Synchronous Induction Motor .....	201
25-2 Induction Motor with Rotating Flux Produced by a D-C Excited Rotating Pole-Structure (Electromagnetic Coupling) .....	202
25-3 Self-Synchronizer (Selsyns, Synchrotic Apparatus, Autosyn, etc.) .....	202
25-4 Position Indicators .....	210
25-5 The Induction Voltage Regulator .....	211
25-6 Resolvers .....	213
Problems .....	215

## CHAPTER 26 THE SINGLE-PHASE INDUCTION MOTOR

	PAGE
26-1 The Single-Phase Windings .....	216
Problems .....	218
26-2 Mechanical Elements of the Single-Phase Motor .....	219
26-3 Application of the Operational Characteristics of the Polyphase Motor to the Single-Phase Motor .....	219
26-4 Torque of the Single-Phase Induction Motor .....	220
26-5 Kirchhoff's Mesh Equations of the Stator and Rotor Circuits .....	222
26-6 The Equivalent Circuit of the Single-Phase Induction Motor .....	223
26-7 The Circle Diagram of the Single-Phase Induction Motor .....	226
26-8 Justification of the Two Rotating Field Theory .....	227

CHAPTER 27 DETERMINATION OF THE PARAMETER OF THE SINGLE-PHASE  
INDUCTION MOTOR FROM A NO-LOAD AND A LOCKED-ROTOR TEST

27-1 The No-Load Test .....	228
27-2 The Locked-Rotor Test .....	230
27-3 Influence of the Parameters on the Performance of the Motor .....	231
Example 27-1 .....	231
Example 27-2 .....	233
Problems .....	236

CHAPTER 28 STARTING THE SINGLE-PHASE MOTOR. TYPES OF  
SINGLE-PHASE MOTORS

28-1 Starting by Means of a Rotating Flux .....	238
28-2 Starting by Means of a Commutator and Brushes .....	241
28-3 The Shaded-Pole Motor .....	243

## CHAPTER 29 LOSSES IN INDUCTION MOTORS HEATING AND COOLING

29-1 Losses in Induction Motors .....	244
29-2 Heating and Cooling of Induction Motors .....	249
Problems .....	253

## CHAPTER 30 MECHANICAL ELEMENTS OF THE SYNCHRONOUS MACHINE

30-1 The Salient-Pole Machine .....	256
30-2 The Cylindrical Rotor Machine .....	260

## CHAPTER 31 GENERAL CONSIDERATIONS OF THE SYNCHRONOUS MACHINE

31-1 The No-Load Characteristic .....	264
31-2 The Main Flux Reactance .....	266
31-3 Effect of Saturation .....	267

CHAPTER 32 PHASOR DIAGRAMS OF GENERATOR AND MOTOR WITH CYLINDRICAL ROTOR. ARMATURE REACTION		PAGE
32-1	Phasor Diagram of Synchronous Generator and Motor with Cylindrical Rotor. Armature Reaction .....	268
CHAPTER 33 GENERATOR CHARACTERISTICS. VOLTAGE REGULATION		
33-1	Generator Characteristics .....	273
33-2	Voltage Regulation .....	277
	Example 33-1 .....	279
	Problems .....	281
CHAPTER 34 THE TWO-REACTION THEORY		
34-1	Essence of the Two-Reaction Theory .....	283
34-2	Effective Armature MMF in Both Axes .....	285
CHAPTER 35 PHASOR DIAGRAMS OF THE GENERATOR AND MOTOR WITH SALIENT POLES. ARMATURE REACTION. GENERAL CHARACTERISTICS		
35-1	Phasor Diagram of the Generator and Motor with Salient Poles. Armature Reaction .....	288
35-2	Generator Characteristics. Voltage Regulation .....	292
	Example 35-1 .....	294
	Example 35-2 .....	295
	Problems .....	296
CHAPTER 36 TORQUE AND POWER RELATIONS. SYNCHRONIZING GENERATORS		
36-1	Torque and Power Relations .....	299
36-2	Synchronizing of Synchronizing Generators .....	301
CHAPTER 37 PARALLEL OPERATION OF SYNCHRONOUS GENERATORS		
37-1	Parallel Operation of Synchronous Generators .....	303
	Example 37-1 .....	305
	Problems (for Chapters 36 and 37) .....	308
CHAPTER 38 CIRCLE DIAGRAMS OF THE SYNCHRONOUS MACHINE. V-CURVES. SYNCHRONOUS CONDENSER. STARTING A SYNCHRONOUS MOTOR		
38-1	Circle Diagrams for Constant Developed Torque and Variable Field Current .....	310
38-2	Circle Diagrams for Variable Torque and Constant Field Current .....	312
38-3	Influence of Field Current on Overload Capacity and Power Factor. V-Curves of the Synchronous Motor. Synchronous Capacitor .....	315

38-4	Starting of a Synchronous Motor .....	318
	Problems .....	319

## CHAPTER 39 EFFECT OF THE EMF HARMONICS

39-1	Resultant EMF .....	321
39-2	Effect of the 3rd Harmonic .....	322
39-3	Time and Space Harmonics .....	323
	Example 39-4 .....	323
	Problems .....	324

## CHAPTER 40 HUNTING OF A SYNCHRONOUS MACHINE

40-1	The Synchronizing Torque .....	326
40-2	Ratio of the Amplitude of Oscillation in Parallel Operation to the Amplitude of Oscillation of the Single Machine. (The Amplification Factor) .....	328
40-3	The Natural Frequency of the Synchronous Machine. The Danger of Resonance .....	331
40-4	Improvement of Parallel Operation by Means of a Damper Winding ....	331

## CHAPTER 41 LOSSES IN SYNCHRONOUS MACHINES. HEATING AND COOLING

41-1	The Losses in the Synchronous Machine .....	333
41-2	Heating and Cooling of the Synchronous Machine .....	335
	Problems .....	335

## CHAPTER 42 SMALL SYNCHRONOUS MOTORS

42-1	The Reluctance Motor .....	337
42-2	The Hysteresis Motor .....	338

## CHAPTER 43 THE SYNCHRONOUS CONVERTER. VOLTAGE AND CURRENT RELATIONS. COPPER LOSSES COMPARED WITH THOSE OF THE D-C MACHINE

43-1	Operation of the Synchronous Converter .....	341
43-2	Voltage and Current Ratios in the Synchronous Converter .....	344
43-3	The Copper Losses in the Synchronous Converter .....	345
43-4	Comparison with the D-C Machine .....	347
	Problems .....	348

## CHAPTER 44 COMMUTATION OF THE SYNCHRONOUS CONVERTER. VOLTAGE REGULATION. STARTING. PARALLEL OPERATION

44-1	Commutation of the Synchronous Converter .....	350
44-2	Voltage Regulation of the Converter .....	350
44-3	Starting and Parallel Operation of Converters .....	351
44-4	Comparison with the Motor Generator Set .....	352

### CHAPTER 45 THE D-C ARMATURE IN AN ALTERNATING MAGNETIC FIELD

	PAGE
45-1 The EMF of Rotation and the EMF of Transformation in the Armature Winding .....	353
45-2 The Torque of the Single-Phase Commutator Motor. The Compensating Winding .....	356
45-3 The Transformer EMF of a Short-Circuited Winding Element and the Commutating Fluxes in the Single-Phase Commutator Motor .....	358
Problems .....	361

### CHAPTER 46 THE SINGLE-PHASE SERIES COMMUTATOR MOTOR

46-1 The Voltage Diagram of the Single-Phase Series Commutator Motor .....	362
46-2 Commutation of the Single-Phase Series Commutator Motor .....	363
46-3 Torque and Characteristic Curves of the Single-Phase Series Commutator Motor .....	365
46-4 The Universal Motor .....	366
Problems .....	366

### CHAPTER 47 THE REPULSION MOTOR

47-1 The Voltage Diagram of the Repulsion Motor .....	368
47-2 Commutation of the Repulsion Motor .....	370
47-3 Characteristic Curves of the Repulsion Motor .....	371

### CHAPTER 48 THE 3-PHASE SHUNT COMMUTATOR MOTOR (THE SCHRAGE MOTOR)

48-1 Connection Diagram and Speed Control of the 3-Phase Shunt Commutator Motor .....	371
48-2 Power-Factor Correction of the 3-Phase Shunt Commutator Motor .....	377
48-3 Commutation of the 3-Phase Shunt Motor .....	377
Problems .....	378

### CHAPTER 49 MOTOR APPLICATION. STARTING. SPEED CONTROL. PROTECTION

49-1 Characteristics of Loads .....	379
49-2 Motor Types, Sizes and Costs .....	382
49-3 Applications of Various Types of Motors .....	385
49-4 NEMA Classification of Induction Motors .....	386
49-5 Wound-Rotor Induction Motor Application .....	391
49-6 Polyphase Induction Motors as Multi-Speed Motors .....	393
49-7 Synchronous Motor Characteristics and Application .....	394
Problems .....	398
49-8 Fractional-Horsepower Motors .....	399
49-9 Definitions .....	399
49-10 Starting Induction Motors .....	406

## PAGE

49-11	Starting Synchronous Motors .....	415
49-12	Factors Governing the Type of Controller or Starter to Be Used. Manual or Magnetic .....	416
49-13	Motor Protection .....	418
49-14	Definitions .....	422

## CHAPTER 50 DETERMINATION OF THE NO-LOAD MMF

50-1	The Five Parts of the Magnetic Circuit .....	427
50-2	The Air-Gap MMF .....	428
50-3	The Teeth MMF .....	431
50-4	The Core MMF .....	434
50-5	The Pole and Yoke MMF .....	435

CHAPTER 51 THE ROTATING POLYPHASE INDUCTION MOTOR AS A STATIONARY TRANSFORMER. THE PRIMARY AND SECONDARY CURRENT. THE  
CIRCLE DIAGRAM OF THE POLYPHASE INDUCTION MOTOR

51-1	The Rotating Polyphase Induction Motor as a Stationary Transformer. Kirchhoff's Equation .....	440
51-2	Primary and Secondary Current. Power Factor .....	442
51-3	Geometric Loci .....	443
51-4	Circle Diagram of the Polyphase Induction Motor—Slip Line .....	446
51-5	The Torque Line .....	449
51-6	Influence of Variation of Leakage Reactances and Secondary Resistance on the Shape of the Geometric Locus of the Primary Current .....	451

CHAPTER 52 DERIVATION OF THE TORQUE OF THE POLYPHASE INDUCTION  
MOTOR FROM THE LAW OF FORCE ON A CONDUCTOR IN A MAGNETIC FIELD  
(BIOT-SAVART'S LAW) .....

452

## CHAPTER 53 THE UNSYMMETRICAL TWO-PHASE INDUCTION MOTOR

53-1	Current in the Main Winding Only .....	454
53-2	Current in the Starting Winding Only .....	456
53-3	Both Windings Carry Current .....	457
53-4	Kirchhoff's Equations of the Stator Circuit and Currents in the Stator Windings .....	458
53-5	The Power of the Rotating Field and the Torque .....	461

CHAPTER 54 THE PERMANENT-SPLIT CAPACITOR MOTOR UNDER  
BALANCED AND UNBALANCED CONDITIONS

54-1	Balanced Conditions .....	463
54-2	Unbalanced Conditions .....	466



## CHAPTER 55 FRACTIONAL-SLOT WINDINGS

	PAGE
55-1 General Consideration .....	470
55-2 The Slot Star .....	471
55-3 Layout of a Fractional-Slot Winding with Respect to the Main Wave. The Coil Grouping .....	474
55-4 Simplification of the Determination of the Coil Grouping .....	476
55-5 Conditions of Balance .....	479
55-6 Beginnings of Phases .....	480
55-7 Layout of a Fractional-Slot Winding with Respect to Harmonics .....	481

## CHAPTER 56 HARMONIC MMF'S AND FLUXES OF THE INDUCTION MOTOR

56-1 Stator Windings with Integral Number of Slots per Pole per Phase ( $q = \text{Integer}$ ) .....	482
56-2 Rotor Windings .....	485
56-3 Introduction of a Fundamental with the Wave Length Equal to $p\tau = \pi D$ .....	488
56-4 Balanced Fractional-Slot Stator Windings .....	490
Examples .....	491
56-5 The Distribution and Pitch Factors .....	492
56-6 The Skew Factor .....	494
56-7 The Rotor Current .....	495

CHAPTER 57 THE LEAKAGE REACTANCES AND MAIN FLUX REACTANCES  
OF WINDINGS EMBEDDED IN SLOTS

57-1 General Formulae for the Coefficients of Self- and Mutual-Inductance ..	499
57-2 Slot Leakage (Single-Layer Windings) .....	500
57-3 Slot Leakage (Two-Layer Windings) .....	503
Example .....	506
57-4 Tooth-Top Leakage .....	509
57-5 End-Winding Leakage .....	510
57-6 Slot Leakage, Tooth-Top Leakage, and End-Winding Leakage with Re- spect to Harmonics .....	511
57-7 Harmonic Leakage of an Integral-Slot Winding .....	512
57-8 Harmonic Leakage of a Fractional Slot-Winding .....	515
57-9 Influence of the Rotor Winding on the Harmonic Leakage Reactance of the Stator Winding .....	517
57-10 Harmonic Leakage of the Rotor Winding with Respect to the Main Wave ..	518
57-11 Harmonic Leakage of a Squirrel-Cage Winding with Respect to the Har- monic $\mu' = v'$ .....	521
57-12 Summary of Main Flux Reactances and Harmonic (Differential Leakage Reactances) .....	522
57-13 Influence of the Slot Openings .....	523

## CHAPTER 58 PARASITIC TORQUES OF THE POLYPHASE INDUCTION MOTOR

58-1	Parasitic Tangential Forces and Parasitic Torques .....	529
58-2	The Asynchronous Parasitic Torques (Dips in the Torque-Slip Characteristic) .....	533
58-3	The Synchronous Parasitic Torques (Cusps in the Torque-Slip Characteristic) .....	535

## CHAPTER 59 RADIAL FORCES, VIBRATION, AND MAGNETIC NOISE IN POLYPHASE INDUCTION MOTORS

59-1	General Considerations .....	540
59-2	The 2-Pole Wave ( $p' = 1$ ) .....	545
59-3	Magnitude of the Force Waves ( $p' = 1$ ) .....	546
59-4	The Sound Intensity .....	549
	Example .....	553

## CHAPTER 60 TRANSIENT AND SUBTRANSIENT REACTANCES. SUDDEN SHORT CIRCUIT OF A SYNCHRONOUS GENERATOR

60-1	Transient Currents with Resistances and Reactances of Both Windings Neglected .....	559
60-2	Transient Currents with Resistances Not Neglected .....	561
60-3	Maximum Transient Currents .....	563
60-4	Transient and Subtransient Reactance in Quadrature Axis .....	566
60-5	Determination of Subtransient Reactances from a Locked Test .....	567

## CHAPTER 61 PULLING INTO STEP OF SYNCHRONOUS MOTORS

61-1	Equation of Motion of the Synchronous Motor Pulling into Step .....	568
61-2	Solution of the Equation of Motion for $\alpha = 0$ (Most Favorable Pole Position) .....	570
61-3	Solution of the Equation of Motion for $\alpha \neq 0$ .....	575

## CHAPTER 62 DESIGN PRINCIPLES OF AN ELECTRIC MACHINE—SPECIFIC TANGENTIAL FORCE

62-1	Magnitude of the Tangential Force .....	578
62-2	Output Constant .....	579
62-3	Range of Tangential Force .....	582

## CHAPTER 63 TANGENTIAL FORCES AND POWER FLOW IN ELECTRICAL MACHINES

63-1	The Tangential Forces .....	584
63-2	The Power Flow .....	584

REFERENCES .....	592
ANSWERS TO PROBLEMS .....	595
INDEX .....	601



# Chapter 1

## ELECTRIC MACHINES · POWER CONVERTERS · FUNDAMENTAL LAWS TO WHICH THE OPERATION OF THE ELECTRIC MACHINES ARE SUBJECT · METHOD OF APPROACH

**1-1. The electric machine as power converters.** All rotating electric machines are dynamic power converters. Either they convert mechanical power into electrical power (generators), or they convert electrical power into mechanical power (motors) or they convert electrical power into electrical power (rotary converter). It is to be remembered that each of the conversion processes is subject to the principles of conservation of energy.

**1-2. The fundamental laws.** The operation of all electric machines is subject to the same fundamental laws. From the electromagnetic point of view, the understanding of four laws suffices for the understanding of the behavior of the electric machines. These laws are

- a. Faraday's law of induction
- b. Kirchhoff's mesh law
- c. Circuital law of the magnetic field (Ampere's law)
- d. Law of force on a conductor in the magnetic field (Biot-Savart's law)

These laws will be briefly repeated.

(a) *Faraday's law of induction.* This law states:

$$e = - \frac{d\phi}{dt} 10^{-8} \text{ volt} \quad (1-1)$$

i.e., *the emf induced in a closed circuit is equal to the rate of decrease of the flux  $\phi$  interlinked with the circuit.*

When a conductor moves relative to a flux which is constant with time, at a speed  $v$ , it may be expedient to use Faraday's law in the form

$$e = - Blv 10^{-8} \text{ volt} \quad (1-2)$$

which can be interpreted as follows: *The emf induced in the conductor is equal to the flux cut by it per second.*

In Eq. 1-2,  $B$  is the flux density in gausses,  $l$  the length of the conductor

within the flux in cm and  $v$  the relative speed between conductor and flux in cm/sec. When  $B$  is expressed in lines per square inch,  $l$  in inches, and  $v$  in feet per minute, the right side of Eq. 1-2 must be multiplied by  $1/5$ .

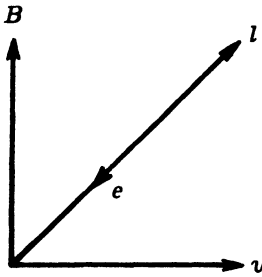


FIG. 1-1. Direction of the induced emf.

The minus sign in Eq. 1-2 means that, when the positive directions of  $v$ ,  $l$ , and  $B$  are assumed as those of an orthogonal system of coordinates (Fig. 1-1) the direction of  $e$  is opposite to the positive direction of  $l$ .

Consider Fig. 1-2. A coil mounted on an iron core rotates between a north and a south pole. Representing by a dot a current flowing toward the observer and by a cross current flowing away from the observer, the direction of the emf induced in the coil is

as shown in Fig. 1-2. It should be noticed that  $B$  is perpendicular to the iron core and  $v$  tangential to it.

The following simple rule, useful for the study of electric machines, can be derived from Fig. 1-2: If the *relative motion of the conductors* with respect to  $B$  is *clockwise*, the direction of the emf in all conductors lying under the North-pole is *inward* (cross), in all conductors lying under the south-pole it is *outward* (dot).

Another rule for the determination of the direction of the induced emf is: open the right hand, keep the fingers together and the thumb in the same plane as the palm but pointing at right angles to the fingers. If the flux enters the palm at right angles to it and the thumb points in the direction of motion of the conductor, the fingers then point in the direction of the induced emf.

The *average emf* induced in the coil of Fig. 1-2 can be readily determined from Eq. 1-1. When the coil lies in the horizontal, it is interlinked with the total pole-flux  $\Phi$ . When it moves from the horizontal position a quarter of a revolution, it lies in the vertical and its flux interlinkage is zero. A quarter of a revolution further in the same direction brings the coil again in the

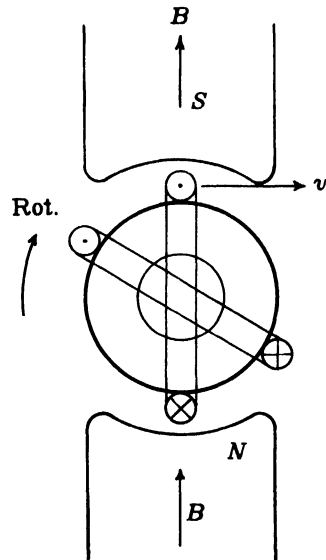


FIG. 1-2. Direction of the induced emf. in a coil of an electric machine.

horizontal; the flux interlinkage is again  $\Phi$  but in the opposite direction. Thus, during a half revolution,  $\Delta\phi = 2\phi$ . If the speed of the armature is  $n/60$  rps, ( $n$  in rpm), the duration of a half-revolution is  $\Delta t = 30/n$  seconds and

$$E_{av} = \frac{2\Phi}{30/n} 10^{-8} = 4\Phi \frac{n}{60} 10^{-8} \text{ volt.} \quad (1-3)$$

The average emf depends upon the total flux per pole and is independent of the flux distribution around the periphery of the armature, i.e., of the magnitude of the flux density  $B$  around the armature. The instantaneous values of the induced emf, on the contrary, depend upon the distribution of  $B$ , as indicated by Eq. 1-2.

Eq. 1-3 assumes that there are only two poles and that the coil consists of two conductors making one turn. If the number of poles is  $p$ , then, the change  $\Delta\phi = 2\Phi$  is accomplished during  $1/(p/2)$  of a half revolution, and  $E_{av}$  becomes  $p/2$  times the value given by Eq. 1-3. Furthermore, if the number of series-connected turns of the coil is  $N$  and these  $N$  turns are so concentrated that they are interlinked with the same number of flux lines at any instant of time, then  $E_{av}$  is  $N$  times larger than the value given by Eq. 1-3, so that

$$E_{av} = \left(4\Phi \frac{p}{2}\right) N \frac{n}{60} 10^{-8} \text{ volt} \quad (1-3a)$$

Consider Fig. 1-3 which shows the normal flux distribution of a salient-pole synchronous machine (Fig. 14-4).  $B$  is zero in the middle of the interpolar space (see Fig. 1-2) and is a maximum in the center of the pole. If both coil sides lie at all times in fields of the same strength, the *instantaneous* value of the emf induced in the coil is (Eq. 1-2)

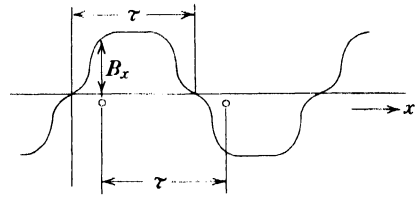


FIG. 1-3. Flux distribution in a salient-pole machine.

$$e = 2B_x lv 10^{-8} \text{ volt} \quad (1-4)$$

i.e., it is proportional to  $B_x$ , and the emf curve has exactly the same shape as the  $B$  curve.

If  $D$  = diameter of the armature and  $p$  = number of poles, then the *arc*

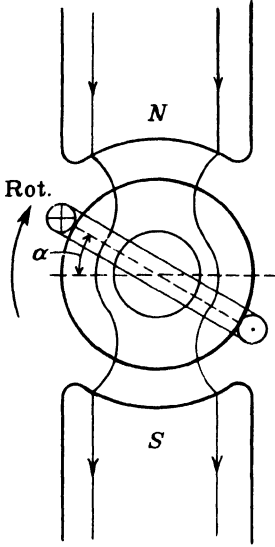
$$\frac{\pi D}{p} = \tau \quad (1-5)$$

is the *pole pitch*. In order that both sides of a coil lie in flux densities of the same strength, its coil span, measured as an arc, must be equal to the pole pitch. This is the case in Fig. 1-2.

When the flux distribution along the armature is *sinusoidal*, the emf of

the coil also will be sinusoidal. The *amplitude and the effective value* of the emf for sinusoidal flux distribution will now be determined for this case.

Consider Fig. 1-4. When the angle between the plane of the coil and the



horizontal ( $\alpha$ ) is zero, the coil is interlinked with the total pole-flux  $\Phi$ ; when this angle is equal to  $\pi/2$ , i.e., the plane of the coil coincides with the pole-axis, the flux interlinkage of the coil is zero. In any intermediate position the flux interlinkage is  $\Phi \cos \alpha$ . This can be seen from Fig. 1-5. When the coil sides (a-b) have the position  $\alpha = 0$  and  $\alpha = \pi$ , the flux interlinked with the coil is proportional to

$$\int_{\alpha=0}^{\alpha=\pi} B_{\alpha} d\alpha$$

When the coil sides have the position  $\alpha$  and  $(\alpha + \pi)$ , the flux interlinked with the coil is proportional to

$$\int_{\alpha}^{(\alpha+\pi)} B_{\alpha} d\alpha$$

FIG. 1-4. Determination of flux interlinkages

The ratio of the latter integral to the former integral is  $\cos \alpha$ , since  $B_{\alpha} = B_{\max} \sin \alpha$ . The flux interlinked with the coil at any position angle  $\alpha$  is therefore  $\phi = \Phi \cos \alpha$ . The curve of flux interlinkage  $\phi$  is shown in Fig. 1-5.

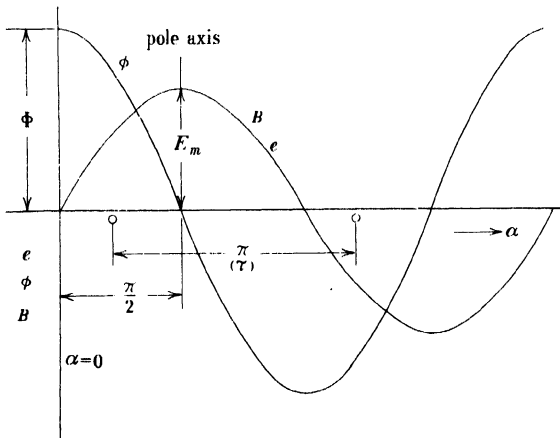


FIG. 1-5. Sinusoidal flux distribution. Flux interlinkage and emf as functions of time.

From Eq. 1-1:

$$e = -\frac{d\phi}{dt} 10^{-8} = -\frac{d}{dt} (\Phi \cos \alpha) 10^{-8} = \Phi \sin \alpha \frac{d\alpha}{dt} 10^{-8} \text{ volt} \quad (1-6a)$$

where  $d\alpha/dt$  is the angular velocity  $\omega$  of rotation of the coil. For a uniform angular velocity of the coil,  $\alpha = \omega t$  and

$$e = \omega \Phi 10^{-8} \sin \omega t \quad (1-6b)$$

It can be seen from Fig. 1-5 that the induced emf  $e$  lags the flux interlinkage  $\phi$  by  $90^\circ$ ; when  $\phi$  is maximum ( $\alpha = 0$ ),  $e$  is zero, and  $e$  becomes a maximum, when  $\alpha = \pi/2$  and  $\phi$  is zero. These same conclusions follow from Eq. 1-6. The instantaneous flux interlinkage is

$$\phi = \Phi \cos \omega t = \Phi \sin \left( \omega t + \frac{\pi}{2} \right)$$

which is a function of  $\sin \left( \omega t + \frac{\pi}{2} \right)$ , while the instantaneous emf  $e$  is a function of  $\sin \omega t$ .

Representing the amplitudes (or the effective values) of the sinusoidal functions  $\phi$  and  $e$  by phasors, *that is, quantities whose values are represented by complex numbers, the emf phasor must lag the flux phasor by  $90^\circ$ .*

The amplitude of the induced emf is (Eq. 1-6b)

$$E_m = \omega \Phi 10^{-8} \text{ volt} \quad (1-7a)$$

The period of a sine function is  $2\pi$ . If  $T$  is the time of a period in seconds and  $f$  the frequency in cycles per second, then

$$2\pi = \omega T \quad \text{where} \quad f = \frac{1}{T}$$

and

$$\omega = \frac{2}{T} \pi = 2\pi f$$

Hence

$$E_m = 2\pi f \Phi 10^{-8} \text{ volt} \quad (1-7b)$$

and the effective value of  $e$  is

$$E = \frac{2\pi}{\sqrt{2}} f \Phi 10^{-8} = 4.44 f \Phi 10^{-8} \text{ volt} \quad (1-8)$$

The frequency  $f$  can be expressed in terms of the revolutions per minute of the armature and the number of poles. Consider Fig. 1-4. While the coil is making one revolution, it generates one cycle of the emf (Fig. 1-5). If the armature rotates at  $n$  revolutions per minute, the frequency in cycles per second will be  $f = n/60$ . This applies to a 2-pole machine. If the number of poles is  $p$  instead of 2, it still holds that the emf goes through a complete cycle when the coil passes two poles of the machine and therefore the fre-



quency is

$$f = \frac{p}{2} \frac{n}{60} = \frac{pn}{120} \text{ cps} \quad (1-9)$$

It has been assumed in Eqs. 1-6a to 1-8 that the coil consists of two conductors making one turn. If the number of series connected turns of the coil is  $n_c$  and the  $n_c$  turns are so concentrated that they are interlinked with the same number of flux lines at any instant of time, the induced emf will be  $n_c$  times that given by Eqs. 1-7 and 1-8, i.e.,

$$E_m = \omega n_c \Phi 10^{-8} = 2\pi f n_c \Phi 10^{-8} \text{ volt} \quad (1-10)$$

and

$$E = 4.44 n_c f \Phi 10^{-8} \text{ volt} \quad (1-11)$$

**Example 1-1.** A coil with five series-connected turns rotates in a sinusoidally distributed flux at a speed of 1200 rpm. The flux per pole is  $\Phi = 3 \times 10^6$  maxwells; the number of poles is  $p = 6$ . What is the average emf induced in the coil? What is the amplitude and the effective value of the emf induced in the coil? What is the frequency of the emf induced in the coil?

From Eq. 1-3a, with  $p = 6$  and  $n_c = 5$

$$E_{av} = 4 \times 3 \times 10^6 \times \frac{6}{2} \times 5 \times \frac{1200}{60} \times 10^{-6} = 36 \text{ volts}$$

From Eq. 1-9

$$f = \frac{6 \times 1200}{120} = 60 \text{ cps}$$

From Eq. 1-10

$$E_m = 2\pi \times 60 \times 5 \times 3 \times 10^6 \times 10^{-8} = 56.6 \text{ volts}$$

$$E = \frac{56.6}{\sqrt{2}} = 40 \text{ volts}$$

Since the flux is sinusoidally distributed,  $E_{av}$  must be  $\frac{2}{\pi} \times E_m$ .

Faraday's law of induction, Eq. 1-1, can also be interpreted in another manner. In this equation  $e$  is the total emf induced in the closed circuit; i.e., if the circuit were opened somewhere and an oscillograph inserted, the value of  $e$  measured at each instant would be for the entire circuit. In reality,  $e$  is the sum of all elemental emf's  $de$  which are induced in the individual elements  $dl$  of the circuit, and Eq. 1-1 can be written:

$$e = \oint E_t dl = - \frac{d\phi}{dt} 10^{-8} \text{ volt} \quad (1-12)$$

where  $E_t$  is the component of the electric field intensity  $E$  in the direction of  $dl$ . This equation states that every change in the lines of flux linking a circuit produces an electric field within the circuit, and that the line integral

of the intensity of this electric field (the induced emf) is equal to  $-\frac{d\phi}{dt}$ .

(Ref. A11.)

In the previous examples (Figs. 1-1 to 1-3), the flux is produced by a magnet, and the change of flux interlinkage is caused by a relative movement of a coil and a magnet. According to Faraday's law of induction, it is only the *change of flux interlinkage* that causes an emf to appear in a circuit, no matter what the source of the flux. Therefore, an emf will be induced in a circuit if its own flux is changed by changing its current, or if the flux of an adjacent circuit is changed by changing the current in this latter circuit. In the first case this will be an emf of *self-induction*; in the second case, an emf of *mutual induction*.

In the case of self-induction, the flux interlinkages of the circuit are determined by its own current:

$$\sum N_x \phi_x = Li \quad (1-13)$$

$$L = \sum N_x \phi_x / i$$

where  $N_x$  is the number of turns interlinked with a flux  $\phi_x$ .  $L$  is the *coefficient of self-inductance*. According to Eq. 1-13 it is the *flux interlinkage per unit current*. The magnitude of  $L$  depends upon the geometrical arrangement of the conductors, upon the number of turns, and upon the magnetic nature of the surroundings. The last-mentioned factor plays a great part in the magnitude of the flux  $\Phi$  and the flux interlinkage. If the surroundings contain ferromagnetic materials, the magnetic resistance (reluctance) is much lower and the flux  $\Phi$  is much larger for the same current than in the case when there are no ferromagnetic materials. This is discussed in Art. 1-3. It is also shown that when there are no ferromagnetic materials, the flux is directly proportional to the magnetizing force (the current), and therefore, in this case, the coefficient of self-inductance  $L$  in Eq. 1-13 is a constant. On the other hand, in ferromagnetic materials flux and magnetizing force are coordinated through the magnetization curve of the material (Fig. 1-8) which has a non-linear character; therefore the coefficient of self-inductance  $L$  is not a constant in this case, but varies with the magnetizing force. For constant  $L$ , according to Eq. 1-1, the emf of self-induction is

$$e_s = -\frac{d\phi}{dt} 10^{-8} = -L \frac{di}{dt} \text{ volt} \quad (1-14)$$

where  $L$  is measured in henries.

If  $i$  is sinusoidal,

$$i = I_m \sin \omega t$$

the emf of self-induction becomes

$$e_s = -I_m \omega L \cos \omega t = I_m \omega L \sin (\omega t - 90^\circ) = I_m N \phi \sin (\omega t - 90^\circ) \quad (1-14a)$$

i.e., the amplitude of the emf of self-induction is equal to  $I_m \omega L$  and the emf of self-induction lags the current by  $90^\circ$ . Note that Eq. 1-14a is in complete accordance with Eq. 1-6b. The latter equation states that the amplitude of the induced emf is equal to  $\omega$  times the maximum flux interlinkage; in Eq. 1-14a,  $I_m L$  is nothing more than the maximum flux interlinkage, for, according to Eq. 1-13,  $L$  is the flux interlinkage per unit current.

In the case of mutual induction, the flux interlinking circuit 1 (the circuit considered) is:

$$(\sum N_x \phi_x)_1 = M i_2 \quad (1-15)$$

The coefficient of mutual inductance  $M$  depends upon the same quantities as does  $L$ , and also upon the relative position of both circuits with respect to each other. For constant  $M$ , according to Eq. 1-1, the emf of mutual induction is:

$$e_{M1} = -M \frac{di_2}{dt} \text{ volt} \quad (1-16a)$$

and vice versa

$$e_{M2} = -M \frac{di_1}{dt} \text{ volt} \quad (1-16b)$$

where  $M$  is measured in henries.

**Example 1-2.** A solenoid with 400 turns carries a 60-cycle current of  $I = 6$  amp. The maximum flux interlinked with each of the 400 turns is  $4 \times 10^6$  maxwells. The surrounding is air. What is the coefficient of self-inductance of the coil? What is the effective value of emf of self-induction?

From Eq. 1-13

$$L = \frac{400 \times 4 \times 10^6}{\sqrt{2} \times 6} \times 10^{-8} = 1.886 \text{ henries}$$

From Eq. 1-14a

$$E_s = 6 \times 2\pi \times 60 \times 1.886 = 4270 \text{ volts}$$

**Example 1-3.** The field circuit of a d. c generator has an inductance of 4 henries. Its field current of 8 amp is interrupted in 0.06 sec. What is the average emf induced in the winding?

From Eq. 1-14

$$e_{s,av} = 4 \frac{8}{0.06} = 534 \text{ volts}$$

(b) *Kirchhoff's mesh law.* This law states: In each mesh of a network, the sum of all impressed and induced emf's taken with proper consideration to signs is equal to the sum of all resistive voltage drops.

$$\sum (V + E) = \sum IR \quad (1-17)$$

(1) *R-L circuit.* Applying Kirchhoff's law to an *R-L* circuit with a constant *L* and an impressed voltage *v*, the equation obtained is

$$v - L \frac{di}{dt} = iR \quad (1-18a)$$

$$v = iR + L \frac{di}{dt} \quad (1-18b)$$

where *v* and *i* are the instantaneous values of impressed voltage and current, respectively.

Eq. 1-18b, which is identical with Eq. 1-18a, can be interpreted in the following way: at any instant of time, the impressed voltage must overcome the resistive voltage drop and the emf of self-induction. While this interpretation is physically correct, it would be entirely wrong to conclude from Eq. 1-18b that  $L(di/dt) = -e_s$  is of the same nature as the resistive voltage drop *iR*. It should not be forgotten that *L* is flux interlinkage associated with an induced emf, but nothing else.

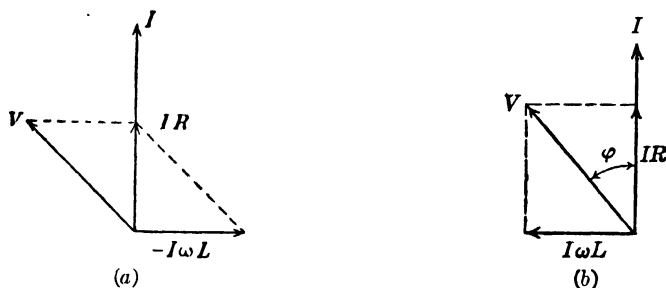


FIG. 1-6. Phasor diagram of voltages in an *R-L* circuit.

If *v* in Eq. 1-18 is sinusoidal, *i* will also be sinusoidal. A sinusoidal quantity can be represented either by the projections of a rotating phasor on a fixed line or by the projections of a fixed phasor on a rotating line (*time line*). It is customary in the first case to select the counter-clockwise rotation of the phasor; therefore, the time line must rotate clockwise in the second case. The magnitude of the phasor is equal to the amplitude of the sinusoidal quantity. Using this phasor representation, the phasor diagram (Fig. 1-6a) is obtained for Eq. 1-18a. *IR* is the resistive voltage drop in phase with *I*;  $-I\omega L$  is the emf of self-induction, 90° behind *I* in accordance with Eq. 1-14a. The geometric sum of *V* and  $-I\omega L$  is equal to *IR* corresponding to Kirchhoff's law, Eq. 1-17.

The phasor representation of Eq. 1-18b is given by Fig. 1-6b. Here  $I\omega L$  is drawn 90° ahead of *I* and is interpreted as the component of *V* necessary to overcome the emf of self-induction. The geometric sum of *IR* and  $I\omega L$  then yields the impressed voltage *V*.

The phasor diagram of Fig. 1-6b is the representation usually presented in textbooks.

In the representation of sinusoidal quantities by complex notation, multiplication by  $+j$  rotates the phasor  $90^\circ$  in a positive direction, and multiplication by  $-j$  rotates the phasor  $90^\circ$  in a negative direction. If the current phasor  $I$  is used as a reference, then the phasor diagram of Fig. 1-6a can be expressed as

$$\dot{V} - j\dot{I}\omega L = \dot{I}R \quad (1-19a)$$

and the phasor diagram of Fig. 1-6b as

$$\dot{V} = \dot{I}R + j\dot{I}\omega L \quad (1-19b)$$

Since the emf of self-induction lags the current which produces it by  $90^\circ$ , its amplitude is multiplied by  $-j$  in Eq. 1-19a where the left side represents the sum of  $V$  and  $E_s$ . The component of the impressed voltage necessary to overcome  $E_s$  is shifted  $180^\circ$  with respect to  $E_s$  and is therefore  $90^\circ$  ahead of  $I$ . For this reason  $I\omega L$  appears with multiplier  $+j$  in Eq. 1-19b.

It is customary to use the symbol  $x$ , called *reactance*, for  $\omega L$ . It should be remembered that  $L$  means flux interlinkages per unit current and is associated with an induced emf; therefore the reactance  $x$  always is *associated with an induced emf*. Introducing  $x$ , Eqs. 1-19a and 1-19b become

$$\dot{V} - j\dot{I}x = \dot{I}R \quad (1-19c)$$

$$\dot{V} = \dot{I}R + j\dot{I}x \quad (1-19d)$$

(2) *R, L, and M circuit with constant L and M.* Applying Kirchhoff's law to an  $R, L, M$ -circuit with an impressed voltage  $v$ , the voltage equation for the instantaneous values is

$$v_1 - L_1 \frac{di_1}{dt} - M \frac{di_2}{dt} = i_1 R_1^* \quad (1-20)$$

For sinusoidal voltages and currents, the voltage equation for effective values is, corresponding to Eq. 1-19a,

$$\dot{V}_1 - j\omega L_1 \dot{I}_1 - j\omega M \dot{I}_2 = \dot{I}_1 R_1 \quad (1-21a)$$

and, corresponding to Eq. 1-19b,

$$\dot{V}_1 = \dot{I}_1 (R_1 + j\omega L_1) + j\omega M \dot{I}_2 \quad (1-21b)$$

Introducing the symbol  $x_1$  for  $\omega L_1$  (primary reactance) and the symbol  $x_m$

\* The emf of mutual induction is introduced here as  $-M(di_2/dt)$ , i.e., with a positive sign for  $M$ . The sign of  $M$  depends, in general, upon the assumed directions of current flow in the coils and upon the manner in which the coils are wound (see references on A-c Circuits). In this text, the directions of the currents and the manner in which the coils are wound will each be assumed so as to yield a positive value for  $M$ .

for  $\omega M$  (mutual reactance), Eqs. 1-21 become

$$\dot{V}_1 - jx_1 \dot{I}_1 - jx_m \dot{I}_2 = \dot{I}_1 R_1 \quad (1-22a)$$

$$\dot{V}_1 = \dot{I}_1 (R_1 + jx_1) + jx_m \dot{I}_2 \quad (1-22b)$$

In Eqs. 1-19b, 1-21b, and 1-22b, the emf's of self- and mutual induction appear as voltage drops. As pointed out previously, it should not be forgotten that the symbols  $\omega L$ ,  $\omega M$ , and  $x$  are always associated with an induced emf.

It should be noted that Eqs. 1-18 to 1-22 apply only when  $L$  and  $M$  are constants, i.e., when the surroundings do not contain ferromagnetic materials. The case of electric circuits surrounded by iron is treated in connection with the transformer (Art. 12-1).

(c) *Circuital law of the magnetic field (Ampere's law).* A relation similar to Eq. 1-12 also holds for the magnetic circuit, i.e., for a closed magnetic circuit carrying a magnetic flux.

If  $H_i$  is the magnetic field intensity at the element  $dl$  of the magnetic circuit,  $N$  the number of turns which are linked by the magnetic flux, and  $I$  the current which flows in the winding, then the equation referred to above is

$$\oint H_i dl = NI \quad (1-23)$$

This equation states that *the line integral of the magnetic field strength along a closed path is equal to the sum of the ampere-turns with which this path is linked.* (See references on Electromagnetic Field Theory.)

Fig. 1-7 shows a solenoid and the flux produced by it. The line integral  $\oint H_i dl$  is the same for all three closed lines (1, 2, and 3) because all three are linked by the entire turns of the solenoid and therefore  $NI$  is the same for all three. The value of the integral  $\oint H_i dl$  is not affected by the shape or the length of the force line selected. For a long line, such as 3, the number of terms  $dl$  appearing in the sum will increase, but the field intensity becomes smaller as the distance from the coil increases.

Eq. 1-23 can be put easily into a form which is similar to Ohm's law for

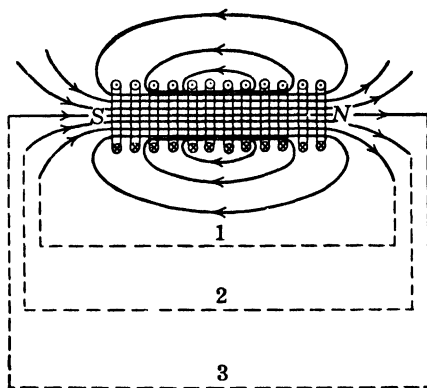


FIG. 1-7. Flux produced by a solenoid.

the electric circuit. For the flux density  $B$ , the relation holds that

$$B = \mu_0 \mu H \quad (1-24)$$

$\mu_0$  is the permeability of a vacuum. Its magnitude depends upon the system of units used.  $\mu$  is the relative permeability of the material, i.e., the ratio of its permeability to that of free space (vacuum). If in Eqs. 1-23 and 1-24, the current  $I$  is expressed in amperes,  $H$  in ampere-turns per centimeter, which, as far as fundamental dimensions are concerned, is the same as amperes per centimeter,  $B$  in gauss,  $\mu_0$  is then in gauss centimeter per ampere, and numerically equals  $0.4 \pi$ .

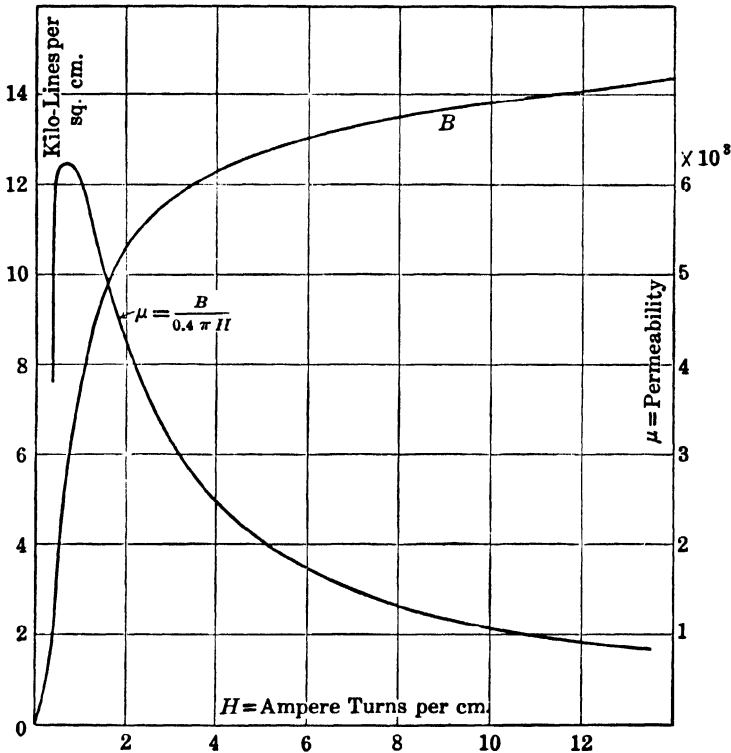


FIG. 1-8. Flux density  $B$  and permeability  $\mu$  as functions of field intensity  $H$ .

For air  $\mu = 1$ , while for iron  $\mu$  is a variable which depends upon the saturation. As an example, Fig. 1-8 shows the value of  $\mu$  as a function of the field strength  $H$  for electrical sheet steel (1.0% silicon); in this case  $\mu$  has a maximum value of 6100. The values of  $B$  are also shown in Fig. 1-8. The  $BH$  curve is called the *magnetization curve* of the material in question. This curve is used in making calculations for magnetic circuits.

The relation between magnetic flux  $\phi$ , cross-section  $A$ , and the flux density

$B$  is given by:

$$\phi = BA \quad (1-25)$$

Substituting Eqs. 1-24 and 1-25 in Eq. 1-23, there results:

$$\phi = \frac{0.4\pi NI}{R_m} \quad (1-26)$$

where

$$R_m = \int \frac{dl}{\mu A} = \sum \frac{l}{\mu A} \quad (1-27)$$

Eq. 1-26 is *Ohm's law of the magnetic circuit*. The factor  $NI$  is analogous to the emf in the electric circuit and is called the *magnetomotive force*. It is usually symbolized by  $M$  or by  $AT$ .  $R_m$  is the magnetic resistance or reluctance of the magnetic circuit.  $R_m$ , similar to the electric resistance, depends upon the length, cross-section, and magnetic conductivity or permeability of the flux path. Notice that  $R_m$  depends upon the value of  $\mu$ . Since in ferromagnetic materials  $\mu$  varies with the magnetizing force,  $R_m$  also varies with the magnetizing force in these materials. An example of the magnetic field is given in Chapter 4.

(d) *Forces on conductors in a magnetic field (Biot-Savart's law). Magnitude and direction of the force.* When a current-carrying conductor is properly oriented in a magnetic field, a force is exerted upon it. If the direction of the lines of induction make an angle  $\alpha$  with the direction of the current-carrying conductor (Fig. 1-9), this force is

$$f = 8.85 \times 10^{-8} B l_e I \sin \alpha \quad \text{lb} \quad (1-28a)$$

where  $l_e$  is the effective length of the conductor in inches, i.e., the length of the conductor lying within the flux,  $I$  the current in amperes, and  $B$  the density of the flux (in lines per square inch) in which the conductor is located.

In electric machines, the lines of induction and the conductors are practically always perpendicular to each other. Thus, in electric machines,

$$f = 8.85 \times 10^{-8} B l_e I \quad \text{lb} \quad (1-28b)$$

The direction of the force  $f$  on the conductor can be determined with the aid of the left-hand rule; open the left hand, keep the fingers together and the thumb in the same plane as the palm but pointing at right angles to the fingers. If the fingers point in the direction of current, and the flux enters the

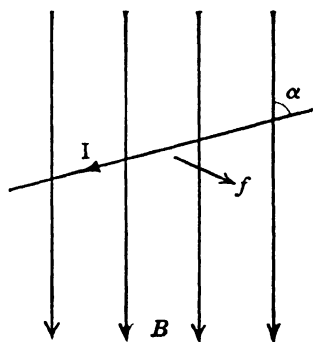


FIG. 1-9. Force on a current-carrying conductor in a magnetic field.



palm at right angles to it, the thumb points in the direction of the force. (Compare with the rule for the direction of the induced emf.)

Another rule for the determination of the direction of the force  $f$  is the following (Fig. 1-10): draw some lines of induction  $B$ , draw a circle between the lines to represent the cross-section of the conductor, and show by two arrows  $aa$  the direction of the field due to the current within the conductor. The conductor will tend to move *toward the region of opposing fields*.

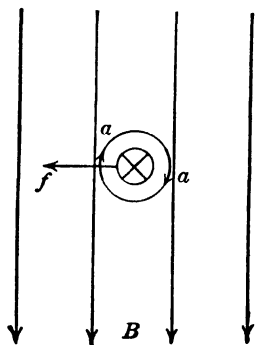


FIG. 1-10. Determination of the direction of the force on a current-carrying conductor in a magnetic field.

It follows from these rules that the force  $f$  is always perpendicular to the plane through  $I$  and  $B$ .

The force on the coil between two poles in Fig. 1-2 will be considered. Fig. 1-11 shows the direction of the forces exerted upon the two coil sides. Because of the large difference between the permeabilities of air and iron, the lines of induction in the air-gap are perpendicular to the iron and therefore the forces are *tangential* to the armature. The forces on both sides act as a couple and tend to rotate the coil about the armature axis. The torque on each conductor, corresponding to the force  $f$ , is equal to  $fR$ , when  $R$  is the radius of the armature. In accordance with the law of

action and reaction, this torque acts not only upon the conductors but also upon the magnetic poles.

In the case of an alternating field and a conductor carrying alternating current, the instantaneous values of the flux density  $B$  and the current  $I$  must be used in Eq. 1-28. If the average value of the force is calculated for a single period, it is found to depend upon the effective values of  $B$  and  $I$ , and upon the time phase displacement between these quantities, i.e.,

$$F_{av} = 8.85 \times 10^{-8} B_{eff} l_c I \cos(B, I) \quad (1-29)$$

The torque produced by the couple in Fig. 1-11 is greatest when the flux and current are in time phase. This point will be considered later.

Eq. 1-28 for the force shows that the direction of the torque changes if the direction of *either* the flux *or* the current is changed. Changing the direction of the current and flux simultaneously does not change the direction of the torque. This explains why a unidirectional torque is possible in an a-c machine.

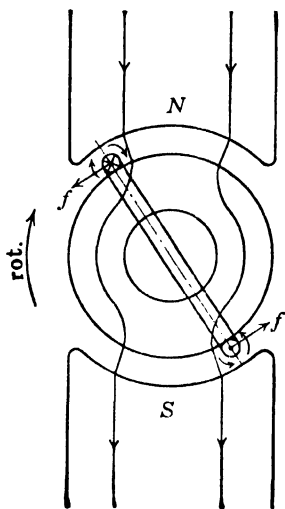


FIG. 1-11. Force on a coil of an electric machine.

The forces shown in Fig. 1-11 refer to a generator driven (by a prime mover) in clockwise direction. Fig. 1-11 also shows the direction of the torque produced by the generated current: it is counterclockwise. Thus, in the case of a generator, the torque developed between the conductors and the flux (the electromagnetic torque) acts in a direction opposite to the direction of rotation and it has to be overcome by the prime mover. In the case of a motor, the torque developed between the conductors and the flux is in the same direction as the direction of rotation and is delivered to its shaft. The balance of torques thus occurs in such a manner that in the generator the torque delivered by the prime mover is balanced by the opposing electromagnetic torque of the armature; in the motor the electromagnetic torque produced by the armature is balanced by the opposing torque of the load. It is well to remember that the generator converts mechanical power into electrical power and the motor converts electrical power into mechanical power.

Eq. 1-29 which gives the average value of the tangential force permits the derivation of a useful formula for the *electromagnetic power* of the electric machine. The torque produced by both sides of the coil (Fig. 1-11) is, in lb-ft,

$$T = 2 \times 8.85 \times 10^{-8} l_e B_{\text{eff}} I \cos(B, I) \times \frac{R}{12} \quad \text{lb-ft} \quad (1-30)$$

where  $R = D/2$  is the radius of the rotor in inches. The relation between torque and power is given by the fundamental equation of mechanics:

$$T = \frac{5250}{n} P_{\text{hp}} = \frac{7.04 P_{\text{watts}}}{n} \quad \text{lb-ft} \quad (1-31)$$

Observe that the *area of the flux distribution curve*, i.e., of the  $B$  curve (Fig. 1-4 or Fig. 1-5), is the *flux per pole per unit length of the armature*, so that for a sinusoidal flux distribution

$$\Phi = \frac{2}{\pi} \tau l_e B \quad (1-32)$$

where  $B$  is the amplitude of the sinusoidal  $B$  curve. The pole pitch  $\tau$  is given by Eq. 1-5. The speed  $n$  in Eq. 1-31 can be expressed by the frequency  $f$  using Eq. 1-9 with  $p = 2$ , since a 2-pole structure is considered.

Combining Eqs. 1-30, 1-31, and 1-32 and introducing Eq. 1-11 the following result is obtained for the power  $P$ :

$$P = EI \cos(B, I) \text{ watts}$$

It is seen from Fig. 1-5 that  $E$ , being  $90^\circ$  behind  $\Phi$ , is in phase with  $B$ , so that the electromagnetic power of the electric machine is

$$P = EI \cos \psi \text{ watts} \quad (1-33)$$

where  $\psi$  is the angle between  $E$  and  $I$ . Combining Eqs. 1-31 and 1-33, then will result

$$T = \frac{7.04 EI \cos \psi}{n} \text{ lb-ft} \quad (1-34)$$

Eq. 1-33, although derived for an elementary machine with two poles and a single coil under the assumption of a sinusoidal flux distribution, applies also to the actual electric machine. It will be seen later that the angle  $\psi$  is smaller than  $90^\circ$  in a generator and larger than  $90^\circ$  in a motor.

**1-3. Method of approach.** All the electric machines consist of magnetically coupled electric circuits. The transformer consists of exactly these same elements. It appears logical, then, to start with the transformer. It is true that the windings of the transformer are at standstill with respect to each other, while the windings of the electric machines move with respect to each other. It will be shown that this relative movement of the windings can be easily introduced as an additional factor into the equations of the transformer. Furthermore, it will be shown that the machines treated in this text can be considered as consisting of only two magnetically coupled electric circuits the basis for which is then the single phase transformer.

Using the transformer as the basis for the treatment of the electric machines, the sequence in which these machines should be studied is

1. Induction motors
2. Synchronous machines
3. Direct-current machines
4. Rotary converters
5. A-C commutator motors.

This sequence follows the degree of similarity between the transformer and the electric machine type.

## PROBLEMS

1. A conductor 10 in. long is moving with a velocity of 80 fpm perpendicular to a magnetic flux whose average density is 60,000 lines per sq. in. Determine the average voltage generated.
2. Determine the velocity of a conductor 15 in. long moving perpendicularly across a magnetic flux of 40,000 lines per sq. in. average density if an average voltage of 0.05 volt is to be induced.
3. A 4-pole generator having a coil of 60 turns on the armature produces a maximum coil voltage of 28.3 volts with a pole flux of  $10^6$  maxwells. The flux distribution is sinusoidal. Determine the generator speed.
4. A conductor is "cutting flux" at an average rate of 150,000 lines per sec. Determine the average voltage induced in the conductor.
5. It is desired to induce an average voltage of 3.5 volts in a coil linking a

certain magnetic circuit. The flux changes from  $+200,000$  lines to  $-200,000$  lines in a time interval of  $1/3$  sec. Determine the number of turns on the coil.

6. A 6-pole generator has a flux per pole of  $2 \times 10^6$  maxwells. The armature rotates at 720 rpm. The flux distribution is sinusoidal. Determine the average emf and the maximum emf induced in a full pitch coil of 5 turns.

7. A square coil 10 in. on each edge has 25 turns and rotates at a speed of 1000 rpm in a magnetic field of 2000 lines per sq. in. Determine the maximum flux passing through the coil, and the average emf induced in the coil. What is the voltage if flux and speed are both increased 50%.

8. A 4-pole generator has a flux of  $3.5 \times 10^6$  maxwells per pole. The armature rotates at 600 rpm. (a) Calculate the average voltage generated in a turn when it travels one pole pitch. (b) What is the average voltage generated in one conductor in  $1/4$  revolution of the armature?

9. An armature conductor 15 in. long moves in a flux the density of which is 50,000 lines per sq. in. under the center of the pole. The diameter of the coil of which the conductor is a part is 15 in. and the armature rotates at 1200 rpm. What is the emf induced in the conductor when it lies under the center of the pole?

10. At what speed must the armature of Problem 9 move in order that the emf induced in the conductor be 12 volts.

11. A square coil, 8 in. on each edge, has 50 turns and its plane lies perpendicular to a uniform magnetic flux with a density of 5000 lines per sq. in. The coil rotates  $\frac{1}{4}$  turn about its axis in 0.08 sec. Determine: (a) maximum flux interlinked with the coil; (b) average emf induced during this 0.08 sec; (c) average emf induced if the coil is made to rotate at 150 rpm; (d) instantaneous emf when coil is perpendicular to the flux and also when it is parallel to the flux.

12. A current of 10 amp flowing in a 400-turn coil produced a flux of 8000 lines interlinking these 400 turns. Determine: (a) the flux linkages in maxwell turns; (b) the self-inductance in henries.

13. If the number of turns in the coil of Problem 12 is doubled and the current remains the same, determine the flux linkages and self-inductance in henries. Assume all flux lines link all turns.

14. 1000 turns are wound upon an iron core magnetic circuit of 3 sq. in. cross-section. A current of 9 amp produces a flux density of 85,000 lines per sq. in. and a current of 4 amp produces 65,000 lines per sq. in. Determine the coefficient of self-inductance for each current.

15. The field of a shunt generator has a self-inductance of 35 henries. The current in the field winding is changed from 1.5 amp to 0.80 amp in 0.01 sec. Determine the emf of self-induction.

16. What is the emf of self-induction in Problem 15 if the current changes to zero in the same time?

17. The four shunt field coils of a generator are connected in series and each has 1000 turns. A direct current of 4.0 amp produces  $0.5 \times 10^6$  lines of flux linking each coil. Determine: (a) the coefficient of self-inductance of the entire winding; (b) the total energy storage. If the field circuit is opened and the current decays to zero in 0.25 sec, what is the average value of voltage generated across the field?

18. Two field coils of a 2-pole machine are wound with 1500 turns each. A field current of 3.0 amp produces a flux of  $3 \times 10^6$  maxwells linking each coil. What is the self-inductance of the field circuit?

19. A 4-pole generator having 2000 field turns per pole produces a pole flux of  $3 \times 10^6$  maxwells when the field current is 2.80 amp. Determine: (a) maxwell-turn linkages per pole; (b) total maxwell-turn linkages; (c) coefficient of self-inductance of the field circuit.

20. A mutual inductance of 3.1 henries magnetically couples two circuits. If the current in the first circuit changes from 2.75 to 1.0 amp in 0.015 sec, what is the average voltage induced in the second circuit?

21. A cast-iron ring has a mean diameter of 12 in. and a circular cross-section of 3.5 sq. in. area. Determine the number of ampere-turns required to produce a total flux of 110,000 maxwells.

22. Solve Problem 21 for the case where an air gap 0.10 in. is cut in the cast-iron ring. (Neglect fringing.)

23. How many additional ampere-turns are required in Problem 21 if the total flux is (a) increased 20%, (b) decreased 20%.

24. A cast-steel ring having a mean diameter of 5.5 in. and a circular cross-sectional area of 0.85 sq. in. has an air gap 0.10 in. long cut in the ring. (a) Determine the number of ampere-turns necessary to produce fluxes of 30, 50, 80, 100 and 105 kilolines per sq. in. (b) if the winding on the ring has 250 turns, plot the curve of total flux vs. exciting current.

25. A 200-turn, single-layer coil is wound uniformly upon the entire of a wooden toroidal ring having a mean diameter of 6 in. and a square cross-section of 1 sq. in. area. Determine: (a) flux density in core when coil current is 4 amp; (b) flux density if the wooden ring is replaced by a cast-steel ring of the same dimensions and the coil carries 4 amp.

26. A cast-steel ring having a mean radius of 10 in. and a circular cross-section 2 in. in diameter is wound with a coil of 700 turns carrying 10 amp. Determine the flux density and the total flux.

27. If an air gap 0.50 in. long is cut in a cast-iron ring of 10 in. mean radius and 3.5 sq. in. circular cross-section, determine the total flux and flux density when 2500 ampere-turns are impressed upon the magnetic circuit.

28. A conductor 25 in. long carries a current of 15 amp and is acted upon by a force of 2 lb when placed in a magnetic flux perpendicular to the flux lines. Determine the flux density in gausses and in lines per square inch.

29. Determine the current carried by a conductor 15 in. long if a force of 0.001 lb acts upon it when it is placed in a magnetic flux of 5000 lines per sq. in. flux density so that the lines of flux make an angle of  $45^\circ$  with the normal to the conductor.

30. A flat, square coil of 20 turns having an area of 60 sq. in. is placed in a uniform magnetic flux, so that the plane of the coil is parallel to the flux lines and the two active coil sides lie perpendicular to the lines of flux. The flux density is 5000 lines per sq. in. and the coil current is 10 amp. Determine: (a) the force in pounds acting on each side of the coil; (b) the torque in pound-feet acting to turn the coil.

31. The coil in Problem 30 is replaced by a 25-turn rectangular coil having dimensions  $12" \times 18"$ , with the longer sides being the active conductors. Determine the turning torque in pound-feet when the current is 15 amp.

32. Repeat Problem 31 with the plane of the coil making an angle of  $45^\circ$  with the direction of the flux lines.

33. Repeat Problem 31 with the plane of the coil making an angle of  $60^\circ$  with the direction of the flux lines.

34. A 15-in. conductor carrying 20 amp lies in a uniform magnetic flux. A force of 0.25 lb tends to move the conductor perpendicular to the flux and to itself. Determine the flux density.

## Chapter 2

---

### TRANSFORMER CONSTRUCTION

Since a-c electric machines are normally built for low frequencies only the low-frequency power transformer will be considered in this text. For transformers operating at higher frequencies, such as those used in transformer-coupled audio amplifiers, and as impedance matching devices in communication circuits, see the listed references.

The American Institute of Electrical Engineers gives the following definition for a transformer: "A transformer is an electric device, without continuously moving parts, which by electromagnetic induction transforms electric energy from one or more circuits at the same frequency, usually with changed values of voltage and current."

**2-1. Transformer types.** The construction of single-phase transformers may be divided into three main types: *core type*, *shell type*, and *spiral-core type*. In all types the core is constructed of laminations using transformer *sheet* steel assembled to provide a continuous magnetic circuit with a minimum of air-gap included. The steel used is of high silicon content, sometimes heat-treated to produce a high permeability and a low core loss at the operating flux density.

In core- and shell-type transformers the individual laminations are L or E shaped. The laminations are varnished or coated to insulate them from each other and thereby reduce the circulating eddy currents. Fig. 2-1a shows the general assembly of laminations and coils of the core-type transformer. Fig. 2-1b shows the manner in which high- and low-voltage coils are grouped together on the legs of a core-type transformer. Figs. 2-2a and 2-2b show the general arrangement of coils and laminations in the shell-type transformer. The shell-type transformer may have a simple form of core such as in Fig. 2-2a or a distributed form (cruciform). In the shell-type transformer the magnetic circuit encloses most of the windings. Figs. 2-3a and 2-3b show the core of the *distributed* shell-type transformer; Fig. 2-4 is a view of such a transformer showing laminations, coils, insulation, cooling ducts, and high- and low-voltage leads.

The choice of core- or shell-type construction is usually one of cost, for similar characteristics can be obtained with both types. For high-voltage

transformers or for multi-winding design some manufacturers prefer the shell-type construction. Usually in this type the iron path is shorter and the mean length of coil turn is longer than in a comparable core-type design. Both core and shell forms are used, and selection is based upon many factors such as voltage rating, kva rating, weight, insulation stress, mechanical stress, and heat distribution.

The spiral core transformer shown in Fig. 2-5 is the newest development in core construction. The core is assembled either of a *continuous* strip of transformer steel wound in the form of a circular or elliptical cylinder, or of a group of short strips assembled to produce the same elliptical-shaped core. By using this construction the core flux always follows along parallel with the grain of the iron. Cold-rolled steel of high silicon content enables the designer to use higher operating flux densities with lower loss per pound. The higher flux density reduces the weight per kva.

**2-2. Windings.** The coils used in transformers are usually form wound and are of either the *cylindrical* or *disc* type. The general form for these types may be circular, oval, rectangular, etc. Fig. 2-6 shows a multi-coil rectangular cylindrical type winding, and Fig. 2-7 shows the manner in which a large round cylindrical coil is wound. The circular cylindrical coil has greater mechanical strength and is employed in most core-type power transformers. Cylindrical coils are wound in helical layers with the layers insulated from each other by paper, cloth, micarta board, or cooling oil ducts. Figs. 2-1a and 2-1b show the general arrangement of these coils with respect to the core. Insulating cylinders of fuller board separate the cylindrical windings from the core and from each other. Since the low-voltage winding is the easiest to insulate, it is placed nearest the core.

Disc coils, such as that shown in Fig. 2-8, may be of one turn per layer or

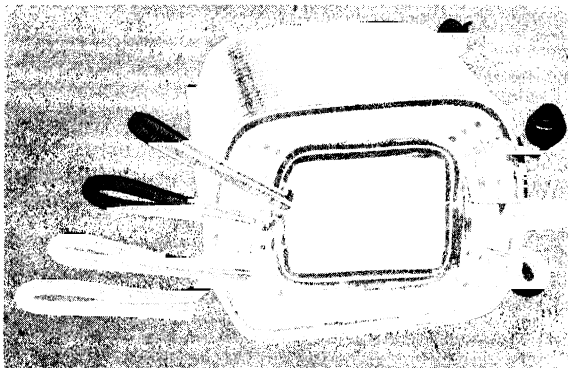


FIG. 2-6. Cylindrical or helical-type of form-wound coil (multi-coil winding).



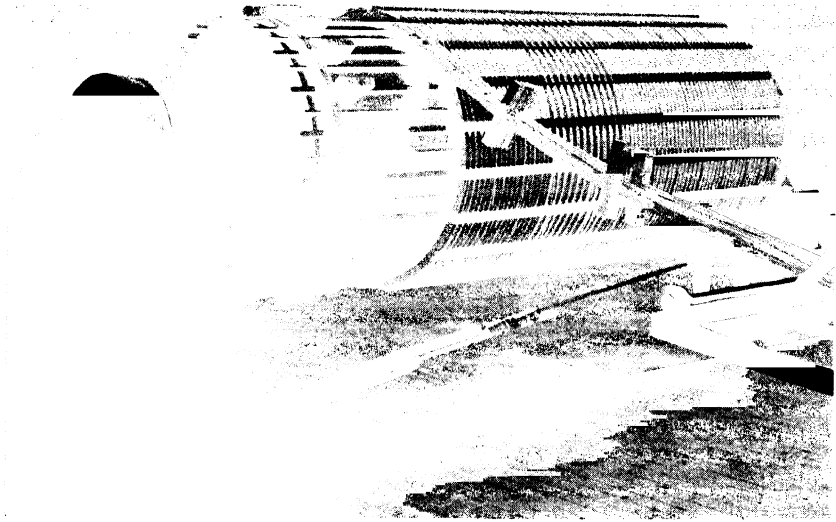


FIG. 2-7. Winding a round cylindrical coil for a 55,000-kva, 287,500/16,320-volt transformer.

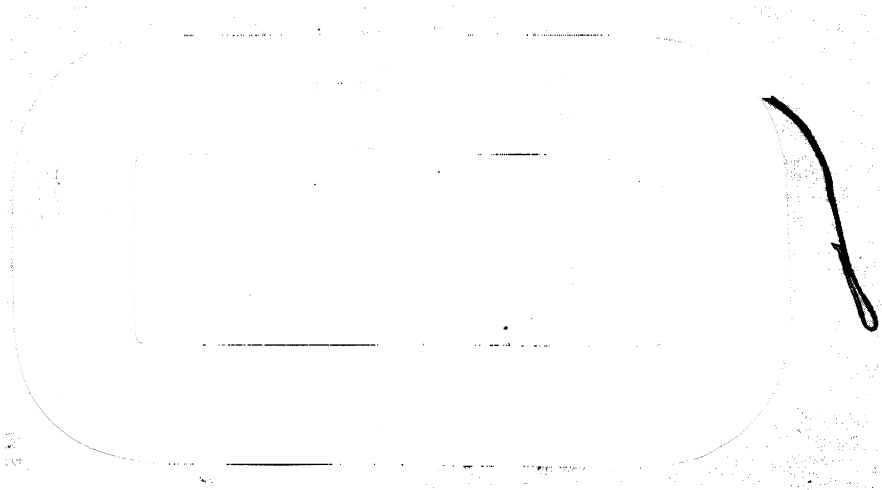


FIG. 2-8. Disc or pancake coil.

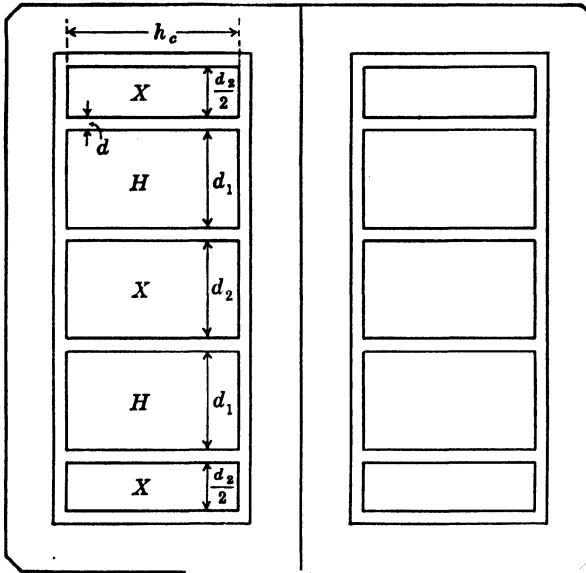


FIG. 2-9. Shell-type transformer showing disc coils.

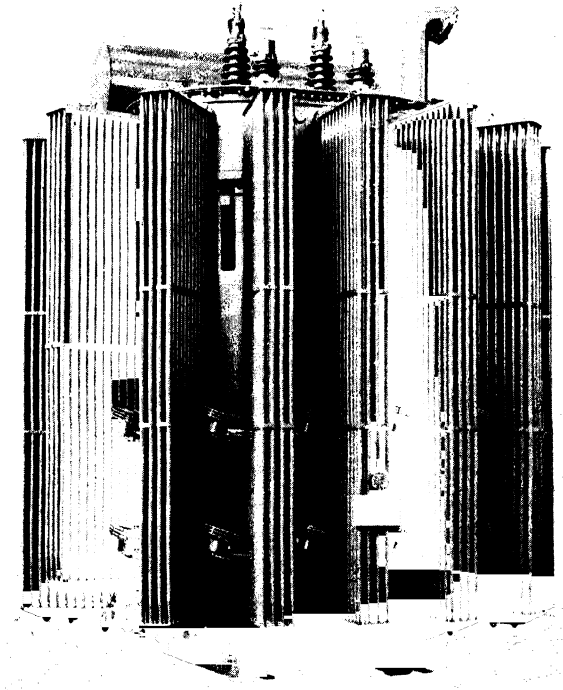


FIG. 2-10. Three-phase, 31,250-kva transformer with radiators and cooling fans.

many turns per layer. Multi-layer discs have the separate layers insulated from each other by paper. A complete winding consists of discs stacked with insulation spaces between the coils as shown in Fig. 2-9; the spaces form horizontal cooling and insulating oil ducts. The low- and high-voltage windings are subdivided into a number of discs and stacked alternately, with the end discs being a part of the low-voltage winding. The leakage reactance is reduced if the end discs contain one half as many turns as the remaining low-voltage discs.

Cores and coils must be provided with mechanical bracing to prevent movement and possible insulation damage. Good bracing also reduces vibration and noise during operation.

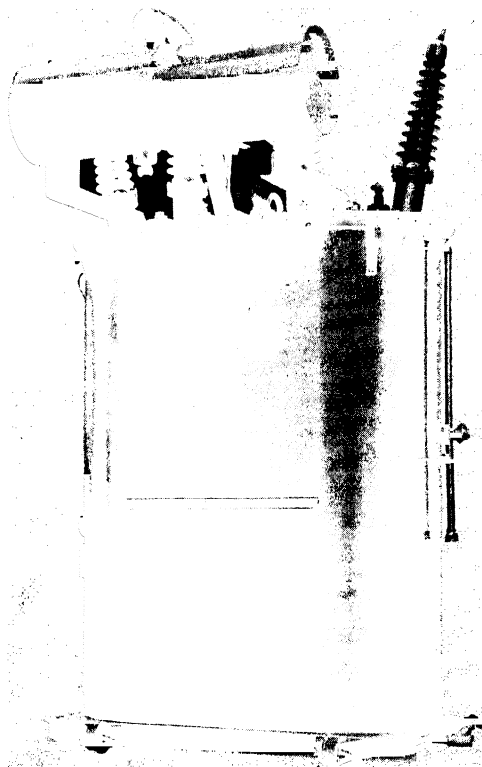


FIG. 2-11. Three-phase, 9,000-kva, 67,560/6,900-volt water-cooled transformer with conservator tank.

**2-3. Cooling.** Transformers may be air-cooled, oil-cooled, or water-cooled. Whatever the method of cooling, the essential problem is that of the heat transfer from the iron and copper of the transformer to the cooling medium. This heat transfer is accomplished by natural oil or air convection, forced oil

or air convection, oil-to-air heat transfer or oil-to-water heat transfer. The tanks may be smooth-sided or corrugated to increase the radiating surface area. Fig. 2-10 shows the use of cooling fans with external radiators. Fig. 2-11 shows a water-cooled transformer with an oil conservator tank. The conservator tank serves as an oil reservoir and also limits the surface area of oil exposed to air, thus reducing the formation of sludge within the oil: with the conservator tank, the main tank can be completely filled with oil. Although the oil is used as a cooling medium, it is also employed for its *insulating qualities* and must be dirt and moisture free. Non-inflammable liquids sold under trade names of Pyranol, Inertol, etc. have been developed to remove the hazard of fire associated with oil.

## Chapter 3

### THE TRANSFORMER AT NO-LOAD

The single-phase transformer described in the following paragraphs consists of two electric circuits and one magnetic circuit. Therefore its study must be based on Kirchhoff's mesh law for the electric circuits and on the circuital law of the magnetic field (Ampere's law) for the magnetic circuit.

Once Kirchhoff's mesh equations for the electric circuits and the relations following from Ampere's law are established, the phasor diagram, the equivalent circuit and the operational characteristics of the transformer can be readily determined. However, a preliminary study is necessary in order to set up the basic relations of the electric and magnetic circuits. The transformer will be considered first at no-load, then under load.

**3-1. The transformer primary.** Fig 3-1 shows an iron core assembled of laminations; two coils are wound on the legs. Coil II, the secondary winding, will be considered open in this article. If an alternating voltage is impressed upon the primary winding, coil I, an alternating current  $I_0$  will flow in it, and this current will produce an alternating magnetic flux.

The current  $I_0$ , the *no-load current*, will lag behind the impressed voltage  $V_1$  by an angle  $\phi_0$  which is about  $90^\circ$ . The active component of  $I_0$ , i.e.,  $I_0 \cos \phi_0$ , supplies the hysteresis and eddy current losses ( $P_{h+e}$ ) in the core iron and the small amount of copper losses in the primary winding. The reactive component of  $I_0$ , i.e.,  $I_0 \sin \phi_0$ , which is much larger than the active component  $I_0 \cos \phi_0$ , is necessary to sustain the alternating flux. This reactive current  $I_0 \sin \phi_0$  is small in comparison with the rated primary current of the transformer, because the magnetic circuit of the transformer consists almost entirely of iron (the air gaps at the joints amount to only about 0.0010 to 0.0015 in.). Such a magnetic circuit has a small reluctance and requires a low magnetizing current in order to produce the flux.

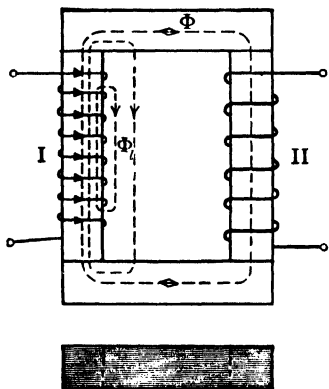


FIG. 3-1. Elementary single-phase transformer.

The flux alternates at the same frequency as the current and induces an emf of self-induction in the primary winding, coil I. Kirchhoff's equation of the primary is therefore (see Eq. 1-19a).

$$\dot{V}_1 - j\dot{I}_0\omega L_1 = \dot{I}_0 r_1 \quad (3-1)$$

$L_1$  is the coefficient of self-inductance of the primary winding, i.e., the flux interlinkages of this winding per ampere. Examining the flux lines, it is found that there are two parts of the flux with two different paths. By far the greatest part of the flux lines (part  $\Phi$ ) is in the iron. Another part ( $\Phi_l$ ) of the flux, small in comparison to that in the iron, exists in parallel paths through the air as indicated in Fig. 3-1. The part of the flux in the air is directly proportional to the current (see Art. 1-2) because the path for these lines consists essentially of air, for which the permeability is a constant ( $\mu = 1$ ); on the other hand, the relationship existing between the current and the flux  $\Phi$  in the iron is given by the magnetization curve for the particular kind of laminations used, which has a non-linear character. As has been explained previously (Art. 1-2), the coefficient of self-inductance is not a constant for the flux in the iron.

A considerable simplification in the study of the transformer behavior is achieved, when the two parts of the flux are considered separately.

The flux in the air is then referred to as the *leakage flux* ( $\Phi_l$ ) and that in the iron as the *main flux*  $\Phi$ . It is only the main flux which links with the turns of secondary coil II and induces there an emf.

Corresponding to the division of the flux into two parts, the coefficient of self-inductance  $L_1$  and the emf of self-induction  $-j\dot{I}_0\omega L_1$  are also divided into two components. The two components of  $L_1$  are  $L_{l1}$  and  $L_m$  and the two components of  $-j\dot{I}_0\omega L_1$  are  $-j\dot{I}_0\omega L_{l1}$  and  $-j\dot{I}_0\omega L_m$ .  $L_{l1}$  is the coefficient of self-inductance of the primary *leakage flux* and  $L_m$  the coefficient of self-inductance of the main flux.

In transformers with iron core, as considered here, the variation of the main flux is connected with losses in the core, namely, hysteresis and eddy current losses. The relation between the main flux, the emf induced by it in the primary winding (which will be denoted by  $E_1$ ) and the current  $I_0$  is shown in Fig. 3-2.

The emf  $E_1$  induced in the primary winding by the main flux  $\Phi$  lags this flux by  $90^\circ$ . To produce the flux  $\Phi$  a current component *in phase with*  $\Phi$ , i.e., a current component leading  $E_1$  by  $90^\circ$  is required. Another current component which is supplied by the lines and *in counter-phase with*  $E_1$  (see

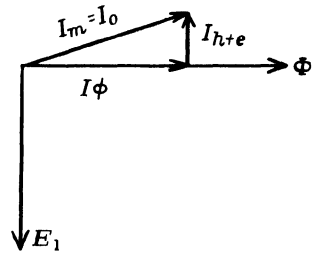


FIG. 3-2. Relation between main flux, emf induced in the primary winding, and magnetizing current.

Fig. 3-3) is required to supply the hysteresis and eddy current losses due to the main flux. The first current component, designated by  $I_\phi$ , is the reactive component of the magnetizing current  $I_m$ ; the second current component, designated by  $I_{h+e}$ , is the active component of the magnetizing current  $I_m$ . Thus

$$\dot{I}_m = \dot{I}_\phi + \dot{I}_{h+e} \quad (3-2)$$

The active component of the no-load current  $\dot{I}_0$ ,  $\dot{I}_0 \cos \phi_0$ , is larger than  $\dot{I}_{h+e}$  by a small amount corresponding to the copper loss  $I_0^2 r_1$  in the primary winding. Since this copper loss at no-load is negligible in comparison with the iron loss in the core, with very close approximation  $\dot{I}_m \approx \dot{I}_0$ .

In order to get the relation between  $E_1$  and the magnetizing current  $\dot{I}_m = \dot{I}_\phi + \dot{I}_{h+e}$  we write, according to Fig. 3-2.

$$\dot{I}_\phi = jc_1 \dot{E}_1$$

$$\dot{I}_{h+e} = -c_2 \dot{E}_1$$

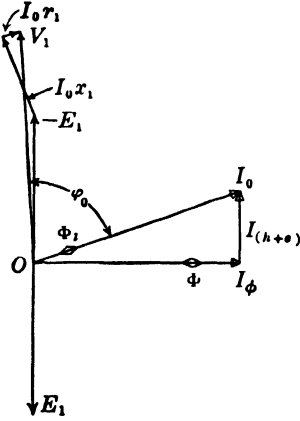


FIG. 3-3. No-load phasor diagram.

so that

$$\dot{I}_m = \dot{I}_\phi + \dot{I}_{h+e} = -\dot{E}_1(c_2 - jc_1)$$

The quantity in parentheses is an admittance. It is called the *main flux admittance* and will be denoted by  $Y_m$ . Instead of  $c_1$  and  $c_2$  the symbols  $b_m$  and  $g_m$  will be used; thus

$$\dot{I}_m = -\dot{E}_1 \dot{Y}_m = -\dot{E}_1(g_m - jb_m) \quad (3-4)$$

$g_m$  is the main flux *conductance*;  $b_m$  is the main flux *susceptance*. Writing

$$-\dot{E}_1 = \frac{\dot{I}_m}{\dot{Y}_m} = \dot{I}_m \dot{Z}_m = \dot{I}_m(r_m + jx_m) \quad (3-5)$$

$r_m$  takes into account the iron losses produced by the main flux and  $x_m = \omega L_m$  is the *main flux reactance*.  $Z_m$  is the *main flux impedance*. Since  $Z_m = 1/Y_m$

$$r_m = \frac{g_m}{g_m^2 + b_m^2} \quad x_m = \frac{b_m}{g_m^2 + b_m^2} \quad (3-6)$$

With  $E_1$  as the emf induced in the primary winding by the main flux, Kirchhoff's mesh equation for the primary circuit becomes (see Eq. 1-19a)

$$\dot{V}_1 + \dot{E}_1 - j\dot{I}_1 \omega L_{l1} = \dot{I}_1 r_1 \quad (3-7)$$

The subscript 1 indicates the primary circuit. Since no-load is considered,  $I_1 = I_0$ . Introducing the *primary leakage reactance*  $x_1$ ,

$$\omega L_{11} = x_1 \quad (3-8)$$

Eq. 3-7 becomes

$$\dot{V}_1 + \dot{E}_1 - j\dot{I}_1 x_1 = \dot{I}_1 r_1 \quad (3-9)$$

$E_1$  is given by Eq. 3-4 or 3-5. Eq. 3-9 can be written as

$$\dot{V}_1 = -\dot{E}_1 + j\dot{I}_1 x_1 + \dot{I}_1 r_1 \quad (3-9a)$$

In the latter form  $-E_1$  is the component of the primary voltage necessary to overcome the emf induced in the winding by the main flux;  $+jI_1 x_1$  is the component of the primary voltage necessary to overcome the emf induced by the primary leakage flux; and  $I_1 r_1$  is the component of the primary voltage necessary to drive the current  $I_1$  through the resistance  $r_1$ .

Eq. 3-9a also can be interpreted in the following way: the voltage impressed on the primary winding  $V_1$  is balanced by the negative value of the emf induced in it by the main flux,  $-E_1$ , and by the voltage drops due to the leakage reactance and the resistance.

The complete phasor diagram at no-load is shown in Fig. 3-3. If the reactive component  $I_\phi$  of the magnetizing current is drawn along the horizontal and is directed to the right, the flux  $\Phi$  is in phase with  $I_\phi$ ; the emf  $E_1$  lags  $\Phi$  by  $90^\circ$  and is therefore directed downward; and consequently the voltage component necessary to overcome  $E_1$  ( $-E_1$ ) leads the flux and the current  $I_\phi$  by  $90^\circ$  and is directed upward. The leakage reactance drop  $I_\phi x_1$ , i.e., the component of the terminal voltage necessary to overcome the emf due to the leakage flux, is perpendicular to  $I_\phi$  and leads  $I_\phi$  by  $90^\circ$ , and the component to overcome the ohmic resistance drop  $I_\phi r_1$  is in phase with the current. The geometric sum of the three voltages,  $-E_1$ ,  $I_\phi x_1$ , and  $I_\phi r_1$ , is the primary applied voltage  $V_1$ . The phase displacement angle between the current  $I_\phi$  and the terminal voltage  $V_1$  is nearly  $90^\circ$ ;  $I_\phi$  is *almost* a pure reactive current with respect to  $V_1$ . It should be realized that the values of  $I_\phi r_1$  and  $I_\phi x_1$  are in reality *very much smaller* in proportion to  $-E_1$  and  $V_1$  than those shown in Fig. 3-3. Also  $I_\phi x_1$  is usually larger than  $I_\phi r_1$ .

**3-2. The transformer secondary.** Consider coil II, the secondary winding, with the winding open (no-load) just as in the foregoing discussion. The lines of force of the alternating main flux  $\Phi$  go through the iron, link this secondary winding, and induce an emf  $E_2$  in it. Since the main flux and its frequency are the same for both primary and secondary windings, the emf's induced in the two windings are respectively proportional to their numbers of turns  $N_1$  and  $N_2$ :

$$\frac{E_1}{E_2} = \frac{N_1}{N_2} = a \quad (3-10)$$



According to Eq. 1-11,

$$E_1 = 4.44 N_1 f \Phi 10^{-8} \text{ volt} \quad (3-11)$$

$$E_2 = 4.44 N_2 f \Phi 10^{-8} \text{ volt} \quad (3-12)$$

The ratio  $N_1/N_2$  is called the *ratio of transformation*. Since the no-load current  $I_0$  is small, the resistance drop as well as the leakage reactance drop is small at no-load, and  $E_1$  is almost equal to the terminal voltage  $V_1$ . Accordingly, the ratio of transformation is often given with sufficient accuracy by the ratio of terminal voltages at no-load:

$$\frac{N_1}{N_2} = \frac{E_1}{E_2} \approx \frac{V_1}{V_2} \quad (3-13)$$

### PROBLEMS

1. A transformer having 480 primary turns and 120 secondary turns takes a power input of 80 watts and a current of 1.40 amp when the primary is connected to a 120-volt, 60-cycle line and the secondary is on open circuit. The primary resistance is 0.25 ohm. Determine the iron loss in watts, the no-load power factor, and the maximum core flux assuming the resistance and reactance drops as negligible. Draw the phasor diagram.

2. A 5-kva, 110/220-volt, 60-cycle transformer has 120 turns on the primary winding, and a core having a cross-section of 4.70 sq. in. and a mean length of 31 in. Using the curves for transformer steel given on page 33, determine the effective value of the magnetizing current and the maximum value of the flux density.

3. If the flux density in a given 2300/230-volt, 60-cycle transformer is not to exceed 60,000 lines per sq. in., determine the number of primary turns when the core cross-section is 26.5 sq. in.

4. A 7.5-kva, 1100/110-volt, 60-cycle transformer is connected across an 1100-volt line with the secondary open. The power input is 120 watts and the no-load current  $I_0$  is 0.40 amp.  $N_1 = 800$  turns,  $N_2 = 80$  turns,  $r_1 = 4$  ohms and  $r_2 = 0.04$  ohm. (a) If the primary leakage reactance drop is neglected, what is the magnitude of the primary and secondary induced voltages? (b) Draw the phasor diagram to scale. (c) What is the maximum value of core flux?

5. If, in Problem 4, the primary leakage flux at no-load is 0.15% of the total flux calculated in part (c), determine the primary and secondary induced voltages. Draw the phasor diagram to scale.

6. A 50-kva, 2300/230-volt, 60-cycle transformer takes 200 watts and 0.30 amp at no-load when 2300 volts is applied to the high-voltage side. The primary resistance is 3.5 ohms. Neglecting the leakage reactance drop determine: (a) no-load power factor; (b) primary induced voltage  $E_1$ ; (c)  $I_{h+c}$ ; (d)  $I_\phi$ . Draw the phasor diagram to scale.

7. A 1000-kva, 25-cycle, 27,000/2200-volt transformer is designed to operate at a maximum flux density of 75,000 lines per sq. in. and an induced voltage of 20

volts per turn. Determine the primary turns  $N_1$ , secondary turns  $N_2$ , and the cross-section area of the core in square inches.

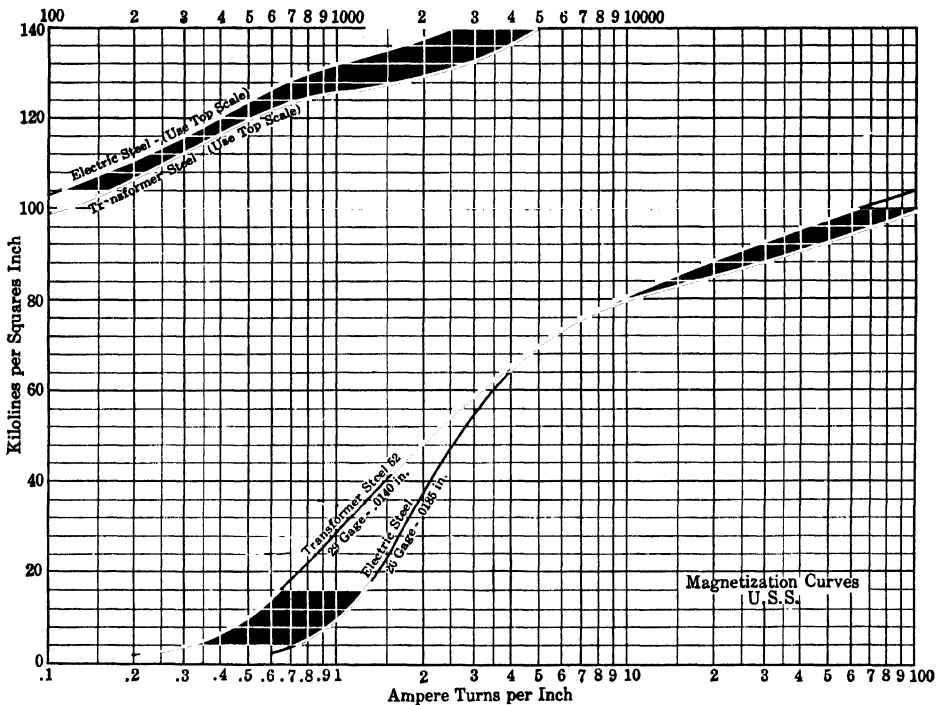
8. Repeat Problem 7 for a 25-cycle, 66,000/1100-volt transformer.

9. The core of a 500-kva transformer has a mean length of 66 in. and a cross-section of 260 sq. in. The primary consists of four identical coils.

(a) If 15,000 volts at 60 cycles is impressed across the four primary coils in series, and the maximum flux density is to be 75,000 lines per sq. in., determine  $I_{h+c}$ ,  $I_\phi$ ,  $I_0$  and the no-load power factor. Use the curves for transformer steel given below.

10. Repeat Problem 9 if 7500 volts at 60 cycles is impressed across two coils connected in series.

11. Repeat Problem 9 if 3750 volts at 60 cycles is impressed across the four coils in parallel.



Magnetization curves for transformer steel and dynamo steel.

## Chapter 4

### THE TRANSFORMER UNDER LOAD

**4-1. The behavior of the transformer primary under load.** Consider the transformer to be loaded, i.e., with a consumer of electric energy placed across the secondary terminals. Since an induced emf ( $E_2$ ) exists in the secondary winding, a current  $I_2$  will flow through the load resistance and the secondary winding. When the transformer losses (copper losses in both windings and hysteresis and eddy-current losses in the core iron) are disregarded, then, according to the law of conservation of energy, the power taken by the primary winding from the lines is equal to the power delivered to the external circuit placed across the secondary winding: i.e., if the secondary is loaded, the current taken by the primary winding from the lines must change as the secondary load current is changed.

As a result of the change in the primary current due to the load, the three components of voltage which balance the primary terminal voltage (Eq. 3-9) also change: the resistance drop and the leakage reactance drop increase or decrease with load change and therefore the voltage  $E_1$  induced by the main flux  $\Phi$  becomes correspondingly smaller or greater. However (in ordinary power transformers) the resistance and leakage reactance drops are usually small in comparison to the emf  $E_1$  even at rated load, so that  $E_1$  has approximately the same value for the loaded as well as the unloaded transformer; since the main flux  $\Phi$  is determined by  $E_1$  (see Eq. 3-11), this means that the main flux  $\Phi$  varies only slightly between no-load and full load. Therefore, practically the same magnetomotive force ( $I_\phi N_1$ , see

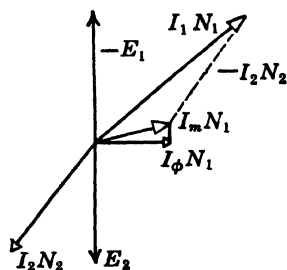


FIG. 4-1. Mmf diagram under load.

Fig. 3-2) and the same magnetizing mmf ( $I_m N_1$ ) are necessary to produce the main flux  $\Phi$  under conditions of load and no-load. The main flux  $\Phi$  is largest at no-load and becomes smaller as short-circuit conditions are approached (see Art. 2).

When the secondary is loaded, *two mmf's act on the transformer*, the mmf of the primary winding and the mmf of the secondary winding; the magnitude of the main flux is determined by the *resultant* of these two mmf's. As explained, this mmf changes little between no-load and full load. Fig. 4-1 shows

the mmf diagram of a loaded transformer in which, assuming a resistive load, the secondary current  $I_2$  lags the emf  $E_2$  induced in the secondary winding by the main flux.  $E_2$  as well as  $E_1$  lags behind the flux  $\Phi$  by  $90^\circ$ . The geometric sum of the primary mmf  $I_1 N_1$  and the secondary mmf  $I_2 N_2$  yields the resultant magnetizing mmf  $I_m N_1$  which is necessary to produce the main flux  $\Phi$ .

Since the reluctance of the magnetic circuit of the transformer is comparatively low, the magnetizing mmf is only about 5 to 10% of the total primary mmf under conditions of rated load; this is the same as saying that the magnetizing current is about 5 to 10% of the rated line current. Therefore, it can be approximated that  $I_1 N_1 \approx I_2 N_2$ , or

$$\frac{I_2}{I_1} \approx \frac{N_1}{N_2} = \frac{E_1}{E_2} \quad (4-1)$$

The currents in the two windings, therefore, are approximately inversely proportional to the induced emf's. This is in conformity with the law of conservation of energy (disregarding losses), for according to this law  $V_1 I_1 \cos \phi_1 = V_2 I_2 \cos \phi_2$ . It will be seen from the following text that  $\cos \phi_1 \approx \cos \phi_2$  for the fully loaded transformer.

**4-2. Reduction of the secondary voltage, current, and parameters to the primary.** The mmf diagram of Fig. 4-1, the phasor diagram of the loaded transformer, and its equivalent circuit become simpler if the assumption is made that *the secondary winding has the same number of turns as the primary winding*, i.e., that  $N_2 = N_1$ . Such an assumption will be permissible if care is taken that the secondary quantities, with  $N_1$  turns, are such that:

1. The mmf of the secondary winding retains its original value, i.e., that the resultant mmf and the main flux  $\Phi$  remain unchanged,
2. The kva of the secondary retain the original value,
3. The  $I^2 R$  loss of the secondary retains its original value,
4. The magnetic energy ( $\frac{1}{2} L_{12} I_2^2$ ) of the secondary leakage flux which appears when the secondary carries current retains its original value.

The secondary quantities expressed in  $N_1$  turns are designated as *referred to the primary* or *reflected into the primary*. They will be indicated by a *primed* letter.

The first condition means that the secondary current referred to the primary ( $I_2'$ ) must be such that

$$I_2' N_1 = I_2 N_2 \quad (4-2)$$

or

$$I_2' = I_2 \frac{N_2}{N_1} = \frac{I_2}{a} \quad (4-2a)$$

where  $a = N_1/N_2$

The second condition requires that

$$E_2' I_2' = E_2 I_2 = E_2' I_2 \frac{N_2}{N_1}$$

or

$$E_2' = E_2 \frac{N_1}{N_2} = E_2 a = E_1 \quad (4-3)$$

This means that the secondary and primary emf's induced by the main flux are equal. This corresponds to the assumption that the number of turns of the secondary winding is equal to that of the primary winding.

The third condition means that

$$I_2'^2 r_2' = I_2^2 r_2$$

Inserting the value of  $I_2'$  from Eq. 4-2a

$$r_2' = \left( \frac{N_1}{N_2} \right)^2 r_2 = a^2 r_2 \quad (4-4)$$

the fourth condition requires that

$$\frac{1}{2} I_2'^2 x_2' = \frac{1}{2} I_2^2 x_2$$

where  $x_2$  is the actual leakage reactance of the secondary. Inserting the value of  $I_2'$  from Eq. 4-2a

$$x_2' = \left( \frac{N_1}{N_2} \right)^2 x_2 = a^2 x_2 \quad (4-5)$$

Thus, calculating with the referred quantities  $E_2'$ ,  $I_2'$ ,  $r_2'$  and  $x_2'$  instead of the actual quantities  $E_2$ ,  $I_2$ ,  $r_2$ , and  $x_2$  does not change anything in the magnetic and electric behavior of the transformer.

It follows from Eqs. 4-2 to 4-5 that the reduction factors to the primary are:  $N_1/N_2 = a$ , for voltage,  $N_2/N_1 = 1/a$  for current, and  $(N_1/N_2)^2 = a^2$  for resistance and reactance.

**4-3. Kirchhoff's mesh law for the secondary.** Kirchhoff's mesh law for the primary is given by Eq. 3-9 or 3-9a. Kirchhoff's mesh equation for the secondary is

$$\dot{E}_2 = \dot{I}_2(r_2 + jx_2) + \dot{I}_2(R_L + jX_L) = \dot{I}_2(r_2 + jx_2) + \dot{V}_2 \quad (4-6)$$

where  $R_L$  and  $X_L$  are the load resistance and reactance respectively and  $V_2$  is the voltage at the load terminals. With all quantities referred to the primary, Eq. 4-6 becomes

$$\dot{E}_2' = \dot{E}_1 = \dot{I}_2'(r_2' + jx_2') + \dot{I}_2'(R_L' + jX_L') = \dot{I}_2'(r_2' + jx_2') + \dot{V}_2' \quad (4-7)$$

**4-4. The emf  $E_1 = E_2'$  induced by the main flux under load.** According to Eq. 4-2,  $I_2' N_1 = I_2 N_2$ . By introducing  $I_2' N_1$  for  $I_2 N_2$  it is possible to

replace the mmf diagram under load, shown in Fig. 4-1, with a *current* diagram, because the secondary and primary mmf's have the same number of turns. It follows from Fig. 4-1

$$\dot{I}_1 N_1 + \dot{I}_2 N_2 = \dot{I}_m N_1 \quad (4-8)$$

Introducing  $I_2' N_1$  for  $I_2 N_2$

$$\dot{I}_1 N_1 + \dot{I}_2' N_1 = (\dot{I}_1 + \dot{I}_2') N_1 = \dot{I}_m N_1 \quad (4-8a)$$

or

$$\dot{I}_1 + \dot{I}_2' = \dot{I}_m \quad (4-9)$$

At no-load the core is magnetized by the mmf  $I_m N_1 \approx I_0 N_1$ . At load the core is magnetized by  $(\dot{I}_1 + \dot{I}_2') N_1$ . At no-load the reactive component of  $I_0(I_\phi)$  produces the main flux and the active component of  $I_0(I_{h+e})$  supplies the iron losses due to the main flux. At load the reactive component of  $(\dot{I}_1 + \dot{I}_2')$  produces the main flux and the active component of  $(\dot{I}_1 + \dot{I}_2')$  supplies the iron losses. Therefore Eqs. 3-4 and 3-5 apply also to the loaded transformer, if  $(\dot{I}_1 + \dot{I}_2')$  is substituted for  $I_0$  i.e., for load,

$$\dot{I}_m = \dot{I}_1 + \dot{I}_2' = -\dot{E}_1 \dot{Y}_m = -\dot{E}_2' \dot{Y}_m \quad (4-10)$$

or

$$-\dot{E}_1 = -\dot{E}_2' = (\dot{I}_1 + \dot{I}_2') \dot{Z}_m = \dot{I}_m \dot{Z}_m \quad (4-10a)$$

$Y_m$  and  $Z_m$  are given by Eqs. 3-4 and 3-5. The relations between  $g_m$ ,  $b_m$ ,  $r_m$ , and  $x_m$  are given by Eq. 3-6.

Eq. 4-8 has been derived from Fig. 4-1 which refers to a resistive load. This equation and the following equations derived from it apply to any kind of load.

Eq. 4-10 contains the parameters of the magnetic circuit  $r_m$  and  $x_m$  (or  $g_m$  and  $b_m$ ). Ampere's law of the magnetic circuit in its direct form  $\oint H_l dl = NI$

(Eq. 1-23) has not been applied to the magnetic circuit of the transformer in the previous considerations. However, it is directly involved in  $I_\phi$  and  $x_m = \omega L_m$ . The magnitude of the main flux can be determined from Eq. 3-11. If  $A$  is the cross-section of the core, then the flux density in the core is  $B = \Phi/A$ . The magnetization curve of the iron used yields then  $H$ . If  $l$  is the length of the magnetic path in the core, then, according to Ampere's law,  $Hl = N_1 \sqrt{2} I_\phi$ . This yields  $I_\phi$ . Corresponding to the definition of  $L$  (Eq. 1-13),  $L_m = N_1 \Phi / \sqrt{2} I_\phi$ , where  $\Phi$  is the maximum value of the flux.

The single-phase transformer consists of two magnetically coupled electric circuits and, therefore, mutual inductance between the two circuits must exist. This mutual inductance has not been treated in the previous considerations. It will be shown that also it is contained in  $x_m$ .

**4-5. The mutual inductance of the transformer.** It will be assumed that the saturation of the transformer is very low so that not only the mmfs but also the fluxes of both windings can be added. The iron losses are also assumed to be negligible. The *total* coefficient of self-inductance of the primary winding will be denoted by  $L_1$ . It includes the interlinkages of the *total* flux  $\Phi_1$  produced by the primary winding, i.e., of the part  $\Phi_{1m}$  which goes through the core as well as of the part  $\Phi_{1l}$  which goes through the air and does not link with the secondary coil (leakage flux). Likewise the *total* coefficient of self-inductance of the secondary winding will be denoted by  $L_2$ . Then the differential equations for the voltages of both windings are (see Eq. 1-20)

$$v_1 = i_1 r_1 + L_1 \frac{di_1}{dt} + M \frac{di_2}{dt} \quad (4-11)$$

$$0 = i_2 r_2 + L_2 \frac{di_2}{dt} + M \frac{di_1}{dt} + v_2 \quad (4-12)$$

Assuming sinusoidal voltages and currents, the equations for the effective values (see Eq. 1-21) become

$$V_1 = I_1(r_1 + j\omega L_1) + jI_2\omega M \quad (4-13)$$

$$0 = I_2(r_2 + j\omega L_2) + jI_1\omega M + V_2 \quad (4-14)$$

The coefficient of self-inductance of the primary winding is (see Eq. 1-13)

$$L_1 = \frac{N_1 \Phi_1}{i_1} 10^{-8} = \frac{N_1(\Phi_{1m} + \Phi_{1l})}{i_1} 10^{-8} \quad (4-15)$$

where (Eq. 1-26)

$$\Phi_{1m} = 0.4\pi N_1 I_1 A_m \quad \text{and} \quad \Phi_{1l} = 0.4\pi N_1 i_1 A_{1l} \quad (4-16)$$

$A_m$  is the permeance of the iron core,  $A_{1l}$  the permeance of the primary leakage path. Thus,

$$L_1 = 0.4\pi N_1^2 (A_m + A_{1l}) 10^{-8} \quad (4-17)$$

For the secondary winding,  $L_2$  is obtained in the same way

$$L_2 = 0.4\pi N_2^2 (A_m + A_{2l}) 10^{-8} \quad (4-18)$$

The coefficient of mutual inductance is (see Eq. 1-15)

$$M_{21} = M_{12} = M = \frac{N_1 \Phi_{2m}}{i_2} 10^{-8} = \frac{N_2 \Phi_{1m}}{i_1} 10^{-8} = 0.4\pi N_1 N_2 A_m 10^{-8} \quad (4-19)$$

If  $N_2$  is made equal to  $N_1$ , i.e., all secondary quantities are referred to the primary, Eqs. (4-13) and (4-14) become

$$V_1 = I_1(r_1 + j\omega L_1) + jI_2'\omega M' \quad (4-20)$$

$$0 = I_2'(r_2' + j\omega L_2') + jI_1\omega M' + V_2' \quad (4-21)$$

and also (see Eqs. 4-18 and 4-19)

$$L_2' = 0.4\pi N_1^2(A_m + A_{2l})10^{-8} \quad (4-22)$$

$$M' = 0.4\pi N_1^2 A_m 10^{-8} \quad (4-23)$$

Inserting these two equations and also Eq. (4-17) into Eqs. (4-20) and (4-21) and introducing

$$L_{1l} = 0.4\pi N_1^2 A_{1l} 10^{-8} \quad \text{and} \quad L_{2l}' = 0.4\pi N_1^2 A_{2l}' 10^{-8} \quad (4-24)$$

there results

$$\dot{V}_1 = \dot{I}_1(r_1 + j\omega L_{1l}) + j(\dot{I}_1 + \dot{I}_2')\omega M' \quad (4-25)$$

$$0 = \dot{I}_2'(r_2' + j\omega L_{2l}') + j(\dot{I}_1 + \dot{I}_2')\omega M' + \dot{V}_2' \quad (4-26)$$

Since the iron losses are neglected,  $I_{h+e} = 0$  and (see Eq. 4-9)

$$\dot{I}_1 + \dot{I}_2' = \dot{I}_\phi. \quad (4-27)$$

Further,

$$\omega L_{1l} = x_1 \quad \text{and} \quad \omega L_{2l}' = x_2' \quad (4-28)$$

then from Eq. (4-25)

$$\dot{V}_1 = \dot{I}_1(r_1 + jx_1) + j\dot{I}_\phi\omega M' \quad (4-29)$$

and from Eq. (4-26)

$$-j\dot{I}_\phi\omega M' = \dot{I}_2'(r_2' + jx_2') + \dot{V}_2' \quad (4-30)$$

Comparing these equations with Eqs. (3-9) and (4-7), it is seen that

$$j\dot{I}_\phi\omega M' = -\dot{E}_1 = -\dot{E}_2' \quad (4-31)$$

From this equation and Eq. (3-5) with  $r_m = 0$  ( $I_m = I_\phi$ )

$$x_m = \omega M' \quad (4-32)$$

Thus the main flux reactance  $x_m$ , implies the mutual inductance between the windings.

$$\delta = \frac{L_1 L_2 - M^2}{L_1 L_2}$$

is the *total leakage coefficient*. The smaller  $\delta$  is, the closer is the inductive coupling of the two circuits.

$$k = \frac{M}{\sqrt{L_1 L_2}} = \sqrt{1 - \delta^2} < 1$$

is the *coefficient of coupling*.

**4-6. Application of the fundamental equations.** Equations 3-9, 4-7, and 4-10

$$\dot{V}_1 + \dot{E}_1 - j\dot{I}_1 x_1 = \dot{I}_1 r_1 \quad (4-33)$$



$$\dot{E}_2' - j\dot{I}_2'x_2' = \dot{I}_2'r_2' + \dot{V}_2' \quad (4-34)$$

$$\dot{E}_1 = \dot{E}_2' = -\dot{I}_m\dot{Z}_m = -(\dot{I}_1 + \dot{I}_2')\dot{Z}_m \quad (4-35)$$

are the fundamental equations of the transformer. Calculations referring to the performance of the transformer are determined by them or by relations derived from them.

The three equations 4-33 to 4-35 contain three unknown quantities,  $\dot{E}_1 = \dot{E}_2'$ ,  $\dot{I}_1$ , and  $\dot{I}_2'$ . Eliminating any two of them, the third quantity can be expressed as a function of the primary voltage  $V_1$ , the six parameters of the transformer ( $r_1, x_1, r_m, x_m, r_2', x_2'$ ) and the load parameters  $R_L'$  and  $X_L$ .

It is evident that the three equations 4-33 to 4-35 can be reduced to two equations with two unknown quantities  $\dot{I}_1$  and  $\dot{I}_2'$ , if Eq. 4-35 is introduced into Eqs. 4-33 and 4-34.

Multiplying Eq. 4-34 by  $I_2'$ , there results

$$E_2'I_2' - jI_2'^2x_2' = I_2'^2r_2' + I_2'V_2'$$

The first term represents the total power, active and reactive, of the secondary circuit (its total volt-amperes). The second term is the reactive power contained in the secondary leakage flux. The third term is the copper loss of the secondary winding. The last term is the total power, active and reactive, of the load.

The three fundamental equations 4-33 to 4-35 will be used to

(a) set up the phasor diagram of voltages and currents (mmfs) of the transformer.

(b) derive the equivalent circuit of the transformer.

It should be noted that phasor diagrams, equivalent circuits, etc., must be derived from the fundamental equations and not vice versa. This is a general statement which applies not only to the specific case of a transformer but to the investigation of the performance of other electrical apparatus.

## Chapter 5

### THE PHASOR DIAGRAM AND EQUIVALENT CIRCUIT OF THE TRANSFORMER UNDER LOAD

**5-1. The phasor diagram of the transformer under load.** In the phasor diagram,  $E_2'$  and  $E_1$  are in phase since both emf's are induced by the same flux  $\Phi$ . The phase displacement between the secondary terminal voltage  $V_2'$  and the secondary current  $I_2'$  is determined entirely by the character of the external load circuit. The component of the secondary emf  $E_2'$  necessary to overcome the secondary leakage reactance drop  $I_2'x_2'$  leads the current  $I_2'$  by  $90^\circ$ . The ohmic voltage drop  $I_2'r_2'$  is in phase with  $I_2'$ . According to Eq. 4-7, the geometric sum of  $I_2'r_2'$ ,  $I_2'x_2'$ , and  $V_2'$  must yield  $E_2' = E_1$ .

Fig. 5-1 shows the phasor diagram of the transformer loaded with a pure resistance. The phasors  $I_\phi$ ,  $I_{h+e}$ ,  $I_m$ ,  $\Phi$ , and  $E_1$  are drawn as for the unloaded transformer (see Fig. 3-3).  $E_2'$  is equal to and in phase with  $E_1$ . Since the load is purely resistive, the secondary current  $I_2'$  and the terminal voltage  $V_2'$  are in phase, so that  $V_2'$  and  $I_2'$  are drawn in the same direction. The

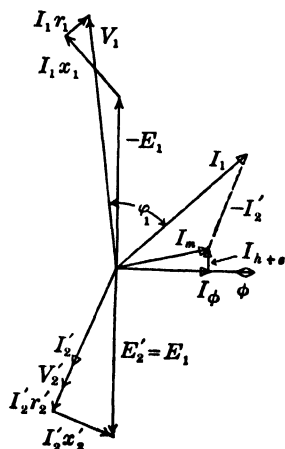


FIG. 5-1. Voltage and (mmf) current diagram of the transformer loaded with a pure resistive load.

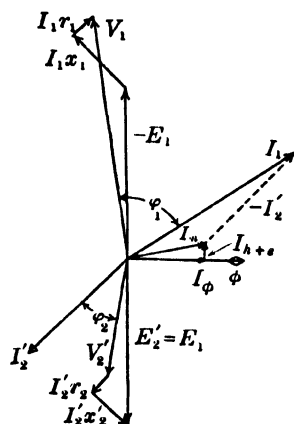


FIG. 5-2. Voltage and (mmf) current diagram of the transformer loaded with an inductive load.

emf  $E_2$  induced in the secondary by the main flux is obtained by adding to  $V_2'$  the quantities  $I_2'r_2'$  in phase with  $I_2'$  and  $I_2'x_2'$  perpendicular to  $I_2'$  and leading it by  $90^\circ$ .

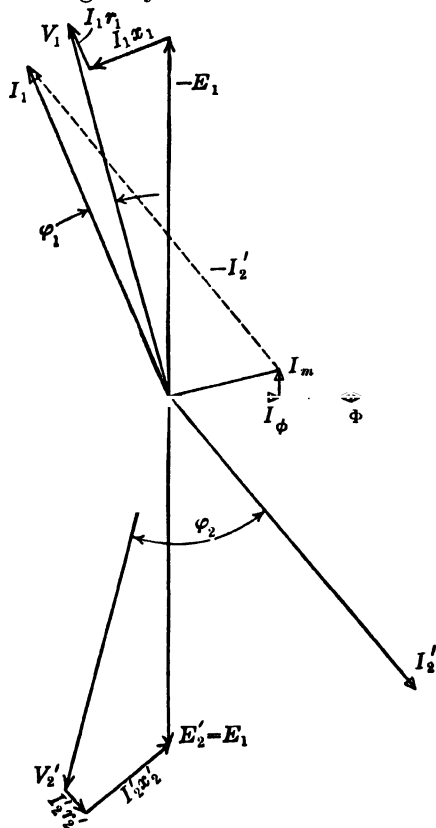


FIG. 5-3. Voltage and (mmf) current diagram of the transformer loaded with a capacitive load.

$\phi_1$  increases with increased inductive load, i.e., with increased angle  $\phi_1$ . For a capacitive load the situation may be reversed, as shown in Fig. 5-3.

From Eq. 4-9

$$\dot{I}_1 = \dot{I}_m + (-\dot{I}_2') \quad (5-1)$$

Thus, in the phasor diagram of Fig. 5-1, the current  $I_1$  is obtained by adding  $-I_2'$  to  $I_m$ . The phasor  $-E_1$ , which is the component of the primary voltage necessary to overcome the emf induced in it by the main flux, is drawn upward and  $90^\circ$  ahead of  $\Phi$ . Adding to  $-E_1$  the primary resistance drop  $I_1r_1$  in phase with  $I_1$  and the leakage reactance drop  $I_1x_1$  perpendicular to  $I_1$  and leading it by  $90^\circ$ , the primary voltage  $V_1$  is obtained.

$\phi_1$  is the phase-displacement angle of the primary, i.e., the angle between primary terminal voltage  $V_1$  and current  $I_1$ . Despite the in-phase condition of voltage and current at the secondary terminals, the magnetizing current and the leakage of both windings cause a slight phase displacement between the primary terminal voltage and current.

Fig. 5-2 shows the voltage and current (mmf) diagram for a transformer with an inductive load, i.e., the secondary current lags the secondary terminal voltage  $V_2'$  by an angle  $\phi_2$ , the secondary phase displacement angle;

**5-2. The equivalent circuit of the transformer.** From the phasor diagrams shown by Figs. 5-1 to 5-3 it may be observed that the application of the voltage  $V_1$  to the primary of the transformer results in a primary current  $I_1$  lagging behind or leading  $V_1$  by an angle  $\phi_1$ . The angle  $\phi_1$  depends upon the load as well as upon the internal action within the transformer. As far as the source of power is concerned, the transformer and load appear as an equivalent impedance of such value that it takes the current  $I_1$  at the

angle  $\phi_1$ . The character or make-up of this equivalent impedance may be obtained from Kirchhoff's mesh equations for the two electric circuits (Eqs. 4-33 and 4-34) and from Eq. 4-35 which characterizes the magnetic circuit. These equations are:

$$\dot{V}_1 = -\dot{E}_1 + \dot{I}_1(r_1 + jx_1) \quad (5-2)$$

$$\dot{E}_2' = \dot{E}_1 = \dot{I}_2'(r_2' + jx_2') + \dot{I}_2'(R_L' + jX_L') \quad (5-3)$$

$$\dot{I}_1 + \dot{I}_2' = \dot{I}_m = -\dot{E}_1 \dot{Y}_m = -\dot{E}_2' \dot{Y}_m \quad (5-4)$$

These are three equations with three unknown quantities ( $E_1$ ,  $I_1$ , and  $I_2'$ ). The solution for  $I_1$  by eliminating  $E_1$  and  $I_2'$  will yield the equivalent impedance, i.e., the equivalent circuit. Introducing the abbreviations

$$r_1 + jx_1 = \dot{Z}_1 \quad (5-5)$$

$$(r_2' + R_L') + j(x_2' + X_L') = \dot{Z}_2' \quad (5-6)$$

Eqs. 5-2 to 5-6 yield

$$\begin{aligned} \dot{E}_1 = \dot{I}_2' \dot{Z}_2' = (\dot{I}_m - \dot{I}_1) \dot{Z}_2' &= -\dot{E}_1 \dot{Y}_m \dot{Z}_2' - \dot{I}_1 \dot{Z}_2' \\ \dot{E}_1(1 + \dot{Y}_m \dot{Z}_2') &= -\dot{I}_1 \dot{Z}_2' \quad \text{or} \quad \dot{E}_1 = -\frac{\dot{I}_1}{(1/\dot{Z}_2') + \dot{Y}_m} \end{aligned} \quad (5-7)$$

Therefore,

$$\dot{V}_1 = \dot{I}_1 \dot{Z}_1 + \frac{\dot{I}_1}{(1/\dot{Z}_2') + \dot{Y}_m} = \dot{I}_1 \left[ \dot{Z}_1 + \frac{1}{(1/\dot{Z}_2') + \dot{Y}_m} \right] \quad (5-8)$$

Eq. 5-8 gives the relation between the primary applied voltage, primary current, and the parameters of the transformer and the load. The quantity in the brackets is the *total impedance, looking into the primary terminals*. It includes the primary and secondary impedance of the transformer, the load impedance, and the main flux admittance  $Y_m$ .

Eq. 5-8 is the equation which applies to a circuit such as that represented in Fig. 5-4. This circuit is the *equivalent circuit* of the transformer and load. In this circuit, as Eq. 5-8 shows, the secondary impedance  $Z_2'$  is in parallel with the main flux admittance  $Y_m$ , giving a resultant admittance  $Y_m + 1/Z_2'$  or a resultant impedance  $1/(Y_m + 1/Z_2')$ . Breaking up  $Z_1$  and  $Z_2'$  into their components according to Eqs. 5-5 and 5-6 and introducing from Eq. 3-4 or 3-5

$$\dot{Y}_m = g_m - jb_m \quad (5-9)$$

or

$$\dot{Z}_m = 1/\dot{Y}_m = (r_m + jx_m) \quad (5-10)$$

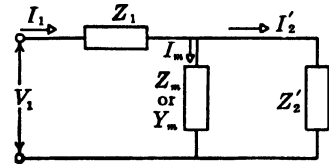


FIG. 5-4. Equivalent circuit of the transformer.

the circuit of Fig. 5-4 becomes that shown in Figs. 5-5 and 5-6 which is more commonly known as the equivalent circuit of the transformer.

It has been pointed out in Art. 3-1 that the magnitude of  $x_m(b_m)$  depends upon the saturation of the iron which is dependent upon the magnitude of the main flux  $\Phi$ . Since the main flux of the transformer remains almost constant between no-load and full-load (Art. 4-1),  $x_m(b_m)$  can be considered as a constant for this range of operation.

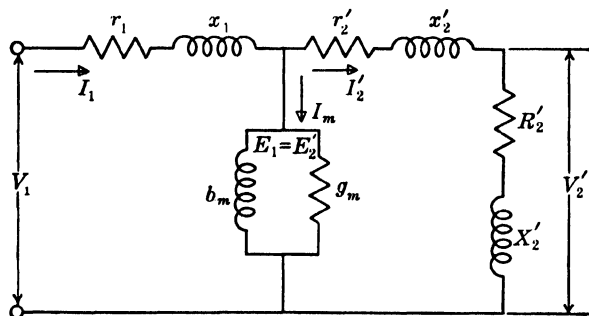


FIG. 5-5. Equivalent circuit of the transformer.

It will be shown in Chapter 8 how the parameters  $r_1$ ,  $x_1$ ,  $r_2'$ ,  $x_2'$ ,  $r_m$  and  $x_m$  (or  $g_m$  and  $b_m$ ) can be determined from no-load and short-circuit tests.

Having an equivalent circuit is of great assistance in making performance calculations of the transformer such as current, power factor, power, etc., especially when a calculating board is used on which the equivalent circuit can be set up.

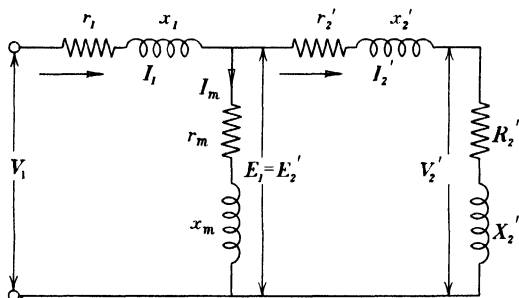


FIG. 5-6. Equivalent circuit of the transformer.

Of course, everything that can be determined from the equivalent circuit can also be determined from the fundamental equations 4-33 to 4-35, because the equivalent circuit has been derived from these equations.

Notice that the equivalent circuit Fig. 5-5 or 5-6 shows

$$I_1 = I_m + I_2'$$

This does not exactly correspond to Eq. 5-4. It should not be forgotten that the equivalent circuit is a circuit as seen from the primary terminals. In this circuit  $I_2'$  is not the actual secondary current (referred to the primary) but a current which, flowing in the primary winding, will produce the same mmf as the actual secondary current flowing in the secondary winding.

**Example.** The parameters of the equivalent circuit of a 100-kva, 2200/220-volt, 60-cycle transformer are given at 75°C as follows:

$$r_1 = 0.286 \text{ ohm}$$

$$x_1 = 0.73 \text{ ohm}$$

$$r_2' = 0.319 \text{ ohm}$$

$$x_2' = 0.73 \text{ ohm}$$

$$r_m = 302 \text{ ohms}$$

$$x_m = 1222 \text{ ohms}$$

It will be shown in Arts. 8-1 and 8-2 how the above parameters have been determined from no-load and short-circuit tests. If the load impedance on the low-voltage side of the transformer is  $Z_L = 0.387 + j0.290$  ohm, solve the equivalent circuit when the voltage  $V_1$  is 2300 volts.

$$a = \frac{2200}{220} = 10 \quad (\text{Eq. 4-3})$$

$$\dot{Z}_L' = R_L' + jX_L' = a^2(R_L + jX_L) = 38.7 + j29.0 = 48.4/36.8$$

From Eq. 5-6

$$\dot{Z}_2' = (0.319 + 38.7) + j(0.73 + 29.0) = 39.02 + j29.73 = 49.0/37.3$$

$$\dot{Z}_m = 302 + j1222 = 1258/76.1$$

$$\dot{Y}_m = 1/\dot{Z}_m = 0.795 \times 10^{-3}/-76.1$$

From Eq. 5-8

$$\begin{aligned} I_1 &= \frac{\dot{V}_1}{\dot{Z}_1 + (1/\dot{Z}_2') + \dot{Y}_m} \\ &= \frac{2300/0}{\left[ 0.286 + j0.73 + \frac{1}{[1/(49.0/37.3)] + 0.795 \times 10^{-3}/-76.1} \right]} = \frac{2300/0}{48.2/39.2} \\ &= 47.7/-39.2 \end{aligned}$$

$$\begin{aligned} \dot{I}_2' &= \dot{I}_1 \times \frac{\dot{Z}_m}{\dot{Z}_2' + \dot{Z}_m} = 47.7/-39.2 \times \frac{1258/76.1}{1258/76.1 + 49.0/37.3} \\ &= 46.2/-40.5 \end{aligned}$$

$$I_m = I_1 \times \frac{Z_2'}{Z_m + Z_2'} = 1.80/-76.7$$

Input power factor	= $\cos 39.2^\circ$	= 0.775 lagging
Power input	= $2300 \times 47.7 \times 0.775$	= 85.0 kw
Power output	= $(46.2)^2 \times 38.7$	= 82.7 kw
Primary copper losses	= $(47.7)^2 \times 0.286$	= 650 watts
Secondary copper losses	= $(46.2)^2 \times 0.319$	= 680 watts
Core losses	= $(1.80)^2 \times 302$	= 980 watts
$\eta$ efficiency	= $\frac{82.7}{85.0} \times 100 = 97.3\%$	
Voltage across load	= $46.2 \times 48.4 = 2240$ volts	
Voltage Regulation (see Chap. 7)	= $\frac{2300 - 2240}{2240} \times 100 = 2.68\%$	
	= 0.0268 pu.	

### PROBLEMS

Equivalent circuit parameters are listed below for four transformers. Assume all values to be corrected to 75°C.

	A	B	C	D
	10 kva	15 kva	500 kva	1000 kva
	240/120	2300/230	11,000/2300	66,000/6600
<i>ohms</i>	60 <i>cycles</i>	60 <i>cycles</i>	60 <i>cycles</i>	60 <i>cycles</i>
$r_1$	0.14	2.5	0.830	22
$x_1$	0.20	10	3.80	105
$r_2$	0.03	0.022	0.035	0.20
$x_2$	0.048	0.095	0.160	1.12
$r_m$	80	1500	2800	25,000
$x_m$	250	8850	11,500	165,000
$a$	2	10	4.78	10

#### LOAD IMPEDANCE (ohms)

$R_L$	1.40	3.54	9.5	35
$X_L$	0	0	5.0	26

1. For transformer A, determine the primary current, primary power factor, magnetizing current, and efficiency. Assume  $V_1$  fixed at nameplate value.
2. Repeat Problem 1 for transformer B.
3. Repeat Problem 1 for transformer C.
4. Repeat Problem 1 for transformer D.

## Chapter 6

### THE 3-PHASE TRANSFORMER

**6-1. Advantages, disadvantages, construction.** Transformation of 3-phase voltages may be accomplished by means of three single-phase transformers arranged in banks so that each phase requires a separate transformer, or by means of a single 3-phase transformer unit. The first method was common practice years ago, for it enabled the use of a single reserve unit of one-third the bank capacity for stand-by or emergency spare. Thus the replacement investment is only  $33\frac{1}{3}\%$  of the first cost of the bank. However, the reliability of modern transformers is such that the necessity for reserve capacity is no longer a demand in many cases. System interconnection frequently provides all the necessary reserve needed. Also, it is sometimes a simple matter to install small or medium portable substations as reserve when required.

Considerable advantages are to be gained from the use of a single-unit 3-phase transformer in place of three single-phase units of the same total capacity. The advantages are: increased efficiency, reduced size, reduced

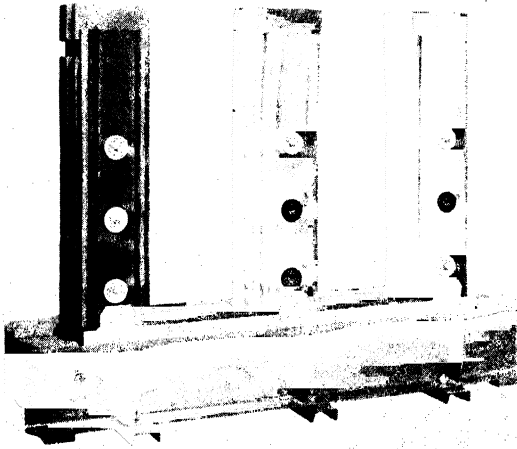


FIG. 6-1. Core of a three-phase transformer.



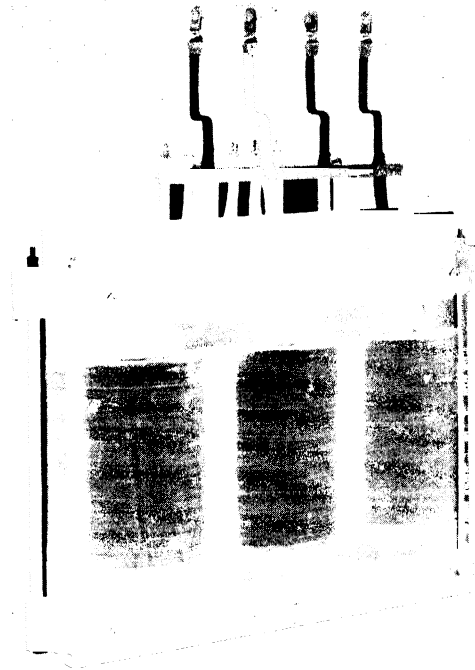


FIG. 6-2. Three-phase, core-type distribution transformer, 37.5 kva, 2400/240 volts-Y-connected.

weight, and less cost. A reduction in space is an advantage from the structural point of view in generating stations or substations.

Disadvantages include the greater cost of spares where spare capacity is demanded, usually a greater repair cost when subject to a short-circuit fault, and greater weight and size for reserve than a single-phase unit of a bank of transformers.

Fig. 6-1 shows the core of a large 3-phase core-type transformer. An assembled 3-phase core-type unit is shown in Fig. 6-2 where the low-voltage cylindrical coils are nearest the core and the high-voltage coils are on the outside. The shell-type as well as the distributed shell-type core construction, discussed in Article 2-1, may also be used for 3-phase transformers. The shell-type construction is one in which the windings are embedded within the iron core. Fig. 6-3 shows the general arrangement of coils in the shell-type 3-phase transformer.

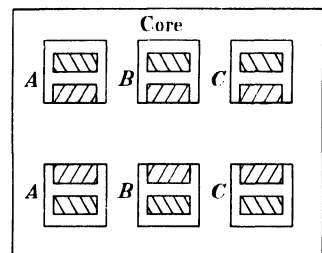


FIG. 6-3. Shell-type construction.

**6-2. Magnetic circuit.** The three cores of the 3-phase transformer are connected on both ends by common yokes. This is permissible. It should be remembered that the three voltages impressed upon the three primary windings make a symmetrical 3-phase voltage system, and this means that the three fluxes due to the three voltages also make a symmetrical system, i.e., the three fluxes are shifted in time by  $120^\circ$  and  $240^\circ$  respectively. Since the sum of the instantaneous values of the three fluxes is therefore equal to zero at any instant of time, it follows that the three magnetic circuits can be connected just as the three current circuits of a 3-phase electric system, for instance in a star in which the return conductor can be omitted.

It is seen from Fig. 6-1 that the magnetic path is not the same for all three fluxes, being longer for the outer cores than for the inner core. As a consequence, the magnetizing current is not the same in the three phases. However, since the magnetizing current is small, the 3-phase transformer can be considered as a symmetrical 3-phase system, i.e., the three phases can be treated as being equal. It then follows that the voltage diagrams derived in Chapters 3, 4, and 5 for the single-phase transformer also apply to *one phase* of the 3-phase transformer. The same is true of the equivalent circuit of the single-phase transformer. Also the no-load and short-circuit tests used to determine the parameters of the single-phase transformer (see Chapter 8) hold equally well for the 3-phase transformer.

If, in general,  $m_1$  is the number of primary phases and  $m_2$  the number of secondary phases, then the power output of the secondary of the transformer is

$$P_2 = m_2 V_2 I_2 \cos \phi_2 \quad (6-1)$$

and the primary power input

$$P_1 = m_1 V_1 I_1 \cos \phi_1 \quad (6-2)$$

$V_1$ ,  $V_2$ ,  $I_1$ , and  $I_2$  are respectively phase voltages and currents.

# Chapter 7

## VOLTAGE REGULATION: THE KAPP DIAGRAM

**7-1. Voltage regulation: the Kapp diagram.** An important factor in transformer operation is the *voltage regulation*. The regulation is defined as the change in secondary voltage, expressed as a percent of rated secondary voltage, which occurs when rated kva output (as a specified power factor) is reduced to zero, with the primary impressed terminal voltage maintained constant. The defining equation for percent regulation is

$$\epsilon = 100 \frac{V_{2 \text{ no-load}} - V_{2 \text{ rated}}}{V_{2 \text{ rated}}}$$

If the multiplying factor 100 is omitted, the regulation will be given in per-unit (the per-unit method of calculation is explained in detail in Chapter 8). If all voltages are referred to the primary, as in the phasor diagrams previously used, the regulation will be

$$\epsilon = 100 \frac{V_1 - V_2' \text{ rated}}{V_2' \text{ rated}} \quad (7-1)$$

Since the voltage regulation is defined in terms of full-load conditions and since the full-load current is large in comparison to the magnetizing current  $I_m$ , it frequently is permissible to neglect the effect of  $I_m$  in considering the voltage regulation. This may not be done, however, if calculations are made for small loads, or in *very small* KVA transformers.

If  $I_m$  is neglected, it will be observed from Eq. 3-4 that this means  $Y_m$  is assumed zero, or in other words that  $Y_m \ll 1/Z_2'$  which is practically true at full-load. Eq. 5-8 then becomes

$$\dot{V}_1 = \dot{I}_1(\dot{Z}_1 + \dot{Z}_2') \quad (7-2)$$

Since

$$\dot{Z}_2' = r_2' + jx_2' + R_2' + jX_2'$$

Eq. 7-2 may be written as

$$\dot{V}_1 = \dot{I}_1[(r_1 + r_2') + j(x_1 + x_2')] + I_1(R_2' + jX_2') = I_1 Z_e + V_2' \quad (7-3)$$

where

$$\dot{Z}_e = (r_1 + r_2') + j(x_1 + x_2') = R_e + jX_e \quad (7-4)$$

$Z_e$  is the *equivalent impedance* of the transformer referred to the primary,  $R_e$  is the *equivalent resistance*, and  $X_e$  the *equivalent leakage reactance*. How these values may be determined from a short-circuit test is explained in Chapter 8. The phasor diagram for Eqs. 7-3 and 7-4 is shown in Fig. 7-1; it is often referred to as the *Kapp Transformer Diagram*. In this diagram the current  $I_2' = I_1$  is assumed to be the rated full-load current, and  $V_2' = OA$  is rated secondary terminal voltage, drawn at angle  $\phi_2$  to  $I_2'$ , as given by the load power factor. Further  $AB = I_2' R_e$  and  $BC = I_2' X_e$ .  $V_1 = OC$  is the primary-terminal voltage. If a circle with radius  $OC$  and center at  $O$  cuts  $OA$  extended at  $D$ , then the regulation in per-unit is  $\epsilon = AD/V_2'$ . It is not feasible to graphically determine the regulation from this diagram since ordinarily  $V_2'$  and  $V_1$  are very large compared to  $e_r$  and  $e_x$ . Hence an analytical method such as given in the following is usually required.

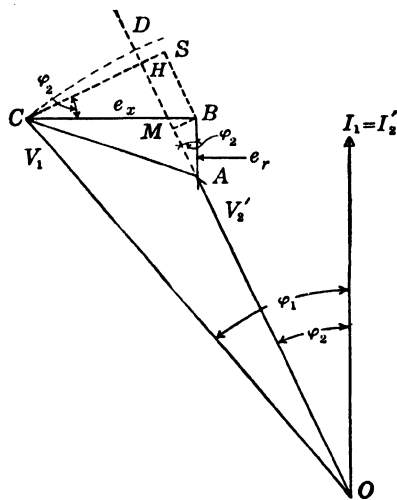


FIG. 7-1. Kapp diagram of a transformer.

In order to calculate the regulation, the quantities may be expressed either in volts, amperes and ohms, or in per-unit values. If per-unit values, then  $e_r$  and  $e_x$  are calculated as  $e_r = I_2' R_e / V_2'$  and  $e_x = I_2' X_e / V_2'$ , where  $I_2'$  is in amperes,  $V_2'$  in volts,  $R_e$  and  $X_e$  in ohms. In the per-unit calculations then  $V_2' = 1$  and  $I_2' = I_1 = 1$ , and  $V_1$  will be in per-unit, for rated loads.

In calculating the regulation, it is always assumed that  $V_2'$  and  $I_2'$  are at rated full-load values as per nameplate data. The problem is then to determine  $V_1$  and then the regulation, Eq. 7-1. In the operation of a transformer  $V_1$  may be fixed and the problem will be then to determine  $V_2'$ . Both problems are outlined in the following.

Referring to Fig. 7-1 in which the quantities may be in volts—amps—ohms, or in p-u:

$$OH = OA + AH = V_2' + AH$$

$$V_1 = \sqrt{(OH)^2 + (CH)^2} = \sqrt{(V_2' + AH)^2 + (CH)^2}$$

where  $AH = AM + MH$ , and  $MH = SB = e_x \sin \phi_2$ , therefore

$$AH = e_r \cos \phi_2 + e_x \sin \phi_2$$

and

$$CH = CS - MB = e_x \cos \phi_2 - e_r \sin \phi_2$$

$$\text{hence } V_1 = \sqrt{(V_2' + e_x \sin \phi_2 + e_r \cos \phi_2)^2 + (e_x \cos \phi_2 - e_r \sin \phi_2)^2} \quad (7-5)$$

also

$$V_1 = \sqrt{(V_2' \cos \phi_2 + e_r)^2 + (V_2' \sin \phi_2 + e_x)^2} \quad (7-5a)$$



TABLE 7-1

APPROXIMATE REGULATION FOR 60-CYCLE,  
3-PHASE, POWER TRANSFORMERS AT FULL-LOAD

kv	Lagging Power Factor	Percent Regulation		
		100 kva	10,000 kva	100,000 kva
15	80	4.2	3.9	
	90	3.3	3.1	
	100	1.1	0.7	
34.5	80	5.0	4.8	
	90	4.0	3.7	
	100	1.2	0.8	
69	80	6.1	5.7	5.5
	90	4.9	4.4	4.2
	100	1.4	0.9	0.6
138	80	7.7	7.2	7.0
	90	6.2	5.6	5.4
	100	1.8	1.2	0.9
230	80		9.7	9.4
	90		7.6	7.3
	100		1.7	1.3

$V_1 = OC_a$ . For  $\phi_{2b}$ , current lagging,  $V_2' = BC_b$  and  $V_1 = OC_b$ . For  $\phi_{2c}$  current leading,  $V_2' = BC_c$  and  $V_1 = OC_c$ . It is seen that numerically  $BC_a = BC_b = BC_c$  ( $B$  being center of circle  $C_b, C_a, C_c$ , for constant  $V_2'$ ), and  $OC_b > OC_a > OC_c$  are the required primary terminal voltages  $V_1$  for the various load powerfactors. The student should construct a similar diagram assuming  $V_1 = \text{constant}$  to show corresponding variation in  $V_2'$  with  $\phi_2$ .

## Chapter 8

### DETERMINATION OF PARAMETERS FROM A NO-LOAD AND A SHORT-CIRCUIT TEST

It is possible with a no-load test and a short-circuit test to determine the six parameters of the transformer and, from these, its regulation and efficiency.

**8-1. The no-load test.** In this discussion only the 2-winding transformer will be considered. Rated voltage  $V_1$  is impressed upon either winding of the transformer, with the other winding open, and the no-load power input  $P_0$  and the no-load current  $I_0$  are recorded. Usually, rated voltage is applied to the low-voltage winding. Fig. 8-1 shows the test circuit used.  $r_1$ , the resistance of the winding excited, is measured with d-c, and the temperature of the cooling medium is recorded.

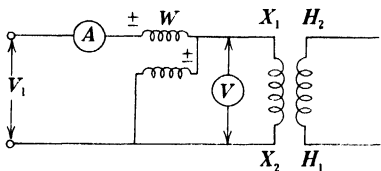


FIG. 8-1. Circuit for no-load test.

Fig. 8-2 shows the equivalent circuit of the transformer at no-load. This may be easily deduced from Fig. 5-6; at no-load the load impedance is infinite and the circuit reduces to that of Fig. 8-2. Given  $V_1$ ,  $P_0$ ,  $I_0$ , and  $r_1$ , the parameters  $x_m$  and  $r_m$  may be determined.

The core loss  $P_{h+e}$  is approximately equal to the no-load loss  $P_0$  since the copper loss  $I_0^2 r_1$ , due to the no-load current, is usually small. From Eq. 3-9

$$\dot{E}_2' = \dot{E}_1 = \dot{V}_1 - \dot{I}_0 \dot{Z}_1$$

or

$$E_1 \approx V_1 \pm I_0 x_1 \quad (8-1)$$

where  $x_1$  is the leakage reactance of the primary winding, the determination of which is discussed in Art. 8-2 which follows.

Since  $E_1$  is the voltage across the main flux impedance  $Z_m$  (Fig. 8-2), and  $r_m$  is small in comparison with  $x_m$ ,

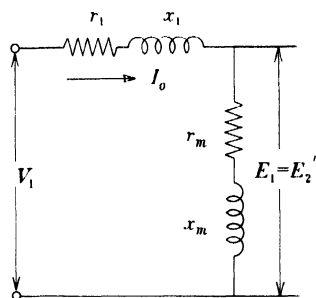


FIG. 8-2. Equivalent circuit for no-load condition.

$$x_m \approx E_1/I_0 \quad (8-2)$$

The main flux resistance  $r_m$  is given by Eqs. 5-9 and 5-10

$$r_m = \frac{g_m}{g_m^2 + b_m^2} \approx \frac{g_m}{b_m^2} \approx g_m x_m^2 \quad (8-3)$$

where  $g_m$ , the main flux conductance is

$$g_m = \frac{P_{h+e}}{E_1^2} \approx \frac{P_0}{V_1^2} \quad (8-4)$$

Thus both  $r_m$  and  $x_m$  can be readily determined if  $x_1$  is known. It should be noted that the parameters determined from the no-load readings are in terms of the winding in which the readings were taken.

**8-2. The short-circuit test.** In this test a reduced voltage is applied to one winding, usually the high-voltage winding, with the other winding solidly short-circuited. The reduced voltage  $V_{sc}$ , frequently called the impedance voltage, is selected so that the short-circuit current  $I_{sc}$  will not damage the windings.  $I_{sc}$  will usually be chosen as full load current.

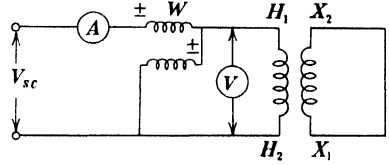


FIG. 8-3. Circuit for short-circuit test.

Fig. 8-3 shows the circuit employed for this test, and Fig. 8-4 shows the equivalent circuit for short-circuit conditions.

Since  $V_2 = 0$  and  $(r_2' + jx_2')$  is small in comparison with  $x_m$ , very little current will flow through the magnetizing branch. Therefore, the main flux and the

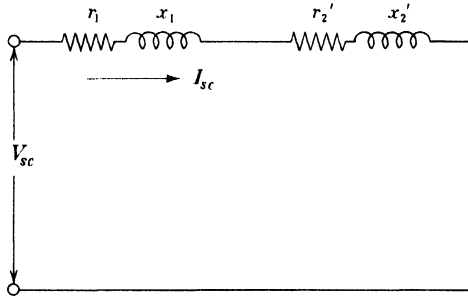


FIG. 8-4. Equivalent circuit for short-circuit condition.

iron losses are very small, and the power  $P_{sc}$  consists essentially of the copper losses in both windings.

The power at short circuit is the total copper loss of the transformer. Because of skin effect,  $P_{sc}$  may be greater than the ohmic copper losses. The skin effect will be neglected in this chapter.



From Fig. 8-4

$$Z_e = \frac{V_{sc}}{I_{sc}} \quad (8-5)$$

$$R_e = \frac{P_{sc}}{(I_{sc})^2} \quad (8-6)$$

$$X_e = \sqrt{Z_e^2 - R_e^2} \quad (8-7)$$

$Z_e$ ,  $R_e$ , and  $X_e$  are called *equivalent impedance*, *equivalent resistance*, and *equivalent leakage reactance* respectively. It is generally assumed that

$$x_1 = x_2' = \frac{X_e}{2} \quad (8-8)$$

Once again it should be noted that the parameters are in terms of the winding in which the instrument readings were taken.

Since the equivalent resistance  $R_e$  is the sum of  $r_1$  and  $r_2'$ , it follows that

$$r_2' = R_e - r_1 \quad (8-9)$$

According to AIEE Standards the resistances must be corrected to 75°C when calculating the regulation and efficiency from the equivalent circuit. This will be shown in the example of Art. 8-4.

Normally at rated current the voltage  $V_{sc}$  is 2 to 4% of rated voltage for low-voltage transformers (up to 2300 volts) and from 5 to 16% for high voltage transformers (up to 275 kv).

**8-3. Transformer efficiency.** The efficiency of a transformer may be obtained by direct loading or by the method of losses. The method of losses is used exclusively in commercial work. If the no-load losses ( $P_0 \approx P_{h+e}$ ) and the load losses ( $\approx I_1^2 R_e$ ) are known, at rated voltage and rated current respectively, the efficiency is

$$\eta = \frac{\text{output}}{\text{output} + \text{losses}} = \frac{\text{kva} \times 10^3 \times \cos \phi}{\text{kva} \times 10^3 \times \cos \phi + I_1^2 R_e + P_{h+e}} \quad (8-10)$$

**8-4. Per unit calculation.** When the parameters, voltage drops, losses, etc., of a transformer are expressed in ohms, volts, and watts, they apply only to the transformer being considered. It is possible to express the parameters, voltage drops, etc., of the transformer so that these quantities, although determined for a certain case, become general, i.e., applicable to a wide range of ratings, sizes, voltages, etc. For this reason certain *units* (base values) have to be defined and the quantities mentioned above expressed as fractions of these units. The quantities so expressed are then referred to as resistances, reactances, voltage drops, etc., on a per-unit basis or in *p-u*.

It is usual to assume the following units:

Unit voltage = primary voltage

Unit current = primary full-load current

$$\text{Unit impedance} = \frac{\text{unit voltage}}{\text{unit current}} = \frac{\text{primary voltage}}{\text{primary full-load current}}$$

Unit power = primary input

The advantages of the per-unit calculation are shown by the following example:

Consider two 500 kva transformers designed for different voltages and having the following data:

(a) 500 kva, 42,000/2400 volts, 60 cycles,

$$r_1 = 19.5 \text{ ohms}, r_2 = 0.055 \text{ ohm}, x_1 = 39.5 \text{ ohms}, x_2 = 0.120 \text{ ohm}, \\ a = 42,000/2400 = 17.5, a^2 = 306.3, r_2' = 0.055 \times 306.3 = 16.84 \text{ ohms}, \\ x_2' = 0.120 \times 306.3 = 36.8 \text{ ohms, and}$$

(b) 500 kva, 84,000/2400 volts, 60 cycles,

$$r_1 = 78.0 \quad r_2' = 67.4 \quad x_1 = 158 \quad x_2' = 147.2 \text{ ohms}, a = 35$$

If each of these transformers is treated on the p-u basis, the results will be:

(a) Unit current =  $500/42 = 11.91$  amp; unit impedances =  $42,000/11.91 = 3528$  ohms.

Therefore

$$r_1 = 19.5/3528 = 0.00553 \quad r_2' = 16.84/3528 = 0.00478$$

$$x_1 = 39.5/3528 = 0.0118 \quad x_2' = 36.8/3528 = 0.01043.$$

(b) Unit current =  $500/84 = 5.95$ ; unit impedance =  $84,000/5.95 = 14130$  ohms.

$$r_1 = 78/14,130 = 0.00552 \quad r_2' = 67.4/14,130 = 0.00478$$

$$x_1 = 158/14,130 = 0.0118 \quad x_2' = 147.2/14,130 = 0.01043.$$

Both transformers have different ratings and therefore different constants when expressed in ohms. However, when expressed in p-u, the parameters of both transformers are equal.

**Example.** A 100-kva, 2200/220-volt, 60-cycle transformer is tested on open-circuit at no-load and short-circuit at 25°C and the following readings are recorded:

*Open circuit* (H.V. winding open)

$$V_1 = 220 \text{ volts}$$

$$I_0 = 18 \text{ amp}$$

$$P_0 = 980 \text{ watts}$$

*Short circuit* (L.V. winding short-circuited)

$$V_{sc} = 70 \text{ volts}$$

$$I_{sc} = 45.5 \text{ amp} = I_1 \text{ rated}$$

$$P_{sc} = 1050 \text{ watts}$$

The resistance of the high-voltage winding after the short-circuit test was 0.24 ohm, and the temperature was 25°C.  $a = 2200/220 = 10$ .

*Required:* the parameters of the equivalent circuit, the regulation at full-load unity p.f. and 0.80 p.f. lagging, and the efficiency at unity p.f. and 0.80 p.f. lagging:

$$I_1(\text{rated}) = \frac{100,000}{2200} = 45.5 \text{ amp}$$

$$Z_e(25^\circ\text{C}) = \frac{70}{45.5} = 1.54 \text{ ohms}$$

$$R_e(25^\circ\text{C}) = \frac{1050}{(45.5)^2} = 0.507 \text{ ohm}$$

$$X_e = \sqrt{(1.54)^2 - (0.507)^2} = 1.46 \text{ ohms}$$

$$R_e(75^\circ\text{C}) = 0.507 \times \frac{234.5 + 75}{234.5 + 25} = 0.605 \text{ ohm}$$

$$r_1(75^\circ\text{C}) = 0.24 \times \frac{234.5 + 75}{234.5 + 25} = 0.286 \text{ ohm}$$

$$r_2' = R_e - r_1 = 0.605 - 0.286 = 0.319 \text{ ohm}$$

$$x_1 = x_2' = 0.73 \text{ ohm}$$

$$P_{h+e} = 980 - (1.80)^2 \times 0.24 = 979 \text{ watts}$$

$$E_1 = 2200 - 1.80 \times 0.73 = 2200 \text{ volts}$$

$$x_m = \frac{2200}{1.80} = 1222 \text{ ohms}$$

$$g_m = \frac{979}{(2200)^2} = 0.000202 \text{ mho}$$

$$r_m = 0.000202 \times (1222)^2 = 302 \text{ ohms}$$

$$\text{Unit voltage} = 220 \times 10 = 2200 \text{ volts } (V_2')$$

$$\text{Unit current} = 45.5 \text{ amp}$$

$$\text{Unit impedance} = 48.4 \text{ ohms}$$

$$e_r = \frac{0.605}{48.4} = 0.0125$$

$$e_x = \frac{1.46}{48.4} = 0.0302$$

Regulation at unity p.f. (Eq. 7-8):

$$\text{Reg.} = 0.0125 + \frac{(0.0302)^2}{2}$$

$$= 0.0125 + 0.000455 = 0.0130$$

Regulation at 0.80 p.f. lagging (Eq. 7-8):

$$\text{Reg.} = 0.80 \times 0.0125 + 0.60 \times 0.0302 + \frac{(0.80 \times 0.0302 - 0.60 \times 0.0125)^2}{2}$$

$$= 0.0100 + 0.0181 + 0.000139$$

$$= 0.0282$$

Efficiency:

$$\text{Load losses (75°C)} = 1050 \times \frac{234.5 + 75}{234.5 + 25} = 1252 \text{ watts}$$

Efficiency at rated load unity p.f.:

$$\eta = \frac{100}{100 + 0.989 + 1.25} = 0.977$$

Efficiency at rated load 0.80 p.f. lagging:

$$\eta = \frac{100 \times 0.80}{100 \times 0.80 + 0.980 + 1.25} = 0.973$$

Efficiency at  $\frac{3}{4}$  load 0.80 p.f. lagging:

$$\eta = \frac{100 \times \frac{3}{4} \times 0.80}{100 \times \frac{3}{4} \times 0.80 + 0.980 \times (\frac{3}{4})^2 + 1.25} = 0.972$$

### PROBLEMS

Open-circuit and short-circuit tests were taken on three single-phase transformers, and the following data were recorded.

	E	F	G
	10 kva	90 kva	5000 kva
	2200/110	11,000/2200	14,000/4000
	60 cycles	60 cycles	60 cycles
$V_1$ volts	110	2200	4000
$I_0$ amp	18	1.70	55.3
$P_0$ watts	68	1010	28,100
$V_{sc}$ volts	112	550	895
$I_{sc}$ amp	4.55	8.18	357
$P_{sc}$ watts	218	995	37,800
$r_1$ ohms (at 25°C)	5.70	8.0	0.16

1. Determine the six parameters of the equivalent circuit for transformer *E*.
2. Repeat Problem 1 for transformer *F*.
3. Repeat Problem 1 for transformer *G*.
4. Determine the regulation and efficiency of transformer *E* at rated load current, unity and 0.80 lagging p.f. Determine the efficiency at  $\frac{1}{4}$ ,  $\frac{1}{2}$  and  $\frac{3}{4}$  load unity and 0.80 lagging p.f.
5. Repeat Problem 4 for transformer *F*.
6. Repeat Problem 4 for transformer *G*.
7. Using the Kapp diagram, determine the regulation of transformer *A*, Chapter 5 (p. 46), at unity, 0.80 lagging and 0.80 leading p.f.
8. Repeat Problem 7 for transformer *B*, Chapter 5 (p. 46).
9. Repeat Problem 7 for transformer *C*, Chapter 5 (p. 46).

10. Repeat Problem 7 for transformer *D*, Chapter 5 (p. 46).

11. A 500-kva 42,000/2400-volt, 60-cycle transformer has parameters  $r_1 = 19.5$ ,  $r_2 = 0.055$ ,  $x_1 = 39.5$ , and  $x_2 = 0.120$ . The core loss and copper loss are equal at full-load. Determine the regulation and efficiency at unity, 0.80 lagging and 0.80 leading p.f.

12. A 500-kva, 2300/230-volt, 60-cycle transformer services both a lighting and a power load. The copper loss is 0.0105 p-u and the core loss 0.0102 with rated full-load current. The transformer is connected continuously to the supply mains. The load is 350 kw at 0.80 p.f. lagging for 10 hr, 450 kw at 0.95 p.f. lagging for 2 hr, and idle the remainder of the day. What is the all-day efficiency?

$$\text{All-day efficiency} = \frac{\text{Total kw-hr output in 24 hr}}{\text{Total kw-hr input in 24 hr}}$$

13. Determine the all-day efficiency of a 100-kva transformer having core and copper losses at full-load current equal to 0.011 p-u, and supplying the following load cycle

<i>kw</i>	<i>p.f.</i>	<i>hr</i>
80	0.85	5
45	0.75	4
100	1.0	2
idle		13

14. A 75-kva 230/115-volt 60-cycle single-phase transformer was tested at no-load and short-circuit, and the following p-u data were recorded:

$V_1 = 1.0$	$V_{sc} = 0.041$
$I_0 = 0.025$	$I_{sc} = 1.0$
$P_0 = 0.01$	$P_{sc} = 0.016$

Determine the regulation and efficiency at full-load, unity p.f., 0.80 p.f. lagging and 0.80 p.f. leading.

What is the efficiency of this transformer at  $\frac{1}{4}$ ,  $\frac{1}{2}$ ,  $\frac{3}{4}$ , and 1 load current, 0.80 p.f. lagging?

15. Prove by means of the calculus that maximum transformer efficiency occurs when copper losses are equal to core losses.

16. What is the primary voltage  $V_1$  required if the transformer of Problem 14 is to deliver 50 kva at 115 volts at 0.80 p.f. lagging?

## Chapter 9

### SHAPE OF THE NO-LOAD AND LOAD-CURRENT WAVE

**9-1. Shape of the no-load and load-current wave.** It has been explained that at no-load the primary applied voltage is practically balanced by the counter emf  $-E_1$  because the resistance drop and leakage reactance drop are negligible at no-load. At any instant therefore  $v_1 \approx -e_1$ . Since the supply line voltages are usually sinusoidal,  $v_1$  and therefore also  $e_1$  can be assumed sinusoidal. Thus

$$v_1 = -e_1 = -E_m \sin \omega t = N_1 \frac{d\phi}{dt}. \quad (9-1)$$

From this it follows that the main flux

$$\phi = - \int \frac{e_1}{N_1} dt = \frac{E_m}{N_1 \omega} \cos \omega t = \Phi_m \cos \omega t, \quad (9-2)$$

i.e., the sinusoidal primary voltage produces a sinusoidal flux at no-load. The primary current, however, will not be sinusoidal, but will be distorted. This is due to the fact that the flux is not directly proportional to the magnetizing current but is determined by the magnetization curve of the steel used for the laminations.

Assume at first that there is no hysteresis loss in the iron. Then  $\phi$  and  $i_\phi$  are related to each other by the magnetization curve in Fig. 9-1a. In Fig. 9-1b,  $\phi$  represents the sinusoidal flux necessary to balance the primary

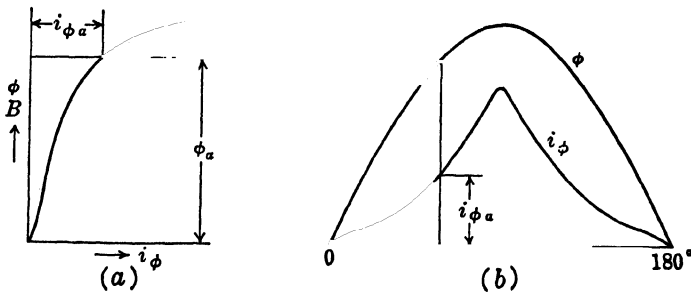


FIG. 9-1. Shape of the reactive component of the no-load current of the transformer. (Eddy current and hysteresis loss neglected.)

voltage. If to each value of  $\phi$  the magnetizing current is taken from Fig. 9-1a and plotted as in Fig. 9-1b a peaked curve for  $i_\phi$  will be found. Although the flux is sinusoidal,  $i_\phi$  is not sinusoidal. On resolving the curve of  $i_\phi$  into a Fourier series a large 3rd harmonic will be found.

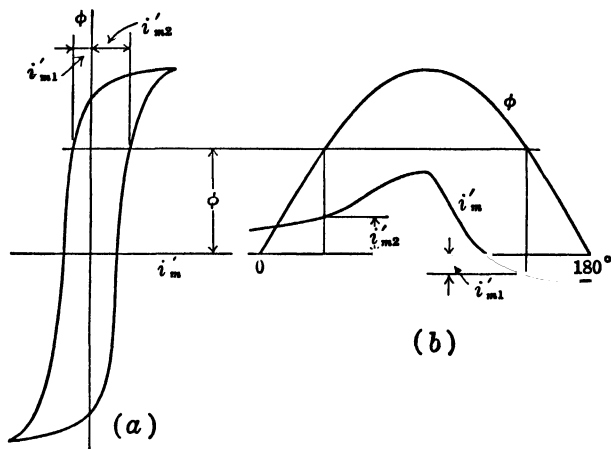


FIG. 9-2. Shape of the reactive and hysteresis components of the no-load current of the transformer. (Hysteresis loss considered.)

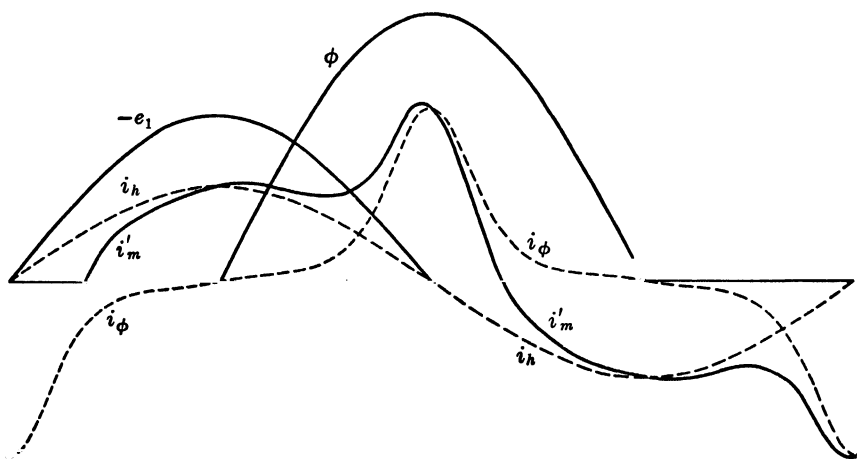


FIG. 9-3. Magnetizing current component  $i_\phi$  and hysteresis current component  $i_h$  of the no-load current of a transformer.

Considering now the case where hysteresis is present,  $\phi$  and  $i_m'$  are related to each other by the hysteresis loop (Fig. 9-2a). Applying the same method of construction as before, a curve for the current ( $i_m'$ ) will be obtained (Fig. 9-2b) which is no longer symmetrical about its peak but is of the same

general shape as in Fig. 9-1b. Here also a large 3rd harmonic is observed.

The current wave  $i_m'$  contains the magnetizing current component  $i_\phi$  and the hysteresis current component  $i_h$  (see Fig. 3-2). The latter current is an active current in phase with  $-e_1$ . In Fig. 9-3  $i_h$  is drawn in phase with  $-e_1$ . Subtracting the curve  $i_h$  from the curve  $i_m'$ , the same curve for  $i_\phi$  results as in Fig. 9-1b; it is in phase with the flux  $\phi$ . In order to get the total no-load current  $i_m$ , the eddy-current component  $i_e$ , which is also in phase with  $-e_1$ , has to be added to the current curve  $i_m'$ .

The results found in the foregoing apply to no-load. When the transformer is loaded and the load current is sinusoidal as it ordinarily is, the load current will smooth out the primary current, since the primary current at any instant is equal to the sum of the secondary current and magnetizing current.

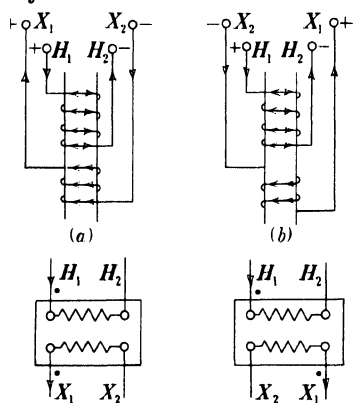


## Chapter 10

### TRANSFORMER POLARITY POLYPHASE CONNECTIONS

**10-1. Transformer polarity.** Transformers, single-phase or polyphase, have all leads marked with a standard system of lettering designating the transformer polarity. In order to connect windings of the same transformer in parallel, or to interconnect two or more transformers in parallel, or to connect single-phase transformers for polyphase transformation of voltages, it is necessary to know the lead marking. Transformer manufacturers usually follow a standard marking scheme.

Transformer *polarity marking designates the relative instantaneous directions of current* in the transformer leads. High-voltage leads are designated with the letter *H*, low-voltage leads with *X*, and



Subtractive Polarity

Additive Polarity

FIG. 10-1. Transformer polarity designation.

tertiary leads with *Y*, each with a suitable subscript 1, 2, 3, 4, etc., depending upon the number of leads. Fig. 10-1 shows the directions of instantaneous currents and induced voltages for power supplied to the high-voltage winding and a load connected to the low-voltage winding. In Fig. 10a both windings are wound in the same direction; in Fig. 10b, in opposite directions. The currents are indicated by closed arrows, and the induced voltages by open arrows. A high- and a low-voltage lead have the same polarity if, at a given instant, the current enters the high-voltage lead and leaves the low-voltage lead (or vice versa), thus giving the effect as though the two leads belonged to a

continuous circuit. Thus, in Fig. 10-1,  $H_1$  and  $X_1$  have the same polarity. This means that in single-phase transformers the marking of the leads is such that when  $H_1$  and  $X_1$  are connected together and voltage applied to either side of the transformer, the voltage measured between the highest subscript *H*-lead and the highest subscript *X*-lead is always less than the voltage of the com-

plete high-voltage winding. Instantaneously the terminal voltage from  $H_1$  to  $H_2$  in Fig. 10-1 is in time phase with the voltage  $X_1$  to  $X_2$ .

Viewing the transformer from the high-voltage side, the  $H_1$ -lead is usually brought out on the right side as shown in Fig. 10-1. When the  $H_1$  and  $X_1$  leads are adjacent, the polarity is said to be *subtractive*, and when  $H_1$  is diagonally opposite  $X_1$ , the polarity designation is *additive*. Fig. 10-1 shows both subtractive and additive polarity designations.

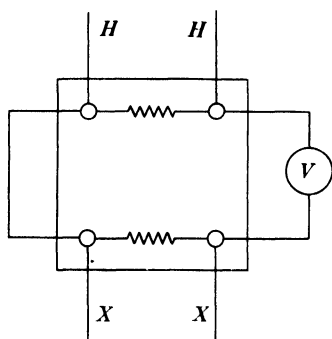


FIG. 10-2. A-c polarity test of a transformer.

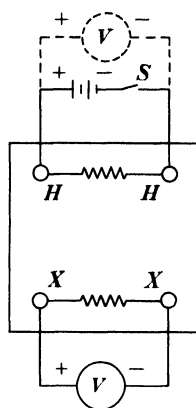


FIG. 10-3. D-c polarity test of a transformer.

Tests to determine the polarity of unmarked transformers are quite simple to perform. An adjacent high- and low-voltage terminal are connected together, as shown in Fig. 10-2, and the voltage between the other two adjacent terminals measured when an a-c voltage is impressed on the high-voltage winding. If the voltmeter reading is greater than the voltage impressed on the high-voltage winding, the polarity is additive; if less, the polarity is subtractive.

Fig. 10-3 shows a method of determining polarity using a dry cell, a switch, and a d-c voltmeter. Either winding of the transformer is placed across the battery with the switch  $S$  in the circuit, and the voltmeter is placed across the same terminals to read upscale. The voltmeter terminals are then transferred directly across to adjacent terminals of the other winding. The switch  $S$  is suddenly opened, and the meter deflection is observed: an upscale deflection indicates additive polarity; a downscale deflection, subtractive polarity. This test is advantageous when the turn ratio is very high but must be used with caution because of the high voltages of self-induction which may appear when the switch is opened.

Fig. 10-4 shows the manner of connection for a transformer having a single H-V winding and two L-V windings, such as a transformer rated at 440-220/110 volts. Fig. 10-4a shows the L-V winding connected in series for

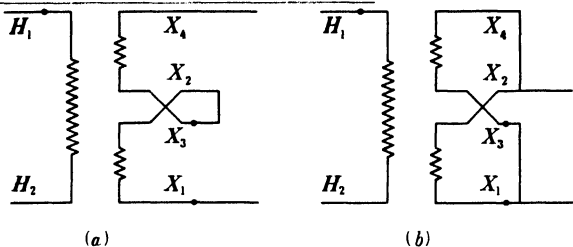


FIG. 10-4. Series and parallel connection of the secondary windings of dual voltage transformer.

220 volts and Fig. 10-4b shows the parallel connection for 100 volts. In instrument transformers the windings terminals are frequently merely *dotted*, as shown in Figs. 10-1 and 10-4. The dots are indicative of terminals having the same polarity. The sequence  $X_1, X_3, X_2, X_4$ , in Fig. 10-4 is deliberate in order to simplify the scheme of connections for either series or parallel operation of the L-V windings.

**10-2. Polyphase connections (3-phase-3-phase).** The generation of large-scale power is usually 3-phase at generator voltages of 13.2 kv or slightly higher. Transmission is accomplished at higher voltages (66, 110, 132, 220, 275 kv), and transformers are therefore necessary to step-up the voltages from the generators to that of the transmission line. At load centers the transmission voltage must be reduced to distribution voltages (6600, 4600, 2300 volts) and, at most consumers, the distribution voltages must be reduced to utilization voltages of about 440, 220, or 110 volts.

Polyphase transformation of 3-phase voltages may be accomplished either by using banks of interconnected single-phase transformers or by using polyphase transformers. Years ago the use of single-phase transformers in banks was the accepted method, but today, with improvement in transformer design and manufacture, the polyphase transformer is commonly used. Various methods of transforming 3-phase voltages to higher or lower 3-phase voltages are available. The most common connections are: (a) delta-delta; (b) wye-wye; (c) delta-wye; (d) wye-delta; (e) open-delta; (f) T.

(a) *Delta-delta ( $\Delta$ - $\Delta$ ) connection.* Fig. 10-5 shows the  $\Delta$ - $\Delta$  connection of three identical single-phase transformers. The secondary winding  $ab$  corresponds to the primary  $AB$ ; the polarity of terminal  $a$  is the same as that of  $A$ . The phasor diagrams neglect the magnetizing current and impedance drops in the transformers and are drawn for unity power factor between *phase* voltage and *phase* current. Thus  $I_{AB}$  is in phase with  $V_{AB}$ . As in previous diagrams, primary and secondary terminal voltages, and also primary and secondary currents, are opposite in phase so that  $V_{ba}$  corresponds to  $V_{AB}$ . Corresponding to  $\cos \phi = 1$  between phase voltage and phase current,  $I_{ba}$  is in phase with  $V_{ba}$ . The phasor diagrams are shown for a balanced load. It

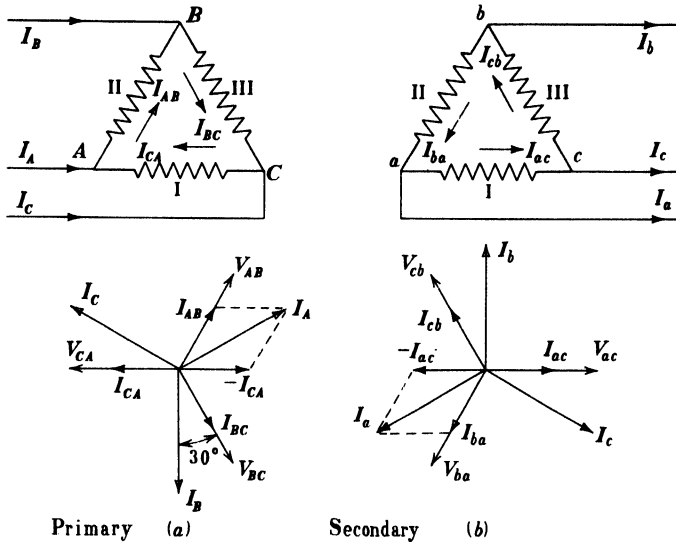


FIG. 10-5. Delta-Delta connection of transformers.

should be noted that the line currents are  $\sqrt{3}$  times the phase currents and are displaced  $30^\circ$  behind the phase currents; the  $30^\circ$  displacement angle always exists for all balanced loads regardless of power factor. For identical transformers, having equal ratios of transformation and equal impedances, no circulating current exists within either primary or secondary delta, and the transformers will share the total load equally; for example, three transformers supplying a 300-kva load will each assume 100 kva of the load. The ratio of transformation between banks is the same as that of the individual transformer.

In order for the output voltage to be sinusoidal, the magnetizing current of a transformer must contain a third-harmonic component (see Art. 9-1). Since the third-harmonic components of current of the three phases are displaced from each other by  $3 \times 120 = 360^\circ$ , they are all in phase and produce a single-phase third-harmonic current circulating within the  $\Delta$ ; this component of current helps to produce the sinusoidal flux, and the secondary voltage is therefore sinusoidal.

The  $\Delta$ - $\Delta$  connection offers an added advantage in that it may be operated in open-delta should one transformer be lost; the capacity available is then reduced: this is explained under (e).

(b) *Wye-Wye (Y-Y) connection.* For this connection the phasor diagrams can be drawn in the same manner as for the  $\Delta$ - $\Delta$  connection. The line voltage is  $\sqrt{3}$  times the phase voltage, and the two are displaced from each other by  $30^\circ$ . The transformation ratio between primary and secondary line voltages or line currents is the same as that of the individual transformer.

Y-Y banks are operated with grounded neutrals, i.e., the neutral of the primary is connected to the neutral of the power source. With an isolated neutral any unbalance in load or any single-phase load connected across one transformer or between lines will cause the electrical neutral to shift position and the phase voltages will become unbalanced. A grounded neutral prevents

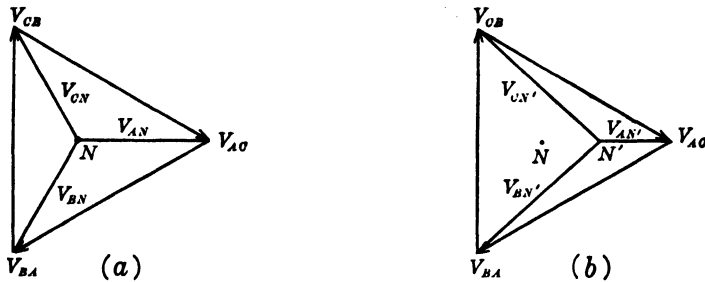


FIG. 10-6. Wye-Wye connection with isolated neutral;  
(a) balanced load; (b) unbalanced load.

this very unsatisfactory condition of operation. Fig. 10-6 shows the conditions existing when the neutral is isolated. In Fig. 10-6a the load is balanced, and in Fig. 10-6b the load is unbalanced.

With an isolated neutral the third-harmonic components of current in the primary cancel one another within the phases and the transformer flux is then non-sinusoidal, thus producing non-sinusoidal phase voltages; however, the line voltages are sinusoidal. Such harmonic voltages are undesirable because of the stresses which they may produce on the insulation of the windings. The use of a grounded neutral or a tertiary  $\Delta$  winding will allow a path for the third-harmonic current and thus produce a sinusoidal flux and a sinusoidal phase voltage.

(c) *Delta-wye ( $\Delta$ -Y) connection.* Fig. 10-7 shows the connections and phasor diagrams for the  $\Delta$ -Y arrangement supplying a balanced unity power factor load. The phasor diagrams may be deduced from the diagram of Fig. 10-5. Primary and secondary line voltages and line currents are observed to be out of phase with each other by  $30^\circ$ . The ratio of primary to secondary line voltages is  $1/\sqrt{3}$  times the transformation ratio for one transformer of the bank. No difficulty regarding third-harmonic currents appears since the existence of a  $\Delta$  connection allows a path for these currents. The use of such a bank permits a grounded neutral on the secondary side, thus providing a 4-wire 3-phase service. Unbalance in loadings causes very slight voltage unbalance since the transformer primaries are connected in delta.

Because of the  $30^\circ$  shift in primary and secondary voltages, it is not possible to parallel such a bank with a  $\Delta$ - $\Delta$  or Y-Y bank of transformers.

The secondary phasor diagrams of Fig. 10-7 may not appear to be completely consistent with those of Fig. 10-5 unless rotated through  $180^\circ$ , thus

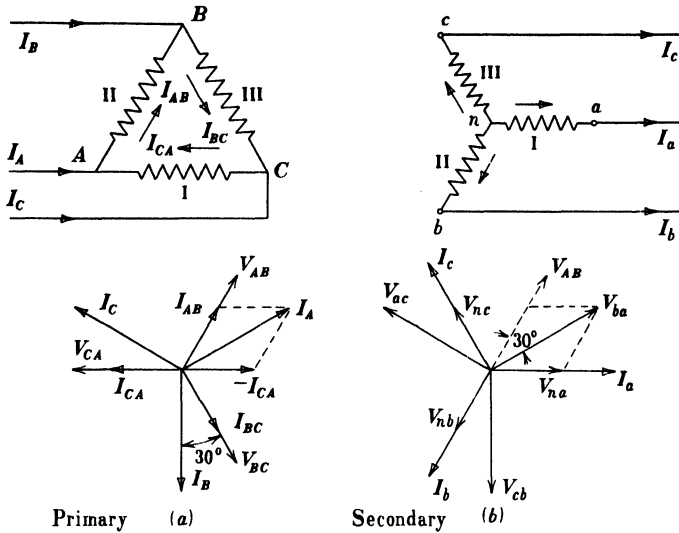


FIG. 10-7. Delta-Wye connection of transformers.

causing  $V_{ba}$  to be  $(180^\circ + 30^\circ)$  out of phase with  $V_{AB}$ . This is entirely due to the arbitrarily assumed positive directions of currents in the wye.

(d) *Wye-delta (Y- $\Delta$ ) connection.* This connection is very similar to that of the  $\Delta$ -Y connection. A  $30^\circ$  shift in line voltages appears between primary and secondary, and third-harmonic currents flow within the  $\Delta$  to provide a sinusoidal flux. The ratio between primary and secondary voltages is  $\sqrt{3}$  times the transformer turn ratio. When operated in Y- $\Delta$ , it is customary and desirable to ground the primary neutral, thus connecting it 4-wire.

(e) *Open-delta (V-V) or V connection.* An advantage of the  $\Delta$ - $\Delta$  connection is found in the fact that if one of the transformers be removed from the bank, due to a fault or otherwise, the remaining two will continue to deliver a 3-phase output to the load. If transformer I be removed from the bank on both primary and secondary sides in Fig. 10-5, the same line voltages  $V_{AB}$ ,  $V_{BC}$ ,  $V_{CA}$ ,  $V_{ba}$ ,  $V_{cb}$ ,  $V_{ac}$ , appear in the phasor diagrams.  $V_{AB}$  and  $V_{ba}$  appear as the sum of the voltages of transformers II and III. If the same unity-power-factor load is applied as in the discussion for the  $\Delta$ - $\Delta$  bank, the currents  $I_a$ ,  $I_b$  and  $I_c$  must appear in the same phase relationship to the line voltages as in Fig. 10-5. Therefore, the phase voltages and phase currents are out of phase by  $30^\circ$ , since phase and line currents are identical in the V connection. As a result, at unity-power-factor the transformers II and III operate at a power factor of 0.866.

In the open-delta connection the combined capacity of the two transformers, i.e.,  $\frac{2}{3}$  of the 3-phase output, is not available if the transformers are not to be overloaded. If the  $\Delta$ - $\Delta$  bank supplies a load of  $\sqrt{3} V_L I_L$  volt-amperes, then the open-delta bank is able to supply  $\sqrt{3} V_L (I_L / \sqrt{3})$

volt-amperes at the same copper losses since the line current becomes the transformer current in the open-delta connection. The ratio of the open-delta to  $\Delta$ - $\Delta$  volt-amperes is thus  $1/\sqrt{3} = 0.577$ . Hence only 0.866 of the combined single-phase capacity is available ( $0.577/0.667$ ) when two transformers are used in open-delta. This factor is sometimes called the *utility factor*.

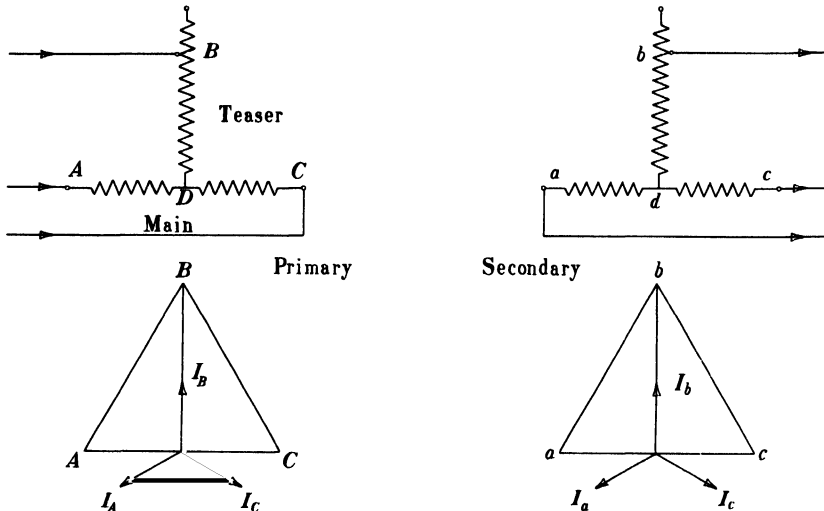


FIG. 10-8. T-connection of transformers.

(f) *T connection* (Fig. 10-8) employing two transformers for 3-phase to 3-phase transformation. The main transformer  $AC$  requires a center tap and the teaser transformer  $DB$  an 0.866 tap, or it may be wound with 86.6% of the turns on the main transformer. For loads of unity power-factor the teaser and each half of the main transformer all operate at different power factors, thus producing voltage unbalance. Where the teaser is wound with the proper number of turns (no tap), the utility factor is 0.928; when the tap is employed and 0.134 turn is unused, the utility factor is 0.866. The student should prove these relations. It is possible to use (in cases of emergency) two identical transformers having the same number of turns in main and teaser if some slight unbalance is not objectionable.

**10-3. Polyphase connection: 2-phase to 3-phase, or vice versa.** This connection known as the *Scott Connection* is shown in Fig. 10-9. Modern distribution systems are 3-phase, but where older 2-phase systems are in use the Scott Connection enables transformation to 3-phase power, either 3- or 4-wire. The connection is best studied with an example: in Fig. 10-9 the main transformer is rated at 2400/208 volts and has a center tap  $d$  on the secondary side; the teaser transformer can be identical but requires an 86.6% tap point  $b$ , providing a voltage of 180 volts. For these transformers supplying a

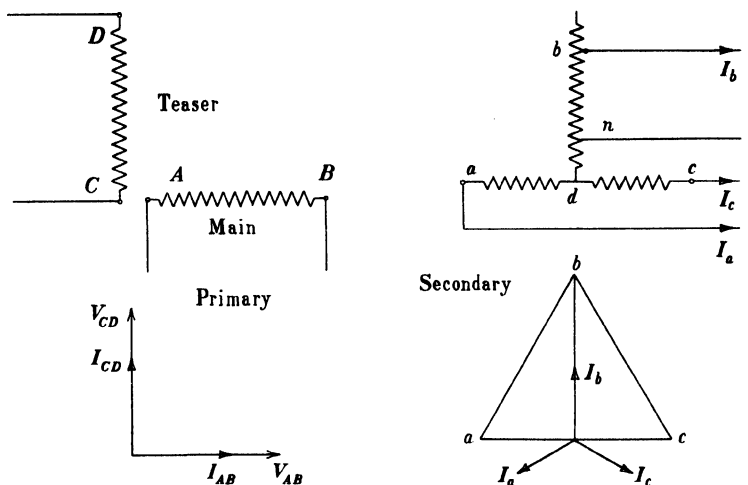


FIG. 10-9. Scott-connection (2- to 3-phase transformation, or vice versa).

100-kw unity-power-factor load with losses neglected, the following results are tabulated:

$I_b$ load	$= \frac{100,000}{\sqrt{3} \times 208} = 278 \text{ amp}$
Teaser power factor	= unity
Main power factor (dc)	= 0.866
Main power factor (da)	= 0.866
Power (teaser)	$= 180 \times 278 = 50 \text{ kw}$
Power (main)	$= 2(104 \times 278 \times 0.866) = 50 \text{ kw}$
Ratio of transformation (teaser)	$= 2400/180 = 13.33$
Ratio of transformation (main)	$= 2400/208 = 11.53$
Primary current (teaser)	= 20.8 amp
Primary current (main)	= 24.1 amp

It is noted that the teaser operates at unity p.f. while each half of the main operates at a p.f. of 0.866. Had the load p.f. been 0.866 lagging, the current phasors on the load phasor diagram would rotate  $30^\circ$  clockwise and the power factors would become: teaser 0.866, one half of main 0.50, other half of main 1.00. Because of the different power output from the teaser and the two halves of the main transformer, some voltage unbalance then results.

**10-4. Polyphase connections: 3-phase to 6-phase.** Where synchronous converters or mercury arc rectifiers require 6-phase power, transformation may be accomplished by one of the following three common schemes of connections: (a) diametrical connection; (b) double-wye; (c) double-delta.



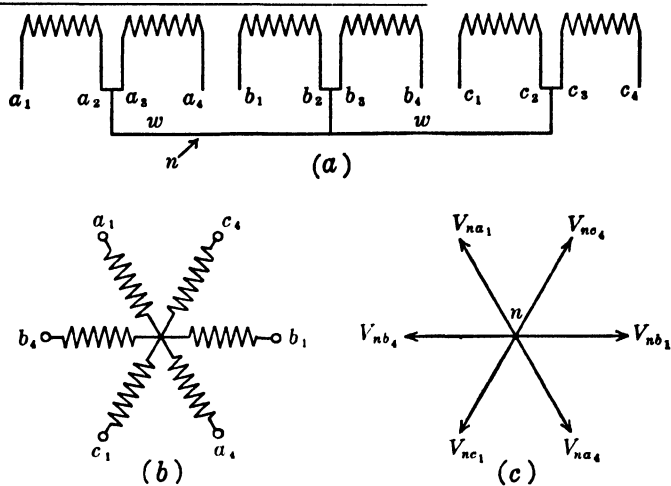


FIG. 10-10. Three- to six-phase transformation; diametrical connection.

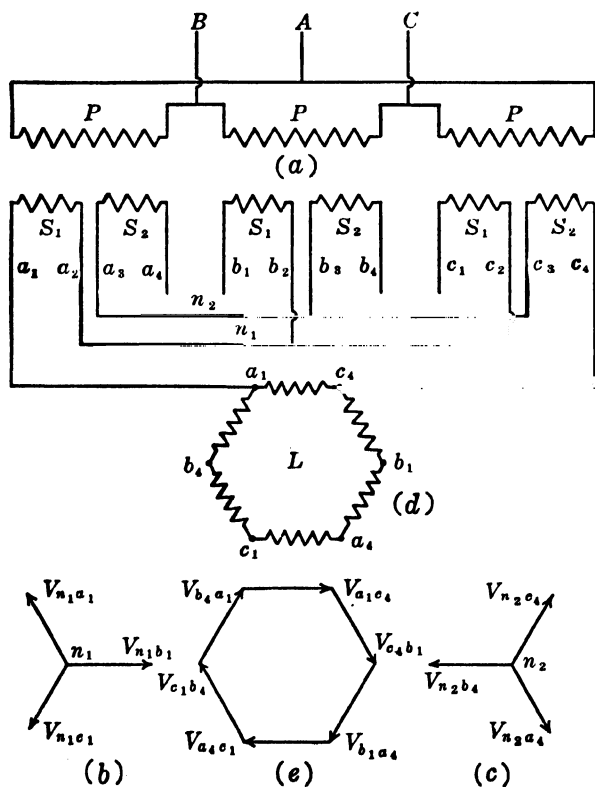


FIG. 10-11. Three- to six-phase transformation; double-wye connection.

(a) Fig. 10-10 shows the *diametrical connection* (only the secondaries shown). Three transformers, having center-tapped secondaries, are necessary. The leads  $a_1c_1b_1a_4c_4b_4$  are connected to the rings of a 6-phase converter or the anodes of a mercury arc rectifier. This connection is a *true* 6-phase connection which yields 6-phase voltages between the six leads regardless of whether or not a load is connected. The neutral of the bank may be grounded and used as the neutral wire of a 3-wire d-c system employing a converter. When the transformers are used with a mercury arc rectifier, the neutral constitutes the negative side of the d-c output.

(b) Fig. 10-11 shows the *double-wye* connection. Each transformer requires two identical secondary windings. Two separate wye connections are arranged as shown in Fig. 10-11 so that the voltages available from terminals  $a_1b_1c_1$  are opposite in phase to the voltages available from  $a_4b_4c_4$ . With the neutrals  $n_1$  and  $n_2$  connected, the system becomes identical with the diametrical arrangement of the previous discussion and is a *true* 6-phase system yielding voltages between terminals both with and without a load connected. With the neutrals  $n_1$  and  $n_2$  separate, the two secondary wyes are not interconnected until a symmetrical 6-phase load is applied to terminals  $a_1c_1b_1a_4c_4b_4$ . Such an arrangement is not considered *true* 6-phase, but operates 6-phase

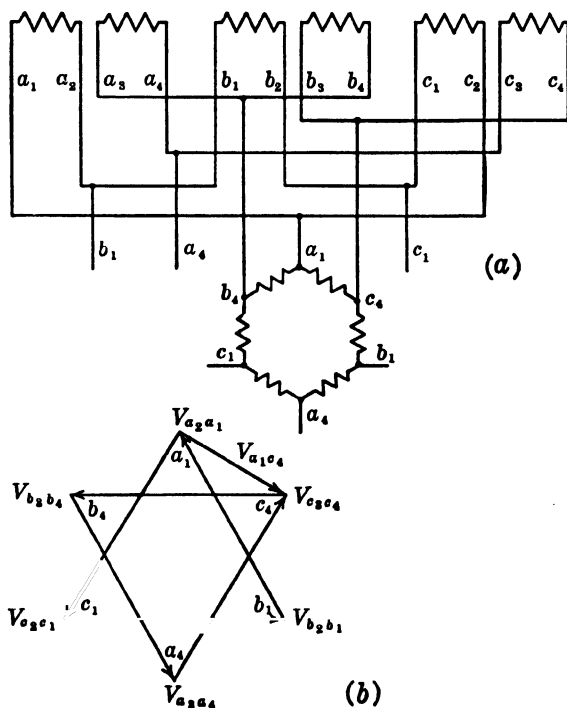


FIG. 10-12. Three- to six-phase transformation; double-delta connection.

when the load is present. When used with a 6-phase mercury arc rectifier, the double-wye connection is employed with a center-tapped reactance coil (called an interphase transformer) connecting  $n_1$  and  $n_2$ . The center tap constitutes the negative side of the d-c output. By using this arrangement two anodes are always firing together, each overlapped with the other by 60 electrical degrees. With a solid connection between  $n_1$  and  $n_2$  just one anode fires at a time.

(c) Fig. 10-12 shows the *double-delta* connection. Again two identical secondaries are necessary on each transformer. Two independent deltas are formed, and the load is necessary to make 6-phase operation complete. Without the load, 6-phase voltages are not obtainable between the terminals  $a_1c_4b_1a_4c_1b_4$ .

A double-T connection employing two transformers also may be used for 3- to 6-phase transformation. The *main* requires a center-tapped primary and two identical center-tapped secondaries; the *teaser* requires an 86.6% tap on the primary and similar taps on each of two identical secondaries.

By means of the Scott connection it is possible to transform from 2- to 6-phase, using main and teaser transformers each having a single primary winding and two secondary windings, the main with center-tapped secondaries, and the teaser with 86.6% tapped windings.

It should be noted here that phase transformation from single phase to polyphase cannot be accomplished with static transformers, and requires rotating equipment.

### PROBLEMS

1. A 10,000-kva, 13,200-volt, 3-phase generator supplies power to a 3-phase, 220-volt load by means of three single-phase transformers connected in a 3-phase bank. Determine the voltage, current, and kva ratings. and also the ratio of transformation for:

- (a) Y- $\Delta$  bank
- (b) Y-Y bank
- (c)  $\Delta$ -Y bank
- (d)  $\Delta$ - $\Delta$  bank

2. Three identical 60-cycle power transformers are connected in a Y- $\Delta$  bank to transform voltages from a 440-volt, 3-phase, 3-wire distribution system, in order to supply a 220-volt 3-phase 3-wire load. If the operating flux density is 70,000 lines per sq in. and the mean core area 40 sq in., determine the number of turns in the primary and secondary windings.

3. Three single-phase transformers are to be arranged in a 3-phase bank to supply a 120-volt, 4-wire system from a 3-wire, 6600-volt distribution line. The transformers are connected  $\Delta$ -Y with the neutral grounded on the secondary side. If a balanced 300-kw unity power factor lighting load is supplied by this bank, determine:

- (a) Primary current and voltage ratings.
- (b) Secondary current and voltage ratings.
- (c) Ratio of transformation.

4. A Y- $\Delta$  bank of transformers supplies a balanced load of 500 kw, 1100 volts 0.85 power factor lagging. Determine primary and secondary voltages and currents. Draw a complete phasor diagram for primary and secondary. Line voltage = 11,000.

5. Repeat Problem 4 for a  $\Delta$ -Y connection.

6. Repeat Problem 4 for a  $\Delta$ - $\Delta$  connection.

7. The leads of three special 220/81-volt transformers lack polarity markings and it is necessary to connect them in a  $\Delta$ -Y bank in order to supply a 3-phase synchronous converter requiring a ring voltage of 140 volts. How would you proceed to connect the transformers using a single lamp as the only test equipment available?

8. If a fully loaded 50-HP, 208-volt, 4-pole induction motor having an efficiency of 91% and a power factor of 90% is placed in parallel with the lighting load of Problem 3 above determine:

(a) Secondary current.

(b) Primary current.

(c) Transformer power factor.

9. A 4600/440-volt Y- $\Delta$  bank of three identical transformers supplies three balanced 3-phase loads connected in parallel: (a) 75 kw at unity power factor; (b) 100 kva at 0.90 power factor lagging; (c) 50 kva at 0.85 power factor leading. Determine the transformer ratings necessary.

10. A  $\Delta$ - $\Delta$  bank of identical transformers carries a balanced 3-phase load of 100 kva, 0.866 power factor lagging, and a single-phase load of 40 kw, unity power factor. Specify the kw and kva of each transformer.

11. A 300-kw, 440-volt, 3-phase, 3-wire balanced load operating at 0.85 power factor lagging is to be supplied from a 4600-volt, 2-phase, 4-wire system. Determine the ratio of transformation and kva ratings for both the main and teaser transformers.

12. How much power is delivered by each transformer in Problem 11?

13. It is necessary to supply a balanced 2-phase, 220-volt load of 50 kw, 0.90 power factor lagging from a 3-phase, 1100-volt system. Specify the voltages and currents for the transformers necessary.

14. A  $\Delta$ - $\Delta$  bank of transformers supplies a balanced unity power load of 150 kw. If one transformer is removed, specify the operating power factor and kw load for each of the two remaining transformers operating in open delta.

15. Repeat Problem 14 for a balanced load of 150 kw operating at 0.866 power factor lagging.

16. A 3-phase, 1100-volt system supplies 1000 kva to a 220-volt balanced 3-phase load by means of T-connected transformers. Specify the voltage and current ratings of the transformers and the ratios of transformation.

17. Two 230/115-volt transformers having center taps on both primary and secondary windings, but lacking 86.6% taps, are connected in T on both primary and secondary sides. If the primary side is connected to a balanced 230-volt, 3-phase system, determine the line to line voltages on the secondary side, and specify the displacement angles between them. Neglect exciting currents and impedance drops.

18. A 2-phase, 440-volt, 60-cycle, 50-HP motor having an efficiency of 91% and operating at a power factor of 0.88 takes power from a 2300-volt, 3-phase

system through a Scott-connected bank of transformers. Determine the kva loading for each transformer on both primary and secondary sides.

19. Two 50-kva transformers are connected in open delta and supply a balanced load of 0.80 power factor lagging. What is the maximum kw load permitted if the transformers are allowed to operate at 15% overload?

20. How much additional load of the same 0.80 power factor can be carried if a third 50-kva transformer is added in Problem 19 to produce a full  $\Delta$ - $\Delta$  bank?

21. A 6-phase, 625-volt synchronous converter receives power from an 11,500-volt 3-phase distribution system. If the power input is 500 kva at unity power factor, and the transformer bank supplying the converter is connected  $\Delta$  on the primary side and diametrical on the secondary, determine the voltage, current, and kva ratings of both primary and secondary windings. Also specify the ratio of transformation.

22. Repeat Problem 21 for a  $\Delta$ -double  $\Delta$  transformer bank.

23. Repeat Problem 21 for a  $\Delta$ -double Y transformer bank.

# Chapter 11

## PARALLEL OPERATION OF TRANSFORMERS

**11-1. Parallel operation of transformers.** When two or more transformers are to be operated in parallel in order to deliver power to a load over common bus-bars, it is necessary to satisfy very definite conditions of operation. In the analysis of this chapter just two transformers will be considered in parallel.

The first condition to be satisfied is that primary and secondary windings be connected to their respective bus-bars with due regard to the polarity:

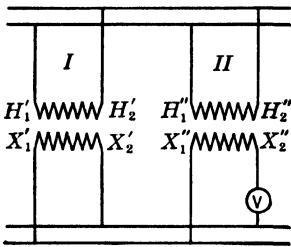


FIG. 11-1. Two transformers in parallel.

at any instant all transformer *terminals connected to a given bus must have the same polarity*. In Fig. 11-1 two transformers are shown in parallel and a voltmeter  $V$  is shown between the terminal  $X_2''$  (or  $X_1''$  or  $X_2'$  or  $X_1'$ ) and the bus-bar to which this terminal is to be connected: it is assumed that the  $H$  terminals constitute the primary windings and the  $X$  terminals are connected to the common bus-bars supplying the load. If the voltmeter  $V$  reads zero, the condition of proper polarities is satisfied; otherwise, the voltmeter would read double secondary voltage indicating improper polarities.

Further conditions for parallel operation can be derived from the current voltage relations of the simplified Kapp diagram (Fig. 7-1) and the corresponding equivalent circuit of Fig. 11-2 which neglects the magnetizing current. In this discussion the influence of the transformation ratio will also be introduced. For this purpose the secondary voltage will be expressed as  $V_2 = aV_t$  where  $V_t$  is the actual secondary voltage. All currents and impedances are referred to the primary side. Thus for transformer I designated with '

$$\dot{V}_1' = a' \dot{V}_t' + \dot{I}_2' \dot{Z}_{e1}' \quad (11-1)$$

and for transformer II

$$\dot{V}_1'' = a'' \dot{V}_t'' + \dot{I}_2'' \dot{Z}_{e1}'' \quad (11-2)$$

But since primaries and secondaries are connected to common buses

$$\dot{V}_1' = \dot{V}_1'' = \dot{V}_1 \quad \text{and} \quad \dot{V}_t' = \dot{V}_t'' = \dot{V}_t \quad (11-3)$$

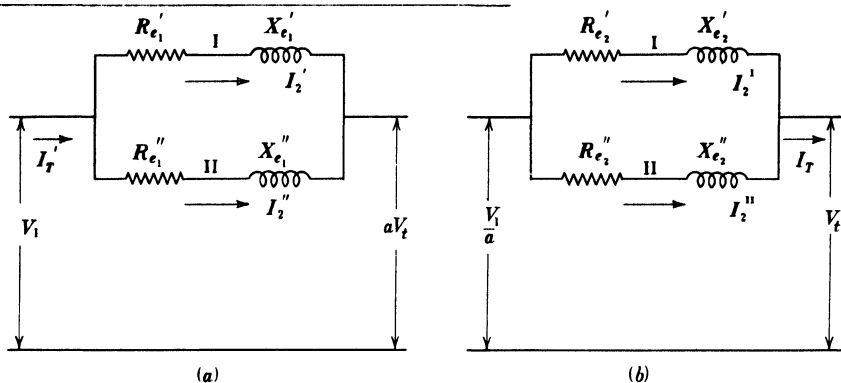


FIG. 11-2. Equivalent circuit of two transformers in parallel:  
(a) in terms of primary; (b) in terms of secondary.

$Z_{e1}'$  and  $Z_{e1}''$  are the equivalent impedances in terms of the primary (short-circuit impedances with secondary short-circuited). The total load current (on the primary side) is the sum of the transformer currents, or

$$\dot{I}_T = \dot{I}_2' + \dot{I}_2'' \quad (11-4)$$

From Eqs. 11-1 to 11-4 the following relations may be obtained:

$$\dot{I}_2' = \frac{-\dot{V}_t(a' - a'') + \dot{I}_T \dot{Z}_{e1}''}{\dot{Z}_{e1}' + \dot{Z}_{e1}''} \quad (11-5)$$

$$\dot{I}_2'' = \frac{+\dot{V}_t(a' - a'') + \dot{I}_T \dot{Z}_{e1}'}{\dot{Z}_{e1}' + \dot{Z}_{e1}''} \quad (11-6)$$

The only quantity in Eq. (11-1) to 11-6) not referred to the primary is  $V_t$ . All other quantities are, as mentioned previously, referred to the primary.

If  $Z_{e2}'$  and  $Z_{e2}''$  are the equivalent impedances referred to the secondary and  $I_T$  is the total load current on the secondary side and  $I_2'$  and  $I_2''$  are now the actual currents in the secondary coils, the voltage equations become

$$\frac{\dot{V}_1'}{a'} = \dot{V}_t' + \dot{I}_2' \dot{Z}_{e2}' \quad (11-7)$$

$$\frac{\dot{V}_1''}{a''} = \dot{V}_t'' + \dot{I}_2'' \dot{Z}_{e2}'' \quad (11-8)$$

and

$$\dot{I}_T = \dot{I}_2' + \dot{I}_2'' \quad (11-9)$$

Eq. 11-3 and Eqs. 11-7 to 11-9 yield

$$\dot{I}_2' = \frac{-\dot{V}_t(a' - a'') + a'' \dot{I}_T \dot{Z}_{e2}''}{a' \dot{Z}_{e2}' + a'' \dot{Z}_{e2}''} \quad (11-10)$$

$$\dot{I}_2'' = \frac{+\dot{V}_t(a' - a'') + a'\dot{I}_T\dot{Z}_{e2}'}{a'\dot{Z}_{e2}' + a''\dot{Z}_{e2}''} \quad (11-11)$$

where  $I_2'$  and  $I_2''$  are now the *actual* transformer currents on the load or secondary side. Equations 11-10 and 11-11 are directly applicable when the total load current on the secondary is given, as is usually the case.

The equations 11-5, 11-6, 11-10, and 11-11 for  $I_2'$  and  $I_2''$  show that the current of each transformer consists of two components. The magnitude of the first component is the same in each transformer but opposite in phase, i.e., these two currents represent an *internal current* circulating between the transformers and never reaching the external circuit. The sum of the second components of  $I_2'$  and  $I_2''$  gives the load current at the primary or secondary bus-bars, depending upon which set of equations is employed.

The circulating current results from a difference in the transformation ratios ( $a' - a''$ ) and is independent of the load current. It also exists at no-load ( $I_T'$  or  $I_T = 0$ ).

From Eqs. 11-5 and 11-6 with transformers having equal transformation ratios ( $a' = a''$ )

$$\frac{I_2'}{I_2''} = \frac{Z_{e2}''}{Z_{e2}'} \quad (11-12)$$

i.e., if two transformers of the same rating and same transformation ratio are to divide the load equally, their short-circuit impedances must be equal. In general, for transformers of different rating but the same transformation ratio, the equivalent impedances must be inversely proportional to the ratings, if each transformer is to assume a load in proportion to its rating. Thus, a transformer in parallel with another of twice the capacity must have an impedance twice that of the larger transformer in order that the load be properly divided between them.

It should be noted that satisfying Eq. 11-12 does not necessarily require equal power factors for the currents  $I_2'$  and  $I_2''$ . Consider two transformers of the same rating and same transformation ratio having  $Z_{e2}' = Z_{e2}''$  (Fig. 11-3). It is assumed that the short-circuit resistances (equivalent resistances) are not equal; consequently the short-circuit reactances are also unequal. Since  $I_2'R_{e2}'$  and  $I_2''R_{e2}''$  make different angles with  $V_t' = V_t''$ , then  $I_2'$  and  $I_2''$  must have different angles with  $V_t$ , i.e., the transformers operate with equal currents at different

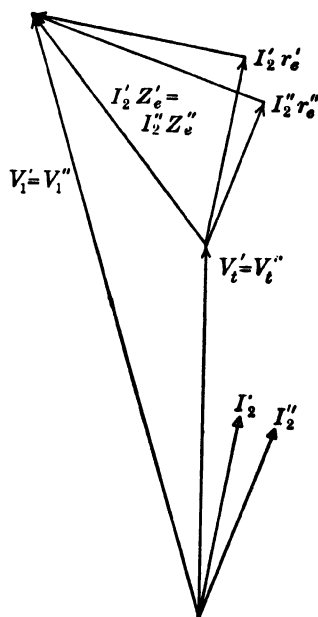


FIG. 11-3. Phasor diagram of two transformers in parallel.



power factors (Fig. 11-3). Thus the proper distribution of active and reactive current components requires that the ratios of short-circuit resistances and reactances be equal, i.e.,  $X_e'/R_e' = X_e''/R_e''$ . If this condition is not satisfied, the total loss of the two transformers will not be a minimum.

Summarizing, the conditions for proper parallel operation of single-phase transformers are the following: (a) proper connections to the bus-bars with regard to polarity, (b) identical voltage ratings, (c) equal transformation ratios, (d) ratio of the equivalent impedances inversely proportional to the ratio of current ratings, (e) ratio of equivalent resistances equal to ratio of equivalent reactances.

For parallel operation of 3-phase transformers, conditions have to be satisfied similar to those for single-phase transformers. The secondary voltages of 3-phase transformers to be connected in parallel are in phase if, for the same winding directions of primary and secondary, the connections of primary and secondary windings are the same: for example, all primaries connected star and all secondaries connected delta, or vice versa. Consider a single-3-phase transformer; if its primary and secondary windings are connected the same (both star or both delta), then the line voltages are displaced from each other by almost  $180^\circ$ . On the other hand, if the primary winding is connected in star and the secondary in delta, or vice-versa, the line voltages are displaced from each other by about  $(180^\circ \pm 30^\circ)$ . It therefore follows that transformers having the same primary connections (all star or all delta) and different secondary connections (some star and some delta) cannot be connected in parallel. However, a transformer with its windings connected in star may be connected in parallel with a transformer having its windings connected in delta.

**Example.** The data below apply to two single-phase transformers:

Transformer	Rating (kva)	Voltage	Short-circuit test (at rated current)	
			Voltage	Watts
A .....	200	2300/230	160	1400
B .....	300	2300/225	100	1700

The transformers operate in parallel on both sides and deliver a total load of 400 kva at 0.80 power factor lagging. Determine: (a) the current delivered by each to the load bus; (b) the power delivered by each; (c) the power factor of each.  $V_t = 230$  volts.

Transformer A

$$I_1 = \frac{200,000}{2300} = 87$$

$$a' = \frac{2300}{230} = 10$$

Transformer B

$$I_1 = \frac{300,000}{2300} = 130.5$$

$$a'' = \frac{2300}{225} = 10.22$$

$$Z_{e1}' = \frac{160}{87} = 1.84$$

$$Z_{e1}'' = \frac{100}{130.5} = 0.767$$

$$R_{e1}' = \frac{1400}{(87)^2} = 0.185$$

$$R_{e1}'' = \frac{1700}{(130.5)^2} = 0.0998$$

$$X_{e1}' = 1.83$$

$$X_{e1}'' = 0.760$$

$$\dot{Z}_{e1}' = 0.185 + j1.83 = 1.84 / 84.23$$

$$\dot{Z}_{e1}'' = 0.0998 + j0.760 = 0.767 / 82.5$$

$$\dot{Z}_{e2}' = \frac{Z_{e1}'}{(a')^2} = 0.00185 + j0.0183$$

$$\dot{Z}_{e2}'' = \frac{\dot{Z}_{e1}''}{(a'')^2} = 0.000955 + j0.00727$$

$$\dot{Z}_{e2}' = 0.0184 / 84.23$$

$$\dot{Z}_{e2}'' = 0.00734 / 82.5$$

$$I_T = \frac{400,000}{230} = 1740 \text{ amp}$$

$$I_T = 1740 / -36.8 = 1392 - j1044$$

$$\dot{i}_2' = \frac{-230 / 0(10 - 10.22) + 1740 / -36.8 \times 10.22 \times 0.00734 / 82.5}{10 \times 0.0184 / 84.23 + 10.22 \times 0.00734 / 82.5}$$

$$= \frac{50.6 + j0 + 91.2 + j93.5}{0.0283 + j0.0257} = \frac{170 / 33.4}{0.259 / 83.73}$$

$$= 657 / -50.33 = 418 - j506$$

$$\dot{i}_2'' = \frac{230 / 0(10 - 10.22) + 1740 / -36.8 \times 10 \times 0.0184 / 84.23}{0.259 / 83.73}$$

$$= \frac{-50.6 + j0 + 216 + j235}{0.259 / 83.73} = \frac{288 / 54.8}{0.259 / 83.73}$$

$$= 1112 / -28.93 = 974 - j538$$

(check)

$$\dot{i}_2' + \dot{i}_2'' = 1392 - j1044$$

$$\text{Power Factor A} = \cos 50.33^\circ = 0.638 \text{ lagging}$$

$$\text{Power Factor B} = \cos 28.93^\circ = 0.875 \text{ lagging}$$

$$\text{Power A} = 230 \times 657 \times 0.638 = 96 \text{ kw}$$

$$\text{Power B} = 230 \times 1112 \times 0.875 = 224 \text{ kw}$$

(check)

$$96 + 224 = 320 = 400 \times 0.80$$

If the load on these transformers was reduced to zero the currents would become

$$\dot{i}_2' \text{ (no-load)} = \frac{-230 / 0(10 - 10.22)}{0.259 / 83.73} = \frac{50.6 / 0}{0.259 / 83.73}$$

$$= 195.5 / -83.73 = 21.3 - j194$$

$$\dot{i}_2'' \text{ (no-load)} = \frac{230 / 0(10 - 10.22)}{0.259 / 83.73} = \frac{50.6 / 180}{0.259 / 83.73}$$

$$= 195.5 / 96.27 = -21.3 + j194$$

The current above is the circulating current and exists under all conditions of loading. Thus, under load, the component of  $I_2'$  supplying the load is

$$\begin{aligned}\dot{I}_2' \text{ (load component)} &= (418 - j506) - (21.3 - j194) \\ &= 396.7 - j312\end{aligned}$$

and 
$$\begin{aligned}\dot{I}_2'' \text{ (load component)} &= (974 - j538) - (-21.3 + j194) \\ &= 995.3 - j732\end{aligned}$$

The sum of the above two currents is as it should be,  $I_T = 1392 - j1044$ .

If the transformation ratios of the two transformers had been the same, and if the equivalent impedances  $Z_{e2}'$  and  $Z_{e2}''$  were unchanged, the circulating current would disappear and  $I_2'$  and  $I_2''$  would become:

$$\begin{aligned}I_2' &= \frac{91.2 + j93.5}{0.259/83.73} = \frac{131/45.7}{0.259/83.73} \\ &= 506/-38.0 = 397 - j312 \\ I_2'' &= \frac{216 + j235}{0.259/83.73} = \frac{319/47.4}{0.259/83.73} \\ &= 1233/-36.33 = 995 - j732\end{aligned}$$

The sum of the above two currents is  $\dot{I}_T = 1392 - j1044$ .

## PROBLEMS

1. The short-circuit test data for two single-phase, 22,000/440-volt, 60-cycle transformers are given below in p-u:

Transformer	Rating (kv)	Short-circuit Test		
		Voltage	Current	Power
I .....	100	0.025	1.0	0.01
II .....	500	0.035	1.0	0.008

Unit voltage = 22,000

Unit current = rated current

Unit power = rated kva

Determine for each transformer

- Impedance, resistance, and reactance in ohms and p-u.
- Full-load efficiency at unity, 0.80 lagging and 0.80 leading factor power, assuming the core loss and copper loss equal at full load.
- Regulation at unity, 0.80 lagging and 0.80 leading power factor.

2. The transformers of Problem 1 are operated in parallel on both the primary and secondary sides and supply a load of 500 kw at unity power factor at 440 volts. Determine:

- Current delivered by each transformer.
- Power output of each transformer.
- Power factor at which each transformer operates.
- Circulating current.

3. Repeat Problem 2 above for a 500-kva load at 0.8 power factor lagging. Carry out all calculations in p-u. Use common base of 600 kva.

4. Two single-phase, 66,000/6600-volt, 60-cycle, transformers are tested on short circuit, and the following p-u data are recorded (unit power = transformer rating in kva):

<i>Transformer</i>	<i>Rating</i>	<i>Voltage</i>	<i>Current</i>	<i>Watts</i>
I.....	1000	0.05	1.0	0.008
II.....	3000	0.06	1.0	0.007

The transformers are connected in parallel on both sides and supply a load of 3500 kva at 0.85 power factor lagging, 6600 volts. Determine:

- Current delivered by each transformer.
- Power output of each transformer.
- Power factor of each transformer.
- Circulating current.

Carry out all calculations on a p-u basis using a common base of 4000 kva.

5. The data of short-circuit tests at *rated current* on two transformers are given as:

<i>Transformer</i>	<i>Kva</i>	<i>Rating</i>	<i>S.C. Test</i>	
		<i>Voltage</i>	<i>Volts</i>	<i>Power (watts)</i>
A .....	100	11,000/2300	265	1000
B .....	500	11,000/2350	340	3400

The transformers are connected in parallel on both sides to 11,000- and 2300-volt buses, and supply a total load current of 275 amp at 0.90 power factor lagging to the 2300-volt bus. Determine:

- Current delivered by each transformer.
- Power delivered by each transformer.
- Power factor of each transformer.
- Circulating current.

6. If the ratios of transformation of the transformers in Problem 5 were the same, namely, 11,000/2300, determine:

- Current delivered by each transformer.
- Power delivered by each transformer.
- Power factor of each transformer.
- Circulating current.

7. Compare the transformer copper losses in Problems 5 and 6. Explain the difference.

## Chapter 12

### THE AUTOTRANSFORMER · INSTRUMENT TRANSFORMERS · CONSTANT-CURRENT TRANSFORMER

**12-1. The autotransformer.** The previous chapters discussed the general theory of the 2-winding transformer. The *autotransformer* using a single winding on an iron core, with a part of the winding common to both the primary and secondary, is frequently used. For certain types of service the autotransformer is superior to the 2-winding transformer, offering better regulation, reduced weight and size per kva, lower cost, higher efficiency, and lower magnetizing current.

In the autotransformer only a part of the kva input is transformed from the primary to the secondary by transformer action, while the remainder is transferred directly from the primary lines to the secondary lines. The relative amounts of power transformed and power transferred depend upon the ratio of transformation. Autotransformers offer the greatest advantage

when the ratio of transformation is small; the smaller the ratio of transformation, the smaller the physical size of the autotransformer required to supply a given load.

However, the autotransformer has a disadvantage in that the low-voltage side has a metallic connection to the high-voltage side contrary to the 2-winding transformer. Thus a ground on the high-voltage side of an autotransformer may subject the low-voltage circuit to the high voltage of the high-voltage line.

Fig. 12-1 shows the schematic diagram of an autotransformer with a primary impressed voltage  $V_1$  and a load voltage  $V_2$ . Just as in the 2-winding transformer

the core flux is determined by the induced emf  $E_1 (\approx V_1)$ , the number of primary turns  $N_1$ , and the line frequency. The ratio of transformation is given by:

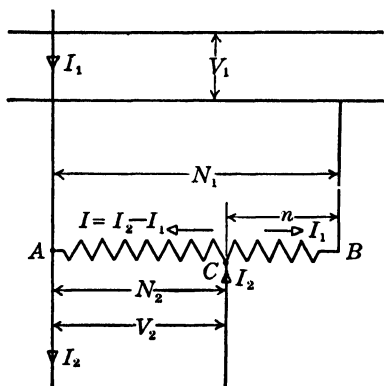


FIG. 12-1. Schematic diagram of an autotransformer.

$$a = \frac{E_1}{E_2} = \frac{N_1}{N_2} \approx \frac{V_1}{V_2} \approx \frac{I_2}{I_1} \quad (12-1)$$

The common part of the winding between *A* and *C* carries a current which is the difference between  $I_2$  and  $I_1$ . If the magnetizing current is ignored the difference  $I_2 - I_1$  may be taken algebraically.

It follows from Fig. 12-1 that:

$$\begin{aligned} \frac{I_2}{I_1} &= a & \frac{E_1}{E_2} &= a \\ \frac{I}{I_1} &= a - 1 & \frac{E_n}{E_1} = \frac{n}{N_1} &= \frac{a - 1}{a} \\ \frac{I}{I_2} &= \frac{a - 1}{a} & \frac{E_n}{E_2} &= a - 1 \end{aligned} \quad (12-2)$$

$$\frac{\text{Rating as an autotransformer}}{\text{Rating as a 2-winding transformer}} = \frac{a}{a - 1} \quad (12-3)$$

$$\frac{\text{Full-load losses in \% of autotransformer rating}}{\text{Full-load losses in \% of 2-winding transformer rating}} = \frac{a - 1}{a} \quad (12-4)$$

$$\frac{\text{Magnetizing current as an autotransformer}}{\text{Magnetizing current as a 2-winding transformer}} = \frac{a - 1}{a} \quad (12-5)$$

$$\frac{\text{Impedance drop as an autotransformer}}{\text{Impedance drop as a 2-winding transformer}} = \frac{a - 1}{a} \quad (12-6)$$

$$\frac{\text{Short-circuit current as an autotransformer}}{\text{Short-circuit current as a 2-winding transformer}} = \frac{a}{a - 1} \quad (12-7)$$

$$\frac{\text{Regulation as an autotransformer}}{\text{Regulation as a 2-winding transformer}} = \frac{a - 1}{a} \quad (12-8)$$

**12-2. Instrument transformers.** Instrument transformers are divided into two classes: potential transformers and current transformers. Each serves two purposes: (1) to insulate the high-voltage circuit from the measuring circuit, in order to protect the measuring apparatus and the operator; (2) to make possible the measurement of high voltages, with low-voltage instruments (usually 115 volts), or large currents with low-current ammeters (usually 5 amp), which procedure simplifies the measuring problem greatly. These transformers also are used to operate relays, solenoids, circuit-breakers, or other controlling devices. The principle of the instrument transformer is fundamentally the same as that of the power transformer.

The potential transformer has the high voltage applied to the primary, and the secondary, usually rated at 115 volts, is connected to the voltmeter.

From Figs. 5-1 and 5-2 it is observed that the ratio of primary to secondary terminal voltage is not the same as the turn ratio, but also depends upon the character of the load, upon the impedance of the windings, and upon the magnetizing current  $I_m$ . The phase angle between primary and secondary terminal voltages is not exactly  $180^\circ$ , or zero if the phasor  $V_2'$  is reversed (see Fig. 7-1). In order to keep the ratio of primary to secondary voltage constant, or practically so, the potential transformer is designed with as small a leakage reactance and resistance as possible. The flux density in the core is also lower than that used in power transformers. Thus, in order to keep the ratio and phase-angle errors small, the instrument transformer is much larger than a power transformer of the same rating. Instrument transformers usually are rated from 25 to 500 volt-amperes according to the *burden* or secondary load. As far as heating is concerned, their rating as a power transformer would be from two to four times the rating as instrument transformers.

From Fig. 5-1 it should be clear that  $V_1/V_2'$  is more nearly unity, or  $V_1/V_2$  more nearly equal to  $a$ , the smaller the load current, or the greater the load impedance. Also  $\phi_1$  is more nearly equal to  $\phi_2$  under these same conditions. It also is clear that, for a given secondary burden, the ratio and phase angle can be specified accurately. Thus, the ratio and phase angle of instrument transformers usually are specified for a certain burden, and correction factors are applied, if necessary, for other burdens. Usually the departure from the specified values is very small. Fig. 12-2 shows a typical correction curve for a potential transformer. The phase-angle error is the angle of departure of  $V_1$  from  $V_2$  reversed, so it is nearly zero and not  $180^\circ$ . The phase-angle error is of importance only in power measurements, while the ratio error is important in both voltage and power measurements. Fig. 12-3 shows a typical volt-

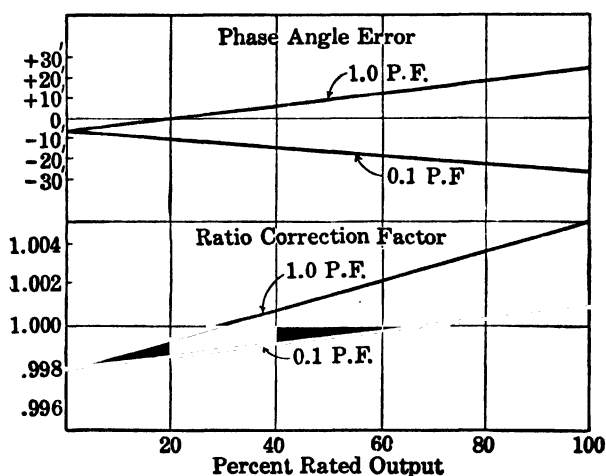


FIG. 12-2. Potential transformer, correction curves.



FIG. 12-3. Potential transformer, 2400/120 volts.

age transformer, rated 2400/120 volts. Note the fuses and bushings on the primary side. The low-voltage secondary terminals are shown on the front of the case.

Current transformers perform somewhat the same service in a-c measurements as shunts do in d-c, and in addition they perform the important function, in high-voltage circuits, of insulating the measuring devices from the high-voltage lines. The important characteristic required in a current transformer is a constant ratio between secondary and primary current, as well as a small phase angle between primary and secondary current. From the discussion of Art. 4-1 and from Figs. 5-1 and 5-2, it is observed that  $I_2'$  and  $I_1$  are more nearly equal, or  $I_2 = aI_1$  when the magnetizing current  $I_m$  is small in comparison to  $I_2'$ . The ratio of  $I_2$  to  $I_1$  differs from the turn ratio  $a$  when  $I_m$  is large, although it is

not affected appreciably by the impedance of the windings. Ratio and phase-angle correction often must be applied to current transformers also, and the manufacturers will supply them when required. Thus, in instrument transformers, it is necessary to use high-grade laminations for the core, and to operate at relatively low flux densities.

The secondary current of the current transformer depends mainly upon the primary current, and is nearly independent of the impedance of the instruments connected to the secondary. Primary current flows independent of whether the secondary circuit is open or closed; it is determined entirely by the line current. If the secondary circuit is open, no secondary current can flow, and hence there is no opposing mmf provided by secondary current. The result is that the primary current is then entirely a magnetizing current  $I_m$  (see Fig. 3-3). This results in a very high flux density and a high induced voltage in the secondary, as well as a high impedance drop across the primary. The voltage may be sufficient to damage the secondary insulation, or to shock severely an operator coming in contact with the secondary terminals. *Therefore, it is important that the secondary of current transformers be short-circuited when there are no instruments connected to it. This is an important consideration.* Many portable current transformers have a shorting switch mounted directly on the transformer.



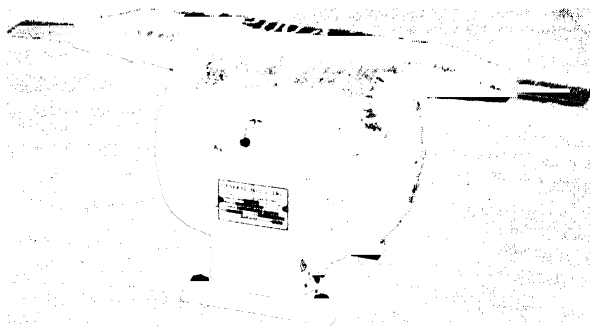


FIG. 12-4. Current transformer, 200/5 amperes.

The primary of the current transformer has only a few turns, often only one, while the secondary has many turns, the number of them depending on the ratio desired. Fig. 12-4 shows a current transformer in which the primary consists only of a single bar of copper around which is placed the secondary winding. The secondary of both the current and potential transformer, as well as the iron core, always should be grounded.

**12-3. The constant-current transformer.** Street lighting circuits, using arc or incandescent lamps, frequently employ lamps connected in series. All lamps in series have the same current which must be carefully regulated and maintained constant in order to insure maximum lamp life. The circuit current is the same as that of the lamps and is much lower than would be the case with lamps in parallel. However, the circuit voltage is usually rather high and depends upon the number of lamps in series.

Constant-current transformers are designed to maintain a constant current in the series lamp circuits, regardless of the number of lamps connected in series across the secondary winding of the transformer. A common secondary current rating is 6.60 amp, but other ratings such as 7.5 or 20 amp also are used. Regulation of the current to within  $\pm \frac{1}{2}\%$  of the rated value between  $\frac{1}{4}$  and  $1\frac{1}{4}$  load is readily accomplished. Primary transformer voltages are usually 2400 or 4800 volts, and the secondary voltages under load may be as high as 4000 volts.

The *moving coil* constant-current transformer may be an oil-immersed transformer, or a dry-type, air-cooled, indoor transformer. The primary winding is stationary and the secondary is free to move with respect to the primary; counterweights are used to effect a balance between the weight of the secondary coil and the force of repulsion between the primary and secondary. Fig. 12-5 shows a constant-current transformer.

In operation a constant voltage is applied to the primary, and the secondary adjusts its position relative to the primary so that the secondary voltage across the series lamp circuit produces the rated lamp current. At this

position a mechanical balance results between coil weight, counterweights, and the electromagnetic force of repulsion. Should a single lamp in the series string burn out, it is automatically shorted by an oxide film device in the lamp base, and the transformer secondary moves farther away from the primary. As the secondary winding moves farther away from the primary winding, the leakage flux increases and the secondary terminal voltage decreases to the value required to produce rated lamp current. At all positions of the coils the force of repulsion is essentially constant.

Constant-current transformers are designed to have a high leakage reactance while power transformers of similar voltage rating have a much lower leakage reactance.

**Example.** A 100-kva, 2300- to -230-volt, 60-cycle, 2-winding transformer is used as an autotransformer having a single winding in order to step up the voltage of a 2300-volt line by 10%. If the transformer has 2% losses, a 2.2% regulation, and a 3.3% impedance ( $Z_r$ ) as a 2-winding transformer, its characteristics as a 2300/2530-volt autotransformer are:

Primary voltage = 2300 volts

Load voltage = 2530 volts

Ratio of transformation =  $\frac{10}{11}$

$I_1$  (as 2-winding transformer) =  $\frac{100,000}{2300} = 43.5$  amp

$I_2$  (as 2-winding transformer) =  $\frac{100,000}{230} = 435$  amp

$I_2$  (as autotransformer) = 435 amp

$I$  (as autotransformer) = 43.5 amp

$I_1$  (as autotransformer) = 478.5 amp

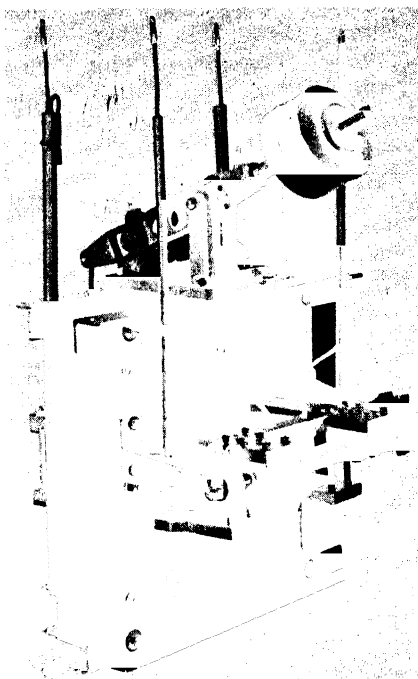


FIG. 12-5. Constant current transformer, 20 kw, 2400-volt primary, 6.6 amp. secondary, 60 cycles, equipped with compound balancing lever and micro-meter weight adjustment. Hinge-end view.

$$\text{Output (as autotransformer)} = 2530 \times 435 = 1100 \text{ kva}$$

$$\text{Losses} = \frac{1}{11} \times 0.02 = 0.00182$$

$$\text{Regulation} = \frac{1}{11} \times 0.022 = 0.002$$

$$\text{Impedance} = \frac{1}{11} \times 0.033 = 0.003$$

Assume 230-volt winding to be insulated for 2300 volts.

### PROBLEMS

1. An autotransformer is required to supply 200 amp at 220 volts from a 240-volt single-phase line. Neglecting losses and impedance drops, determine: (a) ratios  $N_1/N_2$  and  $N_2/n$ ; (b) currents  $I_1$ ,  $I_2$  and  $I$ ; (c) percentage of power transferred directly; (d) percentage of power transformed.

2. A two-winding, 1100/220-volt, 60-cycle transformer is used as an autotransformer to boost the voltage of a single-phase, 1100-volt line 20%. If the transformer was rated at 10 kva (2 winding), determine the output as an autotransformer and the currents  $I_1$ ,  $I_2$  and  $I$ . How much power is transferred directly and how much power is transformed.

3. A short-circuit test is taken on a 10-kva, 2300/115-volt, 60-cycle, two-winding transformer, and the following data are recorded:

$$V_{sc} = 118 \text{ volts}$$

$$I_{sc} = 4.35 \text{ amp}$$

$$P_{sc} = 225 \text{ watts}$$

If this transformer is connected as an autotransformer to boost the voltage of a 2300-volt line 5%, and a short circuit occurs on the 2415-volt output side, determine the theoretical short-circuit current which would flow.

4. Calculate the regulation of the autotransformer in Problem 3 for full-load, 0.80 power factor lagging.

5. A 14-kva, 2300/230-volt, 60-cycle transformer has the following constants:

$$r_1 = 2.5 \text{ ohms}$$

$$r_2 = 0.021 \text{ ohm}$$

$$x_1 = 10.2 \text{ ohms}$$

$$x_2 = 0.10 \text{ ohm}$$

Neglecting the magnetizing current determine the regulation of this transformer when used as an autotransformer to boost the 2300-volt line 10%. The load is 16.5 kw, unity power factor.

6. What voltage impressed across the 2300-volt side of the autotransformer in Problem 5 will produce rated current when the 2530-volt side is short-circuited?

7. Is it possible to arrange two autotransformers in a Scott connection and supply a 2-phase load from a 3-phase system? If a 2-phase, 230-volt, 4-wire, 60-cycle load is to be supplied from a 3-phase, 3-wire, 208-volt, 60-cycle system by

means of two autotransformers, specify the transformer requirements (voltages, taps) and show the manner of connection.

8. Transformation of voltages from 3-phase to 6-phase may be accomplished by means of three autotransformers properly connected. A 6-phase converter requiring ring voltages of 150 volts from a 230-volt, 60-cycle, 3-phase, 3-wire system is to be supplied by means of autotransformers. Specify the transformers necessary and show the diagram of connections.

## Chapter 13

### A-C WINDINGS

**13-1. A-c windings.** A-c windings can be single-phase or polyphase (2 or 3 or more phases). Only the polyphase windings are treated in this chapter. The single-phase windings are treated in connection with the single-phase induction motor (Chap. 26).

Two conductors make one *turn*. Turns placed so closely together that they are all interlinked with the same flux make a *coil*. Thus there are single-turn and multiturn coils.

The coils are placed in *slots* (see, for example, Figs. 16-1, 16-2, 30-2, and 30-11). Polyphase windings are usually *2-layer* (Fig. 13-1), i.e., in each slot

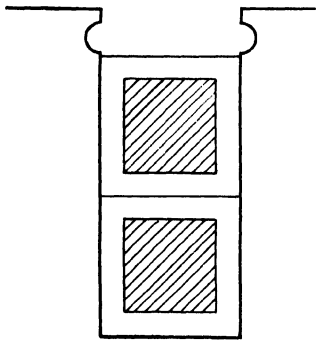


FIG. 13-1. Two-layer winding.

are placed 2 coil sides, one above the other. The single-layer polyphase winding, with one coil side in the slot, is used in the wound rotors of small induction motors (Art. 16-1) but seldom in the stators of these motors.

The polyphase windings can be of *lap* or *wave* type. The wave-type polyphase winding is used mainly in wound rotors of medium size and larger induction motors (Art. 16-1).

Polyphase windings are arranged in *groups* of two or more single coils.

There is *one group per pole per phase*.

For this reason the group is often called *pole-phase group*. The total number of groups is apparently equal to the number of phases times the number of poles:

$$\text{Number of pole-phase groups} = m \times p \quad (m \text{ is the number of phases}). \quad (13-1)$$

The pole-phase group is the *basic unit* of the a-c winding. It determines the number of parallel paths of the winding. The number of single coils of the pole-phase group will be denoted by  $q$ . Thus the total number of slots

$$Q = qmp \quad (13-2)$$

and, vice versa, if the total number of slots ( $Q$ ), the number of phases ( $m$ ), and the number of poles are given, the number of single coils per pole-phase group is

$$q = \frac{Q}{mp} \quad (13-3)$$

$q$  is apparently also the number of slots per pole per phase.

Two examples will be considered. (1) A stator with 12 slots is to be wound for 3 phases and 2 poles. The number of single coils per pole phase group, i.e., the number of slots per pole per phase, is then equal to  $q = 12/(2 \times 3) = 2$ . The total number of pole-phase groups will be  $3 \times 2 = 6$ . Fig. 13-2 shows such a winding. (2) A stator  $Q = 24$  is to be wound for 3 phases and 4 poles. Also in this case the number of single coils per pole-phase group (=the number of slots per pole per phase) is  $2 = 24/(3 \times 4)$ , but the number of pole-phase groups is  $3 \times 4 = 12$ . Fig. 13-5 shows such a lap winding and Fig. 13-9 shows such a wave winding.

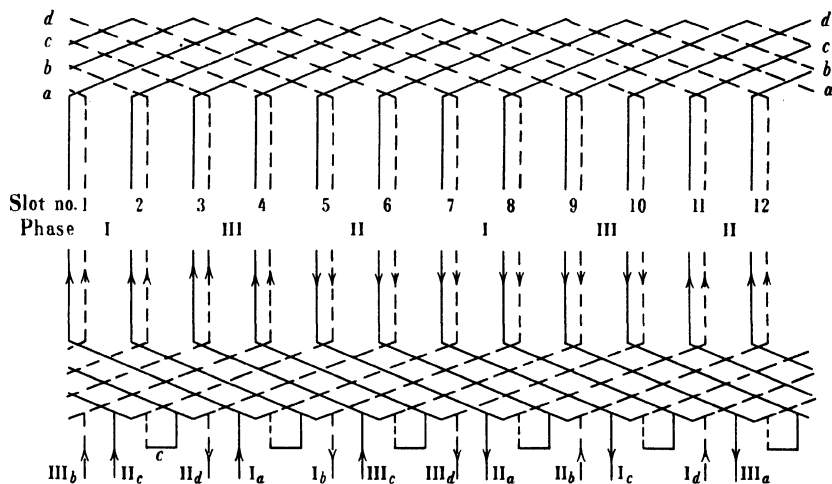


FIG. 13-2. Three-phase, 2-pole, 2-layer, lap winding with two slots per pole per phase. Multiturn coil.

In the previous considerations,  $q$ , the number of slots per pole per phase, is assumed to be an integer (*integral-slot winding*).  $q$  can also be a fractional number (*fractional-slot winding*). These latter windings are not considered in this chapter. They are treated in Chapter 55.

The layout of integral-slot windings will be considered now in some detail. The abbreviation "coil group" for pole-phase group will be used.

(a) *Polyphase lap windings*. Fig. 13-2 shows a 2-pole, 3-phase, 2-layer lap winding placed in 12 slots. The number of slots per pole per phase is  $q = 2$ . If slots 1 and 2 are assigned to phase I, slots 3 and 4 must be assigned to phase

III, slots 5 and 6 to phase II, slots 7 and 8 again to phase I, etc. The reason for the phase sequence I, III, II is given in the following.

Considering the upper coil side in slot 1, the lower coil side which makes a complete coil with it lies in slot 7. The distance between both coil sides, the *coil span*, is  $7 - 1 = 6$  slot pitches. There are  $Q = 12$  slots (total) and the number of poles is  $p = 2$ , i.e., there are 6 slots per pole. Thus the coil span is equal to the pole pitch: the winding is *full-pitch* or *not chorded*. Chorded or fractional-pitch windings will be discussed later in this chapter.

*All coils have the same coil span: this is always the case in a 2-layer winding.* All connections, i.e., those between single coils, between coil groups, and from the winding to the terminals, lie on the same end of the winding. Considering the coils at the end opposite the connections, upper coil side 1 is connected with lower coil side  $1 + 6 = 7$ ; upper coil side 2 with lower coil side  $2 + 6 = 8$ , and so forth. As has been mentioned, a coil may consist of one or more turns. It is assumed in Fig. 13-2 that the coil has more than one turn. The short connectors  $C$  at the connection end connect the last turn of the first coil of a group with the first turn of the second coil of the same group. The second connector  $C$  from the left connects the end of coil (upper 1-lower 7) with the beginning of coil (upper 2-lower 8).

Each phase has two coil groups. Phase I consists of the coil groups terminating in  $I_a I_b$  and  $I_c I_d$ ; phase II of the coil groups terminating in  $II_a II_b$  and  $II_c II_d$ ; and phase III of the coil groups terminating in  $III_a III_b$  and  $III_c III_d$ . In each case  $a$  or  $c$  represents the beginning of a coil group and  $b$  or  $d$  its end. According to the voltage to be produced in the case of a generator, or the voltage impressed in the case of a motor, the coil groups assigned to each phase are connected either in series or in parallel.

The beginnings (as well as the ends) of the three phases must be displaced from each other by 120 *electrical degrees*. That is  $I_a$ ,  $II_a$ ,  $III_a$  in Fig. 13-2 are displaced from each other by 120 electrical degrees. A 2-pole machine corresponds to 360 electrical degrees. Therefore, since a slot pitch is equal to  $360/12$ , or 30 electrical degrees, the beginnings of the three phases must be displaced from each other by  $120/30 = 4$  slots. Hence if slot 1 is taken as the start of phase I, then phase II must start in slot  $1 + 4 = 5$ , and phase III must start in slot  $5 + 4 = 9$ .  $I_a$ ,  $II_a$ , and  $III_a$  are then the beginnings of the three phases.  $I_c$ ,  $II_c$ ,  $III_c$  also could be taken as the beginnings of the three phases since they also are displaced by 120 electrical degrees. Note that it is the displacement of the beginnings of the phases by 120 electrical degrees which makes the sequence of the phases I, III, II, Fig. 13-2.

For any *instant of time*, the direction of currents or emf's in the windings can be found for alternating current *in the same way as for direct current*. However, the currents or emf's in the three phases are displaced in time phase from each other by 120 electrical degrees. For example, if the instant is chosen when the current in phase I is a maximum, Fig. 13-3, the current in the other two phases, II and III, is  $\frac{1}{2}$  the magnitude of the current in phase I

and flows in the opposite direction, i.e., if the current in the coil group  $I_a I_b$  of phase I flows from  $I_a$  to  $I_b$ , the current in the coil group  $II_a II_b$  of phase II flows from  $II_b$  to  $II_a$  and in the coil group  $III_a III_b$  of phase III from  $III_b$  to  $III_a$ . Further, it is important to note that 2 upper (or 2 lower) conductors which lie a pole pitch (in the considered example, 6 slot pitches) apart carry currents of opposite directions. Thus if the arrow goes upward in upper conductor 1, it must go downward in upper conductor  $1 + 6 = 7$ .

In Fig. 13-2 the current directions are shown corresponding to the instant of time assumed in Fig. 13-3. Note that in a 2-pole winding half of the conductors carry currents shown by an upward arrow followed by the other half which carry currents downward. In a  $p$ -pole winding this change occurs  $p/2$  times.

For a series connection of the coil groups of a phase, two coil ends which carry current in opposite directions have to be connected with each other; on the other hand, for a parallel connection of the coil groups, ends carrying current in the same direction have to be connected together. Therefore, for a series connection  $I_b$  is connected to  $I_a$  in phase I,  $II_b$  to  $II_a$  in phase II, and  $III_b$  to  $III_a$  in phase III. For a parallel connection of the coil groups  $I_a$  is connected to  $I_d$ , and  $I_b$  to  $I_c$  in phase I;  $II_a$  to  $II_d$  and  $II_b$  to  $II_c$  in phase II; etc. Notice that the individual coils of a coil group must be connected in series, because they are shifted in space and the emf's induced in them are out

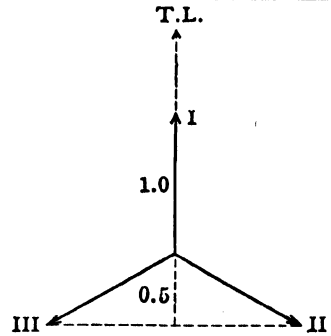


FIG. 13-3. Determination of the direction of current in a 3-phase winding for a fixed instant of time.

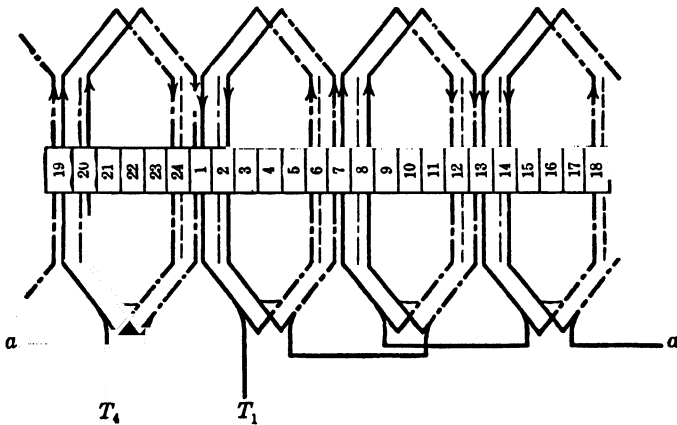


FIG. 13-4. One phase of a 4-pole, 3-phase, 2-layer, fractional pitch lap winding with two slots per pole per phase. Multiturn coil.



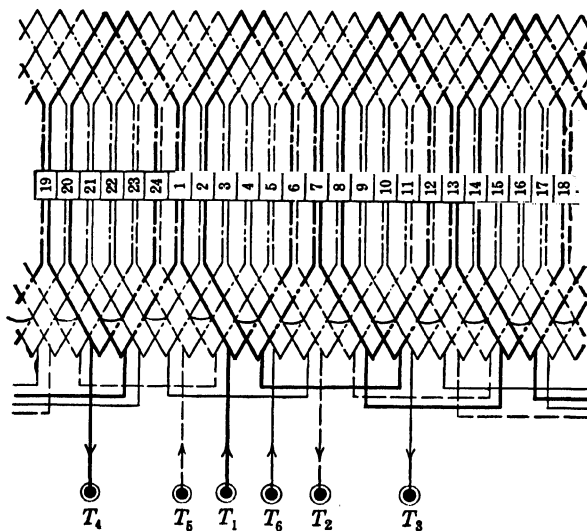


FIG. 13-5. Three-phase, 4-pole, 2-layer, fractional-pitch lap winding with two slots per pole per phase. Multiturn coil.

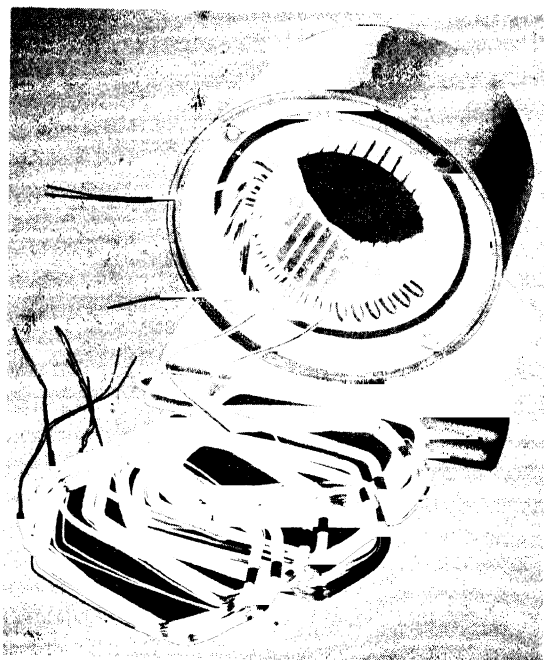


FIG. 13-6. Stator of a small induction motor in process of winding.

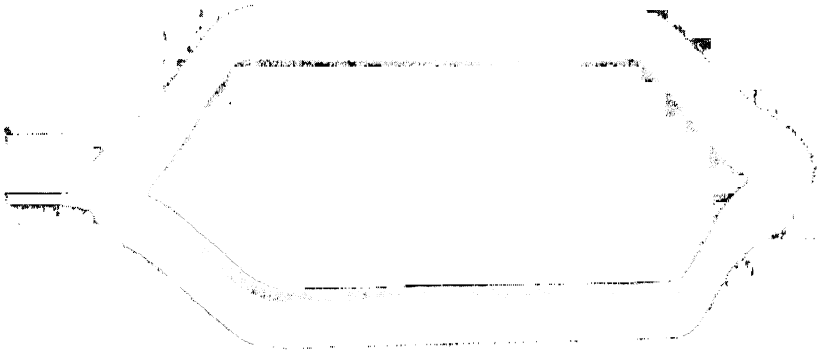


FIG. 13 7 Diamond coil

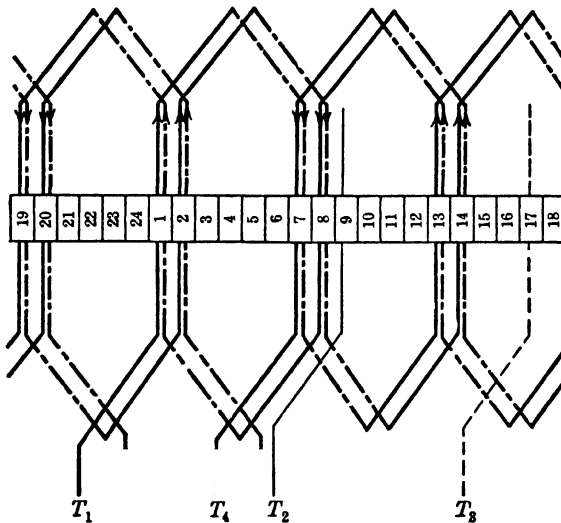


FIG. 13-8. One phase of a 4-pole, 3-phase, 2-layer, wave winding with two slots per pole per phase. Single-turn coil.

of phase. However, all coil groups of a phase can be connected in parallel. Since there are  $p$  coil groups per phase, the *maximum number of parallel paths is  $p$* .

The coil span in Fig. 13-2 is equal to a pole pitch ( $= 6$  slot pitches) and the winding is full pitch. Normally, 2-layer windings are *chorded* (*fractional pitch*). Chording has an advantage in that the shape of the emf induced in the winding and the mmf produced by the winding is closer to a sinusoidal curve than in a full-pitch winding. Fig. 13-4 shows one phase of a 4-pole 2-layer

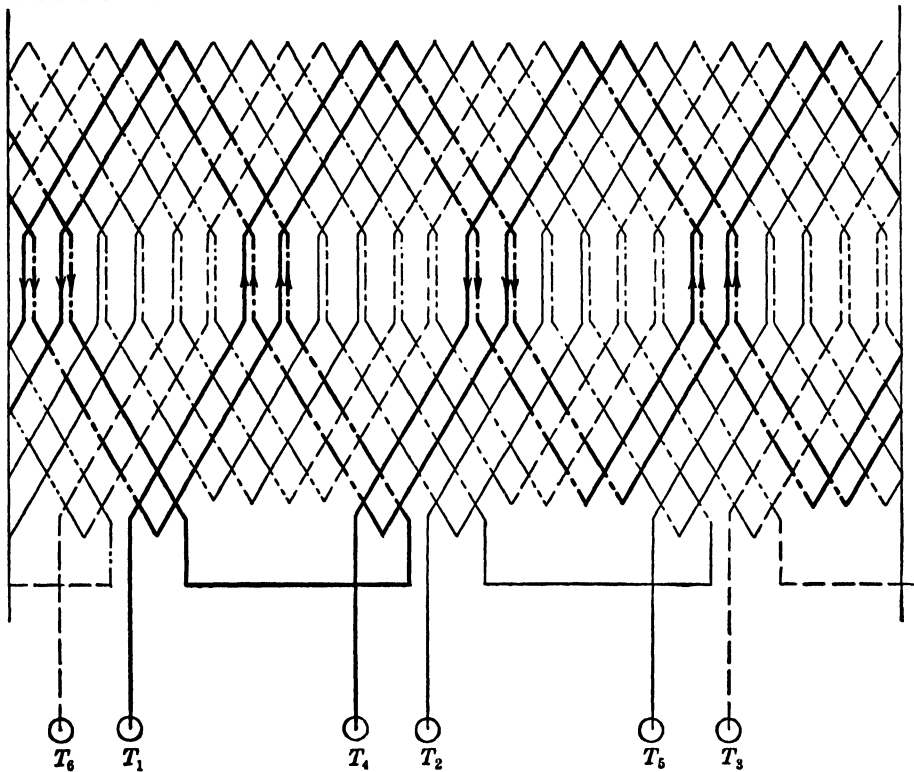


FIG. 13-9. Three-phase, 4-pole, 2-layer, wave winding with two slots per pole per phase. Single-turn coil.

chorded lap winding with  $q = 2$  slots per pole per phase. Upper coil side 1 is connected with lower coil side 6 (not with 7 as in Fig. 13-2). The coil span is equal to  $6 - 1 = 5$  slot pitches. The chording is equal to 1 slot pitch. Fig. 13-5 shows the complete winding. There are  $p \times m = 4 \times 3$  coil groups. The four coil groups of each phase are connected in series, leaving two leads for each phase. The directions of the currents shown in the leads correspond to the instant of time when the current in phase I is a maximum, see Fig. 13-3.

The end-windings as shown in Figs. 13-2, 13-4, and 13-5 are away from the iron of the armature. In smaller machines the coils have a rectangular shape with round ends and the end-windings lie directly at the iron, Fig. 13-6. In larger machines the coils are diamond-shaped, as shown in Fig. 13-7. This coil has 7 turns (7 conductors per coil side) and each conductor consists of 2 parallel strands.

The general considerations outlined in the preceding for 3-phase lap windings also hold for 2-phase lap windings. The only difference is that the 2-phase winding has  $2p$  coil groups while the 3-phase winding has  $3p$  coil groups.

(b) *Polyphase wave windings.* Fig. 13-8 shows one phase of a 4-pole,

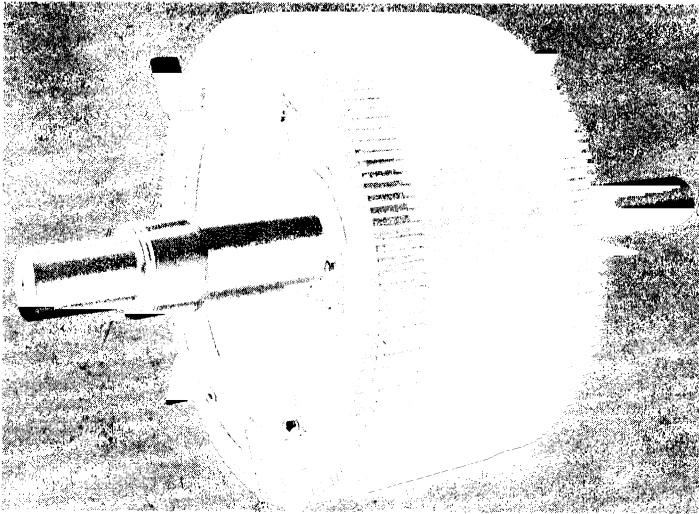


FIG. 13-10. Complete squirrel-cage rotor of a large induction motor.

3-phase, 2-layer, wave winding with  $q=2$  slots per pole per phase; Fig. 13-9 shows the complete winding. If this winding is compared with the lap winding in Fig. 13-5, it is evident that fewer end connections are necessary. While the diamond lap winding has loops on both ends of the coil, Fig. 13-7, the wave winding has a loop on only one end; on the connection side of the coil the ends go in different directions, Fig. 13-8.

(c) *Squirrel-cage windings.* The rotors of most induction and synchronous motors have squirrel-cage windings. These windings have solid, uninsulated bars in the slots and are connected on each end of the rotor by a short-circuiting ring. In small rotors of induction motors (up to 50 HP) the bars and rings are usually die-cast with aluminum, Fig. 16-7; in larger rotors the bars are usually made of copper, Fig. 13-10.

### PROBLEMS

1. Draw the developed winding diagram of a 3-phase, 2-layer lap winding for a 4-pole machine with 3 slots per pole per phase and a 77.8% chording. Single-turn coil.
2. Repeat Problem 1 for a wave winding.
3. Draw the developed winding diagram of a 2-phase, 2-layer lap winding for a 4-pole machine with 4 slots per pole per phase. Chording is 87.5%. Multiturn coil.
4. Suggestions for further armature winding layouts for 3-phase machines are:

	poles $p$	$q$	chording	winding
a.....	2	6	61.1%	lap
b.....	6	2	83.3	lap

---

	<i>poles p</i>	<i>q</i>	<i>chording</i>	<i>winding</i>
c.....	6	2	83.3	wave
d.....	6	4	83.3	lap
e.....	6	4	75	wave
f.....	8	2	83.3	lap
g.....	8	3	77.8	wave

# Chapter 14

## EMF OF AN A-C WINDING

It has been shown in Chap. 1, Eq. 1-11, that the effective value of the emf induced in a coil with  $n_c$  turns is

$$E_c = 4.44 f n_c \Phi 10^{-8} \text{ volt} \quad (14-1)$$

This equation has been derived under the following assumptions:

1. All  $n_c$  turns of the coil are linked with the same flux at any instant.
2. The coil pitch is equal to the pole pitch = 180 electrical degrees (*full-pitch winding*). In this case the maximum flux interlinkage of a turn is equal to the total pole-flux (see Fig. 1-2).
3. The flux ( $B$ -) distribution along the armature is sinusoidal.

Whether or not these three assumptions apply to an a-c winding will be discussed in turn.

**14-1. Distribution factor.** The first assumption that all  $n_c$  turns of the coil are interlinked with the same flux at any instant of time applies to any individual coil of a coil group (pole-phase group), because the  $n_c$  turns lie close together in the same slot and they are all interlinked with the same flux. The emf's induced in them are in phase. It has been mentioned in Art. 13-1 that the emf's induced in individual coils of a pole-phase group are out of phase. They are displaced from each other by the angle  $\alpha_s$  (the *slot angle*)

$$\alpha_s = \frac{180 \times p}{Q} = \frac{180}{mq} \quad (14-2)$$

electrical degrees and the resultant effective emf of the coil group is equal to the geometric sum of  $q$  emf's shifted from each other by  $\alpha_s$  degrees.

Consider as an example a 3-phase winding with  $q = 4$ . The angle between two slots is  $\alpha_s = 180/(3 \times 4) = 15^\circ$ . Fig. 14-1 shows the voltage polygon of the induced emf's in the four coils of the group. Each phasor  $AB$ ,  $BC$ ,  $CD$ ,  $DF$  is equal in magnitude and represents the maximum

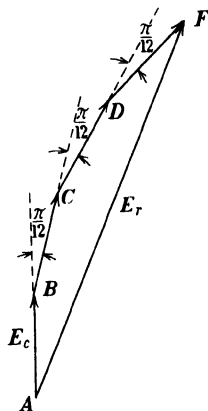


FIG. 14-1. Explanation of the distribution factor.

value of the emf induced in a coil ( $E_c$ ).  $AF$  is the maximum value of the resultant emf ( $E_r$ ), i.e., of the emf induced in the coil group. The ratio

$$\frac{\text{resultant emf}}{\text{sum of emf's of individual coils}} = \frac{E_r}{qE_c} = k_d \quad (14-3)$$

is called the *distribution factor*. It is smaller than 1 and expresses the reduction of the resultant emf of the coil group (winding) caused by the distribution of the turns belonging to a coil group over several ( $q$ ) pairs of slots rather than placing them in one single pair of slots.

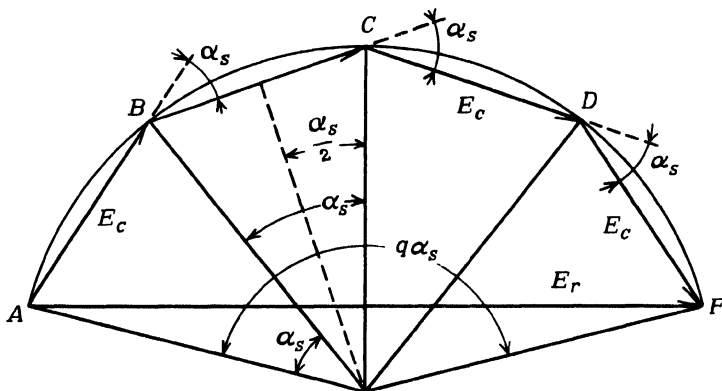


FIG. 14-2. Determination of the distribution factor.

Fig. 14-2, which is the same as Fig. 14-1, is drawn in polar form and yields for the distribution factor

$$k_d = \frac{E_r}{qE_c} = \frac{2R \sin q(\alpha_s/2)}{2Rq \sin (\alpha_s/2)} = \frac{\sin q(\alpha_s/2)}{q \sin (\alpha_s/2)} \quad (14-4)$$

Eq. 14-1 yields now for the effective emf induced in a *coil group of a poly-phase winding*:

$$E_g = qk_d E_c = 4.44 f n_c q k_d \Phi \cdot 10^{-8} \text{ volt} \quad (14-5)$$

where  $n_c q$  is the number of turns in a coil group ( $N_g$ ); therefore,

$$E_g = 4.44 f N_g k_d \Phi \times 10^{-8} \text{ volt} \quad (14-6)$$

It has been also mentioned in Art. 13-1 that all pole-phase groups can be connected in parallel. The reason for this is that the pole-phase groups are shifted a pole pitch = 180 electrical degrees from each other and, therefore, lie in flux densities  $B$  of the same strength. In Fig. 13-2, for example, the upper coil sides 7 and 8 of the second coil group of phase  $A$  are each shifted one pole pitch (= 6 slot pitches) with respect to the upper coil sides 1 and 2

of the first coil group of this phase; also the lower coil sides (1, 2 and 7, 8) of both coil groups are shifted with respect to each other by one pole pitch.

Consider again Fig. 13-2; if the two coil groups of a phase are connected in parallel, the emf induced in the phase is given by Eq. 14-6; if the two coil groups of a phase are connected in series, the emf of a phase will be twice the value given by Eq. 14-6. Consider Fig. 13-5 or 13-9. In both cases the four coil groups are connected in series and the emf induced in a phase is four times the value given by Eq. 14-6. If the four coil groups were connected in two parallel parts, each part consisting of two coil groups in series, the emf of a phase would be twice the value given by Eq. 14-6 and, finally, the emf of a phase would be that given by Eq. 14-6 if the four coil groups were connected in parallel.

The number of *series-connected turns per phase* will be denoted by  $N$ .  $N$  is then equal to  $N_g$  times the number of coil groups connected in series and the emf per phase is

$$E = 4.44fNk_a\Phi 10^{-8} \text{ volt} \quad (14-7)$$

**14-2. Pitch factor.** The assumption that the coil pitch is equal to the pole pitch is seldom true for an a-c winding. Normally the coil pitch is smaller than the pole pitch, i.e., normally a-c windings are *fractional-pitched* or *chorded*, as, for example, in Fig. 13-5, where the coil span is 5 slot pitches while to a pole pitch correspond  $24/4 = 6$  slot pitches.

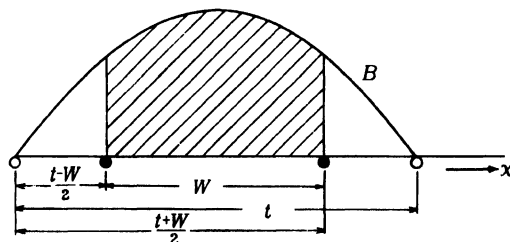


FIG. 14-3. Maximum flux interlinkage of a full-pitch and of a fractional-pitch coil.

Due to the chording, the maximum flux interlinkage with the coil is smaller than the pole flux. Fig. 14-3 shows the maximum flux interlinkage of a full-pitch coil and of a fractional-pitch coil with a coil span  $= W$ . For the full-pitch coil it is the total area of the sinusoidal half wave; for the fractional pitch coil it is equal to the cross-hatched area. The ratio of the latter area to the total area is

$$k_p = \int_{x=(t-W)/2}^{x=(t+W)/2} \sin \frac{\pi}{\tau} x dx \bigg/ \int_{x=0}^{x=\tau} \sin \frac{\pi}{\tau} x dx = \sin \frac{W}{\tau} \frac{\pi}{2} \quad (14-8)$$

$k_p$  is called *pitch factor*. For a full pitch coil,  $W = \tau$  and  $k_p = 1$ .



The emf of the coil is proportional to the maximum flux interlinkage. Therefore, the *general equation* for the emf induced in an a-c winding with  $N$  series turns per phase by a sinusoidally distributed flux is

$$E = 4.44fNk_d k_p \Phi \times 10^{-2} \text{ volt} = 4.44fNk_d k_p \Phi \times 10^{-8} \quad (14-9)$$

$k_{dp}$  is the product of  $k_d$  and  $k_p$ .

The quantity  $Nk_d k_p$  can be considered as the number of *effective turns per phase*. It is smaller than the actual number of turns per phase  $N$ , owing to the distribution of the winding over several slots under each pole and to the chording of the coils. The product  $k_d k_p$  is often called the *winding factor*.

Some values of the distribution factor are given in the following table:

Slots per pole per phase	2	3	4	5	6	8	$\infty$
Three-phase	0.966	0.960	0.958	0.957	0.957	0.956	0.955
Two-phase	0.924	0.910	0.906	0.904	0.903	0.901	0.900

It is seen from this table that the distribution of the winding causes a turn-loss or a voltage loss of 3.5 to 4.5 per cent in 3-phase windings and a loss of 7.5 to 10 per cent in 2-phase windings. The magnitude of the pitch factor  $k_p$  depends upon the ratio of coil span to pole pitch. For  $W/\tau = 5/6$ , for example,  $k_p = 0.966$ .

### 14-3. Non sinusoidal flux (B-) distribution along the armature surface. The preceding considerations are based on the assumption of a

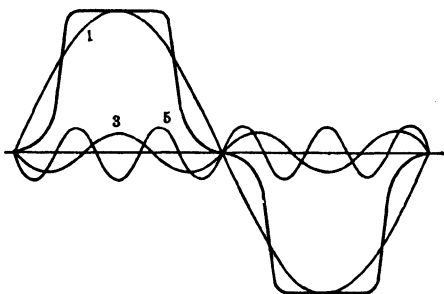


FIG. 14-4. Flux distribution curve at no-load with fundamental and only two harmonics shown.

sinusoidal flux distribution. The induced emf is then a sinusoidal function of time (see Art. 1-2). The low saturated induction motors and the cylinder rotor synchronous machines (Art. 32-1) have a flux distribution close to a sinusoid. The salient pole synchronous machines (Art. 34-1) have a flat flux distribution, as shown in Figs. 1-3 and 14-4. In this latter case, the flux distribution curve is resolved into a Fourier series (Fig. 14-4) and the fundamental and the harmonics are considered separately

(Chap. 39). To each harmonic flux distribution applies then Eq. 4-9. The harmonic emf's of the salient-pole machine will be treated in connection with

the study of this machine (Chap. 39). Harmonic emf's are undesirable. Chording of the coils reduces the harmonics. Also a larger value of  $q$  decreases the harmonics.

### PROBLEMS

1. A 24-pole, 60-cycle, 3-phase synchronous generator has a total of 216 slots, 18 conductors per slot in a 2-layer winding, a 3-parallel wye connection and a coil throw of 0.778. If the no-load generated voltage is 2300 volts between terminals, determine the no-load flux per pole. What is the line voltage for the same pole flux if the machine is reconnected 2-parallel delta?

2. With normal excitation the pole flux in a 60-cycle generator is  $6 \times 10^6$  maxwells per pole and is sinusoidally distributed along the air gap. For a coil pitch of unity determine the generated armature voltage per turn. What is the form factor and shape of this emf? If the coil throw is 0.833, what is the emf induced per turn?

3. With normal excitation the pole flux in a 60-cycle generator is  $10 \times 10^6$  maxwells and is sinusoidally distributed along the air gap. The armature has a 2-layer, 3-phase winding with 12 slots per pole and 6 conductors per slot. What is the emf induced in the winding per pole if the coil throw is: (a) 1.0, (b) 0.833, (c) 0.75? All conductors are connected in series.

4. A 7500-kva, 3-phase, 25-cycle, wye-connected generator is rated to deliver its output at 11,800 volts between terminals. The field structure has 12 poles, and the armature 180 slots containing a 2-layer winding with 4 conductors per slot. All conductors are connected in series. What is the no-load terminal voltage when the pole flux is 52 megalines per pole and the generator is driven at rated speed? The coil throw is 12 slots.

## Chapter 15

### THE MMF OF AN A-C WINDING · ALTERNATING MMF · ROTATING MMF

**15-1. Alternating MMF.** Consider the elementary machine (Fig. 15-1). It is excited by a single coil of  $n_c$  turns which may be considered as one phase

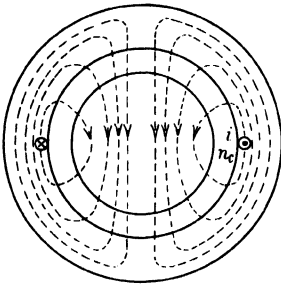


FIG. 15-1. Elementary 2-pole single-phase machine with a single-coil.

of a polyphase winding with  $q=1$  and  $n_c$  conductors in the slot. The machine has two poles, because the flux enters the armature (inner part) once and leaves the armature once. The coil carries a current  $i$ . It is seen from the figure that each line of force is interlinked with all  $n_c i$  ampere turns. Applying Ampere's law of the magnetic

circuit  $\oint H_l dl = NI$  (Eq. 1-23) to this elementary

machine, the line integral  $\oint H_l dl$  is the same for

all lines of force because the mmf  $n_c i$  is the same for all lines of force. Therefore, the representation

of the mmf as a function of space around the stator between the coil sides will be a rectangle with the height  $n_c i$  (Fig. 15-2).

For reasons which will immediately become obvious, it is expedient to

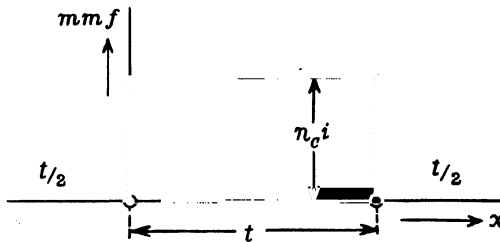


FIG. 15-2. Mmf curve of the elementary machine of Fig. 15-1.

move up the axis of abscissae the distance  $n_c i/2$ , so that the half of the mmf  $n_c i$  which drives the flux *into* the rotor is assumed positive and the half which drives the flux *from* the rotor into the gap is assumed negative (or vice versa). This yields the graphical representation shown in Fig. 15-3.

Since the permeability  $\mu$  of iron is high (see Fig. 1-8) only a small value of field intensity  $H$  in the iron is necessary for any finite value of the flux density  $B = 0.4\pi\mu H$ . This means that the path in the iron contributes but

little to the line integral  $\oint H_c dl$ , and it can be assumed that  $\oint H_c dl = H_g 2g$ ,

i.e.,  $n_c i = H_g 2g$  ( $g$  = length of air gap). Since  $B_g = 0.4\pi H_g$ ,  $B_g = 0.4\pi n_c i/2g = 0.4\pi(n_c i/2)(1/g)$ . Thus if  $g$  is a constant quantity, as is the case in all induction motors, Fig. 15-3 represents not only the mmf-curve but, to another scale, also the flux distribution in the gap (the  $B$  curve). The representation of the latter curve must consist of areas above and below the axis of abscissae which are equal to each other, because the area of the  $B$ -distribution curve is the flux per unit length of the core (see Art. 1-2, Eq. 1-32) and the flux going into the rotor (positive area) must be equal to the flux leaving the rotor (negative area). Thus the representation of the mmf-curve with positive and negative areas, as shown in Fig. 15-3 has the advantage that it also yields the  $B$ -distribution curve which must contain positive and negative areas.

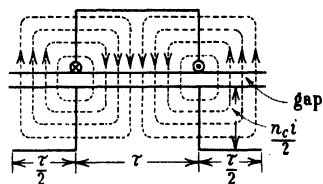


FIG. 15-3. Mmf curve of the elementary machine of Fig. 15-1.

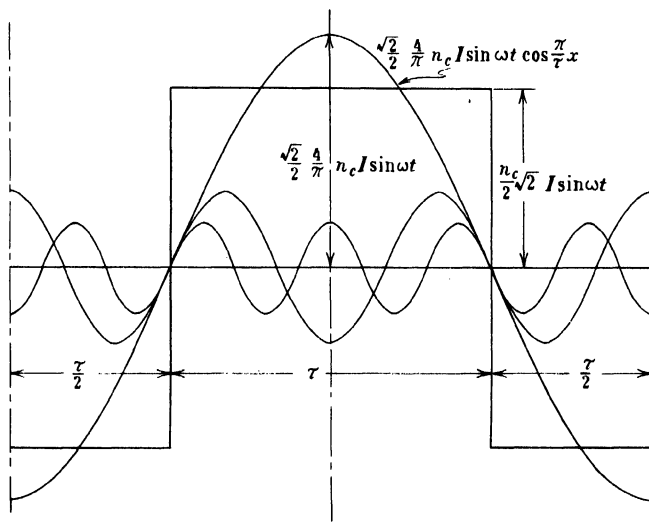


FIG. 15-4. Mmf curve of the 2-pole, single-phase winding of Fig. 15-1 with the fundamental and only two harmonics shown.

If the Fourier series is applied to the rectangular mmf-curve of Fig. 15-3, a fundamental wave and harmonic waves are obtained as shown in Fig. 15-4. The wave length of the fundamental is the same as that of the rectangular mmf-curve, namely,  $2\tau$ . The amplitude of the fundamental wave is  $4/\pi$  times the height of the rectangular wave, i.e.,  $(4/\pi)(n_c i/2)$ . Introducing  $i = \sqrt{2} I \sin \omega t$ , the equation of the fundamental mmf wave becomes

$$f(x) = \frac{\sqrt{2}}{2} \frac{4}{\pi} n_c I \sin \omega t \cos \frac{\pi}{\tau} x = 0.9 n_c I \sin \omega t \cos \frac{\pi}{\tau} x \quad (15-1)$$

For a fixed instant of time  $t$ , this mmf and also the  $B$ -distribution produced by it are *cosine functions of space* ( $x$ ) around the stator. For a fixed point  $x$ , both the mmf and  $B$  are a maximum when the current is a maximum and are zero when the current is zero. If the direction of the current is reversed, the direction of the mmf and  $B$  is also reversed. Such an mmf and flux are referred to as *alternating mmf* and *alternating flux*. The alternating flux thus can be characterized as a flux which is *fixed in space* (standing wave) while its *magnitude varies* from a positive maximum to a negative maximum (standing wave). Such an alternating flux has already been considered in the single-phase transformer.

**15-2. Rotating MMF.** Fig. 15-1 refers to an elementary single-phase machine since there is only one coil fed by a single-phase current. Fig. 15-5 shows an elementary 2-pole 3-phase machine: here three coils are displaced from each other in space by 120 electrical degrees and it will be assumed that they are fed by three currents shifted from each other 120° in time. Each of the three coils will produce a rectangular mmf as that shown in Fig. 15-4 of which only the fundamental will be considered here. The three fundamental waves produced by the three coils will be displaced from each other in space by 120° since the three coils are displaced from each other by this angle. Using coil (phase) I as a reference and placing the  $x=0$  point, as before in Fig. 15-4, in the axis of this coil, the three mmf waves produced by the three coils are

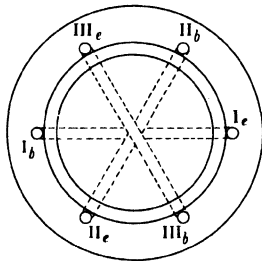


FIG. 15-5. Elementary 2-pole, 3-phase machine.

$$\begin{aligned} f_{\text{I}}(x) &= \frac{\sqrt{2}}{2} \frac{4}{\pi} n_c I \sin \omega t \cos \frac{\pi}{\tau} x \\ f_{\text{II}}(x) &= \frac{\sqrt{2}}{2} \frac{4}{\pi} n_c I \sin (\omega t - 120) \cos \left( \frac{\pi}{\tau} x - 120 \right) \\ f_{\text{III}}(x) &= \frac{\sqrt{2}}{2} \frac{4}{\pi} n_c I \sin (\omega t - 240) \cos \left( \frac{\pi}{\tau} x - 240 \right) \end{aligned} \quad (15-2)$$

The first of these three equations is identical with that derived for the single coil (Eq. 15-1). It is observed that the amplitude of each wave is

$$\frac{\sqrt{2}}{2} \times \frac{4}{\pi} n_c I = 0.9 n_c I$$

In order to obtain the resultant mmf produced by all three phases, the sum  $f_I + f_{II} + f_{III}$  is to be taken. Observing that  $\sin \alpha \cos \beta = \frac{1}{2} \sin (\alpha - \beta) + \frac{1}{2} \sin (\alpha + \beta)$  the final result obtained is:

$$f_{(x)} = \frac{3}{2} \frac{\sqrt{2}}{2} \frac{4}{\pi} n_c I \sin \left( \omega t - \frac{\pi}{\tau} x \right) = 1.35 n_c I \sin \left( \omega t - \frac{\pi}{\tau} x \right) \quad (15-3)$$

The resultant mmf contains a sine function of *time and of space*. The meaning of this function can be seen readily from Fig. 15-6 which represents the position of the resultant around the stator (in the air gap) for three different instants of time. Fig. 15-6a refers to  $t=0$ , Fig. 15-6b refers to  $t=t_1>0$ , and Fig. 15-6c to  $t=t_2>t_1$ . Observe the position of a fixed point of the wave, for example point *A*, at the different instants of time: as time elapses this point moves to the right in the positive direction of the  $x$ -axis. This means that the function  $\sin [\omega t - (\pi/\tau)x]$  represents a *traveling wave*.

Referring to Eq. 15-3, the amplitude of the traveling mmf wave

$$\left( \frac{3}{2} \frac{\sqrt{2}}{2} \frac{4}{\pi} n_c I \right) = 1.35 n_c I$$

is a constant quantity. Thus the resultant mmf of a 3-phase (polyphase) winding is an mmf which travels around the stator (in the gap) with constant amplitude. Such an mmf and the flux produced by it are referred to as a *rotating mmf* and a *rotating flux*.

A comparison of the rotating mmf or flux with the alternating mmf or flux shows that the former has a constant amplitude and moves around in the gap of the machine while the latter has a variable amplitude and is fixed in space.

A rotating mmf and flux can be produced in another way. Consider Fig. 30-3 which shows the rotor of a synchronous machine. The field coils on the salient poles are fed by a direct current. When this pole structure is driven by a Diesel engine or a waterwheel, the effect of its rotation is a rotating mmf and flux. However, a prime mover is necessary to produce this effect, whereas in the discussion considered above the rotating mmf and flux were produced

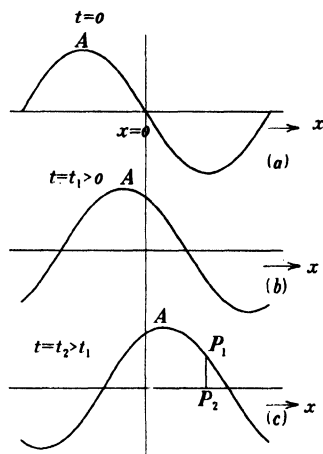


FIG. 15-6. The function  $\sin \left( \omega t - \frac{\pi}{\tau} x \right)$  at different instants of time.

by non-moving coils with polyphase currents flowing in them. The discovery of the possibility of producing a rotating flux by non-moving coils and polyphase currents was a turning point in the development of the electric machine, because the induction motor, which is the most commonly used electric machine, operates on the basic principle of a rotating flux produced by fixed coils.

The velocity of propagation of the mmf wave represented by Eq. 15-3 and of the flux produced by it can be determined from Eq. 15-3. Imagine an observer traveling with the mmf wave and sitting on point  $P_1$  of the wave (see Fig. 15-6c). For this observer, the magnitude of the mmf will always have the same value  $P_1P_2$ , i.e., for him the right side of Eq. 15-3 is a constant quantity. Since the factor  $\frac{3}{2} \frac{\sqrt{2}}{2} \frac{4}{\pi} n_c I$  has a constant value, the condition that exists for the observer is:

$$\sin \left( \omega t - \frac{\pi}{\tau} x \right) = \text{constant}$$

and, therefore,

$$\omega t - \frac{\pi}{\tau} x = \text{constant}$$

Differentiating this equation with respect to  $t$ , the velocity of propagation of the mmf wave  $dx/dt$  is obtained as

$$\frac{dx}{dt} = \omega \frac{\tau}{\pi} = 2f\tau = \frac{2\tau}{T} \quad (15-4)$$

This equation states that the wave moves, during one cycle of the current, a distance  $x$  twice the pole pitch, i.e., its wave length.

For rotating machines it is customary to express the velocity of propagation in rpm rather than as a distance. The distance covered by the wave in one minute is  $2f\tau \times 60$ . The distance which corresponds to one revolution of the rotor is  $p\tau$ . Thus the speed in rpm is

$$n = \frac{2f\tau \times 60}{p\tau} = \frac{120f}{p} \quad (15-5)$$

Note that this is the *same equation* which has been derived for the frequency of the a-c emf induced in an armature winding moving with  $n$  rpm relative to a pole-structure with  $p$  poles (Eq. 1-9).

Applying the relation  $\sin \alpha \cos \beta = \frac{1}{2} [\sin (\alpha - \beta) + \sin (\alpha + \beta)]$  to Eq. 15-1, there results

$$f_{(x)} = \frac{1}{2} \left( \frac{\sqrt{2}}{2} \frac{4}{\pi} n_c I \right) \sin \left( \omega t - \frac{\pi}{\tau} x \right) + \frac{1}{2} \left( \frac{\sqrt{2}}{2} \frac{4}{\pi} n_c I \right) \sin \left( \omega t + \frac{\pi}{\tau} x \right) \quad (15-6)$$

Comparing this equation with Eq. 15-3, it is seen that an alternating mmf can be replaced by two rotating mmf's traveling in *opposite* directions and

each having an amplitude equal to half of that of the alternating mmf. Use of this concept, to replace an alternating mmf by two rotating mmf's, is made in the treatment of the single-phase motor (Chap. 26).

Eqs. 15-1 and 15-3 were derived under the assumption that there is only one coil per pole pair per phase (see Figs. 15-1 and 15-5), i.e., one slot per pole per phase ( $q = 1$ ). If there are  $q > 1$  slots per pole per phase, i.e., the coil group consists of  $q$  individual coils, the resultant mmf is obtained by treating the mmf given by Eq. 15-1 and also that given by Eq. 15-3 as phasors. This is permissible because they are sinusoidal functions. The phasors representing the amplitudes of the mmf's of the individual coils of the coil group are shifted with respect to each other by the electrical angle which corresponds to a slot pitch, and the resultant mmf is obtained by a geometric addition of the mmf's of the  $q$  single coils. This is the same consideration as that applied to the determination of the resultant emf of a coil group with  $q$  coils (see Figs. 14-1 and 14-2). It leads to the introduction of the *distribution factor*  $k_d$  as given by Eq. 14-4, and the resultant mmf is that given by Eq. 15-1 or that given by Eq. 15-3 times  $k_d q$ .

Eqs. 15-1 and 15-3 refer to a full-pitch winding. This can be seen from Figs. 15-1 and 15-5 in which the coil pitch (measured as an arc) is equal to the pole pitch. If the winding is chorded, then the *pitch factor* must be introduced as was done for the determination of the emf of a chorded winding.

Compare Eqs. 15-1 and 15-3. The factor  $\frac{3}{2}$  in Eq. 15-3 is due to the fact that a 3-phase winding has been considered as an example (Fig. 15-5). If an  $m$ -phase ( $m > 1$ ) winding were considered, the factor  $m/2$  would appear in Eq. 15-5. Multiplying Eqs. 15-1 and 15-3 by  $qk_d$  in order to include the case of a coil group with  $q$  single coils, and further, multiplying these equations by the pitch factor  $k_p$  in order to include the case when the coils are chorded, and finally introducing into Eq. 15-3  $m/2$  instead of  $\frac{3}{2}$ , the amplitude of the fundamental of the mmf of a single-phase winding becomes

$$F = 0.9 n_c q k_d p I \quad (15-7)$$

and that of the polyphase winding ( $m > 1$ )

$$F = 0.45 m n_c q k_d p I \quad (15-8)$$

$n_c q$  in Eqs. 15-7 and 15-8 is the number of turns per pole pair. The total number of turns per phase  $N$  is

$$N = \frac{p}{2} n_c q \quad (15-9a)$$

Introducing  $n_c q$  from this equation into Eqs. 15-7 and 15-8 the *amplitude of the fundamental of the mmf of a single phase-winding* is

$$F = 1.8 \frac{N}{p} k_d p I \quad (15-10)$$



and the *amplitude of the fundamental of the mmf of a polyphase winding* ( $m > 1$ ) is

$$F = 0.9m \frac{N}{p} k_{av} I \quad (15-11)$$

Only the fundamental mmf wave has been considered throughout this article. The harmonics (see Fig. 15-4) have been disregarded. An investigation of the harmonic mmf's in the same manner, as has been done for the fundamental wave, shows that a single-phase winding produces harmonic alternating mmf's and fluxes and that a polyphase winding produces harmonic rotating mmf's and fluxes. The speed of the rotating harmonic mmf's and fluxes is different from that of the fundamental wave, Eq. 15-5. Some of the rotating harmonic mmf's (fluxes) travel in the same direction as the fundamental mmf (flux) and some travel in opposite directions. A 3-phase winding does not produce mmf harmonics of the order 3 or a multiple of 3. This will be discussed in Chap. 24.

The useful torque of the machine is produced by the fundamental flux. All harmonic fluxes are undesirable, especially in induction motors, where they produce not only additional losses (see Art. 29-1) but may produce vibration and noise. They may also distort the torque-speed curve and cause locking torques. The harmonic mmf's which produce the harmonic fluxes must be kept as small as possible. This may be achieved by a *chording* of the coils and choosing a value of  $q$  which is not too small. These same means are also used to keep down the harmonics of the induced emf (see foregoing chapter). Chording reduces the harmonics of low order (5th and 7th). *Skewing* of the rotor or stator is very helpful for the reduction of the influence on the rotor of the harmonic fluxes of high order and is used in small and medium-sized induction motors for this purpose (see Fig. 23-5). The influence of the harmonic fluxes on the operation of the induction motor is treated in detail in Chaps. 24 and 58.

**Example 15-1.** The total mmf of a 3-phase 2-pole winding with 2 slots per pole per phase will be determined. It will be assumed that the winding is fractional-pitch, the coil span 5 slot pitches; the mmf will be determined for the instant shown in Fig. 15-7, i.e., when the current in phase III is zero while in phases I and II the currents are equal and of opposite sign.

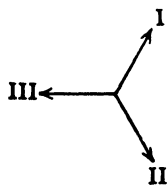
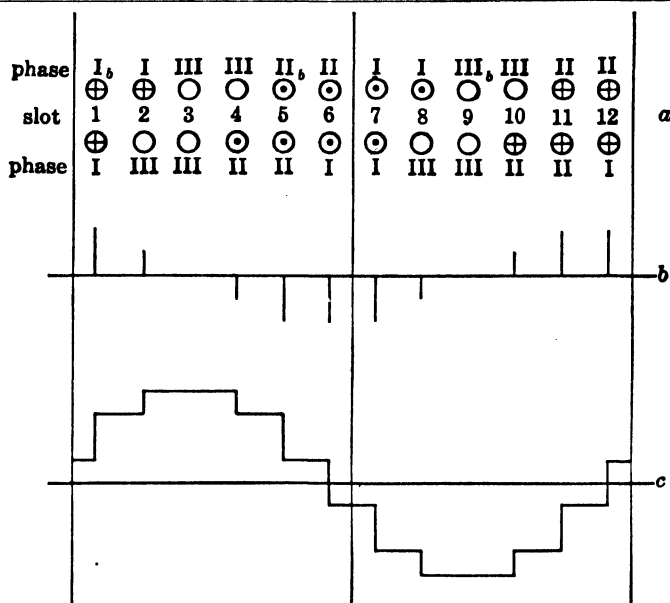


FIG. 15-7. Figure for the example.

The circles in Fig. 15-8a represent coil sides and this figure shows the slot distribution over the two poles.  $I_b$ ,  $II_b$ , and  $III_b$  are the beginnings of the three phases. Since the currents in phases I and II are opposite, the beginning of phase II must be marked by a dot if the beginning of phase I is marked by a cross. This determines the current directions in the top and bottom layers around the machine. Fig. 15-8b is the ampere-conductor

distribution of the winding. It is obtained by adding the currents of Fig. 15-8a, observing the signs and magnitudes of the individual currents. In the case con-

FIG. 15-8. Mmf curve of a 3-phase winding ( $q=2$ ).

sidered, the magnitudes of all currents are equal. Fig. 15-8c is the total mmf of the winding. It is obtained through graphical integration of Fig. 15-8b. The integration can be started at any point and a line then is drawn in such a manner that the positive and negative areas of the mmf curve are equal.

### PROBLEMS

1. Show the shape of the total mmf of the 3-phase winding of Problem 1, Chap. 13, for the instant of time: (a) when the current in phase I is zero; (b) when the current in phase I is a maximum.

2. Repeat Problem 1 for the 2-phase winding of Problem 3, Chap. 21.

*Note*—Problem 4, Chap. 13, offers added suggestions for problems on determining the shape of the mmf wave of 3-phase windings.

## Chapter 16

### MECHANICAL ELEMENTS OF THE POLYPHASE INDUCTION MOTOR AND ITS MAGNETIC CIRCUIT

**16-1.** It follows from Biot-Savart's law (Art. 1-2) that all electric machines must have *two indispensable elements, the magnetic flux and the conductors carrying current* (the armature). In the induction motor the flux is produced by the outer part, the *stator*, while the rotating inner part of the machine, the *rotor*, is its armature. The stator is excited by alternating currents which produce rotating fluxes. The stator iron must be laminated (Art. 29-1).

The armature conductors are placed parallel to the axis of the armature or they are skewed at a slight angle to the axis and the armature iron is also laminated (Art. 29-1).

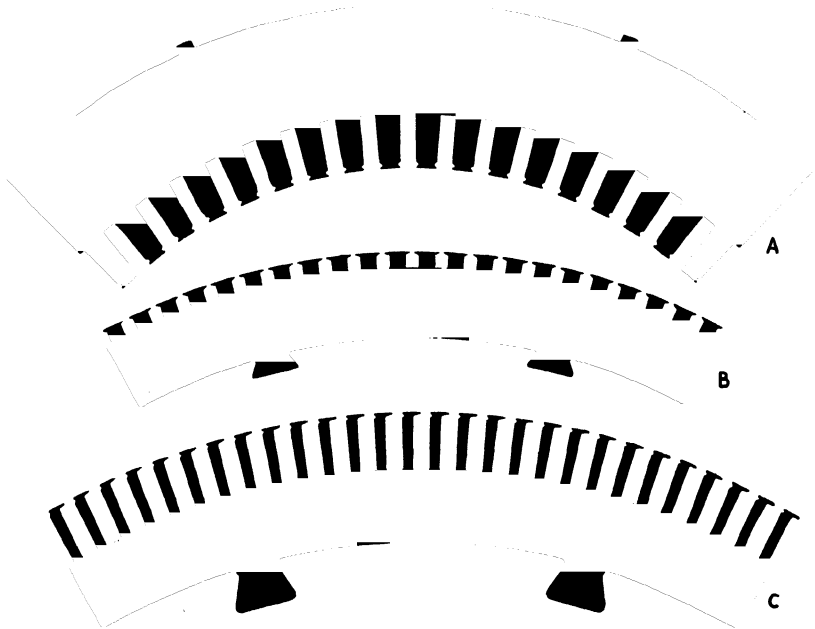


FIG. 16-1. Laminated segments of stator and rotor of large induction motors.

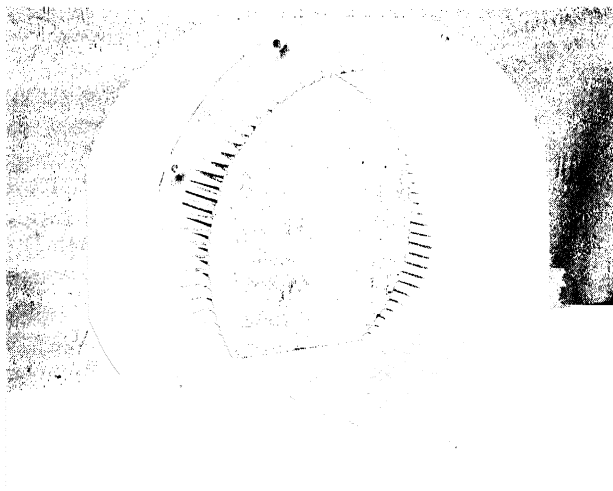


FIG. 16-2. Complete stack of stator laminations of a small induction motor with semi-open slots.

(a) *Stator*. Fig. 16-1 shows laminated segments of large induction motors: *A* represents a stator segment, *B* a segment of a squirrel cage rotor, and *C* a segment of a phase-wound rotor. The difference between these two rotor types is explained later. Fig. 16-2 shows a complete stack of stator laminations for a smaller induction motor with semi-open slots; the laminations of small motors are usually punched from one piece.

The stator or primary winding of the induction motor is connected to a source of power, is placed in the stator slots, and is completely insulated corresponding to the voltage of the power supply. Fig. 16-3 shows the connection end of a partially wound stator, and Fig. 16-4 shows the complete stator for a larger motor.

(b) *Rotor*. The rotor or secondary winding of the induction motor is its armature winding. It is placed in the slots of the rotor. The armature winding is *not connected to a source of power* but gets its power by induction from the flux produced by the stator winding—hence the name *induction motor*.

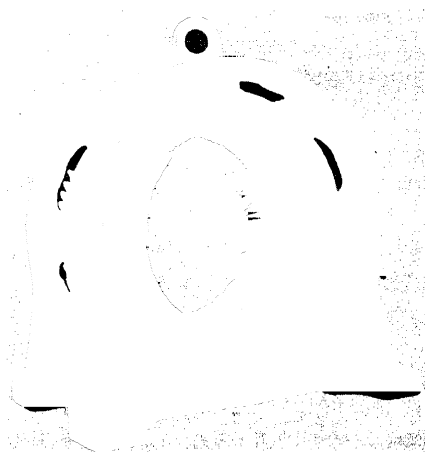


FIG. 16-3. Partially wound stator of an induction motor.

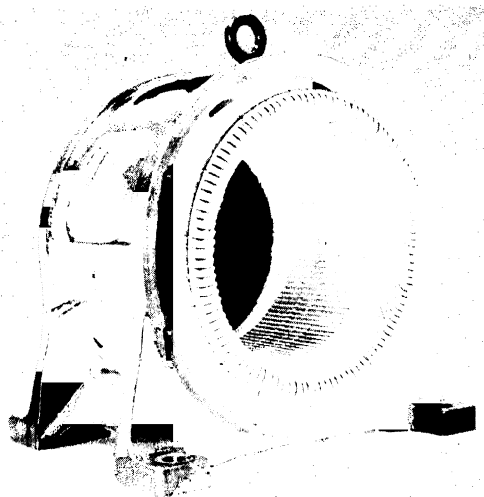


FIG. 16-4. Complete stator of a medium-size induction motor.

There are two general kinds of rotor windings, one the squirrel-cage winding, the other an insulated phase winding similar to that of the stator. The squirrel-cage winding consists of bare bars put in the slots and connected together at each end by a ring. A complete squirrel-cage rotor for a larger induction motor was shown in Fig. 13-10. A laminated segment of a squirrel-cage rotor similar to that shown in Fig. 13-10 is shown in Fig. 16-1B. The slots are shallow and semi-open. This produces a definite speed-torque characteristic. In order to produce a different speed-torque characteristic, the slots and bars often are narrow and much deeper, as shown in Fig. 16-5, which represents a complete rotor of a small induction motor, equipped with ventilating fans. The slots here are skewed in order to produce better starting performance and to reduce noise (Chaps. 58 and 59). Fig. 16-6 shows a squirrel-cage motor with round bars. Fig. 16-7 shows a complete rotor of a

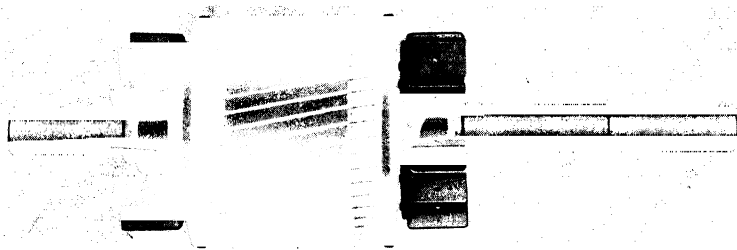


FIG. 16-5. Complete rotor of a squirrel-cage rotor with deep bars.

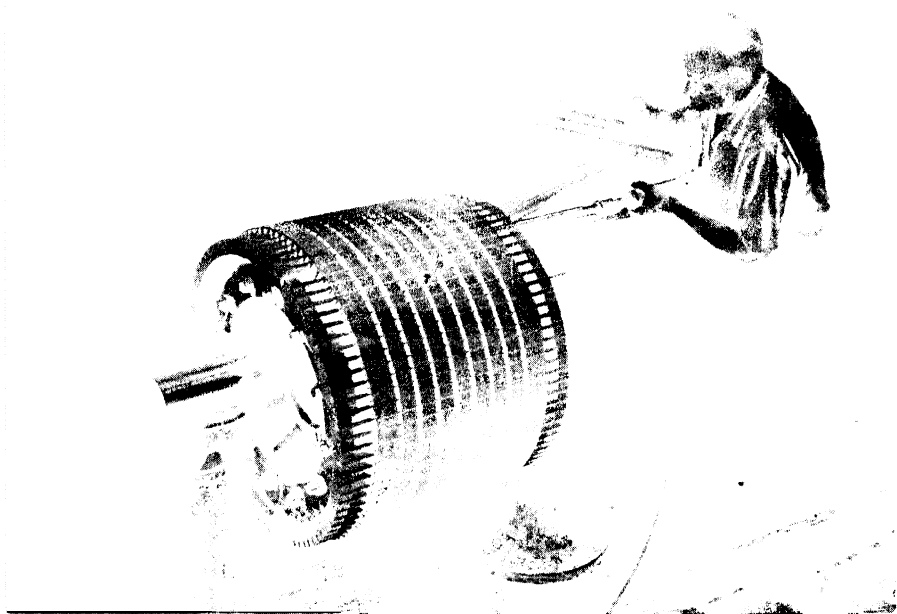


FIG. 16-6. Squirrel-cage rotor with round bars.

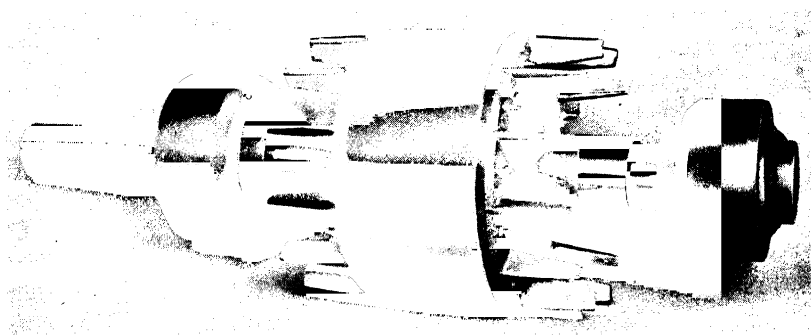


FIG. 16-7. Complete squirrel-cage rotor with die-cast aluminum bars, end rings, and ventilating fans.

smaller motor, in which the rotor bars as well as the rings and ventilating fans are cast in aluminum.

Certain desirable operating characteristics can be achieved by the use of two squirrel cages in the same rotor (Art. 22-5). Different shapes of slots for double-cage rotors are shown in Fig. 22-4. Fig. 16-8 shows the rotor punching for a double-cage rotor, having twice as many slots in the upper cage as in the lower one. Fig. 16-9 shows a complete double-cage rotor.

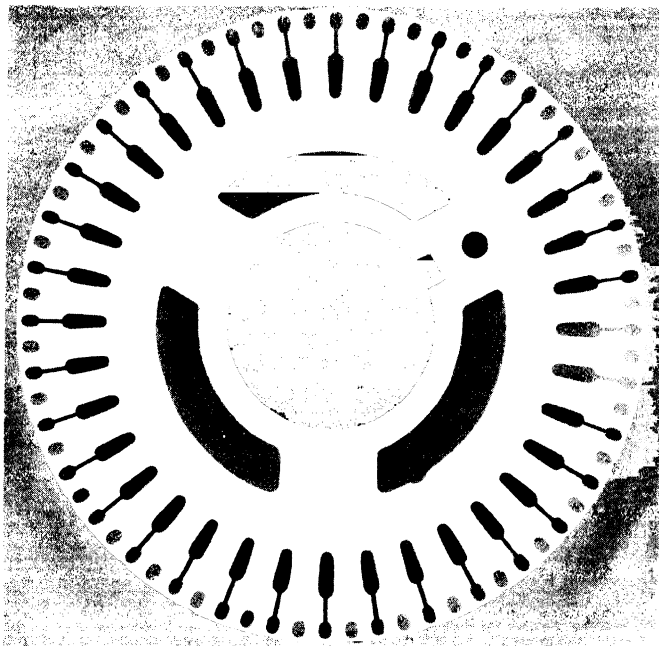


FIG. 16-8. Punching of a double-cage rotor.

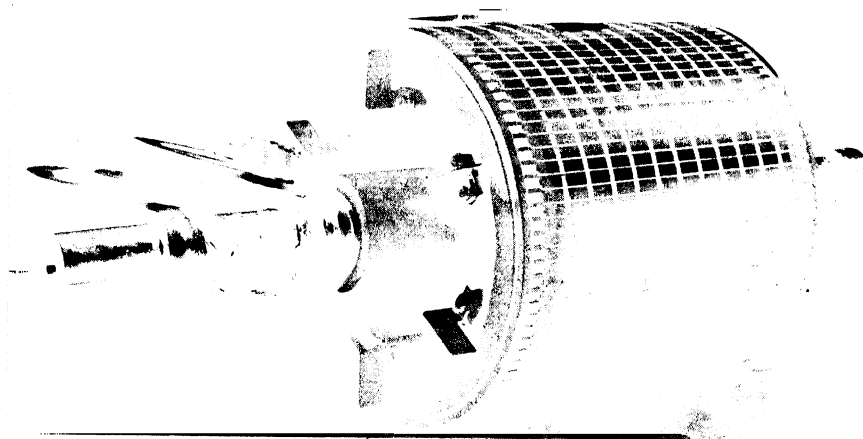


FIG. 16-9. Complete double-cage rotor.

A punching of a phase-wound rotor is shown in Fig. 16-1. Fig. 16-10 shows a partially wound rotor with phase winding, and Fig. 16-11 shows a complete phase-wound rotor. These rotors are usually 3-phase. In order to connect the rotor to an external rheostat, for starting and control purposes, the begin-



FIG. 16-10. Partially wound rotor with phase winding.

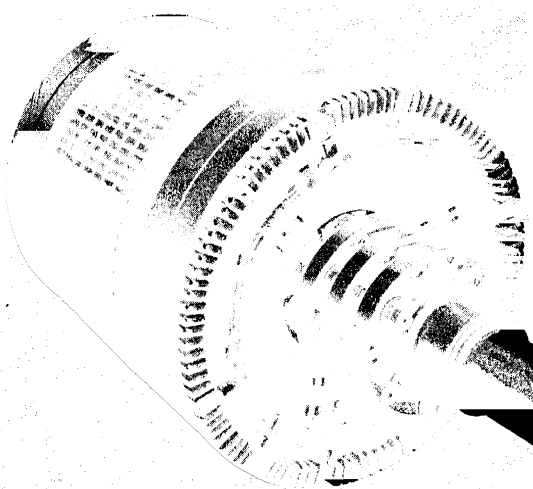


FIG. 16-11. Complete wound rotor of a larger induction motor.

nings of the phases are connected to slip rings; a 3-phase motor has three slip rings. Brushes riding on the slip rings provide the connection to the rheostat. The phase-wound rotor is called simply a *wound rotor* or also *slip-ring rotor*.

Fig. 16-12 shows a cutaway section of a squirrel-cage induction motor, totally enclosed type, fan-ventilated. The flow of air for this motor is shown in Fig. 29-3. Fig. 16-13 shows the parts of a small 3-phase induction motor, with cast-aluminum rotor, and ventilating fan. Fig. 16-14 shows a complete



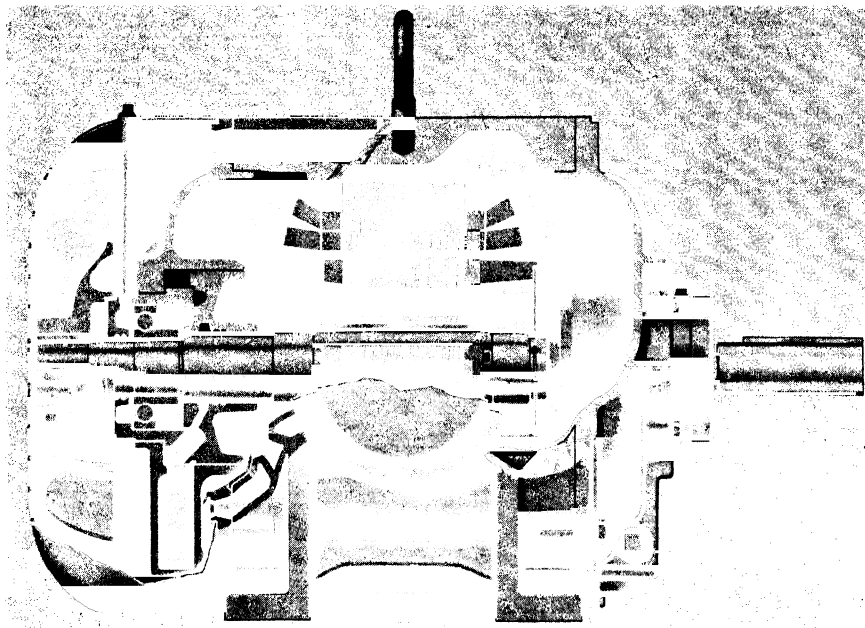


FIG. 16-12. Cutaway section of a totally enclosed fan-ventilated squirrel-cage induction motor.



FIG. 16-13. Parts of a small 3-phase squirrel-cage induction motor with cast aluminum bars.

induction motor, open type, and Fig. 16-15 shows a splash-proof motor. Fig. 16-16 shows a complete medium-sized motor with phase-wound rotor.

The standard ratings of polyphase induction motors are given in Table 49-5.

(c) *The magnetic circuit of the induction motor.* Fig. 16-17 shows the magnetic paths of a 4-pole induction motor. Each of the four paths includes a part of the stator core, two sets of stator teeth, two air-gaps, two sets of rotor teeth, and a part of the rotor core. The circuital law of the magnetic field (Eq. 1-23) is the basic relation for the study of the magnetic circuit of the induction motor. The mmf necessary to drive a given flux through a given structure is determined in Chap. 50.

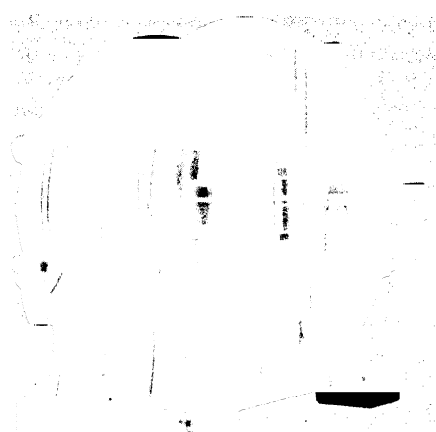


FIG. 16-14. Open-type polyphase induction motor.

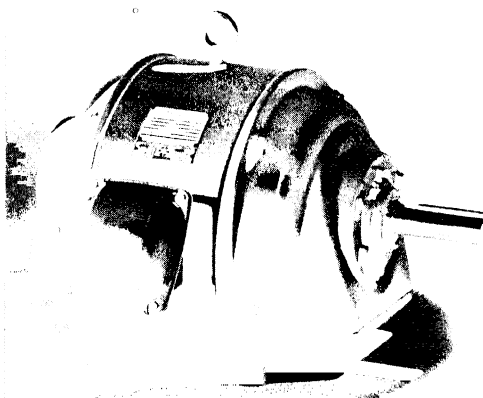


FIG. 16-15. Splashproof, ball-bearing, squirrel-cage induction motor.

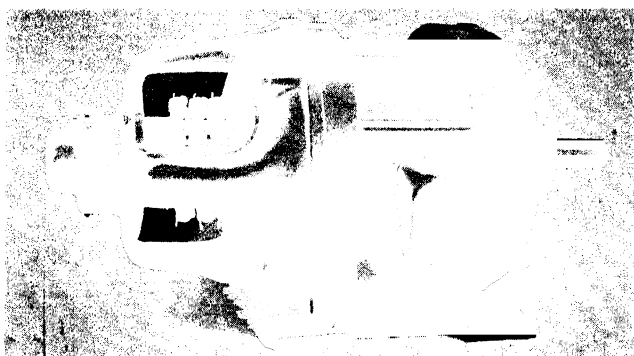


FIG. 16-16. Medium-sized phase-wound induction motor.

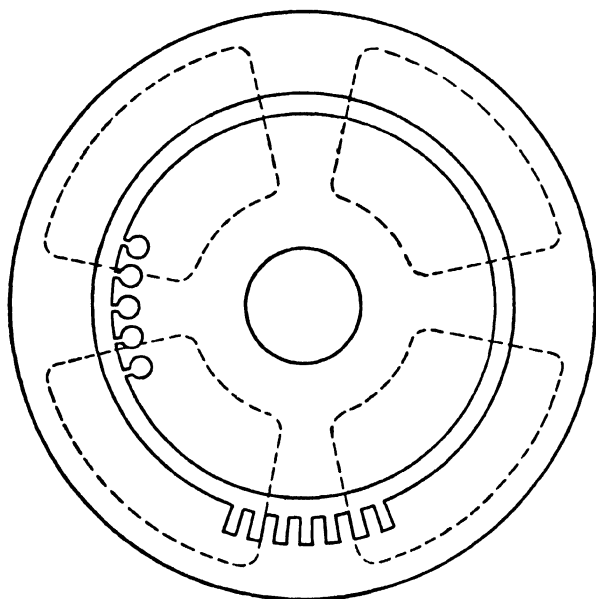


FIG. 16-17. Main flux paths of a 4-pole induction motor.

## Chapter 17

### THE POLYPHASE INDUCTION MOTOR AS A TRANSFORMER

It has been pointed out already that in the induction motor, contrary to other electric machines, only one machine part, the stator, is connected to a source of power. The rotor of the induction motor is not connected to any power line, but receives its emf and current by means of *induction*. This same feature also applies to the transformer, and it will be shown in the following that the *induction motor operates on the transformer principles*.

The stator winding of the polyphase induction motor is usually 3-phase, seldom 2-phase. The rotor winding is either of the squirrel-cage type (Fig. 16-6) or wound 3-phase type (Fig. 16-11) connected to three slip rings. When the rotor winding is phase-wound, it must be wound for the same number of poles as the stator winding. It will be shown in Art. 17-3 that a squirrel-cage winding automatically assumes the same number of poles as the stator.

**17-1. The induction motor at standstill.** (a) *Rotor winding open.* Consider a 3-phase motor with a 3-phase wound rotor, Fig. 17-1, the slip rings of which are at first *open*. In this case the induction motor behaves exactly

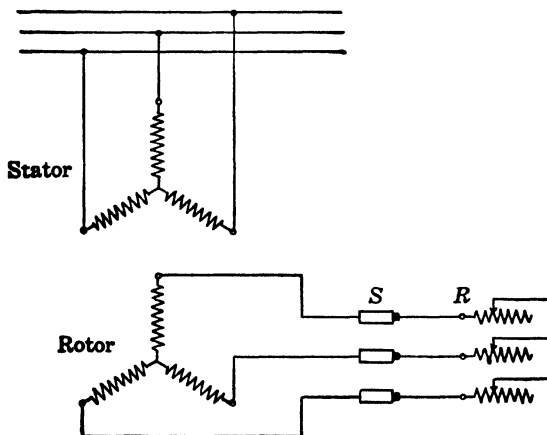


FIG. 17-1. Schematic diagram of a 3-phase, wound-rotor induction motor.

as a transformer with an open secondary (no-load). The impressed line voltage forces currents into the stator windings which produce a rotating flux. The magnitude of the currents and of the flux is such that Kirchhoff's mesh law is satisfied (see Eq. 3-9). There are, besides the impressed voltage, two emf's in the stator circuit, one of them produced by the *main flux*, the other by the *leakage fluxes* of the stator.

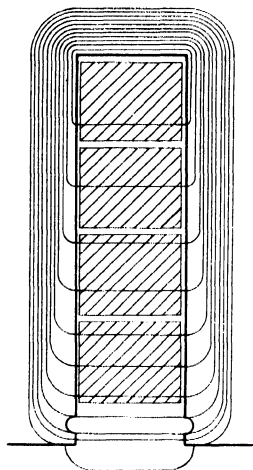


FIG. 17-2. Slot and tooth-top leakage fluxes.

As in the transformer, the main flux is that flux which is interlinked with *both* windings, i.e., the stator and rotor winding. Its path consists of the stator and rotor cores, stator and rotor teeth, and twice the air gap  $g$  (Fig. 16-17). The leakage fluxes of the stator are those fluxes which are interlinked with the stator winding only. The stator winding is embedded in slots, and its leakage fluxes are different from those of the transformer. They are:

1. The slot leakage flux (Fig. 17-2)
2. The tooth-top leakage flux (Fig. 17-2)
3. The end-winding leakage flux (Fig. 17-3)
4. The differential (harmonic) leakage flux.

The slot leakage flux is that which crosses the slot within the slot space. The tooth-top leakage flux is that between the tooth tops in the gap without going through the iron of the rotor. The end-winding leakage flux is that around the end-windings, i.e., around the external connections between the conductors. It has been explained in Art. 15-2 that an a-c winding produces a fundamental mmf wave, the length of which is equal to twice the pole pitch of the machine  $2\tau$ , and harmonic mmf waves. Only the flux produced by the fundamental mmf wave produces the useful torque of the machine. The harmonic fluxes are parasitic fluxes and are to be considered as a leakage flux. This leakage flux is called the *harmonic or differential leakage flux*. The designation "differential" means that the *difference* between the *total* mmf and the *fundamental* wave is to be considered as leakage. The fundamental wave is called the *main wave* or synchronous wave.

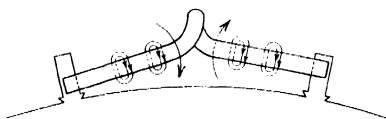


FIG. 17-3. End winding leakage flux.

Only the end-winding flux is a real leakage flux. The three other leakage fluxes together with the fundamental flux constitute the total flux of the machine. Physically only a single flux exists in the machine, namely, the total flux. The division into the main flux and leakage flux is necessary for the same two reasons which were stated for the transformer. The main reason is that it is only the flux interlinked with *both* windings which induces

an emf in the secondary (rotor) winding. The second reason is that the two kinds of flux have paths with entirely different reluctances (see Art. 3-1). While the reluctance of the leakage fluxes is determined mainly by air ( $\mu = 1$ ) resulting in a high reluctance path, (see Eq. 1-27), the main flux path lies in the iron with a high  $\mu$  and in the air gap which is small relative to the air paths of the leakage fluxes 1, 2, and 3.

The fact that the reluctance of the paths of the leakage fluxes is determined mainly by air ( $\mu = 1$ ) and is therefore almost constant makes the magnitude of the leakage fluxes *directly proportional* to the current (mmf) producing them. This does not apply to the main flux, the path of which lies in the air gap and iron (see Art. 3-1). The magnitude of the main flux is determined by the mmf producing it, by the length of the air gap, and by the permeability of the iron. Since the last changes with the mmf according to the saturation curve of the iron used, the main flux is not proportional to the mmf producing it.

Referring again to Fig. 17-1 with the rotor winding open, the two emf's induced in the stator winding are: (a) the emf induced by the main flux; (b) the emf induced by the leakage fluxes. Both emf's lag their fluxes by  $90^\circ$ . As in the transformer (see Art. 3-2) the main flux is produced by the reactive component  $I_\phi$  of the magnetizing current  $I_m$ , while the leakage fluxes are produced by the total stator current which, with the rotor open, is only a little larger than  $I_m$ . As in the transformer, the magnetizing current  $I_m$  has an active component  $I_{h+e}$  in counter-phase with the emf induced by the main flux  $E_1$ , which is necessary to supply the hysteresis and eddy-current losses due to the main flux (Fig. 3-2). As in the transformer,

$$\dot{I}_\phi + \dot{I}_{h+e} = \dot{I}_m \quad (17-1)$$

As in the transformer (see Eq. 3-9), Kirchhoff's mesh law for the stator winding is

$$\dot{V}_1 + \dot{E}_1 - j\dot{I}_1 x_1 = \dot{I}_1 r_1 \quad (17-2)$$

or

$$\dot{V}_1 = -\dot{E}_1 + j\dot{I}_1 x_1 + \dot{I}_1 r_1 \quad (17-2a)$$

The subscript 1 indicates the primary (stator) winding.  $V_1$ ,  $E_1$ ,  $I_1$  and the parameters  $r_1$  and  $x_1$  are assumed to be *phase* values, so that the voltages in Eqs. 17-2 and 17-2a are per-phase quantities.

The relations between  $I_m$  and  $E_1$  are the same as for the transformer, i.e., Eqs. 3-4 to 3-6 also hold here.

The emf  $E_1$  induced by the main flux in the stator winding is equal to (see Eq. 14-9)

$$E = 4.44 N_1 f_1 \Phi k_{dv1} 10^{-8} \text{ volt} \quad (17-3)$$

The main flux induces a voltage not only in the stator winding but also in

the rotor winding. The speed of the rotating flux\* produced by the stator currents is, *with respect to the stator* (see Eq. 15-5),

$$n_s = \frac{120f_1}{p} \quad (17-4)$$

The speed  $120f_1/p$  is called the *synchronous speed*, and the subscript  $s$  indicates this fixed value of the speed. Generally, when the rotor rotates with a speed  $n$  in the direction of the rotating flux, the relative speed between the rotating flux and the rotor winding is  $n_s - n$ . Since the rotor is considered here at standstill  $n = 0$ , the relative speed between the rotating flux and rotor is equal to  $n_s$ , i.e., the frequency of the emf induced in the rotor winding is (see Eq. 1-9)

$$f_2 = \frac{n_s p}{120} = f_1$$

Thus the emf induced in the rotor winding, at standstill, is

$$E_2 = 4.44 N_2 f_1 \Phi k_{dp2} 10^{-8} \text{ volt} \quad (17-5)$$

and

$$\frac{E_2}{E_1} = \frac{N_2 k_{dp2}}{N_1 k_{dp1}} \quad (17-6)$$

i.e., the ratio of the emf's induced in both windings by the main flux is equal to the ratio of their effective turns, just as in the transformer.

The magnetizing current  $I_m$  drawn from the lines by the polyphase induction motor with an open secondary (rotor) is much larger than that drawn by the transformer. This current is from 18 to 40% of the rated current in the induction motor and only 3% to 15% of the rated current in the transformer. The larger magnetizing current of the induction motor is caused by the air gap, i.e., by the higher reluctance of the main flux path of the induction motor: a larger mmf is necessary to drive the same main flux through the induction motor than through the transformer.

(b) *Rotor winding closed.* It will be assumed in this discussion that the rotor winding is closed but that the rotor is *blocked* so that it can not rotate. In this case the emf  $E_2$  induced in the rotor by the main flux, Eq. 17-5, will produce polyphase currents in the rotor winding. These currents yield rotating mmf's consisting of a main wave and harmonics just as the polyphase currents in the stator winding yield a main mmf wave and harmonics. Just as in the stator, the harmonic fluxes of the rotor produced by its harmonic mmf's are considered as leakage fluxes (rotor differential leakage), and only the main wave of the rotor is to be taken into account because only it contributes to the useful torque. For this reason the rotor mmf considered in the following discussion refers to the main wave only.

It has been explained that the frequency  $f_2$  of the rotor currents at stand-

\* Here and in following discussions the rotating flux means the main flux.

still is equal to the stator frequency  $f_1$ . Therefore the speed of the rotor mmf with respect to the rotor, at standstill, is

$$n_s' = \frac{120f_2}{p} = \frac{120f_1}{p} = n_s$$

This equation shows that the speed of the rotor mmf relative to the rotor is identically the same as the speed of the stator mmf relative to the stator, namely,  $n_s' = n_s$ . Thus it follows that at standstill the mmf waves of stator and rotor are stationary with respect to each other. It will be shown in the next article that this is also true when the rotor rotates, no matter what the speed of rotation. *Standstill of stator and rotor mmf waves with respect to each other is a necessary condition for the existence of a uniform torque in the machine.*

The rotor winding is the armature winding of the induction motor. When currents flow in the rotor winding, an mmf wave is produced by them, and this wave reacts upon the stator mmf wave which is always at standstill with respect to the rotor wave. Just as in the transformer the secondary mmf reacts upon the primary mmf (see Art. 4-1). The reaction of the rotor mmf, i.e., the armature reaction, is here such that it opposes the stator mmf and tends to reduce the main flux and  $E_1$ . In accordance with Kirchhoff's equation (Eq. 17-2) the stator is forced to draw more current from the lines, thus compensating for the armature reaction and sustaining the main flux, i.e., the emf  $E_1$ . The terms  $I_1 r_1$  and  $jI_1 x_1$  increase with increasing primary current  $I_1$ . However, these terms are, in the normal range of operation, small in comparison with the emf induced by the main flux,  $E_1$ , so that the main flux varies but little in the *normal* range of operation, just as in the transformer.

When the rotor carries current, *there are two mmf's* in the machine, and the *main flux is determined by the resultant mmf*. The two mmf's are (see Eq. 15-11):

$$F_1 = 0.9m_1 \frac{N_1}{p} k_{a1} I_1 \quad (17-7)$$

and

$$F_2 = 0.9m_2 \frac{N_2}{p} k_{a2} I_2 \quad (17-8)$$

As in the transformer, a simplification of the formulas, the phasor diagram, and the equivalent circuit is achieved when the secondary quantities are "*referred to the primary*" or, in other words, when it is assumed that the rotor winding is identical with the stator winding, i.e., that it has the same number of phases  $m_1$  and the same number of effective turns  $N_1 k_{a1} k_{p1}$  as the stator winding.

Such an assumption will be permissible if care is taken that the referred quantities of the rotor are such that (see Art. 4-2):



1. The rotor retains the original value of its mmf as given by Eq. 17-8, i.e., the main flux is not changed.
2. The kva of the rotor retains its original value.
3. The  $I^2R$  loss of the rotor retains its original value.
4. The magnetic energy of the leakage fluxes of the rotor ( $\frac{1}{2}L_l I^2$ ) retains its original value.

Rotor quantities referred to the stator will be indicated by a *prime*. The first condition above means that the rotor current referred to the stator,  $I_2'$ , must be such that

$$0.9m_1 \frac{N_1}{p} k_{dp1} I_2' = 0.9m_2 \frac{N_2}{p} k_{dp2} I_2$$

or

$$I_2' = \frac{m_2 N_2 k_{dp2}}{m_1 N_1 k_{dp1}} I_2 \quad (17-9)$$

$I_2'$  flowing in the stator winding, will produce the same mmf as the current  $I_2$  produces flowing in the rotor winding. The second condition means that

$$m_1 E_2' I_2' = m_1 E_2' \frac{m_2 N_2 k_{dp2}}{m_1 N_1 k_{dp1}} I_2 = m_2 E_2 I_2$$

or

$$E_2' = \frac{N_1 k_{dp1}}{N_2 k_{dp2}} E_2 = E_1 \quad (17-10)$$

i.e., that the secondary and primary emf's induced by the main flux are equal. This is in accordance with the assumption that the number of effective turns of the secondary winding is equal to that of the primary winding.

The third condition means  $m_1 I_2'^2 r_2' = m_2 I_2^2 r_2$  or, inserting the value of  $I_2'$  from Eq. 17-9,

$$r_2' = \frac{m_1}{m_2} \left( \frac{N_1 k_{dp1}}{N_2 k_{dp2}} \right)^2 r_2. \quad (17-11)$$

The fourth condition means that

$$\frac{1}{2} m_1 I_2'^2 x_2' = \frac{1}{2} m_2 I_2^2 x_2$$

where  $x_2 = \omega L_{l2} = 2\pi f_1 L_{l2}$  is the leakage reactance of the rotor at line frequency  $f_1$ . Inserting into this equation the value of  $I_2'$ ,

$$x_2' = \frac{m_1}{m_2} \left( \frac{N_1 k_{dp1}}{N_2 k_{dp2}} \right)^2 x_2 \quad (17-12)$$

It follows from Eqs. 17-9 to 17-12 that the *reduction factors* from the secondary to the primary are:

$$\frac{N_1 k_{dp1}}{N_2 k_{dp2}} \quad \text{for voltage}$$

$$\frac{m_2 N_2 k_{dp2}}{m_1 N_1 k_{dp1}} \quad \text{for current} \quad (17-13)$$

and

$$\frac{m_1}{m_2} \left( \frac{N_1 k_{dp1}}{N_2 k_{dp2}} \right)^2 \quad \text{for resistance and reactance}$$

Since these reduction factors satisfy conditions 1 to 4, calculations made with the referred quantities  $E_2'$ ,  $I_2'$ ,  $r_2'$  and  $x_2'$  do not change anything in the magnetic or electric behavior of the machine.

The total mmf which produces the main flux  $\Phi$  is given by the geometric sum of the mmf's of both windings  $F_1$  and  $F_2$ , Eqs. 17-7 and 17-8. This geometric sum yields the magnetizing mmf (see Eq. 4-8)

$$0.9m_1 \frac{N_1 k_{dp1}}{p} \dot{I}_1 + 0.9m_2 \frac{N_2 k_{dp2}}{p} \dot{I}_2 = 0.9m_1 \frac{N_1 k_{dp1}}{p} \dot{I}_m \quad (17-14)$$

Substituting for  $\dot{I}_2$  the value from Eq. 17-9, the result is the same as that for the transformer

$$\dot{I}_1 + \dot{I}_2' = \dot{I}_m \quad (17-14a)$$

Therefore, the same considerations apply as for the transformer (see Art. 4-4) and Eq. 4-10 and 4-10a, derived for the transformer, also apply to the induction motor, the secondary of which carries current. However, it should not be forgotten that the rotor is considered here to be at standstill, at which operating condition stator and rotor mmf's are at standstill with respect to each other. Eqs. 4-10 and 4-10a can be considered applicable to the machine during running only when proof is given that stator and rotor mmf's are at standstill with respect to each other at any rotor speed.

Kirchhoff's mesh equations for the stator and rotor are, (see Eq. 17-2)

$$\dot{V}_1 + \dot{E}_1 - j\dot{I}_1 x_1 = \dot{I}_1 r_1 \quad (17-15)$$

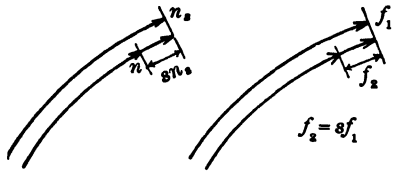
$$\dot{E}_2' - j\dot{I}_2' x_2' = \dot{I}_2' r_2' \quad (17-16)$$

The second equation (17-16) for the rotor applies only to the case considered here, i.e., to the rotor at standstill.

The foregoing considerations refer to the induction motor with a phase wound rotor and an external resistance in the rotor circuit, Fig. 17-1. The same considerations also apply to the squirrel-cage rotor, but in this case no external resistance can be inserted into the rotor; therefore, the squirrel-cage rotor corresponds to the case of a wound rotor with an external resistance equal to zero. The squirrel-cage rotor and the wound rotor with no external resistance behave at standstill as a transformer the secondary of which contains only its own resistance and leakage reactance, i.e. as a transformer at short-circuit. For this condition the main flux of the transformer and induction motor is small, and the current is high and limited mainly by the

leakage reactances and resistances of the primary and secondary windings (see Art. 22-2). Due to the fact that the leakage reactances of the induction motor are much higher than those of the transformer, the short-circuit current (current at standstill) of the induction motor is much smaller than that of the transformer. The short-circuit current is 3.5 to 8 times rated current in the induction motor and 7 to 40 times rated current in the transformer.

**17-2. The induction motor when running. The slip.** When the blocked rotor, with closed winding, is released, it starts rotating because the rotating



$n_s$  = speed of the mmf wave of the stator

$n = (1 - s)n_s$  = rotor speed

$sn_s = n_s - n$  = speed of the rotor mmf wave with respect to the rotor

$n_r = n + sn_s$

FIG. 17-4. Illustration of the speed of the mmf waves of stator and rotor in a polyphase motor.

flux exerts tangential forces on its current-carrying conductors. The direction of rotation of the rotor is the same as that of the rotating flux which rotates at the constant speed  $n_s = 120f_1/p$  relative to the stator, i.e., at synchronous speed (Eq. 17-4). When the rotor is at standstill, the *relative* speed between the rotating flux and rotor is equal to the synchronous speed  $n_s$  and the emf induced in the rotor is  $E_2' = E_1$ . When the rotor rotates at a speed  $n$ , the *relative* speed between the rotating flux and the rotor is  $n_s - n$  (Fig. 17-4). Since it is the relative speed between the flux and rotor winding which determines the

magnitude and frequency of the emf induced in the rotor, the magnitude of the emf induced in the rotor winding at the speed  $n$  is

$$E_{2s}' = \frac{n_s - n}{n_s} E_2' \quad (17-17)$$

and the frequency of this emf is

$$f_2 = \frac{n_s - n}{n_s} f_1 \quad (17-18)$$

The quantity  $(n_s - n)/n_s$  is called the *slip*, i.e., the slip is defined as:

$$s = \frac{n_s - n}{n_s} \quad (17-19)$$

The slip gives the relative speed between the rotating flux and the rotor as a fraction of the synchronous speed  $n_s$ . At standstill,  $n = 0$  and  $s = 1$ ; at synchronous speed  $n = n_s$  and  $s = 0$ . At synchronous speed the relative speed between the rotating flux and the rotor is equal to zero and no emf is induced in the rotor. Therefore, there is no current in the rotor and no tangential force is exerted on the rotor at synchronous speed. An induction motor is

not able to reach the synchronous speed; it will run with a slip sufficient enough to induce the current necessary to produce the tangential force and torque required by the load. *The slip is the basic variable of the induction motor.*

Introducing Eq. 17-19 into Eqs. 17-17 and 17-18, the emf induced in the rotor by the rotating flux as a function of slip  $s$  is

$$E_{2s}' = sE_2' \quad (17-20)$$

and the frequency of this emf is

$$f_2 = sf_1 \quad (17-21)$$

At standstill of the rotor ( $s = 1$ ) the frequency of the rotor emf is equal to the line frequency; this is in accordance with the result obtained previously.

Thus, for the rotor running with the speed  $n$  the quantity  $sE_2' = sE_1$  is to be introduced for  $E_2' = E_1$  in Kirchhoff's mesh Eq. 17-16. In the same equation,  $x_2'$  is the rotor leakage reactance at line frequency  $f_1$ . Since, at the rotor speed  $n$ , the frequency of the rotor current is  $f_2 = sf_1$ , the quantity  $sx_2'$  instead of  $x_2'$  is to be introduced for the running rotor. Hence Kirchhoff's mesh equation of the rotor circuit becomes

$$s\dot{E}_2' - j\dot{I}_2'sx_2' = \dot{I}_2'r_2' \quad (17-22)$$

Eq. 17-16 which applies only to standstill is a special case of Eq. 17-22, obtained from the latter equation by setting  $s = 1$ .

According to Eqs. 17-21, 17-4, and 17-19, the speed of the mmf wave produced by the rotor, *relative to the rotor* is

$$n_s' = \frac{120f_2}{p} = \frac{120f_1s}{p} = sn_s = n_s - n$$

Since the rotor speed is equal to  $n$ , the speed of the rotor mmf wave relative to the stator is  $n + n_s' = n_s$ . This is the same as the speed of the stator mmf wave relative to the stator, i.e., rotor and stator mmf waves are stationary with respect to one another at any rotor speed  $n$ . It has been pointed out in the foregoing article that this is the condition for the existence of a uniform torque in the polyphase machine. *Thus, the polyphase induction motor is able to produce a uniform torque at any rotor speed.* It will be seen later, (see Art. 23-3), that the synchronous motor does not possess the ability to produce a uniform torque at all speeds.

With the proof given that stator and rotor mmf's are at *standstill with respect to each other at any rotor speed*, just as at standstill of the rotor, Eqs. 17-14 and 17-14a also apply to the running motor and consequently Eqs. 4-10 and 4-10a hold for the running motor, i.e., no matter what the speed of the rotor,

$$\dot{I}_m = \dot{I}_1 + \dot{I}_2' = -\dot{E}_1\dot{Y}_m = -\dot{E}_2'\dot{Y}_m \quad (17-23)$$

$$\dot{E}_1 = \dot{E}_2' = -\dot{I}_m\dot{Z}_m = -(\dot{I}_1 + \dot{I}_2')\dot{Z}_m \quad (17-23a)$$

Dividing Eq. 17-22 by the slip  $s$ . Kirchhoff's mesh equation of the rotor becomes

$$\dot{E}_2' = \dot{E}_1 = \left( \frac{r_2'}{s} + jx_2' \right) \dot{I}_2' \quad (17-24)$$

which also can be written as

$$\dot{E}_2' = \dot{E}_1 = (r_2' + jx_2') \dot{I}_2' + \left( \frac{1-s}{s} \right) r_2' \dot{I}_2' \quad (17-24a)$$

Comparing this equation and Eq. 17-15 for the stator with the corresponding mesh equations of the transformer, it is seen that they are of the same character and that the mechanical power of the induction motor can be represented as the power dissipated in a pure resistive load, the resistance being equal to  $[(1-s)/s] r_2'$ , i.e., *the induction motor, when running, behaves as a transformer loaded with a pure ohmic resistance*. It could be expected that the load circuit of the induction motor, considered as a transformer, contains only resistance and no reactance, since the developed power of a rotating induction motor is a mechanical power which can only be represented by a resistance, and not by a reactance.

The similarity of the fundamental equations of the induction motor and the transformer must lead to a similarity of both their phasor diagrams and equivalent circuits.

**17-3. The squirrel-cage rotor. Its number of poles and phases.** Considering the rotor, the number of rotor poles has been assumed to be the same as that of the stator. Stator and rotor must have the same number of poles in all electric machines. In the phase-wound rotor the equality of numbers of poles is achieved simply by winding the rotor for the same number of poles as the stator. It has been mentioned that the squirrel-cage rotor automatically produces the same number of poles as that of the stator.

Consider Fig. 17-5. The rotating flux is sinusoidally distributed as shown by the  $B$ -curve. This flux moves with the speed  $n_s$  while the rotor rotates at speed  $n$ . With respect to the rotor the rotating flux moves at a relative speed  $n_s - n$ . Applying Faraday's law in the  $Blv$  form, the emf's induced in the individual bars of the squirrel cage are also sinusoidally distributed as shown in Fig. 17-5. In order to simplify the explanation, the assumption will be made that the rotor speed  $n$  is close to the synchronous speed  $n_s$ , as is generally the case for operation at rated output.

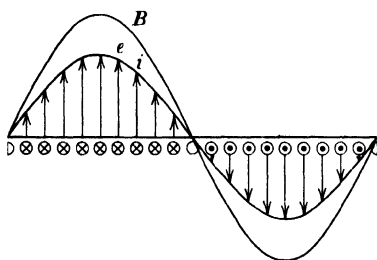


FIG. 17-5. Explanation of the number of poles of a squirrel-cage rotor.

The rotor leakage reactance  $sx_2'$  then becomes very small, and it can then be assumed that the current and emf of the individual rotor bars are in phase.

Therefore the emf's of the individual bars in Fig. 17-5 represent, to another scale, the currents of the individual bars and, if the currents are indicated by crosses under the positive half-wave of the  $B$  curve, they must be indicated by dots under the negative half-wave of the  $B$  curve. It is seen that the flux wave produces a 2-pole current distribution and hence also a 2-pole mmf distribution in the squirrel-cage rotor. Since the number of poles of the flux wave is the same as that of the stator winding, the *squirrel-cage rotor produces the same number of poles as that of the stator*.

The emf's of the individual bars are sinusoidal functions of time, since  $B$  is sinusoidal. As such, they can be represented by phasors. The time angle between the phasors representing two adjacent bars is equal to the space angle between two bars (slot angle  $\alpha_s$ ). The total number of phasors is equal to the number of bars ( $Q_2$ ). Fig. 17-6 shows the phasor diagram of a squirrel-cage rotor with 15 bars. Compare this phasor diagram with that of a 3-phase winding, Fig. 13-3. It is seen that the *squirrel-cage winding is a polyphase winding with  $m_2 = Q_2$  phases*. The number of turns per phase is  $N = 1/2$ , because each phase consists of one conductor. The distribution and pitch factors are equal to 1. Thus, for the squirrel-cage rotor

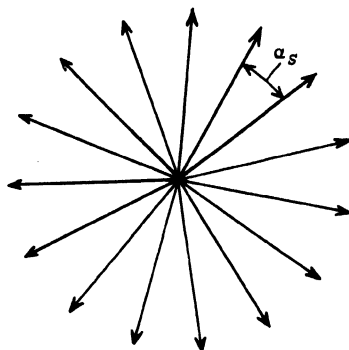


FIG. 17-6. Phasor diagram of a squirrel-cage rotor with 15 bars.

$$m_2 = Q_2; \quad N_2 = 1/2; \quad k_{d2} = 1; \quad k_{p2} = 1 \quad (17-25)$$

The above relations have been derived on the assumption that the stator had a two-pole winding. If the number of poles is  $p$ , then in Eqs. 17-25,  $m_2 = 2Q_2/p$ , since the mmf pattern and current distribution repeat for each pair of poles. These quantities are to be introduced for the squirrel-cage rotor in Eqs. 17-5, 17-6 and 17-8 to 17-14, in order to obtain the secondary quantities referred to the primary (stator).  $E_2$ ,  $I_2$ ,  $r_2$ , and  $x_2$  are the values per bar. If the rotor is skewed,  $N_2$  in the previous equations has to be multiplied by the skew factor (Art. 56-6) which is another distribution factor.

## PROBLEMS

1. Determine the frequency of the rotor currents in an 8-pole, 60-cycle, 3-phase, squirrel-cage induction motor when operating at speeds of 890, 885, 870 and 850 rpm.
2. A 30-HP, 10-pole, 60-cycle induction motor operates at a rated speed of 704 rpm. Determine: (a) full-load slip; (b) the number of space degrees during one cycle.

3. For the motor of Problem 2 determine: (a) the speed of the stator mmf with respect to the stator; (b) the speed of the rotor mmf with respect to the rotor; (c) the speed of the rotor mmf with respect to the stator; (d) the difference between speeds (a) and (c). Remember that the result of (d) is the necessary condition for the existence of a uniform torque in the induction motor.

4. A 4-pole, 3-phase, Y-connected induction motor has 48 stator slots and 10 series conductors per slot. The coil throw is 10 slots. (a) Determine the pitch and distribution factors. (b) Determine the maximum flux per pole when connected to a 230-volt line neglecting resistance and reactance drops in the stator winding.

5. If the rotor of the motor described in Problem 4 has a Y-connected winding with 36 slots, six series conductors per slot, and a coil throw of 9 slots, determine the ratio of transformation.

6. Determine the emf generated in a single conductor rotating in the air gap of the machine of Problem 5 at 1740 rpm. Neglect resistance and reactance drops.

7. A 6-pole, 3-phase, Y-connected induction motor has 54 stator slots, 12 series conductors per slot and a coil throw of 7 slots. (a) Determine pitch and distribution factors; (b) determine the maximum flux per pole when connected to a 230-volt line, neglecting resistance and reactance drops in the stator winding.

8. The rotor of the motor in Problem 7 has four slots per pole per phase with four series conductors per slot. The winding is full pitch. Determine the ratio of transformation.

9. Determine the emf generated in a single conductor rotating in the air gap of the machine of Problem 7 at 1160 rpm. Neglect resistance and reactance drops.

## Chapter 18

### APPLICATION OF THE FUNDAMENTAL EQUATIONS · PHASOR DIAGRAM AND EQUIVALENT CIRCUIT OF THE POLYPHASE INDUCTION MOTOR

**18-1. Application of the fundamental equations.** The equations 17-15, 17-22, and 17-23

$$\dot{V}_1 + \dot{E}_1 - j\dot{I}_1 x_1 = \dot{I}_1 r_1 \quad (18-1)$$

$$s\dot{E}_2' - j\dot{I}_2' s x_2' = \dot{I}_2' r_2' \quad (18-2)$$

$$\dot{E}_1 = \dot{E}_2' = -\dot{I}_m \dot{Z}_m = -(\dot{I}_1 + \dot{I}_2') \dot{Z}_m \quad (18-3)$$

are the fundamental equations of the polyphase induction motor. To them the same considerations apply as to the fundamental equations of the transformer, Art. 4-6. They will be used to

- (a) set up the phasor diagram
- (b) derive the equivalent circuit of the polyphase induction motor
- (c) derive the power and torque relations
- (d) derive the geometric locus of the primary current for variable load (slip).

Examining the fundamental equations 18-1 to 18-3, two questions arise. The first one is related to the fact that, in the transformer, both windings are at standstill with respect to each other and their coefficient of mutual inductance is a constant quantity (except for the saturation influence), while in the induction motor the secondary winding rotates and the coefficient of mutual inductance between primary and secondary is not a constant quantity but is a function of the relative position of the axes of the two windings. This shift between the axes of the two windings which is a function of time does not appear in the fundamental equations 18-1 and 18-3. It is shown in Art. 51-1 that equations 18-1 to 18-3 are correct.

The second question is why, for stator and rotor, only one Kirchhoff's mesh equation is used, while there are several phases (windings) in each of them. The answer to this question is that here only the steady state operation



of the induction motor is considered and that, therefore, voltages and current are the same in each phase. It should further be taken into account that Eq. 18-3 comprises all stator and rotor phases (see Eqs. 17-14 and 17-14a), i.e.,  $E_1$  and  $E_2'$  are emf's induced by fluxes produced by all phase windings of stator and rotor.

**18-2. The phasor diagram of the polyphase induction motor.** Kirchhoff's mesh equations for the primary and secondary electric circuits (Eqs. 18-1 and 18-2) and Eq. 18-3 for the magnetic circuit yield the phasor diagram of (mmf's) currents and voltages shown in Fig. 18-1.

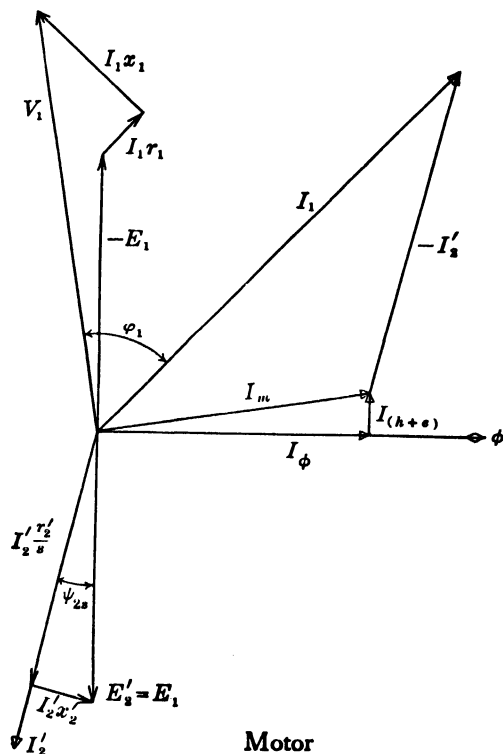


FIG. 18-1. Phasor diagram of voltages and mmf's (currents) of the polyphase induction motor under load.

The main flux  $\Phi$  is in phase with the reactive component of the magnetizing current  $I_\phi$ . The emf's induced by the main flux in both windings,  $E_1$  and  $E_2'$  respectively, are equal and in phase, and lag the main flux  $\Phi$  by  $90^\circ$ .

The active component of the magnetizing current  $I_{h+e}$  which supplies the hysteresis and eddy-current losses due to the main flux is in counter-phase with  $E_1$ . The geometric sum of  $I_\phi$  and  $I_{h+e}$  is the magnetizing current  $I_m$ .

In the transformer this current is practically equal to the no-load current  $I_0$ . In the induction motor, running at no-load, the difference between the no-load current  $I_0$  and  $I_m$  is larger than in the transformer.

The secondary emf  $E_2' = E_1$  is equal to the geometric sum of  $I_2'(r_2'/s) = I_2'[r_2' + r_2'\{(1-s)/s\}]$ , in phase with  $I_2'$ , and the secondary leakage reactance drop  $I_2'x_2'$  which leads  $I_2'$  by  $90^\circ$  (refer to Eqs. 17-24). The angle  $\psi_{2s}$  between rotor (secondary) current  $I_2'$  and rotor emf  $E_2'$  is

$$\psi_{2s} = \tan^{-1} \frac{x_2'}{r_2'/s} = \tan^{-1} \frac{sx_2'}{r_2'} \quad (18-4)$$

The magnitude of  $\psi_{2s}$  depends on the slip. The slip of the induction motor operating at its *rated torque* is usually small, from 0.01 to 0.05; the larger value applies to small motors and the smaller value to large motors. For this slip the angle  $\psi_{2s}$  is very small and the rotor current is almost in phase with its emf  $E_2'$ .

The primary current  $I_1$  is found as the geometric sum of  $I_m$  and  $-I_2'$ . The stator terminal voltage  $V_1$  is the geometric sum of  $-E_1$  (the counter emf) and the voltage drops  $I_1r_1$  and  $I_1x_1$ , the former in phase with  $I_1$  and the latter  $90^\circ$  ahead of  $I_1$ .

The phasor diagram of (mmf's) currents and voltages of the running induction motor is identical with that of a transformer loaded with a pure resistance (see Fig. 5-1). The power factor angle  $\phi_1$  between the primary current  $I_1$  and primary voltage  $V_1$  is *always lagging* in the induction motor, while it can be lagging, zero, or leading in the transformer, depending upon the character of the load (see Fig. 5-3). The lag of  $I_1$  with respect to  $V_1$  is caused by the magnetizing current and by the leakage reactance drops. *Reactive current is required to sustain both the main flux as well as the leakage fluxes.* Induction motors and transformers are the main consumers of reactive current from the power lines. These reactive currents are a necessary evil since they do not contribute to the power transfer but increase the copper losses in the induction motors and transformers, in the wires transferring the power and in the generators producing the power.

**18-3. The equivalent circuit of the polyphase induction motor.** The equivalent circuit of the polyphase induction motor can be derived exactly in the same manner as that of the transformer, namely, from Kirchhoff's mesh equations of both electric circuits (Eqs. 18-1 and 18-2) and from Eq. 18-3 which refers to the magnetic circuit. These equations are

$$\dot{V}_1 = -\dot{E}_1 + \dot{I}_1(r_1 + jx_1) \quad (18-1a)$$

$$\dot{E}_2' = \dot{E}_1 = \dot{I}_2' \left( \frac{r_2'}{s} + jx_2' \right) \quad (18-2a)$$

$$\dot{I}_1 + \dot{I}_2' = \dot{I}_m = -\dot{E}_1 \dot{Y}_m = -\dot{E}_1 / \dot{Z}_m \quad (18-3a)$$

where (see Art. 3-1)

$$\dot{Y}_m = g_m - jb_m \quad (18-5)$$

and

$$\dot{Z}_m = r_m + jx_m \quad (18-6)$$

are the main flux admittance and the main flux impedance respectively. From Eq. 3-6,

$$r_m = \frac{g_m}{g_m^2 + b_m^2} \quad x_m = \frac{b_m}{g_m^2 + b_m^2} \quad (18-7)$$

Kirchhoff's mesh equations, Eqs. 18-1a and 18-2a, can be written as

$$\dot{V}_1 = -\dot{E}_1 + \dot{I}_1 \dot{Z}_1 \quad (18-8)$$

$$\dot{E}_2' = \dot{E}_1 = \dot{I}_2' \dot{Z}_2' \quad (18-9)$$

where

$$\dot{Z}_1 = r_1 + jx_1$$

$$\dot{Z}_2' = \frac{r_2'}{s} + jx_2' = r_2' + r_2' \left( \frac{1-s}{s} \right) + jx_2'$$

These two equations combined with Eq. 18-3a yield

$$\dot{E}_1 = \dot{I}_2' \dot{Z}_2' = (\dot{I}_m - \dot{I}_1) \dot{Z}_2' = -\dot{E}_1 \dot{Y}_m \dot{Z}_2' - \dot{I}_1 \dot{Z}_2'$$

$$\dot{E}_1 (1 + \dot{Y}_m \dot{Z}_2') = -\dot{I}_1 \dot{Z}_2' \quad \text{or} \quad \dot{E}_1 = -\frac{\dot{I}_1}{(1/\dot{Z}_2') + \dot{Y}_m}$$

Therefore,

$$\dot{V}_1 = \dot{I}_1 \dot{Z}_1 + \frac{\dot{I}_1}{(1/\dot{Z}_2') + \dot{Y}_m} = \dot{I}_1 \left[ \dot{Z}_1 + \frac{1}{(1/\dot{Z}_2') + \dot{Y}_m} \right] \quad (18-10)$$

The quantity in the brackets is the total impedance of the polyphase induction motor looking into the primary terminals. This impedance is the same as that of the transformer (see Eq. 5-8).

Hence the equivalent circuit of the polyphase induction motor is, in general, the same as that of the transformer and is given by Fig. 5-4. The main difference lies in the expression for  $Z_2'$ : in the induction motor the resistance  $r_2'$  is associated with the slip  $s$ , while it is a constant in the transformer.

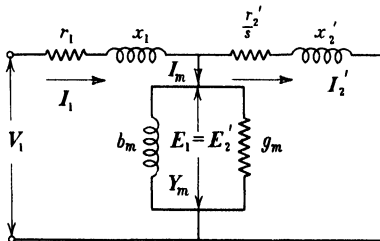


FIG. 18-2. Equivalent circuit of the polyphase induction motor.

Breaking up the impedances  $Z_1$ ,  $Z_2$ ,  $Z_m$ , and the admittance  $Y_m$  into their components, four *identical* forms of the equivalent circuit of the polyphase induction motor are obtained, as shown in Figs. 18-2 to 18-5.

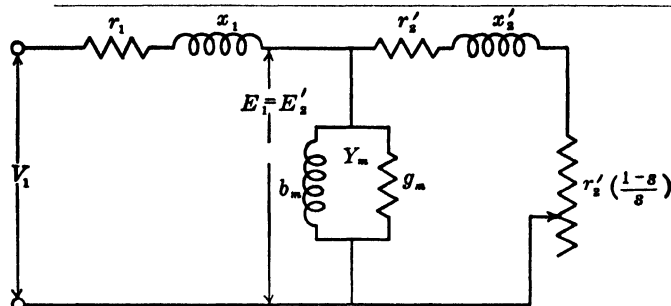


FIG. 18-3. Equivalent circuit of the polyphase induction motor.

It has been pointed out in Art. 4-1 that the magnitude of  $x_m(b_m)$  depends upon the saturation of the iron, i.e., upon the magnitude of the main flux  $\Phi$ . Since the main flux changes little between no-load and full-load,  $x_m(b_m)$  can be treated as a constant, especially for medium-sized and larger-sized motors.

It will be shown in Chapter 22 how the parameters  $r_1$ ,  $x_1$ ,  $r'_2$ ,  $x'_2$ ,  $r_m$  and  $x_m$  (or  $g_m$  and  $b_m$ ) can be determined from the no-load and the blocked rotor tests.

The equivalent circuit is very helpful in making calculations with fixed parameters or with varying parameters, especially when the circuit is set up on a calculating board. It should be kept in mind that an equivalent circuit does not necessarily represent the *actual behavior of all parts* of the apparatus to which it is equivalent. The equivalent circuit of the transformer does not yield the actual values of the secondary voltage and current but "referred" quantities. The equivalent circuit of the induction motor is even further removed from the actual behavior of its

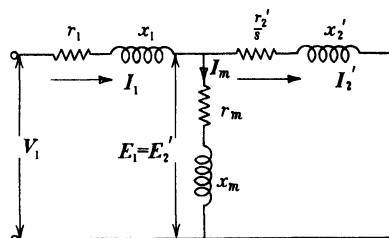


FIG. 18-4. Equivalent circuit of the polyphase induction motor.

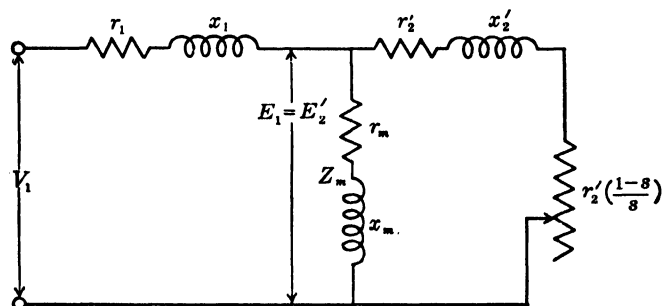


FIG. 18-5. Equivalent circuit of the polyphase induction motor.

secondary circuit than in the transformer. The differences can be seen from the following tabulation:

*Equivalent Circuit*

1. Magnitude of the secondary emf independent of the slip
2. Secondary leakage reactance constant
3. Frequency of secondary emf and current equal to line frequency ( $f_1$ )
4.  $I_1 = I_m + I_2'$

*Actual Behavior*

1. Magnitude of the secondary emf proportional to the slip
2. Secondary leakage reactance proportional to the slip
3. Frequency of secondary emf and current equal to slip frequency ( $sf_1$ )
4.  $I_1 = I_m + (-I_2')$

A polyphase induction motor connected to a 60-cycle line has, at rated load, rotor currents of  $60(0.05 \text{ to } 0.01) = 3 \text{ to } 0.6$  cycles, while the rotor current of its equivalent circuit is line frequency, i.e., 60 cycles. However, calculations based on the equivalent circuit yield correct results. This is due to the fact that in the equivalent circuit  $I_2'$  is not the actual rotor current but a current which, *flowing in the stator winding, produces the same mmf as the actual rotor current flowing in the rotor winding*, see Eq. 17-4. The substitution of an equivalent stator current of line frequency for the actual rotor current of slip frequency is possible because the *rotor mmf is at standstill with respect to the stator mmf at any rotor speed*, i.e., independent of the frequency of the rotor current.

Note that, as in the case of the transformer, the phasor diagram of voltages and mmf's and the equivalent circuit are derived on the basis of Kirchhoff's mesh equations of the electric circuits, and Eq. 18-3a which is based on Ampere's law of the magnetic circuit (see Art. 4-4). Therefore calculations using the basic equations directly yield the same results as calculations using the equivalent circuit. Formulas for the secondary current, primary current, primary power angle, etc., derived from the basic equations are given in Chap. 51. For performance calculations some engineers use the equivalent circuit while others use the basic formulas. The main advantage of the equivalent circuit is that it can be set up on a calculating board.

# Chapter 19

## POWER AND TORQUE RELATIONS POWER BALANCE

**19-1. Developed mechanical power and torque.** Multiplying Kirchhoff's equation of the rotor (Eq. 18-2) by the rotor current  $I_2'$  and the number of phases  $m_1$  leads to expressions for developed mechanical power and torque characteristic for the polyphase induction motor. Eq. (18-2) yields

$$m_1 E_2' I_2' - m_1 j I_2'^2 s x_2' = m_1 I_1'^2 \frac{r_2'}{s} \quad (19-1)$$

The first term represents the total power, active and reactive, of the secondary. The second term is the *reactive* power contained in the secondary leakage fluxes. The third term is the active power of the rotor. Since the emf and current of the rotor are induced by the rotating flux, the active power of the rotor is called *power of the rotating field* ( $P_{\text{rot},f}$ ):

$$P_{\text{rot},f} = m_1 I_2'^2 \frac{r_2'}{s} \text{ watts} \quad (19-2)$$

A part of this power appears as heat in the rotor winding. This part is equal to  $m_1 I_2'^2 r_2'$ . The balance is the *developed* mechanical power of the rotor. Denoting the power loss in the rotor winding by  $P_e$  (electric power of the rotor) and the developed mechanical power by  $P_{\text{m,dev}}$ , yields

$$P_e = m_1 I_2'^2 r_2' = m_2 I_2'^2 r_2 \text{ watts} \quad (19-3)$$

$$\begin{aligned} P_{\text{m,dev}} &= m_1 I_2'^2 \frac{r_2'}{s} - m_1 I_2'^2 r_2' = m_1 I_2'^2 \frac{1-s}{s} r_2' \\ &= m_2 I_2'^2 \frac{1-s}{s} r_2 \text{ watts} \end{aligned} \quad (19-4)$$

Eqs. 19-3 and 19-4 follow also from the equivalent circuit (Figs. 18-3 and 18-5), as they should, because the equivalent circuit has been derived from the fundamental equations 18-1 and 18-3.

From Eqs. 19-2 and 19-3

$$P_e = P_{\text{rot},f} \times s \quad (19-5)$$

From Eqs. 19-2 and 19-4

$$P_{m,dev} = P_{rot,f} \times (1 - s) \quad (19-6)$$

Using the basic relation of mechanics that

$$T = \frac{7.04}{n} P_{watts} \text{ lb-ft} \quad (19-7)$$

the expression for the developed torque of the polyphase induction motor can be derived either from Eq. 19-2 or from Eq. 19-4. Using Eq. 19-2, for  $n$  the synchronous speed  $n_s$  has to be substituted in Eq. 19-7, because the rotating flux has the constant speed  $n_s$ . Using Eq. 19-4, the actual rotor speed  $n = (1 - s)n_s$  (see Eq. 17-19) has to be substituted in Eq. 19-7. Thus, from Eqs. (19-2) and (19-7)

$$T_{dev} = \frac{7.04}{n_s} m_1 I_2'^2 \frac{r_2'}{s} \text{ lb-ft} \quad (19-8)$$

and from Eqs. 19-4 and 19-7

$$T_{dev} = \frac{7.04}{(1 - s)n_s} m_1 I_2'^2 \frac{1 - s}{s} r_2' = \frac{7.04}{n_s} m_1 I_2'^2 \frac{r_2'}{s} \text{ lb-ft} \quad (19-8a)$$

The same result for the developed torque is obtained from both equations (19-2) and (19-4). This could be expected.

From Eqs. 19-2 and 19-8

$$T_{dev} = \frac{7.04}{n_s} P_{rot,f \text{ (watts)}} \text{ lb-ft} \quad (19-9)$$

i.e., the *developed torque* of the polyphase induction motor is *directly proportional to the power of the rotating field*.

The equation for the torque, Eq. 19-8, has been derived from the power equation 19-4. The same equation for the torque can also be obtained from Biot-Savart's law of forces on current-carrying conductors in a magnetic field (Art. 1-2). This is shown in Chap. 52.

Eq. 19-8 for  $T_{dev}$  characterizes the induction motor. It does not apply to the other type of a-c machines (the synchronous machine) because in the synchronous machine both machine parts are connected with a source of power.

Eq. 19-8 yields the *developed* torque. The torque delivered at the shaft is less than the developed by the torque which corresponds to the mechanical losses of the motor (see Art. 19-3).

It follows from Eq. (19-8) that  $T_{dev}$  is a function of slip and secondary current. When the motor parameters ( $r_1$ ,  $x_1$ ,  $r_m$ ,  $x_m$ ,  $r_2'$ ,  $x_2'$ ) are given,  $I_2'$  can be determined for any value of  $s$  from the fundamental equations (18-1 to 18-3) or from the equivalent circuit, and the  $T_{dev}$  can be computed from Eq. 19-8. It has been pointed out previously that the slip is the basic variable of the induction motor.

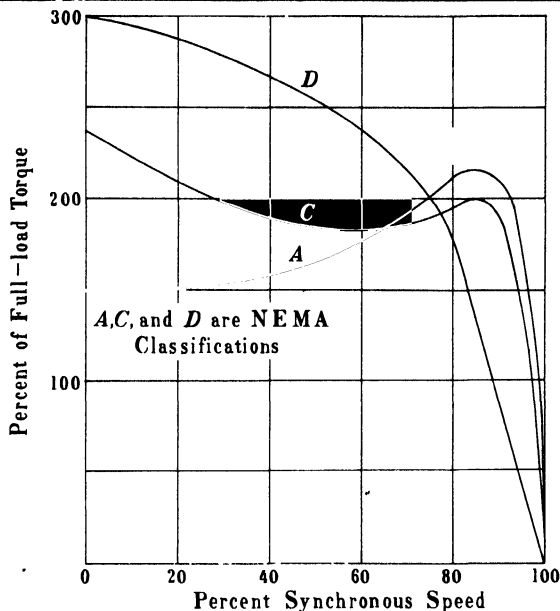


FIG. 19-1. Torque-speed curves of a polyphase induction motor, NEMA classification.

The shape of the torque-speed characteristic depends upon the magnitudes of the machine parameters. Therefore, motors designed for different purposes will have parameters of different magnitudes. Three different shapes of torque-speed characteristics of squirrel-cage motors are shown in Fig. 19-1. *C* and *D* are special machines designed to have high starting torques, i.e., high torques at standstill ( $n=0$ ); design *A* is that of the general-purpose motor, see Table 49-1 ("Characteristics and Applications of Polyphase 60-Cycle A-c Motors").

The motor of design *A* shows a maximum torque, called *pull-out torque*, at a definite slip. When the load torque becomes larger than the pull-out torque, the motor comes to standstill. The slip of the general-purpose motor at rated load is small, between 1% and 5%, i.e., the speed at rated load is between 95% and 99% of the synchronous speed (the larger slip applies to small motors, the smaller slip to large motors). The slip at which the pull-out torque occurs, the *pull-out slip*, is about 5 to 7 times the slip at rated load.

**19-2. The pull-out torque.** The ratio of pull-out torque to rated torque determines the *overload capacity* of the motor and is an important quantity. The Standards of the NEMA prescribe a certain overload capacity for the different motor types (see Table 49-1). In order to determine the pull-out torque, without calculating a number of points of the torque-speed curve, Eq. 19-8 can be used. For this purpose  $I_2'$  must be expressed in terms of the



primary voltage  $V_1$ , the parameters of the motor, and the slip. This can be done by eliminating  $E_1$  and  $I_1$  from Eqs. 18-1 to 18-3 as shown in Chap. 51. This yields

$$I_2' = V_1 \frac{1}{\sqrt{l^2 + m^2}} \quad (19-10)$$

where

$$l = (1 + \tau_2)r_1 + (1 + \tau_1)\frac{r_2'}{s}; \quad m = x_1 + (1 + \tau_1)x_2' - \frac{r_1}{x_m}\frac{r_2'}{s} \quad (19-11)$$

$$\tau_1 = \frac{x_1}{x_m} \quad \tau_2 = \frac{x_2'}{x_m} \quad (19-12)$$

inserting the value of  $I_2'$  from Eq. 19-10 in Eq. 19-8 yields

$$T_{\text{dev}} = \frac{7.04}{n_s s} m_1 \frac{V_1^2 r_2'}{(l^2 + m^2)} \quad (19-13)$$

Differentiating Eq. 19-13 with respect to the slip yields the pull-out slip at which the pull-out torque occurs as

$$s_{\text{p.o.}} \approx \frac{(1 + \tau_1)r_2'}{x_1 + (1 + \tau_1)x_2'} \quad (19-13a)$$

Now the pull-out torque may be calculated from Eq. 19-13, by using the value  $s_{\text{p.o.}}$  as determined from Eq. 19-13a.

**19-3. Power balance.** It has been mentioned previously that the electric machines are energy converters. Any conversion of energy, from one type to another type, is connected with energy losses with the conversion machine. In the induction motor these losses are:

- (a)  $I^2R$ -loss (copper loss) in the stator winding
- (b)  $I^2R$ -loss (copper loss) in the rotor winding
- (c) Iron loss due to the main flux ( $P_{h+e}$ , Art. 3-1)
- (d) Friction loss in the bearings and windage loss ( $P_{F+W}$ ).

While the losses under (a) to (c) are electrical and magnetical losses, the losses under (d) are mechanical losses and as such are proportional to the rotor speed. There are two other types of losses in the induction motor which, although not of mechanical nature, are also proportional to the speed and must be considered as belonging to the category of mechanical losses. These two types of losses are iron losses in the teeth and on the surface of stator and rotor and are caused by the slot-openings of stator and rotor and by the harmonic fluxes of stator and rotor (see Art. 15-2 and Art. 29-1). They are denoted by  $P_{\text{ir,rot}}$  (rotational iron losses).

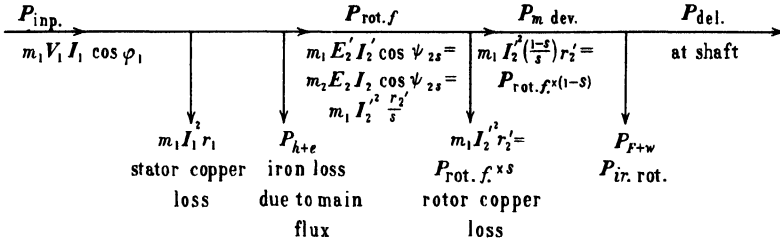


FIG. 19-2. Balance of power in a polyphase induction motor.

The power distribution in the polyphase induction motor is demonstrated by Fig. 19-2. The power input of the stator is

$$P_{in} = m_1 V_1 I_1 \cos \varphi_1 \text{ watts}$$

A part of this power, the stator copper loss  $m_1 I_1^2 r_1$  and the iron loss due to the main flux  $P_{h+e}$  are consumed by the stator. The balance is the power of the rotating field, i.e.,

$$P_{rot.f} = P_{in} - (m_1 I_1^2 r_1 + P_{h+e}) \quad (19-14)$$

From Eq. 19-2 and phasor diagram Fig. 18-1 also

$$P_{rot.f} = m_1 I_2'^2 \frac{r_2'}{s} = m_1 E_2' I_2' \cos \psi_{2s} = m_2 E_2 I_2 \cos \psi_{2s} \quad (19-15)$$

$\psi_{2s}$  is given by Eq. 18-4.

A part of the power  $P_{rot.f}$  is consumed by the rotor as electric power. This is the copper loss of the rotor

$$P_e = m_1 I_2'^2 r_2' = m_2 I_2^2 r_2 = s P_{rot.f} \quad (19-16)$$

(see Eqs. 19-3 and 19-5). The difference between the power of the rotating field and the electric power of the rotor is the developed mechanical power (Eq. 19-4)

$$P_{m,dev} = P_{rot.f} - P_e = (1-s) P_{rot.f} = m_1 I_2'^2 \frac{1-s}{s} r_2' = m_2 I_2^2 \frac{1-s}{s} r_2 \quad (19-17)$$

The mechanical power delivered at the shaft ( $P_{m,del}$ ) is less than the mechanical power developed by the amount of mechanical losses

$$P_{m,del} = P_{m,dev} - (P_{F+w} + P_{ir,rot}) \quad (19-18)$$

**Example 19-1.** A 3-Hp, 440/220-volt, 3-phase, 60-cycle, 4-pole, 1750-rpm squirrel-cage induction motor has the following data and parameters. The data and parameters given will be determined later, in Chapter 22, from a no-load and a locked-rotor test.

(a) *Parameters for starting*

$$r_1 = 2.69 \text{ ohms} = 0.0311 \text{ p-u}$$

$$r_2' = 2.79 \text{ ohms} = 0.0322 \text{ p-u}$$

$$x_1 = x_2' = 3.40 \text{ ohms} = 0.393 \text{ p-u}$$

$$x_m = 103 \text{ ohms} = 1.19 \text{ p-u}$$

$$r_m = 3.66 \text{ ohms} = 0.0423 \text{ p-u}$$

(b) *Parameters for running*

$$r_1 = 2.69 \text{ ohms} = 0.0311 \text{ p-u}$$

$$r_2' = 2.14 \text{ ohms} = 0.0248 \text{ p-u}$$

$$x_1 = 4.36 \text{ ohms} = 0.0505 \text{ p-u}$$

$$x_2' = 4.50 \text{ ohms} = 0.052 \text{ p-u}$$

$$x_m = 103 \text{ ohms} = 1.19 \text{ p-u}$$

$$r_m = 3.66 \text{ ohms} = 0.0423 \text{ p-u}$$

(The difference between starting and running parameters is explained in Chap. 22.)

It is required to determine the performance at start and during running conditions. The friction and windage loss is 44 watts, total no-load iron loss (due to main flux and rotation) 122 watts, and the stray-load loss 48 watts. The no-load current is 2.36 amp at 440 volts. Assume iron loss due to main flux equal one half of total no-load iron losses.

(a) *Starting performance:*

$$r_2' \left( \frac{1-s}{s} \right) = 0$$

$$Z_1 = 2.69 + j3.40 = 4.33 / 51.6$$

$$Z_2' = 2.79 + j3.40 = 4.40 / 50.6$$

$$Z_m = 3.66 + j103 = 103 / 87.96$$

from Eq. 18-10

$$254 / 0 = I_1 \left[ Z_1 + \frac{Z_m Z_2'}{Z_m + Z_2'} \right]$$

$$I_{1(\text{inrush})} = \frac{254 / 0}{8.59 / 51.8} = 29.6 / -51.8$$

$$I_2' = I_1 \times \frac{Z_m}{Z_{r1} + Z_2'} \quad (\text{See Figs. 18-2 to 18-5.})$$

$$I_2' = 29.6 / -51.8 \times \frac{103 / 87.96}{6.45 + j106.4}$$

$$I_2' = 29.6 / -51.8 \times \frac{103 / 87.96}{107.5 / 86.56}$$

$$= 28.4 / -50.4 \text{ amp}$$

$$T_{\text{start}} = \frac{7.04}{1800} \times 3 \times (28.4)^2 \times 2.79 = 26.4 \text{ lb-ft (Eq. 19-8)}$$

(b) *Running performance: assume  $s = 0.03$*

$$r_2' \left( \frac{1-s}{s} \right) = 2.14 \left( \frac{1-0.03}{0.03} \right) = 69.2 \text{ ohms}$$

$$Z_1 = 2.69 + j4.36 = 5.13 / 58.3$$

$$Z_2' = (2.14 + 69.2) + j4.50 = 71.4 / 3.60$$

$$Z_m = 3.66 + j103 = 103 / 87.96$$

from Eq. 18-10

$$I_1 = \frac{254 / 0}{Z_1 + [Z_m Z_2' / (Z_m + Z_2')]} = \frac{254 / 0}{60.8 / 38.2} = 4.18 / -38.2$$

Input power factor =  $\cos 38.2^\circ = 0.785$

$$\begin{aligned} I_2' &= I_1 \times \frac{Z_m}{Z_m + Z_2'} \\ &= 4.18 / -38.2 \times \frac{103 / 87.96}{103 / 87.96 + 71.4 / 3.60} \\ &= 4.18 / -38.2 \times \frac{103 / 87.96}{131 / 55.5} \\ &= 3.28 / -5.74 \text{ amp} \end{aligned}$$

$$T_{\text{dev}} = \frac{7.04}{1800} \times 3 \times (3.28)^2 \times \frac{2.14}{0.03} = 9.0 \text{ lb-ft}$$

$$\text{Mechanical loss torque} = \frac{7.04}{1800} \times (48 + 44 + 61) = 0.60 \text{ lb-ft}$$

$$T_{\text{del}} = T_{\text{dev}} - T_{\text{loss}} = 8.40 \text{ lb-ft}$$

Power input =  $3 \times 254 \times 4.18 \times 0.785 = 2500 \text{ watts}$

Losses

$m_1 I_1^2 r_1$	= 141 watts
$m_1 I_2'^2 r_2'$	= 69
no-load iron (main flux and rotation)	= 122
stray load	= 48
friction and windage	= 44
Total loss	424 watts

Power delivered =  $2500 - 424 = 2076 \text{ watts} = 2.78 \text{ HP}$

$$\text{Efficiency} = \frac{2076}{2500} = 0.83$$

$$\text{Slip} = \frac{69}{2500 - (141 + 61)} = \frac{69}{2298} = 0.03 \text{ (check) (Eq. 19-2)}$$

$$\text{Speed} = \frac{120 \times 60}{4} (1 - 0.03) = 1746 \text{ rpm}$$

$$T_{\text{del}} = \frac{5250}{1746} \times 2.78 = 8.40 \text{ lb-ft}$$

which checks with value previously determined.

It should be noted that normal slip is slightly greater than 0.03 since the calculated output for  $s = 0.03$  is 2.78 HP. An approximation of the normal slip is:

$$s_n = \frac{3.0}{2.78} \times 0.03 = 0.0324$$

From Eq. 19-13a

$$\text{pull-out slip} \approx \frac{1.042 \times 2.14}{4.36 + 1.042 \times 4.50} = 0.246$$

$$\text{at } s = 0.246 \quad r_2' \left( \frac{1-s}{s} \right) = 6.56$$

$$Z_2' = (2.14 + 6.56) + j4.50 = 9.81/27.3$$

$$I_1 = \frac{254/0}{Z_1 + [Z_m Z_2' / (Z_m + Z_2')]} = \frac{254/0}{14.1/41.1} = 18.0/-41.1$$

$$I_2' = I_1 \times \frac{Z_m}{Z_m + Z_2'} = 17.2/-36.6$$

$$T_{\text{p.o.}} = \frac{7.04}{1800} \times 3 \times (17.2)^2 \times \frac{2.14}{0.246} = 30.2 \text{ lb-ft}$$

$$\text{Normal torque} = \frac{3.0}{2.78} \times 8.40 = 9.05 \text{ lb-ft}$$

$$\frac{T_{st}}{T_n} = \frac{26.4}{9.05} = 2.92$$

$$\frac{T_{\text{p.o.}}}{T_n} = \frac{30.2}{9.0} = 3.36$$

## PROBLEMS

Parameters for the starting and running performance for three 3-phase squirrel-cage induction motors are listed below. All values are given in ohms per phase. Also included are the friction and windage, no-load iron, and stray-load losses as a fraction of the output rating. Assume the iron losses due to the main flux =  $\frac{1}{2}$  (total no-load iron losses).

Determine the complete starting and running ( $s = 0.025$ ) performance for each motor.

	Problem 1	Problem 2	Problem 3
	10-HP	15-HP	20-HP
	220-volt	220-volt	440-volt
	2-pole	4-pole	6-pole
	60-cycle	60-cycle	60-cycle
<i>Starting:</i>			
$r_1$ .....	0.142	0.138	0.259
$r_2'$ .....	0.188	0.121	0.352
$x_1 = x_2'$ .....	0.350	0.233	0.842
$x_m$ .....	11.7	8.64	20.7
$r_m$ .....	0.194	0.130	0.390
<i>Running:</i>			
$r_1$ .....	0.142	0.138	0.259
$r_2'$ .....	0.168	0.104	0.324
$x_1$ .....	0.421	0.281	1.04
$x_2'$ .....	0.440	0.302	1.17
$x_m$ .....	11.7	8.64	20.7
$r_m$ .....	0.194	0.130	0.390
<i>Losses:</i>			
Friction and windage .....	0.015	0.01	0.008
No-load iron .....	0.02	0.024	0.024
Stray-load .....	0.02	0.015	0.015

## Chapter 20

### OPERATION OF THE INDUCTION MACHINE AS BRAKE AND GENERATOR

**20-1. Operation as a brake.** No fixed value for the slip  $s$  has been used in the derivation of Kirchhoff's equation for the secondary (see Eq. 17-22). Therefore,  $s$  can be large or small, positive or negative. It is of interest to find the modes of operation which correspond to the different values of  $s$ . The answer to this is given by Eq. 19-4 for the developed mechanical power

$$P_{m,dev} = m_1 I_2'^2 \frac{1-s}{s} r_2' \quad (20-1)$$

and by Eq. 17-19 which defines the slip

$$s = \frac{n_s - n}{n_s} \quad (20-2)$$

At  $s=0$ ,  $n=n_s$  and the relative speed between rotating flux and the rotor is zero. Therefore, at  $s=0$  no emf is induced in the rotor windings; the rotor current ( $I_2'$ ) is zero and  $P_{m,dev}$  is zero. For values of  $s$  larger than zero and smaller than 1; ( $0 < s < 1$ ),  $n$  is smaller than  $n_s$  and  $P_{m,dev}$  is positive, i.e., mechanical power is supplied *by the rotor*. At  $s=1$  ( $n=0$ ),  $P_{m,dev}$  becomes zero, as could be expected, because the rotor is at standstill.

According to Eq. 20-2,  $s > 1$  is possible when  $n$  is negative, i.e., when the rotor rotates in a direction opposite to that of the rotating flux. This condition occurs on a 3-phase motor if, when it is running at a certain speed, two of the three connections to the power lines are suddenly interchanged. The developed power,  $P_{m,dev}$  then becomes negative, i.e., mechanical power is supplied *to the rotor*. Since there is no machine to supply power to the rotor (no prime mover), the mechanical power is taken from the kinetic energy of the rotating mass and the mass soon comes to a standstill. After coming to a standstill the machine again operates as a normal induction motor; it accelerates in the direction of the new rotating flux to a subsynchronous speed corresponding to the load torque. It is evident that during the period from the interchange of line connections to standstill of the rotor the machine operates as a *brake*. This operation is known as *plugging*. Plugging of induction motors for the purpose of stopping, or of stopping and reversing, is used frequently.

**20-2. Operation as a generator.** According to Eq. 20-2, a negative slip ( $s < 0$ ) is possible when  $n > n_s$ . Since the machine when running as a motor cannot reach even the speed  $n = n_s$ , there must be another machine (a prime mover) which brings the rotor up to the speed larger than  $n_s$ . At  $s < 0$ ,  $P_{m,dev}$  becomes negative. This means that at supersynchronous speeds the rotor does not supply mechanical power but *consumes mechanical power*, i.e., the machine operates as a *generator*. Thus an induction motor, driven by a prime mover above its synchronous speed operates as an induction generator. It is a characteristic feature of all electric machines that they are able to operate both as a *motor* and as a *generator*. The following consideration shows that the torque changes its sign when the rotor speed becomes larger than the synchronous speed: at a subsynchronous speed an emf is induced in the rotor winding corresponding to the relative speed between the rotating flux and the rotor,  $(n_s - n)$ . At synchronous speed ( $n = n_s$ ) this emf becomes zero because the relative speed between rotating flux and rotor is zero. At supersynchronous speeds ( $n > n_s$ ) the relative speed between rotating flux and rotor changes its sign as compared to subsynchronous speeds, and therefore  $E_2'$  and  $I_2'$  change their signs. Since torque is determined by the product of flux and armature current, see Eq. 1-28, the torque changes sign at supersynchronous speed. This also follows directly from Eq. 19-8 in which  $s$  is negative for generator operation.

This behavior of the induction generator, derived from the equation for  $P_{m,dev}$  and Biot-Savart's law does not give a complete notion of its operation. Such a notion can be obtained only from Kirchhoff's equations for generator operation. They are (compare with Eqs. 17-2, 17-22, 17-23a)

$$\dot{E}_1 - j\dot{I}_1 x_1 = \dot{I}_1 r_1 + \dot{V}_1 \quad (20-3)$$

$$s\dot{E}_2' - j\dot{I}_2' s x_2' = \dot{I}_2' r_2' \quad (20-4)$$

$$\dot{E}_1 = \dot{E}_2' = -(\dot{I}_1 + \dot{I}_2')\dot{Z}_m \quad (20-5)$$

In the rotor equation (20-4)  $s$  is negative. Fig. 20-1 shows the phasor diagram corresponding to Eqs. 20-3, 20-4, and 20-5. The secondary emf  $E_2'$  leads the flux  $\Phi$  by  $90^\circ$  and is opposite to the direction of  $E_2'$  for the motor (Fig. 18-1). Since  $s$  is negative,  $+j\dot{I}_2' s x_2'$  lags the current  $\dot{I}_2'$  by  $90^\circ$  and  $\dot{I}_2'$  leads  $E_2'$ . The magnitude of the angle  $\psi_{2s}$  between  $\dot{I}_2'$  and  $E_2'$  is given by the same equation as for the motor (Eq. 18-4). The primary current  $\dot{I}_1 = \dot{I}_n - \dot{I}_2'$  is found in the same way as for the motor (Eq. 18-3).  $E_1$  is ahead of  $V_1$  as it should be for a generator (in a motor  $V_1$  is ahead of  $E_1$ , see Fig. 18-1).

As the phasor diagram (Fig. 20-1) shows, the primary current  $\dot{I}_1$  leads the primary voltage,  $V_1$ , i.e., the induction generator, when *singly* operated, can supply a load with leading current (a capacitive load) *only*. The explanation for this is the following: the prime mover can influence only the active component of current and not the reactive component; therefore, the rotor can not supply reactive current. Since a reactive current ( $I_\phi$ ) in phase with the



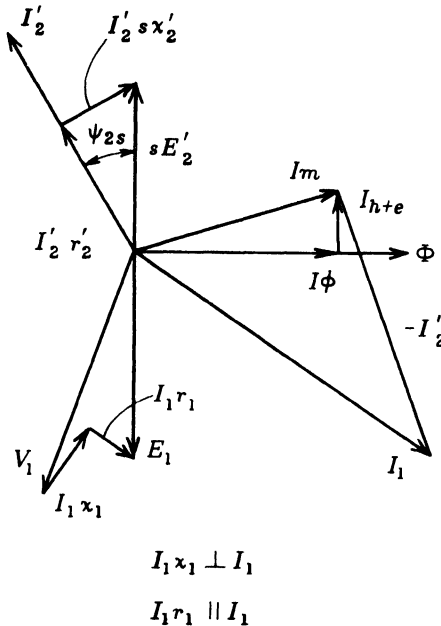


FIG. 20-1. Phasor diagram of an induction generator.

main flux ( $\Phi$ ) is necessary to sustain this flux and another reactive current is necessary to sustain the leakage fluxes, these currents must be supplied by the stator. As the phasor diagram 20-1 shows, only a leading stator current can accomplish this.

If an induction generator operates not singly but in parallel with synchronous generators (these generators are able to supply loads with lagging as well as with leading current, Art. 32-1) and the load is *inductive*, the synchronous generators have to supply the lagging current required by the load and also the lagging current necessary to sustain the fluxes of the induction generator. Loads are ordinarily reactive. Therefore, an induction generator is at dual disadvantage in comparison to the synchronous generator, since it is incapable of delivering a lagging current to the load and moreover takes a lagging current from the line. Induction generators are used seldom.

Curves which show the current  $I_1$  and  $I_2'$  as a function of slip for motor, generator, and brake operation are shown in Fig. 20-2. Both currents change little at high slips. At  $s=0$ ,  $I_1=I_0$ . Fig. 20-3 shows the developed torque  $T$  and the mechanical power at the shaft,  $P_{m,del}$ , as a function of slip for motor, generator, and brake operation.  $T$  and  $P_{m,del}$  are negative at negative values of  $s$  (generator operation).  $T$  is positive for *all* positive values of  $s$  but  $P_{m,del}$  changes its sign at  $s=+1$  where the range of operation as a brake starts. This will be demonstrated once more in Chapter 21 which deals with the circle diagram of the induction motor.

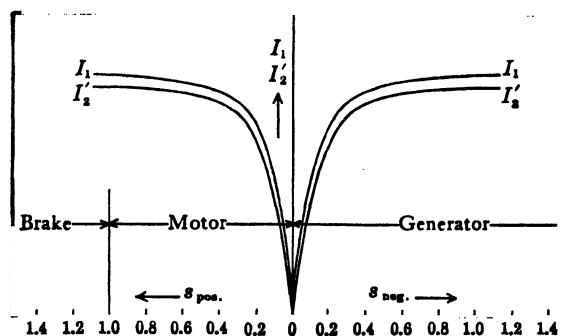


FIG. 20-2. Stator and rotor currents as a function of slip for motor, generator, and brake operation.

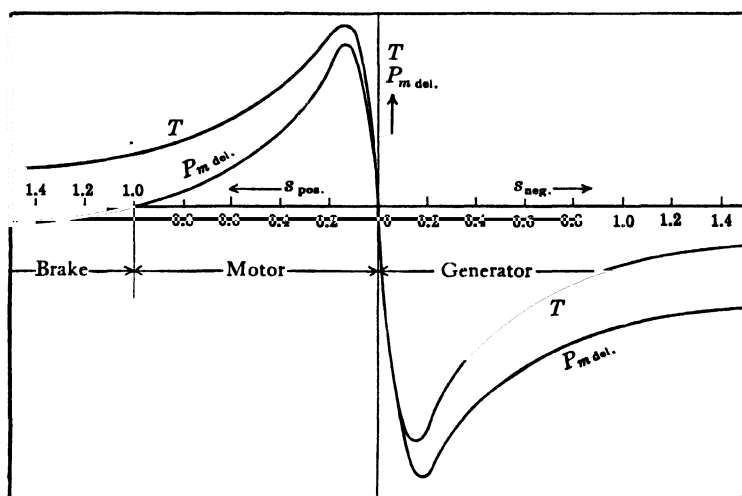


FIG. 20-3. Torque and mechanical power at the shaft as a function of slip for motor, generator, and brake operation.

The following tabulation shows a summary of the magnitudes of the slips and the corresponding modes of operation of the induction machine:

Slip and $n$	Mode of operation	Conversion of energy
$0 < s < 1$ $n_s > n > 0$	Motor	Electrical into mechanical
$s > 1$ $\infty > n > 0$ (but opposite to rotating flux)	Brake	Kinetic into electrical
$s < 0$ $n > n_s$	Generator	Mechanical into electrical

In Kirchhoff's equation of the stator,  $V_1$  is the line voltage in the case of the motor (Eq. 18-1) and an induced voltage in the case of the generator (Eq. 20-3). Considering  $V_1$  to be the line voltage in both cases, the sign of  $V_1$  must be changed in the equation of the generator and Kirchhoff's equations become the same for motor and generator. Therefore, with  $V_1$  to be the line voltage, the equivalent circuit derived for the induction motor (Fig. 18-2 to 18-5) applies also to the induction generator.

## Chapter 21

### CIRCLE DIAGRAM OF THE POLYPHASE INDUCTION MOTOR

**21-1. Determination of the circle diagram.** The same equations of both electric circuits and of the magnetic circuit (Eqs. 18-1 to 18-3) which led to the phasor diagram of mmf's and voltages and to the equivalent circuit of the polyphase induction motor also lead to the geometric locus of the end-point of its primary current. A comprehensive study of this geometric locus is given in Chap. 51. Only a brief explanation is given in this chapter.

Consider Eq. 18-10 derived from the basic equations mentioned above. The quantity in the brackets of this equation represents the *total* impedance of the polyphase induction motor looking into its primary terminals. Eq. 18-10 can be written as

$$\dot{I}_1 = \dot{V}_1 \dot{Y}_t = \dot{V}_1 (g_t - jb_t) \quad (21-1)$$

where  $Y_t$  is the total admittance,  $g_t$  the total conductance, and  $b_t$  the total susceptance, looking into the primary terminals.  $g_t$  and  $b_t$  are functions of the six parameters of the machine and of the slip.

Assuming the real and imaginary axes as shown in Fig. 21-1, and further introducing a Cartesian system of coordinates  $y'$ ,  $x'$  so that  $y'$  lies in the real axis and  $x'$  lies in the imaginary axis, and placing the phasor  $V_1$  arbitrarily in the real axis,

$$\dot{V}_1 = V_1 \quad (21-2)$$

$$\dot{I}_1 = y' - jx' \quad (21-3)$$

In the latter equation,  $y'$  and  $x'$  are the coordinates of the end-point of  $I_1$ . It follows from Eqs. 21-1 and 21-3 that

$$y' = V_1 g_t = \psi_1 \quad (21-4)$$

$$x' = V_1 b_t = \psi_2 \quad (21-5)$$

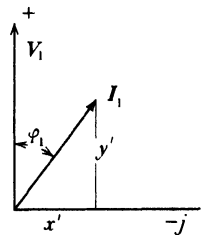


FIG. 21-1. Derivation of the circle diagram.

where  $\psi_1$  and  $\psi_2$  are two different functions of the six parameters and the slip. Eliminating the slip  $s$  from Eq. 21-4 with the aid of Eq. 21-5, or vice versa, a quadratic equation for  $y'$  and  $x'$  is obtained (see Chap. 51) which is the equation of a *circle*, showing that the end-point of the primary current  $I_1$  moves on a circle. Using the rules of analytic geometry, the coordinates of

the center-point and the radius of the circle can be determined. Having the coordinates of the center-point  $C$ , the angle ( $\alpha$ ) which the imaginary axis makes with the line connecting the origin of coordinates and the center-point  $C$  (Fig. 21-2) can be determined:

$$\tan \alpha = \frac{y_c'}{x_c'} \approx \frac{2r_1}{x_m(1 + 2\tau_1 + \tau_2)} \quad (21-6)$$

$\tau_1$  and  $\tau_2$  are given by Eq. 19-12.

In practical problems, two points of the circle are given either by test (see Chapter 22) or by computation. These points are the no-load point  $P_0$  and the short-circuit (locked-rotor) point  $P_L$  (Fig. 21-2).  $P_0$  corresponds to

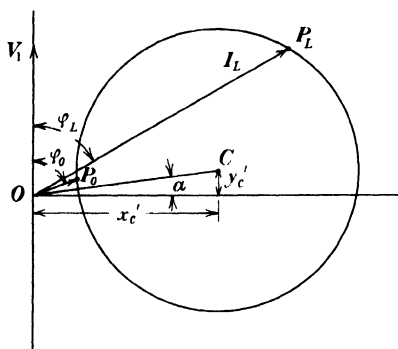


FIG. 21-2. Construction of the circle diagram.

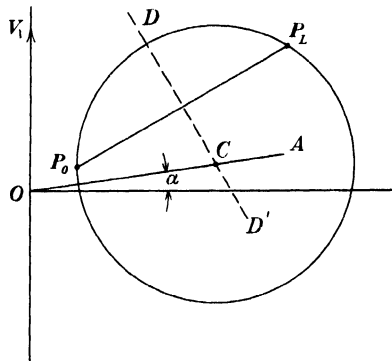


FIG. 21-3. Construction of the circle diagram.

the current  $I_0$  which the motor draws from the lines at no-load;  $P_L$  corresponds to the current which the motor draws from the lines at standstill (rotor locked). The perpendicular bisector  $DD'$  (Fig. 21-3) of the line which connects  $P_0$  and  $P_L$  must go through the center-point of the circle. Since the center-point must also lie on the line  $OA$  which makes the angle  $\alpha$  (Eq. 21-6) with the imaginary axis, the perpendicular bisector  $DD'$  intersects the line  $OA$  in the center-point. Thus the circle on which the end-point of  $I_1$  moves is determined by the no-load and short-circuit (locked rotor) currents and by the angle  $\alpha$ .

Each point of the circle corresponds to a certain value of the primary current  $I_1$  and therefore also to a certain value of the slip  $s$ .

Notice that  $\alpha$  increases with increasing primary resistance. In larger machines,  $\alpha$  is small, and the center-point can be assumed to lie on the imaginary axis.

**21-2. Developed-mechanical-power line and delivered-mechanical-power line.** There are four characteristic points on the circle. These are: the no-load point and the points which correspond to  $s = 0$ ,  $s = 1$  and  $s = \pm \infty$ .

$s=0$  means  $n=n_s$ , i.e., the rotor runs synchronously with the rotating flux and the rotor current is zero (see Art. 20-1). It has been explained that the rotor is not able to achieve this speed by itself but must be brought up to this speed by another machine, and this machine will have to supply the mechanical losses of the rotor, i.e., the friction and windage losses and the rotational iron losses. The active component of the stator current at  $s=0$  is smaller than that at no-load ( $I_0 \cos \varphi_0$ ) by the amount corresponding to these losses. The point on the circle which corresponds to  $s=0$  will be denoted by  $P_0'$ . It lies on the circle below the point  $P_0$  (see Fig. 21-4).

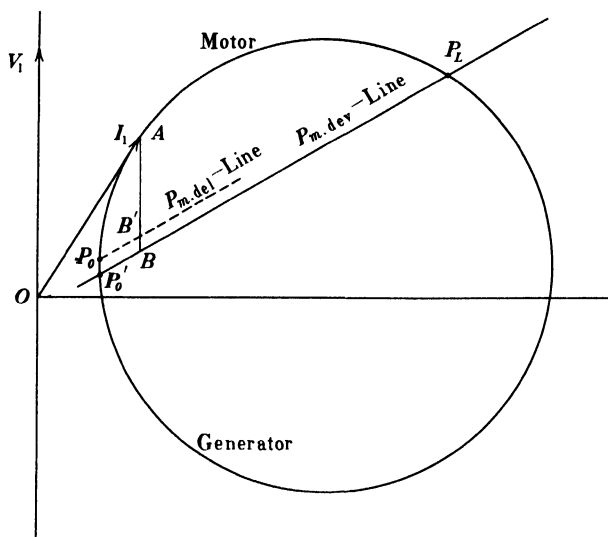


**FIG 21.-4.** Construction of the mechanical-power-lines.

$s=1$  means  $n=0$ , i.e., standstill (locked rotor). The developed mechanical power is zero (see Art. 20-1). This is in agreement with  $n=0$ . Consider Fig. 18-3 or 18-5. The resistance  $[(1-s)/s]r_2'$  which corresponds to the load is zero, and the motor draws a large current from the lines, limited practically only by the resistances and leakage reactances of both windings (see Art. 22-2). The point of the circle which corresponds to  $s=1$  has been denoted by  $P_L$  (Figs. 21-2 and 21-3).

At  $s=0$  the rotor current is zero and the developed mechanical power of the rotor is zero. At  $s=1$ ,  $n=0$  and again the mechanical power is zero. It is shown in Chap. 51 that if a straight line is drawn through the points  $P_0'$  and  $P_L$  (Fig. 21-4), the distance from any arbitrary point on the circle to this line is proportional to the mechanical power developed at the stator current or slip which corresponds to this point of the circle. Thus for the point  $A$  of the circle (Fig. 21-4), i.e., for the current  $OA$  and the slip which correspond to the point  $A$ , the developed-mechanical-power is

proportional to the distance  $AB$ . The line through  $P_0'$  and  $P_L$  is called the *developed-mechanical-power line* ( $P_{m,dev}$ -Line).

The developed mechanical-power is positive for the part of the circle which lies above the  $P_{m,dev}$ -Line and is negative for the part of the circle which lies below this line. This means that mechanical power is available at the shaft, and the machine operates as a *motor* on the part of the circle which lies above the  $P_{m,dev}$ -Line; inversely, the machine accepts mechanical power from the shaft and operates as *generator* or *brake* on the part of the circle below the  $P_{m,dev}$ -Line. The range of operation as a brake will be discussed below.

At no-load the developed-mechanical-power of the motor is equal to its mechanical losses (friction and windage losses and rotational iron losses). At no-load the mechanical power delivered to the shaft is zero. The *delivered-mechanical-power line*,  $P_{m,del}$ -Line, is obtained with good approximation by drawing a straight line parallel to the  $P_{m,dev}$ -Line through the no-load point  $P_0$  (Fig. 21-4). The distance from any point on the circle to the  $P_{m,del}$ -Line is then proportional to the delivered mechanical power. The  $P_{m,del}$ -Line thus drawn applies only up to the maximum value of  $P_{m,del}$ ; the point on the circle corresponding to maximum  $P_{m,del}$  and maximum  $P_{m,dev}$  is determined by the tangent to the circle which is parallel to the  $P_{m,del}$  and  $P_{m,dev}$  lines.

**21-3. The torque-line and the slip-line.** Of interest is the point on the circle at which  $s = \pm \infty$ . Consider the equivalent circuit, Fig. 18-3 or 18-5. The load of the induction motor,  $[(1-s)/s]r_2'I_2'^2$ , which represents its developed mechanical power, is the same at  $s = +\infty$  and  $s = -\infty$ , namely,  $-I_2'^2r_2'$ . This means that  $s = +\infty$  and  $s = -\infty$  are represented by the same point on the circle. The developed mechanical power at this point is negative, i.e., mechanical power is supplied to the shaft. The magnitude of this mechanical power supplied to the machine is equal to  $I_2'^2r_2'$ , which is equal to the copper loss in the rotor. This means that at  $s = \pm \infty$  the rotor copper loss is supplied from outside and that the power of the *rotating field* is zero. Since the power of the rotating field is proportional to the torque on the rotor (see Eq. 19-9) the torque on the rotor is zero at  $s = \pm \infty$ . The torque on the rotor is also zero at  $s = 0$ , because at  $s = 0$  the rotor current is zero. Thus the circle points at which  $s = 0(P_0')$  and  $s = \pm \infty(P_\infty)$  are those at which the torque is zero, and it is shown in Chap. 51 that when a straight line, the *Torque-Line*, is drawn through these two points (Fig. 21-5), the distance from any circle-point to this line represents the developed torque of the machine for the point considered. Thus in Fig. 21-5 the distance  $AC$  from point  $A$  on the circle to the  $T_{dev}$ -Line represents, to a certain scale, the developed torque of the motor at the slip or the primary current which corresponds to the point  $A$ . If a tangent  $BB'$  to the circle is drawn parallel to the  $T_{dev}$ -Line, the distance  $A'C'$  represents the pull-out torque (maximum torque) of the motor.

The circle-point  $P_\infty$  can be found approximately in the manner described





When the primary copper losses are neglected ( $r_1=0$ ), the distance  $P_\infty D$  and also the distance  $HD'$  become zero, i.e., in this case the  $T_{dev}$ -Line coincides with the power-input line.

It has been explained (Art. 20-1) that when the motor operates as a brake the slip is positive and larger than 1. Apparently, the range of operation as a brake lies between the points  $P_L$  and  $P_\infty$ .

Consider point  $G$  in Fig. 21-5. This point lies below the point  $P_0'$  for which  $s=0$  and, therefore, corresponds to a negative slip. The machine operates here as a generator. Accordingly, the active component  $GG'$  of the current  $I_1=OG$  is negative, i.e., power is supplied by the induction machine to the lines. Note that, while the active component of the primary current is reversed, its reactive current component  $OG'$  remains unchanged, and, therefore, reactive current must be supplied by the lines in order to sustain the main flux and the leakage fluxes of the generator, or, when operated singly, the load must be capacitive (Art. 20-1).

The main consumers of reactive currents from power lines are induction motors and transformers and the generators must supply the reactive currents. The *asynchronous (induction) generator* is unable to supply reactive current. This is the reason the induction generator is seldom used.

Fig. 21-6 shows how the slip-line, as well as the slip for any point on the circle, can be determined. The slip-line is found in the following way (see Chap. 51): connect the center-point of the circle  $P_c$  with the point  $P_\infty$  and draw at random a perpendicular  $SS$  to this line  $P_c P_\infty$ . The line  $SS$  is the

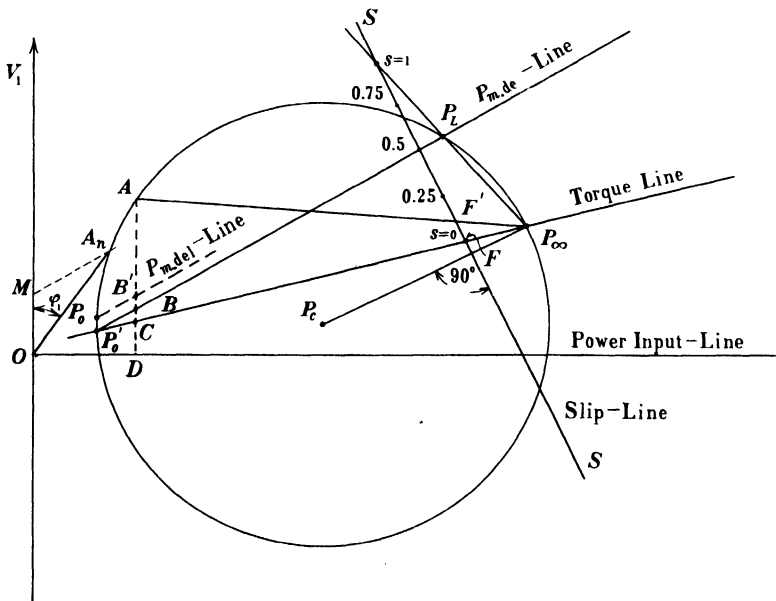


FIG. 21-6. Construction of the slip line.

*slip-line.* The point  $s=0$  is given by the intersection of the slip-line with the line  $P_0'P_\infty$ , i.e., with the torque-line. The point  $s=1$  is given by the intersection of the slip-line and a line drawn through  $P_\infty P_L$ . The slip is distributed uniformly over the slip-line, i.e., the point  $s=0.5$  is in the center between  $s=0$  and  $s=1$ , and so on. The slip for any point  $A$  of the circle (Fig. 21-6) is found by connecting this point with the point  $P_\infty$ ;  $FF'$  is the slip which corresponds to the point  $A$ .

It will be observed in Fig. 21-6 that the following proportionalities exist for the point  $A$ :

$$\begin{aligned} AD &\sim P_1 && \text{(primary power input)} \\ AC &\sim P_{\text{rot},f} && \text{(power transferred by the rotating field)} \\ AC &\sim T_{\text{dev}} && \text{(developed torque)} \\ AB &\sim P_{\text{m},\text{dev}} && \text{(developed mechanical power of the rotor)} \\ AB' &\sim P_{\text{m},\text{del}} && \text{(mechanical power delivered at the shaft)} \end{aligned}$$

$$\begin{aligned} OD &= (AD - AC) \sim (P_1 - P_{\text{rot},f}) && \text{(primary copper losses and iron losses due to the main flux)} \\ &= m_1 I_1^2 r_1 + P_{h+e} \end{aligned}$$

$$\begin{aligned} CB &= (AC - AB) \sim (P_{\text{rot},f} - P_{\text{m},\text{dev}}) && \text{(secondary copper losses)} \\ &= m_2 I_2^2 r_2 \end{aligned}$$

$$\begin{aligned} BB' &= (AB - AB') \sim (P_{\text{m},\text{dev}} - P_{\text{m},\text{del}}) && \text{(friction + windage losses and rotational iron losses)} \\ &= P_{F+W} + P_{\text{ir},\text{rot}} \end{aligned}$$

It should be noted that the geometric locus of the primary current is a circle only when the six parameters of the machine are *constant* quantities, independent of the slip. As it will be shown later (Art. 22-5 and Art. 22-6), this is not the case in medium-size (about 50-HP) and larger machines and often not even in smaller machines, so that the field of application of the circle diagram for the accurate determination of torque, slip, etc., is limited.

#### 21-4. Determination of the scales for the power and torque lines. If

the current scale of the circle diagram is chosen so that  $1'' = a$  amp, the power scale is such that  $1'' = m_1 V_1 a$  watts, since  $m_1$  and  $V_1$  are constant quantities. This power scale applies to the distances between the point on the circle and the power input line (imaginary axis), the  $P_{\text{rot},f}$ -Line (torque line), the  $P_{\text{m},\text{dev}}$ -Line, and the  $P_{\text{m},\text{del}}$ -Line.

The distance between the point of the circle and the  $P_{\text{m},\text{del}}$ -Line which corresponds to the *rated* (normal) output at the shaft is equal to

$$\frac{HP \times 746}{m_1 \times V_1} \text{ amp} = \frac{HP \times 746}{m_1 V_1 a} \text{ inches} = QQ' \quad (\text{Fig. 21-7})$$

where  $HP$  is the rated horsepower of the motor and  $Q$  the intersection point of the  $P_{m,del}$ -Line and the axis of ordinates. Drawing a line  $Q'A_n$  parallel to

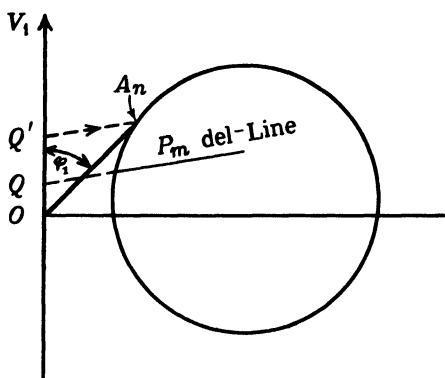


FIG. 21-7. Determination of the normal operating point on the circle diagram.

the  $P_{m,del}$ -Line at the distance  $QQ'$  inches from this line yields the normal operating point on the circle (point  $A_n$ , Fig. 21-7). The rated primary current of the motor is then  $OA_n$  and  $\phi_1$  is the primary power factor angle.

Since (see Eq. 19-9)

$$T_{dev} = \frac{7.04}{n_s} P_{rot,f \text{ (watts)}} \text{ lb-ft}$$

the scale for the developed torque is

$$1'' = m_1 V_1 a \frac{7.04}{n_s} \text{ lb-ft}$$

## PROBLEMS

1. (a) Construct the circle diagram of the 3-HP, 440/220-volt, 3-phase, 60-cycle, 4-pole, squirrel-cage motor treated in the Example of Chapter 19, using the parameters for running, and determine from this diagram the rated primary current, power factor, pull-out torque, starting current, and starting torque.

(b) Construct the circle diagram using the parameters for starting and determine the rated primary current, power factor, pull-out torque, starting current, and starting torque.

(c) Compare the results obtained from the circle diagrams with those obtained from the equivalent circuit in Chap. 19.

2. Repeat Problem 1 for the 10-HP, 220-volt, 3-phase, 60-cycle, 2-pole, squirrel-cage motor the parameters of which are given in Problem 1 of Chap. 19.

3. Repeat Problem 1 for the 15-HP, 220-volt, 3-phase, 60-cycle, 4-pole, squirrel-cage motor the parameters of which are given in Problem 2 of Chap. 19.

4. Repeat Problem 1 for the 20-HP, 440-volt, 3-phase, 60-cycle, 6-pole, squirrel-cage motor the parameters of which are given in Problem 3 of Chap. 19.

These problems will show that the circle diagram constructed with the parameters for running, yields inaccurate values for the starting performance; also, that the circle diagram constructed with the parameters for starting, yields inaccurate results for the running performance and the pull-out torque.

## Chapter 22

### DETERMINATION OF PARAMETERS FROM A NO-LOAD AND A LOCKED-ROTOR TEST · INFLUENCE OF PARAMETERS ON PERFORMANCE · INFLUENCE OF SKIN-EFFECT AND SATURATION ON THE PARAMETERS

It has been mentioned previously that the six parameters of the induction motor can be determined from a no-load and a locked-rotor (short-circuit) test, just as in the case of the transformer. This is shown in the following. The voltage and current are per phase; power is total power.

**22-1. The no-load test.** During this test the load on the motor shaft is zero and the following measurements are taken:

- (a) the primary voltage  $V_1$  which is usually equal to the rated voltage,
- (b) the primary current  $I_0$ ,
- (c) the power input  $P_0$ .

The power  $P_0$  is equal to the motor losses at no-load. These are the copper losses  $m_1 I_0^2 r_1$  in the stator winding, the hysteresis and eddy-current losses due to the main flux  $P_{h+e}$ , the friction and windage losses of the rotor  $P_{F+W}$ , and the rotational iron losses due to the *slot-openings* (see Arts. 19-3 and 29-1), i.e.,

$$P_0 = m_1 I_0^2 r_1 + P_{h+e} + P_{F+W} + P_{ir,rot} \quad (22-1)$$

Since all these losses are small the active component of  $I_0$  is small in comparison with its reactive component  $I_\phi$  and, therefore, the power factor at no-load

$$\cos \varphi_0 = \frac{P_0}{m_1 V_1 I_0} \quad (22-2)$$

is also small, about 0.05 to 0.15.

Only a very small rotor current is necessary to account for  $P_{F+W} + P_{ir,rot}$ , and the secondary circuit can therefore be considered to be open. This may also be deduced from the magnitude of the resistance which represents the mechanical power of the rotor,  $r_2'(1-s)/s$ : this resistance becomes very high

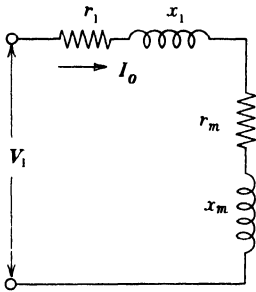


FIG. 22-1. Equivalent circuit of the induction motor at no-load.

because the slip at no-load is negligibly small, i.e., the rotor circuit is practically open at no-load. Thus the equivalent circuit of the motor at no-load is represented by Fig. 22-1.

A knowledge of  $P_{h+e}$  is necessary in order to determine  $r_m$ , for the latter represents these losses.  $P_{h+e}$  can be separated from the other no-load losses by two tests. One test requires that the rotor be driven by another machine at *synchronous speed* ( $s=0$ ). In this case the rotor current is exactly zero and the losses  $P_{F+W}$  and  $P_{I_r, \text{rot}}$  are supplied by the driving machine. The power input of the stator of the induction motor is then equal to

$$P_0' = m_1 I_0'^2 r_1 + P_{h+e} \quad (22-3)$$

where  $P_0'$  and  $I_0'$  are the power input and stator current at  $s=0$ . Having determined  $r_1$  by another test, the loss  $P_{h+e}$  can be calculated. ( $I_0'$  is the current which corresponds to the point  $P_0'$  on the circle diagram (see Fig. 21-6).

The emf  $E_1$  induced by the rotating flux in the stator winding at no-load is approximately

$$E_1 \approx V_1 - I_0 x_1 \quad (22-4)$$

As in the transformer (see Art. 8-1) the conductance of the main flux path is

$$g_m = \frac{P_{h+e}}{m_1 E_1^2} \quad (22-5)$$

From the equivalent circuit at no-load (Fig. 22-1),

$$x_m \approx \frac{E_1}{I_0} \quad (22-6)$$

The main flux resistance  $r_m$  (see Eq. 8-3)

$$r_m = \frac{g_m}{g_m^2 + b_m^2} \approx \frac{g_m}{b_m^2} \approx g_m x_m^2 \quad (22-7)$$

Thus the no-load test yields the main flux parameters  $r_m$  and  $x_m$  (or  $g_m$  and  $b_m$ ), provided that the primary leakage reactance  $x_1$  in Eq. 22-4 is known. This reactance and the secondary parameters  $r_2'$  and  $x_2'$  are obtained with the aid of the short-circuit test.

**22-2. The short-circuit (locked-rotor) test.** During this test the rotor is blocked and the following measurements are taken:

- (a) the primary voltage  $V_L$  which is less than the rated voltage for the reason given below,

(b) the primary current  $I_L$ ,

(c) the power input  $P_L$ .

At standstill the slip  $s$  is equal to unity, and the equivalent circuit of the motor is given by Fig. 22-2. Since the secondary impedance  $r_2' + jx_2'$  is small in comparison with  $x_m$  and the primary voltage drop is large, only a small current flows through the main flux circuit, and the *main flux* and also the iron losses due to the main flux are *small*. At standstill there is no mechanical power [ $\{(1-s)/s\}r_2' = 0$ ] and there are no mechanical losses ( $P_{F+W} = 0$ ,  $P_{ir,rot} = 0$ ) in the machine. Therefore, the power input at standstill  $P_L$  is consumed mainly by the copper losses of both windings.

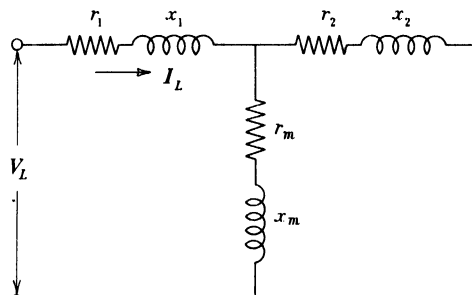


FIG. 22-2. Equivalent circuit of the induction motor at standstill (locked rotor).

It is seen from Fig. 22-2 that at standstill the primary current is practically determined by the sum of the primary and secondary impedances  $r_1 + jx_1$  and  $r_2' + jx_2'$ . It is the counter-emf  $E_1$  which reduces the primary current when the motor runs ( $s \ll 1$ ). But there is only a small counter-emf present at standstill. Therefore, the primary current becomes high, about 4 to 8 times the rated current, if rated line voltage  $V_1$  is applied to the stator during the short-circuit test. In order to avoid over-heating of the windings the short-circuit test is taken at a voltage  $V_L$  which is about 30 to 50% of rated voltage.

The power factor at standstill

$$\cos \varphi_L = \frac{P_L}{m_1 V_L I_L} \quad (22-8)$$

is larger than that at no-load (see Fig. 21-2) but is still small due to the high reactive current component necessary to produce the stator and rotor leakage fluxes.

The measured quantities  $V_L$ ,  $I_L$ , and  $P_L$  determine the short-circuit impedance  $Z_L$ , the short-circuit resistance  $R_L$ , and the short-circuit reactance  $X_L$ .

$$Z_L = \frac{V_L}{I_L} \quad R_L = \frac{P_L}{m_1(I_L)^2} \quad X_L = \sqrt{Z_L^2 - R_L^2} \quad (22-9)$$

On the other hand, the equivalent circuit Fig. 22-2 yields

$$R_L \approx r_1 + r_2' \quad X_L = \frac{x_1}{1 + \tau_2} + x_2' - \frac{r_1 r_2'}{x_m} \quad (22-10)$$

where  $\tau_2 = x_2'/x_m$  (Eq. 19-12)

The stator resistance  $r_1$  is normally measured in connection with the no-load test. Since  $R_L$  is known from Eq. 22-9

$$r_2' \approx R_L - r_1 \quad (22-11)$$

For the separation of  $x_1$  and  $x_2'$  observe that  $\tau_2$  is small, about 0.03 to 0.06, and also that the quantity  $r_1 r_2'/x_m$  is small (especially for medium-size and larger machines) so that with fair approximation

$$X_L \approx x_1 + x_2' \quad \text{and} \quad x_1 \approx x_2' \approx \frac{X_L}{2} \quad (22-12)$$

With this value of  $x_1$  the main flux parameters  $x_m$  and  $r_m$  can now be determined (Eqs. 22-4 to 22-7).

**22-3. Per-unit values of the parameters.** The parameters can be expressed either in ohms or in "per-unit", i.e., as fractions of a fixed unit of impedance. The advantage of the "per-unit" expression of the parameters for transformers has been explained in Art. 8-4. The same advantage exists here. When expressed in "per-unit", the parameters apply to a wide range of induction motors, i.e., to induction motors of different sizes, different speeds, different voltages, etc. When expressed in ohms, the parameters apply to a specific motor having a fixed speed, fixed output, fixed voltage, etc. The unit of impedance in which the parameters of induction motors are expressed, is defined as follows:

Unit voltage = rated voltage per phase.

Unit current = current per phase which corresponds to the output at the shaft

$$= I_{HP} = \frac{HP \times 746}{m_1 V_1}$$

Unit impedance = unit voltage/unit current.

Unit power = unit current  $\times$  unit voltage.

When expressed as fractions of the so defined unit of impedance, the parameters of polyphase induction motors (at rated loads) are approximately:

$$r_1 = 0.01 \text{ to } 0.05 \quad r_2' = 0.01 \text{ to } 0.05 \quad r_m = 0.02 \text{ to } 0.03$$

$$x_1 = 0.06 \text{ to } 0.12 \quad x_2' = 0.08 \text{ to } 0.12 \quad x_m = 1.5 \text{ to } 3.5$$

The larger values of  $r_1$  and  $r_2'$  apply to small motors, the smaller values to large motors. The smaller values of  $x_1$  and  $x_2'$  apply to high-speed machines; the larger values, to lower-speed machines. The lower values of  $x_m$  apply to lower-speed machines; the higher values, to high-speed machines.

#### 22-4. Influence of the parameters on the performance of the motor.

The performance of an induction motor is characterized by the following six quantities:

- (a) Heating of the windings and iron.
- (b) Efficiency.
- (c) Power factor.
- (d) Pull-out torque.
- (e) Starting current (inrush).
- (f) Starting torque.

The requirements with respect to the magnitudes of the parameters, are not the same for all six quantities; they partially contradict each other, so that *compromises must be made by the designer*. These contradictions should be noted in the discussions below.

(a) The heat of the windings and iron depends upon the  $I^2r$  losses and the iron losses. Since the currents are determined by the load the  $I^2r$  losses become small when  $r_1$  and  $r_2'$  are made small, i.e., when as much winding material as possible is arranged in the available space. It will be shown under (f) that a certain value of  $r_2'$  is necessary to produce the desirable starting torque. In order to make the iron losses due to the main flux small, it is necessary to make the main flux small. However, since the torque is determined by the main flux and the rotor currents, a small main flux requires high currents and high  $I^2R$  losses. Also with respect to the pull-out torque, a small flux is not permissible. With respect to heating the rotational iron losses should be made as small as possible.

(b) The efficiency is determined by the total losses of the motor. The lower the losses at a given load the higher will be the efficiency at this load. The consideration for low  $I^2R$  and iron losses is given under (a).

(c) Consider Fig. 22-3. The point  $A$  on the circle corresponds to a certain load:  $OA$  is the total current at this load and  $BA$  is the reactive current component of  $OA$ . At no-load (point  $P_0$ ) the current  $I_0$  is almost equal to the current  $I_\phi$  which sustains the main flux (see Art.

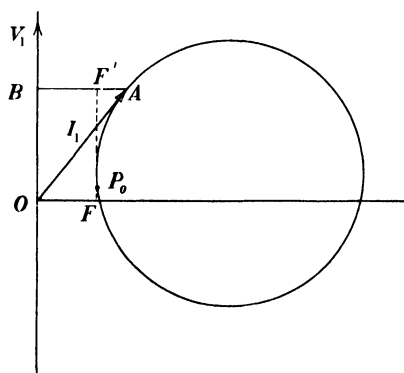


FIG. 22-3. Reactive current of the induction motor.



22-1). In the circle diagram  $I_\phi$  is practically equal to the reactive current  $OF$ . Considering the reactive current at load  $BA$ , it consists of two parts,  $BF' = OF = I_\phi$  and  $F'A$ . The first part is necessary to sustain the main flux, and the second part is necessary to sustain the leakage fluxes of stator and rotor. If there were no leakage fluxes, only the reactive current  $I_\phi$  would appear (at all loads) and the geometric locus of the end-point of the primary current  $I_1$  would be a straight vertical line through the point  $F$ . These are the leakage fluxes which make the geometric locus of the end-point of  $I_1$  become a circle.

For a high power factor a low reactive current is necessary, i.e., a low value of  $I_\phi$  and small leakage reactances  $x_1$  and  $x_2'$  are necessary. For a low value of  $I_\phi$  the air gap must be small and the flux must be small. For this reason the air gap of induction motors is kept as small as mechanically permissible. A small flux is not permissible with respect to the considerations under (a). It will be seen under (e) that the leakage reactances cannot be made too small if the starting current (inrush) requirements are to be satisfied.

(d) Consider Fig. 21-5. The distance between the point  $P_\infty$  and the imaginary axis,  $P_\infty D$ , is equal to the primary copper losses  $m_1 I_1^2 r_1$ . The higher these copper losses, the more the point  $P_\infty$  moves up the circle, and the smaller becomes the pull-out torque. With respect to a high pull-out torque the primary resistance must be small. Physically this can be explained in the following way: the torque is determined by the power of the rotating field, and the higher the primary losses for a given power input, the smaller is the power of the rotating flux field.

It can be seen from Fig. 21-5 that the pull-out torque increases with increasing diameter of the circle, just as the locked-rotor current (starting current) increases with increasing diameter of the circle. Consider Fig. 22-2 which represents the equivalent circuit of the motor at locked rotor. Here, as at all large slips, the magnitude of the primary current is determined mainly by the stator and rotor leakage reactances. The smaller the values of  $x_1$  and  $x_2'$ , the larger is the diameter of the circle and the pull-out torque. However, small values of  $x_1$  and  $x_2'$  are not permissible with respect to the locked-rotor (starting) current.

The secondary resistance  $r_2'$  has no influence on the magnitude of the pull-out torque because  $r_2'$  has no influence on the power of the rotating field. The magnitude of  $r_2'$  influences only the slip at which the pull-out torque occurs (the pull-out slip, see Eq. 19-13).

(e) It has been explained under (d) that the starting current is determined mainly by the leakage reactances  $x_1$  and  $x_2'$  (in the smallest polyphase motors also by  $r_1$  and  $r_2'$ ). A high starting current is not desirable because of the voltage drop which it produces in the supply lines, and standards, limiting the inrush current, have been established for small and medium-size motors by the NEMA (National Electric Manufacturers Association). The leakage reactances  $x_1$  and  $x_2'$  must have certain values in order to meet these stand-

ards. Thus the limitations with respect to the starting current are contrary to the requirements for a high power factor and high pull-out torque.

(f) Eq. 19-8 for the torque shows that at standstill the torque is directly proportional to the copper losses of the rotor  $m_1 I_2'^2 r_2'$ . A high starting torque is only possible when the copper losses of the rotor at standstill are high. At standstill  $I_2' \approx I_1$ , i.e., at standstill  $I_2'$  is almost equal to the locked-rotor current. This current is limited by the source of power supply. Therefore, for a high starting torque the rotor resistance  $r_2'$  must be high. A high rotor resistance contradicts the requirements for a high efficiency.

**22-5. Skin-effect rotors.** Influence of skin effect on rotor parameters  $r_2'$  and  $x_2'$ . The requirements for a large  $r_2'$  with respect to the starting torque and a small  $r_2'$  with respect to the efficiency can be easily realized with the wound rotor motor by inserting a resistor between the slip rings for starting and cutting out this resistance during running. However, there are certain rotor-slot arrangements which make it possible to achieve a high resistance at starting and a low resistance during running also for the squirrel-cage rotor.

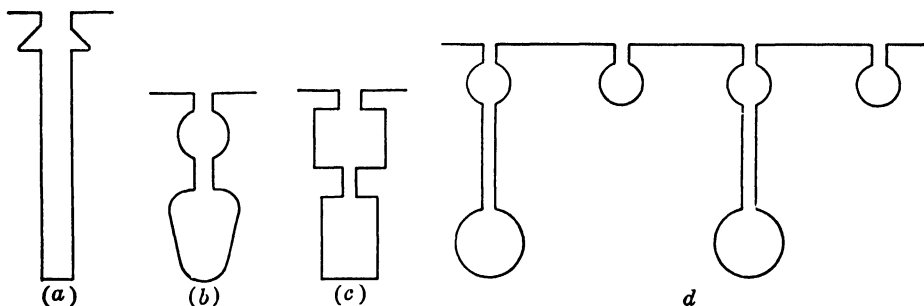


FIG. 22-4. Slot shapes of squirrel-cage rotors for skin effect.

These rotor-slots arrangements are shown in Fig. 22-4. The first one (a) consists of a deep bar (*deep-bar rotor*), and the second one (Fig. 22-4, b and c) consists of two cages (*double-cage or Boucherot rotor*). The operation of these rotors is based upon the *skin-effect* phenomenon which, at *higher frequencies*, allows the current to flow only in the top part of the conductor in the case of the deep-bar rotor and mainly in the upper conductor in the case of the double-cage rotor.

For the skin-effect phenomenon in the deep bar, the following explanation can be given. Consider Fig. 22-5 which shows a slot with a bar and the *slot-leakage flux* produced by the current in the bar. The main flux has its path through the core *below* the slot. Assume that the bar is divided into many strands across the slot. The strands which lie at the bottom of the slot are interlinked with a much larger leakage flux than the strands which

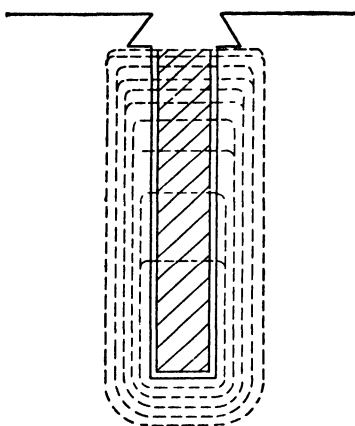


FIG. 22-5. Explanation of the skin effect in conductors due to the cross flux in the slot.

lie at the top of the slot. Therefore, the leakage reactance of the bottom strands is much larger than the leakage reactance of the top strands. Since all strands are linked by the same main flux and, therefore, the induced emf is the same in all strands, a much larger current will flow in the top strands than in the bottom strands. This effect is more noticeable the *higher the frequency*, because the leakage reactance is proportional to the frequency. At standstill the rotor frequency is highest (equal to the line frequency, Eq. 17-21) and at this frequency the rotor current flows only in the upper part of the rotor conductor and the rotor resistance appears to be high.

In the double-cage rotor each conductor is divided essentially in two parts, one part lying in the top cage, the other part in the bottom cage. Both cages are separated by a relatively long and narrow slit and therefore the bottom part of the bar is interlinked with a much higher leakage flux than the top part, i.e., the leakage reactance of the bottom bar is much larger than that of the top bar. The effect of higher frequency thus is the same as in the deep-bar motor. At standstill, current flows mainly in the top bar whereas the bottom bar carries only a small current. The top bar usually has a higher resistance than the bottom bar. For this reason the top cage often is referred to as the high-resistance-low-reactance and the bottom cage as the low-resistance-high-reactance cage.

As the motor comes up to speed, the rotor frequency decreases and therefore the leakage reactance of the assumed single strands in the deep-bar rotor or of the two bars in the double-cage rotor decreases. The influence of the skin effect becomes smaller. At low slips and at normal slip the frequency of the rotor current is very small and the leakage reactance of the single strands of the deep bar or of the two cages of the double cage is negligible as compared with the resistance. The current now is distributed uniformly over the deep bar or divided in the ratio of the resistances of both cages in the double-cage rotor.

The starting action in the skin-effect squirrel-cage rotors is similar to that of the slip-ring rotor: the resistance of the rotor circuit decreases with increasing speed. At normal speed the resistance of both kinds of rotors is equal to the d-c resistance of the rotor winding.

**22-6. Influence of saturation on the parameters  $x_1$  and  $x_2'$ .** It has been explained in Arts. 3-1 and 17-1 that the magnitude of the main flux reactance,  $x_m$ , depends upon the saturation of the main flux path. However this react-

ance changes but little between no-load and full-load. At high slips, for example at starting, the magnitude of the main flux reactance is of little importance since it is always large in comparison with the rotor impedance at high slips (see Fig. 22-2), so that little current flows through it and its presence can be disregarded (see Art. 22-2). The result is that  $x_m$  can be treated as a constant parameter, although it may have different values at full-load and at high slips.

The leakage reactances,  $x_1$  and  $x_2'$ , have been tacitly treated as constants (except the case of the skin-effect motor in which  $x_2'$  is a variable, see foregoing article). The magnetic path of the leakage fluxes lies, to a great part, in the air for which the permeability  $\mu$  is a constant (see Art. 17-1), so that  $x_1$  and  $x_2'$  are practically constant between no-load and over-load, i.e., as long as the stator and rotor currents are not too high. At larger slips, and especially at standstill, these currents are high and they more or less saturate the iron part of the leakage-flux path. Because of this fact,  $x_1$  and  $x_2'$  may be considerably smaller at starting than at running with full-load, namely, about 75 to 85% of the latter values.

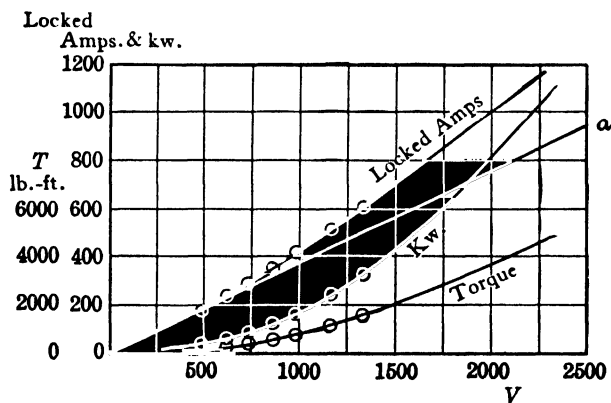


FIG. 22-6. Influence of saturation on the leakage reactances. Locked rotor characteristics of a 600-HP, 6-pole motor with squirrel-cage rotor.

The short-circuit (locked) test usually is made at reduced voltage ( $V_L$ ), i.e., at a relatively small locked-rotor current ( $I_L$ ) at which the saturation is not yet noticeable. Therefore, the determination of the locked current at rated voltage ( $V_1$ ) by multiplying the tested current  $I_L$  by the ratio  $V_1/V_L$  may yield a value too small for the locked current; the real locked current at full voltage may be much larger. Fig. 22-6 shows the locked current  $I_L$  as a function of voltage  $V_L$  for a 600-hp 6-pole motor. The straight line  $a$  would be obtained if there were no saturation. Due to saturation the locked current at normal voltage is 35% higher than without saturation, i.e., the equivalent leakage reactance at normal voltage is about 35% smaller than without saturation.

Since the influence of saturation in the leakage paths occurs only at high current (at high slip) while at normal current there is no saturation in the leakage paths, then for calculating the performance (currents, power factor) at small slips the non-saturated leakage reactances have to be used. On the other hand, for calculating the performance at high slips (starting current and starting torque) the saturated leakage reactances have to be used. The current at pull-out slip is also relatively high and the saturation of the leakage paths may affect the magnitude of the pull-out torque.

**22-7. Summary on variation of parameters with the slip.** It follows from Arts. 25-5 and 22-6 that, due to

	$x_1$	$x_2'$	$r_2'$
<i>Skin effect in rotor bars</i>	no influence	decreases with increasing slip	increases with increasing slip
<i>Saturation of the leakage</i>	decreases with increasing slip	decreases with increasing slip	no influence

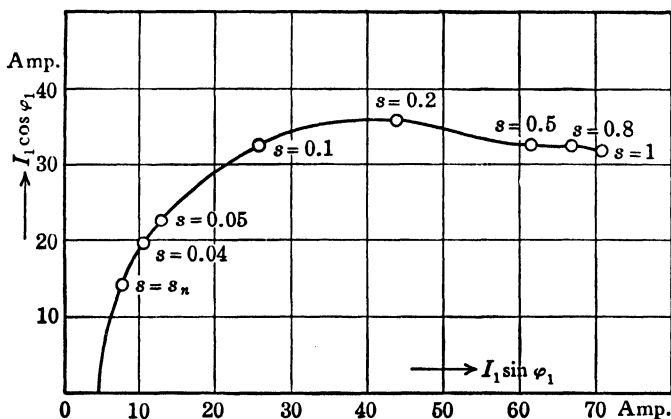


FIG. 22-7. Current diagram of a 20-HP, 6-pole, 50-cycle squirrel-cage motor with deep bars.

It has been mentioned previously (Art. 21-3) that when the parameters of the machine are not constant quantities but change with the slip, the geometric locus of the endpoint of the primary current is not a circle. Fig. 22-7 shows the current diagram of a 20-HP deep-bar motor with six poles at 50 cycles. Fig. 22-8 shows the current diagram of a 20-HP double-cage motor with four poles at 50 cycles.

Fig. 22-9 shows the characteristic curves of a 3-HP, 4-pole, 3-phase,

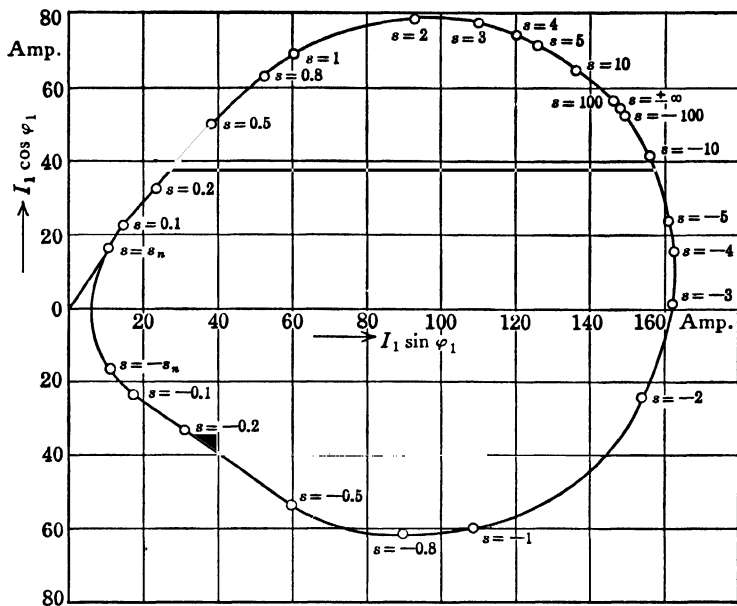


FIG. 22-8. Current diagram of a 20-HP, 4-pole, 50-cycle squirrel-cage motor with double cage.

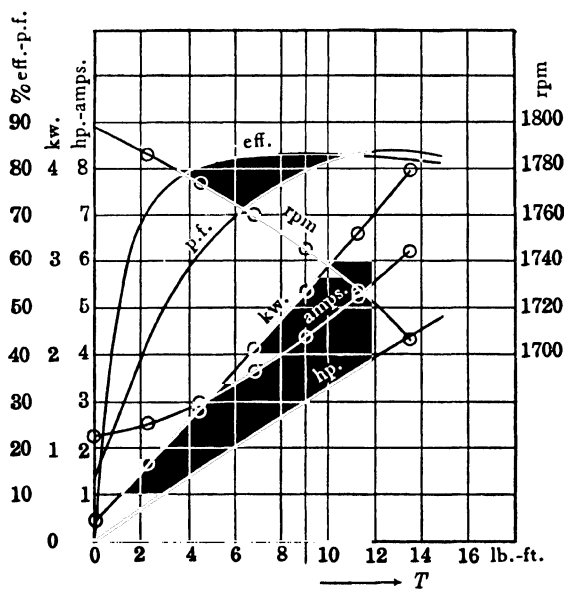


FIG. 22-9. Characteristic curves of a 3-HP, 3-phase, 4-pole motor with squirrel-cage rotor.

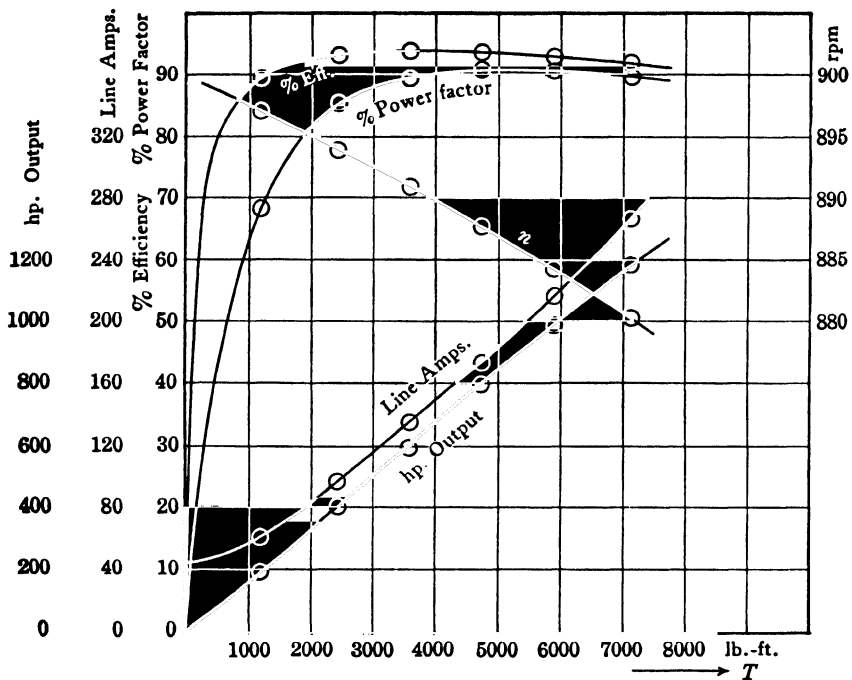


FIG. 22-10. Characteristic curves of an 800-HP, 8-pole, 3-phase motor with squirrel-cage rotor.

220-volt, 60-cycle, 1745-rpm squirrel-cage motor. Fig. 22-10 shows the characteristics of an 800-HP, 8-pole, 3-phase, 2300-volt, 60-cycle, 888-rpm squirrel-cage motor. Up to about  $1\frac{1}{2}$  times rated torque the slip is proportional to the torque.

The influence of voltage and frequency variation on the performance of polyphase induction motors is shown in Table 22-1.

**Example 22-1.** The six parameters of a 3-HP, 440/220-volt, 3-phase, 60-cycle, 4-pole squirrel-cage induction motor will be determined from a no-load and a locked-rotor test. The stator resistance at 25°C is 2.26 ohms, and the friction and windage loss is 44 watts. Stray load loss = 48 watts

*No-load test—75°C*

$$V_1 = 440 \text{ volts}$$

$$I_0 = 2.36 \text{ amp}$$

$$P_0 = 211 \text{ watts}$$

*Locked-rotor test (full voltage)—75°C*

$$V_L = 440 \text{ volts} = V_1$$

$$I_L = 29.1 \text{ amp}$$

$$P_L = 13.92 \text{ kw}$$

*Locked-rotor test (reduced voltage)*

$$V_L = 76 \text{ volts}$$

$$I_L = 4.25 \text{ amp}$$

The skin-effect factor for  $r_2'$  is 1.30 and for  $x_2'$  is 0.97 (see Fig. 22-11).

TABLE 22-1. GENERAL EFFECT OF VOLTAGE AND FREQUENCY VARIATION ON INDUCTION-MOTOR CHARACTERISTICS  
+ = Increase  
- = Decrease

	Starting and Maximum Running Torque	Synchro-nous Speed	% Slip	Full-load Speed	EFFICIENCY		POWER FACTOR			Full-load Current	Starting Current	Temperature Rise, Full Load	Max-imum Overload Capacity	Mag-netic Noise, No-Load in Partic-ular
					Full Load	$\frac{1}{2}$ Load	Full Load	$\frac{1}{2}$ Load	$\frac{1}{4}$ Load					
VOLT-AGE VARI-ATION	120% Voltage	No change	-30%	+ 1.5%	Small +	$\frac{1}{2}$ to 2 points	5 to 15 points	10 to 30 points	15 to 40 points	-11%	+25%	— 5 to 6 C	+44%	Notice-able +
	110% Voltage	No change	-17%	+1%	+ $\frac{1}{2}$ to 1 point	Prac-tically no change	1 to 2 points	3 to 4 points	5 to 6 points	-7%	+ 10 to 12%	— 3 to 4 C	+21%	Slight +
	Func-tion of Voltage	Con-stant	1 (Voltage) <sup>2</sup>	(Syn speed, slip)							Voltage		(Voltage) <sup>2</sup>	
FRE-quency VARI-ATION	90% Voltage	No change	+23%	-11%	- 2 points	Prac-tically no change	1 to 2 points	+ 2 to 3 points	+ 4 to 5 points	+11%	— 10 to 12%	+ 6 to 7 C	-19%	Slight —
	105% Fre-quency	+5%	Practically no change	+ 5%	Slight +	Slight +	Slight +	Slight +	Slight +	Slight —	— 5 to 6%	Slight —	Slight —	
	Func-tion of Fre-quency	Fre-quency		(Syn speed, slip)							1 Frequency			
	95% Fre-quency	-5%	Practically no change	- 5%	Slight —	Slight —	Slight —	Slight —	Slight —	Slight +	+ 5 to 6%	Slight +	Slight +	Slight +

NOTE: This table shows general effects, which will vary somewhat for specific ratings.



## Saturated reactances

$$Z_L = \frac{440}{\sqrt{3} \times 29.1} = 8.73 \text{ ohms}$$

$$R_L = \frac{13,920}{3 \times (29.1)^2} = 5.48 \text{ ohms}$$

$$X_L = \sqrt{Z_L^2 - R_L^2} = 6.80 \text{ ohms}$$

$$r_1(\text{at } 75^\circ\text{C}) = 2.26 \times \frac{234.5 + 75}{234.5 + 25} = 2.69 \text{ ohms}$$

$$r_2' = 5.48 - 2.69 = 2.79 \text{ ohms}$$

$$x_1 = x_2' = 3.40 \text{ ohms}$$

## Unsaturated reactances

$$Z_L = \frac{76}{\sqrt{3} \times 4.25} = 10.3 \text{ ohms}$$

$$X_L = \sqrt{(10.3)^2 - (5.48)^2} = 8.72 \text{ ohms}$$

$$x_1 = \frac{8.72}{2} = 4.36 \text{ ohms}$$

The ratio of unsaturated leakage reactance to saturated leakage reactance (4.36/3.40) is called the *saturation factor*, and equals 1.28.

In order to determine the running performance from the equivalent circuit it is necessary to correct  $r_2'$  and  $x_2'$  for skin-effect since the unsaturated parameters above were taken at 60 cycles.

$$(\text{corrected}) = \frac{2.79}{1.30} = 2.14 \text{ ohms} = r_2'$$

$$(\text{corrected}) = \frac{4.36}{0.97} = 4.50 \text{ ohms} = x_2'$$

$$x_m = \frac{254 - 2.36 \times 4.36}{2.36} = \frac{243.7}{2.36} = 103 \text{ ohms}$$

$$P_{h+e} + P_{\text{ir.rot}} = 211 - 3(2.36)^2 \times 2.69 - 44 = 122 \text{ watts}$$

It will be assumed that one half of the iron losses are due to the main flux so that:

$$P_{h+e} = 61 \text{ watts}$$

$$g_m = \frac{61}{3 \times (243.7)^2} = 3.43 \times 10^{-4} \text{ mho}$$

$$r_m = g_m x_m^2 = 3.43 \times 10^{-4} \times (103)^2 = 3.66 \text{ ohms}$$

(check)

$$m_1 I_0^2 r_m = 3 \times (2.36)^2 \times 3.66 = 61 \text{ watts}$$

$$r_m = \frac{61}{3 \times (2.36)^2} = 3.66 \text{ ohms}$$

The parameters determined above are tabulated in Ex. 19-1.

**Example 22-2.** The example of Chap. 19 will now be solved on a per-unit basis.

$$\text{Unit voltage} = \frac{440}{\sqrt{3}} = 254 \text{ volts}$$

$$\text{Unit current} = \frac{3 \times 746}{3 \times 254} = 2.94 \text{ amp} = I_{\text{HP}}$$

$$\text{Unit impedance} = \frac{254}{2.94} = 86.5 \text{ ohms}$$

$$\text{Unit power} = 254 \times 2.94 = 746 \text{ watts} = 1 \text{ HP}$$

$$\text{Unit speed} = 1800 \text{ rpm}$$

$$\text{Unit torque} = 7.04 \times 3 \times \frac{\text{unit power}}{\text{unit speed}} = 8.80 \text{ lb-ft}$$

(a) *Parameters for starting (p-u)*

$$r_1 = 0.0311$$

$$r_2' = 0.0322$$

$$(x_1 = x_2') = 0.0393$$

$$x_m = 1.19$$

$$r_m = 0.0423$$

(b) *Parameters for running (p-u)*

$$r_1 = 0.0311$$

$$r_2' = 0.0248$$

$$x_1 = 0.0505$$

$$x_2' = 0.0520$$

$$x_m = 1.19$$

$$r_m = 0.0423$$

(a) *Starting performance (p-u)*

$$r_2' \left( \frac{1-s}{s} \right) = 0$$

$$\dot{Z}_1 = 0.0500 / \underline{51.6}$$

$$\dot{Z}_2' = 0.0508 / \underline{50.6}$$

$$\dot{Z}_m = 1.19 / \underline{87.96}$$

From Eq. 18-10

$$1/\underline{0} = \dot{I}_1 \left[ 0.0500 / \underline{51.6} + \frac{0.0508 / \underline{50.6} \times 1.19 / \underline{87.96}}{0.0508 / \underline{50.6} + 1.19 / \underline{87.96}} \right]$$

$$\dot{I}_1 = 10.05 / \underline{-51.8} \text{ (p-u)}$$

(check)  $I_1(\text{amp}) = 10.05 \times 2.94 = 29.6$

$$\begin{aligned}\dot{I}_2' &= 10.05 / -51.8 \times \frac{1.19 / 87.96}{0.0508 / 50.6 + 1.19 / 87.96} \\ &= 9.66 / -50.4\end{aligned}$$

The starting torque on a p-u basis is the same as  $P_{\text{rot.f}}$  on a p-u basis (see Eq. 19-9):

$$P_{\text{rot.f}} = (9.66)^2 \times \frac{0.0322}{1.0} = 3.0$$

$$T_{\text{st p-u}} = 3.0$$

$$(check) \quad T_{\text{st}} (\text{lb-ft}) = 3.0 \times 8.80 = 26.4$$

$$(b) \text{ Running performance} \quad s = 0.03$$

$$\begin{aligned}r_2' \left( \frac{1-s}{s} \right) &= 0.80 \\ \dot{Z}_1 &= 0.0593 / 58.3 \\ \dot{Z}_2' &= 0.825 / 3.60 \\ \dot{Z}_m &= 1.19 / 87.96\end{aligned}$$

from Eq. 18-10

$$\begin{aligned}\dot{I}_1 &= \frac{1.0 / 0}{0.0593 / 58.3 + \frac{0.825 / 3.60 \times 1.19 / 87.96}{0.825 / 3.60 + 1.19 / 87.96}} \\ &= 1.42 / -38.2\end{aligned}$$

$$\text{Input power factor} = \cos 38.2^\circ = 0.785$$

$$\begin{aligned}\dot{I}_2' &= 1.42 / -38.2 \times \frac{1.19 / 87.96}{0.825 / 3.60 + 1.19 / 87.96} \\ &= 1.115 / -5.74\end{aligned}$$

$$P_{\text{rot.f}} = (1.115)^2 \times \frac{0.0248}{0.03} = 1.025$$

$$T_{\text{dev}} = 1.025$$

$$(check) \quad T_{\text{dev}} (\text{lb-ft}) = 1.025 \times 8.80 = 9.05$$

$$\text{Mech. loss torque (p-u)} = \frac{7.04 \times \frac{(48 + 44 + 61)}{1800}}{8.80} = 0.068$$

$$T_{\text{del}} (\text{p-u}) = 1.025 - 0.068 = 0.957$$

$$(check) \quad T_{\text{del}} (\text{lb-ft}) = 0.957 \times 8.80 = 8.40$$

$$\text{Power input} = 3 \times 1.0 \times 1.42 \times \cos 38.2^\circ = 3.35$$

## Losses

$$m_1 I_1^2 r_1 = 0.189$$

$$m_1 I_2'^2 r_2' = 0.093$$

$$\text{no-load iron} = 0.163$$

$$\text{stray load} = 0.064$$

$$\text{Friction and windage} = 0.059$$

$$\text{Total} = 0.568$$

$$P_{\text{del}} = 3.35 - 0.568 = 2.78$$

(check)

$$P_{\text{del}} (\text{watts}) = 2.78 \times 746 = 2076 = 2.78 \text{ HP}$$

$$\text{Efficiency} = \frac{2.78}{3.35} = 0.83$$

$$\text{slip} = \frac{0.093}{3.35 - (0.189 - 0.082)} = 0.03 \quad (\text{check})$$

$$s_{\text{normal}} = \frac{3.0}{2.78} \times 0.03 = 0.0324$$

From Eq. 19-13

$$s_{\text{p.o.}} = \frac{1.042 \times 0.0257}{0.0505 + 1.042 \times 0.0520} = 0.246$$

$$r_2' \left( \frac{1-s}{s} \right) = 0.0758$$

$$\dot{Z}_2' = 0.1133 / 27.3$$

From Eq. 18-10

$$\dot{I}_1 = 6.12 / -41.4$$

$$\dot{I}_2' = 5.85 / -36.6$$

$$P_{\text{rot.f}} = (5.85)^2 \times \frac{0.0248}{0.246} = 3.44$$

$$T_{\text{p.o.}} = 3.44$$

(check)

$$T_{\text{p.o.}} (\text{lb-ft}) = 3.44 \times 8.80 = 30.2$$

The normal torque delivered by this machine at 3.0 HP output,  $s = 0.0324$ , is

$$T = \frac{5250}{1800(1 - 0.0324)} \times 3 = 9.05 \text{ lb-ft}$$

$$= 1.025 \text{ p-u}$$

$$\frac{T_{\text{st}}}{T_n} = \frac{3.0}{1.025} = 2.92$$

$$\frac{T_{\text{p.o.}}}{T_n} = \frac{3.44}{1.025} = 3.36$$

## PROBLEMS

For the influence of skin-effect on  $r_2'$  and  $x_2'$  use Fig. 22-11. For saturation factors use Fig. 22-12.

The *saturation factor* is defined as the ratio of the unsaturated values of  $x_1$  and  $x_2'$ , to the saturated values of these reactances.

1. For the motor of Examples 22-1 and 22-2 calculate the primary current and primary power factor for slips of 1.0, 0.8, 0.6, 0.4, 0.2, 0.1, and 0.03.

2. Determine the developed torque-speed characteristic for the motor of Examples 22-1 and 22-2, using the slips specified in Problem 1. Calculate on a p-u basis.

3. Repeat Problem 1 for 115% rated voltage.

4. Repeat Problem 1 for 85% rated voltage.

5. Repeat Problem 2 for 115% rated voltage.

6. Repeat Problem 2 for 85% rated voltage.

7. Construct the circle diagram for the motor of Examples 22-1 and 22-2, using the unsaturated values of  $x_1$  and  $x_2'$ . From this diagram determine the developed torque-speed characteristic for slips of 1.0, 0.8, 0.6, 0.4, 0.2, 0.1, and 0.03 and compare with Problem 2.

8. The motor of Examples 22-1 and 22-2 is required to develop a higher starting torque. To do this the end rings of the squirrel cage were turned down in a lathe so that the rotor resistance at standstill, as well as at running, was increased 25%. Determine the starting performance.

9. Determine the running performance of the motor in Problem 8 at a slip of 0.04.

10. Determine the pull-out slip and pull-out torque for the motor in Problem 8.

11. It is required to reduce the starting line current of the motor in Examples 22-1 and 22-2 by 20%.

(a) If an autotransformer is used determine the turn ratio.

(b) If series reactors are used determine their value in ohms.

(c) What is the new starting torque developed (express as a percentage of starting torque developed in Examples 22-1 and 22-2).

12. The six parameters of an 800-HP, 2300-volt, 3-phase, 60-cycle, 8-pole, shallow-bar, squirrel-cage induction motor are to be determined from the no-load and locked-rotor tests given below. The stator resistance is 0.103 ohm per phase at 75°C; the stator is wye-connected. (Neglect skin effect.)

<i>No-load test</i>	<i>Locked-rotor test (full voltage)</i>
$V_1 = 2300$ volts	$V_L = 2300$ volts
$I_0 = 43$ amp	$I_L = 1200$ amp
$P_0 = 12.5$ kw	$P_L = 1060$ kw

*Locked-rotor test (reduced voltage)*

$V_L = 600$  volts

$I_L = 240$  amp

The friction and windage loss is 4.4 kw, and the iron losses due to the main flux are 40% of the total no-load iron losses. Assume the temperature of the stator winding at no-load and locked-rotor tests is 75°C.

13. The stray-load losses of the motor of Problem 12 are 5.0 kw. Determine the running performance for a slip of 0.013. Calculate throughout in p-u.

14. Determine the starting performance of the motor of Problem 12.

15. Determine the primary current and power factor at slips of 1.0, 0.8, 0.6, 0.4, 0.2, 0.1, and 0.013 for the motor of Problem 12. Plot.
16. Plot the developed torque-speed characteristic for the motor of Problem 12 at slips of 1.0, 0.8, 0.6, 0.4, 0.2, 0.1 and 0.013.
17. Repeat Problem 15 for 115% rated voltage.
18. Repeat Problem 15 for 85% rated voltage.
19. Repeat Problem 16 for 115% rated voltage.
20. Repeat Problem 16 for 85% rated voltage.
21. Determine the pull-out slip and pull-out torque for the motor of Problem 12.
22. It is desired to reduce the starting current of the motor in Problem 12 by 30%. (a) Determine the series resistors which will accomplish this reduction in current. (b) For reactor starting what magnitude of reactance is needed?
23. No load and locked-rotor tests were taken on a  $7\frac{1}{2}$ -HP, 440-volt, 3-phase, 60-cycle, 6-pole, wye-connected, squirrel-cage induction motor, and the following data were recorded:

<i>No-load test</i>	<i>Locked-rotor test (full voltage)</i>
$V_1 = 440$ volts	$V_L = 440$ volts
$I_0 = 5.84$ amp	$I_L = 60.4$ amp
$P_0 = 600$ watts	$P_L = 24.16$ kw
<i>Locked-rotor test (reduced voltage)</i>	
	$V_L = 210$ volts
	$I_L = 13.5$ amp

The stator resistance per phase is 1.2 ohms at 75°C. The friction and windage loss is 60 watts and the iron losses due to the main flux are 50% of the total no-load iron losses. Assume the temperature of the stator winding at both no-load and locked-rotor tests to be 75°C.

Determine the six parameters of the equivalent circuit in ohms and p-u for both starting and running performance.

24. The stray load losses of the motor in Problem 23 are 93 watts. Determine the running performance at  $s = 0.024$ .
25. Determine the starting performance of the motor in Problem 23.
26. Determine the primary current and power factor for the motor of Problem 23 for slips of 1.0, 0.8, 0.6, 0.4, 0.2, 0.1 and 0.024. Calculate in p-u. Plot.
27. Determine the developed speed-torque characteristic in p-u for the motor of Problem 23 at slips of 1.0, 0.8, 0.6, 0.4, 0.2, 0.1 and 0.024.
28. Calculate the pull-out slip and pull-out torque (in p-u) for the motor of Problem 23.
29. Repeat Problem 26 for 115% rated voltage.
30. Repeat Problem 26 for 85% rated voltage.
31. Repeat Problem 27 for 115% rated voltage.
32. Repeat Problem 27 for 85% rated voltage.
33. Fig. 22-13 refers to 3-phase, 4-pole, 60-cycle, 230-volt induction motors. This figure can be used for preparation of problems on performance of polyphase induction motors. Resistances and reactances are in per-unit. Losses are given as a fraction of power output.  $x_1$  and  $x_2'$  are saturated values.

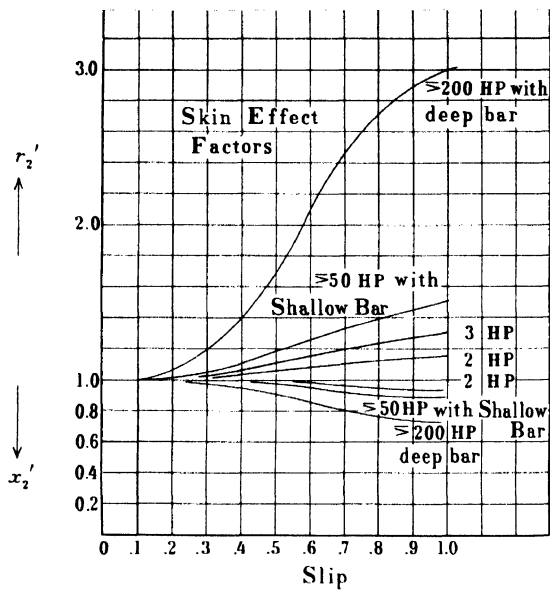


FIG. 22-11. Skin effect factors for problems.

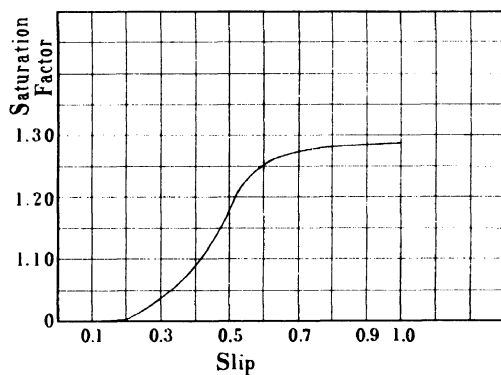


FIG. 22-12. Saturation factor for problems.

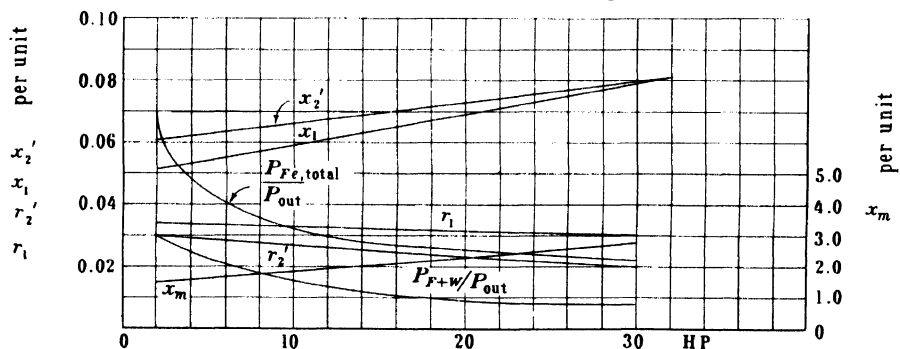


FIG. 22-13. Motor parameters and losses for 3-phase, 4-pole, 60-cycle motors.

## Chapter 23

### STARTING AND SPEED CONTROL OF THE POLYPHASE INDUCTION MOTOR

**23-1. Starting a squirrel-cage motor.** Curve  $T_M$  in Fig. 23-1 represents the torque-speed curve of a typical squirrel-cage motor. Once the squirrel-cage motor is constructed, its parameters cannot be changed, and its torque-speed characteristic is fixed. (In a wound-rotor motor, resistance can be inserted in the rotor circuit, changing  $r_2'$ .) During the starting period the motor goes through the total torque-speed curve  $T_M$ , Fig. 23-1, until it reaches the speed at which the motor torque is equal to the load torque. At no speed below rated should the load torque  $T_L$  be larger than the motor torque  $T_M$ ; otherwise the motor will be unable to reach its rated speed. The difference  $(T_M - T_L)$  is used to accelerate the rotating masses. The larger this difference, the shorter is the accelerating period.

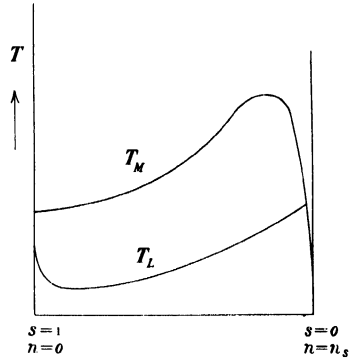


FIG. 23-1. Torque-speed characteristics of a squirrel-cage motor and its load.

Referring to Fig. 21-4, the position of point  $P_L$  determines the starting current and the starting torque. For a squirrel-cage motor, the *starting current is the same as the short-circuit current*. As the squirrel-cage motor starts, it draws at first its locked current from the line. As it speeds up and approaches its load condition, the current  $I_1$  in Fig. 21-4 moves along the circle from point  $P_L$  to the point corresponding to the load condition. The developed torque moves along the curve  $I_M$  in Fig. 23-1, first increasing up to pull-out torque and then decreasing to the value which corresponds to the load torque. The variation of the current and torque during the starting period depends solely upon the parameters of the motor and are independent of the opposing torque of the load.

When an induction motor with squirrel-cage rotor is connected to a distribution system which also supplies incandescent lamp loads, the high



starting current of the motor is undesirable since it may produce a considerable voltage drop and hence a variation in light intensity. When the voltage drop is large, other motors may "pull-out". In many cases, such as ventilating fans and centrifugal pumps, where the required starting torque is small, the starting current of the motor can be reduced, thereby decreasing the starting torque. This may be accomplished by the following means:

- (a) Series resistor
- (b) Series reactor
- (c) Autotransformer
- (d) Star-delta connection
- (e) Part-winding starting.

It follows from Eqs. 19-8 and 19-10 that the *torque* of the induction motor varies with the *square of its terminal voltage*. Thus an increase in the terminal voltage of 10 per cent raises the torque curve  $T_M$ , Fig. 23-1, 21 per cent and, vice versa, a decrease of the terminal voltage of 10 per cent lowers the torque curve 19 per cent. A reduction of the terminal voltage of the motor, in order to reduce the starting current, is used in the methods (a) to (d).

When a series resistor or reactor is used, the starting current of the motor, which in this case is equal to the line current, is reduced directly with its terminal voltage while the starting torque is reduced with the square of the terminal voltage. For example, with a series resistor or reactor which produces a voltage drop of 30 per cent, the line (motor) current will be 70 per cent of its full voltage value and the starting torque of the motor will be 49% of its original value.

When an autotransformer is used, Fig. 23-2, the line current and the motor current are not equal; the line current is the primary current of the transformer while the motor current is the secondary current; therefore, the

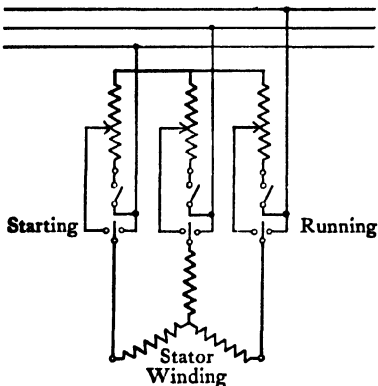


FIG. 23-2. Starting of a squirrel-cage motor with the aid of an autotransformer.

ratio of line current to motor current must be the same as the ratio of motor voltage (secondary voltage of the transformer) to line voltage (primary voltage of the transformer), for the primary and secondary kva must be the same ( $V_1 I_1 \approx V_2 I_2$ ). For example, if the secondary voltage of the transformer is 70% of the line voltage, the motor current is 70% of its original value and the line current is  $0.7(V_2/V_1) = 0.7 \times 0.7 = 0.49 = 49\%$  of the motor current at full voltage. At 70% voltage the motor torque is 49% of its original value as in the case of the series resistor or reactor. The autotransformer reduces the line current with the square of the motor terminal voltage

while the resistor or reactor reduces the line current, at the same starting torque, directly with the terminal voltage. For the same starting torque the autotransformer yields a larger reduction of the line current than the resistor or reactor but is more expensive than the latter.

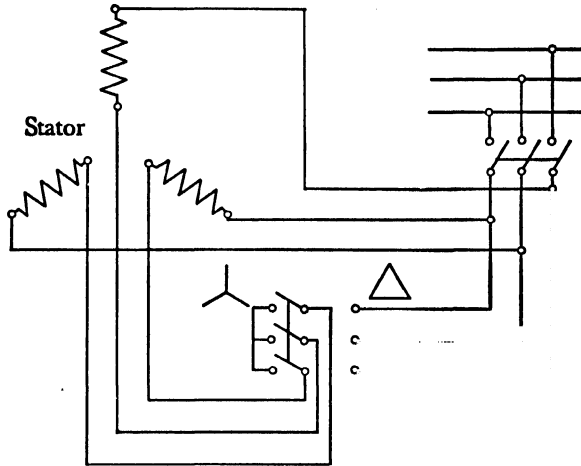


FIG. 23-3. Wye-Delta (Y-Δ) starting of a squirrel-cage motor.

The application of the star-delta connection is as follows: Normally, the motor operates with a delta-connected stator. At start, however, the winding is connected in star (Fig. 23-3). If the motor starts with a star-connected stator, the line current is  $\frac{1}{3}$  of the line current with a delta-connected stator. This is due to the fact that the phase voltage in the star connection is  $1/\sqrt{3}$  times the phase voltage in delta connection and the line current in star connection is also  $1/\sqrt{3}$  times the line current in delta connection. Also, the starting torque is decreased to  $\frac{1}{3}$  of its value with a delta-connected stator, since the change from delta to star decreases the phase voltage to  $1/\sqrt{3}$  of its original value and the torque is proportional to the square of the phase voltage. The delta-star transformation is used principally to start smaller motors.

In the part-winding starting method, the stator winding must consist, for normal operation, of two or more parallel circuits in each phase. For starting, first one of the parallel circuits is used and then the other circuits are switched separately onto the line. Using one of the parallel circuits increases the impedance of the stator winding and reduces starting current and starting torque.

The simplest arrangement for part-winding starting is that with only two parallel circuits in the stator winding. The distribution of the coil groups belonging to each of the two circuits can be made in different ways. For

example, assigning to the first coil group of a phase the number 1, all odd coil groups can be connected in series, making one circuit, and all even coil groups are then connected in series, making the other circuit. With this arrangement, called *alternate pole connection*, the motor draws from the line about 75 per cent of its full-winding starting current and develops 50 to 60 per cent of its full-winding starting torque. Two contactors are necessary for the two-circuit starting: a main contactor for connecting to the line the first circuit and a paralleling contactor which, after the motor comes up to speed, connects to the lines the second circuit (see Fig. 23-3a).

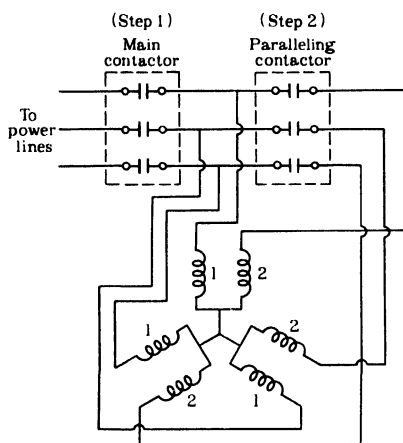


FIG. 23-3a. Part-winding starting.

**23-2. Starting of a wound-rotor (slip-ring) motor.** In the wound-rotor motor, the resistance of the rotor circuit is not fixed as is the case in the squirrel-cage motor; it can be varied between an infinitely large value (open slip rings) and the resistance of the rotor winding  $r_2'$  (slip rings short-circuited). The secondary resistance of the wound-rotor motor is in general  $r_2' + r_{ext}' = r_t'$ , where  $r_{ext}'$  is the external rotor resistance referred to the stator.

Consider a motor running with *constant* load torque. According to Eq. 19-9 this means that  $P_{rot,f}$  is constant. The electric power of the rotor is  $P_e = sP_{rot,f}$ . Since  $P_{rot,f}$  is a constant quantity, the electric power of the rotor must be, for constant load torque,

$$P_e = s \times \text{constant} \quad (23-1)$$

Assume now that the rotor resistance of the motor under consideration has been doubled, from  $r_2'$  to  $2r_2'$ , by reducing the cross-section of the bars. The copper loss of the rotor winding ( $P_e$ ) corresponding to  $2r_2'$  must be twice that due to  $r_2'$ . It is seen from Eq. 23-1 that for constant torque,  $P_e$  will be doubled when  $s$  is doubled, i.e., *for a given torque, the slip is proportional to the rotor resistance*, or, what is the same, for a given torque, the ratio  $r_t'/s$ , is

a constant quantity. The same can be seen from the equivalent circuit, Fig. 18-4. The performance of the circuit remains the same as long as the ratio  $r_t'/s$  is constant. Vice versa, for a fixed performance there must be a fixed ratio  $r_t'/s$ : for a fixed torque, the motor will adjust its slip corresponding to the value of  $r_t'$ .

In a squirrel-cage motor the rotor resistance is fixed ( $=r_2'$ ) and the ratio  $r_2'/s$  is determined only by the slip  $s$ . This yields a *single* torque-speed curve as shown in Fig. 23-1. In the wound-rotor motor the rotor resistance ( $=r_2' + r_{ext}'$ ) can be varied. Since the slip for a given torque is proportional to the rotor resistance, each value of  $r_{ext}'$  determines another torque-speed curve. Fig. 23-4 shows several such torque-speed curves. Curve 1 corresponds to  $r_{ext}' = 0$  (this is the normal torque-speed curve) while the other three curves correspond to  $r_{ext}' = 3r_2'$ ,  $5.5r_2'$  and  $8.5r_2'$  respectively.

The pull-out torque is independent of the rotor resistance and is therefore the same for all torque-speed curves (see Art. 22-4d). A line drawn parallel to the axis of ordinates shows that different torques can be developed at the same slip.

The latter statement applies also to standstill ( $s = 1$ ): it is possible to start a wound-rotor motor with any torque between 0 and the pull-out torque, while the starting torque of the squirrel-cage motor is fixed. The external resistance necessary to start a wound-rotor motor with a given value of torque can be easily determined. As an example, the case will be considered where it is desirable that the motor develop rated torque at standstill ( $s = 1$ ). Refer to the equivalent circuit Fig. 18-4. At rated torque it is desirable that  $r_{ext} = 0$  in order to avoid a reduction in efficiency through additional copper losses in the external resistance. If the slip at rated torque is equal to  $s_n$ , then at rated torque the ratio  $r_t'/s$  is equal to  $r_2'/s_n$ . In order that rated torque appear at standstill where  $s = 1$ , the ratio  $r_t'/s$  must be the same as at rated torque, i.e.,

$$\frac{r_2' + r_{ext}'(s=1)}{1} = \frac{r_2'}{s_n} \quad \text{or} \quad r_{ext}'(s=1) = r_2' \left( \frac{1-s_n}{s_n} \right)$$

If  $s_n = 0.02$ , the external resistance must be  $0.98/0.02 = 49$  times the resistance of the rotor winding (skin effect included).

The squirrel-cage motor must go through its whole torque-speed curve during the starting period, up to the point where the motor torque is equal

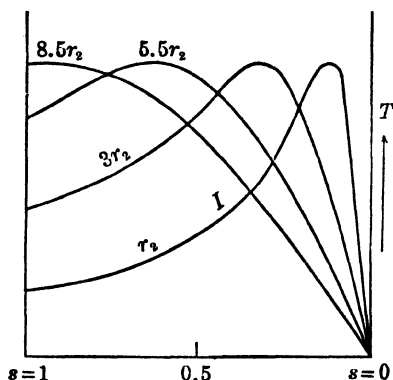


FIG. 23-4. Torque-speed characteristics of a wound-rotor motor for various values of secondary resistance.

to the load torque. On the other hand, it is possible to keep the torque of a wound-rotor motor constant during the entire starting period. This is achieved by keeping the ratio  $r_t'/s$  constant, i.e., by a gradual reduction of the external resistance during acceleration. The torque during the starting period is then a line parallel to the axis of abscissae in Fig. 23-4. Since the starting resistance cannot usually be changed gradually but in steps, the torque and current during starting also change in steps, as shown in Fig. 23-5.

**23-3. Speed control of the polyphase induction motor.** Gradual speed control over a wide range is possible only with the wound-rotor motor. The

speed of the squirrel-cage motor can be changed only in a few large steps. The speed regulation can be achieved in several ways, some of which will be described in the following paragraphs.

(a) *Speed regulation by means of a resistance in the rotor circuit.* Consider Fig. 23-4. Any line parallel to the axis of abscissae corresponds to speed regulation at constant torque. Assume that a wound-rotor motor has to drive a mill which requires a constant torque at variable speed. At the highest speed the motor operates on its natural torque-speed curve (Curve I,

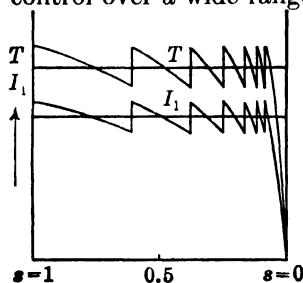


FIG. 23-5. Starting of a wound-rotor motor.

$r_{ext}' = 0$ ), and a fixed point on this curve corresponds to the required torque. Let the slip at this point be  $s_1$ ; the ratio  $r_t'/s$  for this point is then equal to  $r_2'/s_1$ . If the rotor resistance ( $r_2' + r_{ext}'$ ) is now changed, the motor automatically assumes a slip of  $s_2$  of such a magnitude that the ratio  $(r_2' + r_{ext}')/s_2$  is equal to  $r_2'/s_1$ , because to a fixed value of torque there corresponds a fixed ratio of  $r_t'/s$  (see foregoing article). Thus variable speed can be obtained by means of a variable resistor in the rotor circuit.

However, this kind of speed control is not economical. Consider Eq. 19-5 which states that the electric power of the rotor, i.e., the power dissipated in the rotor as copper losses, is equal to the slip times the power of the rotating field. In the case of the constant-torque drive considered above the power of the rotating field remains constant, i.e., independent of the slip, since, according to Eq. 19-9, the torque is equal to a constant quantity times the power of the rotating field. Also the power input to the motor does not change with rotor speed when the torque remains constant (see Eq. 19-14). Therefore, the higher the slip, the larger the part of the power input dissipated as copper losses in the rotor circuit and the lower the efficiency of the motor. The percent decrease in efficiency is almost equal to the percent decrease in speed.

(b) *Speed control by changing the number of poles.* Assuming a constant line frequency, speed variation in a few steps may be obtained by varying the number of poles of the motor, since, according to Eq. 17-4,

$$n_s = \frac{120f}{p}$$

Special windings are capable of producing different numbers of poles by a regrouping of coils. The most common winding of this kind is that with the pole ratio 1 : 2. Such a winding for 4 and 8 poles with  $f_1 = 60$  cycles yields two synchronous speeds of 1800 and 900 rpm respectively. If more than two speeds are desired, two separate windings can be arranged in the stator slots. Normally a squirrel-cage rotor is used for this kind of speed variation, or otherwise the rotor must have the same kind of winding as the stator, which then necessitates a larger number of slip rings than the normal three. If a slip-ring rotor is used, variation of speed between steps (synchronous speeds) can be accomplished by inserting resistance in the rotor circuit.

(c) *Speed control with the aid of a special regulating set.* With the aid of a regulating set it is possible to obtain a continuous and economic speed regulation of the wound-rotor motor. The operation of such a set is based upon the considerations discussed in the following paragraphs.

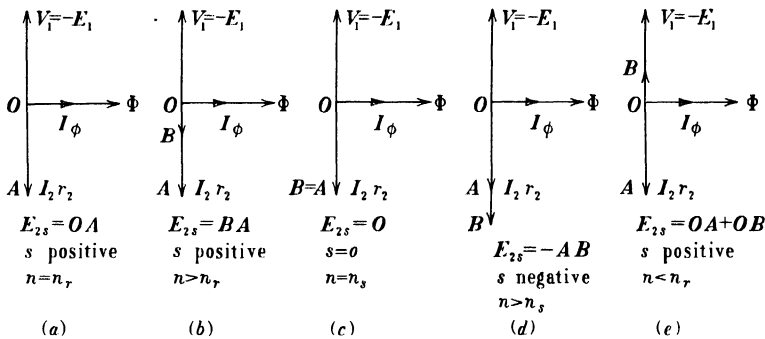


FIG. 23-6. Phasor diagrams for explanation of speed control of a polyphase wound-rotor induction motor.

To overcome a given opposing torque at the shaft of the motor a definite rotor current is necessary, i.e., there must be a definite induced emf  $E_{2s}$  and with it a corresponding slip. Consider Fig. 23-6a which represents a simplified phasor diagram of the induction motor with  $r_1$ ,  $x_1$  and  $x_2$  assumed to be negligible. In this case, the induced emf  $E_{2s}$  is consumed by the resistance drop  $I_2 r_2$ . In Fig. 23-6b, the value of  $I_2 r_2$  is the same as in Fig. 23-6a and, therefore, the values of  $I_2$  and of the torque are the same as for Fig. 23-6a. However, in Fig. 23-6b a voltage  $OB$  is impressed upon the slip rings of the rotor in phase with  $I_2 r_2$ . Since the total emf necessary to produce the current  $I_2$  is equal to  $OA$ , and since a voltage  $OB$  is introduced from the outside through the slip rings, the emf to be induced in the rotor by the rotating flux of the machine must be  $OA - OB = BA$ . This is less than  $OA$ , and therefore the slip will be less than in the case of Fig. 23-6a.

Figs. 23-6c, d, and e refer to the same current  $I_2$ , i.e., to the same torque as Figs. 23-6a and b. In Fig. 23-6c, the voltage impressed upon the slip rings,  $OB$ , is equal to  $OA = I_2 r_2$  and no emf induced in the rotor by the rotating flux is necessary; in this case the slip will be zero and the rotor speed will be the same as that of the rotating flux, namely, the synchronous speed  $n_s$ . In Fig. 23-6d, the impressed voltage  $OB$  is larger than the voltage drop  $I_2 r_2$  necessary for the required torque. This forces the rotor to run above the synchronous speed, i.e., with a negative slip so that  $E_{2s}$  becomes negative. The magnitude of  $E_{2s}$  is equal to  $OB - OA$ . Here the machine operates as a motor above the synchronous speed. In Fig. 23-6e the impressed voltage  $OB$  is in counter-phase with  $I_2 r_2$ . This forces the rotor to run with a higher slip than without the impressed voltage, because the induced rotor emf has to overcome the opposing voltage  $OB$  and also supply the voltage drop  $I_2 r_2$ .

Thus it is possible to regulate the speed of a wound-rotor induction motor below as well as above its synchronous speed, if a variable voltage is impressed on its rotor which is opposite in-phase to or in-phase with the emf induced in the rotor by the rotating flux.

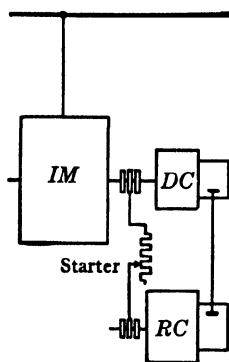


FIG. 23-7. Speed regulation of a wound-rotor motor with the aid of a rotary converter and a d-c machine (Kramer cascade).

Fig. 23-7 shows a regulating set consisting of a synchronous converter ( $RC$ ) and a d-c machine ( $DC$ ).  $IM$  is the induction motor the speed of which is to be regulated. The synchronous converter is a combination of a synchronous machine and a d-c machine (see Art. 43-1). The slip rings of the induction motor are connected with the slip rings of the synchronous converter. The commutator of the synchronous converter is connected with the commutator (armature) of the d-c machine, which is coupled to the induction motor. The starter is short-circuited during running.

When the induction motor operates at a certain slip  $s$ , the electric power of the rotor ( $sP_{\text{rot.f}}$ , see Eq. 19-5) is consumed by the synchronous converter ( $RC$ ) and delivered to the d-c machine ( $DC$ ). The synchronous part of the converter consumes power from the induction motor and operates as a synchronous motor. Therefore the d-c part of the synchronous converter operates as a d-c generator, and the d-c machine ( $DC$ ) which consumes power from the converter operates as a d-c motor. Thus the electric power of the rotor of the induction motor is delivered back to its shaft as mechanical power.

The speed variation is accomplished by varying the excitation of the d-c machine ( $DC$ ). The greater the excitation, the lower the speed of the induction motor. The regulating set does not operate near synchronous speed because the voltage at the slip rings becomes too small to cause the rotary converter to rotate.

The arrangement shown in Fig. 23-7 in which the d-c machine is coupled to the induction motor is used when increasing torque with decreasing speed is required (constant HP drive). When the torque is constant or decreases with speed (fan drive), the d-c machine (*DC*) is not coupled with *IM*, but with a synchronous machine which then operates as a generator and delivers the electric power of the rotor of the induction motor back to the line.

It is possible to correct the power factor of the induction motor with the aid of the excitation of the synchronous converter, because a synchronous motor when over-excited is able to deliver reactive current (see Art. 38-3). At a certain excitation of the synchronous converter the total reactive power required by the induction motor is supplied to its rotor by the converter, and the phase displacement at the stator terminals of the induction motor becomes zero ( $\cos \varphi_1 = 1$ ).

The synchronous converter set is able to vary the speed only below synchronism. There are other sets employing a-c commutator machines which permit speed control below and above synchronism.

With all these sets the rotor frequency is determined by both the induction motor and the regulating set. The rotor frequency (rotor slip) varies with the load just as in the ordinary induction motor. In Fig. 23-8 curve *a* shows the natural torque-speed characteristic of an induction motor, i.e., the characteristic for no impressed voltage on the slip rings (see Fig. 23-6a). The slip increases, i.e., the speed decreases slightly with increasing torque (as in a d-c shunt motor). Curve *b* of Fig. 23-8 shows the torque-speed characteristic when a constant voltage is impressed upon the rotor which is opposite in-phase to the emf induced in the rotor by the rotating flux. Such a voltage forces the rotor to increase the slip at all values of torque (see Fig. 23-6e). However, the trend of the torque-speed characteristic remains the same as for the natural characteristic, i.e., the speed decreases slightly with increasing torque.

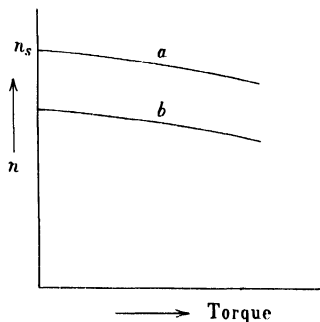


FIG. 23-8. Torque-speed characteristics of an induction motor controlled by a regulating set.

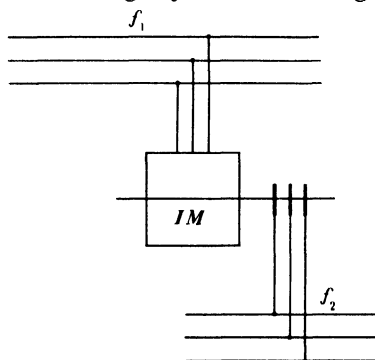


FIG. 23-9. Doubly fed induction motor.



(d) *Speed control by double feeding.* The machine behaves entirely differently when the secondary frequency is determined not by the induction motor and its regulating set but by another source of power with *fixed* frequency. In this case the induction machine is referred to as a *doubly fed induction motor*. Fig. 23-9 shows such an arrangement. The rotor as well as the stator is connected to a source of power. The fixed frequencies of both sources are  $f_1$  and  $f_2$ , respectively. It will be assumed, as an example, that the motor has four poles and that  $f_1 = 60$  cycles while  $f_2 = 25$  cycles.

It has been previously explained, see Art. 17-1, that, for the development of a uniform torque, stator and rotor mmf waves must be at standstill with respect to each other. In the example considered, the speed of the stator mmf with respect to the stator is  $n_{s1} = (120 \times 60)/4 = 1800$  rpm, and the speed of the rotor mmf with respect to the rotor is  $n_{s2} = (120 \times 25)/4 = 750$  rpm. If the rotor is fed in such a manner that its mmf rotates in the same direction as the stator mmf, then the condition for a uniform torque is satisfied only when the rotor speed is  $n_{s1} - n_{s2} = 1800 - 750 = 1050$  rpm. On the other hand, if the rotor is fed in such a manner that its mmf rotates in opposite direction to the stator mmf, then the condition for a uniform torque is satisfied only when the rotor speed is  $n_{s1} + n_{s2} = 1800 + 750 = 2550$  rpm.

Thus the doubly fed induction motor has *two fixed speeds* at which a uniform torque exists. Expressed by a formula, these two speeds are

$$n = \frac{120(f_1 \pm f_2)}{p} \quad (23-2)$$

At each of these two speeds the machine is able to develop uniform torques of different magnitudes, as shown in Fig. 23-10. Apparently a continuous speed control can be achieved if one of the two frequencies of Eq. 23-2 can

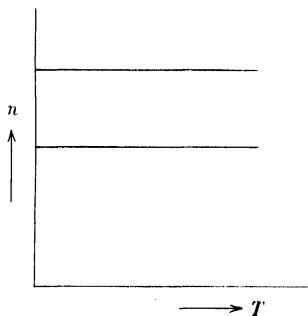


FIG. 23-10. Torque-speed characteristics of a doubly fed induction motor.

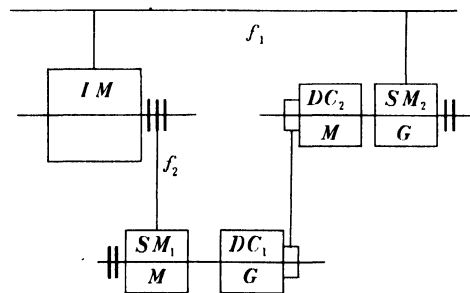


FIG. 23-11. Speed control of an induction motor by double feeding.

be continuously varied. Such an arrangement is shown in Fig. 23-11. *IM* is the induction motor the speed of which is to be controlled. The stator is

connected to the supply lines; its rotor is connected to a synchronous machine  $SM_1$ , which is coupled to a d-c machine  $DC_1$ . The latter is connected electrically with another d-c machine  $DC_2$ , which is coupled to a synchronous machine  $SM_2$ , connected to the lines. The electric power of the rotor of the induction motor is consumed by the synchronous machine  $SM_1$  which operates as a motor. The d-c machine  $DC_1$ , therefore, operates as a generator, and the d-c machine  $DC_2$  operates as a motor. The synchronous machine  $SM_2$  operates as a generator and returns the electric power of the induction motor to the lines.

The speed control of the induction motor in the above arrangement is accomplished by changing the excitation of the d-c machine  $DC_2$ . This produces a change in speed of the set  $SM_1 - DC_1$  and therefore a change in the frequency  $f_2$ .

If  $f_2$  is zero, i.e., if one of the sources of power is d-c, Eq. 23-2 yields only a *single speed* at which the machine is able to produce a uniform torque. This is the case in the *synchronous machine* which will be treated later.

### PROBLEMS

1. A 15-HP, 4-pole, 3-phase, 60-cycle, 440-volt, Y-connected wound-rotor induction motor has the following per-unit parameters at  $s = 1$  ( $x_1, x_2'$  sat. values):

$$\begin{array}{lll} r_1 = 0.018 & r_m = 0.17 & r_2' = 0.023 \\ x_1 = 0.09 & x_m = 3.5 & x_2' = 0.085 \end{array}$$

Determine the external resistance (in ohms per phase) necessary to start this motor with 130% rated torque. The rated speed is 1756 rpm.

2. For the wound-rotor motor of Problem 1 determine the external resistance (in ohms per phase) necessary to start the motor with its pull-out torque. Can the motor start with a torque larger than the pull-out torque? (Sat. factor = 1.2.)

3. Determine the starting torque of the motor of Problem 2 for an external resistance three times as large as that necessary to start the motor with its pull-out torque.

4. Determine the starting performance of the motor of Problem 1 for an external resistance = 0. Is the starting performance with external resistance = 0 satisfactory?

5. For the motor of Problem 1 determine the external resistance necessary to start the motor with rated torque, and also the stator current which occurs at this resistance. Compare this stator current with that of a squirrel-cage motor.

6. A 125-HP, 6-pole, 3-phase, 60-cycle, 2300-volt, Y-connected, squirrel-cage induction motor has the following per-unit parameters at  $s = 1$  ( $x_1, x_2'$  unsat. values):

$$\begin{array}{lll} r_1 = 0.017 & r_m = 0.20 & r_2' = 0.018 \\ x_1 = 0.095 & x_m = 3.1 & x_2' = 0.10 \end{array}$$

The saturation factor of the leakage paths at  $s = 1$  and starting with full voltage is 1.23. Determine the voltage ratio of an autotransformer necessary to reduce the starting current to 60% of the value which occurs at starting with full voltage.

(Assume that the saturation of the leakage paths at 60% starting current is 1.1.) What will be the starting torque at that voltage ratio?

7. Determine for the motor of Problem 6 the series ohmic resistance in the stator circuit necessary to reduce the starting current to 60% of the value which occurs at starting with full voltage. What is the loss in this resistance?

8. Refer to Problem 7. What is the starting torque with the resistance which reduces the starting current to 60% of the value which occurs at full voltage?

9. Determine for the motor of Problem 6 the series inductive reactance in the stator circuit necessary to reduce the starting current to 60% of the value which occurs at starting with full voltage.

10. Refer to Problem 9. What is the starting torque with the inductive reactance which reduces the starting current to 60% of the value which occurs at full voltage?

11. With 2300 volts at the terminals of a 3-phase, wound-rotor induction motor the emf measured at the open-rotor slip rings at standstill is 640 volts. For a blocked rotor test with 780 volts at the stator terminals and the slip rings short-circuited, the line current is 275 amp and the power input is 115 kw. What resistance (in ohms) should be connected, (a) in star and (b) in delta, to the rotor slip rings so that, with 2300 volts applied to the stator, the rotor current at standstill will be unchanged? What is the ratio of the torques developed in the two cases? (Neglect the magnetizing branch and assume that the stator and rotor parameters are equal. Further, neglect the voltage drops in the stator for the open-rotor test.

12. It is to be decided whether to start a squirrel-cage induction motor by means of an autotransformer or a series resistance in the stator circuit. In each case, the line current at full voltage must be equal to the rated current of the motor. For a blocked rotor test with 25% rated voltage at the terminals of the motor, the motor current is equal to the rated current and the power factor is 0.20. Compare the starting torques for the two methods of starting. (Neglect the magnetizing branch and assume equal parameters for stator and rotor.)

13. A 500-HP, 3-phase, 25-cycle, 2300-volt, 12-pole induction motor has a slip of 1.8% at full-load. The resistance of the rotor winding per phase, referred to the stator, is 0.5 ohm. What is the rotor current at full-load? What is the ratio of delivered to developed torque? What is the starting torque, if the terminal voltage is adjusted so that the rotor current is twice its full-load value? (Total rotational losses = 2.5%.)

14. A 500-HP, 3-phase, 60-cycle, 2300-volt induction motor has full-load copper losses in the stator and rotor windings equal to 2.4% and 2.6%, respectively. The total iron loss is 8.6 kw. The iron loss due to the fundamental flux is 3.5 kw. The friction and windage losses are 8 kw. The magnetizing current is 20 amp. The leakage reactances of the windings at  $s = 1$  are 4.5 times their resistances. Determine the terminal voltage of this motor if the starting current is to be 200 amp. (Neglect the skin-effect in the rotor winding. Stray load loss = 5.5 kw.) (Full-load  $\cos \phi = 0.90$  in.)

15. A 2000-HP, 24-pole, 3-phase, 60-cycle, 6600-volt, star-connected wound-rotor induction motor has a turn ratio 8.05. The rotor is star-connected. The speed of this motor is controlled by a 3-phase a-c commutator machine set between rated speed and -30% of rated speed. Determine the approximate values of voltage and the kva of the commutator machine, neglecting voltage drops due to resistance and leakage reactance of the stator winding, and leakage reactance of the rotor winding.

## Chapter 24

### INFLUENCE OF HARMONIC FLUXES ON THE TORQUE-SPEED CHARACTERISTIC

**24-1. Order and speed of the harmonic mmf's and fluxes.** In Chap. 15, the mmf of an elementary machine having one phase, one slot per pole ( $q = 1$ ) and a full-pitch winding (Fig. 15-1) was considered. The mmf of this winding has been found to be a rectangular curve, Fig. 15-3. The Fourier series has been applied to this curve and only the fundamental wave, with the wave length  $2\tau$ , has been considered. This fundamental wave is (Eq. 15-1)

$$f_1 = \frac{\sqrt{2}}{2} \frac{4}{\pi} n_c I \sin \omega t \cos \frac{\pi}{\tau} x \quad (24-1)$$

$n_c$  is the number of conductors in the slot. If the harmonic mmf's are also considered (see Fig. 15-4), the mmf equation is

$$f_1 = \frac{\sqrt{2}}{2} \frac{4}{\pi} n_c I \sin \omega t \left[ \cos \frac{\pi}{\tau} x - \frac{1}{3} \cos 3 \frac{\pi}{\tau} x + \frac{1}{5} \cos 5 \frac{\pi}{\tau} x - \frac{1}{7} \cos 7 \frac{\pi}{\tau} x + \dots \right] \quad (24-2)$$

i.e., the winding considered produces in addition to the main (fundamental) wave also harmonic mmf's of the order  $\nu = 3, 5, 7 \dots$  (see Fig. 15-4), the wave lengths of which are respectively  $2\tau/3, 2\tau/5, 2\tau/7 \dots$ , or in general  $2\tau/\nu$ , and the amplitudes of which are  $1/\nu$  times the amplitude of the fundamental.  $\nu = 1$  is the fundamental. These are all *alternating mmf's* producing pulsating fluxes. The subscript I indicates that the machine has only one phase.

In Chap. 15 an elementary 3-phase machine was also considered, the three windings of which are displaced from each other by  $2\tau/3 \times \pi/\tau = 120$  electrical degrees and are fed by three currents shifted from each other by  $120^\circ$  in time. The space displacement of  $120^\circ$  refers to the fundamental wave, as can be seen from the factor  $2\tau/3$  ( $2\tau$  is the wave length of the main wave; the factor  $\pi/\tau$  converts the distance  $2\tau/3$  into degrees). If the space displacement between the three windings is equal to  $120^\circ$  with respect to the main, it will be equal to  $3 \times 120^\circ = 360^\circ$  with respect to the third harmonic, to  $5 \times 120^\circ = 600^\circ$  with respect to the fifth harmonic, and so forth, because the third

harmonic has a wave length equal to 1/3 of that of the fundamental, the fifth harmonic has a wave length equal to 1/5 of that of the fundamental.

If we refer Eq. 24-2 to phase I of the 3-phase machine, then the mmf of phase II of this machine is

$$f_{II} = \frac{\sqrt{2}}{2} \frac{4}{\pi} n_c I \sin(\omega t - 120) \\ \times \left[ \cos\left(\frac{\pi}{\tau} x - 120\right) - \frac{1}{3} \cos\left(3 \frac{\pi}{\tau} x - 360\right) + \frac{1}{5} \cos\left(5 \frac{\pi}{\tau} x - 600\right) - \dots \right] \quad (24-3)$$

and the mmf of phase III (with phase I as reference)

$$f_{III} = \frac{\sqrt{2}}{2} \frac{4}{\pi} n_c I \sin(\omega t - 240) \\ \times \left[ \cos\left(\frac{\pi}{\tau} x - 240\right) - \frac{1}{3} \cos\left(3 \frac{\pi}{\tau} x - 720\right) + \frac{1}{5} \cos\left(5 \frac{\pi}{\tau} x - 1200\right) - \dots \right] \quad (24-4)$$

In order to find the resultant mmf, the fundamental and each harmonic has to be considered separately, because they have different wave lengths. The resultant fundamental mmf and the resultant mmf of each harmonic is then found by adding the three corresponding terms of Eqs. 24-2, 24-3, and 24-4.

The addition of the three fundamental ( $\nu=1$ ) mmf's yielded (Art. 15-1, Eq. 15-3)

$$f_{\nu=1} = \frac{3}{2} \frac{\sqrt{2}}{2} \frac{4}{\pi} n_c I \sin\left(\omega t - \frac{\pi}{\tau} x\right) \quad (24-5)$$

and it has been found that this is a sinusoidal wave traveling in the positive direction of the  $x$ -axis (Fig. 15-6) with the velocity of propagation (Eq. 15-4)

$$\frac{dx}{dt} = \omega \frac{\tau}{\pi} = 2f\tau = \frac{2\tau}{T} \quad (24-6)$$

or the speed in rpm (Eq. 15-5)

$$\frac{120f}{p} = n_s = \text{synchronous speed} \quad (24-7)$$

If the three terms of the 3rd harmonic are added up, the resultant mmf is

$$f_{\nu=3} = 0 \quad (24-8)$$

i.e., a 3-phase winding does not produce a 3rd harmonic mmf. The addition of the three terms of the 5th harmonic yields

$$f_{\nu=5} = \frac{1}{5} \frac{3}{2} \frac{\sqrt{2}}{2} \frac{4}{\pi} n_c I \sin\left(\omega t + 5 \frac{\pi}{\tau} x\right) \quad (24-9)$$

Applying the same method of consideration as that applied to the fundamental wave in Art. 15-1, it is found that the resultant 5th harmonic is a wave traveling in the negative direction of the  $x$ -axis, i.e., opposite to the direction of the fundamental wave, with the speed in rpm  $= n_s/5$ .

The resultant of the three terms of the 7th harmonic is

$$f_{\nu=7} = \frac{1}{7} \frac{3}{2} \frac{\sqrt{2}}{2} \frac{4}{\pi} n_c I \sin \left( \omega t - 7 \frac{\pi}{\tau} x \right) \quad (24-10)$$

This is a wave which travels in the positive direction of the  $x$ -axis, i.e., in the same direction as the fundamental wave, with the speed  $n_s/7$  rpm.

Summarizing, a polyphase winding produces a series of traveling waves, some of them traveling in the same direction as the fundamental (main) wave, some traveling in the opposite direction from the fundamental wave. The speed of the fundamental wave is the synchronous speed  $n_s$ . The speed of  $\nu$ -th harmonic is  $n_s/\nu$ .

It seems to follow from Eqs. 24-5, 24-9, and 24-10, that the amplitude of the  $\nu$ -th harmonic is equal to  $1/\nu$  times the amplitude of the fundamental. However, it should be kept in mind that the foregoing considerations refer to an elementary machine with  $q = 1$  and full-pitch winding. The consideration of a winding with  $q > 1$  makes it necessary to introduce the distribution factor (see Art. 15-1) and Eqs. 24-5, 24-9, and 24-10 must be multiplied by  $q$  times distribution factor. The magnitude of the distribution factor is determined by the value of  $q$  and by the slot angle  $\alpha_s$ . For the fundamental (main) wave,  $\alpha_s = 180^\circ/mq$ . Since for the  $\nu$ -th harmonic to  $180^\circ$  of the fundamental correspond  $\nu \times 180^\circ$ , the slot angle for the  $\nu$ -th harmonic is  $\nu 180/mq$  and the distribution factor of the  $\nu$ -th harmonic is (Eq. 14-4)

$$k_{d\nu} = \frac{\sin \nu q (\alpha_s/2)}{q \sin \nu (\alpha_s/2)} \quad (24-11)$$

If the other limitation imposed by the elementary winding, namely  $W/\tau = 1$  (full-pitch winding), is dropped, the pitch factor must be introduced. For the fundamental wave, the pitch factor is  $\sin$  of the angle  $(W/\tau)\pi/2$ , (Eq. 14-8). For the reason mentioned above, this angle is for the  $\nu$ -th harmonic  $\nu$  times as large and the pitch factor of the  $\nu$ -th harmonic is

$$k_{p\nu} = \sin \nu \frac{W}{\tau} \frac{\pi}{2} \quad (24-12)$$

Eqs. 24-5, 24-9, and 24-10 must be multiplied by this factor. Having multiplied these equations by  $q k_{d\nu} k_{p\nu}$ , the mmf of the  $\nu$ -th harmonic of a coil group (polyphase group) is obtained and it is seen that the ratio of the amplitude of the mmf of the  $\nu$ -th harmonic to that of the fundamental (main) wave is

$$\frac{F_\nu}{F_{(\nu=1)}} = \frac{1}{\nu} \frac{k_{d\nu} k_{p\nu}}{k_{d\nu=1} k_{p\nu=1}} \quad (24-13)$$

**24-2. Influence of the harmonic fluxes on the torque-speed characteristic.** The rotating harmonic mmf's produce rotating harmonic fluxes just as the fundamental mmf wave produces a rotating flux. The slip-ring rotor is wound for a fixed number of poles (same as that of the stator) and is less sensitive to the harmonic fluxes than the squirrel-cage rotor which adjusts its number of poles to that of the rotating flux (see Art. 17-2, Fig. 17-4). The squirrel cage reacts to each harmonic flux in the same manner as to the fundamental wave, i.e., it produces with each harmonic flux a complete torque-speed characteristic consisting of all three ranges of operation (as a brake, as a motor, and as a generator, see Fig. 20-3). The pull-out slip is different for the different harmonics.

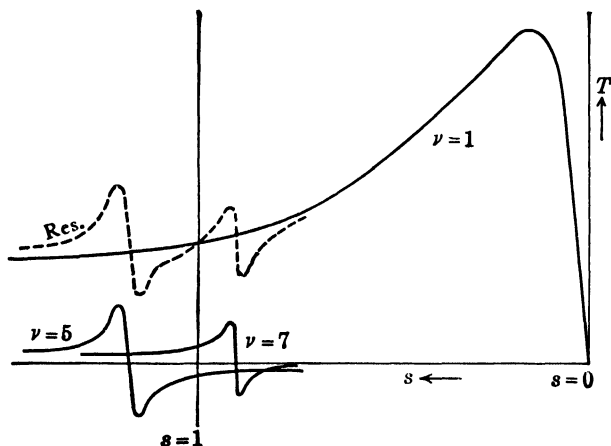


FIG. 24-1. Parasitic asynchronous torques in the speed-torque curve.

Fig. 24-1 shows the torque-speed characteristics of the fundamental wave ( $\nu=1$ ) and of the 5th and 7th harmonics. The resultant torque-speed characteristic shows dips. If the dip (in Fig. 24-1 it is due to the 7th harmonic) is large enough so that the resultant torque is smaller than or equal to the load torque at the slip at which the dip occurs, the motor will not be able to come up to speed; it will crawl with the speed which corresponds to the intersection point of the motor torque-curve and the load torque-curve.

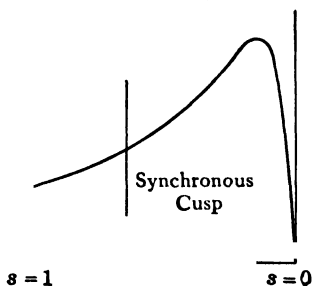


FIG. 24-2. Parasitic synchronous torque in the speed-torque curve ( $s < 1$ ).

In addition to the parasitic torques shown in Fig. 24-1 which have the same character as the working ( $\nu=1$ ) torque-speed characteristic and for this reason can be called induction motor torques or *asynchronous torques*, there is another

type of parasitic torque in the induction motor. These are *synchronous torques* which characterize the other type of a-c motor, the synchronous motor (see Chap. 36). A synchronous torque appears in the torque-speed curve of the induction motor in the shape of a cusp. Fig. 24-2 shows a torque-speed characteristic with such a cusp. If the dip produced by the cusp is large, the motor will not be able to come up to speed, for the same reason as for a large dip produced by a parasitic asynchronous torque.

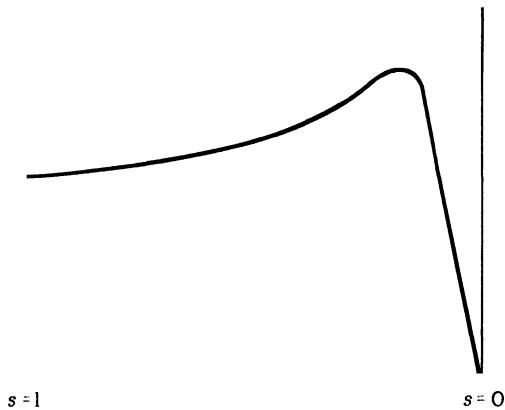


FIG. 24-3. Parasitic synchronous torque in the speed-torque curve ( $s = 1$ ).

A synchronous cusp may also appear at standstill (Fig. 24-3). If it is large enough, the motor will not be able to start at all; it is said then that the motor has *locking torques* or *dead points*.

**24-3. Means to reduce or to avoid the parasitic torques.** Synchronous cusps can be avoided by a proper selection of the number of stator and rotor slots (Chap. 58). Asynchronous torques cannot be avoided, but they can be reduced. One of the means of reduction is given by Eq. (24-13): the factor  $k_{av}$  must be kept small. The distribution factor of the harmonics is normally fixed, but the pitch factor can be influenced by the selected coil span ( $W/\tau$ ). A coil span of 83 per cent ( $W/\tau = 5/6$ ) reduces considerably the 5th and 7th harmonics which produce the largest asynchronous torques. An example of the influence of the coil pitch upon the dip in the torque-speed characteristic is shown in Fig. 24-4.

It is not only the harmonics of low order (the 5th and 7th) which produce asynchronous torques. Some harmonics of high order may also produce considerable asynchronous torques as well as synchronous torques, if the number of slots of stator and rotor cannot be chosen so as to avoid the synchronous torques entirely. The influence of high-order harmonics can be reduced by skewing the rotor or stator slots (Chap 58).



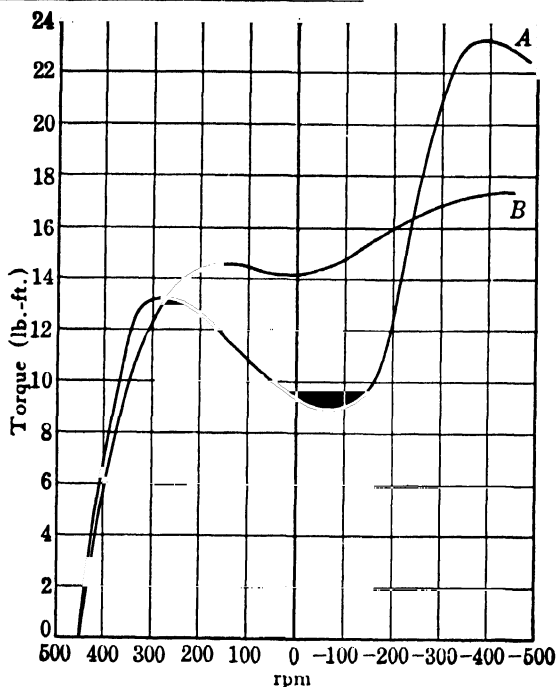


FIG. 24-4. Influence of coil pitch. Speed-torque curves of a 2-speed 1/2-HP 60-cycle motor for 8 and 16 poles. Slot combination 54/82. Rotor skewed. The speed-torque curves apply to the 16-pole connection.

A. coil width = 5 slot pitches.

B. coil width = 4 slot pitches.

The parasitic torques are normally of no importance for the wound-rotor motor, because this motor can be started with its pull-out torque by inserting resistance in the rotor circuit (see Fig. 23-4).

The harmonics of high order may produce disturbing magnetic noise in both types of induction motors, the squirrel-cage and wound-rotor motors (see Chap. 59).

## Chapter 25

### SOME SPECIAL INDUCTION MACHINES

Some of the machines described below have only the construction but not the behavior in common with the induction motor. This is pointed out in the discussion of the individual machines.

**25-1. The synchronous induction motor.** Consider Eq. 23-2. If the frequency  $f_2$  of the line to which the rotor is connected is equal to zero, the rotor speed becomes

$$n = \frac{120f_1}{p} = n_s$$

i.e., *there is only one speed*, the synchronous speed, at which a uniform torque is developed. Thus a wound-rotor motor, the rotor of which is excited with direct current, runs at synchronous speed and operates as a synchronous motor (see Art. 23-3d). Fig. 25-1 shows the connection diagram of the synchronous induction motor.  $R$  is the starting resistance which is cut out during running;  $DC$  is the exciter of the induction motor. Field current is applied by the exciter after the motor comes up to speed. The d-c excitation then pulls the motor into "step", i.e., into synchronous speed (see Chap. 61).

The synchronous induction motor has been used for many applications,

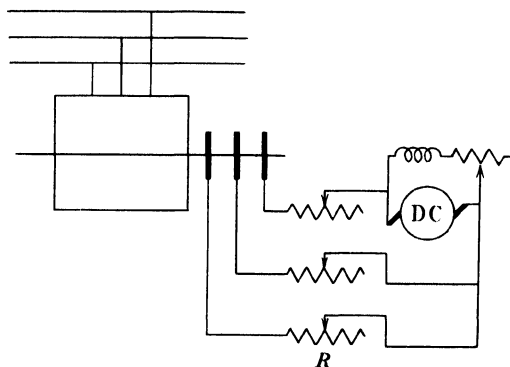


FIG. 25-1. Connection diagram of the synchronous induction motor.

especially in Europe. The advantage of this type of machine lies in a better starting performance as compared with that of the salient pole synchronous motor. On the other hand, low-voltage exciter with high current ratings have to be used for these machines; this is necessitated by the limited starting voltage at the slip rings of induction motors; such a limited voltage requires a small number of rotor turns and therefore a low rotor resistance so that  $I_2 r_2$  is small.

**25-2. Induction motor with a rotating flux produced by a d-c excited rotating pole-structure (electromagnetic coupling).** The rotating flux of the conventional induction motor is produced by polyphase windings carrying polyphase currents. A rotating flux can also be produced by a rotating pole-structure excited by direct current, and such a rotating flux has the same effect as that produced by polyphase a-c windings. Use is made of this where an a-c source is not available, as for example, on shipboard. An induction motor of this kind must have additional bearings so that *both* members, the primary and the secondary, can rotate independently. The primary has a d-c excited pole-structure, while the secondary member has a single- or double-cage winding. When placed between a Diesel and a geared propeller shaft on shipboard, this machine prevents the transmission of torque pulsations to the gears.

**25-3. Self-synchronizers (Selsyns, Synchrotie Apparatus, Autosyn, etc.).** In many power applications, as for example in lift-bridge drives, printing-press drives, etc., it is desirable to tie together two or more parallel drives, by a *pure electrical* interconnection, in such a manner that the speeds as well as the space-phase alignments of the different drives are the same. For this purpose wound-rotor induction motors can be used. Consider Fig.

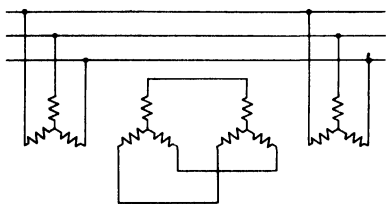


FIG. 25-2. Connection diagram of two three-phase self-synchronizers.

25-2 in which the stators of two 3-phase wound-rotor induction motors are connected to a *common* source of power and the rotors are electrically interconnected. Since each of the machines is connected to two sources of power, both will behave as synchronous machines (see Art. 23-3d), and each machine will influence the speed of the other machine in such a manner that both machines will always run synchronously.

Assume, for example, that the line frequency in Fig. 25-2 is 60 cycles, that the machines are 2-pole, and that the rotor of one machine operates at a speed  $n_1 = 1780$  rpm while the rotor of the other machine runs at speed  $n_2 = 1820$  rpm. The rotor frequencies corresponding to these two speeds are (see Eq. 17-18)

$$f_{r1} = \frac{3600 - 1780}{3600} 60 = 30.35$$

$$f_{r2} = \frac{3600 - 1820}{3600} 60 = 29.65$$

The first rotor which runs at the lower speed will be urged, by the second machine, to assume the speed (see Eq. 23-2)

$$n_1' = \frac{60 - 29.65}{2} 120 = 1820 \text{ rpm}$$

i.e., to increase its speed, and the second rotor which has the higher speed will be urged by the first machine to assume the speed

$$n_2' = \frac{60 - 30.35}{2} 120 = 1780 \text{ rpm}$$

i.e., to decrease its speed. Thus, synchronizing forces will make both machines always run synchronously *with the same speed*.

Now consider the machines at a fixed speed. There is only *one* relative position of both rotors at which the secondary emf's will be exactly opposed with respect to the circuit of the two rotors, so that no current will flow in the secondary windings (Fig. 25-3a). For all other positions of the two rotors, there will be a resultant voltage ( $\Delta E$ , Fig. 25-3b) which will produce a current and torque tending to turn the rotors to that position where the rotor emf's are opposed. One of the two machines operates as a *generator* (*transmitter*) and the other as *motor* (*receiver*), the generator tending to reduce the angle by which its rotor is advanced, and the motor tending to reduce the angle by which its rotor is behind.

Since one machine operates as a generator and the other as a motor, the a-c source of power has to deliver only the losses to the self-synchronizers. This applies also to a system with more than two units.

It is evident that the torques which line up the self-synchronizers will be small, when their rotors run in the direction of their rotating fields at low slip, because at low slip the rotor emf's and currents are small. Large rotor emf's are obtained when the rotors run opposite to the direction of the rotating fields.

Consider Fig. 25-4 in which a tie of two parallel drives is shown having two *identical* d-c motors as main motors and two self-synchronizers. When both motors are equally loaded, no current will flow in the synchronizers. Assume that the load of main motor 2 is dropped to 80% of that of main motor 1. Since both main motors have the same speed-torque characteristic,

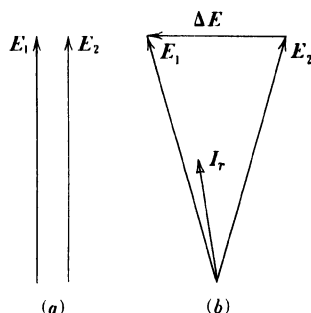


FIG. 25-3. Phasor diagram of the rotors of two self-synchronizers.

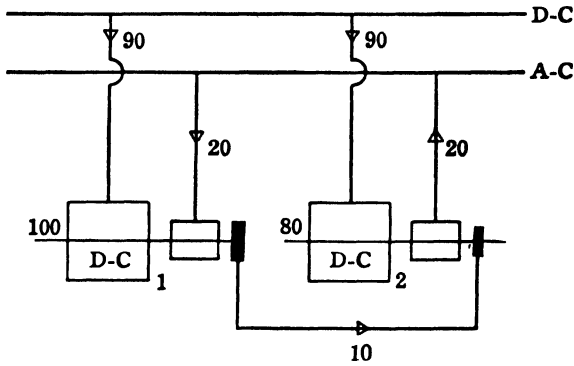


FIG. 25-4. Load distribution for two self-synchronizers rotating in the direction of their rotating fields.

main motor 2 will tend to increase its speed corresponding to the decrease of load. However, the self-synchronizers will force both main motors to maintain the same speed and therefore each of the main motors will draw from the d-c line half of the total power necessary for the drive, i.e.,  $(100 + 80)/2 = 90\%$ . This power distribution between the main motors does not correspond to the load at the shafts, and the synchronizers will restore the power balance. Synchronizer 1 will operate as a motor and deliver to its shaft the deficient 10% of power, while synchronizer 2 will operate as a generator and take from its shaft 10% of the power. The mechanical power for each synchronizer will be 10%.

Although the self-synchronizers as doubly fed machines behave as synchronous machines, the fundamental power equations of the induction motor (Eqs. 19-5 and 19-6) also apply to them, for in these machines as in the induction motor the power transfer from stator to rotor occurs at the speed of the rotating field, while the rotors run with a speed different from that of the rotating field. Thus, if the losses in the synchronizers are neglected, and the power input of the motor is considered as positive,

$$P_{st, 1} = P_m \frac{1}{1-s}, \quad P_{st, 2} = -P_m \frac{1}{1-s}, \quad (25-1)$$

$$P_{rot, 1} = P_m \frac{s}{1-s}, \quad P_{rot, 2} = -P_m \frac{s}{1-s}.$$

Assume that the synchronizers in the example Fig. 25-4 run in the direction of their rotating fields with half synchronous speed, i.e.,  $s = 0.5$ . Since  $P_m = 10\%$ ,

$$P_{st, 1} = 10 \frac{1}{1-0.5} = 20\%, \quad P_{st, 2} = -20\%,$$

$$P_{rot, 1} = 10 \frac{0.5}{1-0.5} = 10\%, \quad P_{rot, 2} = -10\%.$$

and the power flow in both units will be such as shown in Fig. 25-4.

Assume now that the self-synchronizers run opposite to their rotating fields with the same speed. Then  $s = 1.5$  and

$$P_{st, 1} = 10 \frac{1}{1 - 1.5} = -20\%, \quad P_{st, 2} = 20\%,$$

$$P_{rot, 1} = 10 \frac{1.5}{1 - 1.5} = -30\%, \quad P_{rot, 2} = 30\%.$$

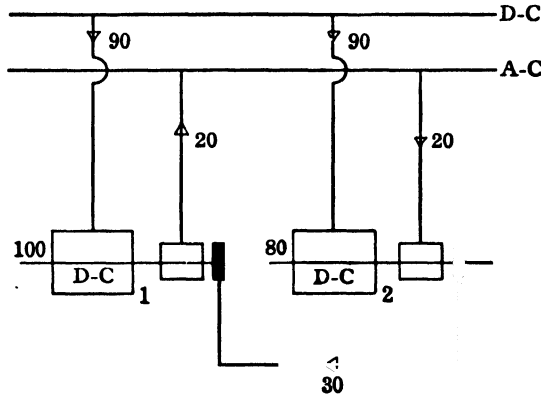


FIG. 25-5. Load distribution for two self-synchronizers rotating opposite to the direction of their rotating fields.

The power flow for this case is shown in Fig. 25-5. Contrary to Fig. 25-4, self-synchronizer 1 now operates as a generator (transmitter) and self-synchronizer 2 as a motor (receiver).

The following data were obtained from tests on 2 units consisting of identical d-c main motors and identical self-synchronizers with the rating:

7.5 hp, 4 poles, 50 cycles,  $n_s = 1500$ , 380 volts

$n = 1020$ in the direction of the rotating field	$n = 1000$ opposite to the direction of the rotating field
$P_{st, 1} = 3.8$	2.7 kw
$P_{st, 2} = 2.1$	3.45 kw
$I_{st, 1} = 6.4$	8.7 amp
$I_{st, 2} = 11.7$	7.4 amp
$\cos \varphi_{st, 1} = 0.94$	0.47
$\cos \varphi_{st, 2} = 0.26$	0.73
$V_{rot} = 50$	245 volts
$I_{rot} = 17$	13.1 amp
$\cos \varphi_{rot} = 0.62$ leading	0.95 leading

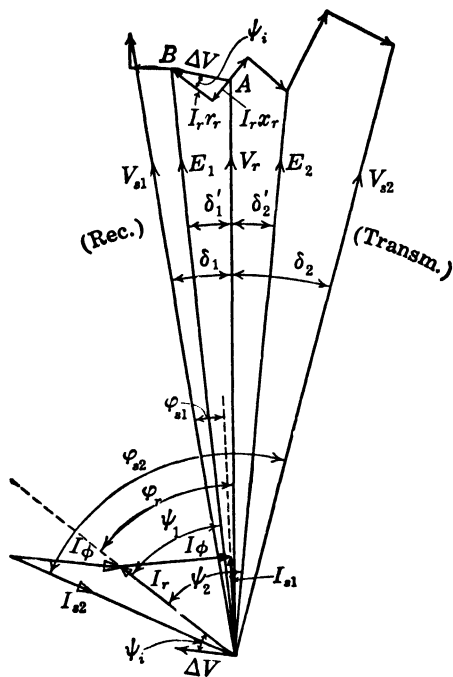


FIG. 25-6. Phasor diagram for the load distribution of Fig. 25-4.

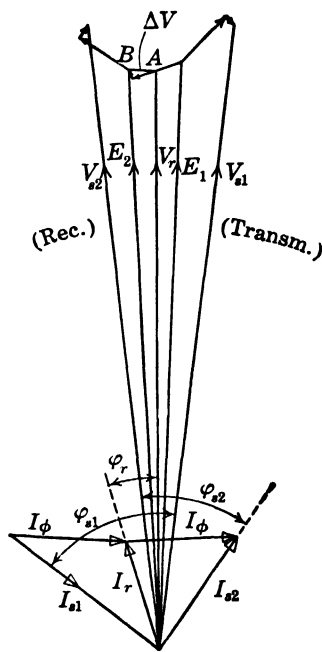


FIG. 25-7. Phasor diagram for the load distribution of Fig. 25-5.

Figs. 25-6 and 25-7 are the phasor diagrams corresponding to both tests. Consider Fig. 25-6, left side.  $V_r$  is the common rotor voltage,  $I_r$  is the common rotor current shifted with respect to  $V_r$  by an angle  $\varphi_r$ , corresponding to  $\cos \varphi_r = 0.62$ . The angle  $\delta_1' + \delta_2' = \delta$  is the displacement of both rotors with respect to each other.

$\delta_1'$  is the angle by which the emf  $E_1$  of synchronizer 1 (i.e., of the motor, receiver) leads the rotor voltage  $V_r$ . The magnitude of the rotor current  $I_r$  is determined by the magnitude of the voltage drop  $\Delta V$  in the rotor winding and the resistance and leakage reactance of the rotor winding. Corresponding to the direction of  $\Delta V$ , the current  $I_r$  leads the rotor voltage  $V_r$ .

The primary current  $I_1$  of the receiver (motor) is obtained by adding the reactive component of the magnetizing current  $I_\phi$  to the rotor current  $I_r$ .  $I_\phi$  is perpendicular to  $E_1$ . The primary voltage  $V_{s1}$  of the receiver (motor) now can be determined by adding the voltage drops in the stator winding due to resistance and leakage reactance to  $E_1$ .

The voltage diagram of synchronizer 2 (i.e., of the generator, transmitter) is obtained in the same way as for synchronizer 1. Both constructions must yield the same magnitude for  $V_{s1}$  and  $V_{s2}$ , since both stators are connected to the same line. As should be expected, the stator voltage leads the induced

emf in the motor diagram and lags the induced emf in the generator diagram.

Again in Fig. 25-7 the left side of the diagram represents the receiver and the right side of the diagram the transmitter.

Note that in Figs. 25-6 and 25-7 the stator voltages  $V_{s1}$  and  $V_{s2}$  appear displaced with respect to each other although they are in-phase, since both stators are connected to the same source of power. The displacement between both rotors ( $\delta_1' + \delta_2'$ ) must appear between the emf's  $E_1$  and  $E_2$ , and this leads to the fictitious phase angle between the primary voltages. Assuming that the angle between the stator voltages is the same as that between the emf's, i.e., between the rotors, the equivalent circuit shown in Fig. 25-8 can be derived from the fundamental equations of the two units. The solution of this circuit for rotation against the rotating fields, leads to the following expressions. (Ref. B3.)

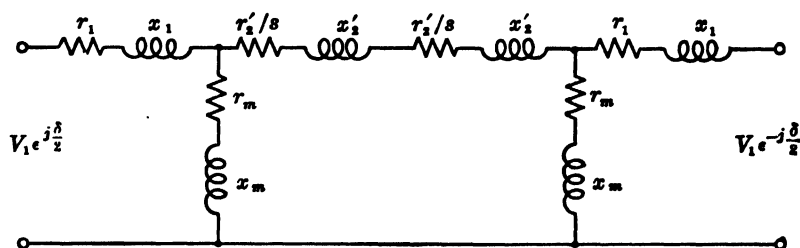


FIG. 25-8. Equivalent circuit of two self-synchronizers.

$$T_{tr} = \frac{6.09}{n_s} V(I - I_m) \sin \varphi \sin \delta + T_{as} \sin^2 \frac{\delta}{2} \quad \text{lb-ft}, \quad (25-2)$$

$$T_{rec} = \frac{6.09}{n_s} V(I - I_m) \sin \varphi \sin \delta - T_{as} \sin^2 \frac{\delta}{2} \quad \text{lb-ft}, \quad (25-3)$$

where  $V$  is the line voltage,  $I$  the stator current of the induction motor for slip  $s$ ,  $I_m$  the magnetizing current of the induction motor,  $\cos \varphi$  the power factor of the induction motor for slip  $s$ ,  $T_{as}$  the induction-motor torque for slip  $s$ , and  $\delta$  the displacement between both rotors.

Figs. 25-9 and 25-10 refer to two 25-hp 8-pole 60-cycle 3-phase self-synchronizers. Fig. 25-9 shows the torques as a function of slip for a fixed value of  $\delta$ . Fig. 25-10 shows the torque as a function of  $\delta$  for a fixed value of slip larger than 1.0.

Fig. 25-11 is determined by test. It refers to a set of two and a set of three 9-hp 4-pole 50-cycle synchronizers. It shows, as a multiple of rated induction motor torque, the maximum permissible difference in the load torques for which the system still is stable. Curve 1 refers to two units. Curve 2 refers to three units, one of which has a larger load torque than the two others. Curve 3 refers to three units, two of which have larger (but equal) load torques than the third.



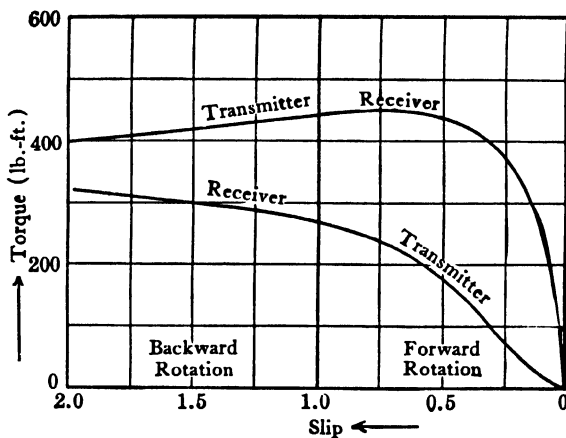


FIG. 25-9. Torque as a function of slip for two self-synchronizers.

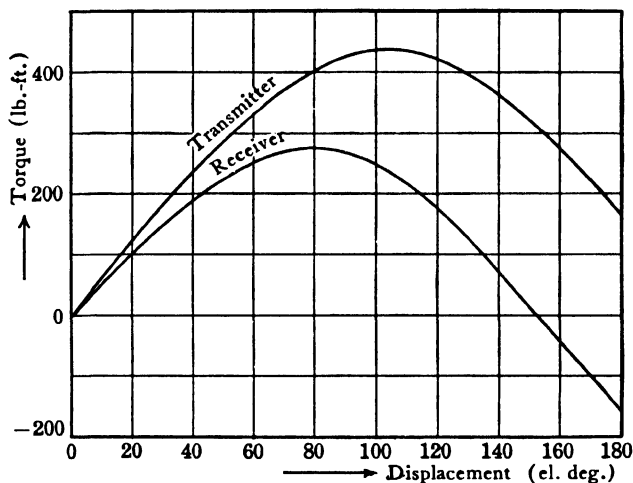


FIG. 25-10. Torque as a function of displacement for two self-synchronizers.

The self-synchronizers must be *lined up before starting*. Otherwise, if the initial angle of displacement is large and both units are unrestrained, they may come up to speed in the direction of their rotating fields, one machine serving as a short circuit for the rotor of the other. If one unit is restrained, the other may come up to speed. The lining-up occurs best when single-phase excitation instead of 3-phase excitation is applied to the stators, since the single-phase motor is not able to start and to come up to speed. If for lining up the connection scheme Fig. 25-12 is used, the torque-displacement curve will be as shown in Fig. 25-13. It refers to the same machines as Figs. 25-9 and 25-10.

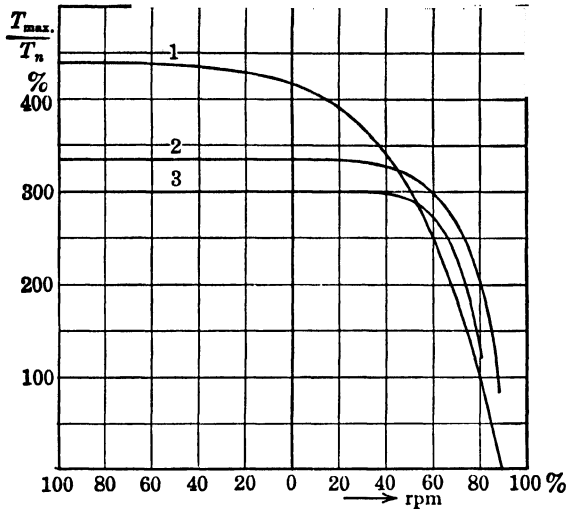


FIG. 25-11. Overload capacity as a function of speed for two and three self-synchronizers.

While lining up with single-phase excitation in the stators, the rotor emf's will not constitute a 3-phase system. Since the stator current is single-phase, the emf's in the three rotor phases will be in-phase and a single unit will not be able to produce torque. However, when the rotors of *two* units are not in juxtaposition, a component of the secondary current creates a *cross flux* in each machine, and torques result which tend to turn the rotors into juxtaposition.

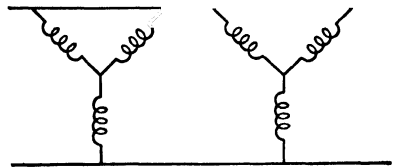


FIG. 25-12. Single-phase connection for lining up self-synchronizers.

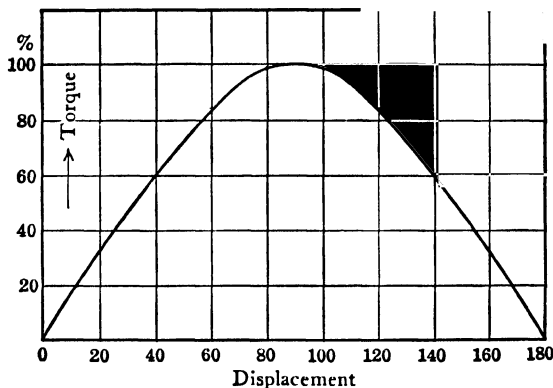


FIG. 25-13. Torque as a function of displacement for the single-phase connection

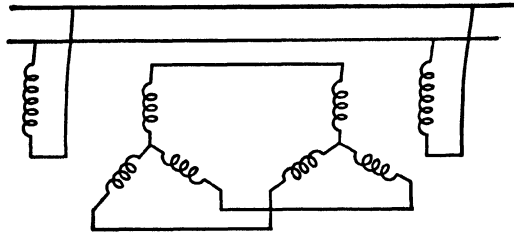


FIG. 25-14. Connection for two single-phase position indicators.

**25-4. Position indicators.** In many applications, as, for example, elevators, hoists, generator rheostats, gates or valves, etc., an indication of the position is desirable. In these cases single-phase units are used, the rotors of which are of the salient-pole type as in the synchronous machine (Ref. B2). The rotors have single-phase windings excited by a-c. The 3-phase stator windings are connected directly together (Fig. 25-14). The saliency of the poles gives the advantage of increasing the synchronizing torque by the reluctance torque (see Art. 36-1). This kind of unit is usually of fractional horsepower rating, while the 3-phase self-synchronizers for power applications of the wound-rotor induction-motor type are built as larger units (up to 100 hp). A typical torque-displacement curve of a single-phase salient-pole unit is shown in Fig. 25-15.

If the rotor of the transmitter is turned by a certain angle, the rotor of the receiver will turn by the same angle. When it is desirable to indicate a *difference between two angles*, the differential system as shown by Fig. 25-16 can be used. The differential position indicator has two 3-phase windings, each connected to one of the secondary windings of the single-phase units. It will indicate the difference of the rotor positions of the 2 units. A differen-

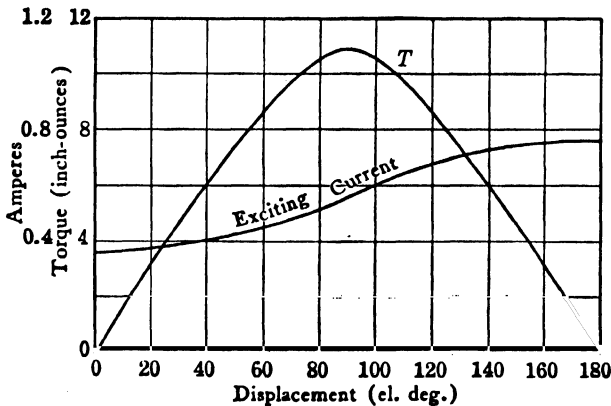


FIG. 25-15. Torque as a function of displacement for two single-phase salient-pole position indicators.

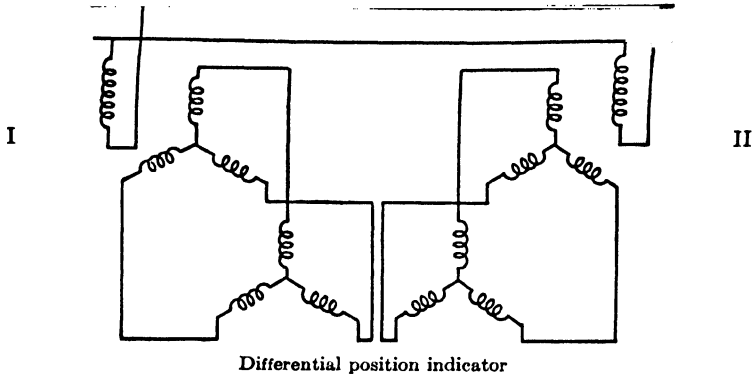


FIG. 25-16. Connection diagram for a differential system.

tial unit in connection with a single-phase transmitter also can be used in order that the receiver indicates the sum or the difference of the angles applied to the transmitter and differential unit.

**25-5. The induction voltage regulator.** The induction voltage regulator is an induction motor which is used as a transformer to regulate the voltage of an outgoing circuit from a central station having many single circuits. The rotor does not rotate continuously but may be rotated through a range of 180 electrical degrees.

As in the case of the induction motor the induction voltage regulator may be either single-phase or polyphase. Since it has to add or subtract an increment of line voltage, *its secondary is in series with the line*. Fig. 25-17 shows the coil arrangement of a single-phase induction regulator with single-phase windings on both the stator and the rotor. The primary  $P$  (usually the rotor) is connected to the power line as in the ordinary transformer. The secondary  $S$  is in series with the line.  $V_1$  is the non-regulated voltage;  $V_2$ , the regulated.  $V_s$  is the secondary voltage of the induction regulator. Thus

$$V_2 = V_1 \pm V_s \quad (25-4)$$

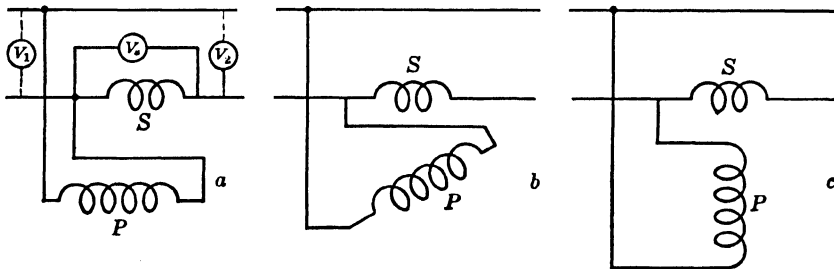


FIG. 25-17. Schematic diagram showing the principle of operation of a single-phase induction regulator.

The magnitude of  $V_s$  depends upon the mutual inductance between the secondary and primary windings of the induction regulator, i.e., upon the angle between the axes of the windings  $P$  and  $S$ .  $V_s$  is a maximum when the axes of the two windings coincide (Fig. 25-17a);  $V_s$  is zero when the axes of the two windings are shifted 90 electrical degrees with respect to each other (Fig. 25-17c). The angle between the positions for the positive and negative maximum of  $V_s$  is 180 electrical degrees.

Consider Fig. 25-17c in which the axes of the windings are perpendicular to each other. The voltage  $V_s$  of the secondary winding due to the transformer flux is zero, but, since this winding carries the load current which is an alternating current, an emf of self-induction is induced in it. Hence, the secondary winding appears in the load circuit as a reactor which would reduce the load voltage  $V_2$  if its reactive voltage drop were not nullified. Fig. 25-18 shows the actual coil arrangement of the single-phase induction regulator. The rotor has, in addition to the primary winding  $P$  which is connected to the line, a short-circuited winding  $SC$  the axis of which is

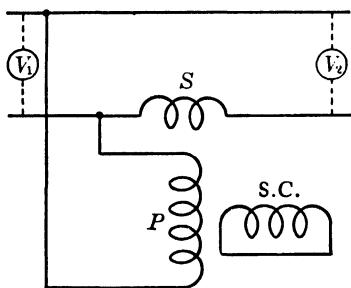


FIG. 25-18. Coil arrangement in the single-phase induction regulator.

shifted 90 electrical degrees with respect to the primary winding. Fig. 25-18 shows the primary and secondary windings in the same position as Fig. 25-17c. However, it can be seen from Fig. 25-18 that the flux produced by the load current in the secondary winding  $S$  also will link the short-circuited winding  $SC$ , because the axes of these windings coincide. Since the winding  $SC$  is short-circuited, the secondary winding  $S$  and the winding  $SC$  behave as a transformer under short-circuit conditions, i.e., the flux in the axis of the secondary winding  $S$  is small and the voltage

drop in the line is caused only by the relatively small leakage fluxes of the secondary winding  $S$  and the winding  $SC$ .

The voltage drop in the line due to the secondary  $S$  of the regulator at the position shown in Fig. 25-17c could appear to a lesser degree (corresponding to the sine of the angle between the axes of the coils  $P$  and  $S$ ) at any intermediate position between those of Fig. 25-17a and Fig. 25-17c. However, since the compensating winding  $SC$  has a fixed position with respect to the primary winding  $P$ , it has the same effect on the secondary  $S$  and the line at intermediate positions as for the position shown in Fig. 25-18.

Fig. 25-19 shows the coil arrangement of a 3-phase induction regulator. The primary winding can be connected star or delta while the secondary is again in series with the line. The action is somewhat different from that of the single-phase induction regulator. The primary currents produce a *rotating flux* which induces a voltage  $V_s$  in the secondary winding. The magnitude of this induced voltage is constant and independent of the relative

position of the windings. However, the relative position of the windings determines the *phase* of the secondary voltage  $V_s$  with respect to the primary voltage  $V_1$ . The relation here is

$$\dot{V}_2 = \dot{V}_1 + \dot{V}_s \quad (25-5)$$

i.e., the regulated voltage is the geometric sum of  $V_1$  and  $V_s$ . Fig. 25-20 shows the voltage diagram of the polyphase induction regulator. As in the single-phase induction regulator, the maximum regulated voltage is  $V_1 + V_s$ , and the minimum regulated voltage is  $V_1 - V_s$ . For intermediate positions of rotor and stator the end-point of  $V_s$  and also of  $V_2$  moves on a circle. A short-circuited compensating winding (see Fig. 25-18) is not required for the polyphase induction regulator.

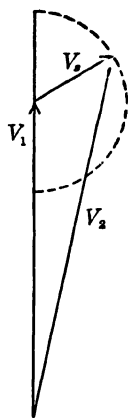


FIG. 25-20. Voltage diagram of the polyphase induction regulator.

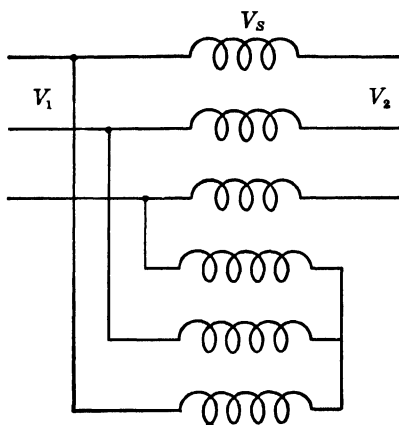


FIG. 25-19. Schematic diagram for a 3-phase induction regulator.

Induction regulators usually are built as vertical 2-pole machines, or in the larger sizes as vertical 4-pole machines. The smaller the number of poles, the larger the mechanical angle which corresponds to 180 electrical degrees, and the easier the voltage adjustment. The gradual rotation of the rotor is accomplished by a worm-gear drive with the gear on the shaft of the rotor. The worm is usually operated by a motor controlled automatically by voltage relays. Since the rotor of the induction regulator does not rotate, it may be cooled by oil just as any ordinary transformer. This is of decided advantage when the induction regulator is used to regulate a high-voltage line.

**25-6. Resolvers.** Resolvers are used to perform trigonometric operations in analog computing devices and control systems. One of the common operations is the production of a *pure sinusoidal* voltage as a function of the angle between stator and rotor windings.

Resolvers are built 2-pole for an output of few millivolt-amperes. Both stator and rotor have two single-phase windings. Fig. 25-21 shows a schematic diagram of the windings of a resolver. As in the induction voltage regulator the rotor does not rotate continuously but may be rotated through a range of 180 electrical degrees.

The single-phase voltage impressed upon the two primary windings (stator or rotor windings) produce two alternating fluxes shifted 90 degrees with respect to each other in space. It will be assumed that the primary

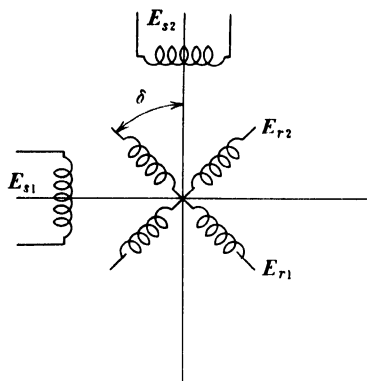


FIG. 25-21. Winding arrangement of a resolver.

windings lie in the stator and the secondary windings in the rotor. If the emf's induced by the two stator fluxes in the stator windings are  $E_{s1}$  and  $E_{s2}$ , then for a displacement  $\delta$  of the axes of stator and rotor windings, the emf's induced in the rotor windings are (Fig. 25-21)

$$E_{r1} = aE_{s1} \cos \delta + aE_{s2} \sin \delta \quad (25-6)$$

$$E_{r2} = -aE_{s1} \sin \delta + aE_{s2} \cos \delta \quad (25-7)$$

where  $a$  is the ratio of rotor turns to stator turns.

It is required that the secondary voltages  $E_{r1}$  and  $E_{r2}$  be purely sinusoidal. This necessitates sinusoidal flux distribution and a *sinusoidal distribution* of the rotor (secondary) conductors. The sinusoidal flux distribution can be achieved through a sinusoidal distribution of the stator (primary) conductors. Fig. 25-22 shows such a conductor distribution for a rotor with 12 slots. One of the two windings lies in the slots 1-7, 2-6, 12-8, 3-5, and 11-9 and has its pole axis through the slots 4-10; the other winding lies in the slots 4-10, 5-9, 3-11, 6-8, and 2-12 and has its pole axis through the slots 1-7. The angle between 2 slots is  $360/12 = 30$  degrees. Considering the first winding (Fig. 25-22a), the number of turns in slots 1-7 is  $2N$ , the number of turns in slots 2-6 and 12-8 is  $2N \cos 30^\circ = \sqrt{3}N$ , the number of turns in slots 3-5 and 11-9 is  $2N \cos 60^\circ = N$ , and the number of turns in slots 4 and 10 is  $2N \cos 90^\circ = 0$ . The second winding has exactly the same distribution but shifted 90 degrees.

In order to eliminate the influence of the harmonics of high order, rotor or stator slots must be skewed (see Art. 24-3).

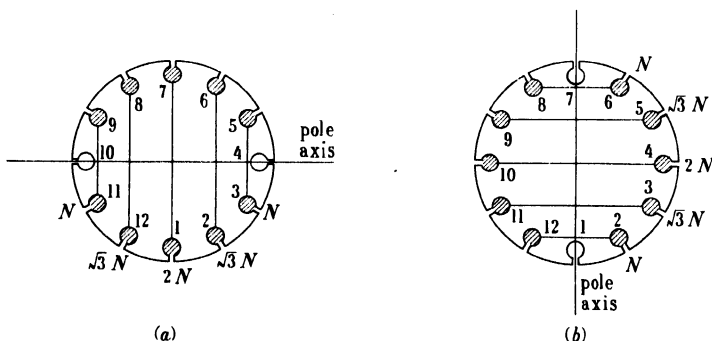


FIG. 25-22. Conductor distribution in the primary of a resolver for sinusoidal flux distribution.

### PROBLEMS

1. A 40-kw, unity power factor, 440-volt, single-phase load is fed through an induction voltage regulator which is boosting the primary line voltage 15%. Determine the currents in each winding of the regulator neglecting the magnetizing current.

2. A 2-kva induction voltage regulator is designed to operate on either a 115-volt or a 230-volt supply circuit. There are two primary windings and two secondary windings which give 100% buck or boost on the load side when voltage is applied to the regulator. Specify the coil currents for each connection and show properly labeled diagrams of connections. Neglect magnetizing current.

3. A 230-volt, 3-phase, 60-cycle, wound-rotor, Y-connected induction motor has a slip-ring voltage of 120 volts at standstill with the slip rings open. This motor is to be used as a 3-phase induction voltage regulator to boost the 230-volt line voltage 15%. Determine the angle between stator and rotor voltages necessary to achieve this boost, neglecting the magnetizing current and the resistance and reactance drops in the machine.

4. Repeat Problem 3 for 5% and 10% boost in voltage.

5. Repeat Problem 3 for 5, 10, and 15% voltage buck.

6. Referring to Problem 3, what are the maximum and minimum voltages (available on the regulated side) which this machine can produce? Neglect the magnetizing current and the resistance and reactance drops.



## Chapter 26

### THE SINGLE-PHASE INDUCTION MOTOR

**26-1. The single-phase windings.** Any 3-phase induction motor can be made to operate as a single-phase induction motor by opening one of the three stator phases. The two remaining stator phases constitute a single-phase winding distributed over  $\frac{2}{3}$  of the pole pitch. A 3-phase winding is ordinarily a 2-layer winding (Art. 13-1), while the actual single-phase winding which is used in the stator of fractional-horsepower single-phase induction motors is single-layer.

It is designed in the form of the *hand* or *mould* winding, Fig. 26-1, or the *skein* winding, Fig. 26-2. The single coils are connected in groups as in the polyphase windings, but the coils belonging to a group have *different coil spans*, Fig. 26-1. There are as many coil groups as there are poles.

In the hand winding, the wire is placed in the slot one turn at a time, starting with the inner coil (coil with the smallest span). In the mould

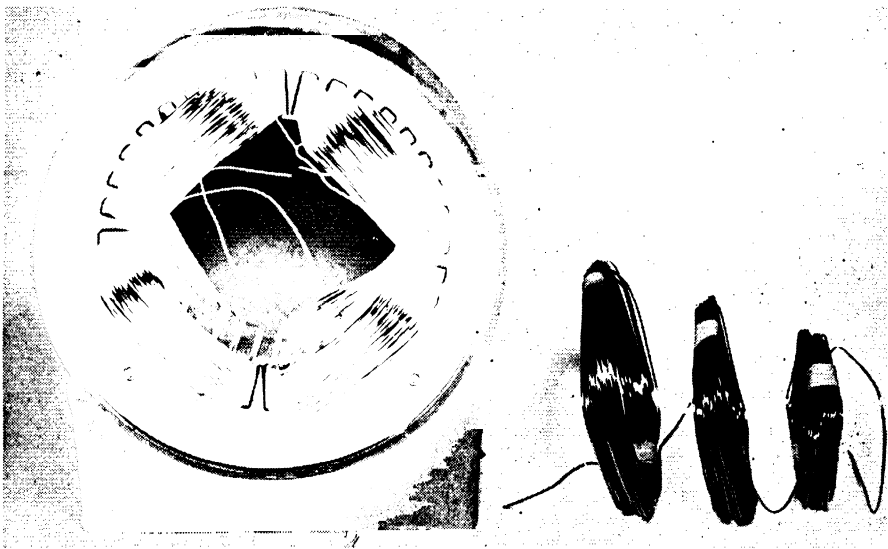


FIG. 26-1. Mould winding.



FIG. 26-2. Skein winding.

winding, the coils are first wound on a mould and then placed in the slots. In the skein winding, a skein of wires is looped a number of times through the slots to form a pole.

Single-phase induction motors have two single-phase windings, the *main* winding and the *starting* winding, see Art. 28-1. For the main winding, any

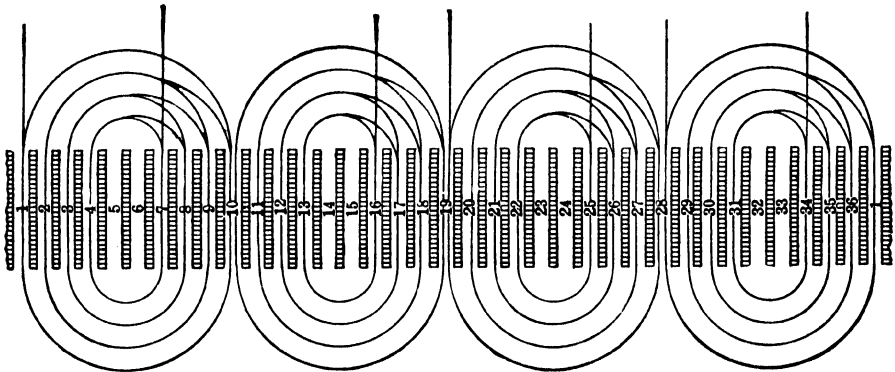


FIG. 26-3. Mould winding diagram for a single-phase, 4-pole motor with 36 slots. Main winding only.

one of the three kinds of windings discussed is used; for the starting winding, the skein winding is preferred.

Fig. 26-3 shows the diagram of a mould winding for a 4-pole motor with 36 slots. Only the main winding is shown. There are  $p=4$  coil groups each with 4 coils of different coil spans. Notice that the winding is not placed in all slots.

Slot No.	1	2	3	4	5	6	7	8	9	10	11	12	13	14	15	16	17	18	19	20	21	22	23	24	25	26	27	28	29	30	31	32	33	34	35	36
Main Winding	1	2	2	1			1	2	2	1	2	2	1			1	2	2	1	2	2	1			1	2	2	1	2	2	1			1	2	2
Starting Winding				1	1	1	1							1	1	1	1						1	1	1	1					1	1	1	1		

FIG. 26-4. Winding distribution for a single-phase 4-pole motor with 36 slots.

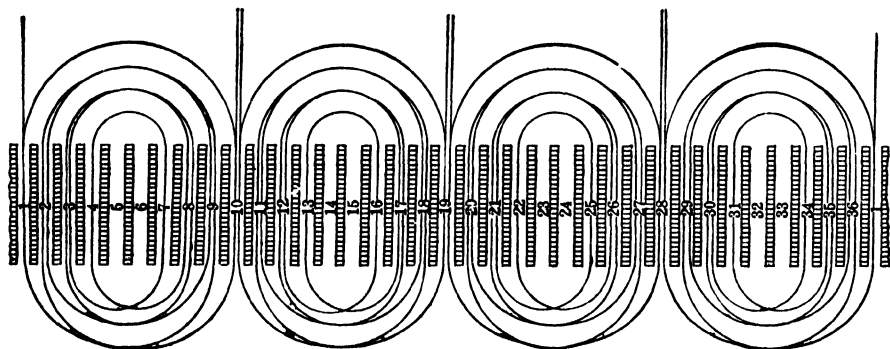


FIG. 26-5. Skein winding diagram corresponding to the winding distribution of Fig. 26-4. Main winding only.

Figs. 26-4 and 26-5 show the winding distribution and winding diagram for a 4-pole 36-slot motor with a skein winding. The numbers in the second row of Fig. 26-4 indicate the number of times the loop of the skein passes through the slot. The numbers in the third row indicate the same for the starting winding. Fig. 26-5 shows the main winding only. Here, also, each of the two windings is placed only in a part of the slots. The axes of the two windings are displaced by 90 electrical degrees.

The rotor of the single-phase induction motor normally has a squirrel-cage winding.

## PROBLEMS

1. A 2-pole, 24-slot, single-phase motor has the following winding distribution: Draw the main winding diagram for the skein winding.

2. Draw the main winding diagram for a mould winding for the motor of Problem 1. The numbers in the table indicate in this case the ratios of turns in the individual coils.

**26-2. Mechanical elements of the single-phase motor.** Fractional-horsepower motors are usually single-phase, and there are many types of such single-phase motors. The differences between them are described in Chap. 28. However the mechanical elements of the single-phase induction motor are the same as those of the polyphase induction motor, except that a centrifugal switch is used in certain types of single-phase motors, in order

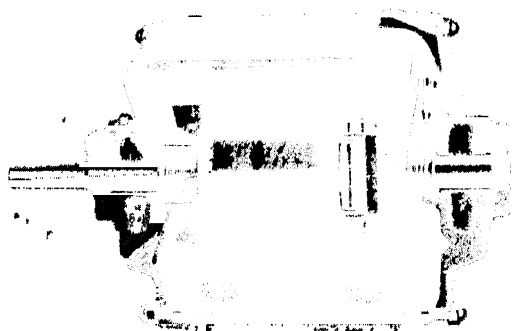


FIG. 26-6. Cutaway view of a single-phase induction motor with centrifugal switch.

to cut out the winding which is used only for starting (see Chap. 28). Fig. 26-6 shows the cutaway view of a single-phase motor with centrifugal switch. As has been mentioned, the rotor of the single-phase induction motor is usually of the squirrel-cage type.

**26-3. Application of the operational characteristics of the polyphase motor to the single-phase motor.** It has been shown previously (Art. 15-2) that the main flux of the polyphase induction motor is a *rotating flux*. On the other hand, the main flux of the single-phase motor is an *alternating flux* (Art. 15-1), fixed in space. It is possible to set up the fundamental equations of the single-phase motor and derive its operational characteristics on the basis of the alternating flux. (Ref. C2, C3 and C4.) However, it is also possible to set up the fundamental equations and derive the characteristics of the single-phase motor on the basis of the operational characteristics of the polyphase motor. This latter possibility is based on the fact that an alternating mmf (or flux) can be replaced by two rotating mmf's (fluxes).

It was found in Chap. 15 (Eqs. 15-1 and 15-10) that an alternating mmf is given by the equation

$$f = 1.8 \frac{N}{p} k_a I \sin \omega t \cos \frac{\pi}{\tau} x \quad (26-1)$$

Applying to this equation the relation  $\sin \alpha \cos \beta = \frac{1}{2} \sin (\alpha - \beta) + \frac{1}{2} \sin (\alpha + \beta)$ , there results

$$f = 0.9 \frac{N}{p} k_{ap} I \sin \left( \omega t - \frac{\pi}{\tau} x \right) + 0.9 \frac{N}{p} k_{ap} I \sin \left( \omega t + \frac{\pi}{\tau} x \right) \quad (26-2)$$

i.e., the *alternating mmf can be replaced by two rotating mmf's* (see Eq. 15-3) traveling in *opposite* directions (the terms with  $x$  have in Eq. 26-2 different signs) and each having an amplitude equal to half of that of the alternating mmf. Use will be made of this property for the analysis of the single-phase motor.

To these two rotating mmf's there correspond two fluxes rotating in opposite directions, each with synchronous speed.

The rotating flux which travels in the same direction of rotation as the rotor is called the *forward rotating flux*, while the rotating flux which travels in the opposite direction to the rotor is called the *backward rotating flux*.

Contrary to the polyphase induction motor, where the rotor emf is induced by only one rotating flux, it is induced here by two rotating fluxes, and the influence of each flux on the rotor is to be considered separately. The effect of *each* of the two rotating fluxes on the rotor of the single-phase motor is the same as that of the single rotating flux on the rotor of the polyphase motor.

Assume that the rotor has a speed  $n$  rpm. Then, according to the definition of the slip  $s$  (see Eq. 17-19), the slip of the rotor with respect to the forward rotating flux is

$$s_f = \frac{n_s - n}{n_s} = 1 - \frac{n}{n_s} \quad (26-3)$$

Since the backward rotating flux rotates opposite to the rotor, the slip of the rotor with respect to this backward rotating flux is

$$s_b = \frac{n_s - (-n)}{n_s} = 1 + \frac{n}{n_s} = 2 - s \quad (26-4)$$

In order to make clear the influence of the two rotating fluxes on the rotor it will be assumed that  $n < n_s$ . Then, with respect to the forward rotating flux, and according to Eq. 26-3,  $s$  is positive and smaller than 1. Considering Fig. 20-3, it is seen that the rotor, under the influence of the forward rotating flux, operates as in a *motor*. With  $s$  positive and smaller than 1, the slip of the rotor with respect to the backward rotating flux is, according to Eq. 26-4, positive and larger than 1. Again considering Fig. 20-3 it is seen that the rotor, under the influence of the backward rotating flux, operates in the region of brake operation. Thus the two rotating fluxes have an opposite influence upon the rotor.

**26-4. Torque of the single-phase induction motor.** The relation for the *developed* torque, Eq. 19-8, derived for the polyphase induction motor can be applied to each of the two rotating fluxes of the single-phase induction

motor. Thus the torque developed by the rotor under the influence of the forward rotating flux is

$$T_f = \frac{7.04 I_{2f}'^2 r_2'}{n_s s} \text{ lb-ft} \quad (26-5)$$

and the torque developed by the rotor under the influence of the backward rotating flux is

$$T_b = -\frac{7.04 I_{2b}'^2 r_2'}{n_s (2-s)} \text{ lb-ft} \quad (26-6)$$

$I_{2f}'$  and  $I_{2b}'$  are the currents produced in the rotor by the forward and backward fluxes respectively. The *resultant* developed torque is the sum of  $T_f$  and  $T_b$ . Thus

$$T_r = T_f + T_b \quad (26-7)$$

Fig. 26-7 shows both torques and the resultant torque for slips between 0 and +2. The resultant torque is *zero at standstill* in accordance with the fact that an alternating flux is not able to start an induction motor: only a

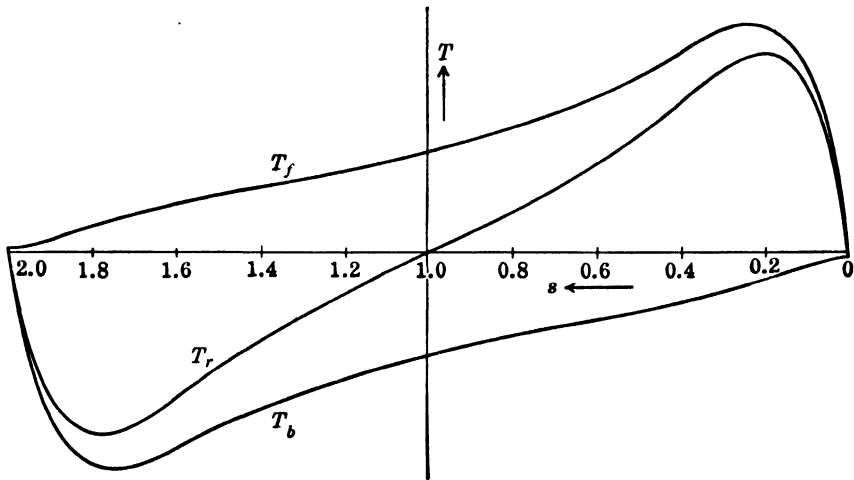


FIG. 26-7. Forward, backward, and resultant torque of a single-phase induction motor.

rotating flux is able to do this. At standstill  $s=1$  and  $2-s=1$  and both rotating fluxes have equal but opposite influence on the rotor; therefore  $T_f = -T_b$  and  $T_r = 0$ . However, at any other slip,  $|T_f| \neq |T_b|$  and there exists a driving torque  $T_r$ . This means that there is no torque on the rotor when it is at standstill ( $s=1$ ), but as soon as the rotor starts rotating ( $n > 0$ ), *regardless of the direction of rotation*, a driving torque is present which will bring the rotor up to about synchronous speed ( $n_s = 120f_1/p$ ) as in the poly-phase motor. At synchronous speed ( $s=0$ ) the resultant torque has a small negative value.

The secondary quantities in Eqs. 26-5 and 26-6 are referred to the primary. The reduction factors are found in the same manner as for the polyphase induction motor.

The reduction factor for voltage is  $N_1 k_{dp1}/N_2 k_{dp2}$  where  $N_1$  is the *total* number of turns of the stator and  $N_2$  the number of turns of the rotor *per phase*. The alternating mmf of the stator per pole is (Eq. 15-10)

$$F_a = 0.90 \frac{N_1 k_{dp1}}{p/2} I_1 \quad (26-8)$$

and the mmf of each of the two rotating fluxes

$$F_1 = 0.45 \frac{N_1 k_{dp1}}{p/2} I_1 \quad (26-9)$$

The mmf of the  $m_2$  phase rotor per pole is (Eq. 15-11)

$$F_2 = 0.45 m_2 \frac{N_2 k_{dp2}}{p/2} I_2. \quad (26-10)$$

In order that

$$I_2' \times 0.45 \frac{N_1 k_{dp1}}{p/2} = 0.45 m_2 \frac{N_2 k_{dp2}}{p/2} I_2,$$

the reduction factor for currents to the primary must be

$$a_I = \frac{m_2 N_2 k_{dp2}}{N_1 k_{dp1}}; \quad (26-11)$$

thus

$$I_{2f}' = \frac{m_2 N_2 k_{dp2}}{N_1 k_{dp1}} I_{2f}, \quad (26-12)$$

$$I_{2b}' = \frac{m_2 N_2 k_{dp2}}{N_1 k_{dp1}} I_{2b}. \quad (26-13)$$

The reduction factor for  $r_2$  and  $x_2$  is given by the ratio of the reduction factor for voltage to the reduction factor for current. Therefore

$$r_2' = \frac{1}{m_2} \left( \frac{N_1 k_{dp1}}{N_2 k_{dp2}} \right)^2 r_2, \quad x_2' = \frac{1}{m_2} \left( \frac{N_1 k_{dp1}}{N_2 k_{dp2}} \right)^2 x_2. \quad (26-14)$$

For the squirrel-cage rotor (see Art. 17-3)

$$m_2 = Q_2 N_2 = \frac{1}{2}, \quad k_{dp2} = 1. \quad (26-15)$$

If the rotor is skewed,  $N_2$  in the previous equations has to be multiplied by the skew factor (Art. 56-6).  $I_2$ ,  $r_2$ , and  $x_2$  are the values per bar. For the single-phase windings, the winding factor  $k_w$  is to be used for  $k_{dp1}$  (Art. 56-5).

**26-5. Kirchhoff's mesh equations of the stator and rotor circuits.** It is now simple to derive, on the basis of the foregoing, Kirchhoff's mesh equa-

tions for both rotor and stator. The two rotating fluxes induce two emf's and two currents ( $I_{2f}'$  and  $I_{2b}'$ ) of the frequencies of  $sf_1$  and  $(2-s)f_1$  respectively, in the rotor. Since the *frequencies are different*, the two emf's and their currents must be considered separately, i.e., two Kirchhoff's mesh equations must be set up for the rotor, namely, (see Eq. 18-2)

$$\dot{E}_{2f}' - j\dot{I}_{2f}'x_2' = \dot{I}_{2f}'\frac{r_2'}{s} \quad (26-16)$$

and

$$\dot{E}_{2b}' - j\dot{I}_{2b}'x_2' = \dot{I}_{2b}'\frac{r_2'}{2-s} \quad (26-17)$$

The emf's  $E_{2f}'$  and  $E_{2b}'$  become, according to the Eq. 18-3

$$\dot{E}_{2f}' = -j(\dot{I}_1 + \dot{I}_{2f}')\dot{Z}_m \quad (26-18)$$

and

$$\dot{E}_{2b}' = -j(\dot{I}_1 + \dot{I}_{2b}')\dot{Z}_m \quad (26-19)$$

( $I_1 + I_{2f}'$ ) is the resultant mmf, i.e., the magnetizing current of the forward rotating flux; ( $I_1 + I_{2b}'$ ) is the magnetizing current of the backward rotating flux. All quantities in Eqs. 26-16 to 26-19 are referred to the stator. Therefore the emf's induced in the stator winding by the two rotating fluxes are also equal to  $E_{2f}'$  and  $E_{2b}'$  (see Eq. 17-10), and Kirchhoff's mesh equation for the stator is (see Eq. 18-1)

$$\dot{V}_1 = \dot{I}_1(r_1 + jx_1) + j(\dot{I}_1 + \dot{I}_{2f}')x_m + j(\dot{I}_1 + \dot{I}_{2b}')x_m \quad (26-20)$$

**26-6. The equivalent circuit of the single-phase induction motor.** The equivalent circuit of the single-phase motor is obtained from Eq. 26-20 by eliminating the rotor currents  $I_{2f}'$  and  $I_{2b}'$  with the aid of Eqs. 26-16 to 26-19. Introducing the abbreviations

$$\begin{aligned} \dot{Z}_1 &= r_1 + jx_1, \quad \dot{Z}_{2f}' = \frac{r_2'}{s} + jx_2'; \\ \dot{Z}_{2b}' &= \frac{r_2'}{2-s} + jx_2' \quad \text{and} \quad r_m + jx_m = \dot{Z}_m \end{aligned} \quad (26-21)$$

Eq. 26-20 becomes

$$\dot{V}_1 = \dot{I}_1 \left[ \dot{Z}_1 + \frac{\dot{Z}_m \dot{Z}_{2f}'}{\dot{Z}_m + \dot{Z}_{2f}'} + \frac{\dot{Z}_m \dot{Z}_{2b}'}{\dot{Z}_m + \dot{Z}_{2b}'} \right] \quad (26-22)$$

The second term in the bracket is the impedance of  $Z_m$  and  $Z_{2f}'$  connected in parallel; the third term in the bracket is the impedance of  $Z_m$  and  $Z_{2b}'$  connected in parallel. Therefore, the equivalent circuit of the single-phase induction motor is as shown in Fig. 26-8, or more explicitly as shown in Fig. 26-9.

With the parameters given, it is possible to determine from the equivalent circuit the primary current, the primary power factor, and the rotor currents



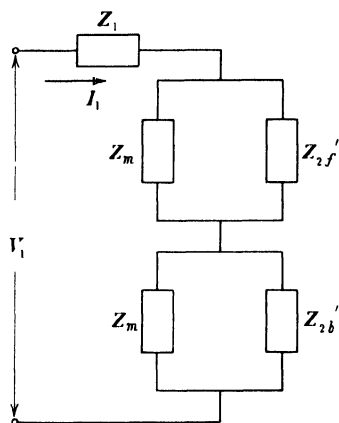


FIG. 26-8. Equivalent circuit of the single-phase induction motor.

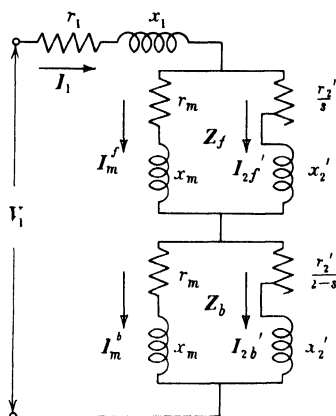


FIG. 26-9. Equivalent circuit of the single-phase induction motor.

$I_{2f}'$  and  $I_{2b}'$ . Then, with the aid of Eqs. 26-5 to 26-7, the forward and backward torques and the resultant torque can be calculated.

Fig. 26-10 shows the forward rotor current  $I_{2f}'$ , the backward rotor current  $I_{2b}'$ , and the stator current  $I_1$  as a function of slip. The backward current  $I_{2b}'$  is a mirror image of the forward current  $I_{2f}'$  with respect to the axis of ordinates through  $s = 1$ .  $I_{2f}'$  is zero at  $s = 0$ ;  $I_{2b}'$  is zero at  $s = 2$ .

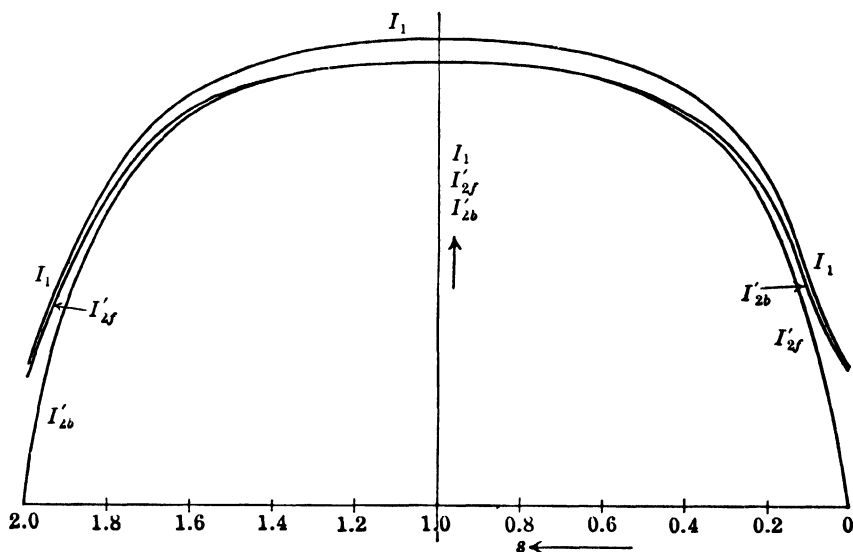


FIG. 26-10. Forward rotor current, backward rotor current, and primary current as a function of slip.

Consider the *characteristic points*  $s=0$ ,  $s=2$ , and  $s=1$ . For  $s=0$  and  $s=2$ , the equivalent circuit yields the same total impedance, i.e., the same primary current  $I_1$ . This impedance is

$$\dot{Z}_{1(s=0)} = jx_m; \quad \dot{Z}_{1(s=2)} \approx \frac{r_2'}{2k_2^2} + j\frac{x_2'}{k_2} \quad (26-23)$$

and the total impedance

$$\dot{Z}_{1(s=0)} \approx \left( r_1 + \frac{r_2'}{2k_2^2} \right) + jx_m \frac{k_1k_2 - 1}{k_2}. \quad (26-24)$$

where

$$k_2 = 1 + \tau_2 \quad \text{and} \quad \tau_2 = \frac{x_2'}{x_m}$$

and

$$k_1 = 1 + \tau_1 \quad \text{and} \quad \tau_1 = \frac{x_1}{x_m}$$

(see Eqs. 27-1, 2, 3).

The stator current at  $s=0$  is with fair approximation

$$I_{1(s=0)} = I_{1(s=2)} = V_1 \frac{1}{\sqrt{\left( r_1 + \frac{r_2'}{2k_2^2} \right)^2 + \left( \frac{x_m}{k_2} \right)^2 (k_1k_2 - 1)^2}}, \quad (26-25)$$

$$\tan \varphi_{1(s=0)} = \frac{x_m(k_1k_2 - 1)}{k_2 \left( r_1 + \frac{r_2'}{2k_2^2} \right)}. \quad (26-26)$$

When the rotor circuit is open at  $s=0$

$$I_{1(s=0, \text{ open})} = \frac{V_1}{\sqrt{r_1^2 + k_1^2 x_m^2}}. \quad (26-27)$$

The ratio between these two currents is approximately

$$\frac{I_{1(s=0)}}{I_{1(s=0, \text{ open})}} \approx \frac{k_1k_2}{k_1k_2 - 1} \approx 1.8 \text{ to } 1.9. \quad (26-28)$$

When the rotor is open at  $s=0$  the reactive component of the stator current is equal to  $I_\phi$  (see Art. 22-1). When the rotor is closed at  $s=0$  the reactive component of the stator current is nearly twice as large. This is due to the backward rotating field. This field induces an emf and current in the rotor also at  $s=0$  and the stator must draw more current from the line in order to sustain the main flux. In the polyphase machine there is no difference between the two currents; their ratio is equal to 1. Since the reactive component of the no-load current of the single-phase motor is nearly twice the current  $I_\phi$  necessary to produce the flux, the power factor of the single-phase motor is less than that of the polyphase motor.



There is a small negative torque at  $s=0$  due to the backward rotating flux. However, the line through  $P_0'$  and  $P_L$  represents with fair approximation the  $P_{m,dev}$ -Line (see Fig. 21-4), and the distance from any point of the circle to this line is a measure of the developed mechanical power. As in the polyphase motor, the  $P_{m,del}$ -Line can be found by drawing a line parallel to the  $P_{m,dev}$ -Line, through the point  $P_0$  (see Fig. 21-4).

The circle diagram of the single-phase motor does not include a torque line since the torque of the single-phase motor is zero not only at a point close to  $s=0$  ( $P_0'$ ) and  $s=\infty$  ( $P_\infty$ ) but also at standstill ( $s=1$ ,  $P_L$ ). The determination of the torque-speed curve from the circle diagram is not possible for the single-phase motor; as a result the circle diagram of the single-phase motor is of little value.

The single-phase motor can operate as a generator, but it *cannot operate as a brake* (dotted part of the circle between  $P_L$  and  $P_\infty$ ). Operation as a brake means that the rotor rotates in a direction opposite to that of the rotating flux. Considering the fact that the forward and backward fluxes rotate in opposite directions, the single-phase motor has no defined direction of rotation; it is capable of coming up to speed from standstill ( $s=1$ ) in either direction and there is no possibility for its rotor to run against its rotating flux (see Art. 26-4)—References on the operation of single-phase motors are given under *D*.

**26-8. Justification of the two rotating field theory.** The theory of the single-phase motor developed in this chapter is based on Eq. 26-2, i.e., on a *mathematical* operation which replaces a stationary wave by two rotating waves.

One could be in doubt whether this mathematical operation yields the actual physical phenomena occurring in the single-phase motor, for example, whether there are really two currents of different frequency in the rotor. Kirchhoff's equations 26-16 to 26-20 which are the basis for the theory of the single-phase motor derived in the previous articles is based on the assumption of two rotor currents of different frequency. If there are no two such currents in the rotor, the theory would be invalid.

The answer is that the mathematics do not fail. There are two currents of different frequencies in the rotor. This can be proved by test and also by using the constant flux theorem (Art. 60-1 and Ref. C9).

## Chapter 27

### DETERMINATION OF THE PARAMETERS OF THE SINGLE-PHASE INDUCTION MOTOR FROM A NO-LOAD AND A LOCKED-ROTOR TEST

**27-1. The no-load test.** The no-load test is run at rated voltage  $V_1$  with the starting winding open (see Art. 28-1), and  $I_0$  and  $P_0$  are measured.

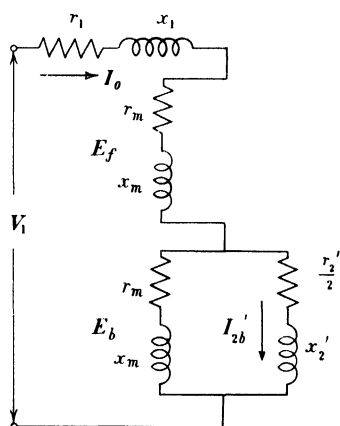


FIG. 27-1. Equivalent circuit of the single-phase motor at no-load.

Fig. 27-1 shows the equivalent circuit for no-load ( $s \approx 0$ ). At synchronous speed no current flows in the rotor of the *polyphase* motor (see Fig. 22-1) because the relative speed between the rotating flux and the rotor is zero. However, it is quite different with the single-phase motor, for at  $s = 0$  there is no difference in speed between the rotor and the forward rotating flux, but there is a difference in speed equal to twice the synchronous speed between the rotor and the backward rotating flux. Therefore current  $I_{2b}'$  flows in the rotor of the single-phase motor at  $s = 0$ . At no-load the rotor current of the polyphase motor is negligible. As can be seen from Fig. 27-1 this is not the case with the single-phase motor.

At no-load the stator of the polyphase motor carries only the magnetizing current necessary to sustain the main flux since there is no armature reaction from the rotor. The stator current of the single-phase motor at no-load is about twice the magnetizing current, owing to the armature reaction from the rotor current  $I_{2b}'$ . As a result, the stator copper losses of the single-phase motor at no-load are larger than those of the polyphase motor. At no-load the copper losses in the rotor of the polyphase motor are  $\approx 0$ , but there are copper losses at no-load in the rotor of the single-phase motor due to the current  $I_{2b}'$ .

Since  $(r_m + jx_m)$  is large in comparison with  $[(r_2'/2) + jx_2']$ ,  $I_{2b}' \approx I_0$  at no-load (see Fig. 27-1 and also Fig. 26-10). It will be shown in the following article

that  $r_2' \approx r_1/2$ . Hence the rotor copper losses at no-load can be assumed equal to  $0.5r_1I_0^2$ .

Thus the power input at no-load  $P_0$  consists of the iron losses due to the main flux, the friction and windage losses, the rotational iron losses, the copper losses in the stator winding  $I_0^2r_1$  and the copper losses in the rotor winding  $\approx 0.5I_0^2r_1$ . Subtracting from  $P_0$  the sum  $(P_{F+W} + I_0^2r_1 + 0.5I_0^2r_1)$ , the remainder is the sum of  $P_{h+e} + P_{ir,rot}$ . It can be assumed with fair approximation that the iron losses due to the main flux are equal to  $\frac{1}{2}(P_{h+e} + P_{ir,rot})$ . Thus the iron losses due to the main flux, which are necessary for the determination of the parameter  $r_m$ , are known.

It follows from the equivalent circuit of Fig. 27-1 that, for no-load ( $s \approx 0$ ),

$$V_1 \approx I_0 \frac{x_m}{k_2} (2k_2^2 - 1) \quad (27-1)$$

where

$$k_2 = 1 + \frac{x_2'}{x_m} \quad (27-2)$$

or

$$x_m \approx \frac{V_1}{I_0} \frac{k_2}{2k_2^2 - 1} \quad (27-3)$$

$x_m$  cannot be determined from Eq. 27-3 because  $k_2$  is unknown. However,  $k_2$  varies within narrow limits, usually between 1.03 and 1.07, and a certain value for  $k_2$  can be assumed at first. This value can be checked later (see the following article). A knowledge of  $x_m$  is necessary for the determination of  $r_m$ .

As for the polyphase motor, Eqs. 22-5 and 22-4,

$$g_m = \frac{P_{h+e}}{E_1^2} \quad (27-4)$$

$$E_1 \approx V_1 - I_0 x_1 \quad (27-5)$$

$E_1$  consists here of two parts: the voltage across the forward branch  $E_{2f}'$ , and the voltage across the backward branch  $E_{2b}'$ , Fig. 27-1. Since  $(r_m + jx_m)$  is large in comparison with  $(r_2'/2 + jx_2')$ , the voltage  $E_{2b}'$  is large in comparison with the voltage  $E_{2b}$ . It can be assumed that the ratio of the two voltages is the same as that of the two impedances  $(r_m + jx_m) \approx jx_m$  and  $[(r_2'/2) + jx_2']$ , i.e.

$$\frac{E_{2f}'}{E_{2b}'} = \frac{x_m}{\sqrt{(r_2'/2)^2 + x_2'^2}} = C \quad (27-6)$$

Since  $E_1 = E_{2f}' + E_{2b}'$

$$E_{2f}' \approx E_1 \frac{C}{1+C} \quad (27-6a)$$

Assuming that the iron losses are produced by the forward rotating flux only, because the backward emf is small and the backward rotating flux therefore weak

$$g_m \approx \frac{P_{h+e}}{E_{2f}'^2} \quad (27-7)$$

Further from Eq. 22-7

$$r_m \approx g_m x_m^2 \quad (27-8)$$

Thus the no-load test yields the main flux parameters  $x_m$  and  $r_m$ , provided that the resistances  $r_1$  and  $r_2'$  and the leakage reactances  $x_1$  and  $x_2'$  are known. These parameters can be obtained from the short-circuit (locked-rotor) test.

**27-2. The locked-rotor test.** This test is made with the starting winding open, and  $V_L$ ,  $I_L$ , and  $P_L$  are measured. As for the polyphase motor, Eq. 22-9,

$$Z_L = \frac{V_L}{I_L} \quad R_L = \frac{P_L}{I_L^2} \quad X_L = \sqrt{Z_L^2 - R_L^2} \quad (27-9)$$

The equivalent circuit for the locked rotor, Fig. 27-2, yields with fair approximation

$$Z_{(s=1)} \approx \left( r_1 + \frac{2r_2'}{k_2^2} \right) + j(x_1 + 2x_2') \quad (27-10)$$

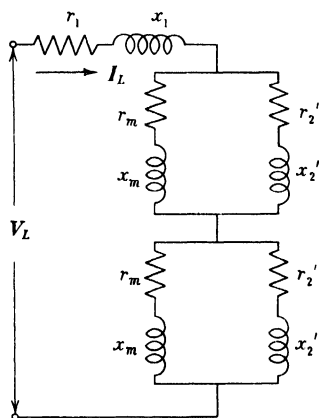


FIG. 27-2. Equivalent circuit of the single-phase motor at standstill.

i.e., at locked rotor, the equivalent resistance of the motor is approximately equal to the primary resistance plus twice the rotor resistance, and the equivalent reactance of the motor is approximately equal to the primary reactance plus twice the rotor reactance.

$r_1$  is measured separately. Then, using the measured locked-rotor resistance  $R_L$ ,

$$r_2' = \frac{R_L - r_1}{2} k_2^2 \quad (27-11)$$

For the separation of  $x_1$  and  $x_2'$ , it is usually assumed that

$$x_1 \approx 2x_2' = \frac{X_L}{2} \quad (27-12)$$

With these values of  $x_1$  and  $x_2'$ , the previously assumed value for  $k_2$  can be checked, and the resistance  $r_2'$ , the quantity  $C$  (Eq. 27-6), and the resistance  $r_m$  can be determined.

### 27-3. Influence of the parameters on the performance of the motor.

The influence of the parameters on the performance of the single-phase motor is, in general, the same as that on the polyphase motor. However, the existence of the backward rotor current  $I_{2b}'$  results in an increase in the stator current and mainly of its reactive component. This makes the *power factor* of the single-phase motor *lower* than that of the polyphase motor. Also the efficiency of the single-phase motor is influenced by the increased copper losses in both the stator and rotor.

A further difference between the polyphase and single-phase motor appears in the influence of the secondary resistance on the pull-out torque. The rotor resistance does not affect the magnitude of the pull-out torque in the polyphase motor (see Art. 22-4d); it affects only the pull-out slip, i.e., the slip at which the pull-out torque appears. Because of the backward rotating flux, the rotor resistance influences not only the pull-out slip of the single-phase motor but also the magnitude of the pull-out torque. Fig. 27-3 shows speed-torque curves of a single-phase motor for different values of  $r_2'$ . The larger the rotor resistance, the smaller is the pull-out torque. Speed control of a single-phase motor with a wound rotor by means of a resistance in the rotor circuit is therefore possible only within a narrow range.

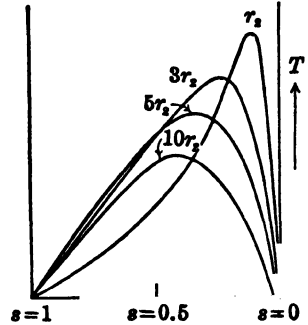


FIG. 27-3. Influence of the rotor resistance on the torque-speed curve of the single-phase motor.

**Example 27-1.** The determination of the parameters from a no-load and locked-rotor test will be demonstrated on  $\frac{1}{8}$ -HP 6-pole 60-cycle split-phase motor for 110 volts.

(a) *No-load test* (starting winding open) shows

$$V_1 = 110 \text{ volts}, \quad P_0 = 63.0 \text{ watts}, \quad I_0 = 2.70 \text{ amp}$$

$r_1$  after the test = 2.65 ohms;  $P_{F+} = 3.0$  watts (ball-bearing motor)

(b) *Locked-rotor test* (starting winding open) shows

$$V_L = 110 \text{ volts}; \quad P_L = 851 \text{ watts}; \quad I_L = 11.65 \text{ amp}$$

$r_1$  after the test = 2.54 ohms.

(The difference in the magnitude of  $r_1$  is due to the fact that the tests were made at different times and at different ambient temperatures.)

Assume  $k_2 = 1.05$ ; then from Eq. 27-3

$$x_m = \frac{110}{2.70} \cdot \frac{1.05}{2 \times (1.05)^2 - 1} = 35.5 \text{ ohms}$$

$r_m$  can be determined when the other parameters are known.



From Eq. 27-9

$$Z_L = \frac{110}{11.65} = 9.44 \text{ ohms}; \quad R_L = \frac{851}{(11.65)^2} = 6.27 \text{ ohms};$$

$$X_L = \sqrt{(9.44)^2 - (6.27)^2} = 7.03 \text{ ohms}$$

From Eq. 27-12

$$x_1 \approx 2x_2' \approx \frac{7.03}{2} = 3.51 \text{ ohms}$$

$$x_2' = 1.75 \text{ ohms}$$

Checking (Eq. 27-2)

$$k_2 = 1 + \frac{1.75}{35.5} = 1.0493$$

which value is very close to the assumed  $k_2 = 1.05$ .

From Eq. 27-11

$$r_2' = \frac{6.27 - 2.54}{2} \times (1.05)^2 = 2.06$$

The five parameters as determined from the no-load and locked-rotor tests are (in ohms)

$$\begin{array}{ll} r_1 = 2.54 & r_2' = 2.06 \\ x_m = 35.5 & \\ x_1 = 3.51 & x_2' = 1.75 \end{array}$$

For the calculation of the performance of the motor the hot resistances of the windings at full-load should be used; if full-load data are not available the resistances at 75°C must be used. For the motor considered,  $r_1$  at full-load was 2.85 ohms, while in the locked-rotor test the resistance was 2.54 ohms. It can be assumed that the resistance of the rotor is increased by the load in the same ratio as the stator resistance. Thus at full-load  $r_2' = 2.06(2.85/2.54) = 2.31$ , and the motor parameters for performance calculations are (in ohms)

$$\begin{array}{ll} r_1 = 2.85 & r_2' = 2.31 \\ x_m = 35.5 & \\ x_1 = 3.51 & x_2' = 1.75 \end{array}$$

$r_m$  can now be determined. The no-load losses of the motor are 63 watts. They consist of copper losses in both windings, iron losses (due to the main flux + rotational losses), and friction and windage losses. The latter losses are 3.0 watts. The resistance of the stator winding after the no-load test was 2.65 ohms, and thus the loss in the stator copper is

$$P_{co,1} = 2.65 \times (2.7)^2 = 19.3 \text{ watts}$$

From the locked-rotor test,  $r_1 = 2.54$  and  $r_2' = 2.06$ . Since at no-load  $r_1 = 2.65$ , it can be assumed that at no-load

$$r_2' = 2.06 \frac{2.65}{2.54} = 2.15 \text{ ohms}$$

It has been explained previously (see Art. 27-1 and Fig. 26-10) that the rotor current at no-load is approximately equal to  $I_0(I_{2b}' \approx I_0)$ . Therefore the losses in the rotor winding at no-load are

$$P_{co, 2} = 2.15 \times (2.7)^2 = 15.7 \text{ watts}$$

The total iron losses are then

$$P_{ir} = 63.0 - (3.0 + 19.3 + 15.7) = 25.0 \text{ watts}$$

The rotational iron losses at no-load are relatively larger in the single-phase motor than in the polyphase motor. As in the latter motor, the slot openings cause tooth-surface and tooth-pulsation losses in the single-phase motor (see Art. 29-1a). However, contrary to the polyphase motor, the single-phase motor has a large no-load current which does not differ very much from the full-load current. In consequence of this, the harmonics produce additional tooth-surface and tooth-pulsation losses (see Art. 29-1b) at no-load. As has been explained, all of these additional iron losses are caused by the rotation of the rotor and must be supplied by the rotor. It can be assumed that the losses due to the main flux are approximately half of the total iron losses, i.e.,  $P_{h+c} \approx 13$  watts. This loss determines the magnitude of  $r_m$ . From Eqs. 27-5, 27-6, and 27-6a

$$E_1 = 110 - 2.70 \times 3.51 = 100.6$$

$$C = \frac{35.5}{\sqrt{(2.15/2)^2 + (1.75)^2}} = 17.3 \quad E_{2f}' = 100.6 \frac{17.3}{18.3} = 95.2$$

Eqs. 27-7 and 27-8 yield

$$g_m = \frac{13}{(95.2)^2} = 0.0014$$

$$r_m = 0.0014 \times (35.5)^2 = 1.77 \text{ ohms}$$

The six parameters for performance calculations are (in ohms)

$$\begin{array}{lll} r_1 = 2.85 & r_m = 1.77 & r_2' = 2.31 \\ x_1 = 3.51 & x_m = 35.5 & x_2' = 1.75 \end{array}$$

*Note.*—In general the saturation of the leakage paths should be taken into account when evaluating the locked-rotor test (see Art. 22-6 and Ex. 22-1). The saturation of the leakage paths has been neglected here.

**Example 27-2.** The parameters computed in Example 27-1 for a  $\frac{1}{8}$ -HP 6-pole split-phase motor will be used to determine the performance of the motor.

(a) First the iron losses due to the main flux will be neglected, i.e., assume  $r_m = 0$ , and the primary current, power factor, and torque will be determined for approximately normal slip. Since no simple formula is available for the normal slip of a single-phase motor, a value of slip will be assumed, the torque corresponding to this slip will be computed, and finally the real slip will be determined from the ratio of rated output to calculated output. The normal slip of the single-phase motor lies between 0.025 and 0.05, the smaller value occurring in larger motors.

The calculations below will be carried through for a slip of  $s = 0.038$ . Since the iron losses are neglected, the resultant impedance of the forward branch of the equivalent circuit is

$$\begin{aligned}\dot{Z}_f &= \frac{\dot{Z}_m \dot{Z}_{2f}'}{\dot{Z}_m + \dot{Z}_{2f}'} = \frac{35.5/90[(2.31/0.038) + j1.75]}{j35.5 + [(2.31/0.038) + j1.75]} \\ &= \frac{35.5/90 \times 60.8/1.65}{60.8 + j37.25} = \frac{2160/91.65}{71.4/31.5} \\ &= 30.3/60.15 = 15.1 + j26.2\end{aligned}$$

and the impedance of the backward branch

$$\begin{aligned}\dot{Z}_b &= \frac{\dot{Z}_m \dot{Z}_{2b}'}{\dot{Z}_m + \dot{Z}_{2b}'} = \frac{35.5/90[(2.31/1.962) + j1.75]}{[j35.5 + (2.31/1.962) + j1.75]} \\ &= \frac{35.5/90 \times 2.11/56.0}{1.178 + j37.25} = \frac{74.9/146.9}{37.3/88.2} \\ &= 2.01/57.8 = 1.07 + j1.70\end{aligned}$$

$$\dot{Z}_t = \dot{Z}_1 + \dot{Z}_f + \dot{Z}_b = 19.0 + j31.4 = 36.8/58.8$$

$$\dot{I}_1 = \frac{110/0}{36.8/58.8} = 2.99/-58.8$$

$$\cos 58.8^\circ = 0.517$$

$$V_{2f}' = I_1 Z_f = 2.99 \times 30.3 = 90.6 \text{ volts}$$

$$V_{2b}' = I_1 Z_b = 2.99 \times 2.01 = 6.01 \text{ volts}$$

$$I_{2f}' = \frac{V_{2f}'}{Z_{2f}'} = \frac{90.6}{\sqrt{(2.31/0.038)^2 + (1.75)^2}} = 1.49 \text{ amp}$$

$$I_{2b}' = \frac{V_{2b}'}{Z_{2b}'} = \frac{6.01}{\sqrt{(2.31/1.962)^2 + (1.75)^2}} = 2.85 \text{ amp}$$

From Eqs. 26-5, 26-6 and 26-7 the developed torque is

$$T = \frac{7.04}{1200} \times 2.31 \left[ \frac{(1.49)^2}{0.038} - \frac{(2.85)^2}{1.962} \right] \times 16 = 11.8 \text{ oz-ft}$$

Since part of this developed torque is necessary to supply the iron losses due to rotation and the friction and windage losses, the load torque is therefore less than the 11.8 oz-ft developed.

(b) The iron losses due to the main flux will now be taken into account and the resultant impedance determined as in part (a), Fig. 26-9.

$$\begin{aligned}\dot{Z}_m &= r_m + jx_m = 1.77 + j35.5 \\ \dot{Z}_f &= \frac{(1.77 + j35.5)[(2.31/0.038) + j1.75]}{1.77 + j35.5 + (2.31/0.038) + j1.75} \\ &= \frac{35.5/87.15 \times 60.8/1.65}{62.6 + j37.25} = \frac{2160/88.8}{72.8/30.8} \\ &= 29.7/58.0 = 15.7 + j25.2\end{aligned}$$

$$\dot{Z}_b = \frac{35.5 \angle 87.15 [(2.31/1.962) + j1.75]}{1.77 + j35.5 + (2.31/1.962) + j1.75}$$

$$= \frac{35.5 \angle 87.15 \times 2.11 \angle 56.0}{2.95 + j37.25} = \frac{74.9 \angle 143.2}{37.3 \angle 85.46}$$

$$= 2.01 \angle 57.7 = 1.07 + j1.70$$

$$\dot{Z}_t = \dot{Z}_1 + \dot{Z}_f + \dot{Z}_b = 19.6 + j30.4$$

$$= 36.2 \angle 57.2$$

$$\dot{I}_1 = \frac{110 \angle 0}{36.2 \angle 57.2} = 3.04 \angle -57.2$$

$$\cos 57.2^\circ = 0.542$$

$$V_{2f}' = I_1 Z_f = 3.04 \times 29.7 = 90.2 \text{ volts}$$

$$V_{2b}' = I_1 Z_b = 3.04 \times 2.01 = 6.11 \text{ volts}$$

$$I_{2f}' = \frac{V_{2f}'}{Z_{2f}'} = \frac{90.2}{\sqrt{(2.31/0.038)^2 + (1.75)^2}} = 1.49 \text{ amp}$$

$$I_{2b}' = \frac{V_{2b}'}{Z_{2b}'} = \frac{6.11}{\sqrt{(2.31/1.962)^2 + (1.75)^2}} = 2.89 \text{ amp}$$

The developed torque is

$$T = \frac{7.04}{1200} \times 2.31 \left[ \frac{(1.49)^2}{0.038} - \frac{(2.89)^2}{1.962} \right] \times 16 = 11.67 \text{ oz-ft}$$

The iron losses due to rotation were assumed to be 12 watts and the friction and windage loss 3.0 watts, totaling 15 watts. The delivered torque for the assumed slip of 0.038 is therefore

$$T_{\text{del}} = 11.67 - \frac{7.04}{1200} \times 15 \times 16 = 10.26 \text{ oz-ft}$$

To determine the efficiency at slip  $s = 0.038$

$$P_{\text{co},1} = (3.04)^2 \times 2.85 = 26.3 \text{ watts}$$

$$P_{\text{co},f} = (1.49)^2 \times 2.31 = 5.1$$

$$P_{\text{co},b} = (2.89)^2 \times 2.31 = 19.3$$

$$P_{\text{ir, total}} = 25$$

$$P_{\text{F+W}} = 3$$

$$\text{Total} = 78.7 \text{ watts}$$

$$\text{Input} = 110 \times 3.04 \times 0.542 = 181.4 \text{ watts}$$

$$\text{Output} = 181.4 - 78.7 = 102.7 \text{ watts}$$

$$= 0.137 \text{ HP}$$

$$\eta = \frac{102.7}{181.4} \times 100 = 56.6\%$$

Since the rated output is 0.166 HP, the normal slip is approximately

$$\frac{0.166}{0.137} \times 0.038 = 0.046$$

Therefore normal speed is approximately

$$1200(1 - 0.046) = 1144 \text{ rpm}$$

It should be noted that no stray load losses were included in the efficiency calculation. This is justified by the fact that the no-load current of the single-phase motor is high and therefore stray load losses occur at no-load and are included with the rotational iron losses.

### PROBLEMS

In all problems following take into account the iron losses due to the main flux and neglect saturation of leakage paths.

1. Determine the running performance of the motor of Examples 27-1 and 27-2 at a slip of 0.045.

2. Calculate and plot for the motor of Examples 27-1 and 27-2 the primary current and power factor for slips of 0.30, 0.25, 0.20, 0.10, 0.075 and 0.046.

3. Calculate and plot for the motor of Examples 27-1 and 27-2 the developed torque-speed characteristic for slips of 0.30, 0.25, 0.20, 0.10, 0.075, and 0.046.

4. Repeat Problem 3 for a 25% increase in  $r_2'$ .

5. The no-load test and locked-rotor test of a  $\frac{1}{4}$ -hp split-phase motor for 110 volts, 60 cycles, 4 poles, and approximately 1725 rpm, show the following:

#### *No-load Test*

$$V_1 = 110 \quad I_0 = 3.55 \quad P_0 = 86.0 \\ r_1 = 1.58$$

#### *Locked-rotor Test*

$$V_L = 110 \quad I_L = 21.0 \quad P_L = 1592 \\ r_1 = 1.55$$

Friction and windage losses = 7.0 watts. Hot resistance at full-load:  $r_1 = 1.71$ . Determine for this motor its six constants. Assume that half of the iron losses are due to the main flux.

6. Determine for the motor of Problem 5 the running performance at a slip  $s = 0.043$ .

7. For the motor of Problem 5 calculate and plot the primary current and power factor for slips of 0.30, 0.25, 0.20, 0.10, 0.075 and 0.043.

8. Calculate and plot the developed torque-speed characteristic for the motor of Problem 5 at slips of 0.30, 0.25, 0.20, 0.10, 0.075 and 0.043.

9. A  $\frac{1}{8}$ -hp split-phase motor designed for 100 volts, 60 cycles, 4 poles, and approximately  $n = 1720$  has the following constants:

$$r_1 = 3.8, \quad r_2' = 2.325, \quad I_0 = 1.86 \\ x_m = 52.9, \quad x_2' = 2.1, \quad r_2' = 2.1 \text{ at no-load} \\ x_1 = 4.2,$$

Friction and windage losses = 10 watts. Total iron losses = 19 watts of which half can be assumed as main flux losses. Determine the main flux resistance  $r_m$ .

10. Determine the running performance for the motor of Problem 9 at a slip of 0.045.

11. Calculate and plot for the motor of Problem 9 the primary current and power factor for slips of 0.30, 0.25, 0.20, 0.10, 0.075 and 0.045.

12. Calculate and plot the developed torque-speed characteristic for the motor of Problem 9 at slips of 0.30, 0.25, 0.20, 0.10, 0.075, and 0.045.

13. The no-load and locked-rotor tests of a  $\frac{1}{4}$ -hp split-phase motor for 110 volts, 60 cycles, 4 poles, and approximately 1725 rpm, show the following:

*No-load Test*

$$V_1 = 110 \quad I_0 = 2.75 \quad P_0 = 59.5 \\ r_1 = 2.41$$

*Locked-rotor Test*

$$V_L = 110 \quad I_L = 14.6 \quad P_L = 1123 \\ r_1 = 2.21$$

Friction and windage losses = 5.4 watts. Hot resistance at full-load:  $r_1 = 2.44$ . Determine for this motor its six constants. Assume that half of the iron losses are due to the main flux.

14. Determine the running performance of the motor in Problem 13 for a slip of 0.045.

15. Calculate and plot the primary current and power factor of the motor in Problem 13 for slips of 0.30, 0.25, 0.20, 0.10, 0.075 and 0.045.

16. Calculate and plot the developed torque-speed characteristic for the motor of Problem 13 at slips of 0.30, 0.25, 0.20, 0.10, 0.075, and 0.045.

## Chapter 28

### STARTING THE SINGLE-PHASE MOTOR TYPES OF SINGLE-PHASE MOTORS

It has already been mentioned that in contrast to the polyphase motor or the a-c commutator motor, the single-phase motor has *no starting torque*. In order to start the single-phase motor, either a *rotating flux* such as that in the polyphase motor has to be produced, or a *commutator* with brushes has to be included with the rotor. The split-phase motor (Fig. 28-1) and the repulsion start motor (Fig. 28-5) are examples of these two methods of starting the single-phase motor.

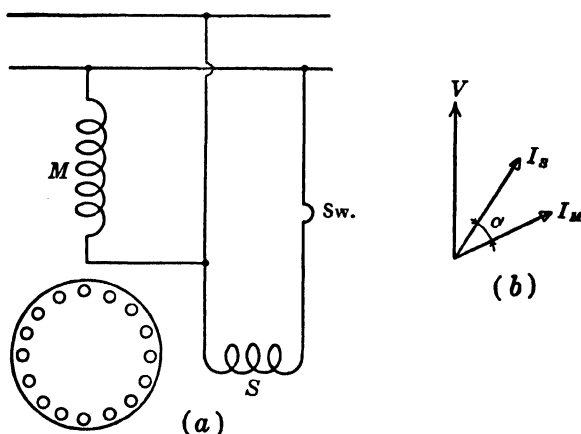


FIG. 28-1. Connection and current diagram of the split-phase motor (for starting).

**28-1. Starting by means of a rotating flux.** In order to produce a rotating flux at standstill a second winding (*starting or auxiliary winding*) is necessary in the stator in addition to the main winding. The axis of the starting winding has to be *displaced in space* with respect to the axis of the main winding, and the current in the starting winding has to be *out of time phase* with the current in the main winding.

The main winding leaves one slot or several slots empty and several slots only partly filled (see Fig. 26-4). The starting winding is placed in these

empty and partly filled slots so that the axes of both windings are displaced by 90 electrical degrees.

A number of different methods are employed to achieve the time phase shift between the currents in the main and starting windings.

(a) *Split-phase motor*. The connection diagram for this type of motor is shown in Fig. 28-1.  $M$  is the main winding,  $S$  is the starting winding,  $Sw$  is a centrifugal switch. The main winding has a relatively low resistance and high reactance, while the starting winding has a high resistance and low reactance. This results in an angle  $\alpha$  of about  $30^\circ$  between the currents in the two windings (Fig. 28-1b) and in a small rotating flux superimposed on the alternating flux. The starting torque is therefore limited. The starting winding cannot remain in the circuit continuously, or overheating and noise will occur. Usually a centrifugal switch on the rotor (see Fig. 26-6) automatically disconnects the starting winding at about 70% of the synchronous speed.

It is shown (see Art. 53-5) that the starting torque is approximately

$$T = \frac{450.8}{n_s} \frac{r_2'}{[1 + (x_2'/x_m)]^2} \frac{N_S k_{WS}}{N_M k_{WM}} I_M I_S \sin \alpha \text{ oz-ft} \quad (28-1)$$

where the subscripts  $M$  and  $S$  refer to the main and starting windings respectively.  $k_{WM}$  and  $k_{WS}$  are the winding factors of both windings (see Chap. 14).  $r_2'$  and  $x_2'$  are both referred to the main winding, and  $\alpha$  is the angle between the currents  $I_M$  and  $I_S$ .

The magnitude of the current drawn from the line ( $I_M + I_S$ ) is limited and fixed by the NEMA standards. Hence higher starting torques can be achieved mainly by increasing the angle  $\alpha$  between  $I_M$  and  $I_S$ .

(b) *Resistance-start split-phase motor*. An increase of the angle  $\alpha$  and of the starting torque can be achieved by inserting a resistance in series with the starting winding. This resistance must be cut out together with the starting winding at about 70% of the synchronous speed.

(c) *Reactor-start split-phase motor*. Inserting of a reactor in series with the main winding has the same effect as the insertion of a resistance in series with the starting winding. This reactor must be short-circuited, or otherwise made ineffective, when the starting winding circuit is opened by the centrifugal switch.

(d) *Capacitor-start motor*. A very considerable increase of the angle  $\alpha$  between  $I_M$  and  $I_S$  can be achieved when a capacitor is placed in series with the starting winding (Fig. 28-2a). The capacitor causes the current in the starting winding to lead the terminal voltage (Fig. 28-2b) and, with an appropriate capacitor, the angle  $\alpha$  may approach  $90^\circ$ .

Capacitor-start motors are built from  $\frac{1}{8}$  to 10 HP. For a line voltage of 110 volts the size of the capacitor is 70–90 $\mu$ f for  $\frac{1}{8}$ -HP motors, 120–150 $\mu$ f for the  $\frac{1}{4}$ -HP motor, 230–280 $\mu$ f for the  $\frac{1}{2}$ -HP motor, and 340–410 $\mu$ f for the 1-HP motor. The starting torques, which depend on the size of the capacitor,



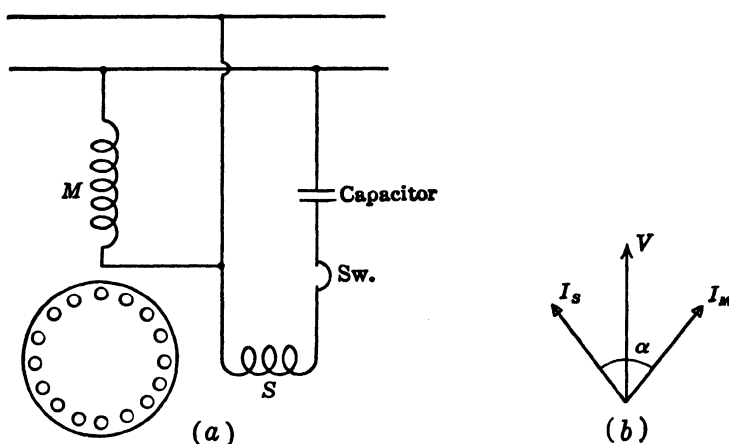


FIG. 28-2. Connection and current diagram of the capacitor-start motor.

are about 350 to 400% of rated torque for  $n=3450$  rpm, 400 to 475%  $n=1725$  rpm, and 285 to 390% for  $n=1140$  rpm, motors.

The capacitor used for starting purposes is the relatively inexpensive electrolytic capacitor which is fit for intermittent duty only. As in the split-phase motor the starting winding of the capacitor motor is opened by a centrifugal switch at about 70% of the synchronous speed.

(e) *Permanent-split capacitor motor.* In this type of motor the starting winding and the capacitor are designed for *permanent operation*, giving an unbalanced 2-phase motor. For satisfactory running performance only a small capacitance is necessary. For example, for 110 volts the capacitor of a  $\frac{1}{20}$ -HP motor is  $3\mu f$ , of a  $\frac{1}{8}$ -HP motor  $5\mu f$ , of a  $\frac{1}{4}$ -HP motor  $8\mu f$ , of a  $\frac{1}{2}$ -HP motor  $15\mu f$ . This is much less than the capacitance necessary for high starting torque (see "Capacitor-start motor"). However, the permanent-split capacitor motor uses the same capacitor for starting and running and, therefore, has a small starting torque of about 35 to 50% of the rated torque.

Since the electrolytic capacitor cannot be used for continuous operation, the more expensive oil or pyranol-insulated foil-paper capacitor must be used for this type of motor.

(f) *Two-value capacitor motor.* In order that the 2-phase motor described under (e) be able to develop a high starting torque and at the same time have a satisfactory running performance, it is necessary to use different values of capacitance for starting and running. This can be accomplished either by using two capacitors, an electrolytic capacitor for starting and an oil capacitor for running, or by using a single oil capacitor in connection with an autotransformer.

The arrangement with two separate capacitors is shown in Fig. 28-3.  $A$  is an oil capacitor;  $B$  is an electrolytic capacitor. A centrifugal switch ( $Sw$ ) on

the rotor shaft or a relay disconnects the electrolytic capacitor after starting is accomplished.

The arrangement with one capacitor and an autotransformer is shown in Fig. 28-4. The capacitor is connected across the terminals of the autotransformer which has a mid-tap used for starting. When starting, the voltage across the capacitor is twice as large as when running, thus giving an effective capacitance at start which is four times the running capacitance.

The permanent-split capacitor motor and the 2-value capacitor motor both operate as unbalanced 2-phase motors and offer advantages in comparison with the split-phase motor and capacitor-start motor, which are pure single-phase motors. The latter motors produce a pulsating torque resulting in vibration and noise under certain conditions. The former motors develop a more uniform torque and are, therefore, quieter than the pure single-phase motors.

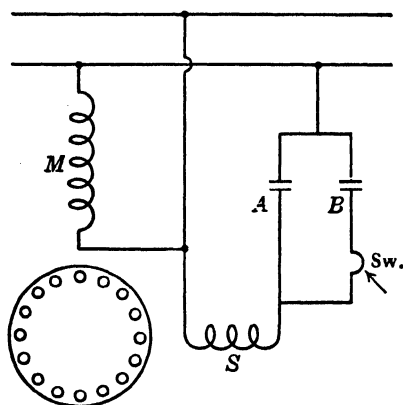


FIG. 28-3. Connection diagram of the 2-value capacitor motor with two capacitors.

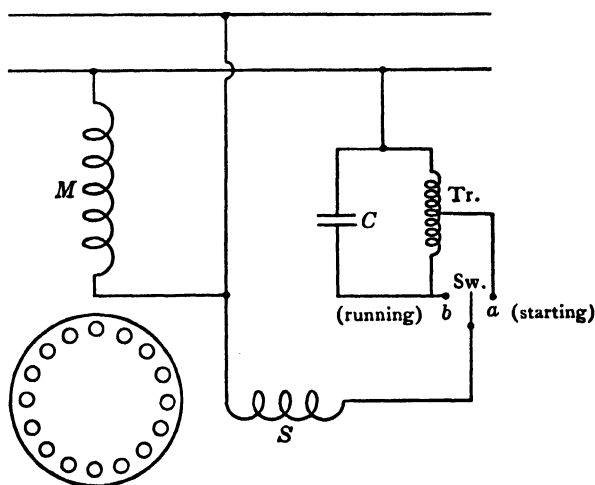


FIG. 28-4. Connection diagram of the 2-value capacitor motor with transformer.

**28-2. Starting by means of a commutator and brushes.** This method of starting a single-phase induction motor is based upon the properties of the *repulsion motor* which is a single-phase a-c commutator motor. Its connection diagram is shown in Fig. 28-5. The stator has a single-phase winding

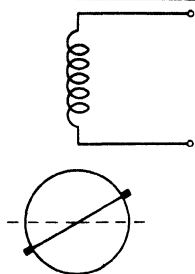


FIG. 28-5. Connection diagram of the repulsion motor.

similar to that of the single-phase induction motor, and the rotor has a d-c armature winding with commutator and brushes. The *brushes are short-circuited*. It will be shown in Art. 47-3 that this motor has series-motor characteristics and is, therefore, able to develop a high starting torque.

Reversal of the repulsion motor can be achieved either by shifting the brushes (see Art. 47-3), or by arranging two identical single-phase windings in the stator, one for each direction of rotation.

Two types of single-phase motors employing the repulsion motor properties for starting are available: the repulsion-start induction motor and the repulsion induction motor.

(a) *Repulsion-start induction motor*. This motor is built exactly as the repulsion motor. However, when the rotor has reached about  $\frac{2}{3}$  of the synchronous speed, a centrifugal mechanism short-circuits the commutator segments so that the armature acts as a squirrel-cage winding in a single-phase stator. A view of such a motor, disassembled, is shown in Fig. 28-6. The centrifugal mechanism is sometimes designed to lift the brushes from the commutator at the same time that a bracelet short-circuits the commutator segments. The repulsion-start induction motor starts as a repulsion motor but operates as an induction motor with an approximately constant-speed characteristic.

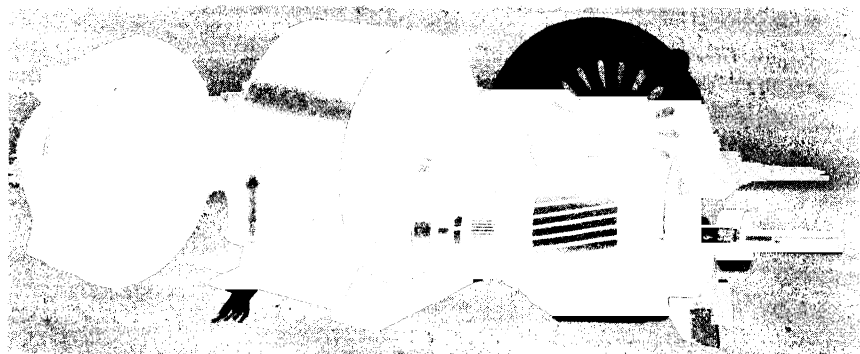


FIG. 28-6. Disassembled small repulsion-start single-phase motor.

(b) *Repulsion-induction motor*. The stator is the same as that of the repulsion (single-phase) motor. In addition to the d-c armature winding with commutator and brushes a squirrel-cage winding is also included in the rotor. No centrifugal mechanism is used to short-circuit the d-c armature winding so that both rotor windings always operate in parallel. Depending upon the design of the windings, the motor may have either an approximately

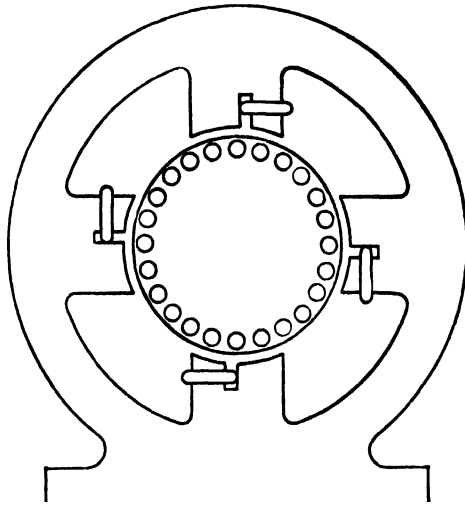


FIG. 28-7. Shaded-pole motor.

constant speed characteristic, as the induction motor, or a varying speed characteristic, as the repulsion (series) motor. The capacitor start motor has practically replaced the repulsion type motors.

**28-3. The shaded-pole motor.** For a very small output and a small starting torque the construction shown in Fig. 28-7 is used. The main winding, not shown in the figure, is a concentrated single-phase winding placed on salient poles. Around a portion of each pole a copper strap (called *shading coil*) is placed, thus forming a short circuit. The rotor is of the squirrel-cage type.

The main winding produces an alternating flux. However, the flux will not be in time-phase over the whole pole area: within the part of the pole lying *inside* the shading coil the flux will be delayed with respect to the flux in the part of the pole lying outside the shading coil. This is due to the induced current in the shading coil which delays the change of flux interlinkage within this coil. This means that the flux is a maximum in the shaded portion of the pole later than in the unshaded portion, which is identical with a progressive shift of the flux in the direction of the unshaded pole-portion to the shaded pole-portion. The effect of this progressive shift of the flux is the same as that of a weak rotating flux.

## Chapter 29

### LOSSES IN INDUCTION MOTORS HEATING AND COOLING

**29-1. Losses in Induction Motors.** The conversion of energy, from electrical into mechanical in the motor and from mechanical into electrical in the generator, is connected with losses. These losses are caused by the magnetic flux, the currents in the conductors of stator and rotor and by the mechanical rotation. Because of these losses, the input to the machine must, of necessity, be larger than the output. The efficiency of a machine is defined as:

$$\eta = \frac{\text{output}}{\text{input}} = \frac{\text{input} - \text{losses}}{\text{input}} = \frac{\text{output}}{\text{output} + \text{losses}} = 1 - \frac{\text{losses}}{\text{input}}$$

The different kinds of losses which appear in the electric machine and especially in the induction motor are considered in the discussions which follow.

(a) *Losses due to the main flux.* Since the main flux moves with respect to the stator and rotor iron, the particles of the iron are alternately magnetized, first in one direction and then in the other. This leads to the *hysteresis losses*. The magnitude of the hysteresis loss depends upon the area of the hysteresis loop, the number of magnetic cycles per second, and the quality of the iron.

The iron is laminated perpendicular to the direction of the current flow in the armature conductors in order to avoid parasitic (eddy) currents in the iron running parallel to the conductors and causing losses (see Chap. 16). However, eddy currents do appear in the single laminations and produce heat losses. The eddy-current losses depend upon the flux density, the number of magnetic cycles per second, the thickness of the laminations, and the quality of the iron.

According to Steinmetz, the hysteresis losses per unit weight can be represented by the following equation:

$$P_h = \sigma_h f B^{1.6} \quad (29-1)$$

where  $B$  is the maximum value of flux density and  $f = pn/120$  is the number of magnetic cycles per second.  $\sigma_h$  is a constant depending upon the quality

of the iron. Steinmetz's equation yields low values for the losses when  $B > 65,000$  lines per sq in. A more accurate equation proposed by R. Richter is:

$$P_h = afB + bfB^2 \quad (29-2)$$

where  $a$  and  $b$  are constants corresponding to  $\sigma_h$ . In practice  $B > 65,000$  lines per sq in. In this case the first term of Eq. 29-2 can be disregarded and the following equation used:

$$P_h = \sigma_h \frac{f}{60} \left( \frac{B}{64,500} \right)^2 \quad \text{watts/lb} \quad (29-3)$$

The eddy-current losses are:

$$P_e = \sigma_e \left( \Delta \frac{f}{60} \frac{B}{64,500} \right)^2 \quad \text{watts/lb} \quad (29-4)$$

The constant  $\sigma_e$  depends upon the electric resistivity of the iron.  $\Delta$  is the thickness of the laminations in inches. The total iron losses per pound are

$$P_{h+e} = \sigma_h \frac{f}{60} \left( \frac{B}{64,500} \right)^2 + \sigma_e \left( \Delta \frac{f}{60} \frac{B}{64,500} \right)^2 \quad \text{watts/lb} \quad (29-5)$$

In practice, iron-loss curves are used which represent the loss in watts per pound as a function of the flux density  $B$ . Such curves for different kinds of iron are given at the end of the book. It follows from Eq. 29-5 that the iron loss is proportional to the square of the flux density  $B$  and to the frequency of magnetization  $f$  in first or second degree. Eq. 29-5 and the iron-loss curves are based on sinusoidal variation of  $B$ .

The frequency of magnetization is constant for the stator, namely, equal to the line frequency  $f_1$ , and variable for the rotor, since it is the relative speed between the rotating flux of the machine and the rotor which determines the frequency of magnetization of the rotor. In the rotor the frequency is  $f_2 = sf_1$ . At rated speed  $s$  is small and there are practically no hysteresis or eddy-current losses due to the main flux in the rotor.

The iron losses due to the main flux are larger than those obtained from Eq. 29-5, or from the iron loss curves, due to the non-sinusoidal flux distribution (non-sinusoidal  $B$  curve) at higher saturation of the iron, non-uniform distribution of the flux over the cross-section of the armature core, punching of the laminations, and the filing of the laminations in order to remove the burrs. The increase of the iron losses due to these factors may be as high as 30 to 40%.

(b) *Losses due to slot-openings.* Consider Fig. 29-1. It refers to a smooth rotor (with closed slots) and shows the influence of the stator slots on the flux distribution curve. The flux density is larger at points opposite the teeth than at points opposite the slots, owing to the difference of the magnetic reluctance. Superimposed on the average flux density is a *ripple*, the wave length of which is equal to a slot pitch. This ripple moves with respect to the

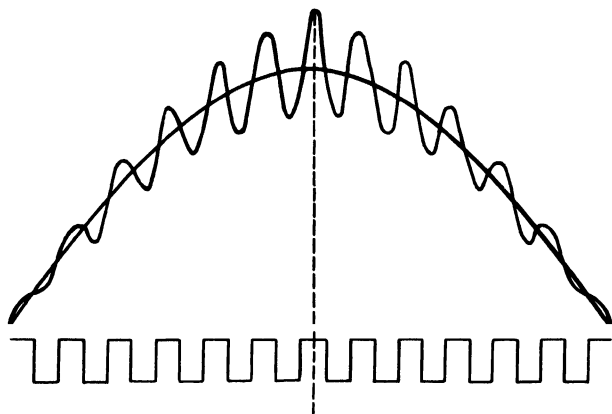


FIG. 29-1. Flux ripple produced by slot openings.

rotor and induces eddy currents in the rotor surface. The amplitude of the ripple depends upon the width of the slot-opening. In induction motors both the stator and the rotor are slotted. Therefore, the stator slot-openings produce surface losses in the rotor and the rotor slot-openings produce surface losses in the stator. Medium-sized and larger induction motors have open slots in the stator and semi-open slots in the rotor; smaller induction motors have semi-open slots in both parts. The surface losses are larger in machines with open slots.

Due to the fact that both the rotor and stator have slots, another kind of loss appears in the induction motor: the flux pulsation due to the slot openings *penetrates the teeth* themselves and produces eddy currents as well as hysteresis losses in the teeth. The frequency of these pulsations is the same as that of the tooth surface losses, i.e., for the stator  $Q_2 n/60$  and for the rotor  $Q_1 n/60$ . The magnitude of the variation of the flux density in the teeth depends upon the saturation in the teeth. The total losses due to the slot openings are larger in induction motors than in d-c machines (and synchronous machines). These losses, as a percentage of the iron losses due to the main flux, (Eq. 10-5), are approximately: 80 to 120% in squirrel-cage motors with semi-open slots in stator and rotor, 150 to 200% in squirrel-cage motors with open slots in stator and semi-open slots in rotor, and 180 to 220% in wound rotor motors.

The flux ripple produced by the slot openings induces parasitic currents not only in the iron but also in the bars of a squirrel-cage rotor. The currents induced in these bars may become considerable and the copper losses in the bars high, if the slot pitch of the cage is much different from the stator slot pitch. A difference up to 30% between the slot pitches keeps the losses at a low level. Equal slot pitches cannot be used because this would produce locking torques which may prevent starting of the motor.

(c) *Losses due to the load currents.* The load currents produce  $I^2R$  losses in the stator and rotor windings. Furthermore, the *cross-flux in the slot* may produce additional copper losses through *skin-effect* (see Art. 10-1) which forces the current to flow in the top part of the conductor, thus decreasing the effective area of the conductor and increasing its resistance which results in an increase of the copper losses. The skin-effect is proportional to the square root of the frequency. It is negligible at rated load in the rotor since the frequency of the rotor currents at rated load is very small. Although the stator frequency is always equal to the line frequency, i.e., usually 60 cycles, the skin-effect loss in the stator is usually small (in medium-sized and larger motors about 5 to 15% of the stator  $I^2R$  losses).

(d) *Losses due to harmonic fluxes.* It has been shown in Art. 24-1 that the mmf of a distributed winding consists of a main wave and harmonics. While the main wave produces the main flux, the harmonics produce parasitic fluxes which travel with different speeds than the main flux and some in an opposite direction to the main flux. The amplitudes of these rotating fluxes are proportional to the current in the winding and inversely proportional to the length of air-gap. Since the induction motor has a smaller air-gap than the other a-c machines, in order to keep down its magnetizing current, the harmonic fluxes are stronger in it than in the other a-c machines with larger air-gaps.

At no-load the stator current of the induction motor is small and, therefore, the stator mmf and the harmonic fluxes are also small. At full-load the harmonic fluxes may become considerable, depending upon the design of the winding (see Art. 24-3). Since the stator harmonic fluxes travel with respect to the rotor, they produce rotor surface losses and tooth-pulsation losses in the same way as the slot opening ripple produces losses (Fig. 29-1). The same consideration also applies to the rotor: at load the rotor currents produce harmonic fluxes which travel with respect to the stator and cause stator tooth-surface and tooth-pulsation losses. These losses are mainly eddy-current losses.

In well-designed induction motors the losses due to the harmonic fluxes of stator and rotor mmf are 0.6 to 3.0% of the motor output. The larger value applies to small motors; the lower value, to large motors. A motor of 1000-HP output has about 1% harmonic losses. In poorly designed induction motors the harmonic losses may be 4 to 5 times as high as the values given above.

Just as the flux ripple due to the slot openings induces currents in the bars of the squirrel-cage rotor, the flux harmonics of the stator induce currents in the squirrel-cage bars. In well-designed induction motors these current losses usually are small, about 0.03 to 0.05% of the output.

In large machines the leakage fluxes around the end-windings of the stator, due to the load current, are considerable and, since they move with respect to the stator, they induce eddy currents in metallic parts, such as the end



plates, finger plates, bolts, etc. These losses can be neglected in small machines. The losses under (c) and (d) are the rotational iron losses (see Art. 19-3).

(e) *Friction and windage losses.* Because of rotation, bearing friction losses occur in all machines. The amount of the bearing friction losses depends upon the pressure on the bearing, the peripheral speed of the shaft at the bearing, and the coefficient of friction between bearing and shaft.

Windage losses also occur because of rotation. The amount of these losses depends upon the peripheral speed of the rotor, the rotor diameter, the core length, and largely upon the construction of the machine.

(f) *No-load and load losses: stray-load losses.* The losses which appear at no-load and those which appear at load are shown in Table 29-1.

TABLE 29-1

No-load losses	Iron losses in the stator due to the main flux.	Surface and tooth pulsation losses in stator and rotor due to slot openings.	Copper losses in the squirrel cage due to the slot openings.	Windage and bearing friction losses.
Load losses	$I^2R$ losses in the stator and rotor windings.	Surface and tooth pulsation losses in stator and rotor due to harmonic fluxes.	Skin-effect losses in the stator winding.	Losses in the structural parts due to leakage fluxes.

The additional losses due to the load (these are items 2, 3, and 4 of the second row) are called *stray load losses*.

(e) *Examples of loss distribution and efficiencies.* The following tabulation shows the loss distribution of three induction motors, one of which is single-phase and the other two polyphase.

$\frac{1}{8}$ -HP, 4 poles, single phase, 60 cycles, 110 volts, $n = 1720$ rpm	
Stator winding $I^2R$ .....	25 watts
Rotor winding $I^2R$ .....	20
Total iron loss (including stray load-loss) .....	20
Bearing friction and windage loss .....	10
	<hr/> 75 watts (Total)

Output  $\frac{1}{8}$  HP = 124.5 watts

$$\text{Efficiency} = 100 \frac{124.5}{124.5 + 75} = 62.3\%$$

3 HP, 4 poles, 60 cycles,

3 phase, 220/440 volts, 1745 rpm

250 HP, 8 poles, 60 cycles,

3 phase, 2300 volts, 883 rpm

<i>Aluminum cast squirrel-cage Rotor</i>		<i>Squirrel-cage Rotor</i>
Stator winding . . . . .	140 watts	4300 watts
Rotor winding . . . . .	80	3600
Stray load-loss . . . . .	50	1900
Iron loss . . . . .	120	2700
Bearing friction and windage loss . . . . .	50	2000
	440 watts (Total)	14,500 watts (Total)

Output =  $746 \times 3 = 2238$  watts

Output =  $746 \times 250 = 186.5$  kw

Efficiency =  $100 \frac{2238}{2238 + 440} = 83.6\%$

Efficiency =  $100 \frac{186.5}{186.5 + 14.5} = 92.8\%$

**29-2. Heating and cooling of induction motors.** The losses treated in the the previous article are of different kinds, but all of them appear in the electric machine in the form of heat. Since the losses are produced mainly in the active parts of the machine, i.e., in the iron which carries the flux and in the conductors which carry the currents, the heat appears mainly in these machine parts. The result is an increase in the temperature of the iron and copper above that of the surroundings.

Tests on various kinds of *insulating* materials have shown that for each material there is a safe continuous-operating temperature which cannot be exceeded without impairing the life of the material. Table 29-2 shows the limiting temperatures for the different kinds of insulation as specified by the AIEE.

The table distinguishes four classes of insulation. Class O insulation consists of cotton, silk, paper, and similar organic materials when neither impregnated nor immersed in oil. Class A insulation consists of cotton, silk, paper, and similar organic materials when impregnated or immersed in oil; also enamel, as applied to conductors. Class B insulation consists of inorganic materials, such as glass, or mica and asbestos in built-up form, combined with binding substances.

A relatively new development in the field of insulating materials is represented by the *silicon* binders and varnishes. These binders and varnishes when used together with the inorganic materials of Class B insulation yield an insulation which is able to withstand much higher temperatures than the standard Class B insulation for the same life of the winding (see class H insulation).

The temperature rise of any part of the machine decreases as the heat conductivity to the surface of the machine part and the heat transfer from the surface of the machine part to the cooling medium (normally air, or hydrogen in some large machines) are increased. *High heat conductivity* of all materials used, i.e., of the laminations, conductor material, and insulating

materials, and *high heat transfer* from the surfaces of windings and iron to the cooling medium are the necessary conditions for low temperature rises. The heat conductivity of the insulating materials is low.

There are two ways for the heat transfer from the surface to the cooling medium to occur: (1) through radiation and (2) through convection, i.e., heat transportation by the moving air or hydrogen. The radiation is affected by the frame. In totally enclosed machines without an air supply from the outside, convection is also affected only by the frame. In open-type machines and in totally enclosed machines with an air supply from the outside, the

TABLE 29-2

Class	Material Classification	Limiting Temperatures, °C for Industrial Apparatus		
		Ther- mometer	Embedded Detector	Hot- spot
O Untreated organics	Untreated fabrics of cotton, silk, linen. Untreated paper, fiber, wood, etc.	75	85	90
A Treated or impregnated organics	Oil, varnish, wax, or compound impregnated fabrics or sheets of cotton, silk, linen, paper, wood, fiber; oil, varnish, bakelite, organic filler compounds.	90	100	105
B Treated or impregnated inorganics	Asbestos, fiberglas, mica tape, oxide films, inorganic fillers, asbestos boards. (A limited amount of organic materials may be used for binding purposes.)	110	120	130
H Treated or impregnated inorganics	Mica, asbestos, fiberglas and similar inorganic materials in built-up form with binding substances composed of silicone compounds, or materials with equivalent properties; silicone compounds in rubbery and resinous forms, or materials with equivalent properties in minute proportions. Class A material may be used only where essential for structural purposes during manufacture.	—	—	180

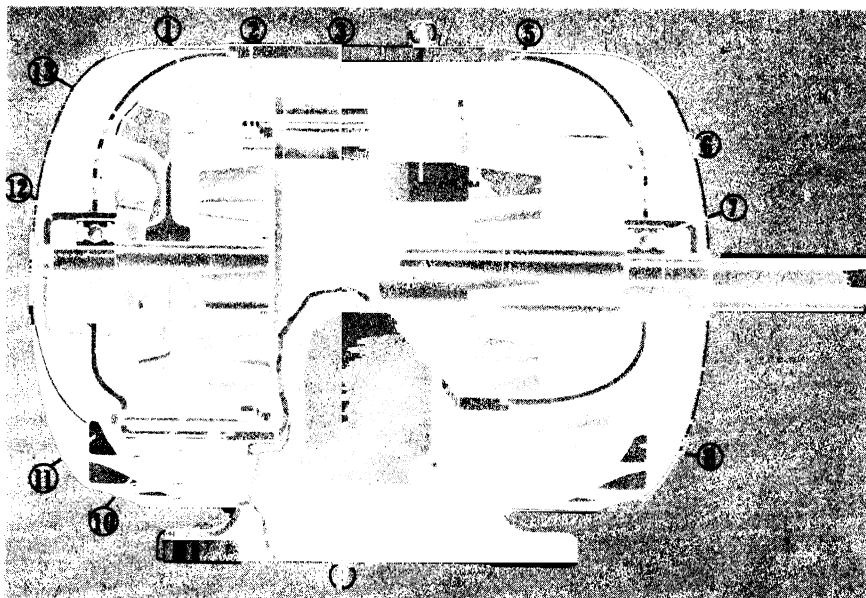


FIG. 29-2. Cutaway view of a splash proof ball-bearing, squirrel-cage motor.

- |                            |                               |
|----------------------------|-------------------------------|
| 1. End turn of stator coil | 7. Prelubricated ball bearing |
| 2. Locking bar             | 8. Ventilation openings       |
| 3. Stator core             | 9. Conduit box                |
| 4. Rotor                   | 10. End plates                |
| 5. Balancing lug           | 11. End brackets              |
| 6. Rotor blades            | 12. Bearing hub               |
|                            | 13. Fan                       |

winding and the laminations, as well as the frame, are included in the heat transfer by convection. The heat transfer by convection is much larger than that by radiation.

Sufficient ventilation (cooling by convection) of the machine is necessary in order to keep the temperature rises of the iron and copper within the prescribed limits. This ventilation can be achieved when care is taken in the design to insure that good heat transfer will take place from the active iron and copper, where the losses originate, to the cooling medium. The ventilation can be radial or axial. In medium-size and larger machines it is normally radial. In this case the armature with cores larger than 5 inches are divided into stacks of laminations about 2 in. wide, separated by  $\frac{3}{8}$ -in. ventilating ducts through which the air is forced (see Figs. 16-4 and 16-6). Forcing air through radial or axial ducts facilitates the transfer to the air of the heat due to the losses in the iron and also in the embedded parts of the windings. Sufficient air circulation must also be present around the end-windings and field coils so that the heat developed there can be transferred to the air.

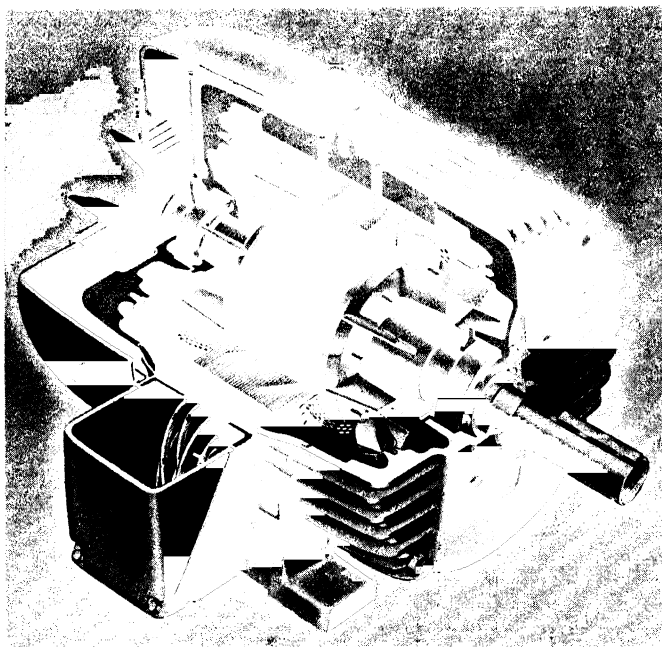


FIG. 29-2a. Cutaway view of totally enclosed fan-cooled ball-bearing polyphase induction motor.

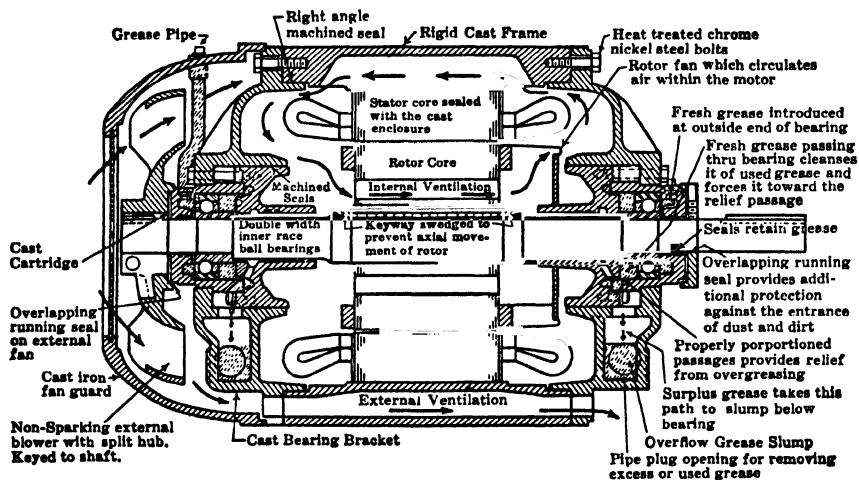


FIG. 29-3. Air flow in a totally enclosed fan-cooled, squirrel-cage motor.

Of the various kinds of machine construction, the open machine, i.e., one in which there is no restriction to ventilation other than that necessitated by good mechanical construction, is preferred for the medium-sized and

larger motors. Smaller motors are made open or totally enclosed, fan-ventilated. On account of the environment, more or less complete enclosure may be necessary. The different types of enclosures are defined in the NEMA (National Electrical Manufacturers Association) Standards.

Fig. 29-2 shows a cutaway section of an open splash-proof squirrel-cage motor. Fig. 29-3 shows the air flow in a totally enclosed fan-cooled squirrel-cage motor. Note the internal and external ventilation separated from each other and flowing in opposite directions. A cutaway section of a totally enclosed fan-cooled squirrel-cage motor is shown in Fig. 16-12 and in Fig. 29-2a. For a method of calculating the temperature rises of copper and iron, see Ref. A11.

### PROBLEMS

1. A 7.5-HP, 230-volt, 4-pole, 3-phase, 25-cycle, squirrel-cage induction motor was loaded by means of a Prony brake and the following data were recorded for three different loads. Power was measured by the 2-wattmeter method.

	(1)	(2)	(3)
Voltage . . . . .	230	230	230
Line current . . . . .	25.1	14.4	9.55
Watts $W_1$ . . . . .	5500	2950	1550
Watts $W_2$ . . . . .	2920	1120	- 490
Scale reading(lb) . . . . .	36.8	17.3	4.0
Speed(rpm) . . . . .	682	710	733

A brake arm 24 in. long was used, and the tare reading on the scale was 1.61 lb. Determine the performance for each point including HP output, slip, torque, power factor, and efficiency.

2. A 5-HP, 230-volt, 4-pole, 60-cycle, 3-phase, squirrel-cage induction motor is delivering rated output. The iron loss is 150 watts of which 65 watts are due to the main flux; stator copper loss, 125 watts; rotor copper losses, 130 watts; friction and windage losses, 90 watts; stray load losses, 95 watts. Determine: (a) power transferred by rotating field; (b) mechanical power in watts developed by rotor; (c) power input in watts; (d) efficiency; (e) slip; (f) torque in pound-feet.

3. Repeat Problem 2 for a 6-HP output assuming the following: stator copper loss, rotor copper loss and the stray load-loss vary as the square of the output, and the core and friction and windage loss remain constant.

4. A 100-HP, 3-phase, 4-pole, 440-volt, 60-cycle, squirrel-cage induction motor is operating at full-load at a slip  $s = 0.02$ . The full-load stator current is 11.35 amp and the stator hot resistance is 0.032 ohm per phase. The no-load current is 1135 amp and the no-load power input 4580 watts. Forty percent of the total iron losses can be assumed to be the iron losses due to the main flux. The friction and windage losses are 1.7% of the output and the stray load-loss 1.5% of the output. Determine the full-load efficiency and power factor.

5. The motor of Problem 4 takes 92 amp when delivering  $\frac{3}{4}$  rated output and 150 amp when delivering  $\frac{5}{8}$  rated output. The iron losses due to the main flux can be assumed the same as at full-load. Also, the friction and windage losses remain unchanged. The stray load-losses vary as the square of the primary current, and

the slip is proportional to the output. Determine the efficiency and power factor at  $\frac{3}{4}$  and  $\frac{1}{4}$  load. Combine with Problem 4 and draw curves of efficiency and power factor vs. load.

6. A 2300-volt, 3-phase, 8-pole, 60-cycle, squirrel-cage induction motor takes a power input of 361 kw when delivering rated output. The rated line current is 193 amp and the speed 879 rpm. At rated output, friction and windage losses are 4.40 kw, stray load-losses 3.36 kw, and the iron losses are 5.0 kw of which 2.2 kw are due to the main flux. The stator resistance at 75°C is 0.158 ohm per phase. Determine the output, efficiency and power factor at full-load.

7. Determine the output, efficiency and power factor of the motor in Problem 6 for power inputs of 275 and 450 kw. The respective line currents are 80 and 129.5 amp. The stray load-losses are proportional to the square of the power input; the iron losses, iron losses due to main flux, and friction and windage losses are the same as for full-load in Problem 6. Assume slip proportional to power input. Combine with Problem 6 and draw curves of efficiency and power factor vs. output.

## *Chapter 30*

### MECHANICAL ELEMENTS OF THE SYNCHRONOUS MACHINE

As in the d-c machine, the flux of the synchronous machine is produced by a direct current. However, quite different from the d-c machine, the pole structure of the synchronous machine is the inner part of the machine which rotates, while the armature is the outer part and is stationary. As in the induction motor, the stationary part is called the stator and the rotating part the rotor. Thus, of the three main kinds of electric machines—namely the d-c machine, induction motor, and synchronous machine—in the d-c machine and the synchronous machine the flux is produced by a direct current, while in the induction motor the flux is produced by an alternating current.

It will be explained in the following that the synchronous machine is a special case of the induction motor. On the other hand, the d-c machine is nothing more than a synchronous machine with an added special device, the commutator.

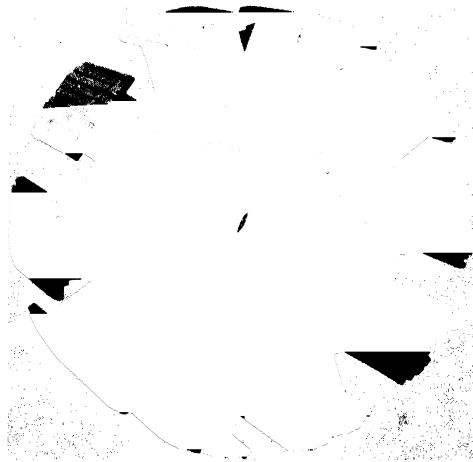


FIG. 30-1. Salient-pole rotor of a 10-pole synchronous machine (field coils not shown).



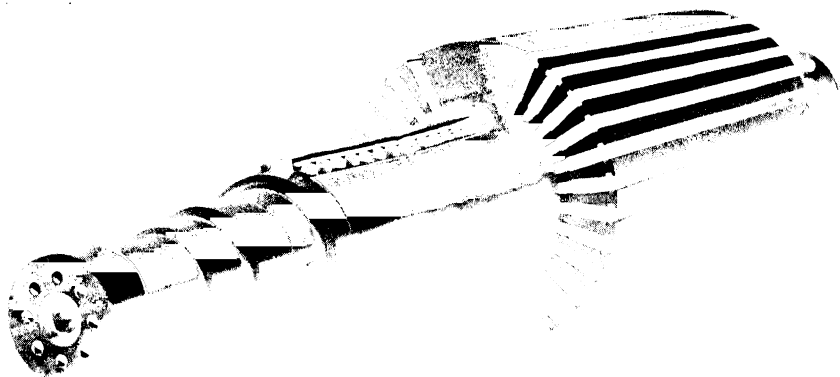


FIG. 30-2. Cylindrical rotor of a 2-pole synchronous machine.

A distinction must be made between synchronous machines having six or more poles and those having two and four poles. The rotors of the former are of the salient-pole type (*salient-pole rotors*), as in the d-c machine. Fig. 30-1 shows a salient-pole rotor, without the field coils, for a 10-pole synchronous machine. Two-pole and 4-pole 60-cycle machines rotate at 3600 and 1800 rpm respectively. When used as generators, they are driven by steam turbines. The rotors are subject to high mechanical stresses and for this reason are built of high-grade steel in a cylindrical shape (*cylindrical rotors*). Fig. 30-2 shows a cylindrical rotor (without winding) of a 2-pole synchronous machine. The d-c field winding is placed in slots and held in place by heavy metal wedges. The two large teeth correspond to the salient poles of the salient-pole rotor. It should be mentioned that small 4-pole machines are built with salient poles.

While the field winding of the salient-pole machine consists of concentrated coils as in the d-c machine, the field winding of the cylindrical rotor machine is distributed similar to a single-phase winding (see Fig. 26-1).

**30-1. The salient-pole machine.** Fig. 30-3 shows the main flux paths of a 4-pole salient-pole machine. The general shape and construction of the stator is very similar to that of the induction motor. The core is laminated just as in the induction motor and the d-c machine, and for the same reason. Fig. 30-4 shows a partially wound stator of a larger salient-pole machine, and Fig. 30-5 shows a complete stator.

Fig. 30-6 shows a punching of a salient-pole machine, with slots for a squirrel-cage winding which is called a *damp*er or an *amortisseur* winding. This winding is necessary in all synchronous motors for starting purposes (see Art. 38-4) and is often used in synchronous generators to damp out oscillations which may occur during parallel operation (see Art. 40-4).

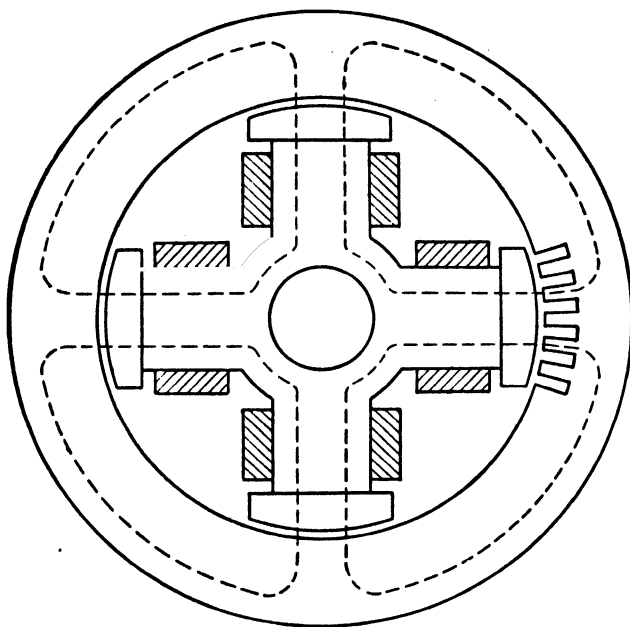


FIG. 30-3. Main flux paths of a 4-pole, salient-pole synchronous machine.

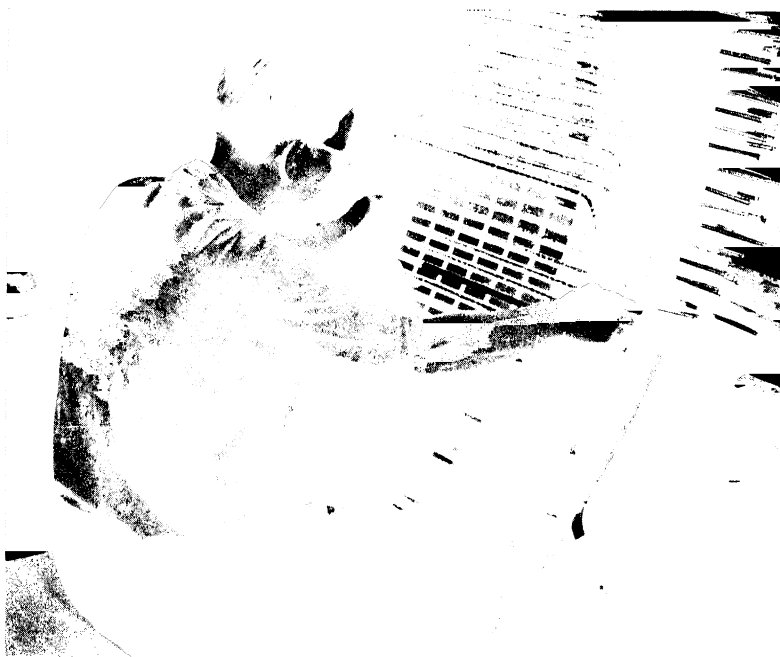
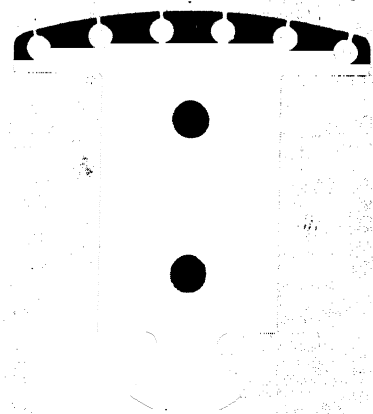


FIG. 30-4. Partially wound stator of a large synchronous machine with salient poles.



**FIG. 30-5.** Complete stator of a 3-phase, salient-pole synchronous motor, 1000 HP, 2200 volts, 514 rpm.



**FIG. 30-6.** Pole punching of a salient-pole machine with slots for the damper winding.

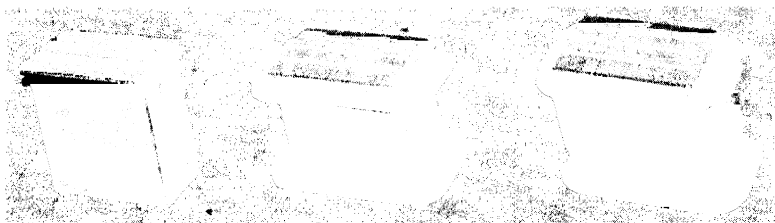


**FIG. 30-7.** Salient pole in three stages of assembly.

Fig. 30-7 shows a salient pole in three stages of assembly: the bare pole, the insulated pole, and the complete pole. Fig. 30-8 shows details of a damper winding: the bars of each pole are connected to segments which (in all

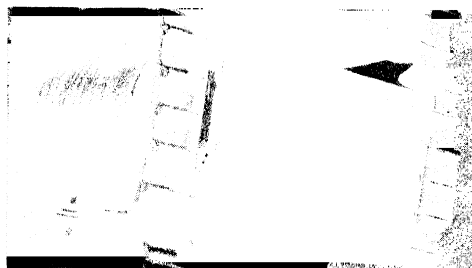


FIG. 30-8. Details of a damper winding.

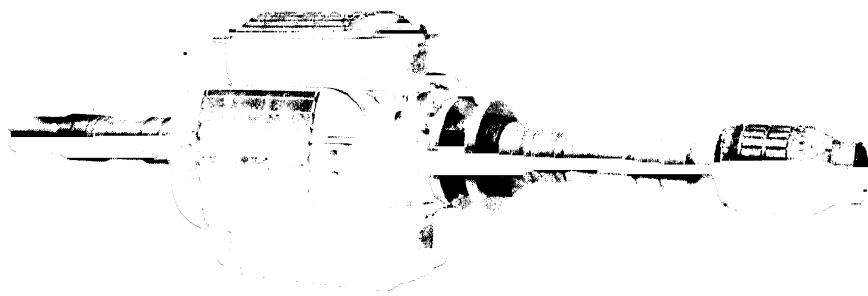


FIG. 30-9. Complete rotor of a 4-pole, salient-pole, synchronous machine.

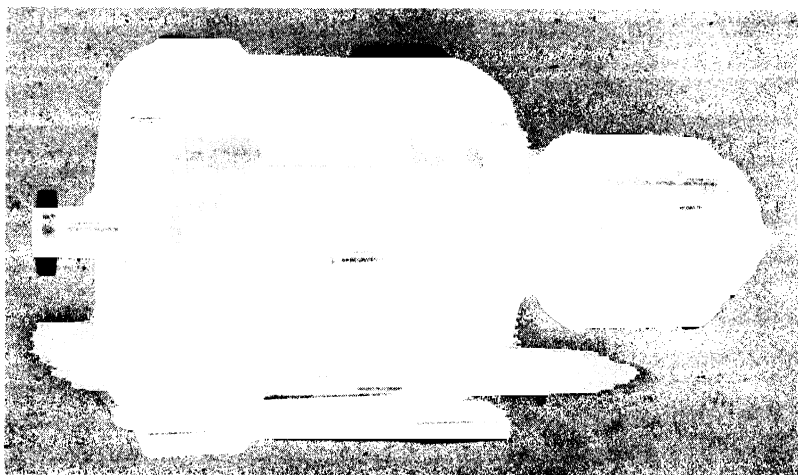


FIG. 30-10. Complete synchronous machine coupled with exciter.

motors) are bolted together making a complete ring connection around the rotor. Fig. 30-9 shows a complete salient-pole rotor of a 4-pole generator. Fig. 30-10 shows a complete synchronous machine coupled with its d-c exciter.

**30-2. The cylindrical rotor machine.** Fig. 30-11 shows a punched stator segment of a 2-pole machine with a cylindrical rotor. Fig. 30-12 shows a stator core assembly of a cylindrical rotor machine without winding. Fig. 30-13 shows the complete stator of a 3-phase cylindrical rotor generator, rated at 80,000 kw, 1800 rpm, 22,000 volts.

A complete 2-pole rotor, without winding, was shown in Fig. 30-2. In this figure the bottom part of each slot does not contain conductors but is open and used for ventilation purposes. The grooves at the top of each slot are designed to hold the wedges.

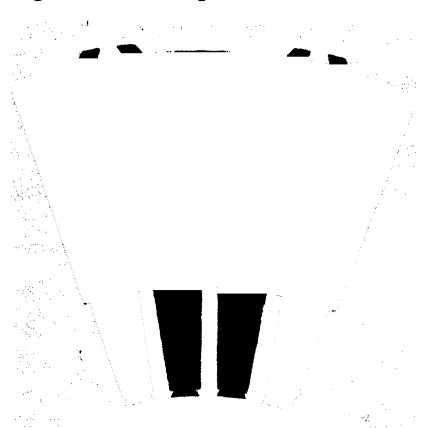


FIG. 30-11. Punched stator segment of a 2-pole machine with cylindrical rotor.

Fig. 30-14 demonstrates the process of assembling the rotor winding. Fig. 30-15 shows a rotor with the winding and wedges assembled. Fig. 30-16 shows part of a complete rotor: to the

left, the end-winding retaining ring; in the center, the ventilation fan; to the right, the slip rings through which the d-c exciting current is introduced.

Fig. 30-17 shows a 2-pole cylindrical rotor generator with its turbine

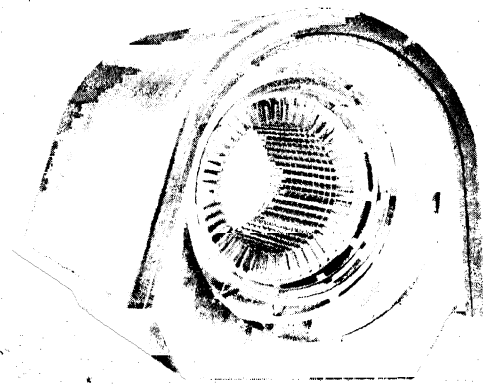


FIG. 30-12. Stator core assembly without winding, for a cylindrical rotor machine.

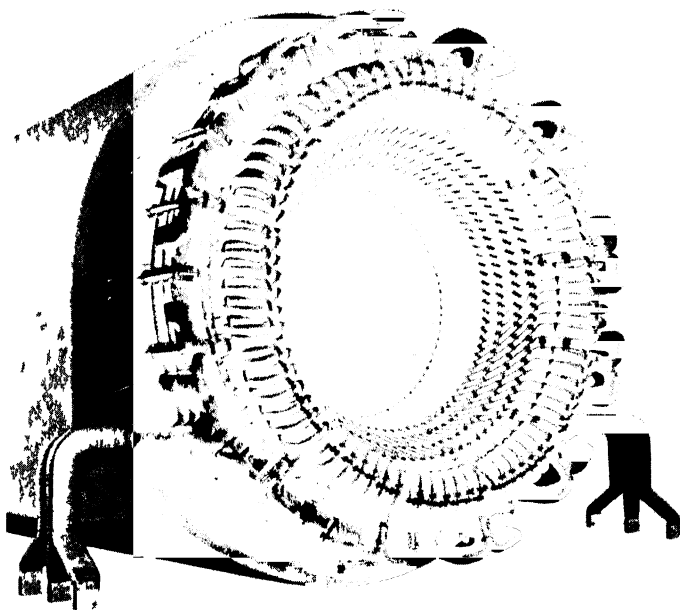


FIG. 30-13 Complete stator of a 3 phase cylindrical rotor generator, 80,000 kw, 85 per cent p f, 22,000 volts, 1800 rpm.



FIG. 30-14. Winding the coils of a 2 pole cylindrical rotor.

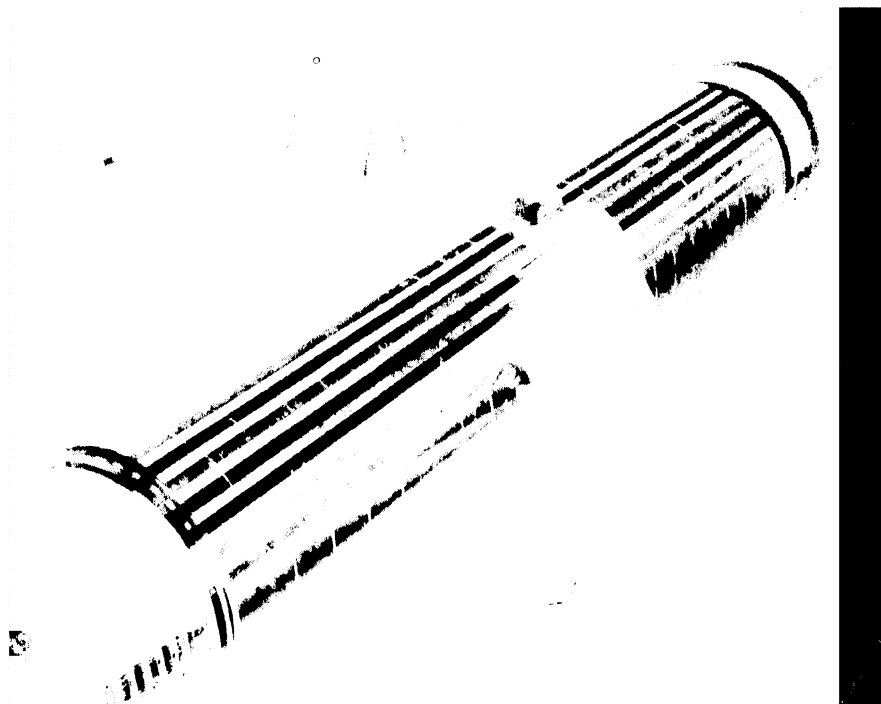


FIG. 30-15. Cylindrical rotor complete with winding and slot wedges.

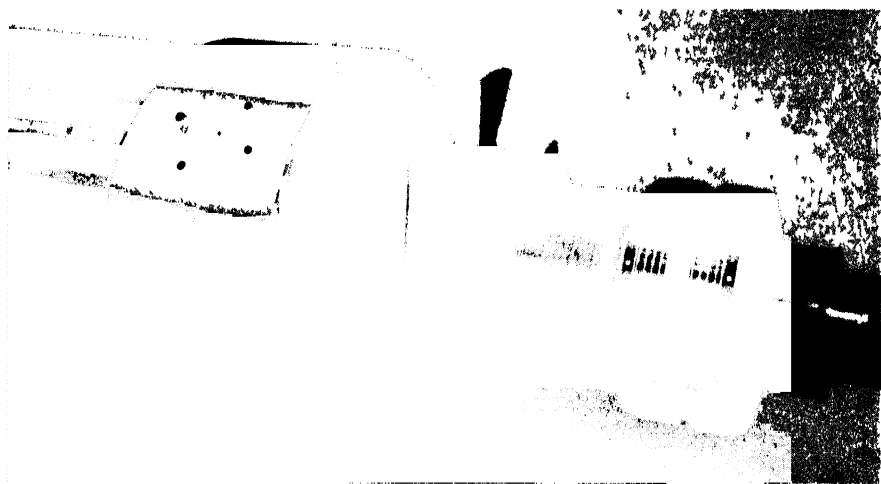


FIG. 30-16. Part of a cylindrical rotor for a 12,500-kva machine showing the end winding retaining ring, ventilating fan, and slip rings



FIG. 30-17. Three-phase cylindrical rotor generator, 31,250-kva, 14,440 volts, 80 per cent p.f., 3600 rpm, with turbine and exciter.

and exciter. The rating of this unit is 31,250 kva at 14,440 volts, 0.80 power factor, 60 cycles.

No distinction has been made in the foregoing between the synchronous generator and synchronous motor because the synchronous machine is able to operate both as a generator and as a motor, just as the d-c machine. The cylindrical rotor machine is chiefly used as a generator while most synchronous motors are of the salient-pole type.



## Chapter 31

### GENERAL CONSIDERATIONS OF THE SYNCHRONOUS MACHINE

**31-1. The no-load characteristic.** The stator as well as the rotor of the synchronous machine is connected to a source of power. Therefore, as for the doubly fed induction motor (see Art. 23-3d), a uniform torque cannot be developed at all rotor speeds, because the stator and rotor mmf's are not at standstill with respect to each other at all rotor speeds. In general, the doubly fed machine has two speeds at which the torque is uniform. These speeds are given by Eq. 23-2:

$$n = \frac{120(f_1 \mp f_2)}{p} \quad (31-1)$$

Since the rotor is connected to a d-c source of power in the case of the synchronous machine,  $f_2 = 0$ , and there is only a *single speed* at which a uniform torque exists, namely,

$$n_s = \frac{120f_1}{p} \quad (31-2)$$

This is the *synchronous* speed of the machine. The synchronous machine is bound to its synchronous speed. Its torque-speed characteristic is a vertical line, as shown in Fig. 31-1. For comparison, the torque-speed characteristic of the induction machine is also shown in this figure.

When a synchronous generator is operating as a single unit, i.e., not in parallel with other machines, it is necessary for the rotor speed to remain *constant* in order that the *frequency* remain constant.

The synchronous machine represents a special case of the doubly fed induction machine and is therefore a special case of the transformer. However, it has the character of a *current transformer*, while the induction machine has the character of a *voltage transformer*. The voltage transformer oper-

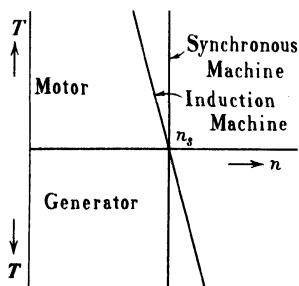


FIG. 31-1. Torque-speed characteristic of the synchronous machine and the induction machine.

ates with a constant primary voltage and therefore with almost a constant flux from no-load to full-load, since its voltage drop is small. The current transformer when operated with a constant primary current has a large flux variation between no-load and full load: at no-load its flux is fixed by the mmf of the primary current alone; at load its flux is determined by the resultant of the primary *and* secondary mmf's. The primary current of the synchronous machine is the direct current of the field winding; the secondary current is the armature current.

Since there is not a direct proportionality between mmf and flux in iron, the magnetization curve of the material has to be used for a study of the current transformer. The same reasoning applies to the synchronous machine, i.e., the saturation curve (*no-load characteristic*) of the magnetic circuit of the synchronous machine has to be used for the study of its behavior and performance. This is the same as in the d-c machine, which also operates with a variable flux. The no-load characteristic was not mentioned in the foregoing study of the induction motor. It was not necessary in the case of the induction motor because this machine behaves as a voltage transformer and operates with almost a constant flux between no-load and full-load, i.e., it operates at a single point of the no-load characteristic and the entire curve is therefore unnecessary.

Curve *Olb* in Fig. 31-2 is a no-load characteristic: as for the d-c machine, the field ampere-turns (field mmf,  $M_f$ ) of the field current  $I_f$  is shown on the axis of abscissae and the pole-flux  $\Phi$  or the armature (stator) emf  $E$  is shown on the axis of ordinates. At low values of  $\Phi$  the no-load characteristic is a straight line because the mmf required for the iron parts of the magnetic

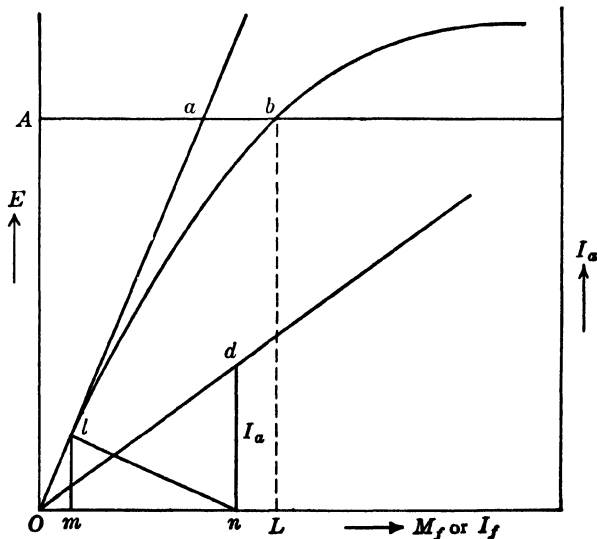


FIG. 31-2. No-load and short-circuit characteristic of a synchronous machine.

path is negligible in comparison with the mmf required to maintain the flux  $\Phi$  in the air-gap between the rotor and stator. The straight line  $Oa$  which coincides with the lower part of the no-load characteristic is called the *air-gap line*. The field mmf necessary to induce a certain emf  $OA$  in the stator winding is equal to  $Ab$ . The part  $Aa$  of this mmf is necessary to drive the flux, which corresponds to  $E = OA$ , through the air-gap, and the part  $ab$  is necessary to drive the flux through the iron parts of the magnetic path.

**31-2. The main flux reactance.** The rotor of the synchronous machine runs at the speed given by Eq. 31-2, i.e., if the rotor has  $p$  poles and the stator current has a frequency  $f_1$ , the rotor speed is  $n_r = 120f_1/p$ . The stator winding must be wound for the same number of poles as that of the rotor. The speed of the stator mmf with respect to the stator is given by Eq. 17-4, which is identical with Eq. 31-2, i.e., stator and rotor mmf's are at standstill with respect to each other. This is to be expected since Eq. 31-2 has been derived for the condition of a uniform torque.

Thus the main flux of the machine, which is produced by the stator and rotor mmf's, travels at synchronous speed  $n_s$  with respect to the stator and zero speed with respect to the rotor, i.e., the main flux induces emf's in the stator winding but none whatever in the rotor windings (field winding and damper winding). The rotor windings appear open with respect to the main flux. The same result can be obtained from the equivalent circuit of the induction motor, Fig. 18-4, since for the synchronous machine  $s = 0$ .

In the treatment of the synchronous machine the armature resistance is denoted by  $r_a$ , and the armature leakage reactance by  $x_l$ . The corresponding symbols for the induction machine are  $r_1$  and  $x_1$ . The main flux reactance requires here a special consideration. The main flux reactance ( $\omega L_m$ ) is  $\omega$  times the flux interlinkage with the stator winding, when one ampere flows in it. It will be seen later (Art. 32-1) that the position of the amplitude of the stator mmf with respect to the pole axis (axis going through the center of the pole) depends upon the character of the load. Keeping in mind that the stator mmf is at standstill with respect to the rotor and considering the salient pole machine,  $L_m$  is not a constant: when the load is such that the amplitude of the stator mmf coincides with the pole axis (see Fig. 34-1),  $L_m$  will be a maximum; on the other hand, when the load is such that the amplitude of the stator mmf coincides with the axis of the interpolar space (see Fig. 34-2),  $L_m$  will be a minimum, because in the latter case the reluctance of the main flux path is much larger than in the first case.

The maximum value of the main flux reactance is denoted by  $x_{ad}$  and is called the *armature reaction reactance in the direct axis*; the minimum value of the main flux reactance is denoted by  $x_{aq}$  and is called the *armature reaction reactance in the quadrature axis*. "Direct" axis is identical with pole axis; "quadrature" axis is identical with axis of the interpolar space. These axes are shifted from each other by 90 electrical degrees ( $= \frac{1}{2}$  a pole pitch).

Since the machine with cylindrical rotor has no interpolar spaces, for this type machine  $x_{ad} \approx x_{aq}$ . The two reactances are not *exactly* equal due to the large tooth in the pole axis which makes the reluctance in this axis somewhat smaller than in the axis shifted from it by  $90^\circ$ .

In the consideration of the cylindrical rotor machine, the symbol  $x_{ad}$  will be used for the main flux reactance.

**31-3. Effect of saturation.** Under some conditions of operation the machine is unsaturated (Art. 32-2b) and operates on the air-gap line (Fig. 31-1). The saturation introduces non-linearity between flux (or emf) and magnetizing mmf (or current). In some considerations, for the sake of simplification, the saturation is neglected and the air-gap line is used instead of the no-load characteristic; this linearizes the problem.

When the saturation does not exist or is neglected, i.e., when the no-load characteristic is assumed to be a straight line (the air-gap line), then *two* methods of approach are permissible for treatment of problems with several mmf's magnetizing the same magnetic circuit:

(a) *Each mmf is considered separately.* There are as many fluxes considered as there are mmf's and as many emf's are considered as there are fluxes. The resultant emf is determined by geometrical addition of the individual emf's.

(b) *The resultant mmf is determined by geometrical addition of the individual mmf's.* The flux produced by the resultant mmf is determined and then the emf induced by this flux.

When saturation is considered, *only one* method of approach can be used for treatment of problems with several mmf's magnetizing the same magnetic circuit, namely, method (b). This is due to the non-linearity of the no-load characteristic.

In the following, the synchronous machine will be considered first to be unsaturated and method (a) will be applied; then the saturation will be taken into account and method (b) will be used.

The machine with cylindrical rotor will be considered first, because this machine with  $x_{ad} \approx x_{aq}$ , is closer to the transformer than the salient-pole machine. The transformer diagrams can be applied to this machine.

## Chapter 32

### PHASOR DIAGRAMS OF GENERATOR AND MOTOR WITH CYLINDRICAL ROTOR · ARMATURE REACTION

**32-1. Phasor diagrams of synchronous generator and motor with cylindrical rotor. Armature reaction.** First the unsaturated machine, i.e., the machine operating on its air-gap line, will be considered; then the saturated machine.

(a) *Machine unsaturated.* Applying method (a) of Art. 31-3, the following mmf's, fluxes, and emf's induced by the fluxes in the armature winding are to be considered:

<i>MMF's</i>	<i>Fluxes</i>	<i>Induced EMF's</i>
Field (rotor) mmf ( $M_f$ )	$\Phi_f$	$E_f$
Armature mmf ( $M_a$ )	$\Phi_a$	$-jI_a x_{ad}$ (see Eq. 3-1)
MMF of the leakage (const $\times I_a$ ) flux	$\Phi_l$	$-jI_a x_l$

$I_a$  is the armature current.  $M_a$  is given by Eq. 15-11

$$M_a = 0.9m \frac{N^a}{p} k_{ap} I_a \quad (32-1)$$

Thus, Kirchhoff's mesh equation for generator operation is

$$\dot{E}_f - j\dot{I}_a x_{ad} - j\dot{I}_a x_l = \dot{I}_a r_a + \dot{V} \quad (32-2)$$

or

$$\dot{V} = \dot{E}_f - \dot{I}_a r_a - j\dot{I}_a (x_l + x_{ad})$$

and for motor operation,

$$\dot{V} + \dot{E}_f - j\dot{I}_a x_{ad} - j\dot{I}_a x_l = \dot{I}_a r_a \quad (32-3)$$

$E_f$  is the emf induced in the armature winding by the *field* (rotor) flux. In the case of the generator the sum of the three emf's balances the voltage drop in the armature resistance and in the load. In the case of the motor, the sum of the impressed voltage and the three emf's balances the voltage drop in the armature resistance.

Eq. 32-2 for the generator can be rewritten as

$$\dot{V} + \dot{I}_a r_a + j \dot{I}_a (x_l + x_{ad}) = \dot{E}_f \quad (32-4)$$

and Eq. 32-3 for the motor can be rewritten as

$$\dot{V} = -\dot{E}_f + \dot{I}_a r_a + j \dot{I}_a (x_l + x_{ad}) \quad (32-5)$$

$E_f$  appears in the latter equation with a minus sign, being the counter-emf of the motor, just as in the d-c motor and induction motor.  $x_{ad}$  is the *armature reaction reactance of the direct axis*. The sum

$$x_l + x_{ad} = x_d \quad (32-6)$$

is called the *direct-axis synchronous reactance*.

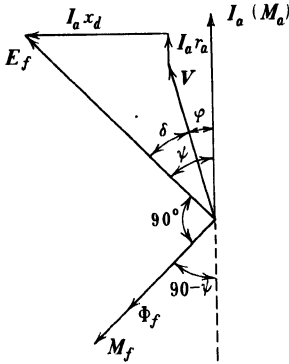


FIG. 32-1. Phasor diagram of an unsaturated synchronous generator with a cylindrical rotor—lagging current.

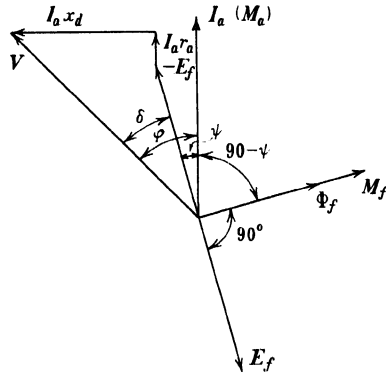


FIG. 32-2. Phasor diagram of an unsaturated synchronous motor with a cylindrical rotor—lagging current.

The phasor diagrams which correspond to Eqs. 32-4 and 32-5 are shown in Figs. 32-1 and 32-2, both for lagging current. Since  $E_f$  is 90 electrical degrees behind the flux  $\Phi_f$  producing it and since this flux is in phase with the field mmf  $M_f$ , both  $\Phi_f$  and  $M_f$  are readily drawn in the phasor diagrams. Figs. 32-3a and 32-3b show the phasor diagrams for a leading current.

The following observations can be made on the four phasor diagrams. First,  $V$  lags behind  $E_f$  in a generator and  $V$  is ahead of  $-E_f$  in a motor. Furthermore, considering the generator

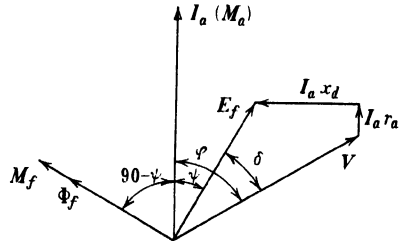


FIG. 32-3a. Phasor diagram of an unsaturated synchronous generator with a cylindrical rotor—leading current.

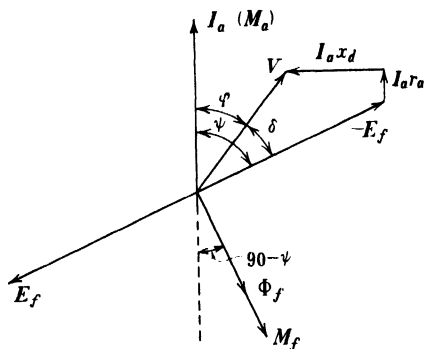


FIG. 32-3b. Phasor diagram of an unsaturated synchronous motor with a cylindrical rotor—leading current.

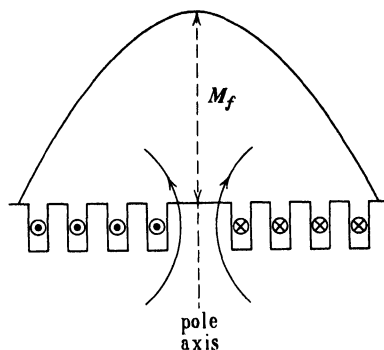


FIG. 32-4. Field mmf distribution and field pole axis.

diagrams of Figs. 32-1 and 32-3a, the angle between the armature mmf  $M_a$  (Eq. 32-1) which is in phase with  $I_a$ , and the field mmf  $M_f$  is larger than  $90^\circ$  for a lagging current and less than  $90^\circ$  for a leading current. This means that a lagging current in a generator opposes its field mmf, while a leading current supports its field mmf. It can be seen from the motor diagrams of Figs. 32-2 and 32-3b that the opposite is true of a motor: lagging current in a motor supports the field mmf, while leading current opposes the field mmf.

These considerations yield the following important *rules of armature reaction* in the synchronous machine: *lagging current opposes the field (rotor) mmf in a generator and supports the field mmf in a motor; leading current supports the field mmf in a generator and opposes the field mmf in a motor.*

However, it should be observed that it is not the power factor angle  $\phi$  between  $I_a$  and  $V$  which determines the character and the magnitude of the armature reaction but *the angle  $\psi$  between  $I_a$  and  $E_f$ , or  $-E_f$* , because the position of  $M_f$  in the phasor diagram is determined by  $E_f$ . It is seen from Figs. 32-1 to 32-3 that the angle between the axes of the field mmf  $M_f$  and the armature mmf  $M_a$  is  $(90 - \psi)^\circ$ . Neglecting harmonics, the field mmf and the armature mmf are sinusoidal waves, the amplitudes of which can be treated as phasors. In the phasor diagrams (Figs. 32-1 to 32-3)  $M_f$  and  $M_a$  are the phasors which *represent the amplitudes* of both mmf's. Since the amplitude of a sinusoidal mmf coincides with the center-line of the flux distribution produced by it, i.e., with its pole axis (see Fig. 32-4), *the angle  $(90 - \psi)^\circ$  is the angle between the pole axes of rotor and stator.*

Attention must be called to the angle  $\delta$  between  $V$  and  $E_f$ , or  $-E_f$ , in the phasor diagrams. It will be shown later (see Art. 36-1) that this angle is the *basic variable* of the synchronous machine, just as the slip is the basic variable of the induction motor. A torque-angle characteristic therefore takes the place of the torque-speed characteristic of the induction motor, and it is the angle  $\delta$  which determines the magnitude of the torque.

(b) *Machine saturated.* When the machine is saturated, the *resultant mmf* of the field and armature windings and the flux produced by it must be considered. The armature reaction reactance  $x_{ad}$  does not appear in this case, because it is taken care of by the armature mmf which is a component of the total mmf. Only the leakage reactance  $x_l$  of the armature is to be considered and a no-load characteristic must be available (see Art. 31-3). The mmf's, fluxes, and emf's induced by the fluxes in the armature winding are

<i>MMF's</i>	<i>Fluxes</i>	<i>Induced EMF's</i>
Resultant of $\dot{M}_f + \dot{M}_a = (\dot{M}_r)$	$\Phi_r$	$E$
MMF of the leakage (const $\times I_a$ ) flux	$\Phi_l$	$-jI_a x_l$

Kirchhoff's mesh equation for generator operation is (see Eq. 32-4)

$$\dot{V} + \dot{I}_a r_a + j\dot{I}_a x_l = \dot{E} \quad (32-7)$$

and for motor operation (see Eq. 32-5)

$$\dot{V} = -\dot{E} + \dot{I}_a r_a + j\dot{I}_a x_l \quad (32-8)$$

Here,  $E$  is entirely different from  $E_f$ .  $E_f$  is the emf induced in the armature winding by the field flux (of an unsaturated machine) *alone*.  $E$  is the emf induced in the armature winding by the flux due to the resultant mmf of armature and rotor.

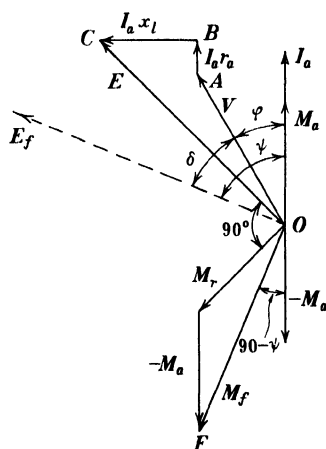


FIG. 32-5. Phasor diagram of a saturated synchronous generator with a cylindrical rotor —lagging current.

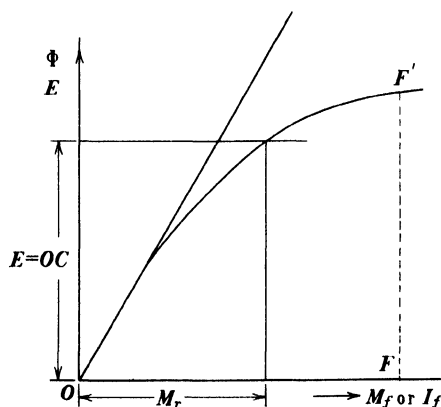


FIG. 32-6. Determination of the resultant mmf from the no-load characteristic.

Fig. 32-5 shows the phasor diagram of a generator with a cylindrical rotor for a lagging current.  $OC$ , the resultant of  $V$ ,  $I_a r_a$ , and  $I_a x_l$ , is the emf  $E$  to be induced in the armature by the flux produced by the *resultant* mmf



( $M_r$ ). This resultant mmf must lead the emf  $OC = E$  by  $90^\circ$ . Its magnitude is to be determined from the no-load characteristic as shown in Fig. 32-6. Having found  $M_r$  from the no-load characteristic, the field mmf  $M_f$  is determined from the equation

$$\dot{M}_r = \dot{M}_f + \dot{M}_a \quad (32-9)$$

or

$$\dot{M}_f = \dot{M}_r + (-\dot{M}_a) \quad (32-9a)$$

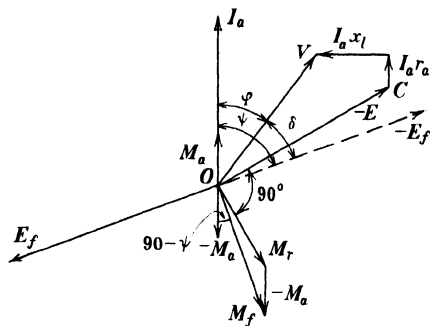


FIG. 32-7. Phasor diagram of a saturated synchronous motor with a cylindrical rotor—leading current.

characteristic in the manner shown in Fig. 32-6 for the generator.  $M_f$  is again determined from Eq. 32-9a.

as shown in Fig. 32-5. The angle between  $M_f$  and  $-M_a$  is  $(90 - \psi)^\circ$ . If the generator, loaded corresponding to the phasor diagram of Fig. 32-5, should suddenly lose its load, the voltage at its terminals would be the no-load voltage  $E_f$ , which corresponds to the field mmf  $M_f = OF$  (equal to  $FF'$  in Fig. 32-6). The direction of  $E_f$  is indicated in the phasor diagram.

The phasor diagram of a motor with a cylindrical rotor and a leading current, taking into account saturation, is shown in Fig. 32-7. The resultant mmf  $M_r$  is found from the no-load

## Chapter 33

### GENERATOR CHARACTERISTICS · VOLTAGE REGULATION

**33-1. Generator characteristics.** The characteristics described in the following paragraphs are of importance for establishing good concepts of generator operation.

(a) *No-load and air-gap characteristic.* These characteristics have already been shown in Fig. 31-2.

(b) *Short-circuit characteristic. Potier triangle.* The short-circuit characteristic represents the armature current  $I_a$  as a function of the field current  $I_f$  or of the field mmf  $M_f$  with the armature terminals short-circuited. It is taken at synchronous speed of the generator. Referring to Fig. 32-5 the short-circuited generator appears to be loaded with an almost pure inductance because the resistance of the armature winding  $r_a$  is small in comparison to its leakage reactance  $x_l$ . Fig. 33-1 shows the phasor diagram of the short-circuited machine using method (b) of Art. 31-3, although the machine is not saturated, as explained in the following. The terminal voltage  $V$  is equal to zero. The emf induced in the armature winding by the flux produced by the resultant mmf is  $AC$ . The resultant mmf, found from the no-load characteristic, is  $M_r$ , and the field mmf  $M_f$  is then  $M_f = M_r + (-M_a)$ . The armature mmf  $M_a$  acts almost directly opposite to the field mmf  $M_f$ , as it should for an inductively loaded generator, according to the rules of armature reaction (see Chap. 32).

The field mmf  $M_f$  must be large enough to overcome the opposing armature mmf  $M_a$  and to induce an emf which balances the impedance drop  $I_a z_a = I_a(r_a + jx_l)$  of the armature winding. If, in the no-load characteristic of Fig. 31-2,  $lm$  is drawn equal to the impedance drop  $I_a z_a$ , then  $Om$  is the field mmf necessary to induce the emf which balances  $I_a z_a = AC$  (Fig. 33-1).

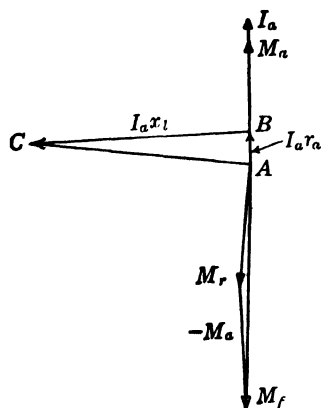


FIG. 33-1. Phasor diagram of a short-circuited generator with a cylindrical rotor.

Further, if in Fig. 31-2,  $On$  is made equal to  $M_f$ , then  $mn = M_f - Om$  is the opposing armature mmf  $M_a$ . Finally, if  $nd$  is made equal to  $I_a$  in Fig. 31-2 and the origin  $O$  is connected with  $d$  by a straight line, the line  $Od$  is the *short-circuit characteristic* of the generator. It is a *straight line* because in the short-circuited machine the emf induced in the armature and the main flux are small; as a result there is no saturation of the iron.

The triangle  $lmn$  in Fig. 31-2 is a characteristic triangle of the synchronous machine: it contains two important quantities, namely, the armature reaction mmf ( $mn = M_a$ ) and the leakage reactance  $x_l \approx z_a = lm/I_a$ . This triangle is called the *Potier triangle*.

(c) *Load characteristic*. This characteristic represents the terminal voltage  $V$  as a function of field current  $I_f$ , or field mmf  $M_f$ , for a constant load current  $I_a$  and a constant phase angle  $\varphi$ . Fig. 33-2 shows three such characteristics for the same constant load current  $I_a$  but for different values of a lagging angle  $\varphi$ .

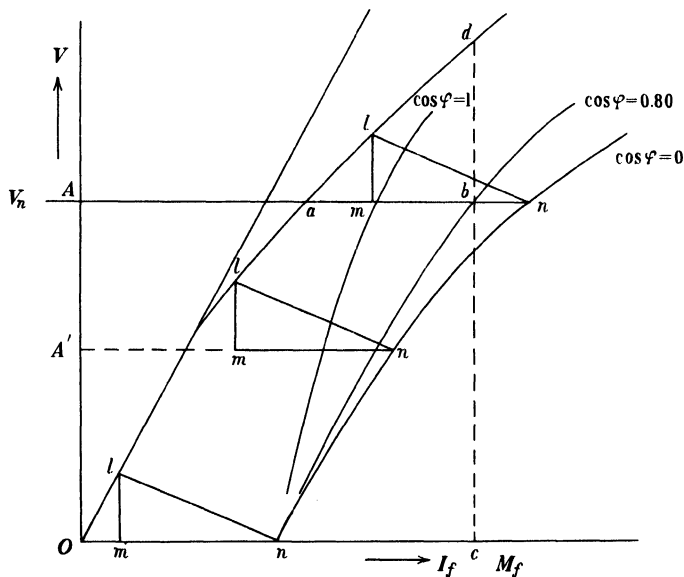


FIG. 33-2. Load characteristics of a cylindrical rotor generator for constant armature current and variable power factor angle  $\varphi$ .

Let  $OA$  be the normal terminal voltage  $V_n$  of the generator. The field current necessary to produce this voltage at no-load is  $Aa$ . At a fixed load current, the field current required to sustain this voltage increases rapidly with decreasing  $\cos \varphi$ . This increase of field current is necessary to counterbalance the voltage drop  $I_a z_a$  but mainly to counteract the armature reaction which increases with increasing lagging angle  $\varphi$ . The  $\cos \varphi = 0$  load characteristic can be readily constructed if the no-load characteristic and the Potier triangle are available. This is based upon the fact that, at  $\cos \varphi = 0$ , the

armature mmf is in almost direct opposition to the field mmf, just as at short-circuit, Fig. 33-1. Then at constant current  $I_a$  the voltage drop remains the same ( $=lm$ ) for all values of  $V$  and the armature reaction mmf also remains the same ( $=mn$ ) for all values of  $V$ . Thus the  $\cos \varphi = 0$  characteristic can be found by moving the Potier triangle  $lmn$  parallel to itself with the vertex  $l$  on the no-load characteristic; the point  $n$  describes the  $\cos \varphi = 0$  characteristic, Fig. 33-2. For the voltage  $OA = V_n$ , as an example, the emf induced by the main flux is  $(OA + ml)$ ; the resultant mmf  $M_r$  is  $Am$  and the field mmf  $M_f$  is  $An$ . For the voltage  $OA'$  the induced emf is  $(OA' + ml)$  and the field mmf is  $A'n$ .

It has been shown that the  $\cos \varphi = 0$  load characteristic can be determined from the no-load characteristic and the Potier triangle. Inversely, the Potier triangle can be determined from the no-load characteristic and two points of the  $\cos \varphi = 0$  load characteristic. It will be noted in Fig. 33-2 that the Potier triangle  $lmn$  fixes the angle  $lOn$ , since  $On$  is parallel to the axis of abscissae and  $Ol$  is parallel to the air-gap line. Let  $n$  and  $n'$  in Fig. 33-3 be two experimentally determined points of the  $\cos \varphi = 0$  load characteristic, the point  $n$  being determined with the armature short-circuited and the point  $n'$  being determined at normal terminal voltage  $V_n$  with full-load current. Then, if  $n'O'$  is made equal to  $nO$  and the line  $O'A$  is drawn through  $O'$  parallel to the air-gap line, the intersection of  $O'A$  and the no-load characteristic will yield the Potier triangle  $lmn$ .  $lm$  is the leakage reactance drop and  $lm/I_a$  is the leakage reactance  $x_l$ .  $mn'$  is the armature reaction mmf  $M_a$ .

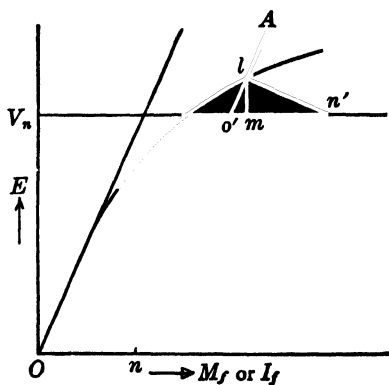


FIG. 33-3. Determination of Potier triangle from no-load characteristic and two points of zero power factor characteristic determined by test.

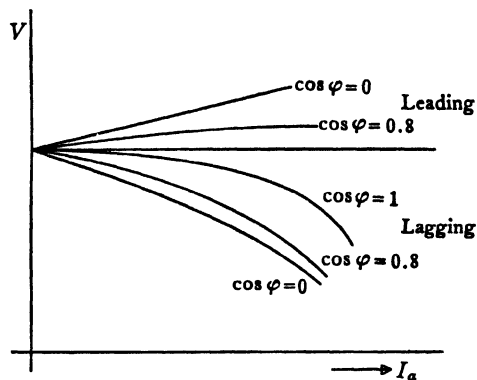


FIG. 33-4. External characteristics for lagging and leading current.

(d) *External characteristic.* This characteristic represents the terminal voltage  $V$  as a function of the load current  $I_a$  at constant field current  $I_f$ , and constant power factor  $\cos \varphi$ . Fig. 33-4 shows the trend of the external

characteristic for lagging as well as leading current. For a lagging current the total voltage drop increases as the power factor decreases.

(e) *Regulation curve.* This curve shows the field current  $I_f$  as a function either of the load current  $I_a$  at constant power factor, or of the power factor at constant load current  $I_a$ . In both cases the terminal voltage is kept constant. Fig. 33-5 shows regulation curves for two fixed values of power factor and variable  $I_a$ ; Fig. 33-6 shows a regulation curve for a fixed value of the load current and variable  $\cos \varphi$ . The trend of these curves, as well as that of the other characteristics of the machine under load, can be explained by the rules of armature reaction (see foregoing article).

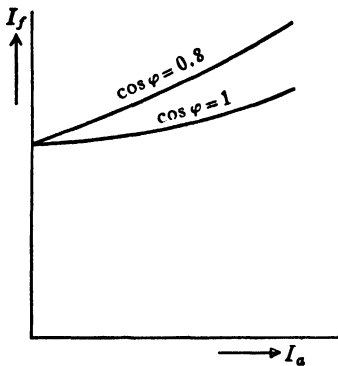


FIG. 33-5. Regulation curves for constant power factor.

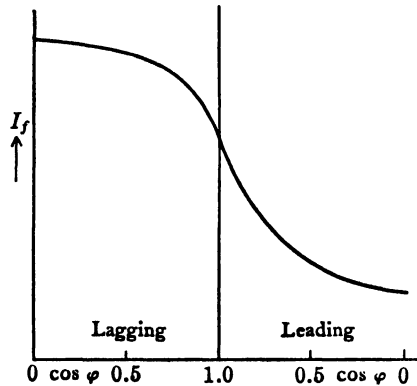


FIG. 33-6. Regulation curve for constant load current.

(f) *Short-circuit ratio.* The short-circuit ratio (SCR) of a synchronous machine is defined as the ratio of field current required to produce rated voltage on *open circuit* to the field current required to produce rated current on *short circuit*. Fig. 33-7 shows a no-load characteristic and a short-circuit characteristic. The armature current is expressed in per-unit of rated current. According to the definition

$$\text{SCR} = \frac{OF_0}{OF_s} = \frac{LF_0}{KF_s} = \frac{LF_0}{1} = LF_0 \quad (33-1)$$

The short-circuit ratio determined in this manner is the *saturated* SCR. The *unsaturated* SCR is equal to  $L'F'_0$ ; it is determined from the no-load field current which corresponds to the air-gap characteristic and is smaller than the saturated SCR which is equal to  $LF_0$ .

The short-circuit ratio is an important factor for the synchronous machine for the following reasons. The field mmf  $OF_s$ , Fig. 33-7, necessary to produce the rated current at short circuit is larger the larger the armature reaction mmf and the  $I_a x_l$  drop (see Fig. 33-1). A small SCR indicates a large armature reaction, i.e., a machine sensitive with respect to load variations. A large

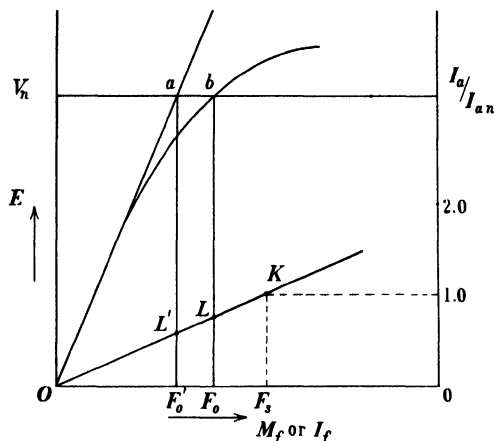


FIG. 33-7. Determination of the SCR.

SCR indicates a small armature reaction, i.e., a machine less sensitive to load variations.

(g) *Determination of the direct-axis synchronous reactance  $x_a$ .* This reactance can be determined from the no-load and short-circuit characteristics. Consider Fig. 33-7. The field current  $OF_0'$  induces the emf  $F_0'a = V_n$  in the stator at open circuit. When the stator is short-circuited at the same field current  $OF_0'$ , the induced emf in the stator is the same but it is consumed by the drop due to the synchronous impedance (see Fig. 32-1) i.e.  $E_f = F_0'a = V_n = I_a z_a$ . Since  $r_a$  is small in comparison with  $x_a$

$$x_a \approx \frac{V_n}{I_a} \approx \frac{V_n}{F_0' L'} \quad (33-2)$$

where  $I_a = F_0' L'$  is the short-circuit current which corresponds to  $I_f = OF_0'$ .  $F_0' L'$  is expressed in Fig. 33-7 in per-unit, the unit being the normal current. If, in Fig. 33-7, the voltage is also expressed in per-unit with the normal voltage  $V_n$  as the unit value

$$x_a \approx \frac{1}{F_0' L'}$$

As has been shown under (f),  $F_0' L'$  is the *unsaturated* short-circuit ratio. Thus

$$x_a = \frac{1}{\text{SCR}} \quad (33-3)$$

i.e., the synchronous reactance in per-unit is equal to 1 divided by the unsaturated short-circuit ratio.

**33-2. Voltage regulation.** The voltage regulation is defined as the per-unit voltage rise which takes place at the terminals when the load is dropped and

the field current and the speed remain unchanged. In this case the no-load voltage corresponding to the field current appears at the machine terminals; this voltage can be determined from the no-load characteristic. In Fig. 33-2 the field mmf which corresponds to the voltage  $V_n$  and  $\cos \varphi = 0.8$  is  $Ab$ . The no-load voltage  $E_f$  produced by this mmf is  $cd$  and consequently the per-unit voltage regulation is:

$$\epsilon = \frac{db}{cb} = \frac{E_f - V_n}{V_n} \quad \text{in p-u} \quad (33-4)$$

or

$$\epsilon = \frac{E_f - V_n}{V_n} \times 100 \quad \text{in percent} \quad (33-4a)$$

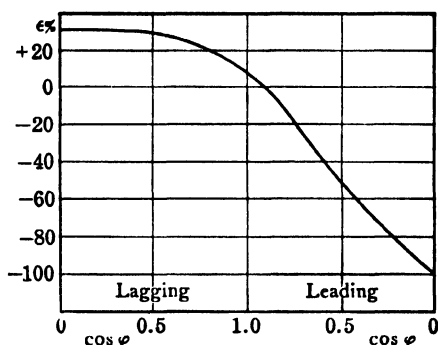


FIG. 33-8. Voltage regulation as a function of power factor for constant lagging and leading current.

The voltage regulation increases with increasing load current  $I_a$  and with increasing lagging angle  $\varphi$ . For capacitive loads the voltage regulation may be negative. Fig. 33-8 shows the voltage regulation for a constant-load current and variable power factor.

Similar to the short-circuit ratio, the voltage regulation is determined partly by the voltage drop  $I_a z_a$  but mainly by the armature reaction. It is an important factor for the synchronous machine. There are several methods employed for the determination

of the magnitude of the voltage regulation. The following empirical method is recommended by the AIEE.

The no-load characteristic and two points of the  $\cos \varphi = 0$  load characteristic are determined by tests, one of the two points being at normal current and short-circuited armature (point  $n$  Fig. 33-3), the other point being at normal current and normal voltage (point  $n'$  Fig. 33-3). From this the Potier triangle can be determined as explained in the foregoing article. Referring to Fig. 33-9a where the load current  $I_a$  is assumed along the horizontal, draw the voltage diagram of the three phasors  $V_n$ ,  $I_a r_a$ , and  $I_a x_l$ , i.e., determine the emf  $E$  to be induced in the armature by the flux due to the resultant mmf (see Fig. 32-5).  $I_{fs}$  is then the difference in field amperes between the air-gap line and the no-load characteristic for the voltage  $E$ , and it represents the effect of saturation.

In order to find the field current  $I_{ft}$  which corresponds to the load current  $I_a$ , the rated voltage  $V_n$ , and the fixed value of the angle  $\varphi$ , draw  $I_{fs}$  horizontally (Fig. 33-9b), lay off the value of the field current  $I_{fsh}$  required to produce the current  $I_a$  in the short-circuited armature ( $On$  Fig. 31-2 or

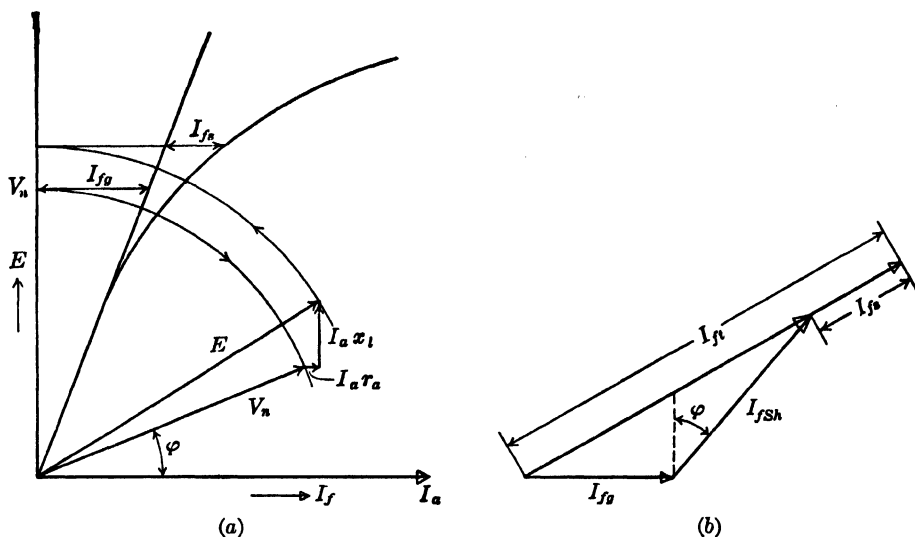


FIG. 33-9. Empirical AIEE method for determination of regulation.

On Fig. 33-2 or  $O'n'$  Fig. 33-3) at the power factor angle  $\varphi$  to the vertical, and add  $I_{fs}$  directly to the phasor sum of these two phasors. The no-load voltage  $E_f$  taken from the no-load curve corresponding to  $I_{f1}$  determines the voltage regulation.

**Example 33-1.** The no-load and the full-load zero-power-factor characteristics of a 3-phase, 6500-kva, 5500-volt, Y-connected turbogenerator are shown in Fig. 33-10. The ordinate is plotted in volts per phase.

$$V_n = \frac{5500}{\sqrt{3}} = 3180 \text{ volts per phase}$$

$$I_a = \frac{6500}{\sqrt{3} \times 5.5} = 683 \text{ amp}$$

Following the methods of Art. 33-1c, the triangle  $O'ln$  is constructed, and the Potier triangle  $lmn$  is determined. From this,  $mn = 71$  is the armature reaction  $M_a$  expressed in terms of field amperes,  $lm = 660$  volts is the leakage-reactance voltage; therefore  $x_l = 660/683 = 0.968$  ohm. The leakage reactance in p-u is  $660/3180 = 0.208$ . The short-circuit ratio (unsaturated) SCR is  $Aa/On = 73/87 = 0.84$ , and the saturated value is  $Ab/On = 80/87 = 0.92$  (for the saturation at rated voltage). Also from the short-circuit characteristic (on per-unit basis) the  $SCR = F_0' L' = 0.84$ ; the saturated value  $SCR = F_0 L = 0.92$ . Therefore  $x_a = 1/0.84 = 1.19$  in per-unit. The unit impedance is  $3180/683 = 4.66$  ohms; therefore  $x_a = 1.19 \times 4.66 = 5.54$  ohms. Also by definition  $x_a = nh/683 = 3780/683 = 5.54$  ohms. The armature-reaction reactance  $x_{ad} = x_a - x_l$  (Eq. 37-5); hence  $x_{ad} = 5.54 - 0.968 = 4.57$  ohms, or  $4.57/4.66 = 0.98$  p-u.



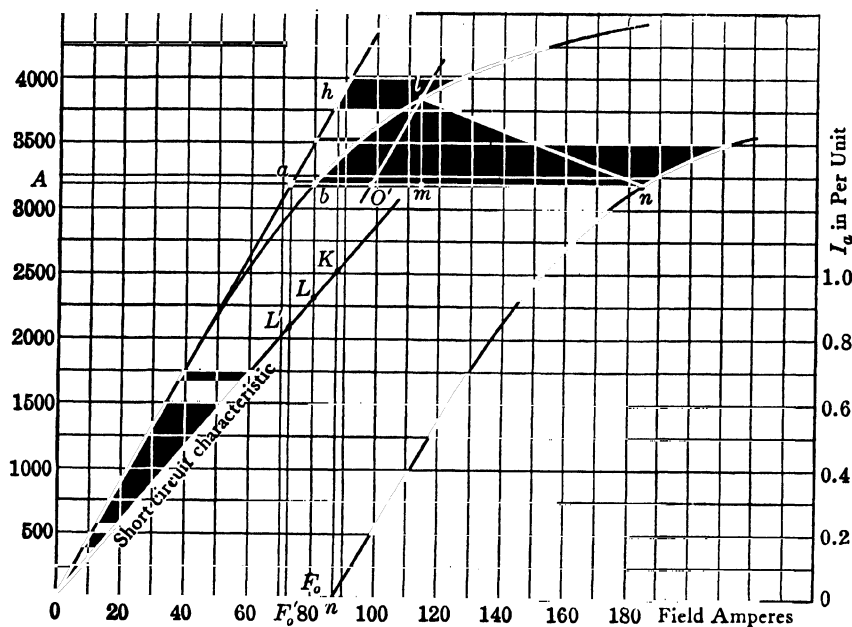


FIG. 33-10.

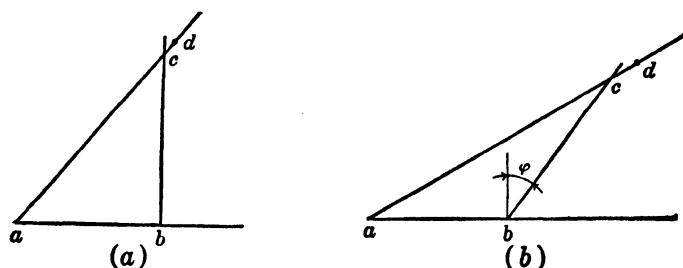


FIG. 33-11.

The per-unit voltage regulation of this machine now will be determined for (1) unity power factor. (2) 0.8 power factor lagging, using the AIEE method described in Art. 33-2 (see also Fig. 33-9). (Armature resistance is neglected.) From Fig. 32-5 it follows that  $E = \sqrt{(V_n \cos \varphi)^2 + (V_n \sin \varphi + I_a x_l)^2}$ ; hence for  $\varphi = 0$ ,  $E = \sqrt{(3180)^2 + (660)^2} = 3250$ . From Fig. 33-10 the value of  $I_{fs} = Aa = 73$ ,  $I_{fsh} = O_n = 87$ , and  $I_{fs} = ab = 8.6$ . Fig. 33-9b is now constructed as shown in Fig. 33-11a in which  $ab = I_{fs} = 73$ ,  $bc = I_{fsh} = 87$ ; then  $ac = \sqrt{73^2 + 87^2} = 113.6$ ,  $cd = 8$ , and hence  $I_{ft} = ad = 121.6$ . This value of field current produces  $E_f = 3950$  at no-load (see Fig. 33-10). Hence  $\epsilon = (3950 - 3180)/3180 = 0.242$  at unity power factor. For  $\cos \varphi = 0.8$  lagging current

$$E = \sqrt{(3180 \times 0.8)^2 + (3180 \times 0.6 + 660)^2} = 3615 \text{ volts}$$

From Fig. 33-10,  $I_{fg} = 73$ ,  $I_{fab} = 87$ ,  $I_{fa} = 16$ . Fig. 33-9b now appears as shown in Fig. 33-11b. Here  $ab = 73$ ,  $bc = 87$ ,  $cd = 16$ ,  $ad = 159.2$  amp. This  $I_f$  produces  $E_f = 4280$  volts at no-load; hence

$$\epsilon = \frac{4280 - 3180}{3180} = 0.346$$

With the information given in this example it is instructive to draw the phasor diagram of Fig. 32-5 for this machine. This is done only for 0.8 power factor lagging (Fig. 33-12). The figure is drawn to scale, so that  $V = 3180$ ,  $E = 3615$ ,  $M_r = 100$ ,  $M_a = 71$ ,  $M_f = 159.2$ ,  $\cos \phi = 0.8$ .

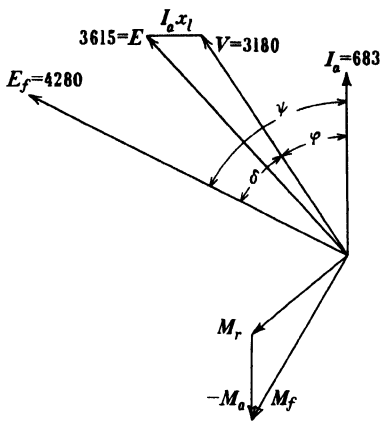


FIG. 33-12.

## PROBLEMS

1. For the machine of Example 33-1, determine the voltage regulation for 0.8 power factor leading, and draw the voltage and mmf diagrams.

2. The no-load and full-load zero-power-factor curves for a 12.0-kv 5000-kva 3-phase Y-connected 60-cycle turbogenerator are as follows, the voltage per-phase (neglect armature resistance):

$I_f$ (amp):	10	20	30	40	43.0	50	60	70	80	90	100	110
$V$ (no-load):	1750	3500	5120	6360	6700	7260	7860	8280	8580	8780	—	—
$V$ (full-load):	—	—	—	—	0	1080	2720	4250	5380	6180	6750	7080

(a) Construct the Potier triangle and determine  $x_l$  in ohms and in per-unit.

(b) Determine the armature reaction  $M_a$  in terms of field amperes.

(c) Determine  $x_d$  in ohms and in p-u.

3. Using the AIEE method, determine the voltage regulation for the machine of Problem 2 in p-u for unity power factor and for 0.8 lagging and 0.8 leading.

4. For the machine of Problem 2 draw the short-circuit characteristic and determine the saturated and unsaturated SCR.

5. The no-load and full-load zero power factor characteristics for a 23,500-kva, 13,800-volt, 3-phase, 60-cycle, 2-pole, 0.85-p.f. lagging hydrogen-cooled turbogenerator are given below in p-u values.

### No-load characteristic

$I_f$ :	0.10	0.20	0.40	0.60	0.80	1.0	1.2	1.4	1.6
$V$ (no-load):	0.13	0.23	0.45	0.69	0.87	1.0	1.09	1.15	1.21

### Zero-power-factor characteristic

$I_f$ :	1.2	1.3	1.4	1.6	1.7	1.8	2.0	2.2	2.4	2.6
$V$ (full-load):	0.015	0.13	0.25	0.49	0.61	0.69	0.83	0.92	0.99	1.25

Unit field amperes = 185

Unit voltage = 13,800

Neglect armature resistance.

(a) Construct the Potier triangle and determine  $x_l$  in ohms and p-u.

(b) Determine the armature reaction  $M_a$  in terms of field amperes.

(c) Determine the value of  $x_a$  in both ohms and p-u.

6. For the machine of Problem 5 determine the voltage regulation for 0.80 p.f. lagging and 0.80 p.f. leading, using the AIEE method.

Draw emf and mmf phasor diagrams.

7. Determine the unsaturated SCR for the machine of Problem 5.

8. A 70,600-kva, 13,800-volt, 3-phase, 60-cycle, 2-pole, 0.85-p.f. lagging hydrogen-cooled turbogenerator has no-load and full-load zero power characteristics identical with those of Problem 5, on a p-u basis. However, for this generator:

$$\text{Unit field amperes} = 350$$

$$\text{Unit voltage} = 13,800$$

(a) Construct the Potier triangle and determine  $x_l$  in ohms and p-u.

(b) Determine the armature reaction  $M_a$  in field amperes.

(c) Determine the value of  $x_a$  in ohms and p-u.

9. For the machine of Problem 8 determine the regulation at unity, 0.80 lagging and 0.8 leading power factor, using the AIEE method.

Construct emf and mmf phasor diagrams.

## Chapter 34

### THE TWO-REACTION THEORY

**34-1. The essence of the two-reaction theory.** It has been found in Art. 32-1 that the amplitude  $M_a$  (pole axis) of the stator mmf makes an angle  $90 - \psi$  with the direct axis (pole axis of the rotor).  $\psi$  is the angle between the armature current  $I_a$  and the emf  $E$ , induced in the armature by the field flux (Fig. 32-1). Its magnitude depends upon the character of the load. Fig. 34-1 shows the relative position of  $M_a$  and the direct axis for  $\psi = 90^\circ$  (pure inductive load). Fig. 34-2 shows their relative position for  $\psi = 0$  (certain capacitive load), (see also Fig. 32-3a). For intermediate values of  $\psi$  ( $90 > \psi > 0$ ), the relative position of  $M_a$  and the direct axis is that between those of Figs. 34-1 and 34-2 (Fig. 34-3).

It has been pointed out in Art. 31-2 that the reluctance with respect to the armature mmf depends upon the position of the amplitude  $M_a$  of the armature mmf with respect to the rotor poles. It is seen from Figs. 34-1 and

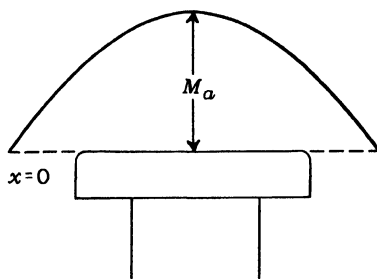


FIG. 34-1. Position of the armature mmf with respect to the direct axis for  $\psi = 90^\circ$ .

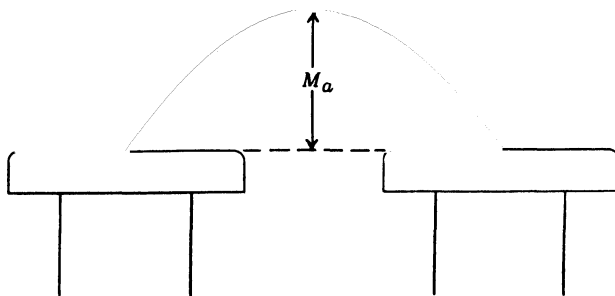


FIG. 34-2. Position of the armature mmf with respect to the direct axis for  $\psi = 0$ .

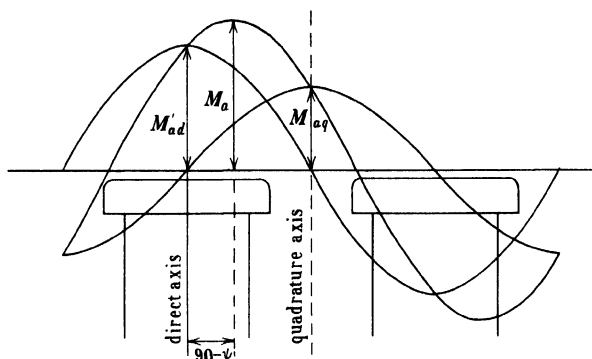


FIG. 34-3. Armature mmf wave and its two component waves in their positions relative to the direct and quadrature axes.

34-2 that this reluctance is minimum for the position Fig. 34-1 and maximum for the position Fig. 34-2. For any intermediate position of the armature mmf with respect to the poles, the reluctance has a value between the minimum and the maximum values. It is relatively simple to determine the effect of the armature mmf for its positions Figs. 34-1 and 34-2 because the direct axis and the quadrature axis are both axes of symmetry for the rotor, but it is difficult to determine the effect which the armature mmf has in intermediate positions. This difficulty can be overcome by the use of *Blondel's two-reaction theory*.

This theory consists essentially of the replacement of the sinusoidal armature mmf of amplitude  $M_a$  by two sinusoidal waves, one of which has its amplitude coinciding with the direct axis, and the other has its amplitude coinciding with the quadrature axis (Fig. 34-3). The amplitudes of these two waves can be determined from the phasor diagrams derived previously. Consider Figs. 32-1 and 32-3b which refer to a generator and motor, the generator running with lagging current, the motor with leading current (these are the normal kinds of operation for a synchronous generator and motor). The relative position of the armature mmf ( $M_a$ ) with respect to the direct axis ( $M_f$ ), as it follows from the two phasor diagrams, is shown in Fig. 34-4. If

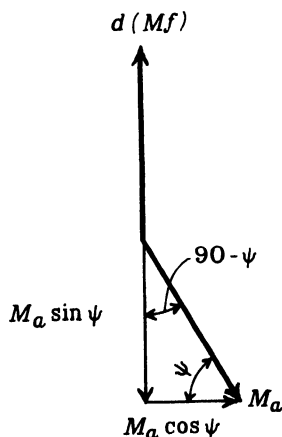


FIG. 34-4. Resolution of the armature mmf into two components, the direct-axis armature mmf and the quadrature axis mmf.

$M_a$  is resolved into the components  $M_a \sin \psi$  and  $M_a \cos \psi$ , then the first component coincides with the direct axis and the second with the quadrature axis, i.e., the replacement wave, the pole axis of which coincides with the direct axis, has the amplitude

$$M_{ad}' = M_a \sin \psi \quad (34-1)$$

and the replacement wave, the pole axis of which coincides with the quadrature axis, has the amplitude

$$M_{aq}' = M_a \cos \psi \quad (34-2)$$

Fig. 34-3 shows the two component waves of the armature mmf wave with the amplitude  $M_a$ . Figs. 34-5 and 34-6 show the component waves and their

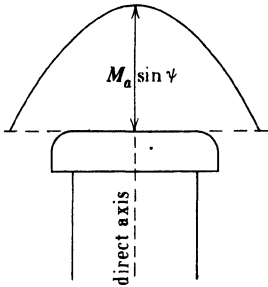


FIG. 34-5. Direct-axis armature mmf in its position relative to the direct axis.

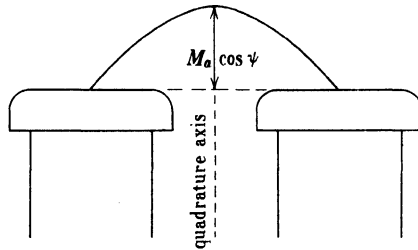


FIG. 34-6. Quadrature-axis armature mmf in its position relative to the quadrature axis.

positions with respect to the direct and quadrature axes separately. It is seen from Fig. 34-5 that the reluctance with respect to armature component-wave with the amplitude  $M_{ad}'$ , the pole-axis of which coincides with the direct axis, is the same as for the rotor (field) mmf. The magnetic path is the same for both mmf's, namely, the path through the salient poles (Fig. 30-3), with the direct axis as symmetry axis. The component of the armature mmf with the amplitude  $M_{aq}'$  has a cross-magnetizing effect on the poles, because its axis is shifted  $90^\circ$  with respect to the direct axis.

**34-2. Effective armature mmf in both axes.** Consider Fig. 34-5. It is seen that the component of the armature mmf with the amplitude  $M_{ad}' = M_a \sin \psi$  will produce very little flux at the edges of the sinusoid due to the interpolar spaces. It can be assumed that only the part of this mmf shown in Fig. 34-7 is effective. Of this part the fundamental alone is to be considered, since the influence of the harmonics is small. The amplitude of the fundamental is given by the equation

$$a_1 = \frac{1}{\pi} \int_0^{2\pi} f(x) \sin x \, dx \quad (34-3)$$

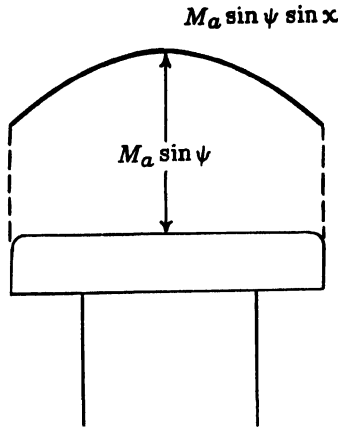


FIG. 34-7. Effective part of the armature mmf of amplitude  $M_{ad}'$ , in the direct axis.

If the ratio between pole arc and pole pitch is denoted by  $\alpha$ , i.e.,

$$\frac{b_p}{\tau} = \alpha$$

then (Fig. 34-1)

$$f(x) = 0 \text{ from } x = 0 \text{ to } x = (1 - \alpha)\pi/2$$

$$f(x) = 0 \text{ from } x = (1 + \alpha)\pi/2 \text{ to } x = \pi + (1 - \alpha)\pi/2$$

$$f(x) = 0 \text{ from } x = \pi + (1 + \alpha)\pi/2 \text{ to } x = 2\pi$$

$$f(x) = M_a \sin \psi \sin x \text{ from } x = (1 - \alpha)\pi/2 \text{ to } (1 + \alpha)\pi/2$$

$$f(x) = -M_a \sin \psi \sin x \text{ from } x = \pi + (1 - \alpha)\pi/2 \text{ to } x = \pi + (1 + \alpha)\pi/2$$

Carrying out the integration Eq. (34-3) yields

$$a_{1a} = M_a \sin \psi \left( \frac{\alpha\pi + \sin \alpha\pi}{\pi} \right) \quad (34-4)$$

Consider now Fig. 34-6. It is seen that the component of the armature mmf with the amplitude  $M_{aq}' = M_a \cos \psi$  will produce but little flux in the interpolar space. Assuming that the effective part of this mmf is as shown in Fig. 34-8 (the height of the line  $cd$  is assumed to be  $\frac{1}{2}$  of the amplitude  $M_a \cos \psi$ ) and again considering only the fundamental of this mmf, the result is

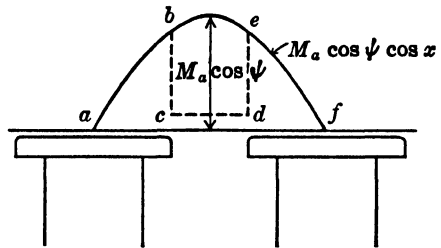


FIG. 34-8. Effective part of the armature mmf of amplitude  $M_{aq}'$  in the quadrature axis.

$$a_{1a} = M_a \cos \psi \left( \frac{\alpha\pi - \sin \alpha\pi + \frac{1}{2} \cos \alpha(\pi/2)}{\pi} \right) \quad (34-5)$$

The factors of Eqs. 34-4 and 34-5 shown in parenthesis are the *effectiveness* factors of the two armature mmf's.

The field mmf of the salient-pole machine is rectangular. For its fundamental the Fourier series yields

$$a_{1f} = I_f \frac{N_f}{p} \frac{4}{\pi} \sin \frac{\alpha\pi}{2} \quad (34-6)$$

$N_1$  is the total number of field turns.

The amplitudes of the armature mmf's,  $a_{1d}$  and  $a_{1q}$ , are used in connection with the no-load characteristic, short-circuit characteristic and load characteristics. In all these characteristics,  $I_f(N_f/p)$  is used as abscissa and not  $a_{1f}$ , the fundamental, i.e., as abscissa is used, the field fundamental divided by  $(4/\pi) \sin (\alpha\pi/2)$ . Therefore, when  $a_{1d}$  and  $a_{1q}$  are used in connection with these characteristics, they also must be divided by the same factor. These lead to the following values of the two armature mmf's to be used in the following considerations:

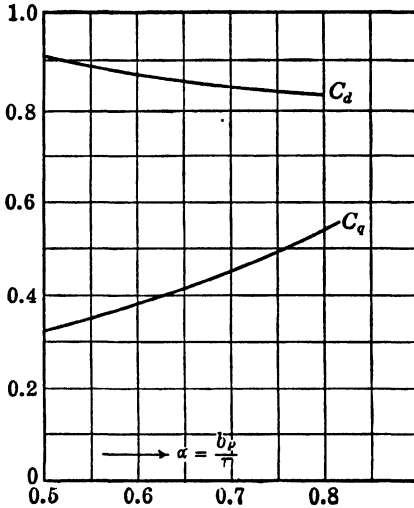


FIG. 34-9. Factors,  $C_d$  and  $C_q$ , for the effective armature mmfs in the direct axis and in the quadrature axis of the salient-pole machine.

$$\begin{aligned} M_{ad} &= a_{1d} \frac{1}{(4/\pi) \sin (\alpha\pi/2)} \\ &= M_a \sin \psi \frac{\alpha\pi + \sin \alpha\pi}{4 \sin (\alpha\pi/2)} \\ &= C_d M_a \sin \psi \end{aligned} \quad (34-7)$$

$$\begin{aligned} M_{aq} &= a_{1q} \frac{1}{(4/\pi) \sin (\alpha\pi/2)} \\ &= M_a \cos \psi \frac{\alpha\pi - \sin \alpha\pi + \frac{1}{2} \cos (\alpha\pi/2)}{4 \sin (\alpha\pi/2)} \\ &= C_q M_a \cos \psi \end{aligned} \quad (34-8)$$

where

$$C_d = \frac{\alpha\pi + \sin \alpha\pi}{4 \sin (\alpha\pi/2)} \quad (34-9)$$

$$C_q = \frac{\alpha\pi - \sin \alpha\pi + \frac{1}{2} \cos (\alpha\pi/2)}{4 \sin (\alpha\pi/2)} \quad (34-10)$$

The values of  $C_d$  and  $C_q$  as functions of  $\alpha = b_p / \tau$  are shown in Fig. 34-9.  $M_a$  is given by Eq. 32-1.

Thus, contrary to the cylindrical rotor machine, where the armature mmf with the amplitude  $M_a$  is considered in total, this mmf must be split into two mmf's with the amplitudes  $M_{ad}$  and  $M_{aq}$  for the consideration of the salient-pole machine (Refs. E1, E4, E6, E8).



## Chapter 35

### PHASOR DIAGRAMS OF THE GENERATOR AND MOTOR WITH SALIENT POLES · ARMATURE REACTION · GENERATOR CHARACTERISTICS

**35-1. Phasor diagrams of the generator and motor with salient poles. Armature reaction.** First the unsaturated machine will be treated.

(a) *Machine unsaturated.* The direct-axis armature mmf  $M_{ad}$  is proportional to  $I_a \sin \psi$ ; the quadrature-axis armature mmf  $M_{aq}$  is proportional to  $I_a \cos \psi$ . The first mmf produces a flux in the direct axis; the second mmf produces a flux in the quadrature. As a consequence, the two fluxes are proportional to, and in phase with,  $I_a \sin \psi$  and  $I_a \cos \psi$  respectively. The emf's induced by the two fluxes in the armature winding are  $-jx_{ad}I_a \sin \psi$  and  $-jx_{aq}I_a \cos \psi$ . The first of these emf's is similar to that which appears in the unsaturated machine with cylindrical rotor (see Eq. 32-2). As in the case of the latter machine,  $x_{ad}$  is the *armature reaction reactance in the direct axis*. Accordingly,  $x_{aq}$  in the second emf,  $-jx_{aq}I_a \cos \psi$ , is the *armature reaction reactance in the quadrature axis*.

Compared with the cylindrical rotor machine,  $x_{ad}$  has the same significance in both kinds of machine and  $x_{aq}$  appears only in the salient-pole machine. Furthermore, two emf's are to be considered in the armature winding of the salient-pole machine, one perpendicular to  $I_a \sin \psi$  and the other perpendicular to  $I_a \cos \psi$ , while only the one emf, perpendicular to  $I_a$ , is to be considered in the armature winding of the cylindrical rotor machine.

As has been explained (Art. 31-2),  $x_{ad}$  is due to a flux the path of which is the same as that of the field winding, i.e., *along* the field poles, and  $x_{aq}$  is due to a flux which goes *across* the main poles; both of these fluxes do not take into account the leakage fluxes of the armature winding.

Thus, in accordance with method (a) of Art. 31-3, the following mmf's, fluxes, and emf's induced by the fluxes in the armature winding are to be considered (see Art. 32-1a):

<i>MMF's</i>	<i>Fluxes</i>	<i>Induced EMF's</i>
Field (rotor) mmf ( $M_f$ )	$\Phi_f$	$E_f$
Armature mmf in the direct axis ( $M_{ad}$ )	$\Phi_{ad}$	$-jI_a x_{ad} \sin \psi$

Armature mmf in the quadrature axis

$$(M_{aq}) \quad \Phi_{aq} \quad -jI_a x_{aq} \cos \psi$$

MMF of the armature leakage flux (const.

$$\times I_a) \quad \Phi_l \quad -jI_a x_l$$

and, therefore, Kirchhoff's mesh equation for generator operation is (see Eq. 32-4)

$$\dot{V} + \dot{I}_a r_a + j\dot{I}_a x_l + jx_{aq}\dot{I}_a \cos \psi + jx_{ad}\dot{I}_a \sin \psi = \dot{E}_f \quad (35-1)$$

or

$$\dot{V} = \dot{E}_f - \dot{I}_a(r_a + jx_l) - j\dot{I}_a(x_{ad} \sin \psi + x_{aq} \cos \psi)$$

and that for motor operation (see Eq. 32-5)

$$\dot{V} = -\dot{E}_f + \dot{I}_a r_a + j\dot{I}_a x_l + jx_{aq}\dot{I}_a \cos \psi + jx_{ad}\dot{I}_a \sin \psi \quad (35-2)$$

Fig. 35-1 shows the phasor diagram of an unsaturated salient-pole generator for lagging current. The phasors  $V = OA$ ,  $I_a r_a = AB$  and  $BC = I_a x_l$  are drawn in the same manner as before (see, for example Fig. 32-1). Then the phasors  $CD = x_{aq} I_a \cos \psi$  and  $DF = x_{ad} I_a \sin \psi$  are drawn. Since, according to Kirchhoff's mesh law, the phasor row  $OAB CDF$  must be balanced by the emf induced in the armature by the field flux, i.e.,  $OF$  is equal to  $E_f$ ,  $E_f$  lies  $90^\circ$  behind  $M_f$ . Fig. 35-2 shows the phasor diagram of an unsaturated salient-pole motor for a leading current.

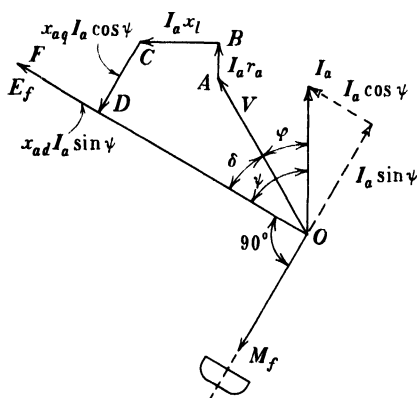


FIG. 35-1. Phasor diagram of an unsaturated, salient-pole generator loaded with lagging current.

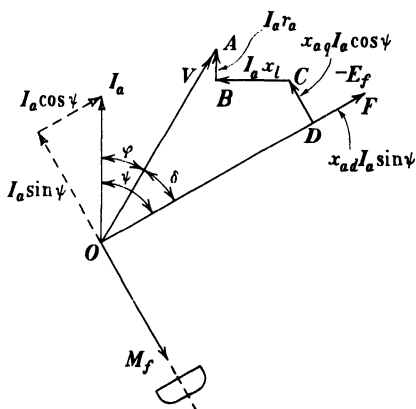


FIG. 35-2. Phasor diagram of an unsaturated, salient-pole motor carrying leading current.

It will be observed from diagrams Fig. 35-1 and 35-2 that a lagging current in a generator opposes the field mmf and also that a leading current in a motor opposes the field mmf. This is the same as in the machine with a cylindrical rotor. In general, the *rules of armature reaction* derived for the cylindrical rotor machine *apply also to the machine with salient poles*.

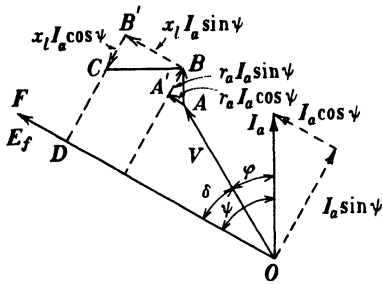


FIG. 35-3. Auxiliary diagram to Fig. 35-4.

The phasor diagrams, Figs. 35-1 and 35-2 can be represented in a somewhat different form. The phasors  $AB = I_a r_a$  and  $BC = I_a x_l$  can each be resolved into two components (Fig. 35-3) so that  $AA' = I_a r_a \cos \psi$ ,  $A'B = I_a r_a \sin \psi$ ,  $BB' = I_a x_l \sin \psi$ , and  $B'C = I_a x_l \cos \psi$ . This changes Kirchhoff's equation 35-1 to

$$\begin{aligned} \dot{V} + \dot{I}_a r_a \cos \psi + \dot{I}_a r_a \sin \psi + j \dot{I}_a x_l \sin \psi \\ + j \dot{I}_a x_l \cos \psi + j \dot{I}_a x_{aq} \cos \psi + j \dot{I}_a x_{ad} \sin \psi \\ = \dot{E}_f, \end{aligned} \quad (35-3)$$

Further introducing the abbreviations  $I_a x_l \cos \psi + I_a x_{aq} \cos \psi = I_a x_q \cos \psi$ ,  $I_a x_l \sin \psi + I_a x_{ad} \sin \psi = I_a x_d \sin \psi$ ,  $I_a \cos \psi = I_q$ , and  $I_a \sin \psi = I_d$ , simplifies Eq. (35-3) to

$$\dot{V} + \dot{I}_d r_a + \dot{I}_q r_a + j \dot{I}_q x_q + j \dot{I}_d x_d = \dot{E}_f, \quad (35-4)$$

and the phasor diagram (Fig. 35-1) for the generator with lagging current becomes as shown in Fig. 35-4.  $x_d = x_l + x_{ad}$  is the *direct-axis synchronous reactance* (see Eq. 32-6), and

$$x_q = x_l + x_{aq} \quad (35-5)$$

is the *quadrature-axis synchronous reactance*.

In constructing the phasor diagrams (Figs. 35-1 to 35-4), it has been tacitly assumed that the angle  $\psi$  between  $I_a$  and  $E_f$  is known. Otherwise it would not be possible to resolve  $I_a$  into the components  $I_a \sin \psi$  and  $I_a \cos \psi$ . The following artifice can be used to find the angle  $\psi$  while constructing the diagram.

In Fig. 35-5 which refers to a generator with lagging current, the phasor  $DC = I_a x_{aq} \cos \psi$  is the emf induced in the stator winding by the cross-flux of the machine, the axis of which is the quadrature axis. Since the path of the cross-flux is unsaturated, the emf  $CD = I_a x_{aq} \cos \psi$  can be found from the lower part of the no-load characteristic (air-gap line) as the emf corresponding to the mmf  $M_f = M_{aq} = C_q M_a \cos \psi$  (Eq. 34-8). If the line  $CB = I_a x_l$  (Fig. 35-5) is extended until it intersects the line in which  $E_f$  lies, the distance  $CC'$  is equal to  $CD / \cos \psi$ . This emf ( $= I_a x_{aq}$ ) is independent of the angle  $\psi$  and can be found just as the emf  $CD$  from the lower part of the no-load characteristic; it is the emf which corresponds to the mmf  $M_{aq} / \cos \psi = C_q M_a$

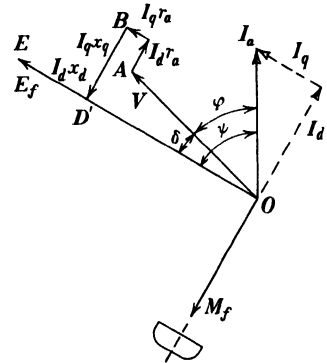


FIG. 35-4. Phasor diagram of an unsaturated, salient-pole generator loaded with lagging current on the basis of the synchronous reactances.

(Fig. 35-6). Hence the angle  $\psi$  can be found in the following way: Draw the phasor row  $OABC$ ; determine, from the no-load characteristic, the emf which corresponds to the mmf  $C_a M_a$ , i.e., the emf  $CC' = I_a x_{aq}$ ; extend  $BC$  by the distance  $CC' = I_a x_{aq}$ ; the line which connects the origin  $O$  with the point  $C'$  coincides with  $E_f$ , and makes the angle  $\psi$  with  $I_a$ .

(b) *Machine saturated.* When the machine is saturated, only *one* flux is to be considered in the direct axis, namely, the flux produced by the resultant of the mmf's  $M_f$  and  $M_{ad}$ . Thus, in accordance with method (b) of Art. 31-3, the following mmf's, fluxes, and emf's induced by the fluxes in the armature winding are to be considered (see Art. 32-1b):

MMF's	Fluxes	Induced EMF's
Resultant of $\dot{M}_f + \dot{M}_{ad}(\dot{M}_r)$	$\Phi_d$	$E_d$
Armature mmf in the quadrature axis ( $M_{aq}$ )	$\Phi_{aq}$	$-jI_a x_{aq} \cos \psi$
MMF of the armature leakage flux (const. $\times I_a$ )	$\Phi_l$	$-jI_a x_l$

Kirchhoff's mesh equation for generator operation is in this case (see Eq. 35-1)

$$\dot{V} + \dot{I}_a r_a + j\dot{I}_a x_l + jx_{aq}\dot{I}_a \cos \psi = \dot{E}_d \quad (35-6)$$

and for motor operation (see Eq. 35-2)

$$\dot{V} = -\dot{E}_d + \dot{I}_a r_a + j\dot{I}_a x_l + jx_{aq}\dot{I}_a \cos \psi \quad (35-7)$$

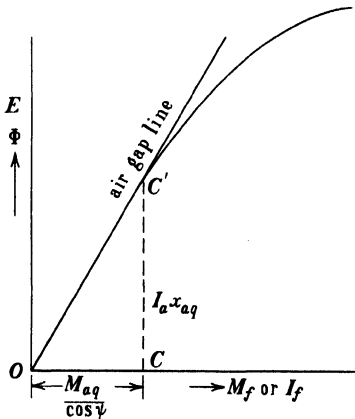


FIG. 35-6. Determination of the angle  $\psi$ .

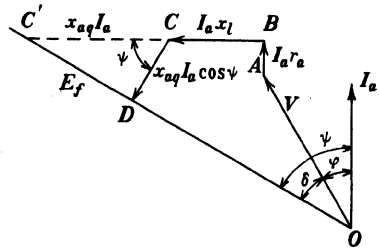


FIG. 35-5. Determination of the angle  $\psi$ .

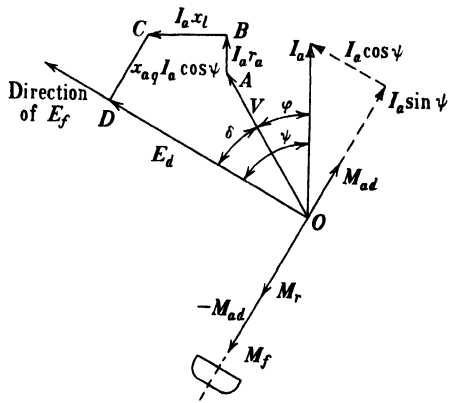


FIG. 35-7. Phasor diagram of a saturated, salient-pole generator loaded with lagging current.



is a quantity peculiar only to the salient-pole machine. When  $x_d$  and  $x_l$  are known, then

$$x_{ad} = x_d - x_l$$

$x_{aq}$  is the armature reaction reactance in the quadrature axis;  $x_{ad}$  is that in the direct axis. The ratio of  $x_{aq}$  and  $x_{ad}$  is the same as the ratio of the armature flux in the quadrature axis and the armature flux in the direct axis, both produced by *unit current* flowing in the armature winding. Since the ratio of fluxes is the same as that of their mmf's the ratio of  $x_{aq}$  and  $x_{ad}$  must be the same as that of  $M_{aq}$  and  $M_{ad}$  at unit current ( $I_a \cos \psi = 1$ ,  $I_a \sin \psi = 1$ ), i.e.,

$$\frac{x_{aq}}{x_{ad}} = \frac{C_q}{C_d} \quad (35-8)$$

from which equation  $x_{aq}$  and also  $x_q = x_l + x_{aq}$  can be determined. It can be seen that  $x_{aq}$  is much smaller than  $x_{ad}$  and therefore  $x_q$  is also much smaller than  $x_d$ .

The following *empirical* method of determining  $x_q$  for a given value of  $x_d$  is recommended by the AIEE

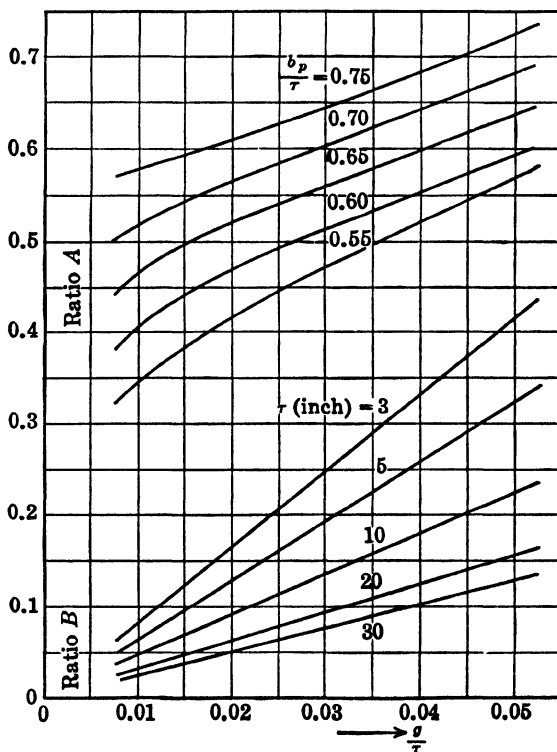


FIG. 35-9. Determination of the synchronous reactance in the quadrature axis ( $x_q$ ) of the salient pole machine by the AIEE empirical method.

$$x_q = x_d \frac{(x_{aq}/x_{ad}) + (x_l/x_{ad})}{1 + (x_l/x_{ad})} = x_d \frac{A + B}{1 + B} \quad (35-9)$$

The ratios  $A$  and  $B$  are given in Fig. 35-9 as functions of the ratio of pole arc to pole pitch  $b_p/\tau$ , of the ratio of air-gap in center of the pole to pole pitch  $g/\tau$ , and of the pole pitch  $\tau$ .

The definition of the *voltage regulation* and the methods for determining its magnitude are the same for the salient-pole machine as for the cylindrical rotor machine. Thus the AIEE method described in Art. 33-2 can also be applied to the salient-pole machine.

**Example 35-1.** Fig. 35-10 is the no-load and gap characteristic for a 20-kva, 60-cycle, 3-phase, 440-volt, Y-connected, 6-pole, salient-pole synchronous generator. Each field pole has 400 turns. The armature is a single-circuit winding, with 72 slots and 8 series conductors per slot, coil pitch 10 slots. The armature resistance  $r_a = 0.13$  ohm, the leakage reactance  $x_l = 0.23$  ohm, and the ratio of pole arc to pole pitch  $b_p/\tau = 0.7$ .

From the armature winding data, the coil pitch is  $\frac{5}{6}$  and  $k_p = 0.966$ ,  $k_d = 0.958$ ,  $k_{dp} = 0.925$ ,  $I_a = 20,000/(440 \times 1.73) = 26.3$  rated armature current.  $C_d = 0.84$  and  $C_q = 0.46$  correspond to  $b_p/\tau = 0.7$ . From Eq. 15-11:

$$M_a = \frac{0.9mN_a I_a k_{dp}}{6} = \frac{0.9 \times 3 \times 96 \times 26.3 \times 0.925}{6} = 1050 \text{ AT per pole}$$

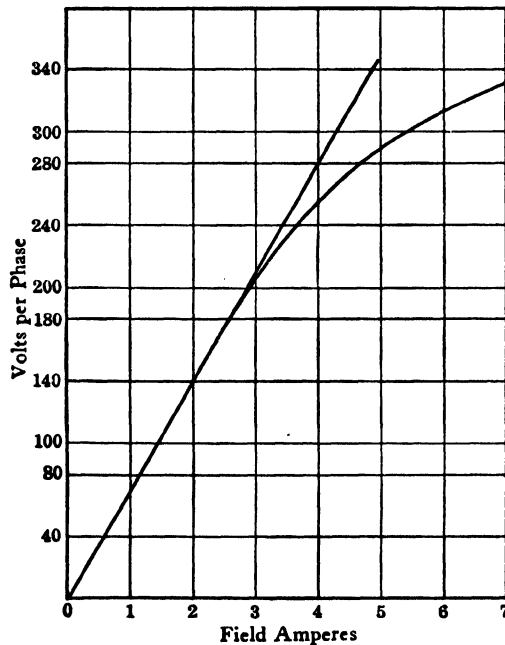


FIG. 35-10.

$M_a = 1050/400 = 2.63$  in terms of field current.  $C_q M_a = 0.46 \times 2.63 = 1.21$ . Fig. 35-5 is now constructed for  $\cos \varphi = 0.8$  lagging current.  $OA = 254$  volts,  $AB = 26.3 \times 0.13 = 3.42$  volts,  $BC = 26.3 \times 0.23 = 6.05$  volts. From Figs. 35-6 and 35-10 with  $OC = C_q M_a = 1.21$ ,  $CC' = x_{aq} I_a = 84$ . This is  $CC'$  in Fig. 35-5. From the latter

$$\tan \psi = \frac{V \sin \varphi + I_a x_l + I_a x_{aq}}{V \cos \varphi + I_a r_a} = \frac{254 \times 0.6 + 6.05 + 84}{254 \times 0.8 + 3.42} = 1.17, \psi = 49.6^\circ$$

$$\cos \psi = 0.648, \sin \psi = 0.761, \psi - \varphi = 12.7^\circ$$

$$\begin{aligned} E_d &= V \cos(\psi - \varphi) + I_a r_a \cos \psi + I_a x_l \sin \psi \\ &= 254 \times 0.975 + 3.42 \times 0.648 + 6.05 \times 0.761 = 254.6 \text{ volts} \end{aligned}$$

From Fig. 35-10,  $I_f$  required for  $E_d = 255$  is 4.05 amp. To this must be added  $M_{ad} = M_a C_d \sin \psi = 1050 \times 0.84 \times 0.761 = 671$  AT or  $671/400 = 1.68$  field amp to overcome  $M_{ad}$ . Hence the field current required is  $4.05 + 1.68 = 5.73$  amp. This value of  $I_f$  produces a no-load voltage of 310. The regulation is  $\epsilon = (310 - 254)/254 = 0.22$  at 0.8 power factor lagging. The characteristic reactances may be determined from the data as follows:  $M_a = 2.63$  in terms of field current for the rated current, 23.6 amp. For this same current  $I_a x_l = 26.3 \times 0.23 = 6.05$  volts. With  $I_a x_l$  and  $M_{ad} = C_d M_a$  the Potier triangle may be drawn in Fig. 35-10. The short-circuit characteristic can now be determined (see Fig. 31-2) with  $mn = M_{ad}$  and  $ml = I_a x_l$ . The no-load characteristic and short-circuit characteristic yield the unsaturated SCR = 1.593. The value for  $x_d$  is therefore 0.628. The unit impedance is  $254/26.3 = 9.66$  ohms and the leakage reactance in p-u =  $0.23/9.66 = 0.0238$ . Hence  $x_{ad} = x_d - x_l = 0.628 - 0.0238 = 0.604$ . From this  $x_{aq} = 0.604 \times 0.46/0.84 = 0.331$ . Therefore  $x_q = x_{aq} + x_l = 0.331 + 0.0238 = 0.355$  p-u.

**Example 35-2.** The synchronous reactances in both axes will be determined for the following generator:

Output: 875 kva,  $\cos \varphi = 0.80$ , 3 phases, 60 cycles, 24 poles, 2300 volts,  $I_a = 220$  amp.

Stator winding: 180 slots, 6 conductors per slot, coil pitch 6 slot pitches, pole pitch  $\tau = 9.52$  in., width of the pole arc  $b_p = 6.0$  in., no-load mmf at 2300 volts  $M_{f0} = 3610$  AT per pole and  $M_{f0g} = 2930$  AT per pole for the gap only. The leakage reactance is 0.826 ohm per phase. For the ratio  $b_p/\tau = 6.0/9.52 = 0.63$ ,  $C_d = 0.86$ ,  $C_q = 0.41$ . The number of slots per pole per phase  $q = 180/(3 \times 24) = 2.5$ ,\*  $k_d = 0.955$ .  $k_p = \sin [(6/7.5) \times \pi/2] = 0.951$ ,  $k_{dp} = 0.908$ . The number of turns per phase

$$N_a = \frac{6 \times 180}{2 \times 3} = 180$$

The total armature mmf in the direct axis at  $\psi = 90^\circ$  (short circuit) is

$$M_{ad} = 0.9 \times 3 \times \frac{180}{24} \times 0.908 \times 220 \times 0.86 = 3480 \text{ AT per pole}$$

From the data given, the air-gap line  $OG$  in Fig. 35-11 may be drawn. Construct the Potier triangle with  $lm = I_a x_l = 220 \times 0.826 = 182$  volts and  $mn = 3480$  AT. To

\* In this example, the value of  $q$  is 2.5. Such a winding is classified as a fractional slot winding and was not considered in Chapters 13 or 14 of this text. Equation 14-4 for the distribution factor does not apply to this kind of winding.



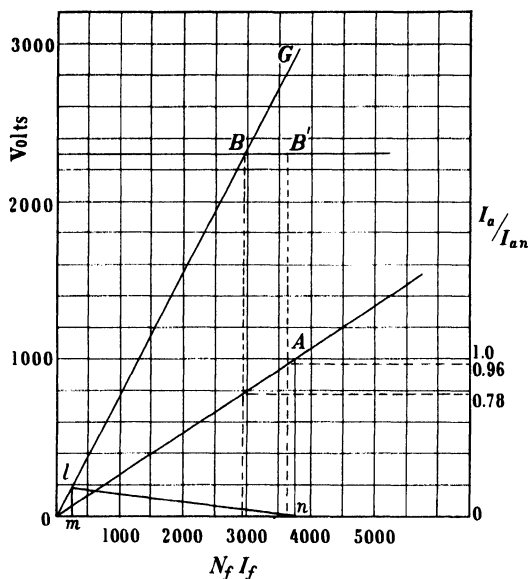


FIG. 35-11.

point  $n$  (3730 AT) corresponds unit armature current ( $nA$ ) on the short-circuit characteristic—draw this latter characteristic as  $OA$ . Corresponding to  $M_{f_{0a}} = 2930$  and  $M_{f_0} = 3610$  (points  $B$  and  $B'$  respectively) the unsaturated SCR may be determined as 0.78. Hence (in p.u.):

$$\begin{aligned}
 x_d &= \frac{1}{0.78} = 1.28 \\
 x_l &= 0.137 \\
 x_{ad} &= 1.28 - 0.137 = 1.14 \\
 x_{aq} &= 1.14 \times \frac{0.41}{0.86} = 0.543 \\
 x_q &= x_l + x_{aq} = 0.137 + 0.543 = 0.680
 \end{aligned}$$

## PROBLEMS

1. Determine the voltage regulation of the machine of Example 35-1, at unity power factor and at 0.8 power factor leading. Draw the voltage and mmf diagram to scale.

2. Determine the synchronous reactances in both axes for the following generator:

Output: 16,500 kva,  $\cos \varphi = 0.85$ , 3 phases, 60 cycles, 52 poles, 6600 volts,  $I_a = 1442$  amp.

Stator winding: 312 slots, 2 conductors per slot, coil pitch = 5 slot pitches, pole pitch = 11.55 in., pole arc = 8.5 in., no-load mmf at 6600 volts  $M_{f_0} = 6380$  AT per pole, and  $M_{f_{0a}} = 5730$  AT per pole for the gap only. Leakage reactance of the armature winding (in p.u.) = 0.187.  $C_d = 0.84$  and  $C_q = 0.48$ , corresponding to  $b_p/\tau = 0.736$ .

3. The no-load characteristic of the machine of Problem 2 is as follows, the voltage being per-phase:

AT per pole:	3020	4500	5520	6380	7080	8350
Volts:	2000	3000	3500	3810	4000	4250

Determine (a) field ampere-turns required per pole to produce rated armature current on short circuit; (b) the saturated SCR; (c) the voltage regulation at unity, 0.80 lagging, and 0.80 leading power factors. ( $r_a$  neglected.)

4. A 3-phase, 15-kva, 220-volt, Y-connected, 6-pole synchronous generator with salient poles has  $r_a = 0.10$  ohm per phase. The no-load characteristic is

$V$ (per phase):	37	70	98.4	109.3	123	142	156	166	174	181	187
$I_f$ (amp):	1.0	2.0	3.5	3.0	4.0	5.0	6	7	8	9	10

The full-load zero-power-factor characteristic is

$V$ :	0	62	88.5	109	127	132
$I_f$ :	4.05	6.35	7.43	8.5	9.7	10

The short-circuit characteristic is

$I_f$ :	2.1	4.05	6.17
$I_a$ :	20	40	60

The ratio of  $x_d$  to  $x_q$  was found to be 1.21. Construct the Potier triangle and determine  $x_l$ , and the value of  $M_a$  expressed in terms of field amperes.

5. Determine the voltage regulation of the machine of Problem 4 at unity power factor and at 0.8 power factor, leading and lagging current.

6. Determine  $x_d$  and  $x_q$  for the machine of Problem 4.

7. The following data apply to a 72-pole, 16,667-kva, 100-rpm, 13.8-kv, Y-connected, waterwheel synchronous generator:  $x_d = 0.895$ ,  $x_q = 0.62$ ,  $x_l = 0.240$  in p-u. The armature reaction  $M_a$  expressed in terms of field amperes is 135. Determine  $x_{aa}$  and  $x_{ad}$  and express all the characteristic reactances in both ohms and per-unit. Determine the value of field current required to circulate rated current in the short-circuited armature, and the SCR (unsaturated).  $I_f = 80$  amp for  $E = 3600$  v.

8. The no-load characteristic for the machine of Problem 7 is

$V$ :	2000	3600	6300	7800	8900	9550	10,000
$I_f$ :	45	80	150	200	250	300	350

The voltage is per-phase. From the data given determine the values  $BC$ ,  $CC'$  and the angles  $\psi$  and  $\delta$  of Fig. 35-5. From  $CC'$  and the no-load characteristic determine  $M_a C_q$ , and then  $C_d$  and  $C_q$ . ( $\cos \varphi = 0.8$  lagging, neglect  $r_a$ .)

9. From the data determined in Problem 8 determine the voltage regulation of the machine, at unity and at 0.8 lagging and leading power factor. Use method described in Example 35-1.

10. Repeat Problem 9, using the AIEE method, and compare results.

11. A 6000-kva, 2400-volt, 3-phase, 60-cycle, 40-pole, salient-pole generator has a resistance of 0.006 ohm per phase and is wye-connected. The characteristic curves are:

$I_f$ (amp):	25	50	75	100	125	150	175	200	255
$V$ (terminal):	690	1330	1900	2320	2600	2770	2900	3020	3160

*Full-load zero power factor*

$I_f$ (amp):	100	125	150	175	200	225	250	275	300	325
$V$ (terminal):	0	650	1170	1580	1890	2090	2240	2350	2450	2520

*Short circuit*

$I_f$ (amp):	0	50	100	150
$I_a$ (amp):	0	720	1450	2160

Construct the Potier triangle and determine  $x_l$  (in ohms and p-u) and  $M_a$  in equivalent field amperes.

12. Determine the voltage regulation for power factors of unity, 0.80 lagging, and 0.80 leading for Problem 11.

13. Determine the SCR,  $x_d$ , and  $x_q$  for the machine of Problem 11.  $C_d = 0.84$  and  $C_q = 0.50$ .

14. A 750-kva, 2400-volt, 3-phase, 60-cycle, 52-pole, salient-pole generator has an armature resistance of 0.15 ohm per phase and is wye-connected. The characteristic curves are:

*No-load*

$I_f$ (amp):	10	20	30	40	50	60	70	80	100	120	140
$V$ (terminal):	470	930	1400	1830	2150	2420	2600	2750	2960	3150	3300

*Full-load zero power factor*

$I_f$ (amp):	70	80	90	100	110	120	140	160	200
$V$ (terminal):	0	550	920	1200	1500	1740	2130	2350	2700

*Short circuit*

$I_f$ (amp):	0	31	62	93
$I_a$ (amp):	0	100	200	300

Construct the Potier triangle and determine  $x_l$  (in ohms and p-u) and  $M_a$  in equivalent field amperes.

15. Determine the voltage regulation for power factors of unity, 0.80 lagging and 0.80 leading for the machine of Problem 14.

16. Determine the SCR,  $x_d$ , and  $x_q$  for the machine of Problem 14.  $C_d = 0.85$ ,  $C_q = 0.45$ .

## Chapter 36

### TORQUE AND POWER RELATIONS SYNCHRONIZING GENERATORS

**36-1. Torque and power relations.** Fig. 36-1a shows the power balance of the synchronous generator. The iron losses ( $P_{h+e}$ ) necessary to sustain the main flux are supplied mechanically by the rotor. The total power input ( $P_{\text{inp,shaft}}$ ) is then consumed by the sum of  $P_{h+e}$ , the rotational iron losses ( $P_{\text{ir,rot}}$ ), the friction and windage losses ( $P_{F+W}$ ), and the electromagnetic power supplied to the stator ( $P_{\text{rot,f}}$ ). A small part of the latter power is consumed by the stator as  $I^2R$  losses, and the balance ( $mVI_a \cos \varphi$ ) goes to the line. The copper losses of the field winding do not appear in the power balance of Fig. 36-1a because they are supplied by a d-c source of power. Fig. 36-1b shows the power balance of the synchronous motor.

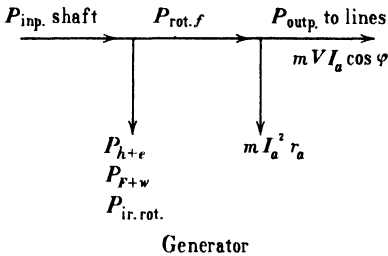


FIG. 36-1a. Power balance of a synchronous generator.

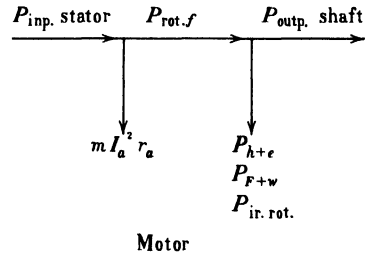


FIG. 36-1b. Power balance of a synchronous motor.

As in all other electric machines, the electromagnetic power ( $P_{\text{rot,f}}$ ) is equal to (see Eqs. 1-33 and 19-15)

$$P_{\text{rot,f}} = mEI \cos \psi \text{ watts} \quad (36-1)$$

The electromagnetic torque is

$$T = \frac{7.04}{n_s} P_{\text{rot,f}} \text{ lb-ft} \quad (36-2)$$

Phasor diagram Fig. 35-4, which refers to an unsaturated salient-pole generator, will be used in order to transform Eq. 36-1 for the electromagnetic

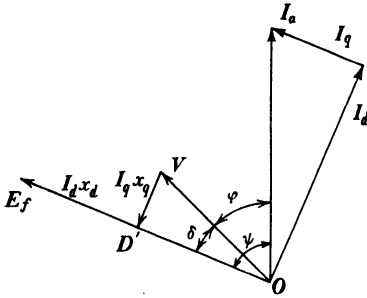


FIG. 36-2. Phasor diagram of an unsaturated, salient-pole generator loaded with lagging current ( $r_a$  assumed zero).

power ( $I_a^2 r_a$  will be neglected). The result obtained also holds with satisfactory accuracy for the saturated machine. The electromagnetic power of the machine with a cylindrical rotor will appear as a special case of the machine with salient poles.

With  $I_a r_a$  neglected, the phasor diagram of Fig. 35-4 becomes as shown in Fig. 36-2. Furthermore, it follows from Figs. 36-1a and 36-1b that for  $r_a = 0$

$$P_{\text{rot.f}} = m V I_a \cos \varphi \quad (36-3)$$

It can be seen from Fig. 36-2 that

$$I_a \cos \varphi = I_d \sin (\psi - \varphi) + I_q \cos (\psi - \varphi) = I_d \sin \delta + I_q \cos \delta$$

$$V \sin \delta = I_q x_q; \quad I_q = \frac{V \sin \delta}{x_q}; \quad V \cos \delta = E_f - I_d x_d$$

$$I_d = \frac{E_f - V \cos \delta}{x_d}$$

Inserting the equations for  $I_a \cos \varphi$ ,  $I_q$ , and  $I_d$  in Eq. 36-3 the equation for the electromagnetic power becomes

$$P_{\text{rot.f}} = m \frac{V E_f}{x_d} \sin \delta + m V^2 \frac{x_d - x_q}{2 x_d x_q} \sin 2\delta \quad (36-4)$$

In the cylindrical rotor machine  $x_d = x_q$  since there are no interpolar spaces. Thus for the cylindrical rotor machine

$$P_{\text{rot.f}} = m \frac{V E_f}{x_d} \sin \delta \quad (36-5)$$

It has been mentioned that the angle  $\delta$  between  $V$  and  $E_f$  is the basic variable of the synchronous machine. It can be seen from Eqs. 36-4 and 36-5 that for constant field current, i.e., for constant  $E_f$ , the electromagnetic power and torque (Eq. 36-2) of the synchronous machine depend solely upon the angle  $\delta$ .

Fig. 36-3 is the torque-angle characteristic of the cylindrical rotor machine. The angle  $\delta$  is arbitrarily assumed positive for generator operation and negative for motor operation. The characteristic is a sinusoidal curve, and maximum torque occurs at  $\delta = \pm 90^\circ$ .

Considering Eq. 36-4 for the salient-pole machine, it is seen that the saliency ( $x_d \neq x_q$ ) appears in the second term which is a function of  $\sin 2\delta$ . Fig. 36-4 shows both terms of the torque of the salient-pole machine, each separately, as well as the total torque as a function of  $\delta$ . Maximum torque occurs at an angle smaller than  $90^\circ$  for both generator and motor.

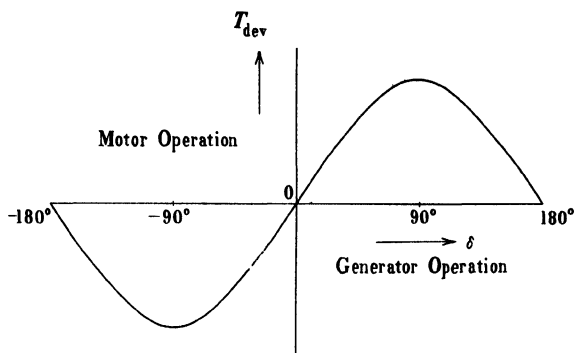


FIG. 36-3. Torque angle characteristic of a cylindrical rotor machine.

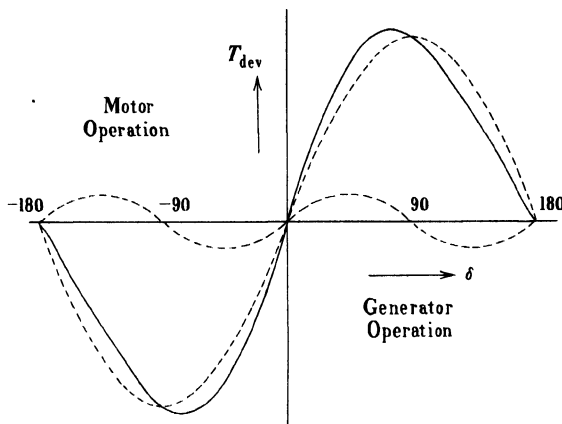


FIG. 36-4. Torque angle characteristic of a salient-pole machine.

An examination of Eqs. 36-4 and 36-5 shows that, when the field current is zero ( $E_f = 0$ ), the torque of the cylindrical rotor-machine is zero while that of the salient-pole machine is not zero but has a definite value. The latter machine is able to produce a torque without field excitation and this torque depends upon the difference between the reluctances in both axes ( $x_d - x_q$ ). Synchronous motors without field windings are used for certain applications as small units; they are called *reluctance motors* (see Art. 42-1).

**36-2. Synchronizing of synchronous generators.** Synchronizing a synchronous generator means connecting the generator to an existing line which has a terminal voltage  $V$  in such a manner that no inrush of current takes place.

As in the case of the d-c generator, several conditions must be fulfilled in order to avoid an inrush of current.

1. The terminal voltage of the incoming machine must be equal to the line voltage  $V$ .

2. Both voltages must be in phase.

3. The frequency of both voltages must be the same.

The first condition means that the voltage of the incoming machine must be exactly equal to the line voltage. If the terminal voltage of the incoming machine is greater or less than the line voltage, a current surge results upon the connection of the new machine, which subsequently causes circulating current through the armature winding of the machine, the bus-bars, and the other generators feeding the line.

The second condition, both voltages in phase, means that at the moment of connection the terminal voltage of the incoming machine and the line voltage must act in opposition to each other in the closed circuit consisting of the incoming machine, the bus-bars, and the other generators. If both voltages are not in phase at the moment of connection, the resulting voltage difference produces a surge of current which, in case of large phase displacements, can damage the machine windings.

The in-phase condition between the line voltage and the voltage of the incoming machine and also the third condition of equal frequencies can be

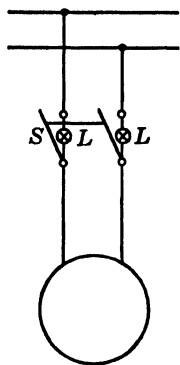


FIG. 36-5. Synchronizing a generator by means of lamps.

determined by means of lamps. Fig. 36-5 shows the arrangement of the lamps for an incoming single-phase machine. The double-pole switch  $S$  is bridged by two lamps  $L$ . If the voltages are equal and in phase, the lamps remain dark. However, if the voltages are equal but the line frequency and the frequency of the incoming machine are not the same, the lamps remain dark for only a short time, then brighten, and later become dark again. The flashing of the lamps occurs in a periodic sequence, and the frequency of fluctuation is an indication of the difference in frequency between the incoming machine and the line. The frequency of the incoming machine must be adjusted so that the flashing of the lamps takes place very slowly, and the switch  $S$  must be closed at the moment when the lamps are dark. For a 3-phase machine, three lamps are connected to a 3-pole switch in the same manner as for the single-phase machine. Instruments called synchroscopes are available for an accurate indication of synchronism. (See end of Chap. 37 for Problems to this Chapter.)

## Chapter 37

### PARALLEL OPERATION OF SYNCHRONOUS GENERATORS

**37-1. Parallel operation of synchronous generators.** Since qualitative rather than quantitative results are important in the consideration of machines operating in parallel, the cylindrical rotor machine, as the simpler of the two types, will be considered. Furthermore, it will be assumed that the saturation of the magnetic path is low and that the armature resistance is zero. Under these simplified conditions the phasor diagram of a generator with lagging current is shown in Fig. 37-1 (see also Fig. 32-1).

It has been shown in the foregoing article that the angle  $\delta$  between the phasors  $V$  and  $E_f$  is a measure of the power developed by the machine. Consider a synchronous generator connected to a line with a constant voltage  $V$ , at no-load. Since  $\delta = 0$  corresponds to the no-load condition, the phasors  $E_f$  and  $V$  in the phasor diagram of Fig. 37-1 must coincide. It will be assumed that the field current is adjusted in such a manner that  $E_f = V$ . The phasor diagram which corresponds to the no-load condition with  $E_f = V$  is shown in Fig. 37-2. Also according to Kirchhoff's mesh law, Eq. 32-2, the armature current  $I_a$  must be zero because  $E_f = V$ . Now let the regulator of the prime mover (for example, a turbine) be influenced in such a manner that the prime mover receives added input (more steam) and seeks to drive the generator at an increased speed. Since the rpm of the synchronous

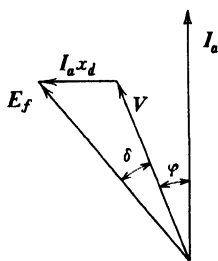


FIG. 37-1. Simplified phasor diagram of a cylindrical rotor generator loaded with lagging current.

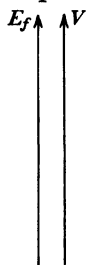


FIG. 37-2. Phasor diagram for no-load and  $E_f = V$ .

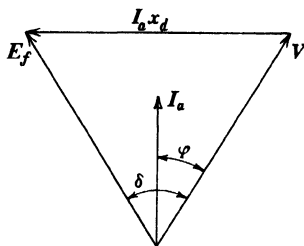


FIG. 37-3. Phasor diagram showing relative position of  $E_f$  and  $V$  of Fig. 37-2 after the input to the prime mover has been increased.



machine is fixed by its number of poles and the line frequency (see Eq. 1-9), the increased input will result in an advance of the pole structure, i.e., considering the phasor diagram of Fig. 37-2, the phasor  $E_f$  will be moved ahead of the line voltage  $V$  to a new angle  $\delta$  (Fig. 37-3) which corresponds to the power input. Since  $E_f \neq V$ , a current  $I_a$  will flow in the armature winding of a magnitude determined by Eq. 32-2, i.e.,  $(E_f - V) = jI_a x_a$ . It follows from Fig. 37-3 that the phase displacement between the current  $I_a$  and the terminal voltage  $V$  is relatively small. This leads to the important statement that the *forward advance of the phasor  $E_f$  (of the pole structure) forces the generator to deliver a current  $I_a$  to the line which is nearly in phase with  $V$ , and which therefore yields an active power output.* ( $\delta$  exaggerated in Fig. 37-3.)

Thus, if the output of a synchronous generator which is operating in parallel with other generators is to be increased, its prime mover must be momentarily accelerated by supplying it with more power (for example, more steam) and, vice versa, if the output is to be reduced, the prime mover must be decelerated by reducing its input. This is entirely different from the operations necessary to change the load of a d-c generator or an induction generator: a change of the field current is necessary in order to change the load of a d-c generator, and a change of the speed (of the slip) of the rotor is necessary to change the load of an induction generator (see Art. 20-2).

Consider again Fig. 37-2 which represents the phasor diagram of a generator at no-load with its field current adjusted in such a manner that  $E_f = V$ . No change will be made in the power input of the prime mover so that the angle  $\delta$  will remain equal to zero. However, a change will be made in the field current, i.e., in  $E_f$ . First let the field current be increased so that  $E_f > V$ , as shown in Fig. 37-4a. According to Kirchhoff's mesh law, Eq. 32-2,  $jI_a x_a$  must then be in phase with  $V$ , i.e., the generator current  $I_a$  must lag  $V$  by  $90^\circ$ . Thus an increase of field current forces the generator to carry a lagging reactive current. If the field current is decreased so that  $E_f$  becomes smaller than  $V$ , as shown in Fig. 37-4b,  $jI_a x_a$  is opposite to  $V$  and the generator is forced to carry a leading reactive current.

The character of the armature current for an increase or decrease of the field current, obtained from the phasor diagrams of Figs. 37-4a and 37-4b, can also be derived from the rules of armature reaction (see Art. 32-1). If a generator or motor is connected to a line with a constant voltage  $V$ , the flux of the machine and therefore its field current are fixed by the load and the voltage  $V$ . If the field current is increased at no-load (as considered in Fig. 37-4) above this fixed value, a generator will react by delivering a lagging current to the line, because in a generator a lagging current opposes the field mmf. If, on the other hand, the field current is decreased below this fixed value, a generator will react by delivering a leading current to the line, because in a generator a leading current supports the field mmf.

The same consideration applies to any load. If the field current of a

generator operating in parallel with other generators at a fixed terminal voltage is increased, the reactive current of the generator will be increased and, vice versa, if the field current is decreased, the reactive current will be decreased. The generator may be even forced to carry a leading current, if the reduction of the field current exceeds a certain value. This will be explained below by an example.

It follows from these considerations that a *variation of the field current*, at fixed load and voltage, *will force the generator to vary its reactive current*.

Care must be taken that generators operating in parallel are loaded in proportion to their ratings. This applies to the active as well as to the reactive current of each generator, i.e., not only the armature current but also the field current must be properly determined and fixed.

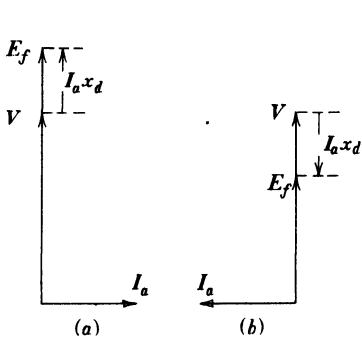


FIG. 37-4. Influence of change in field current (excitation) on behavior of a synchronous generator.

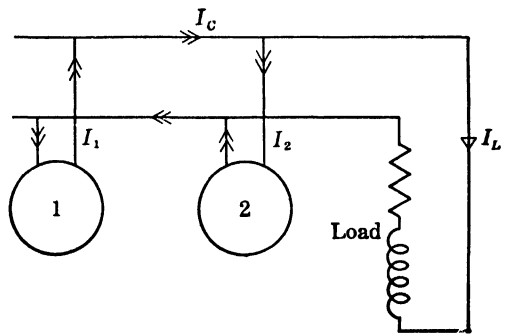


FIG. 37-5. Circulating current between two generators in parallel.

**Example 37-1.** An arrangement consisting of two identical generators and an inductive load (Fig. 37-5) will be considered. If the field currents of both machines are equal and if the load is equally divided between them, then their vector diagrams will be identical:  $I_1 = I_2$ ,  $E_{f1} = E_{f2}$ ,  $\varphi_1 = \varphi_2$ , and  $\delta_1 = \delta_2$  (Fig. 37-6a). The excitation of machine 1 now will be increased and the excitation of machine 2 decreased in such a manner that the terminal voltage remains unchanged; also, the total power output is to be the same and is to be equally divided between both machines. The condition of voltage balance then demands that machine 1 which now is overexcited shall deliver a larger lagging current, and that machine 2 which is underexcited deliver a smaller lagging current. Fig. 37-6a shows the phasor diagram of both machines for this condition of operation. The armature current of each of the two machines, prior to the change of their field currents, was  $OB$  with the active component equal to  $OA$  and the reactive component equal to  $AB$ . The load current is equal to  $OD$ . The emf's induced by the field currents were  $E_{f1} = E_{f2}$ . After the change of the field currents without changing the power (active current) of each of the machines, the armature current of machine 1 becomes equal to  $OP$  and that of machine 2 equal to  $OQ$ . The emf's induced by the field currents become

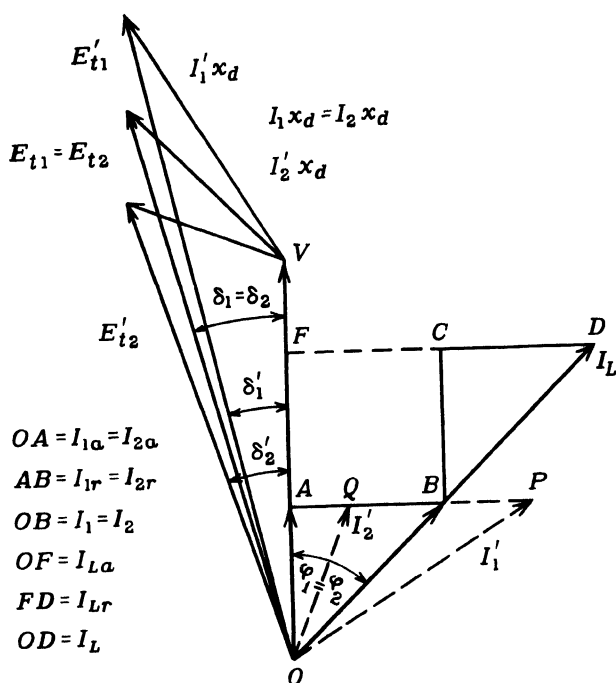


FIG. 37-6a. Influence of change in excitation on two generators in parallel.

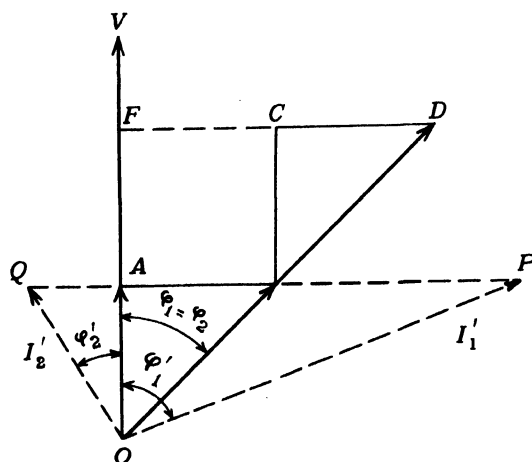


FIG. 37-6b. Influence of change in excitation on two generators in parallel.

$E_{f1}'$  and  $E_{f2}'$ . The angles between the terminal voltage  $V$  and the emf's  $E_{f1} = E_{f2}$  were  $\delta_1 = \delta_2$  before the change of the field currents. After the change they become  $\delta_1'$  and  $\delta_2'$ , i.e., the angle  $\delta$  becomes smaller ( $\delta_1'$ ) for machine 1 and larger ( $\delta_2'$ ) for machine 2. This is in accordance with the requirement that the active power of each machine remains constant (see Eq. 36-5).

Now it will be assumed that, under the same conditions as before (constant terminal voltage and constant active power of each machine), the field current of machine 1 is changed to such an amount that its armature current becomes equal to  $OP$  (Fig. 37-6b), i.e., the reactive current supplied by machine 1 ( $AP$ ) is larger than the reactive current required by the load ( $FD$ ). In order that the terminal voltage remain constant, machine 2 must be underexcited to such a degree that it carries leading current (current  $AQ$ ). Since the load is inductive, the leading current of machine 2 does not appear in the external circuit (load circuit). It flows as an internal or *circulating* current in the armature windings of both machines and in the connecting bus-bars only. Fig. 37-5 shows the direction of the circulating current in both machines at a given instant of time. It is the same in both machines but oppositely directed.

**Example 37-2.** Consider again two identical machines, connected to a unity power-factor load, and initially adjusted to deliver equal currents  $I_1 = I_2$  (Fig. 37-7) at terminal voltage  $V$  and at  $\delta_1 = \delta_2$ . The synchronous impedance drop in each is shown as  $AB$  (resistance neglected). Assume now that the terminal voltages and load power are to remain constant, and that the input power to machine 1

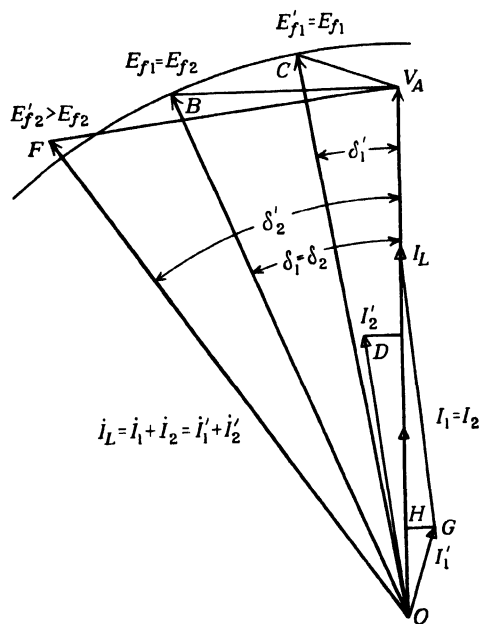


FIG. 37-7. Influence of the change in power input on two generators in parallel.

is reduced, without changing its excitation. As a result, the angle  $\delta_1$  is reduced to  $\delta_1'$ , and the impedance drop becomes  $AC$  as shown in Fig. 37-7. The armature current in machine 1 therefore becomes  $I_1'$ . Note that  $AB/AC = I_1/I_1'$ , and that a lagging current now appears in machine 1. Since the load voltage  $V$  and current  $I_L$  are assumed constant, changes must occur in 2, to offset the changes in 1. The current in 2 now must become greater, and equal to  $I_2' = OD$  such that the vector sum  $I_1' + I_2' = I_L$ . The impedance drop in 2 shown as  $AF$ , drawn perpendicular to  $I_2'$ , therefore is increased in the ratio  $AF/AB = I_2'/I_2$ , thus requiring the voltage  $E_{f2}'$  and the new angle  $\delta_2'$  as shown in Fig. 37-7. Note that more power must be applied to 2, and also that its field current must be increased to accomplish these changes. A circulating current  $GH$  also is now present, which increases the total copper loss. The conclusion can be drawn that identical machines should deliver equal currents and operate at power factors the same as that of the common load.

Circulating currents are undesirable currents because they produce larger  $I^2R$  losses within the machines than are necessary for a given load. Such currents are recognized by the difference in the power factors of the machines operating in parallel. If the machines are identical and the power is equally divided, circulating currents can be recognized by the difference in the armature currents (also by the difference in the field currents).

## PROBLEMS

(Consider all machines unsaturated. Unit current = rated current for generators and =  $I_{HP}$  for motors.)

1. A 1500-HP, 6600-volt, 3-phase, 60-cycle, 6-pole cylindrical-rotor synchronous motor has a rated armature current of 136 amp, and an armature reactance  $x_a = 0.95$  p-u. Neglecting the resistance and assuming the input power to remain constant at 1000 kw, determine the angle  $\delta$  for values of  $E_f = 1.15, 1.20, 1.25, 1.30$  (p-u) volts respectively. Determine the power  $P_{\text{rot.f}}$  in each case.

2. For each value of  $E_f$  and the angle  $\delta$ , determined in Problem 1, calculate (a) the line current, (b) power factor of the motor. Determine the value of  $E_f$  and  $\delta$  to produce a motor power factor of unity.

3. Since  $t_a$  is neglected, the limiting value of  $\delta$  is  $90^\circ$ . For an input of 1000 kw, determine the value of  $E_f$  when  $\delta = 90^\circ$ .

4. Repeat Problem 1 for inputs of 1200 kw and for 500 kw.

5. Repeat Problem 2 for inputs of 1200 kw and for 500 kw.

6. If the motor of Problem 1 is constructed with a salient-pole rotor having an armature resistance of 0.01 p-u,  $x_d = 0.90$  p-u, and  $x_q = 0.65$  p-u, determine the power  $P_{\text{rot.f}}$  for the same  $\delta$  angles calculated using the corresponding values of  $E_f$ . Compare your results with Problem 1. Neglect resistance.

7. Two identical synchronous generators operate in parallel delivering power to a 40,000-kw load at 0.866 power factor lagging and rated terminal voltage. The machines are Y-connected and each is rated 30,000 kva, 13.2 kv and has  $x_d = 0.775$  in p-u. They are adjusted so that each is delivering its proper share of the load, and each operates at the same power factor. Determine for each machine (a) kva; (b) kw; (c) kvars; (d) the voltage  $E_f$  (per phase); (e) the angle  $\delta$ ; (f) the angle  $\psi$ , neglecting  $r_a$ . A combined graphical and analytical solution is suggested for these problems on parallel operation.

8. The excitation of one machine of Problem 7 is increased so that  $E_f = 14,000$  volts per phase, while the terminal voltage, the total load, and the power of each machine remain constant. Determine (a) the power factor of each machine; (b) the current of each machine; (c) the voltage  $E_f$  of the second machine; (d) the angle  $\delta$  for each machine; (e) the angle  $\psi$  for each machine; (f) the kva of each machine; (g) the kvars of each machine.

9. Two synchronous generators are rated as follows: machine 1, 30,000 kva, 13.2 kv,  $x_d = 0.775$  per-unit; machine 2, 12,250 kva, 13.2 kv,  $x_d = 1.0$  per-unit. They both are Y-connected and operate in parallel to deliver a total load of 36,000 kw at 0.866 power factor delivering current in proportion to their rating. Determine for each machine (a) the kw; (b) the kva; (c) the kvars; (d) the current; (e) the power factor; (f) the voltage  $E_f$ ; (g) the angle  $\delta$ .

## Chapter 38

### CIRCLE DIAGRAMS OF THE SYNCHRONOUS MACHINE · V-CURVES · SYNCHRONOUS CONDENSER · STARTING A SYNCHRONOUS MOTOR

As in the case of the induction motor the geometric locus of the stator current of the synchronous machine is a circle when the parameters ( $r_a$ ,  $x_l$ , and the main flux reactance) are constant quantities. Otherwise the geometric locus becomes a curve of higher order than the second order. Only the simplest case with constant parameters, namely, the *unsaturated* machine with constant reluctance around the stator bore, i.e., *with a cylindrical rotor*, will be considered.

**38-1. Circle diagrams for constant developed torque and variable field current.** Considering the synchronous motor, the power input per phase is (Fig. 36-1b)

$$P_{\text{inp, stator}} = VI_a \cos \varphi \text{ watts per phase} \quad (38-1)$$

and the electromagnetic power (the power of the rotating field),  $P_{\text{rot, f}}$ , which is proportional to the developed torque of the machine,

$$P_{\text{rot, f}} = VI_a \cos \varphi - I_a^2 r_a \text{ watts per phase} \quad (38-2)$$

Consider Fig. 38-1. Let  $OL$  be the current  $I_a$  which corresponds to a fixed torque at a fixed field current. Then with a point  $M_T$  on the axis of ordinates chosen so that

$$OM_T = \frac{V}{2r_a} \quad (38-3)$$

$$I_a^2 \sin^2 \varphi = R_T^2 - (\overline{OM_T} - I_a \cos \varphi)^2$$

or

$$VI_a \cos \varphi - I_a^2 r_a = \frac{V^2}{4r_a} - R_T^2 r_a \quad (38-4)$$

The left side of this equation is the power of the rotating field,  $P_{\text{rot, f}}$  (see Eq. 38-2). In order that this power, i.e., the torque, remain constant and

independent of the value of the field current, the quantity on the right side of Eq. 38-4 must also be a constant, i.e.,

$$\frac{V^2}{4r_a} - R_T^2 r_a = \text{constant} = P_{\text{rot},f} \quad (38-5)$$

Since  $V$  and  $r_a$  are constant quantities, the quantity  $R_T$  must also be a constant, if  $P_{\text{rot},f}$ , i.e., the torque, is to remain constant.

Since point  $L$  in Fig. 38-1 changes its position with the value of the field current, it follows that the geometric locus of the stator current for constant torque and variable field current is a circle with  $R_T$  as the radius and  $M_T$  as the center point, whereby  $OM_T = V/2r_a$ . To each value of the constant torque there corresponds another value of  $R_T$ , but the center point  $M_T$  is always the same for all constant-torque circles.

Solving Eq. 38-5 for the radius  $R_T$  at constant torque (constant  $P_{\text{rot},f}$ )

$$R_T = \sqrt{\frac{V^2}{4r_a^2} - \frac{P_{\text{rot},f}(\text{constant})}{r_a}} \quad (38-6)$$

This equation determines the radius of the circle, with  $M_T$  as a center point, which corresponds to the chosen constant value of torque ( $P_{\text{rot},f}$ ).

The radius  $R_T$  which corresponds to zero torque is

$$R_{T0} = \frac{V}{2r_a} \quad (38-7)$$

Since  $OM_T = V/2r_a$ , the zero-torque circle goes through the origin of the coordinates  $O$ . Fig. 38-2 shows several circles for different values of constant torque. The larger the torque, the smaller the radius (see Eq. 38-6). The influence of the variation of the field current shows up in the change of the active as well as of the reactive components of  $I_a$  at the same value of torque. The change in the active component is due to the change of the copper losses  $I_a^2 r_a$ . If these losses are assumed to be zero ( $r_a = 0$ ), then according to Eq. 38-2)

$$P_{\text{rot},f} = VI_a \cos \varphi \quad (38-8)$$

In order that the torque ( $P_{\text{rot},f}$ ) remain constant, the power input  $VI_a \cos \varphi$  must remain constant, i.e., the geometric locus of the primary current  $I_a$  for constant torque at variable field current ( $r_a = 0$ ) becomes a straight line as shown in Fig. 38-3. As to be expected from the rules of armature reaction (see Art. 32-1) the armature current becomes leading when the motor is overexcited, and lagging when the motor is underexcited.

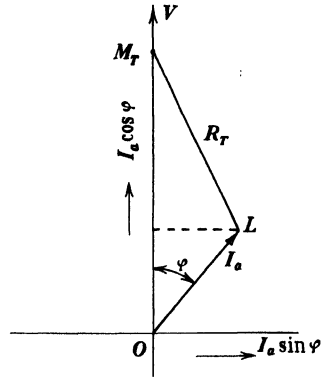


FIG. 38-1. Determination of the circle diagram for constant torque and variable field current.



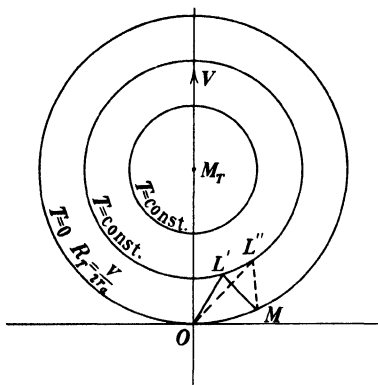


FIG. 38-2. Circle diagrams for constant torque and variable field current ( $r_a$  abnormally large).

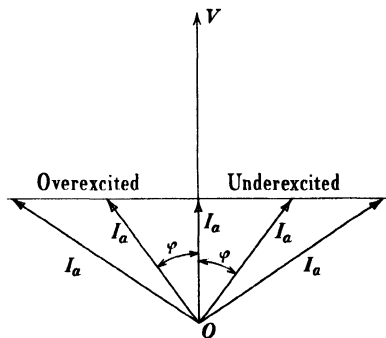


FIG. 38-3. Locus of stator current for constant torque and variable field current ( $r_a=0$ ,  $I_a \cos \varphi = \text{constant}$ ,  $T = \text{constant}$ ).

### 38-2. Circle diagrams for variable torque and constant field current.

The phasor diagram Fig. 38-4 refers to a motor operating with a lagging current (see Fig. 32-2);\* the voltage phasor  $V$  is placed in the vertical. The geometric sum of the voltage drops  $I_a r_a$  and  $j I_a x_d$  is designated as  $I_a z_d$ . This latter phasor is  $\psi_a$  degrees ahead of the current phasor  $I_a$  where

$$\tan \psi_a = \frac{x_d}{r_a} \quad (38-9)$$

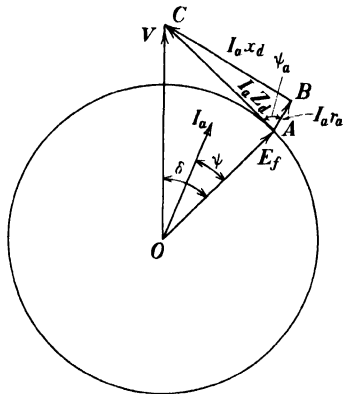


FIG. 38-4. Circle diagram of impedance drop  $I_a z_d$  for constant field current (see footnote on p. 312).

If the torque is varied at constant field current, the magnitude of the phasors  $V$  and  $E_f$  will not be changed, but the torque angle  $\delta$  (see Art. 36-1) will increase with increasing torque and decrease with decreasing torque. Therefore the phasor  $I_a z_d$  changes with changing angle  $\delta$ , and with it the armature current  $I_a$  also changes.

It can be seen from Fig. 38-4 that, when  $\delta$  varies, the end-point of  $E_f$  describes a circle

\* The phasor diagram of Fig. 38-4 refers to a motor, since  $V$  is ahead of  $E_f$ . However,  $E_f$  is shown with a plus sign and not with a minus sign (see Fig. 32-2). This is done in order that a single phasor diagram may be used for both generator and motor operation, in which the phasor  $V$  is common to both types of operation. Since  $V$  is a generated voltage in the case of a generator and an impressed voltage in the case of a motor, the phasors representing  $V$  are opposite in sign. Therefore, when  $V$  is represented by a single phasor for both motor and generator, the sign of  $-E_f$  must be reversed for motor action.

with the origin  $O$  as a center point. Since the end-point  $C$  of the terminal voltage phasor  $V$  is fixed, the end-point  $A$  of the phasor  $I_a z_d$  which coincides with the end-point of  $E_f$ , also moves on a circle. The minimum value of  $I_a z_d$  is

$$I_a z_{d(\min)} = V - E_f \quad (38-10)$$

and the maximum value of  $I_a z_d$  is

$$I_a z_{d(\max)} = V + E_f \quad (38-11)$$

The minimum and maximum values of  $I_a z_d$  lie in the *vertical*, coinciding with the direction of the voltage phasor  $V$ .

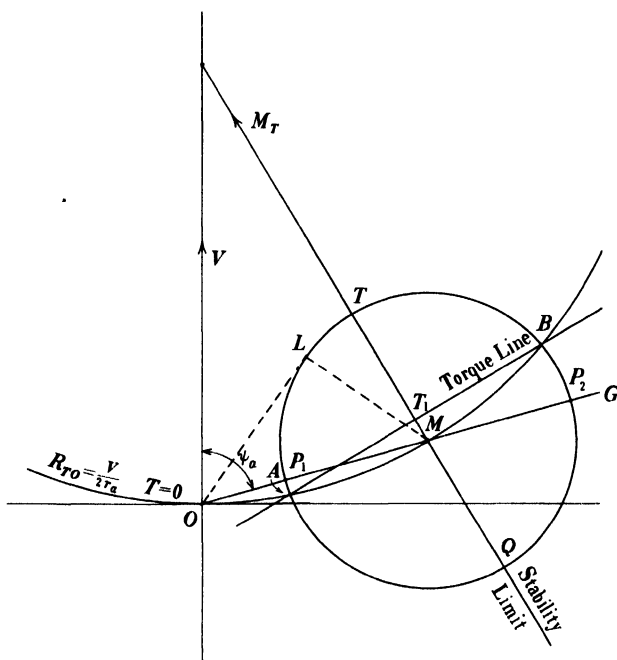


FIG. 38-5. Circle diagram for variable torque and constant field current.

If the end-point of the phasor  $I_a z_d$  moves on a circle, the same must be true of the end-point of the phasor  $I_a$  because  $z_d$  is a constant. The phasor  $I_a z_d$  is  $\psi_a$  degrees ahead of the phasor  $I_a$ . Therefore, the minimum and maximum values of  $I_a$  must lie  $\psi_a$  degrees behind the line on which the minimum and maximum values of  $I_a z_d$  lie, i.e.,  $\psi_a$  degrees behind the terminal voltage  $V$ . Thus, if a line  $OG$  is drawn which lies  $\psi_a$  degrees behind the voltage  $V$  (see Fig. 38-5),  $I_{a(\min)}$  and  $I_{a(\max)}$  lie on this line. The values of  $I_{a(\min)}$  and  $I_{a(\max)}$  are determined by Eqs. 38-10 and 38-11 as

$$I_{a(\min)} = \frac{V - E_f}{z_d}; \quad I_{a(\max)} = \frac{V + E_f}{z_d} \quad (38-12)$$

If, in Fig. 38-5,  $OP_1 = I_{a(\min)}$  and  $OP_2 = I_{a(\max)}$ , then  $P_1P_2$  is equal to the diameter of the circle on which the end-point of  $I_a$  moves, and the center point  $M$  of the circle lies midway between the points  $P_1$  and  $P_2$ . Thus the diameter of the circle is equal to

$$D = I_{a(\max)} - I_{a(\min)} = \frac{2E_f}{z_d} \quad (38-13)$$

and the distance from center  $M$  to the origin  $O$  is

$$OM = I_{a(\max)} - \frac{D}{2} = \frac{V}{z_d} \quad (38-14)$$

i.e., the diameter of the circle depends upon the magnitude of  $E_f$  and therefore upon the field current, while the position of the center of the circle depends upon the magnitude of the terminal voltage  $V$ . The diameter of the circle changes with the field current, but the center is the same for all circles. The diameter of the circle increases with increasing field current. When the field current is zero, the circle degenerates into a point, namely, the center  $M$  for which the torque is zero. Circle diagrams for variable developed torque for three different values of field current are shown in Fig. 38-7 ( $r_a = 0$ ).

In order to determine the *Torque-Line* in Fig. 38-5, two points must be found on the circle for which the torque is zero (see Art. 21-3). In Fig. 38-2, which represents circle diagrams for constant developed torque and *variable field current*, the zero-torque points lie on the circle  $T=0$ . This circle comprises all possible values of field current and therefore includes the field current for which the circle of Fig. 38-5 is drawn. Thus, if in Fig. 38-5 a circle is drawn with the radius  $R_{TO} = V/2r_a$  (Eq. 38-7) from a center  $M_T$  on the axis of ordinates and through the origin  $O$ , this circle will intersect the circle of variable torque in two points ( $A$  and  $B$  Fig. 38-5) for which the torque is zero; the line connecting these two points is the *Torque-Line*. The machine operates as a motor on the arc  $AB$  above the *Torque-Line* and as a generator on the arc  $AB$  below the *Torque-Line*. Since zero torque corresponds to the center  $M$ , this point must also lie on the  $T=0$  circle.

The distance from a point on the circle to the axis of abscissae is proportional to the power input (see Art. 21-3), and the distance from a point on the circle to the *Torque-Line* is proportional to the developed torque of the machine and also to the developed mechanical power of the machine ( $P_{\text{rot.f}}$ ) which includes the windage, friction, and iron losses.

Starting with the point  $A$  (Fig. 38-5), the torque rises and reaches its maximum value (*pull-out torque*)  $TT_1$  at point  $T$ . Beyond the point  $T$  the power input and the armature current increase, but the developed mechanical power and the torque decrease, because the copper losses increase at a greater rate than the power input. If the load torque plus the loss torque is greater than  $TT_1$ , the motor pulls out of step and comes to rest.

At point  $Q$ , which lies diametrically opposite  $T$ , the developed mechanical power of the machine as a generator reaches its maximum value  $T_1Q$ . If the power output from the prime mover is greater than  $T_1Q$  plus the losses, the prime mover runs away with the generator. The line  $TQ$  represents the *stability limits* of the machine as both a motor and a generator.

If the armature resistance  $r_a$  is neglected ( $r_a = 0$ ) in Fig. 38-5, then  $\psi_a = 90^\circ$ , and the points  $P_1$  and  $P_2$  lie on the axis of abscissae (Fig. 38-6). Therefore the center  $M$  of all circle diagrams for variable torque and constant field current lies on the axis of abscissa. Since, for  $r_a = 0$ , the radius of the  $T = 0$  circle ( $R_{T0}$ , Fig. 38-5, Eq. 38-7) becomes infinite, the geometric locus for  $T = 0$  becomes a straight line coinciding with the axis of abscissae. Thus, for  $r_a = 0$ , the Torque-Line as well as the power input line coincide with the axis of abscissae (Fig. 38-6).

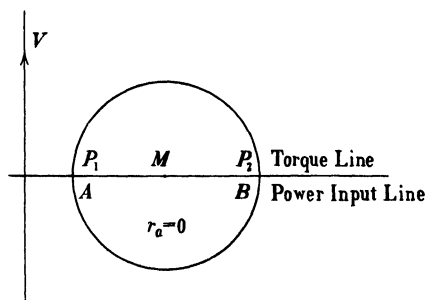


FIG. 38-6. Circle diagram for variable torque and constant field current ( $r_a = 0$ ).

A comparison between Figs. 38-5 and 38-6, which represent the geometric locus of the stator current of the synchronous machine for variable torque, and Figs. 21-3 and 21-5, which represent the geometric locus of the primary current of the stator of the induction machine for variable torque, shows the similarity of both current diagrams. In both cases the position of the center of the circle diagram depends upon the magnitude of the resistance of the stator winding. In both cases the center of the circle lies on the axis of abscissae and the Torque-Line coincides with the axis of abscissae if the resistance of the stator winding is neglected. However, there are differences between the two types of machines. The diameter of the circle of the induction machine is determined by the parameters ( $r$  and  $x$ ) of its stator and rotor winding and by the line voltage and does not vary when the line voltage is fixed. On the other hand, the diameter of the circle of the synchronous machine depends only upon the parameters of its stator winding and not upon the parameters of its rotor windings. This is due to the fact that at synchronous speed no emf's are induced in the rotor windings. Furthermore, the diameter of the current circle of the synchronous machine can be varied, at fixed line voltage, by varying the field current, i.e.,  $E_f$ .

**38-3. Influence of field current on overload capacity and power factor. V-curves of the synchronous motor. Synchronous capacitor.** Fig. 38-7 shows several circle diagrams for variable torque and constant field current with the armature resistance neglected. The larger diameter corresponds to the larger field current. Two statements with respect to the behavior of the synchronous motor can be made on the basis of Fig. 38-7. First, an increase

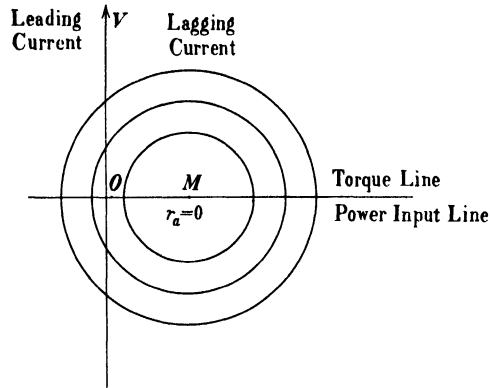


FIG. 38-7. Influence of excitation on overload capacity and power factor ( $r_a = 0$ ).

of the field current increases the pull-out torque, i.e., the ratio of pull-out torque to load torque (*the overload capacity*) increases with increasing field current. (Note that when the armature resistance is not neglected there is a limit to the overload capacity, which does not follow from Fig. 38-7). Second, at a fixed load the power factor of the motor can be changed over a wide range by changing the field current. At a certain value of field current the power factor is unity; decreasing the field current below this value makes the power factor lagging, while an increase makes it leading. Since the field current influences the overload capacity, certain limits are set for the power factor. The field current of the synchronous motor is usually adjusted in such a manner that the motor operates at rated load either with  $\cos \varphi = 1$  or with a leading power factor.

Consider Fig. 38-5. For a given motor the location of the center  $M$  is fixed by the angle  $\psi_a$ , i.e., by the parameters of the armature winding and by the terminal voltage, since  $OM = V/z_a$ . The current which corresponds to an arbitrary point  $L$  on the circle is  $I_a = OL$ . Then the distance  $LM$  must be equal to  $E_f/z_a$ . This can be seen by comparing Fig. 38-5 with Fig. 38-4. In the latter figure  $OC = V$ ,  $CA = I_a z_a$ , and  $AO = E_f$ . Dividing the sides of the triangle  $OCA$  by  $z_a$  a triangle with the sides  $V/z_a$ ,  $I_a$ , and  $E_f/z_a$  results. Since, in Fig. 38-5,  $MO = V/z_a$  and  $OL = I_a$ , the third side of the triangle  $MOL$ , namely  $LM$ , must be  $E_f/z_a$ . It follows from this that when a point of the plane, for example point  $L'$  in Fig. 38-2, is connected with the origin  $O$  and the center  $M$ , which is fixed for a given motor, the distance  $OL'$  represents a current  $I_a$  and the distance  $L'M$  the quantity  $E_f/z_a$ , both for the same field current; this is true because any point of the plane can be considered as belonging to a circle diagram for variable torque and constant field current. It should be noted (as previously stated in Art. 38-2) that the point  $M$  lies on the  $T = 0$  circle and corresponds to  $E_f = 0$ . In cylindrical rotor machines the torque developed is zero when  $E_f = 0$  (see Eq. 36-5).

If the center  $M$  in Fig. 38-5 is fixed for a given motor, then the points on a constant-torque circle (Fig. 38-2) yield currents  $I_a$  ( $OL'$ ,  $OL''$  ...), and the distances from the center  $M$  to these points on the circle yield the corresponding emf's ( $E_f' = L'M \times z_d$ ,  $E_f'' = L''M \times z_d$ ) and so forth. In this way the correlation between the armature currents  $I_a$  and the emf's  $E_f$  corresponding to the currents  $I_a$  can be found for any constant-torque circle. Fig. 38-8 shows  $I_a = f(E_f)$  for three different constant values of  $T$ . These curves have the shape of a V and are called the *V-curves* of the synchronous motor.

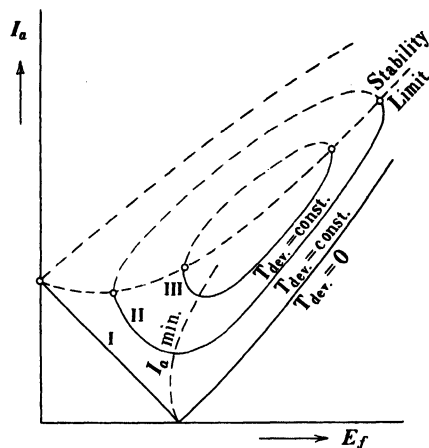


FIG. 38-8. V-curves of a synchronous motor.

Each constant torque circle (Fig. 38-2) has a *minimum* current at which the constant torque is produced: this is the lower intersection point of the circle with the axis of ordinates. The minimum currents for the different constant torque circles are connected in Fig. 38-8 by a dotted line: this minimum-current line is also the unity power factor line as can be seen from Fig. 38-2.

It has been explained previously that the magnitude of the pull-out torque depends upon the field current. For any constant torque  $T$  (Fig. 38-8) there is a field current at which this constant torque becomes equal to the pull-out torque: at this specific field current the stability limit is reached. The field currents (emf's  $E_f$ ) which determine the stability limits are also indicated in Fig. 38-8. At large values of torque  $T$  the stability limit approaches the unity power factor field current. A relatively small underexcitation in this case may cause the motor to fall out of step. It follows that the synchronous motor must be overexcited in the region of maximum output.

If a synchronous motor is overexcited, it is forced to draw a leading current from the line (see Art. 32-1 and Fig. 38-7). The synchronous motor then performs the function of a *static capacitor*, i.e., it compensates for the lagging reactive currents necessary to sustain the fluxes in induction motors and transformers and thus reduces the amount of lagging current to be supplied by the generators; as a result the generators can be made smaller, since they do not have to supply the total amount of lagging current demanded by the load. Overexcited synchronous motors operating at no-load are called *synchronous capacitors* and are used to compensate for lagging reactive currents in large transmission lines. They are built only in large units. Characteristics of unity and 0.8-power factor synchronous motors are shown in Fig. 49-17. Examples for the use of a synchronous motor to improve the over-all power factor of a plant are given in Art. 49-7.

**38-4. Starting of a synchronous motor.** It was pointed out in the treatment of the induction motor (see Art. 17-1) that a uniform torque can be developed only when the mmf waves of both stator and rotor are stationary with respect to each other. This condition is satisfied for the synchronous motor when it runs at synchronous speed; only at this speed the stator mmf and the rotor mmf have the same speed  $n_s = 120f/p$ .

Consider the synchronous motor at standstill. If, in order to start the motor, the stator is connected to the line, the stator mmf achieves synchronous speed immediately, while the rotor mmf is still at standstill. Therefore no starting torque is developed, and the motor will not come up to speed. The conditions are entirely different for the induction motor, because the rotor of this motor is not connected to a source of power but establishes its currents by induction from the stator. As has been explained (in Art. 17-2) the mmf waves of stator and rotor in this case are at standstill with respect to one another at *any* rotor speed, including standstill; therefore, the induction motor is capable of developing a starting torque.

In order to make it possible for a synchronous motor to start, it is supplied with a squirrel cage similar to that of the induction motor. For reasons which will become clear later (see Art. 40-4), the squirrel-cage winding is called the *dampers winding*. The damper bars are placed in slots punched in the pole shoes (see Figs. 30-6 and 30-8); they are connected on both sides of the pole shoes by segments which are joined together to make a ring connection on each side of the poles. The cage is not complete, since there are no bars in the interpolar spaces.

Just as in the squirrel-cage induction motor, the synchronous motor takes a relative large starting current from the lines. However, since the damper winding is to be used only for starting, and not for running as in the case of the induction motor, its resistance and leakage reactance can be freely adjusted to suit the required starting torque and starting current.

The rotating flux cannot induce an emf in the field winding at synchronous speed, because at this speed the flux is stationary with respect to the poles. However, it is quite different during the starting period when the speed of the field structure is less than that of the rotating flux; in this case a high emf is induced in the field winding which has a large number of turns, and this induced emf may lead to a breakdown of the insulation, if the field winding is left open during starting. In order to protect the field winding it is *closed* through a resistor during the starting period. This resistor is removed from the field circuit, and the d-c excitation is applied when the rotor reaches its maximum induction motor speed; the motor then falls into synchronism and runs as a synchronous motor. At synchronous speed the damper winding is ineffective.

The resistance inserted in the field circuit during starting is about 5 to 15 times the resistance of the field winding. Besides protecting this winding it also improves the starting performance of the motor at low slips. Typical

torque-speed and current characteristics of synchronous motors during starting are shown in Fig. 49-13.

When it is necessary to reduce the starting current of a synchronous motor, the same means can be employed as for the induction motor: part-winding starting, an autotransformer, or a reactor in series with the stator winding, is quite effective (see Art. 23-1).

### PROBLEMS

(Consider all machines unsaturated. Unit current =  $I_{HP}$ .)

1. A 700-HP, 6-pole, 3-phase, 60-cycle, 4000-volt (star-connected) synchronous motor has the following data at full-load:

Efficiency	= 93%
Field current	= 25.0 amp
Total iron loss	= 5.6 kw
Friction and windage loss	= 3.2 kw
Stray load loss	= 2.0 kw

Further:

$$r_a = 0.012 \text{ p-u}$$

$$x_l = 0.10 \text{ p-u}$$

$$x_{ad} = 1.08 \text{ p-u}$$

The air-gap line is determined by:

$$I_f = 13.5 \text{ amp} \quad E = 3080 \text{ volts (line-line)}$$

It can be assumed that the rotational iron losses are equal to 2.5 kw. Construct the circle diagram for rated field current and determine the stator current, power factor, and the ratio of pull-out torque to rated torque (developed values).

2. Construct, for the motor of Problem 1, several circle diagrams for constant developed torque and draw the V-curves of the motor.

3. Repeat Problem 1 for  $r_a = 0$ .

4. Repeat Problem 2 for  $r_a = 0$ .

5. A 250-HP, 26-pole, 3-phase, 60-cycle, 2200-volt (star-connected) synchronous motor has the following data at full-load:

Efficiency	= 91%
Field current	= 36 amp
Total iron loss	= 5.0 kw
Friction and windage loss	= 0.7 kw
Stray load loss	= 0.9 kw

Further:

$$r_a = 0.014 \text{ p-u}$$

$$x_l = 0.14 \text{ p-u}$$

$$x_{ad} = 0.74 \text{ p-u}$$

The air-gap line is determined by:

$$I_f = 23.5 \text{ amp} \quad E = 2100 \text{ volts}$$

It can be assumed that the rotational iron losses are equal to 2.5 kw.



Construct the circle diagram for rated field current and determine the stator current, power factor, and ratio of pull-out to rated torque (developed values).

6. Construct, for the motor of Problem 5, several circle diagrams for constant developed torque and draw the V-curves of the motor.

7. Repeat Problem 5 for  $r_a = 0$ .

8. Repeat Problem 6 for  $r_a = 0$ .

9. Repeat Problem 1 for  $I_f = 17$  and 35 amp and draw the curve

$$\frac{T_{\text{dev. p.o.}}}{T_{\text{dev. rated}}} \text{ vs. } I_f.$$

10. Repeat Problem 5 for  $I = 25$  and 43 amp and draw the curve

$$\frac{T_{\text{dev. p.o.}}}{T_{\text{dev. rated}}} \text{ vs. } I_f.$$

## Chapter 39

### EFFECT OF THE EMF HARMONICS

**39-1. Resultant emf.** It has been mentioned in Art. 14-3 that the flux distribution curve of the salient pole synchronous machine is not sinusoidal. When resolved into a Fourier series, it consists of a fundamental and harmonics (Fig. 14-4). It was shown there that the emf induced in the armature by the fundamental wave is (Eq. 14-9).

$$E_1 = 4.44 f_1 N k_{a p 1} \Phi \times 10^{-8} \text{ volt} \quad (39-1)$$

The subscript 1 indicates the fundamental (first harmonic). Accordingly, the magnitude of the  $n$ th harmonic emf is

$$E_n = 4.44 f_n N k_{a p n} \Phi_n \times 10^{-8} \text{ volt} \quad (39-2)$$

$f_n = n f_1$ , because the number of poles of the  $n$ th harmonic is  $n$  times that of the fundamental (Fig. 14-4) and the frequency of the induced emf is proportional to the number of poles (Eq. 1-9).  $k_{a n}$  and  $k_{p n}$  are given by Eqs. 24-11 and 24-12 with the order  $n$  introduced for the order  $\nu$ .

$\Phi_n$  is much smaller than  $\Phi_1$  for two reasons: (1) the amplitudes of the harmonics are much smaller than the amplitude of the fundamental; (2) the pole pitch of the  $n$ th harmonic is only  $1/n$ th part of the pole pitch of the fundamental.

In order to determine the effective value of the resultant emf, it is necessary to evaluate the square root of the average value of the instantaneous values squared taken over a period of the fundamental.

$$E = \sqrt{\frac{1}{2\tau} \int_0^{2\tau} e^2 dx} \quad (39-3)$$

This results in the equation:

$$E = \sqrt{E_1^2 + E_3^2 + E_5^2 + \dots} \quad (39-3a)$$

The effective value of the resultant emf therefore is equal to the square root of the sum of the squares of the effective values of the individual emfs.

Consider as an example a case in which the 3rd and 5th harmonics are much larger than commonly found in machines:

$$E_1 = 1 \quad E_3 = 0.1 \quad E_5 = 0.1.$$

The resultant effective value is:

$$E = \sqrt{1 + 0.01 + 0.01} = 1.01.$$

The harmonics have a negligible influence on the effective emf of the machine and it is permissible to consider only the fundamental of the flux distribution curve:

$$E = 4.44fNk_{ap1}\Phi_1 10^{-8} \quad (39-4)$$

Since it is tedious to determine the value of  $\Phi_1$ , it is customary to use the total flux  $\Phi$  in calculations; normally  $\Phi$  differs only slightly from  $\Phi_1$  so that

$$E = 4.44fNk_{ap1}\Phi 10^{-8} \text{ volts} \quad (39-5)$$

or

$$E = 4f_BfNk_{ap1}\Phi 10^{-8} \text{ volts} \quad (39-6)$$

in which, in order to increase the accuracy, the form factor  $f_B$  of the field distribution curve is introduced in place of the form factor of the fundamental 1.11.  $f_B$  is somewhat smaller than 1.11 and is usually known either from plotted or from experimentally determined field distribution curves.

**39-2. Effect of the 3rd harmonic.** Under some circumstances the 3rd harmonic can lead to difficulties in 3-phase machines. The emf's induced by the fundamental in the three phases of a 3-phase system are

$$\begin{aligned} e_1 &= \sqrt{2} E_1 \sin \omega t, \\ e_2 &= \sqrt{2} E_1 \sin (\omega t - 120^\circ), \\ e_3 &= \sqrt{2} E_1 \sin (\omega t - 240^\circ). \end{aligned} \quad (39-7)$$

The beginnings of phases 2 and 3 are displaced 120 and 240 electrical degrees respectively from the beginning of phase 1. For the third harmonic these displacement angles are  $3 \times 120^\circ$  and  $3 \times 240^\circ$  since the pole pitch for the 3rd harmonic is  $\frac{1}{3}$  of the pole pitch of the fundamental. Consequently, for the 3rd harmonic,

$$\begin{aligned} e_1 &= \sqrt{2} E_3 \sin 3\omega t, \\ e_2 &= \sqrt{2} E_3 \sin (3\omega t - 360^\circ) = \sqrt{2} E_3 \sin 3\omega t, \\ e_3 &= \sqrt{2} E_3 \sin (3\omega t - 720^\circ) = \sqrt{2} E_3 \sin 3\omega t. \end{aligned} \quad (39-8)$$

While the voltages induced in the 3 phases by the fundamental constitute a symmetrical 3-phase system, the voltages induced in these phases by the 3rd harmonic are *all in-phase* and therefore do not constitute a 3-phase system of voltages. With respect to the three winding groups these emf's of triple frequency are such that at each instant they are directed from the beginnings of all 3 phases to their ends or from the ends of all 3 phases to their beginnings.

The triple frequency emf's will not appear at the terminals of a 3-phase star-connected machine since they cancel one another in each 2 phases. This is entirely different for the delta-connected machine where the end of one phase is connected to the beginning of the next phase. Here the triple frequency emf's add up algebraically in the 3 phases, and the resultant emf is 3 times the emf of 1 phase. This produces a *circulating current* which flows through the series-connected phases. The circulating current is nearly independent of the load and under certain conditions can produce a considerable additional heating loss. For this reason the delta connection is avoided and the star connection of the winding groups is employed wherever possible.

**39-3. Time and space harmonics.** In the foregoing, the flux distribution curve produced by the field poles of a synchronous machine was considered with its fundamental wave as well as the harmonics. The latter have a *fixed* position with respect to the fundamental and travel with the same speed as the fundamental. Therefore, they induce harmonic emf's in the armature winding, the frequency of which is  $n$  times the frequency of the fundamental wave

$$e_n = \sqrt{2} E_n \sin n\omega t.$$

Harmonics of the emf curve or current curve are *time harmonics* in contrast to the harmonics of the mmf curve, considered in Art. 24-1, which are *space harmonics*. These latter harmonics are due to the arrangement of the winding and are produced by any single-phase or polyphase winding, even when the current which flows in the ac-winding is sinusoidal.

It has been stated in the foregoing that the harmonics of the flux distribution curve of the synchronous machine are fixed with respect to the fundamental, and travel with the same speed as the fundamental. It has been shown in Art. 24-1 that the space harmonics produced by a polyphase winding have no fixed position with respect to the fundamental wave and that they travel with different speeds, some in the same direction as the fundamental, some opposite to the fundamental.

**Example 39-4.** The flux distribution curve of a synchronous machine is represented at no-load by

$$B_x = 100 \sin \frac{x}{\tau} \pi - 14 \sin 3 \frac{x}{\tau} \pi - 20 \sin 5 \frac{x}{\tau} \pi + 1 \sin 7 \frac{x}{\tau} \pi.$$

Determine the emfs induced at no-load by the harmonics (as fractions of the fundamental).

Let  $\Phi_1 = 100$ . Then, since  $\frac{B_3}{B_1} = 0.14$  and  $\frac{\tau_3}{\tau_1} = \frac{1}{3}$ ,  $\Phi_3 = \frac{1}{3}$ ,  $\Phi_0 = \frac{1}{3} \times 14 = 4.67$ .

Accordingly

$$\Phi_5 = \frac{1}{5} \times 20 = 4, \quad \Phi_7 = \frac{1}{7} \times 1 = 0.143.$$

Further,  $f_1 = 60$ ,  $f_3 = 3 \times 60 = 180$ ,  $f_5 = 5 \times 60 = 300$ ,  $f_7 = 7 \times 60 = 420$ . The distribution factors are (see Eq. 24-11)

$$k_{d1} = +0.966, k_{d3} = +0.707, k_{d5} = +0.259, k_{d7} = -0.259,$$

and the pitch factors (Eq. 24-12)

$$k_{p1} = +0.966, k_{p3} = \sin 3 \times \frac{5}{6} \times 90 = -0.707, k_{p5} = \sin 5 \times \frac{5}{6} \times 90 = +0.259,$$

$$k_{p7} = \sin 7 \times \frac{5}{6} \times 90 = +0.259.$$

The ratios of the emf's are

$$\frac{E_3}{E_1} = \frac{\Phi_3}{\Phi_1} \cdot \frac{f_3}{f_1} \cdot \frac{k_{dp3}}{k_{dp1}} = \frac{4.67}{100} \times 3 \times \frac{0.707 \times 0.707}{0.934} = 0.075,$$

$$\frac{E_5}{E_1} = \frac{\Phi_5}{\Phi_1} \cdot \frac{f_5}{f_1} \cdot \frac{k_{dp5}}{k_{dp1}} = \frac{4}{100} \times 5 \times \frac{0.259 \times 0.259}{0.934} = 0.01435,$$

$$\frac{E_7}{E_1} = \frac{0.143}{100} \times 7 \times \frac{0.259 \times 0.259}{0.934} = 0.00072.$$

## PROBLEMS

1. Determine for the machine of Example 1 the ratios of the emf's at no-load for full-pitch winding.

2. A 24-pole 60-cycle 3-phase synchronous generator has the following data: voltage 2300 volts,  $q = 2.5$  slots per pole per phase, 18 conductors per slot, connection 3 parallel stars,  $k_{d1} = 0.957$ , throw 80%. Determine the no-load flux per pole. What is the line voltage of the generator if the connection is changed to 2 parallel  $\Delta$ ?

3. The armature of a 3-phase 60-cycle alternator has 12 slots per pole. The winding is 2-layer with 4 turns per coil, the pitch is  $\frac{5}{6}$ , and the flux per pole is  $1.2 \times 10^6$  maxwells, distributed according to the equation  $B_x = B_1 \sin x - 0.2B_1 \sin 5x$ , where  $x$  is expressed in electrical degrees. Determine: (a) effective value of the fundamental voltage per phase per pair of poles; (b) effective value of the 5th harmonic voltage per phase per pair of poles; (c) resultant phase voltage per pair of poles.\*

4. The total flux per pole in a 3-phase 60-cycle alternator is 1.3 million maxwells, distributed according to the equation  $B_x = B_1 \sin x - 0.3B_1 \sin 3x$ , where  $x$  is expressed in elec. deg. The winding is 2-layer with 12 conductors per slot, the pitch being  $\frac{5}{6}$ , and there are 9 slots per pole. Determine: (a) flux per pole due to the fundamental; (b) flux per pole due to the 3rd harmonic; (c) voltage per pair of poles due to the fundamental, the 3rd harmonic, and the resultant. If the windings are Y-connected, what is the ratio of the line voltage to phase voltage?\*

5. The flux per pole in a 6-pole 3-phase Y-connected alternator is 1.4 million maxwells. The machine has 90 slots, the coil pitch is 12 slots, the winding is 2-layer: with 4 conductors per slot. The equation for the flux distribution in the gap is  $B_x = B_1 \sin x + 0.3B_1 \sin 3x$ , where  $x$  is expressed in elec. deg. Determine the voltage

\*  $x = 0$  is at the middle of the interpolar space.

per phase and the line voltage due to the fundamental and to the 3rd harmonic in the flux.\*

6. A generator has 6 identical coil groups, displaced 30 electrical degrees apart, each circuit being rated at 220 volts and 100 amp. Determine the kva rating of the machine when all the coils are used to make (a) 6-phase; (b) 3-phase; (c) 2-phase; (d) single-phase. Determine the single-phase rating if only 4 coil groups are used.

$x = 0$  is at the middle of the interpolar space.

## Chapter 40

### HUNTING OF A SYNCHRONOUS MACHINE

**40-1. The synchronizing torque.** Consider a synchronous motor under load with a voltage diagram for  $r_a = 0$  as shown in Fig. 40-1. The pole structure assumes a position such that the emf phasor  $E_f$  lags the terminal voltage  $V$  by an angle  $\delta$ , the magnitude of which is fixed by the load. As is seen from Fig. 40-1, the simplest case, i.e., the unsaturated machine with cylindrical rotor, is being considered again.

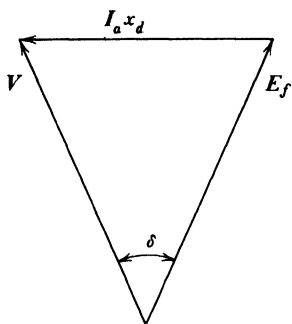


FIG. 40-1. Phasor diagram of a synchronous motor with cylindrical rotor ( $r_a = 0$ ). See footnote on p. 312.

Now assume that the load on the motor shaft is suddenly dropped. Then the angle  $\delta$  must become zero, i.e., the pole structure has to move forward by the angle  $\delta$ . This cannot happen suddenly because of the mass of the rotor (flywheel effect of the rotor). Consequently, in spite of the loss of the load, the armature current will not become zero at once, and the torque produced by this current, which previously served to overcome the load torque, will now accelerate the pole structure.

When the pole structure reaches the zero position ( $\delta = 0$ ), its kinetic energy will cause it to swing ahead of this position. The emf  $E_f$  now leads the terminal voltage  $V$ , and the machine operates as a generator. However, since generator operation cannot continue due to the lack of a prime mover, the angle  $\delta$  must again become zero, and the action repeats itself. The entire sequence of events can be observed on the ammeters and wattmeters.

This kind of oscillation is similar to that of a flywheel (sometimes called a balance wheel) and a torsion spring. If the spring is under tension when the flywheel is at rest, and the flywheel is then released, the force of the spring seeks to bring it first to the zero position. However, since the wheel is accelerated by the force of the spring during the entire travel to the zero position, maximum velocity occurs at  $\delta = 0$  and, therefore, the wheel swings beyond this zero position. The spring is now twisted in the opposite direction. The position of rest (end position) is again reached when the kinetic energy of the flywheel has been converted into the potential energy of the spring. The

action starts again and continues until the original energy stored in the spring is absorbed by the frictional losses of the system.

The fact that the output of a synchronous machine depends upon the position of its pole structure, and that every change in the position of the poles (angle  $\delta$ , Fig. 40-1) involves a corresponding change in the output, causes the synchronous machine to act as an oscillating system. The change in output (or torque), produced by twisting the pole structure through a unit angle, may be compared to the change in the force of the spring in the mechanical system consisting of flywheel and spring, when the flywheel is twisted through a unit angle.

The *change in the torque per unit angle* is called the *synchronizing torque* of the synchronous machine. Therefore, this is the torque with which the pole structure is restored to its mid-position when it is twisted ahead of or behind this position by a unit angle.

The power of the rotating flux of an  $m$ -phase synchronous machine with cylindrical rotor is given by Eq. 36-5 (resistance neglected):

$$P_{\text{rot},f} = m \frac{E_f V}{x_d} \sin \delta \quad (40-1)$$

The torque corresponding to this power is:

$$T = \frac{7.04}{n_s} m \frac{E_f V}{x_d} \sin \delta \quad (40-2)$$

and consequently the synchronizing torque is:

$$T_s = \frac{dT}{d\delta} = \frac{7.04}{n_s} m \frac{E_f V}{x_d} \cos \delta \quad \text{lb-ft/rad} \quad (40-3)$$

Eq. 36-4 yields for the synchronizing torque of the salient-pole machine

$$T_s = \frac{7.04}{n_s} m \left[ \frac{E_f V}{x_d} \cos \delta + V^2 \frac{(x_d - x_q)}{x_d x_q} \cos 2\delta \right] \quad \text{lb-ft/rad} \quad (40-3a)$$

In a manner similar to that of suddenly dropping the entire load on a synchronous motor, every sudden change in load of a synchronous motor or generator produces oscillations. The frequency of these oscillations depends solely upon the magnitude of the synchronizing torque and upon the magnitude of the flywheel mass to be accelerated and decelerated. Since an applied force is absent, the *system oscillates freely at its natural frequency*. These are the same oscillations which the mechanical system, consisting of flywheel and spring, executes when the flywheel is twisted and the system is then allowed to oscillate freely. The directive force of the spring and the mass of the wheel are the factors which determine the frequency of oscillation. Here, as in the synchronous machine, damping has only a negligible influence on the frequency of oscillation.



Of greater importance than the natural oscillations are the *forced oscillations* which appear in the synchronous machine when the prime mover torque of a generator is irregular, as in a gas engine, or when the load torque of a motor is irregular, as in a compressor.

If, in the foregoing example of spring and flywheel, a force is applied which has the same period as that of flywheel and spring, then the amplitude of the oscillations becomes greater and greater; the amplitude would become infinitely great if no damping were present. The magnitude of the imparted torque is of no consequence whatever; the smallest torque suffices to produce violent oscillations. A similar condition appears, although the amplitude of the oscillations does not become as great, when the period of the applied force is not exactly the same as the natural frequency of the system but is very near to it. When an applied force is present, the frequency of oscillations is independent of the natural frequency of the system and is equal to the frequency of the applied force (*forced oscillations*). The case where the frequency of the forced oscillations is equal or close to the natural frequency of the system (resonance) is always dangerous.

It should be noted that a synchronizing torque appears only when the phasor of the terminal voltage  $V$  is fixed, as is the case of a generator operating in parallel with other generators, or of a motor (Fig. 40-1). In a singly operated synchronous generator the phasor  $V$  follows the emf phasor  $E_f$ , and there is no synchronizing torque. Again, considering the system of flywheel and spring with damping, a singly operated generator lacks the spring equivalent or, comparing the synchronous machine with a  $LCR$ -circuit, the singly operated generator behaves like a  $LR$ -circuit, whereas the generator, operated in parallel with other generators, and the synchronous motor behave as an  $LCR$ -circuit.

**40-2. The ratio of the amplitude of oscillation in parallel operation to the amplitude of oscillation of the single machine (the amplification factor).** A singly operated generator follows forced oscillations just as an  $LR$ -circuit follows the magnitude and frequency of the impressed voltage. Comparing the  $LR$  and the  $LCR$ -circuits, for equal impressed terminal voltage and frequency, the frequency of the oscillations (of the current) will be the same in both circuits, but the magnitude of the oscillations (the amplitude of the current) will, in general, be different. The same applies to the singly operated generator and to the generator operated in parallel with other generators. Considering the torque of the prime mover as consisting of a constant term, which produces the average power of the generator, and a superimposed sinusoidally varying term, which produces power oscillations, the generator operated in parallel with other generators will react differently, with respect to the oscillating torque, than the singly operated generator. The ratio of the amplitudes of oscillation for both cases will be considered in the following:

Let

$\Omega = \frac{\omega}{p/2}$  = instantaneous mechanical angular velocity of the machine;

$\Omega_m$  = mean mechanical angular velocity of the machine;

$\omega_m$  = mean electrical angular velocity of the machine;

$J$  = moment of inertia of flywheel mass;

$T_v$  = amplitude of the periodically varying part of the torque curve of the prime mover, having the angular velocity  $\nu\Omega_m$ .

The equation representing the motion of a *singly* operated machine is then

$$\frac{J}{p/2} \frac{d(\omega - \omega_m)}{dt} = T_v \sin(\nu\Omega_m t) \quad (40-4)$$

i.e., the oscillating term of the torque of the prime mover is used to accelerate the flywheel mass when it is positive, and decelerate the flywheel mass when it is negative, thus producing changes in the angular velocity of the rotating mass relative to the mean velocity.

If the machine operates in parallel with other synchronous machines, the terminal voltage produced is common for all. If the machine in consideration is subjected to forced oscillations by the prime mover, the line voltage phasor  $V$  is no longer able to take part in the oscillations as in the case of the singly operated machine, but it must retain its position. As explained in the foregoing, the hunting pole structure will then give rise to variations in the magnitude of the angle  $\delta$ , and consequently a synchronizing force appears. The *synchronizing torque*  $T_s$  is equal to the *change in the machine torque per unit angle*. For a change in the angle from  $\delta_m$  to  $\delta$ , where  $\delta_m$  corresponds to the mean position of the pole structure, the change in the machine torque is  $T_s(\delta - \delta_m)$ . The surplus (or deficiency) torque which the prime mover delivers is used now, on the one hand, for accelerating (or decelerating) the mass of the flywheel and, on the other hand, to balance the synchronizing torque.

Accordingly, the equation of motion of the synchronous machine connected to a constant voltage line is:

$$\frac{J}{p/2} \frac{d(\omega - \omega_m)}{dt} + T_s(\delta - \delta_m) = T_v \sin(\nu\Omega_m t) \quad (40-5)$$

The solution of this latter equation is readily obtained by considering an oscillating circuit consisting of inductance and capacitance. The voltage equation of this circuit is

$$L \frac{di}{dt} + \frac{1}{C} \int i dt = E_m \sin \omega t \quad (40-6)$$

Differentiating this equation:

$$L \frac{d^2 i}{dt^2} + \frac{i}{C} = E_m \omega \cos \omega t \quad (40-7)$$

On the other hand, by differentiating Eq. (40-5),

$$\frac{J}{p/2} \frac{d^2(\omega - \omega_m)}{dt^2} + T_s(\omega - \omega_m) = T_s \nu \Omega_m \cos(\nu \Omega_m t) \quad (40-8)$$

Equations 40-7 and 40-8 are identical in all respects. The mutually corresponding terms are

$$\begin{aligned} (\omega - \omega_m) &\dots i \\ \frac{J}{p/2} &\dots L \\ T_s &\dots \frac{1}{C} \end{aligned} \quad (40-9)$$

In the same manner, where the synchronizing force is zero and only mass is present, Eq. 40-4 corresponds to a circuit containing only inductance.

The similarity of the differential equations offers a means of determining the magnitude of the oscillations of the synchronous machine from the  $L$  and  $LC$ -circuits. Damping has been discounted for the synchronous machine and, therefore,  $R$  must be assumed zero in the electric circuits.

The amplitude of the current in a circuit containing only inductance is given by:

$$I_{m,L} = \frac{E_m}{\omega L}$$

In a circuit containing self-inductance and capacitance the amplitude of the current is:

$$I_{m,LC} = \frac{E_m}{\omega L - (1/\omega C)}$$

The ratio of these currents is:

$$\frac{I_{m,LC}}{I_{m,L}} = \frac{\omega L}{\omega L - (1/\omega C)} = \frac{1}{1 - [1/(2\pi)^2 f^2 LC]} = \zeta \quad (40-10)$$

However,  $1/(2\pi\sqrt{LC})$  is the natural frequency ( $f_n$ ) of oscillation of an  $LC$ -circuit. Consequently, the ratio of the maximum value of current in a circuit containing  $L$  and  $C$  to that in a circuit containing  $L$  alone is given by:

$$\zeta = \frac{1}{1 - (f_n/f)^2} \quad (40-11)$$

The same equation must apply to the hunting of a synchronous machine. The factor  $\zeta$  is called the *amplification factor* or the *modulus of resonance*. It

gives the ratio of the *amplitude* of oscillation of a system containing mass and synchronizing force to that of a system in which only mass alone is present.

**40-3. The natural frequency of the synchronous machine. The danger of resonance.** The natural frequency of oscillation of a synchronous machine obtained by comparing it to a circuit consisting of inductance and capacitance is (Eq. 40-9)

$$f_n = \frac{1}{2\pi} \sqrt{\frac{(p/2)T_s}{J}} \quad (40-12)$$

The amplification factor  $\zeta$  depends on the frequency  $f$  of the forced oscillations of the prime mover, and on  $f_n$ , the natural frequency of oscillation.  $\zeta$  is the ratio of two amplitudes of oscillation, namely, that of a system with synchronizing force and mass to that of a system with mass alone. The amplitude of oscillation of the system containing mass alone has a constant finite magnitude which remains within fixed limits. *The amplification factor  $\zeta$  is, therefore, directly a measure of the magnitude of the oscillations which appear in parallel operation.*

Fig. 40-2 shows the relation between the amplification factor and the ratio  $(f_n/f)$  in which the negative values of  $\zeta$  obtained for  $f_n > f$  are drawn upward.

Equation 40-10 and Fig. 40-2 shows that the amplification factor becomes greater as the natural frequency of the machine and the frequency of the forced oscillations of the prime mover (or of the load in the case of a motor) approach each other. If the natural frequency and the forced frequency are equal (resonance), the amplitude factor  $\zeta$  then becomes infinitely great. *In order to avoid the danger of resonance, the natural frequency of oscillation and the forced frequency of the prime mover (or load) must differ from each other.*

The values of  $\zeta$  which lie between  $\zeta = +3$  and  $\zeta = -2$  (the cross-hatched region, Fig. 40-2) are to be avoided for satisfactory parallel operation.

The adjustment of the appropriate ratio of  $f_n$  to  $f$  is essentially accomplished by a suitable selection of the moment of inertia of the rotating mass (see Eq. 40-12). The synchronizing torque  $T_s$  can be changed only within small limits.

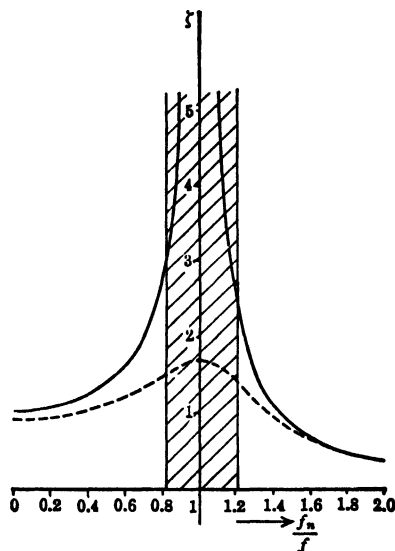


FIG. 40-2. Resonance curves.

**40-4. Improvement of parallel operation by means of a damper winding.** A reduction in the hunting can be achieved by a *damper winding*

which is placed in the pole shoes in the same manner as the starting winding of the synchronous motor (see Art. 38-4), with the individual poles often not connected together. When the machine hunts, the armature flux no longer remains stationary with respect to the pole structure, but a difference in velocity between these two exists. Because of this difference, currents flow in the bars of the damper winding, which serve to reduce the oscillations.

The speed of the armature flux is constant  $=n_s$ . When the rotor speed is below  $n_s$ , the operation of the damper winding is that of a motor and it accelerates the rotor. When rotor speed is above  $n_s$ , the operation of the damper winding is that of a generator and it decelerates the rotor.

Under some circumstances an excessively strong damping effect can be disadvantageous. If the mechanical hunting is prevented by too strong a damping effect, the flywheel mass loses its property as a reservoir of energy necessary to compensate for the torque variations of the prime mover. These torque variations are consequently transmitted to the generator so that its output and current vary in the same manner as the torque of the prime mover. This is not desirable for two reasons: first, the other machines operating in parallel must take over the compensating effect; second, the varying current gives rise to higher copper losses.

If the pole shoes are solid, eddy currents are produced in them as a result of the relative motion between the armature field and the poles; these eddy currents act in a manner similar to a damper winding. On the other hand, in machines with laminated pole shoes the self-damping effect is slight and a damper winding has to be used. A certain amount of damping always is necessary, or otherwise the free oscillations which appear in the case of suddenly applied loads would continue undamped and thereby become of infinitely long duration.

If very strong damping is present, the resonance curve  $\zeta = f(f_n/f)$  flattens out as is indicated by the dotted curve of Fig. 40-2.

From the above it becomes clear why the squirrel cage in the pole structure of the synchronous machine is called a damper or amortisseur winding.

It should be mentioned that when an induction motor is subjected to oscillations of its speed, i.e., to hunting, it also develops a synchronizing and damping torque. (See reference on A-C Machines at end of text.)

## Chapter 41

### LOSSES IN SYNCHRONOUS MACHINES HEATING AND COOLING

**41-1. The losses in the synchronous machine.** Similar to those in the induction motor, the losses in the synchronous machine are as follows:

(a) *Losses due to the main flux.* For the same reasons as given for the induction motor (Art. 29-1), the hysteresis and eddy-current losses due to the main flux are larger than those calculated from Eq. 29-5 or from iron-loss curves (given at end of text). The increase may be as high as 40 to 60% for salient-pole machines, 30 to 40% for 4-pole machines with cylindrical rotor, and 15 to 25% for 2-pole machines with cylindrical rotor.

The ripple due to the slot-openings of the stator causes high-frequency eddy currents in the pole surface. The losses produced by these eddy currents in per cent of the losses due to the main flux are approximately: 50 to 70% in salient-pole machines, 40 to 50% in 4-pole machines with cylindrical rotor, and 25 to 50% in 2-pole machines with cylindrical rotor.

Similar to the induction motor, the ripple produced by the slot openings of the stator causes currents not only in the iron but also in the damper winding of the salient-pole machine. The currents induced in the damper bars and their losses become considerable, if the slot pitch of the cage is much different from the stator slot pitch. A difference of up to 25% in the slot pitches keeps the losses at a low level. The losses are negligible when both slot pitches are equal to each other. Equal slot pitches can be made in salient-pole generators but not in motors, because this would produce locking torques which may prevent starting of the motor.

(b) *Losses due to the load current.* The load current produces  $I^2R$  losses in the stator winding and usually increases the  $I^2R$  losses of the field winding due to armature reaction. The additional losses due to the load current are similar to those of the induction motor.

The *cross-flux* in the slots produces skin-effect which may increase the copper loss considerably. Conductors stranded depthwise or special conductors (Roebel bars) must be used in large machines, in order to reduce the skin-effect losses. An increase of 15 to 20% in the  $I^2R$  losses due to skin-effect is reasonable.

TABLE 41-1. NO-LOAD LOSSES

Salient-pole machines.	Iron losses in the stator due to the main flux.	Pole surface losses due to slot openings.	Copper losses in the damper winding due to slot openings.	Windage and bearing friction losses.
Cylindrical rotor machines.	Iron losses in the stator due to the main flux.	Rotor surface losses due to slot openings.		Windage and bearing friction losses.

The *harmonic fluxes* produced by the stator winding produce surface losses in the rotor, in the same way as the ripple due to the slot openings. In the salient-pole machine these losses appear on the pole surfaces; in the cylindrical rotor machine, on the surface of the solid rotor. Because of the relatively large gap of the synchronous machine, these losses are usually small, about 0.05 to 0.15% of the output.

TABLE 41-2. LOAD LOSSES

Salient-pole machines.	$I^2r$ losses in stator and rotor windings.	Skin-effect losses in the stator winding.	Pole surface losses due to harmonic fluxes.	Losses in structural parts due to leakage fluxes.
Cylindrical rotor machines	$I^2r$ losses in stator and rotor windings.	Skin-effect losses in the stator winding.	Rotor surface losses due to harmonic fluxes.	Losses in structural parts due to leakage fluxes.

As in large induction motors, the *leakage fluxes of the end-windings* produce eddy-current losses in the structural parts (end plates, finger plates, bolts, etc.). The use of non-magnetic iron for the end plates and rotor retaining rings reduces these losses.

(c) *Friction and windage losses.* With respect to the friction and windage losses, the same reasoning applies as for the d-c machine and induction motor. The windage losses are quite high in 2-pole generators with cylindrical rotor. The use of hydrogen instead of air as a cooling medium reduces the windage losses to about 10% of those which appear with air.

(d) *No-load and load losses; stray load losses.* The losses which appear at no-load and at load, respectively, are shown in Tables 41-1 and 41-2. The additional losses due to the load (items 2, 3, and 4 of Table 41-2) are called *stray load losses*.

(e) *Example of loss distribution and efficiency.* In the following tabulation is shown the loss distribution of a salient-pole generator.

875 kva, 24 poles, 60 cycles,  $\cos \varphi = 0.80$

3 phase, 300 rpm, 2300 volts

Stator winding $I^2R$ .....	13,500
Rotor winding $I^2R$ .....	9,000
Stray load loss .....	4,000
Iron loss (total) .....	12,000
Bearing friction and windage loss .....	2,500
	<hr/> 41,000 watts

Output =  $875 \times 0.8 = 700$  kw

$$\text{Efficiency} = 100 \frac{700}{700 + 41} = 94.5\%$$

**41-2. Heating and cooling of the synchronous machine.** With respect to classes of insulation, limiting temperatures, heat conductivity, and heat transfer, the same considerations apply as in the induction motor. As in the d-c machine and induction motor, radial vents are used for cooling the stator of the salient-pole machine. Cylindrical rotor machines are usually long, and the problem of air flow requires very special attention. Hydrogen is normally used as cooling medium in these machines. When forced through hollow conductors of rotor and stator, the heat transfer is increased enormously. Also, liquid cooling is used for the stators of cylindrical rotor machines. (For the computation of the temperature rises of copper and iron of air cooled machines, see Ref. A11.)

## PROBLEMS

1. A 500-kva, 4-pole, 3-phase, 60-cycle,  $\cos \varphi = 0.8$  lagging, 120/208-volt, salient-pole generator has 72 slots, 2 conductors per slot, and each conductor consisting of 16 parallel strands. The bare dimensions of the strand are 0.081 in.  $\times$  0.162 in. The mean length of a turn is 80 in. At 208 volts the winding is connected 4-parallel star. The field current at full-load is 27.2 amp, and the field resistance at 75°C is 4.55 ohms. The friction and windage loss is 4.1 kw, the total iron losses 6.2 kw and the stray load loss 1.5 kw. Determine the efficiency of this generator. Determine the current density of the stator winding.

2. An 1875-kva, 6-pole, 3-phase, 60-cycle,  $\cos \varphi = 0.8$  lagging, 2400/4160-volt, salient-pole generator has 72 slots and 8 turns per coil. At 4160 volts the winding is connected 2-parallel star. The current density in the stator winding is 1835 amp per sq. in. The mean length of a turn is 90 in. and the winding is 2-layer. The leakage reactance of the stator is 0.096 (in p-u, unit current = rated current). The no-load characteristic is given by:

$I_f$ (amp) =	20	30	43	51	60	66	87	100	118
$E_f$ (volts) =	1600	2400	3200	3600	4000	4160	4600	4800	5000



The field current necessary to produce rated armature current with a short-circuited armature is 74 amp. The resistance of the field winding is 0.643 ohm. The friction and windage loss is 12.5 kw. The total iron loss is 17 kw; and the stray load loss, 9.6 kw. Determine the field current at full-load and the efficiency at full-load.

3. Determine, for the generator of Problem 2, the field current and efficiency at  $\frac{3}{4}$  load,  $\cos \varphi = 0.8$  lagging, assuming that the iron loss remains the same as at full-load and that the stray load loss changes with the square of the armature current.

4. Determine, for the generator of Problem 2, the field current and efficiency at  $\frac{1}{2}$  load,  $\cos \varphi = 0.8$  lagging, assuming that the iron loss remains the same as at full-load and that the stray load loss changes with the square of the armature current.

## Chapter 42

### SMALL SYNCHRONOUS MOTORS

Fractional-horsepower synchronous motors are built for a wider range of output and speed than fractional-horsepower induction motors. In miniature ratings (below 0.001 HP) they are used for clocks, timing devices, control apparatus, etc.

There are two basic types of fractional-horsepower synchronous motors which do not need d-c excitation and are self-starting. These are the *reluctance* type motor and the *hysteresis* type motor.

**42-1. The reluctance motor.** The ASA defines the reluctance motor as follows: A reluctance motor is a synchronous motor similar in construction to an induction motor, in which the member carrying the secondary circuit has salient poles, without direct-current excitation. It starts as an induction motor but operates normally at synchronous speed.

Fig. 42-1 shows the rotor punching of a  $\frac{1}{2}$ -HP, 4-pole, 3-phase reluctance motor. Six teeth are removed at four places, yielding four salient poles. Since this motor starts as an induction motor, the rings connecting the rotor bars must be complete, i.e., they must go around the whole rotor. The teeth can be cut out only partially, and the free spaces filled with aluminum in die-cast aluminum rotors, as shown in Fig. 42-2.

It has been shown in Art. 36-1 that a *salient-pole* machine is able to produce torque and run at synchronous speed without field excitation. Use is made of this property in the reluctance motor. Having started as an induction motor and having reached its maximum speed as an induction motor, it pulls into step and runs as a synchronous motor by virtue of its saliency.

As for the d-c excited synchronous motors, pulling-into-step is facilitated when the speed reached as an induction motor is as high as possible. This means that the rotor resistance must be made low. Furthermore, the motor

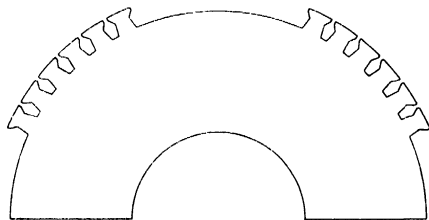


FIG. 42-1. Rotor punching of a reluctance motor.

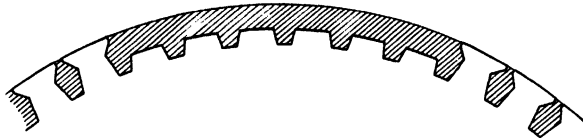


FIG. 42-2. Rotor of a reluctance motor (die-cast aluminum).

pulls into step easier the lower the  $WR^2$  of the rotating mass (rotor + load) (Ref. F1).

The stator of the reluctance motor can be polyphase or single phase. Therefore, there are:

- (a) polyphase reluctance motors,
- (b) split-phase type reluctance motors, and
- (c) capacitor-type reluctance motors.

In the case of the split-phase type, the capacitor-start, and the two-value capacitor motors the usual switch is necessary to cut out the starting winding or to change the capacitance before the motor reaches synchronous speed.

**42-2. The hysteresis motor.** The ASA defines the hysteresis motor as follows: A hysteresis motor is a synchronous motor without salient poles and without direct-current excitation, which starts by virtue of the hysteresis losses induced in the hardened steel secondary member by the revolving field of the primary, and operates at synchronous speed *due to the retentivity of the secondary core*.

In order to explain the operation of the hysteresis motor the induction motor will be considered. During the starting of the latter motor, eddy-current and hysteresis losses appear in the rotor iron. Both kinds of losses are accompanied by torques.

It is obvious that the eddy currents in the rotor iron are able to produce a torque with the machine flux in the same way as the currents in the rotor bars do. Writing, for the eddy-current loss in the rotor (Eq. 29-4),

$$p_e = c_e f_2^2 B^2 = c_e s^2 f_1^2 B^2 \quad (42-1)$$

and applying Eq. 19-8 for the torque, the driving torque which corresponds to the eddy currents in the rotor is

$$T_e = \frac{7.04}{n_s} \frac{c_e s^2 f_1^2 B^2}{s} = \frac{7.04}{n_s} c_e s f_1^2 B^2 \quad (42-2)$$

This torque is proportional to the slip; it decreases with increasing rotor speed and becomes zero at synchronous speed.

The hysteresis losses in the rotor iron can be written (Eq. 29-3),

$$p_h = c_h f_2 B^2 = c_h s f_1 B^2 \quad (42-3)$$

Again applying Eq. 19-8 the torque which corresponds to the hysteresis losses in the rotor is

$$T_h = \frac{7.04}{n_s} c_h f_1 B^2 \quad (42-4)$$

This torque is constant and independent of the rotor speed.

In order to get a physical conception of the torque  $T_h$ , called *hysteresis torque*, consider Figs. 42-3 to 42-5. It will be assumed that the rotor of the induction motor has no secondary winding so that the driving torque is due

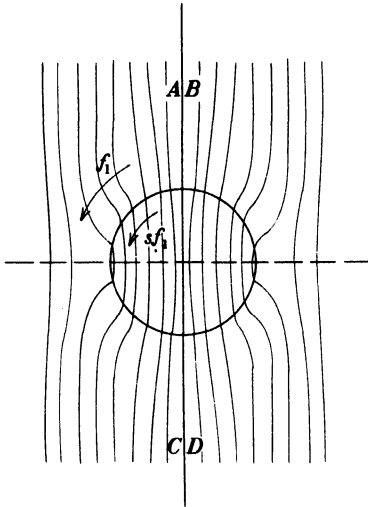


FIG. 42-3. Iron rotor without hysteresis in a magnetic field.

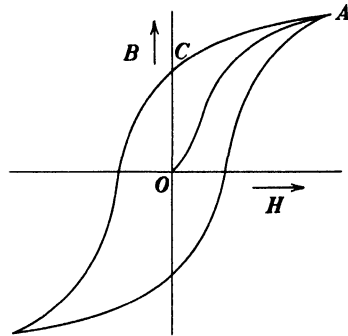


FIG. 42-4. Hysteresis loop.

only to the eddy-current and hysteresis losses. If there are no hysteresis losses, the magnetization of the rotor is in phase with the stator mmf, as shown in Fig. 42-3: the magnetic axis  $AC$  of the rotor coincides with the axis  $BD$  of the stator mmf. Fig. 42-4 shows a hysteresis loop. Conforming to the meaning of the word *hysteresis*, the flux density  $B$  lags behind the magnetizing force when there are hysteresis losses. For example, starting at the point  $A$  of the loop and decreasing the magnetizing force to the value zero, the flux density will not be zero but equal to  $OC$ . If the motor considered has hysteresis losses, this lag of the magnetization behind the magnetizing force due to hysteresis results in a lag of the magnetic axis of the rotor behind the axis of the stator mmf, as shown in Fig. 42-5. The angle of lag  $\alpha$  which causes the hysteresis torque is independent of the frequency of the magnetization of the rotor  $f_2 = sf_1$ ; it depends only upon the hysteresis loop of the material used for the rotor and remains the same at all rotor speeds. Hence the hysteresis torque is constant and independent of the rotor speed (Ref. F2).

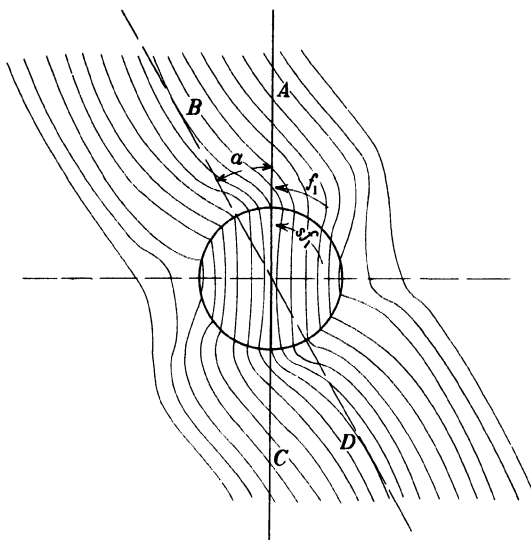


FIG. 42-5. Iron rotor with hysteresis in a magnetic field.

It follows from the foregoing that the rotor iron must have high hysteresis losses, i.e., a large hysteresis loop. The rotor construction of the hysteresis motor is schematically shown in Fig. 42-6. A ring of special magnetic material, such as cobalt or chrome steel, is mounted on an arbor of non-magnetic material such as aluminum. No squirrel cage is used. Starting is produced by the eddy-current *and* hysteresis torques. At synchronous speed, the eddy-current torque is zero, and the operation of the motor is accomplished exclusively by the hysteresis torque. At this speed the rotor develops magnetic poles similar to the d-c excited synchronous motor or reluctance motor. The strength of the poles is determined by the retentivity of the rotor-ring material (*OC* in Fig. 42-4).

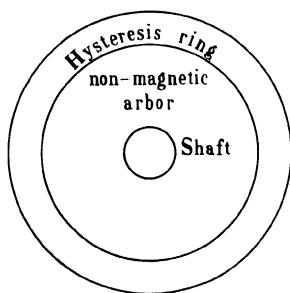


FIG. 42-6. Rotor of a hysteresis motor.

The stator of the hysteresis motor is usually single phase. There are:

- (a) polyphase hysteresis motors
- (b) capacitor type hysteresis motors
- (c) shaded pole hysteresis motors

The hysteresis motor is the most quiet of small motors. (For other types of small synchronous motors see Ref. on A-C Machines at end of text.)

## Chapter 43

### THE SYNCHRONOUS CONVERTER · VOLTAGE AND CURRENT RELATIONS · COPPER LOSSES COMPARED WITH THOSE OF THE D-C MACHINE

---

**43-1. Operation of the synchronous converter.** The d-c machine is nothing more than an a-c machine with a special device, the commutator, which makes it possible to pick up (for generator operation) a fixed instantaneous value of voltage from the winding. It follows, therefore, that the d-c armature winding must also be able to operate as an a-c winding.

Since the beginning and end of each winding element must be connected to a commutator bar, the d-c armature winding must be a closed winding. It is represented schematically in Fig. 43-1 which shows a 2-pole machine with a closed winding wound on a ring. The end of each turn (end of each winding element) is connected to the beginning of the next following turn, and the connection point is connected to a commutator bar as in the actual d-c machine. Furthermore, for 3-phase operation, three equidistant points of the winding, i.e., three points (points *a*, *b*, *c*) shifted 120 electrical degrees from one another, are connected to three slip rings. If such an armature is driven by a prime mover, it is able to supply d-c and a-c power simultaneously. The a-c power is 3-phase corresponding to the three slip rings. In multipole machines *each two consecutive armature paths* must be divided into three equal parts, in order to make the winding 3-phase;  $a/2$  points of the winding are then connected to each slip ring, i.e., each phase of the 3-phase winding consists of  $a/2$  parallel paths ( $a$  = number of d-c paths in the winding).

If the winding in Fig. 43-1 is connected to two slip rings, single-phase a-c power will be obtained. The tap points must be displaced 180 electrical degrees in this case; thus in a 6-phase converter, as an example, the tap points must be displaced 60 electrical degrees, and so forth. In all cases, each phase consists of  $a/2$  parallel paths. A 6-pole, 3-phase rotary converter is shown in Fig. 43-2.

It has been pointed out that a machine with an armature, as shown in Fig. 43-1, is able to operate as an a-c generator-d-c generator (double-current generator). Also, it is capable of operation as an a-c motor-d-c generator or as an a-c generator-d-c motor. In the former case this machine

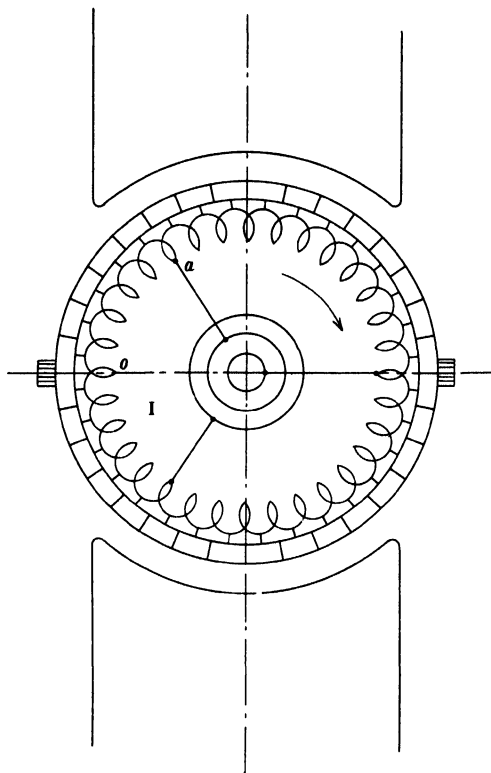


FIG. 43-1. Two-pole, 3-phase synchronous converter (schematic representation).

type is called a *synchronous converter*; in the latter case it is called an *inverted converter*. The normal operation is that as a synchronous converter, i.e., the machine operates as an a-c motor-d-c generator.

Since the poles of the converter are excited with d-c, its *fundamental* character must be the same as that of a synchronous machine. For a constant frequency  $f$  the speed is constant, independent of the load, and given by the familiar equation

$$n_s = \frac{120f}{p} \quad (43-1)$$

Apparently, the rotor must rotate against its rotating flux, in order that the latter be at standstill with respect to the mmf of the poles. It should be remembered that this is the condition for the existence of a uniform torque (see Art. 17-1).

The synchronous converter operates as a synchronous motor on the a-c side and as a d-c generator on the d-c side. The direct current in the armature, therefore, produces a torque which opposes the motion of the rotor, i.e.,



FIG. 43-2. 6-pole, 3-phase synchronous converter: 150 kw, 275 volts, 1200 rpm.

the driving torque produced by the alternating current. Just as in the synchronous motor (see Fig. 35-2), the alternating emf phasor falls behind the phasor which represents the line voltage, and the armature takes an active current from the line of sufficient magnitude to balance the opposing torque of the direct current and the rotational loss torque. This latter torque is comparatively small. Since the mmf of the direct current and the mmf of the *active alternating* current both have their amplitudes (axes) in the interpolar space (see Fig. 34-6), and correspond one to generator operation, the other to motor operation, they oppose and *cancel* each other, i.e., the synchronous converter *has no cross-flux*.

Just as in a synchronous motor, the alternating current and voltage of a synchronous converter are in phase for some one value of excitation. If the field current is increased above this value, the machine is *overexcited* and draws a *leading current* from the line because a leading current opposes the field mmf in a synchronous motor (see Arts. 32-1). If the field current is decreased, the machine is *underexcited* and draws a *lagging current* from the line because a lagging current supports the field mmf in a synchronous motor. For reasons discussed in the following, the excitation of the synchronous converter normally is adjusted so that the voltage and current are in-phase.

Since the direct current of a synchronous converter is taken from the same winding to which the alternating current is supplied, a fixed ratio exists between the d-c and a-c voltages, as well as between the d-c and a-c currents.



**43-2. Voltage and current ratios in the synchronous converter.** In order to determine the ratio between the d-c and a-c voltages of a synchronous converter, it will first be assumed that the machine operates at no-load and is so excited that it draws no reactive current from the line. Therefore, there is no armature reaction and the main flux, produced only by the d-c field mmf, induces a fixed emf in the armature winding.

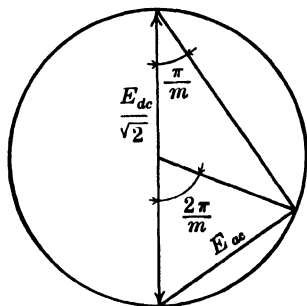


FIG. 43-3. Determination of d-c and a-c voltage ratio for the polyphase converter.

The *amplitude* of the emf induced in the armature winding is picked up at the brushes when the brushes are in the neutral axis. If a sinusoidal flux distribution is assumed, the ratio of the effective value of the emf to the maximum value is  $1/\sqrt{2}$ ; therefore, in a single-phase converter, the ratio of the alternating emf  $E_{a-c}$  (effective value) to the direct emf  $E_{d-c}$  is  $1/\sqrt{2}$ . In

a multi-phase converter, with the same armature winding operating at the same speed, the value of the d-c emf does not change, but the effective value of the a-c emf per phase ( $E_{a-c}$ ) is less than  $E_{d-c}/\sqrt{2}$  and equal to the chord subtending an angle of  $2\pi/m$  radians in a circle having a diameter  $E_{d-c}/\sqrt{2}$  (Fig. 43-3);  $m$  is the number of phases. Consequently, for an  $m$ -phase converter,

$$E_{a-c} = \frac{E_{d-c}}{\sqrt{2}} \sin \frac{\pi}{m} \quad (43-2)$$

This expression and those developed in the following also apply to the single-phase converter if  $m$  is taken as 2.

The emf transformation ratio for single-, 3-, and 6-phase converters, therefore, is

$$E_{a-c}/E_{d-c}$$

$$\text{Single-phase} = 0.707$$

$$\text{3-phase} = 0.612$$

$$\text{6-phase} = 0.354$$

At no-load the terminal voltages are practically equal to the emf's induced in the winding. Therefore, at no-load the transformation ratio of the emf's is the same as the ratio of the terminal voltages at the slip rings and at the brushes. Since the voltage drop in the armature winding of a converter is small, the emf ratio also applies approximately to the terminal voltages under load, so that

$$\frac{V_{a-c}}{V_{d-c}} \approx \frac{1}{\sqrt{2}} \sin \frac{\pi}{m} \quad (43-3)$$

The a-c voltage available from the supply lines does not usually correspond to the d-c voltage desired at the brushes. Therefore, the synchronous converter usually requires a transformer between the line and slip rings in order to transform the line voltage to the proper value. Figs. 10-10 to 10-12 inclusive show three single-phase transformers with three different types of connections which may be used for 6-phase synchronous converters.

The tapped armature winding of a synchronous converter behaves as a closed or mesh polyphase winding. The line voltage is equal to the phase voltage, and the slip-ring current is  $2 \sin (\pi/m)$  times the phase current. If  $I_{d-c}$  is the terminal direct current,  $I_{a-c}$  the alternating current per phase, and the losses are disregarded, then the d-c power output is equal to the a-c power input:

$$V_{d-c} I_{a-c} = m V_{a-c} I_{a-c} \cos \varphi \quad (43-4)$$

From this equation and Eq. 43-3 the ratio of phase current to d-c current becomes

$$\frac{I_{a-c}}{I_{d-c}} = \frac{\sqrt{2}}{m \sin (\pi/m)} \cdot \frac{1}{\cos \varphi} \quad (43-5)$$

The ratio of slip-ring current to direct current, therefore, is:

$$\frac{I_r}{I_{d-c}} = \frac{2\sqrt{2}}{m \cos \varphi} \quad (43-6)$$

Equations 43-5 and 43-6 assume no losses whatever in the converter; they yield for a value of  $\cos \varphi = 1$  the following table of current ratios:

<i>Number of phases</i>	$I_{a-c}/I_{d-c}$	$I_r/I_{d-c}$
1	0.707	1.414
3	0.545	0.943
6	0.472	0.472

In a 3-phase converter the active component of the slip-ring current is approximately equal to the direct current, while in a 6-phase converter it is equal to about one-half the direct current.

**43-3. The copper losses in the synchronous converter.** The superposition of direct current and alternating current in the armature conductors leads to peculiar results in the copper losses.

Consider Fig. 43-1. Each phase covers 120 electrical degrees (in general  $2\pi/m$  electrical degrees). The position of phase I is assumed such that the mid-point  $O$  of the phase coincides with the mid-point of the interpolar space, i.e., with the brush axis. In this position the sum of the flux lines linking phase I is maximum, and the emf induced in this phase is, therefore, zero. It will be further assumed that induced emf and current are in phase; therefore the current is also zero in phase I.

Consider the winding element  $O$ , lying midway between the taps a-c. The alternating current in this element, as well as in the other winding elements within phase I, is zero. Since the mid-element  $O$  lies directly under the brush, the direct current is being commutated. Thus, for this element  $O$ , the direct and alternating currents go through zero at the same instant. Fig. 43-4 shows the relative positions of the d-c and a-c waves for this winding element as a function of time. The resultant current, which is the difference between the direct current and alternating current, is also shown in Fig. 43-4.

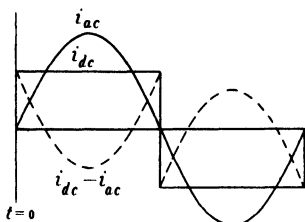


FIG. 43-4. Currents in the winding element midway between taps.

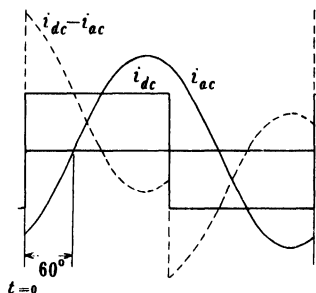


FIG. 43-5. Currents in the winding element at the tap point.

Winding element  $a$  at the tap point, which is displaced  $60^\circ$  from the mid-element in the direction of rotation, carries, at the time when commutation takes place in mid-element  $O$ , exactly the same alternating current as the mid-element but a different direct current, since commutation has taken place  $60^\circ$  earlier. The relative positions of the two current waves for the tap element  $a$  is shown in Fig. 43-5. The resultant current, which is again the difference between the direct and alternating currents, has an entirely different shape than that of the mid-element  $O$ .

The copper losses in each winding element are determined by the *resultant* current in the element. Therefore, the copper losses are different in the individual coils. The losses are least in the winding element mid-way between tap points of a phase and greatest at the tap points.

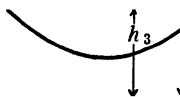


FIG. 43-6. Copper losses in the individual winding elements.

The axis of abscissa in Fig. 43-6 represents the series order of the winding elements of one phase of a 3-phase converter between tap points, and the axis of ordinates represents the copper losses in the individual elements produced by the resultant currents. The heating effect in a winding element at the tap point is 5.4 times as great as the heating effect in the mid-element. The mean value of the losses

for the entire phase, as found by planimeter measurement, is given by the distance  $h_3$  from the axis of abscissa to the straight line  $a$ . The distance  $h_4$  from the axis of abscissa to the straight line  $b$  represents the losses that would be produced by the direct current alone. Consequently  $h_3/h_4$  is the ratio of the copper losses of the machine operating as a 3-phase converter to the copper losses of the same machine operating as a d-c generator. This ratio is equal to 0.56.

**43-4. Comparison with the d-c machine.** It is seen in Fig. 43-6 that the copper losses of a 3-phase converter are much less than those of a d-c machine of the same dimensions and rating. It is shown in the following that the 6-phase and 12-phase converters are still more favourable with respect to losses than the 3-phase converter.

Fig. 43-6 refers to  $\cos \varphi = 1$  operation. When the synchronous converter is overexcited or underexcited, it carries a reactive current which increases the copper losses. The following table shows the ratio ( $r$ ) of the current losses in the synchronous converter to the corresponding losses in a d-c machine of the same dimensions and rating for various power factors on the a-c side.

No. of phases	1	3	6	12
$\cos \varphi = 1.00$	( $r$ ) = 1.38	0.56	0.27	0.21
0.90	1.85	0.84	0.48	0.40
0.80	2.51	1.23	0.77	0.67
0.70	3.46	1.80	1.19	1.06

The copper losses of a converter becomes less as the number of phases is increased. Furthermore, they are least when the excitation is adjusted to give unity power factor on the a-c side.

Since the current losses are proportional to the square of the current, a synchronous converter, assuming equal armature copper losses as a basis, may deliver a direct current output  $\sqrt{1/r}$  times greater than the output of a d-c machine of the same dimensions. Therefore, the magnitude  $\sqrt{1/r}$  gives the ratio of the power output of a converter to that of a d-c machine of equal dimensions. This ratio is shown in the following table:

No. of phases	1	3	6	12
$\cos \varphi = 1.00$	$\sqrt{1/r} = 0.85$	1.33	1.93	2.20
0.90	0.73	1.09	1.46	1.58
0.80	0.63	0.90	1.14	1.22
0.70	0.54	0.74	0.91	0.97

For any number of phases the converter output increases rapidly with an increasing value of  $\cos \varphi$ .

The 12-phase synchronous converter has little advantage over the 6-phase converter; it is quite long since it requires 12 slip rings. For this reason it is

customary to design converters 6-phase. In small converters, up to 250 kw, the saving in material and the increased efficiency produced by a larger number of phases is not so important, and 3-phase design is employed.

### PROBLEMS

1. A 6-phase synchronous converter delivers 625 volts d-c to a traction system. Determine: (a) the diametrical voltage of the armature; (b) the voltage between adjacent slip rings; (c) and the voltage between alternate slip rings.

2. If a converter delivers 350 kw at 625 volts d-c determine the approximate slip-ring current, assuming the a-c supply to be: (a) single-phase; (b) 3-phase; (c) 6-phase. Assume an efficiency of 94.5% and unity power factor.

3. A 250-kw, 230-volt, 3-phase, synchronous converter receives power from a 13,200-volt, 3-phase, 60-cycle power system. The transformer bank supplying the converter is connected  $\Delta$ -Y and has an efficiency of 98%. The full load efficiency of the converter is 93%. Determine for unity power factor: (a) d-c output current of converter; (b) slip-ring current; (c) voltage, current, and kva ratings of transformer secondaries; (d) power input, current, and voltage of transformer primaries when the converter is delivering rated output. Neglect voltage drops in converter and transformers, and transformer magnetizing current.

4. Repeat Problem 3 for the same machine operated 6-phase with the transformer bank connected  $\Delta$ -diametrical.

5. Repeat Problem 3 for the same machine operated 6-phase with the transformer bank connected  $\Delta$ -double  $\Delta$ .

6. Repeat Problem 3 for a power factor of 0.90 leading. The converter efficiency is now 92% and the transformer efficiency 97.5%.

7. If the machine of Problem 3 is operated 6-phase, 0.90 power factor leading, with a  $\Delta$ -double  $\Delta$  bank supplying the power, determine: (a) slip-ring current; (b) voltage, current, and kva ratings of transformer secondaries. Assume converter efficiency 92% and transformer efficiency 97.5%.

8. A 2500-kw, 25-cycle, 500-rpm, 230-volt, 6-phase synchronous converter supplies a 3-wire d-c system. The transformer bank supplying the converter is  $\Delta$ -double Y (neutrals connected) and receives power from a 27,000-volt, 3-phase system. The full-load converter efficiency is 95% and the full-load transformer efficiency 98.5%. For unity power factor determine: (a) d-c output current; (b) slip-ring current; (c) diametrical slip-ring voltage; (d) adjacent slip-ring voltage; (e) slip-ring to neutral voltage; (f) transformer primary current; (g) line current from 27,000-volt system.

9. Three identical single-phase transformers supply a 500-kw, 125-volt synchronous converter. The converter is 3-phase, 25-cycle, and receives power from a 27,000-volt, 3-phase distribution system, with the transformer bank connected  $\Delta$ -Y. If the converter operates at a power factor of 0.95 lagging and an efficiency of 0.94, determine the transformer voltage, current, and kva rating. If the transformer reactance drop is 5% and the converter drops are neglected, determine the d-c output voltage at full-load, unity p.f. and also 0.90 p.f. leading.

10. Three single-phase transformers connected Y-diametrical supply a 6-phase, 200-kw, 625-volt railway synchronous converter from a 13,200-volt, 3-phase line. Determine: voltage, current, and kva ratings of the transformers when the con-

verter delivers full-load at 0.95 p.f. leading and an efficiency of 0.93. What is the ratio of transformation of the transformers?

11. A 1000-kw, 230-volt, 6-phase, 25-cycle synchronous converter supplies a 3-wire d-c system. Power is received from a 13,200-volt, 3-phase system. Write specifications for three single-phase transformers you might order, assuming primaries connected in  $\Delta$ ; (b) primaries connected in Y. Give the reasons for your selection and show connection diagram.

12. Two single-phase transformers connected in open delta supply a 250-kw, 230-volt, 3-phase synchronous converter from an 1100-volt, 3-phase line. Neglecting losses and assuming operation at unity p.f., what are the voltage, current, and kva ratings of the transformers necessary? At what p.f. do the transformers operate?

13. A 250-kw, 230-volt, 6-phase synchronous converter receives power from an 1100-volt, 3-phase line by means of two transformers connected in T-double T. Specify voltage, current, and kva ratings of the transformers necessary when operating at full-load, unity p.f. At what p.f. do the transformers operate? Neglect losses. Show diagram of connections.

14. If the converter of Problem 13 receives power from a 1100-volt, 2-phase line, specify the complete transformer ratings, neglecting losses and assuming rated output at unity p.f. Show diagram of connections.

15. Sketch the wave form of the current in a conductor located 15 electrical degrees from a tap point of a 3-phase synchronous converter for (a) unity p.f., (b) 0.90 p.f. lagging.

16. Repeat Problem 15 for a 6-phase synchronous converter.

17. If the 250-kw, 230-volt, 3-phase converter of Problem 13 receives its power from the 1100-volt, 3-phase line by means of autotransformers, specify the transformers necessary. Give voltages, tap points, and show connection diagram.

18. Specify the voltages of the autotransformers necessary to supply a 250-kw, 230-volt, 6-phase synchronous converter from an 1100-volt, 3-phase, 3-wire supply system. Show connection diagram.

## Chapter 44

### COMMUTATION OF THE SYNCHRONOUS CONVERTER · VOLTAGE REGULATION · STARTING · PARALLEL OPERATION

**44-1. Commutation of the synchronous converter.** As in a d-c generator, the converter needs interpoles for the purpose of improving the commutation. However, there is a difference between the d-c machine and the converter: the latter has no cross-flux (flux in the neutral axis, see Art. 43-1). As a consequence, the mmf required on the interpoles of a converter is much less than that necessary for a d-c machine of the same rating: because of the absence of a cross-flux, the interpoles must produce mainly the counter-emf equal to the emf of self- and mutual-induction in the short-circuited winding element, plus the voltage drop in the brush contact surface. In the d-c machine the interpoles need an additional mmf to suppress the armature cross-flux, which mmf is equal to the entire armature mmf.

The absence of a cross-flux in the synchronous converter is due to the fact that the mmf of the direct current and the mmf of the active component of the alternating current cancel each other (see Art. 43-1). Since there is no mmf in the quadrature axis, a compensating winding which reduces this mmf is *unnecessary* in the rotary converter. This inherent cancellation of the d-c cross flux is of advantage with respect to the interpoles. However, the absence of the compensating winding is a disadvantage under transient conditions, such as change of frequency, sudden short circuit on the a-c side, or suddenly applied d-c load. In these cases the armature flux is not compensated, and high coil voltages and ring fire may appear, leading to possible damage of the commutator, brushes, and brush holders.

**44-2. Voltage regulation of the converter.** Since the ratio of direct and alternating voltages of a converter is fixed, any change in the direct voltage requires a change in the slip-ring voltage. If the field current of a converter is changed, only the reactive component of its current is materially changed; the effect of a change in the field current on the d-c voltage is insignificant. The reactive current may change the d-c voltage slightly by changing the voltage drop in the transformer to which the converter is connected; in

itself, this voltage drop is very small. Different means can be employed in order to adjust the slip-ring voltage: taps on the primary side of the transformer; a synchronous generator booster which is connected in series with the converter; an induction regulator (see Art. 25-5) the secondary winding of which is connected in series with the converter. The generator booster and the induction regulator permit a continuous regulation of the d-c voltage, which cannot be obtained with taps on the transformer. Also, a choke coil on the a-c side of the converter, in connection with variation of the field current, permits voltage regulation on the d-c side. However, in this case the converter carries reactive current which increases the copper losses.

**44-3. Starting and parallel operation of converters.** Starting of a converter can be accomplished on either the a-c or the d-c side. Since the converter behaves as a synchronous motor on the a-c side, it is not capable of starting by itself. It must be equipped, just as the synchronous motor, with a squirrel-cage winding (damper winding) to enable it to start as a squirrel-cage induction motor. In order to keep the starting current low, a reduced voltage of about  $\frac{1}{3}$  to  $\frac{1}{2}$  the rated voltage is impressed across the slip rings during the starting period. For this reason the secondary of the main transformer is suitably tapped to give this reduced voltage. When the converter is brought up to near synchronous speed as an induction motor, it will pull into step as a reluctance motor because of the salient poles (see Art. 36-1), and full voltage can be applied after it has been excited with direct current.

Just as in the conventional synchronous motor (Art. 38-4), care must be taken with the synchronous converter to see that the field winding is not punctured by high induced voltages at start. In order to avoid breakdown, the field winding is short-circuited across the armature at start or broken into several groups; in the latter case the correct connection must be made when the machine has reached synchronous speed.

If a direct-current source is available, the converter can be started from the d-c side in the same manner as a shunt motor. After reaching its rated speed, it is then synchronized with the alternating-current supply. The converter is started from the d-c side wherever this is possible. Very large converters are also started by means of special starting motors.

If several converters operate in parallel with each other, each converter normally has its own transformer. If several converters are supplied from a common transformer, then the armature windings of the machines are connected in parallel on both the a-c and the d-c sides. If, in this case, the brush-contact resistances of the machines are not equal, the direct current may enter the negative brushes of a machine and then, instead of leaving its positive brushes, follow a path through the armature, out the slip ring, over the bus-bars on the a-c side, and out the positive brushes of another machine. The brushes of this latter converter are then decidedly overloaded and sparking at the commutator results.



If a converter operates in parallel with d-c generators or with a bank of batteries, then any sudden additional load will be taken in the greater part by the converter because of its low voltage drop (in the armature winding and in the transformer). In order to obtain a uniform distribution of the load among all machines operating in parallel, and also the battery, under certain circumstances it is necessary to increase the voltage drop in the converter by using a small differentially connected series winding and a choke coil on the a-c side.

The distribution of load among rotary converter operating in parallel can be varied by changing their d-c voltages, using the means described in Art. 44-2.

As has been mentioned, a synchronous converter can also be used to transform from d-c to a-c (*inverted converter*). However, certain difficulties arise here which are not present when the synchronous converter transforms from a-c to d-c. The inverted converter operates either as a shunt or compound motor, and therefore its a-c frequency depends upon its d-c excitation. Consider the inverted converter loaded with an inductive load: an increase of the inductive current weakens the field of the converter (see Art. 32-1) and increases its speed and frequency. The increase of frequency increases the inductive reactance of the load and thus the lag angle of the current. This further reduces the field and increases the speed. The action is cumulative, and for this reason the inverted converter has to be provided with a speed-limiting device. Also, the normal rotary converter has to be provided with such a device when the possibility of inverted operation exists, as for example, in the case of a short circuit on the a-c line of a converter operating in parallel with a storage battery.

**44-4. Comparison with the motor-generator set.** A motor-generator set can be used to convert alternating current to direct current or direct current to alternating current. The motor of the a-c to d-c set can be either an induction motor or a synchronous motor. The disadvantage of the motor-generator set in comparison with the synchronous converter is its low overall efficiency. In a motor-generator set the entire transformed energy is first transformed into mechanical energy by the motor, and then into electrical energy by the generator; in a converter the transformation is accomplished in the same armature, the winding of which carries only the difference of the two currents. The losses in the motor-generator set are, therefore, much larger than those in the synchronous converter.

The motor-generator set and the rotary converter have both been superseded by the mercury-arc rectifier and are now used only in special applications, such as speed regulating sets.

## Chapter 45

### THE D-C ARMATURE IN AN ALTERNATING MAGNETIC FIELD

In the d-c machine and in the synchronous converter the d-c armature rotates in a magnetic field that does not vary with time and that does not move. In contrast, in a-c commutator motors a d-c armature rotates in a magnetic field that either varies with time (single-phase commutator motor), or rotates (polyphase commutator motor). A series of new phenomena, therefore, are introduced which do not appear in the case of a d-c armature rotating in a constant stationary magnetic field. The behavior of a d-c armature in an alternating field will be considered in this chapter.

**45-1. The emf of rotation and the emf of transformation in the armature winding.** In the d-c machine the magnetic axis of the d-c armature is determined by the position of the brushes on the commutator (Fig. 45-1). The same holds true for the d-c armature in an alternating field. However, in

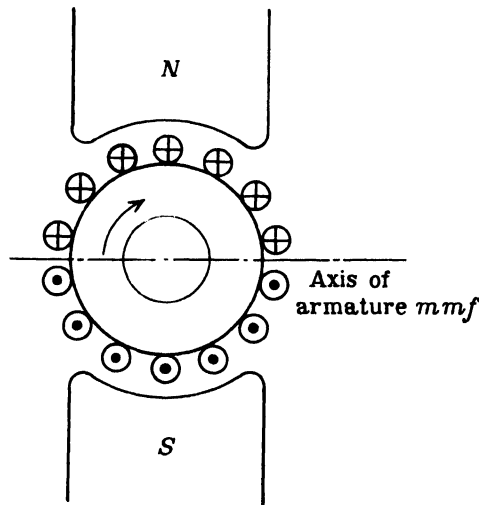


FIG. 45-1. Position of the axis of the armature mmf in a d-c machine.

each armature path of the d-c machine, the magnitude and direction of the currents are constant, and the resulting armature flux, therefore, is constant; in the single-phase commutator motor, on the other hand, the current in each armature path varies with time, since the brushes carry alternating current, and as a result, the armature flux also varies with time; *the armature flux of a single-phase commutator motor is an alternating flux* the axis of which is determined by the position of the brushes on the commutator.

In the single-phase commutator motor the field (pole) winding is either a concentrated winding, similar to that in the d-c machine, or a distributed winding as in the single-phase induction machine; it produces an alternating flux. For the sake of simplicity the field winding is shown as a concentrated winding in all the figures that follow.

(a) *The emf of rotation in the armature winding.* Fig. 45-2 represents schematically the field winding and the armature winding of a single-phase commutator motor. The brush axis is perpendicular to the axis of the pole-flux, and the armature rotates in the alternating flux produced by the field winding. The emf induced in the armature as a result of rotation and appearing at the brushes is, as in the case of the d-c machine, proportional to the rpm of the armature. However, since the flux is alternating, it is not a direct emf but an alternating emf, and its *frequency is independent of the rpm of the armature and always equal to the frequency of the field current* (the frequency of

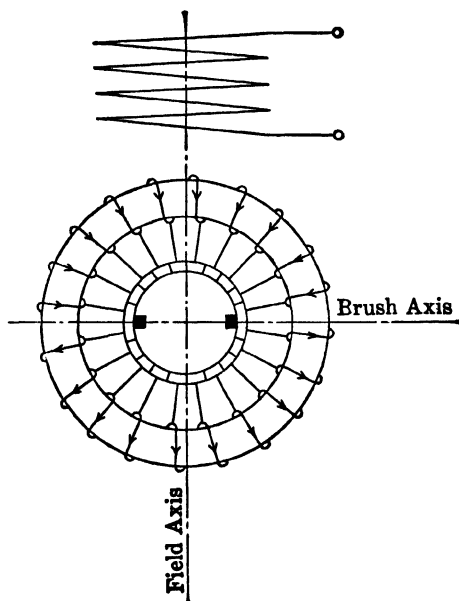


FIG. 45-2. Emf of rotation in a d-c armature winding due to an alternating flux. Brushes in the neutral.

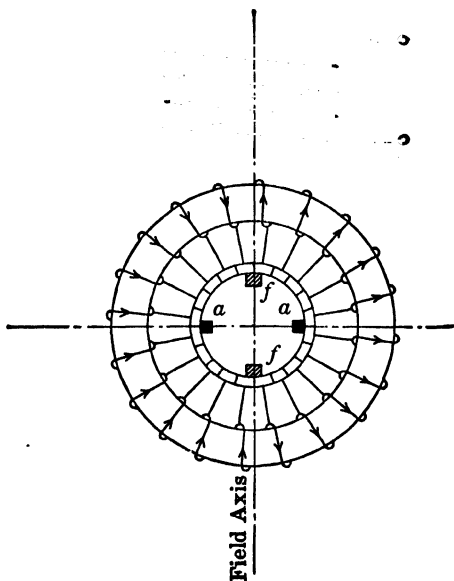


FIG. 45-3. Transformer emf in a d-c armature winding due to an alternating flux.

the line). This is easily understood from the following consideration: The flux of a d-c machine is unvarying with time and, as a result of rotation, a direct emf is induced in the armature the magnitude of which is proportional to the rpm of the armature. If the flux of a d-c machine were to pulsate, then an alternating emf would appear between the brushes on the commutator; the frequency of this emf would correspond to the frequency of the pulsations of the flux, but its *magnitude* would be proportional to the speed of the armature and independent of the frequency of the flux pulsations. From the same consideration it follows that the emf produced *by rotation in an alternating flux is in phase with the flux*: the emf is zero when the flux is zero and a maximum when the flux is a maximum.

(b) *The transformer emf in the armature winding.* In addition to the emf of rotation a second emf is induced in the armature winding *by transformer action* with the main flux. Since the pole-flux linking the individual armature winding elements is an alternating flux, it induces emf's in them just as the primary winding of a transformer induces emf's in the turns of the secondary winding; these emf's are *entirely independent of the speed*. In Fig. 45-3 the direction of the transformer emf's is shown for a certain instant of time. The emf's in the turns to the left of the axis of the field winding and the emf's in the turns to the right of the axis of the field winding have opposite directions with respect to one another, exactly the same as do the emf's of rotation with respect to the brush axis in Fig. 45-2. These transformer emf's cannot produce *internal* (circulating) currents in the armature winding, because, with respect to the closed circuit of the armature winding, the emf's in both halves of the winding cancel one another. Furthermore the transformer emf's are ineffective with respect to the brushes lying in the axis perpendicular to the field winding (brushes *aa*, Fig. 45-3), because they cancel one another within the upper half as well as within the lower half of the armature winding; therefore the transformer emf's produce no current in the armature winding if these brushes (*aa*) are joined together. However, it is different if brushes are placed on the commutator along the field axis (brushes *ff*, Fig. 45-3). Between these brushes the transformer emf's add within both halves of the winding, and current would flow between these brushes if they were joined together.

Thus, the emf of rotation and the transformer emf *both have the same frequency*. However, while the emf of rotation is in phase with the pole-flux producing it, and its magnitude depends upon the rpm of the armature, the transformer emf is displaced in phase  $90^\circ$  behind the flux producing it, as in every trans-

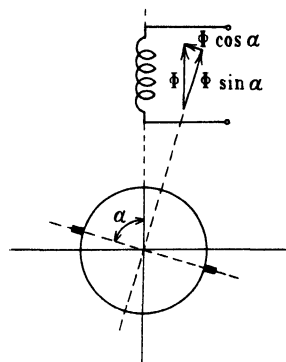


FIG. 45-4. Emf of rotation and transformer emf in a d-c armature winding due to an alternating flux. Brushes not in the neutral.

former, and its magnitude is independent of the rpm of the armature.

If the brushes are shifted so that the angle between the brush axis and the field axis,  $\alpha$ , is  $\geq 90^\circ$  (Fig. 45-4), then, as in the d-c machine, the emf of rotation is less than in the case when  $\alpha = 90^\circ$ ; it is proportional to  $\sin \alpha$ . Furthermore, in this case a transformer emf appears between the brushes which is proportional to  $\cos \alpha$ . This can be seen without further discussion if the flux is divided into two components, one of which,  $\Phi \sin \alpha$ , is perpendicular to the brush axis, and the other,  $\Phi \cos \alpha$ , is parallel to the brush axis (Fig. 45-4).

**45-2. The torque of the single-phase commutator motor. The compensating winding.** By means of Fig. 45-3 and the fundamental law of the force on a conductor in a magnetic field (see Art. 1-2d), it is evident that the currents produced in the armature by the transformer emf's and flowing through the brushes  $ff$  produce no torque in conjunction with the pole-flux: in the left half as well as in the right half of the armature the torque produced by the coils lying in the upper half of the armature oppose the torque produced by the coils lying in the lower half of the armature. It is quite different, however, with the currents produced by the rotational emf's (Fig. 45-2): these currents and the pole-flux produce the useful torque. In the first case, where the armature currents are produced by transformer action, the axis of the armature flux coincides with the axis of the pole-flux. In the second case, where the armature currents are produced by rotation, the axis of the armature flux makes an angle of  $90^\circ$  with the axis of the pole-flux: *the greatest torque appears if the brush axis (axis of the armature flux) and the field axis make an angle of  $90^\circ$  with each other* (as is usually the case in the d-c machine).

The average value of the developed torque is according to Eq. 1-33

$$T = \frac{7.04}{n} E I \cos \psi \quad \text{lb-ft.} \quad (45-1)$$

where  $E$  and  $I$  are the effective values of the emf induced in the armature by rotation and of the armature current.  $\psi$  is the angle between  $E$  and  $I$ . Eq. 45-1 applies also to the d-c machine, however, for the d-c machine  $E$  is the amplitude of the a-c emf ( $E_{d-c} = \sqrt{2}E$ , see Art. 43-2, Fig. 43-3).

If the brush axis makes an angle  $\alpha$  (Fig. 45-4) with the main flux axis, then the value of Eq. 45-1 must be multiplied by  $\sin \alpha$ , since only the component  $\Phi \sin \alpha$  of the flux is effective. Thus the general expression for the average value of the torque is

$$T = \frac{7.04}{n} E I \cos \psi \sin \alpha \quad \text{lb-ft.} \quad (45-2)$$

The torque of the single-phase commutator motor is not constant but varies between a maximum and a minimum value (see Art. 1-2d). Disregarding the

factors  $\cos \psi$  and  $\sin \alpha$ , the average value of the torque of the single-phase commutator motor is less, in the ratio of  $1:\sqrt{2}$ , than the constant torque of a d-c machine with the same flux and the same armature copper losses as in the single-phase commutator motor. If the emf and current are not in phase or if the angle between the brush axis and the field (pole) axis is not equal to  $90^\circ$  ( $\psi \neq 0$ ,  $\alpha \neq 90^\circ$ ), then, in comparison with the d-c machine, the torque is still further less.

*The compensating winding.* The pole-flux induces transformer emf's in the armature winding; yet, a transformer emf appears at the brushes only when the brushes are not placed on the perpendicular to the axis of the field, i.e., are not placed in the neutral axis. If the brushes are on a perpendicular to the field axis, the transformer emf between them is equal to zero, because the emf's of the individual coils in each armature path mutually cancel one another. However, the pole-flux links not only the armature winding but also the field winding; it induces a voltage of self-induction in this winding, the frequency of which is equal to the frequency of the line, and a part of the terminal voltage must be consumed in order to overcome this voltage of self-induction. This component of the terminal voltage leads the field current by  $90^\circ$ .

The armature flux has the same effect on the armature winding as the field flux has on the field winding. As described, the armature flux is an alternating flux the axis of which coincides with the brush axis. Since the armature winding behaves magnetically as a solenoid, the axis of which coincides with the brush axis, the armature flux induces an emf of self-induction in the armature winding by transformer action, and a component of the terminal voltage again must be used to overcome this induced emf.

The emf's of self-induction in the field winding and in the armature winding introduce a phase shift between the terminal voltage and the current and would make the phase displacement of the single-phase commutator motor extraordinarily large if special means were not employed in order to avoid this effect. As in the d-c machine, the armature flux does not contribute to the electromagnetic power (Eq. 1-33) and may be nullified here just as in the d-c machine; in consequence of this fact, *the single-phase commutator motor is, as a rule, supplied with a compensating winding* (see Art. 46-1). By means of this winding the armature flux is reduced to a small residue, the leakage fluxes, so that the emf of self-induction of the armature is small and equal to the emf induced in the armature winding by its leakage fluxes only. On the other hand, the voltage of self-induction in the field winding cannot be avoided, for this is produced by the main flux which creates the effective torque; this flux cannot be eliminated or reduced. In order to diminish the emf of self-induction in the field winding of a single-phase series motor, the number of turns of the field winding is made as small as possible.

Similarly, as in the d-c machine, the compensating winding is made as a distributed winding and placed in slots in the stator. Its magnetic axis must

coincide with the axis of the armature winding, i.e., the brush axis. Since the armature flux is alternating, it is not necessary to connect the compensating winding in series with the armature winding so that it will carry the armature current, as in the case of a d-c machine. The compensating winding will suppress the armature field if it is simply short-circuited on itself, for, with respect to the armature winding as the primary winding it acts as the short-circuited secondary of a transformer.

**45-3. The transformer emf of a short-circuited winding element and the commutating fluxes in the single-phase commutator motor.** If commutation plays an essential role in the d-c machine and affects its performance, then this same problem enters to an even greater measure in the a-c commutator motor, because commutation takes place under much more unfavorable conditions than in the d-c machine: it is the *transformer emf in the short-circuited winding element* which makes the commutation worse in comparison to that of the d-c machine. It is evident from Fig. 45-2 that, during the time a winding element is short-circuited by the brush, the element lies in a plane that is perpendicular to the field (pole) axis, and in consequence of this it is linked by the pole-flux. Thus a transformer voltage results of the magnitude (see Eq. 3-11)

$$e_t = 4.44fN_s\Phi 10^{-8} \text{ volt} \quad (45-3)$$

where  $N_s$  is the number of turns per winding element. The emf  $e_t$  induced in the short-circuited winding element thereby is independent of whether the armature rotates or is at rest and *appears at start as well as during the running of the machine*. While in the d-c machine, with the brushes located in the neutral axis, the pole-flux has no effect on the short-circuited winding element, in this case the effect of the pole-flux is present constantly in the form of a transformer emf in the short-circuited element.

The armature flux has no effect on the short-circuited winding element because it is canceled by the compensating winding. Besides the transformer emf  $e_t$ , the short-circuited element is influenced by the resistance of the short-circuit path and the *emf of self-induction*, which is the result of the change in the current during the movement of the coil from one armature path to another (see Fig. 45-1). Since the armature carries an alternating current, the reversal of current in the short-circuited element can take place at any instantaneous value of the current. The greatest emf of self-induction appears if commutation takes place at the maximum value of the current. If commutation takes place at the moment when the instantaneous value of the current is zero, then the emf of self-induction also is zero. Since maximum value of emf of self-induction occurs at the instant of maximum value of current, and zero value of emf of self-induction occurs at the instant of zero value of current, it follows that the *emf of self-induction in the short-circuited winding element is in phase with the alternating current*.

While the transformer emf in the short-circuited winding element depends upon the pole-flux and the line frequency, and lags  $90^\circ$  behind the pole-flux, the emf of self-induction in the short-circuited winding element depends upon the current and the speed of the armature and is in phase with the current. The fact that the two emf's appearing in the short-circuited element of a single-phase commutator machine have different phase angles with respect to the current, and also depend upon different quantities, make improvement of commutation in the single-phase commutator machine rather difficult.

The cancellation of the emf of self-induction in the short-circuited winding element can be accomplished by means of interpoles in the same manner as in the d-c machine, i.e., by the *rotation* of the short-circuited element *in a commutating flux*. The strength of the commutating flux must be proportional to the current since the emf of self-induction  $e_s$  is proportional to the current. It has been found that the emf induced by *rotation* in an alternating flux is *in phase* with the alternating flux. Therefore, the phase of the commutating flux must be opposite to that of the current; then the emf induced by rotation in this flux will be exactly opposite to  $e_s$ . Fig. 45-5a shows the phasor diagram of the armature current  $I$  and the commutating flux  $\Phi_{is}$  necessary to cancel the emf of self-induction  $e_s$ . The voltage  $e_s$  is in phase with  $I$ , and the flux  $\Phi_{is}$  produces, by rotation, a voltage in the short-circuited winding element which is equal and opposite to  $e_s$ . To produce the commutating flux  $\Phi_{is}$ , the armature current has to be employed just as in the d-c machine; thus, the commutating pole winding has to carry the armature current.

It is quite different, however, with the transformer emf in the short-circuited winding element. In Fig. 45-5b  $\Phi$  is the field flux and  $e_t$  the transformer emf induced in the short-circuited element, lagging  $90^\circ$  behind the field-flux.  $e_t$  cannot be canceled by the transformer effect of a commutating

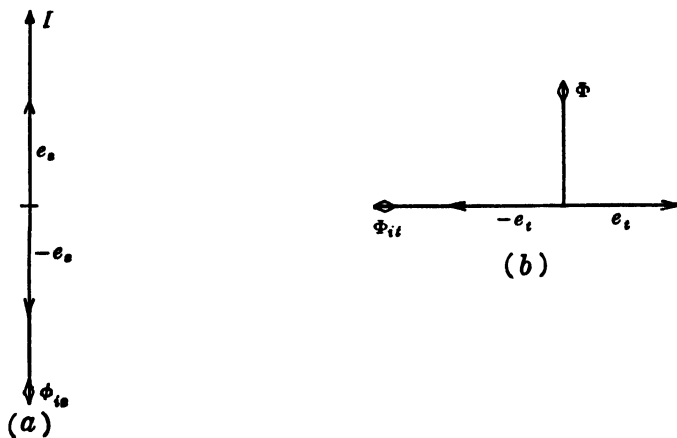


FIG. 45-5. Emf's in the short-circuited winding element and the necessary commutating fluxes.



flux, for this flux would have to be displaced in phase  $180^\circ$  from the field flux, and this would weaken the main flux. If  $e_t$  is to be canceled, this must be accomplished *by rotation* in a commutating flux and this commutating flux must be  $90^\circ$  ahead of the main flux, as shown in Fig. 45-5b. For the cancellation of the transformer emf  $e_t$  in the short-circuited winding element a commutating flux  $\Phi_{it}$  of a different phase and also of a different magnitude is necessary than that required for the cancellation of the emf of self-induction  $e_s$ , because  $e_t$  is proportional to the field-flux and to the line frequency while  $e_s$  is proportional to the current and to the speed of the armature. The manner of producing both of these commutating fluxes is an important consideration in the design of single-phase commutator machines. Both emf's in the short-circuited winding element,  $e_s$  and  $e_t$ , usually are displaced nearly  $90^\circ$  from each other so that the resultant induced emf in the short-circuited path of the single-phase commutator motor is approximately equal to

$$e_r = \sqrt{e_t^2 + e_s^2} \quad (45-4)$$

As will be shown,  $e_r$  is completely canceled by the two commutating fluxes only for a fixed load. For other loads a certain residue remains. Experience shows that for good commutation, i.e., for satisfactory operation of the commutator, this remainder must not exceed 3 volts. This also sets a limit for  $e_t$ . Since the magnitude of the transformer emf  $e_t$  is independent of the armature speed and, on the other hand, since this voltage can be canceled only by *rotation* in a commutating field, it cannot be canceled at low speeds; consequently, *at standstill the transformer emf produces its full effect*. Thus, while starting, there is no means of avoiding the undesirable effect of the transformer emf in the short-circuited winding element, and it must be small (less than 3 volts), unless resistance is inserted between the winding elements and the commutator bars in order to reduce the current in the short-circuited path and the current density under the brush.

From Eq. 45-3 it follows that  $e_t$  can be diminished if the line frequency and the field-flux are made small. This is the reason why, in the case of single-phase traction motors, a frequency of 25 cps ( $16\frac{2}{3}$  cps in Europe) is selected, and why in a-c commutator motors the pole-flux must be kept low in comparison to that of other machines. The low field flux causes a low voltage per winding element. In consequence of this, the commutator of the a-c commutator machine is designed only for low voltage (about 100 volts at 50 to 60 cps, 300 volts at 25 cps, and 500 volts at  $16\frac{2}{3}$  cps). Where the line voltage is higher than these values a transformer is necessary between the line and the armature.

The limit of 3 volts for the residual voltage in the short-circuited coil is determined by the contact resistance between commutator bars and brushes. The greater this contact resistance, the smaller the current in the short-circuited path. Only hard brushes with a high contact resistance are used for

a-c commutator motors; for these brushes a residual voltage of 3 volts is permissible.

### PROBLEMS

1. A 4-pole d-c armature rotates in a sinusoidally distributed alternating flux the maximum value of which is  $1.5 \times 10^6$  maxwells. The armature speed is 1200 rpm. Determine the rotational emf: (a) when the brushes are in the neutral; (b) when the brushes are in the pole axis. The number of turns per path is 80.

2. Determine, for the armature of Problem 1, the transformer emf induced between the brushes: (a) when the brushes are in the neutral; (b) when the brushes are in the pole axis. The frequency of the field current is 25 cycles.

3. Determine, for the armature of Problem 1, the average torque produced if the winding is lap wound, the brushes are in the neutral, and the armature current is 20 amp. The phase angle between armature current and flux is  $20^\circ$ .

4. Determine the ampere-conductors of the compensating winding for the armature of Problem 1 if the armature winding is lap wound and the armature current is 20 amp.

## Chapter 46

### THE SINGLE-PHASE SERIES COMMUTATOR MOTOR

**46-1. The voltage diagram of the single-phase series commutator motor.** The diagram of connections of the single-phase series motor is shown in Fig. 46-1:  $A$  is the armature,  $FW$  the field winding,  $CW$  the compensating winding, and  $IW$  the interpole winding. The brush axis is perpendicular to the field axis, and the axes of the compensating and interpole windings coincide with the brush axis. The connection of the armature, interpole, and compensating windings must be arranged in such a manner that the mmf's of the compensating and the interpole windings act in opposition to the armature mmf (see Arts. 45-2 and 45-3). Since the brush axis is perpendicular to the field (pole) axis, only an emf of rotation ( $E_r$ ) is induced in the armature winding by the pole-flux, between the brushes, but no transformer emf whatever. The compensating winding nullifies the mmf of the armature winding. The field winding  $FW$  as well as the interpole winding  $IW$  is designed as a concentrated winding in a manner similar to the d-c machine.

Kirchhoff's mesh equation for the circuit of Fig. 46-1 is

$$\dot{V} - j\dot{I}\Sigma x = \dot{I}\Sigma r + \dot{E}_r \quad (46-1)$$

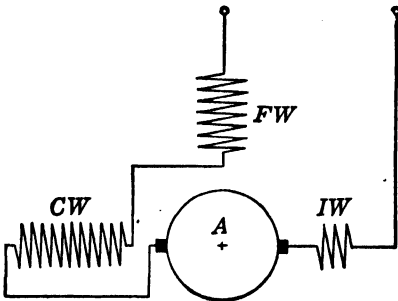


FIG. 46-1. Schematic diagram of the connections of a single-phase series commutator motor.

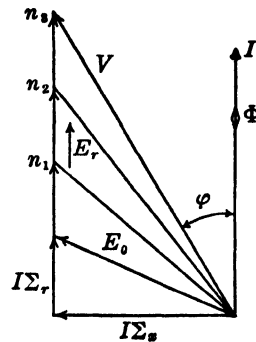


FIG. 46-2. Voltage diagram of the single-phase series commutator motor.

The meaning of  $\Sigma x$  and  $\Sigma r$  is explained below.  $E_r$  (Art. 45-1) is in phase with  $I(\Phi)$ , as is  $I\Sigma r$ , and is placed together with  $I\Sigma r$ .

The voltage diagram corresponding to the connections of Fig. 46-1 can be established easily. All four windings carry the same current  $I$ . The pole-flux  $\Phi$  is produced by, and is in phase with, the current  $I$  (Fig. 46-2). Accordingly, the emf of rotation in the armature winding  $E_r$  is in phase with  $I$ . If  $\Sigma r$  represents the sum of the resistances of the four windings and  $\Sigma x$  the sum of the leakage reactances of armature and compensating winding plus the reactances of the field and interpole winding, then, according to Kirchhoff's mesh equation, the impressed voltage  $V$  is equal to the geometric sum of the voltage drops  $I\Sigma r$  and  $I\Sigma x$  and the emf of rotation in the armature winding  $E_r$ . The iron losses in the stator are considered as an  $I^2R$  loss and are included in  $I\Sigma r$ . On the other hand, the iron losses of the rotor are for the greatest part of a mechanical nature similar to the windage and friction losses (see Art. 29-1b) and are considered as a mechanical power loss. The reactance of the field winding constitutes the greatest part of the sum  $\Sigma x$ . In Fig. 46-2 the emf of rotation  $E_r$ , which is in phase with  $\Phi$  and  $I$ , is drawn for three different speeds. At constant current  $I$  this emf of rotation  $E_r$  is a measure of the developed mechanical power of the rotor (see Art. 1-2d): as such, it behaves as a dissipative resistance and is in phase with  $I\Sigma r$ . The mechanical power delivered at the shaft is less than the product  $E_r I$  by the amount of the rotational iron losses in the rotor plus the windage and friction losses.

As Fig. 46-2 shows, the phase displacement angle  $\varphi$  of the single-phase series motor decreases with decreasing  $I\Sigma x$ ; further, it decreases considerably with increasing rpm, because with increasing rpm  $E_r$  increases in comparison to  $I\Sigma x$ . For high speeds the power factor approaches a value  $\cos \varphi = 0.95$ .

Analogous to the circle diagram of the induction motor, a circle diagram for the current (at constant voltage) can also be derived for the single-phase commutator motor. However, this circle diagram is not of great value because the single-phase series motor, in contrast to the induction motor which operates over the normal working region with an almost constant flux, it has a varying flux, i.e., a varying saturation of the path of the main flux and, therefore, a varying field winding reactance; this factor cannot be taken into consideration in the circle diagram.

#### 46-2. Commutation of the single-phase series commutator motor.

The phasor diagram of fluxes and emf's for the short-circuited winding element is obtained by superposition of Figs. 45-5a and 45-5b where it has to be noted that  $\Phi$  is in phase with  $I$ . Fig. 46-3 shows this diagram. The resulting emf  $e_r$  in the short-circuited element lags the current by a fixed angle. The generation of the oppositely directed emf  $-e_r$  is to be accomplished by means of the resulting commutating flux  $\Phi_i$ , and the task of the interpole

winding is to furnish this flux. The interpoles cannot be excited by the armature current directly, for the resulting interpole flux  $\Phi_i$  and the armature current  $I$  are not in phase. The interpole winding must be excited by a current which lags the armature current  $I$  by the same angle by which  $e_r$  lags  $I$ . This will occur if a resistance  $R$  is connected in parallel with the interpole winding as Fig. 46-4 shows. If  $V_i$  is the voltage common to the interpole winding and the resistance  $R$  (Fig. 46-5), then the current  $I_i$ , which flows in the interpole winding, lags behind  $V_i$  by about  $90^\circ$ , because the reactance of this winding is small in relation to its reactance; on the other hand, the current  $I_R$ , which flows in the resistance  $R$ , is in phase with  $V_i$ . Since the geometric sum of  $I_i$  and  $I_R$  must be equal to the armature current  $I$ , the interpole current  $I_i$  is caused, by the parallel resistance  $R$ , to lag behind the armature current, and it can therefore produce the necessary resulting commutating flux  $\Phi_i$ . It should be

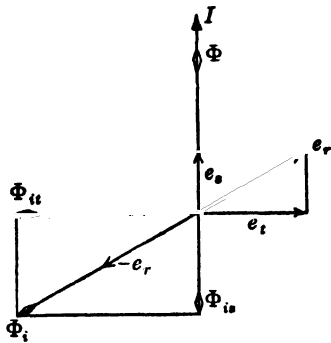


FIG. 46-3. Phasor diagram of the emf's in the short-circuited winding element and of the commutating fluxes.

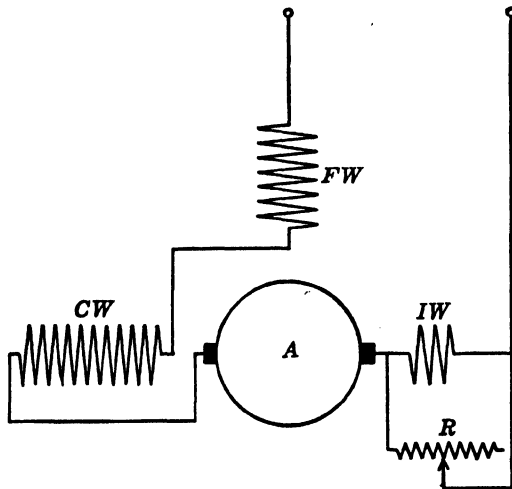


FIG. 46-4. Resistance in parallel with the interpole winding for producing the commutating fluxes according to Fig. 46-3.

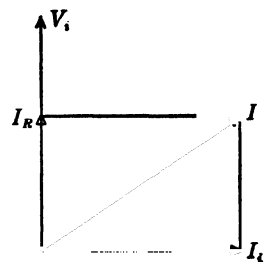


FIG. 46-5. Current diagram for interpole winding and resistance of Fig. 46-4.

remembered (see Art. 45-3) that the arrangement for improving the commutation shown in Fig. 46-4 is effective only within a certain range of motor speed; it is not effective at low speeds.

**46-3. Torque and characteristic curves of the single-phase series commutator motor.** Since the flux in the single-phase series motor is in phase with the armature current, and the brush axis makes an angle of  $90^\circ$  with the field axis, the torque, in accordance with Eq. 45-2, is

$$T = \frac{7.04}{n} E_r I \quad \text{lb.-ft.} \quad (46-2)$$

The magnitude of the armature rotational emf  $E_r$  can be determined from Eq. 14-9, if it is remembered that it is proportional to the frequency of rotation of the armature, though its actual frequency is equal to the line frequency (Art. 45-1a). Thus

$$E_r = 4.44(pn/120)N k_{ap} \Phi \times 10^{-8} \quad (46-3)$$

$N$  is the number of turns per circuit (between two brushes). If  $Z$  is the total number of conductors of the armature

$$N = \frac{Z}{2a} \quad (46-4)$$

For the d-c armature winding  $k_a = 2/\pi$ : when the number of slots in the coil group ( $q$ ) is large, the distribution factor can be defined as the ratio of chord to arc (see Fig. 14-1). For the d-c armature winding this ratio is equal to the ratio of diameter to the length of half a circle  $= 2/\pi$  (Fig. 45-1). The d-c armature windings are almost full-pitch, so that  $k_p = 1$  (Eq. 14-8).

Inserting Eqs. 46-3 and 46-4 and also  $k_a = 2/\pi$  and  $k_p = 1$  into Eq. 46-2, the equation for the torque can be written as

$$T = 0.083(p/a)Z\Phi I \times 10^{-8} \quad \text{lb.-ft.} \quad (46-5)$$

Speed control in the single-phase series motor is accomplished by *voltage control*. For a given torque (given armature current) the counter-emf ( $E_r$ ,

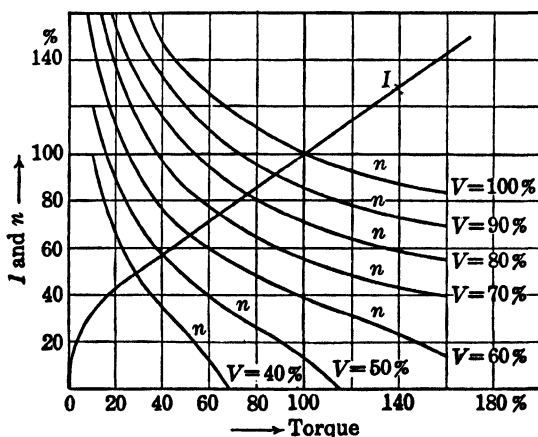


FIG. 46-6. Speed-torque characteristics and torque-current characteristic of the single-phase series motor.

in Fig. 46-2) increases as the voltage increases and, therefore, the speed increases with increasing voltage. For the purpose of speed control the transformer secondary is tapped, and the speed control is accomplished economically.

The relation between torque and current, as well as that between torque and speed for various voltages, is shown in Fig. 46-6. Rated values of torque, speed, etc., are taken as 100%. The general trend of the current as well as of the speed curve is the same as that in a d-c series motor. The greater the voltage, the greater will be the speed for the same torque. The line current for a given torque is independent of the magnitude of the voltage. In order to develop rated torque at start, 45 to 50% of the rated voltage is necessary. For satisfactory commutation the speed range of the single-phase series motor is between 20 and 150% of rated speed.

**46-4. The universal motor.** The A.S.A. definition of a universal motor is as follows:

A universal motor is a series-wound or a compensated series-wound motor which may be operated either on direct current or single-phase alternating current at approximately the same speed and output. These conditions must be met when the direct-current and alternating-current voltages are approximately the same and the frequency of the alternating current is not greater than 60 cps.

As can be seen from this definition, there are two types of universal motors: the non-compensated and the compensated. The non-compensated motor has salient poles just as the d-c machine; the compensated motor has slotted stator punchings, such as the traction motor described in Art. 46-1.

The universal motor is a fractional-horsepower motor and is usually designed for speeds of 3500 rpm or less, but also up to 10,000 or 15,000 rpm. The no-load speed may be as high as 20,000 rpm. The non-compensated motor is less expensive than the compensated motor, but its operating characteristics are not as good as those of the compensated motor.

### PROBLEMS

1. The sum of the resistances of the field winding, compensating winding, armature winding, and interpole winding of a 25-cycle, single-phase series motor is 1.5 ohms. The sum of the reactances of these windings is 4.5 ohms. At a current of 5 amp the flux per pole is  $475 \times 10^3$  maxwells. Determine the speed of the motor, if the number of poles is 4, the number of turns per path is 60, and the terminal voltage is 120 volts.

2. Determine the terminal voltage necessary to reduce the speed of the motor of Problem 1: (a) by 20%; (b) by 30%. Torque remains the same as in Problem 1.

3. Determine the terminal voltage necessary to increase the speed of the motor of Problem 1; (a) by 20%; (b) by 30%. Torque remains the same as in Problem 1.

4. Determine the torque of the motor of Problem 1 if the winding is lap wound. The brushes are in the neutral.

5. A 2-pole, 25-cycle, single-phase series motor has a total field resistance of 0.80 ohm and each pole has 150 turns. A field current of 10.0 amp produces a voltage across the field of 50 volts. Determine the reactance of the field in ohms and the pole flux. Neglect leakage.

6. The armature of the 25-cycle motor in Problem 5 is wound with winding elements having 8 turns. What is the maximum flux permitted to link a winding element if the maximum rms transformer voltage between commutator bars is limited to 3 volts.

7. If the power input to the machine of Problem 1 is 500 watts when  $\cos \varphi = 0.85$  and the terminal voltage is 71 volts, determine the emf of rotation.



## Chapter 47

### THE REPULSION MOTOR

**47-1. The voltage diagram of the repulsion motor.** The circuit of the repulsion motor is shown in Fig. 47-1. The stator winding (field winding *FW* and compensating winding *CW* in series) is connected to the line and is completely detached electrically from the armature winding; the armature is short-circuited on itself by the brushes. Since the commutator is not included in the circuit containing the stator winding, the latter may be designed for any voltage desired.

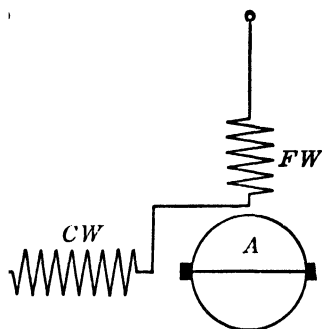


FIG. 47-1. Schematic connection diagram of the repulsion motor.

The compensating winding *CW* and the armature constitute a transformer; by this means the load current which is necessary to produce the torque is transferred by induction from the lines to the armature. The compensating winding, therefore, can be designated as the *stator torque winding*. The torque is produced by the armature current and *main flux*; the brush axis is

perpendicular to the field (pole) axis, exactly as in the series motor. The cross-flux in the load (horizontal) axis cannot produce torque with the armature currents, because its axis coincides with the brush axis, i.e., because with respect to this flux the current distribution in the armature is such that the torques of the individual coils mutually cancel themselves (see Art. 45-2).

*At start* the repulsion motor behaves exactly as the series motor. At start, in both motors, the voltage impressed across the terminals is consumed essentially by the field winding, because of its high reactance. At start the compensating winding and the armature winding require only a small part of the total voltage, namely, the short-circuit voltage of their leakage reactances and resistances, since the fluxes produced by these windings cancel each other. The armature current is displaced practically  $180^\circ$  behind the pole-flux, which is produced by a current of the same phase as the current in the torque winding (winding *CW*); therefore, the conditions for developing a high starting torque are just as favorable as in the series motor.

When running, an emf is induced in the armature by the pole-flux as well as by the cross-flux. The pole-flux produces an emf of rotation  $E_r$  in the armature which is in phase with this flux and the field current, and consequently with the current in the torque winding (winding  $CW$ ), since these currents are always equal. The armature current, produced by transformer action with the torque winding, is displaced in phase nearly  $180^\circ$  from the field current, so that the emf  $E_r$  of rotation and the current transferred by transformer action are likewise displaced in phase nearly  $180^\circ$  from one another. The emf of rotation  $E_r$  consequently acts on the transformer consisting of the torque winding (winding  $CW$ ) and the armature as the *counter-voltage of an ohmic resistance*; when running, the transformer appears non-inductively loaded, and the terminal voltage at the primary of the transformer, i.e., at the torque winding, must rise by an amount corresponding to the emf  $E_r$ ; therefore, when running a voltage, in phase with the current, appears at the terminals of the torque winding  $CW$ , in addition to the short-circuit voltage which appears at standstill. Since this voltage at the torque winding can be produced by transformer action only, its appearance is possible if a *cross-flux* ( $\Phi_q$ ) is developed in the torque axis which is displaced in phase  $90^\circ$  relative to this voltage. Thus two fluxes, the pole-flux and the cross-flux, are to be considered. Kirchhoff's equations of stator and rotor circuits are

$$V_1 + E_{1t} - jI_1(x_f + x_c) = I_1(r_f + r_c) \quad (47-1)$$

$$E_{2t} + E_r - jI_2x_2 = I_2r_2 \quad (47-2)$$

Fig. 47-2 shows the voltage diagram of the repulsion motor. The stator current  $I_1$  and the pole-flux  $\Phi$  are drawn upward along the vertical. The armature emf of rotation  $E_r$  is in phase with  $\Phi$ . The geometric sum of  $E_r$  and the emf  $E_{2t}$  induced in the armature by the transformer action of the cross-flux  $\Phi_q$  must be equal to the resistance and reactance voltage drops in the armature winding  $I_2r_2$  and  $I_2x_2$ . The cross-flux  $\Phi_q$  is produced in the torque winding by a magnetizing current  $I_m$ . Consequently, the stator current  $I_1$  is equal to the geometric sum of  $-I_2$  and  $I_m$ . The stator voltage  $V$  must be large enough to overcome the transformer emf of the compensating winding  $E_{1t}$ , and besides provide for the resistance and reactance voltage drops of the field and compensating windings  $I_1(r_f + r_c)$  and  $I_1(x_f + x_c)$ .

The armature field is canceled in the repulsion motor in the same manner as in the series motor (Fig. 46-1). It is necessary to distinguish between the armature flux and the cross-flux  $\Phi_q$ , for the armature flux is in phase with the current  $I_2$  while the cross-flux is displaced in phase about  $90^\circ$  from the current  $I_2$ .  $x_2$  consists of only the leakage reactance of the armature winding. Correspondingly  $x_c$  consists of only the leakage reactance of the compensating winding; on the other hand,  $x_f$  includes the complete self-inductance of the field winding, as in the series motor.

As was mentioned previously, the cross-flux  $\Phi_q$ , which takes no part in the

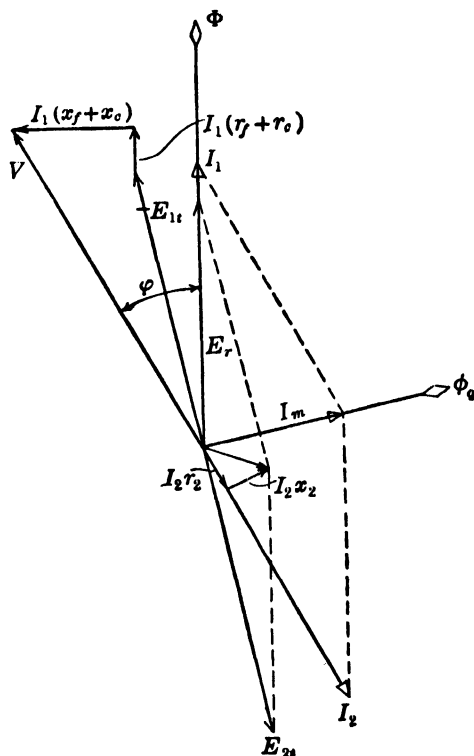


FIG. 47-2. Flux and voltage diagram of the repulsion motor.

production of torque, is absolutely essential for the transfer of power from the stator to the rotor. The pole-flux  $\Phi$  and the cross-flux  $\Phi_q$  are displaced exactly  $90^\circ$  from each other in space phase and almost  $90^\circ$  in time phase. This results in a *rotating flux*. The speed of this rotating flux is

$$n_s = \frac{120f}{p}$$

if  $f$ , as in the discussions preceding, is the line frequency. Thus the repulsion motor at standstill has an alternating flux and develops a rotating flux during running.

**47-2. Commutation of the repulsion motor.** The repulsion motor has no interpoles for improvement of commutation. At standstill the transformer emf appears in the short-circuited winding element, just as in the single-phase series motor, and the current of the short-circuit path is limited by the contact resistance between brush and commutator bars. The fact that the repulsion motor develops a rotating flux while running is of importance for its commutation during running: it is evident that, when the short-circuited

winding element has the same speed as the rotating flux, no voltage is induced in it by the rotating flux. Thus, at synchronous speed of the rotor, no transformer emf appears in the short-circuited winding element. The influence of the transformer emf on commutation is largest at standstill; it decreases as the motor speed increases; it becomes zero at the synchronous speed of the motor, and increases again as the speed becomes larger than the synchronous speed. Consequently, the repulsion motor is *best operated near synchronous speed*.

**47-3. Characteristic curves of the repulsion motor.** Since the ratio of the field current to the armature current is fixed as a result of the series connection of the field and torque windings, the repulsion motor has the *characteristic of a series motor*.

Fig. 47-3 shows the field and compensating windings of Fig. 47-1 combined into a *single* winding. The connections of Figs. 47-1 and 47-3 are entirely equivalent to one another. This becomes evident if the stator winding of Fig. 47-3 is assumed divided into two parts, one of which has its axis in the direction of the brush axis and the other perpendicular to the brush axis. Fig. 47-3 represents the actual coil arrangement of the repulsion motor. By means of a *brush displacement* the stator winding can be distributed in any manner selected into a field and a compensating winding; in this manner the *speed and the torque of the motor can be varied*, since a variation of the number of field turns gives rise to a variation in the flux ( $\Phi$ ) which produces the torque.

The two extreme brush positions are found when the brush axis is perpendicular to the axis of the stator winding ( $\alpha = 0^\circ$ ), and when the brush axis coincides with the axis of the stator winding ( $\alpha = 90^\circ$ ). In the first case ( $\alpha = 0^\circ$ ) the armature current and torque of the motor are zero: this position is the *zero position* of the brushes. In the second case ( $\alpha = 90^\circ$ ) the motor behaves as a short-circuited transformer: this position is the *short-circuit position* of the brushes. Here, in spite of the very large current in both windings, the torque is zero because the torque-producing pole-flux is missing. Because of the large currents which can damage the windings, the motor should not be connected to the line with the brushes in this position.

At start the brushes are placed first at the zero position and then moved in one direction or the other. The *direction of rotation* of the rotor may be determined by the following considerations: if a short-circuited and movable coil is placed in the alternating field produced by a fixed coil, the movable coil seeks to adjust itself *with the shortest travel* so that the flux passing through it becomes a minimum; its axis attempts to take a position perpendicular to

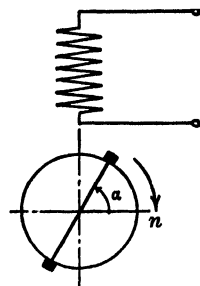


FIG. 47-3. Actual winding arrangement of the repulsion motor.

the axis of the field. Accordingly, the armature shown in Fig. 47-3, which may be taken as a short-circuited solenoid with the same axis as the brush axis, will try, by rotation, to bring its axis (the brush axis) to the right (clockwise) and along the horizontal. Since the brushes are immovable and the armature itself can move under the brushes, the armature itself will turn to the right (clockwise) and continue to rotate because the current distribution in the armature remains unchanged due to the fixed position of the brushes. In Fig. 47-3 the brushes are displaced by an angle  $\alpha$  from the zero position in a counter-clockwise direction and the resulting rotation of the armature is clockwise. If the brushes are shifted from the zero position in a clockwise direction, the armature rotates counterclockwise; i.e., *the direction of rotation of the armature is always opposite to the displacement of the brushes from the zero position*. In order to reverse the direction of rotation of a repulsion motor it is necessary only to place its brushes in an *opposite position* with respect to the zero position.

Fig. 47-4 shows the starting torque of the repulsion motor as a function of the brush position,  $\alpha$ . The maximum torque is obtained at a brush shift of about  $75^\circ$  to  $80^\circ$ . Starting is accomplished by shifting the brushes far enough from the zero position and against the desired direction of rotation until the magnitude of the motor torque exceeds the opposing torque of the load; the motor then runs and carries the load.

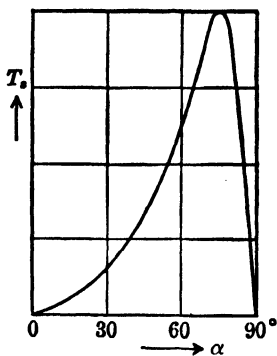


FIG. 47-4. Starting torque of the repulsion motor as a function of the brush angle.

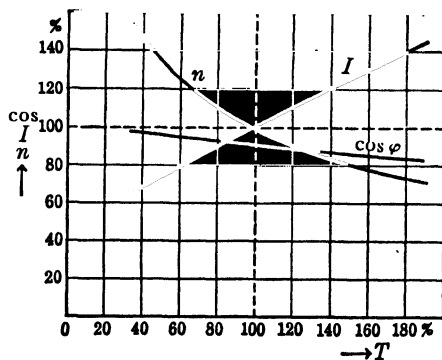


FIG. 47-5. Speed-torque characteristic and torque-current characteristic of the repulsion motor, for a fixed brush position.

At rated load the brush shift depends upon the construction of the motor and is  $67^\circ$  to  $77^\circ$ . The relation between torque, speed, stator current and power factor at the brush position for rated output is shown in Fig. 47-5. As in Fig. 46-6 all quantities are given as a percentage of their value at rated load. The speed-torque characteristic of the repulsion motor follows the same general trend as that of the series motor. Fig. 47-6 shows the relation between torque and speed for various brush positions,  $\alpha$ . This figure is

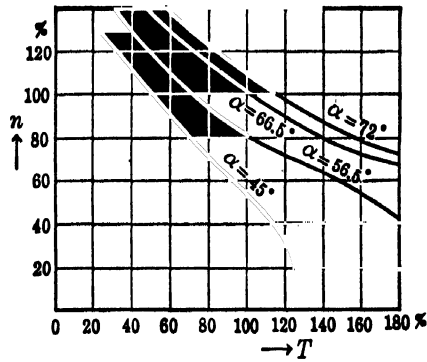


FIG. 47-6. Speed-torque characteristics of the repulsion motor for various brush positions.

similar to Fig. 46-6 which shows the speed of the series motor as a function of the torque for various voltages. The various voltages in Fig. 46-6 (speed control by variation of voltage) correspond to the various brush positions in Fig. 47-6 (speed control by change in the field).

## Chapter 48

### THE 3-PHASE SHUNT COMMUTATOR MOTOR (THE SCHRAGE MOTOR)

Since the 3-phase shunt motor is the most widely used of the polyphase commutator motors, it will be the only one considered in this discussion.

**48-1. Connection diagram and speed control of the 3-phase shunt commutator motor.** As was explained in Art. 23-3c, the speed of an induction motor can be regulated by means of a voltage impressed on its secondary winding which has the same direction and frequency as the emf induced in this winding by the rotating flux. If the voltage impressed upon the secondary winding is in phase with the induced emf, the speed of the rotor will rise, for a smaller induced emf, and consequently a smaller slip is necessary to produce the secondary current required for the opposing torque. On the other hand, if the voltage impressed on the secondary winding is displaced  $180^\circ$  in phase from the induced emf, the speed of the rotor will fall, for a greater secondary emf, and consequently a greater slip is necessary to produce the secondary current required for the opposing torque. By a suitable selection of the phase and magnitude of the impressed voltage, it is possible, therefore, to regulate the speed of an induction motor below as well as above synchronous speed.

The voltage impressed upon the secondary winding, for the purpose of regulating the speed, must have the same frequency as the emf induced in this winding by the rotating flux, i.e., the slip frequency, and it must change its frequency according to the load. In the treatment of the induction motor, it has been mentioned already that such a voltage of variable frequency can be generated by means of a polyphase commutator machine. The 3-phase shunt motor described in the following is a combination of a polyphase rotor-fed induction motor and a polyphase commutator machine in one armature and one stator.

Fig. 48-1 shows the connection diagram of the 3-phase shunt motor. Its rotor has two windings, one of which is connected to slip rings and the other to a commutator; its stator has only one winding. The line is connected to the slip rings *UVW*. Neither the commutator winding of the rotor nor the stator winding is connected to the line. The three separate phase windings of

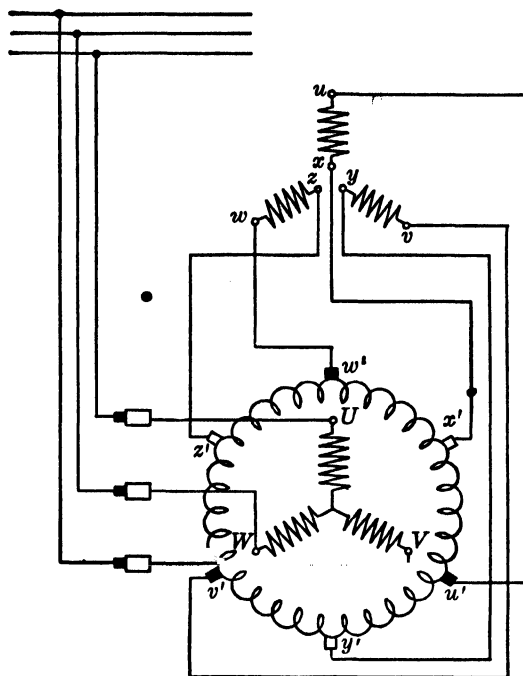


FIG. 48-1. Schematic connection diagram of the 3-phase shunt motor (Schrage motor).

the stator are not connected to each other but are open; each of these phase windings is connected to two brushes which may be moved in *opposite* directions on the commutator. Accordingly, the 2-pole machine has 6 sets of brushes.

Relative to the *rotor* the speed of the rotating flux produced by the rotor (primary) winding is always the same,  $n_s = 120f_1/p$ . The relative velocity of the rotating flux in relation to space (stator) depends upon the speed of the rotor. As in the case of every rotor-fed induction motor, the direction of rotation of the rotor is always opposite to that of its rotating flux, for both motor and generator operation; the speed of the rotating flux relative to the *stator* is  $n_s$  at standstill and zero at synchronous speed. Consequently, the frequency of the emf's induced in the stator windings by the rotating flux is slip frequency, and rotor and stator mmf waves are at standstill with respect to one another at any rotor speed, i.e., the necessary condition for the development of a uniform torque is satisfied.

The frequency of the voltage at the commutator *brushes* can be determined from the following consideration. In a d-c machine the magnetic field is at standstill and the frequency of the current at the brushes is zero and independent of the armature speed ( $n$ ). If the brushes of a d-c machine were made to rotate with a certain speed  $n'$ , an a-c instead of a d-c voltage would be measured at the brushes and the frequency of this a-c voltage would be



determined by the speed of the brushes  $n'$  but not by the armature speed  $n$ . Vice versa, if the magnetic flux (poles) of a d-c machine were made to rotate with a speed  $n'$  relative to the space, again an a-c voltage would be measured at the brushes and the frequency of this voltage would be determined solely by the speed of the magnetic flux relatively to space,  $n'$ . In the 3-phase shunt motor connected according to Fig. 48-1, the magnetic flux rotates with the speed  $(n_s - n) = sn_s$  with respect to space. Therefore the frequency of the voltage at the brushes is  $sf_1$ , i.e., the same as in the stator winding, and brushes and stator winding can be connected together.

The magnitude of the voltage impressed on the stator winding (the brush voltage) is changed in the rotor-fed shunt motor by changing the spacing between the brushes of each brush pair, i.e., the distances  $u'x'$ ,  $v'y'$ , and  $w'z'$  (Fig. 48-1). The commutator voltage increases with the distance between the brushes. The greatest voltage is delivered by the commutator when the distance between the two brushes of the brush pairs is 180 electrical degrees. If both brushes of the brush pairs are on the same commutator bar, the voltage impressed on the stator winding is zero, each of the three stator windings is short-circuited, and the machine behaves as an ordinary induction motor.

The speed control is continuous, and the maximum range of control is determined by the maximum voltage available at the commutator brushes. With respect to commutation this voltage is made about one half of the voltage induced in the open stator winding at standstill: this will produce a

speed range of from  $\frac{1}{2}$  to about  $1\frac{1}{2}$  times synchronous speed, i.e., a speed regulation in the ratio 1:3 is achieved.

If a constant brush voltage is impressed on the stator winding, the speed characteristic is displaced more or less upward or downward according to the magnitude and phase of this voltage. Fig. 48-2 shows three speed-torque characteristics assuming that the regulation at no-load is in the ratio of about 1:3. The upper and lower curves show the same trend as the middle curve for which the brush voltage is equal to zero and which is, therefore, identical with the speed characteristic of the ordinary induction motor. The slip increases and therefore the speed decreases with increasing torque. By inserting resistance in

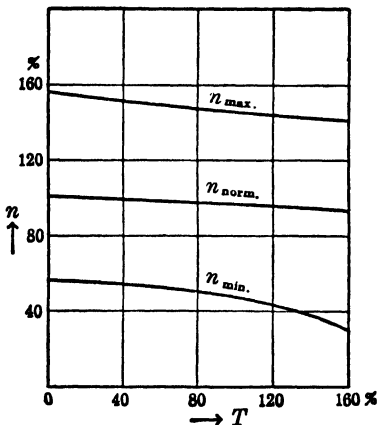


FIG. 48-2. Speed-torque characteristics for a speed ratio of 1:3 at no load.

the stator circuit it is also possible to extend the range of regulation further downward, just as in the induction motor. The appearance of a 3-phase shunt commutator motor is shown in Fig. 48-3.



FIG. 48-3. Three-phase shunt motor (Schrage motor).

**48-2. Power-factor correction of the 3-phase shunt motor.** Power-factor correction can be attained in the induction motor by impressing a voltage on the secondary winding which leads the emf induced in it by the rotating flux by  $90^\circ$ . When speed regulation alone is desired, the axis of each brush pair must coincide with the axis of the proper stator phase. The change in spacing between the brushes, in order to vary the speed, is accomplished by arranging the pairs of brushes in separate brush yokes which may be displaced from each other in opposite directions. In order to obtain power-factor correction the axis of a brush pair must be displaced from the axis of the corresponding stator phase by a fixed angle.

Assuming a regulation at no-load of about 1.3, as shown in Fig. 48-2, the relation between the power factor and the torque of the 3-phase shunt motor is given in Fig. 48-4. The power factor curve for  $n_{\text{normal}}$  is exactly the same as that of the ordinary induction motor: in this case the brush voltage is zero. The curve for the higher speed,  $n_{\text{max}}$ , produces a leading power factor at the larger values of torques in consequence of the power-factor correction. For the curve at the low speed,  $n_{\text{min}}$ , the no-load power factor must be unity or leading in order that the power factor at larger torques does not become too low.

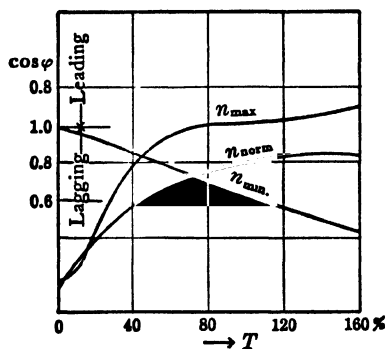


FIG. 48-4. Power factor of the 3-phase shunt motor as a function of torque.

**48-3. Commutation of the 3-phase shunt motor.** Since the rotating flux of the 3-phase shunt motor with power supply through the slip rings has a constant speed ( $n_s$ ) with respect to the armature, the emf induced by it in the short-circuited winding element is constant and independent of the

speed. The emf of self-induction in the short-circuited winding element depends upon the range of speed regulation. At synchronous speed this emf is zero, for at this speed the brushes of each brush pair are placed on the same commutator bar, and commutation of current does not take place. It is low for a small range of speed variation. No special means are available to improve the commutation of a 3-phase shunt motor (such as the interpoles of a d-c motor or of an a-c single-phase series motor). Therefore, the emf of the short-circuited winding must be kept small, and hard brushes with a high contact resistance must be used.

### PROBLEMS

1. The adjustable-speed, 3-phase, slip-ring fed, shunt motor (Schrage motor) is designed to increase the speed at no-load by 40% and to decrease the speed at no-load by 55%. What should be the maximum brush voltage impressed upon the stator winding in percent of the voltage of the open stator winding at standstill? Assume that the line frequency is 60 cycles. What is the frequency of the brush voltage at 140% and 45% of the no-load speed.

2. At constant torque for the motor considered in Problem 1, approximately what will be the power of the commutator winding in percent of the motor power input at 40% higher speed and at 55% lower speed.

3. The secondary frequency of the induction motor is greater than the line frequency only when its rotor runs against the rotating flux. Is it possible to produce a stator frequency in the Schrage motor larger than the line frequency, with the rotor running in the same direction as the rotating flux? If so, what should be the brush voltage, in percent of the voltage at the stator-winding terminals at standstill, in order that the secondary frequency be 130 cycles? The line frequency is 60 cycles.

## Chapter 49

### MOTOR APPLICATION · STARTING SPEED CONTROL · PROTECTION

The problem of motor application consists essentially in finding first the *requirements of the load*, such as horsepower, variation of speed, torque, starting torque, acceleration characteristics, the duty cycle, and the surrounding or operating conditions. In order to specify the motor to fit these requirements, the character of the power supply must be known, as well as the operating characteristics of the various motors which are available. If the motor and its control have been properly chosen and applied it will be able to start the load from rest, and accelerate it to full speed without injury to the motor or the load and without putting an undue strain on the power lines. The load will be carried satisfactorily through whatever duty cycle is required, and the capacity of the motor will be adequate for such momentary overloads as may be required by the load without shutting down the motor or overheating it. Many installations are served satisfactorily by general-purpose motors, which are readily available and standardized according to generally accepted standards set up by NEMA (National Electrical Manufacturers Association). The discussion to follow considers only the general fundamentals of motor application. (See references for additional inf.)

**49-1. Characteristics of Loads.** An important characteristic of motor loads is the *relation of torque to speed*. Many industrial loads are *essentially constant speed*, that is, a variation in speed of 5 to 15% is of not particular importance. Such loads are constant-speed conveyors, pumps, fans, blowers, wood-working machines, metal-working machines, motor generator sets, line shafting, compressors, power-plant auxiliaries, grinders, concrete mixers, laundry machinery, looms in textile mills. Since these loads are essentially constant-speed loads, the *increase in load is brought about by increased torque requirements*, such as are produced by adding load to a motor-generator set, adding material to a conveyor, etc. In this type of load, the output therefore is proportional to the load torque. Any constant-speed motor such as d-c shunt, induction or synchronous with suitable starting torque and pull-out torque may be applied to these loads.

On the other hand many loads require that the *speed be adjustable* over a

wide range for various conditions of operation, but that the speed regulation still be within 10 to 15%. Such loads are fans, blowers, machine tools, some types of printing presses, some textile machinery, paper machines. Adjustable speed loads are of three general types, (1) in which the torque is essentially constant at all speeds, (2) in which the output requirements are practically constant at all speeds, and (3) those in which the torque is inherently variable. Typical of (1) are conveyors (when variable speed is needed) and automatic machine tools; in this type of load the output varies directly with the speed and the motor is called a constant-torque adjustable-speed motor. The best type of control for these devices, i.e., the one requiring the smallest motor, is the d-c shunt motor with an adjustable armature voltage supply. This is not always practical, so a d-c shunt motor designed for adjustable speed by field control may be used for such loads. The wound-rotor induction motor with a resistor in the rotor circuit may be used provided the speed range is not too great, or a brush-shifting commutator motor may be used. Type (2) loads include most machine tools, where the speed is reduced as the size of cut is increased. A d-c shunt motor designed for adjustable speed by field control is well suited for this type of load, although where the range of speed is not more than 1:2 the wound-rotor motor may be used. Type (3) loads include fans, blowers, and centrifugal pumps. In these loads the torque increases with about the square of the speed, so that the power output required varies as the cube of the speed. Loads of this type usually require low starting torque. Where practically constant speed is required, the single phase or polyphase, squirrel-cage induction is indicated. *A d-c motor with field control is best suited for wide speed ranges.*

The *starting torque* required by the load is an important factor in determining the type of motor. Loads such as fans, blowers, centrifugal pumps, unloaded compressors, machine tools, etc., usually require a *low starting torque*, i.e., one considerably less than full-load torque, perhaps 30 to 50%. Other loads, such as loaded compressors, pumps, ball mills used for grinding ore, and conveyors, start under load. In addition to the load there may be considerable standing friction to be overcome, where the machinery has been standing idle for some time. This type of load requires *high starting torque* to break away from standstill, and the starting torque required may be as high as 300% for some loads. Certain loads, such as band saws, centrifugal compressors, wood chippers, and others, have high inertia. While these machines may be started unloaded, the high inertia may require long starting periods and consequent heating of the motor, unless adequate torque is provided for quick acceleration. If high inertia as well as high load torque is encountered, the starting requirement is especially difficult.

Another important factor in motor application, is the surrounding conditions under which the motor must operate. If the ambient temperature is high, special motor insulation may be required, or in any case a larger size than for normal ambient temperature (40° C); or perhaps special ventilating

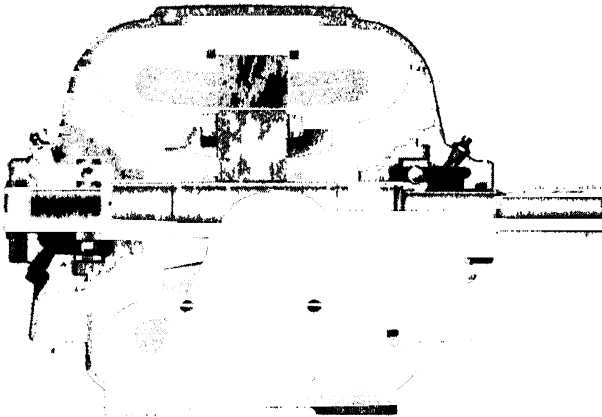


FIG. 49-1. Cut-away view of a splash-proof ball-bearing squirrel-cage induction motor showing baffle and general construction.

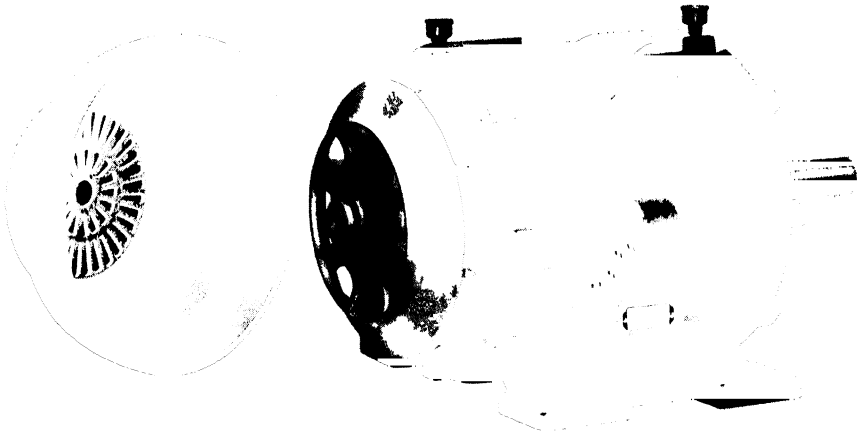


FIG. 49 2. Totally enclosed 7 1/2-hp fan-cooled induction motor.

methods may be required. The new type of plastic insulation (silicon) evidently will make possible operating under higher temperatures. If the surrounding air contains dust, corrosive or explosive gases, salt air, excessive moisture, the motor will require special enclosures to protect the windings and any sliding contacts such as a commutator or slip rings. Motor enclosures are available as splash-proof, drip-proof, dust-proof, explosion proof, etc. (see Definitions, Art. 49-17), to take care of these conditions. Fig. 49-1 shows the features of splash-proof construction applied to an induction motor, and Fig. 49-2 shows a totally enclosed fan-cooled induction motor. Fig. 49-3 shows the application of a totally enclosed fan-cooled motor in a grain elevator.

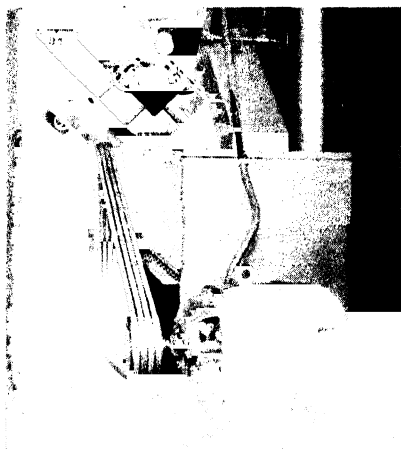


FIG. 49-3. Totally enclosed fan-cooled 10-hp induction motor driving a conveyor in a grain elevator.

The manner of connecting the load to the motor also must be considered. A belt or chain connection requires that the bearings of the motor be adequate to stand the strain caused by the belt or chain. Direct connection through couplings or by gear does not put as much strain on motor bearings as the belt or chain connection, and the former methods are used when possible. The V-belt drive (Fig. 49-3) usually is preferred over the flat belt for short shaft centers.

49-2. Motor Types, Sizes, and Costs. The frame size of a motor depends basically upon such factors as *horsepower, speed, temperature* (both ambient and the allowable rise), the duty cycle of operation, and type of motor enclosure. The horsepower rating required for a driven machine usually can be obtained from the manufacturer. In some cases, such as hoists, pumps, fans, etc., the horsepower can be calculated with considerable accuracy,

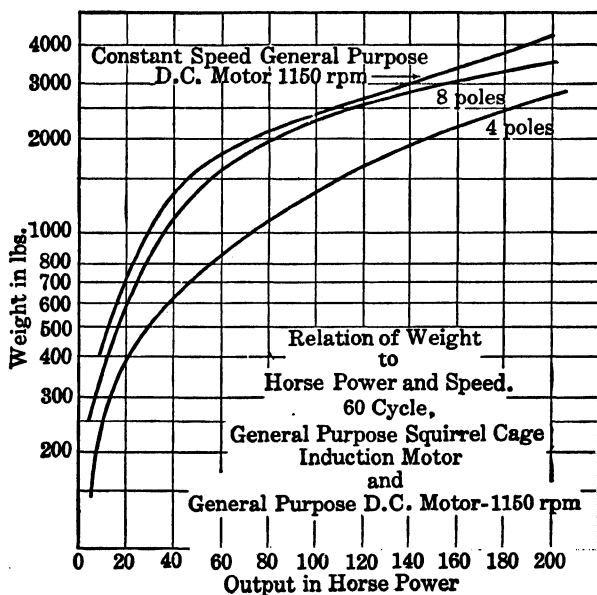


FIG. 49-4. Relation of weight to horsepower and speed for general purpose squirrel-cage induction motors and general purpose d-c shunt and compound motors.

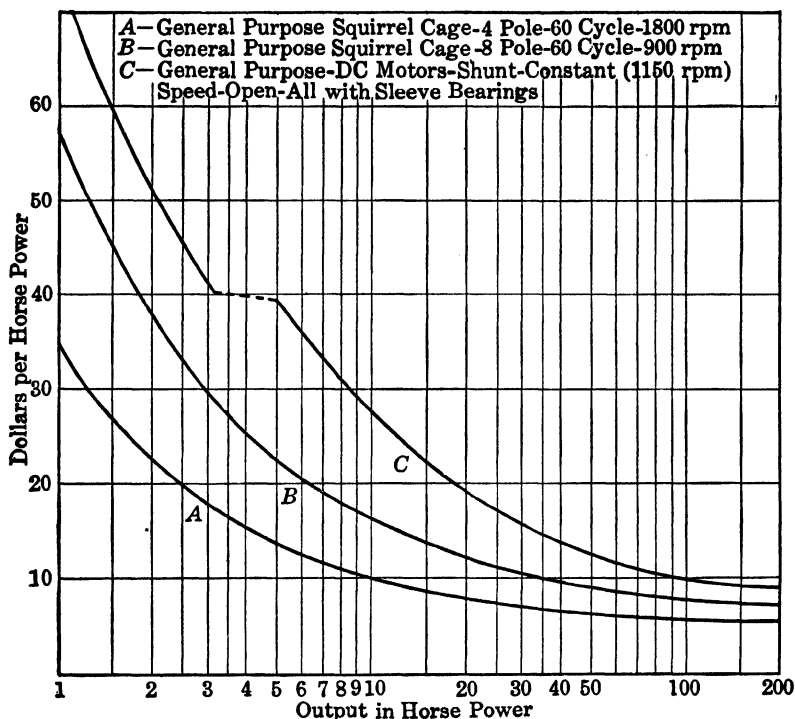


FIG. 49-5. Relation of price to horsepower and speed for general purpose squirrel-cage induction motors and general purpose d-c shunt motors.

while in other cases an actual load test may be required. The cost of a motor depends basically upon the horsepower, speed, type of enclosure, and type of bearings. Generally speaking, higher-speed motors are lighter in weight and less expensive than lower-speed motors.

Very high-speed motors have high costs due to the special mechanical features necessary at the high speeds. Fig. 49-4 shows the relation of horsepower, weight, and speed for d-c motors and polyphase induction motors, while Fig. 49-5 shows typical relation of cost per horsepower to speed and horsepower.

The list prices are representative of a competitive line of NEMA standardized motors. The increase in weight and cost with reduction in speed for induction motors is clearly shown. The lower cost of the squirrel-cage motor in comparison with the d-c motor is observed in Fig. 49-5. A further advantage of the squirrel-cage motor is its simplicity



FIG. 49-6a. Single reduction gear motor, 3-hp, 150-rpm induction motor.



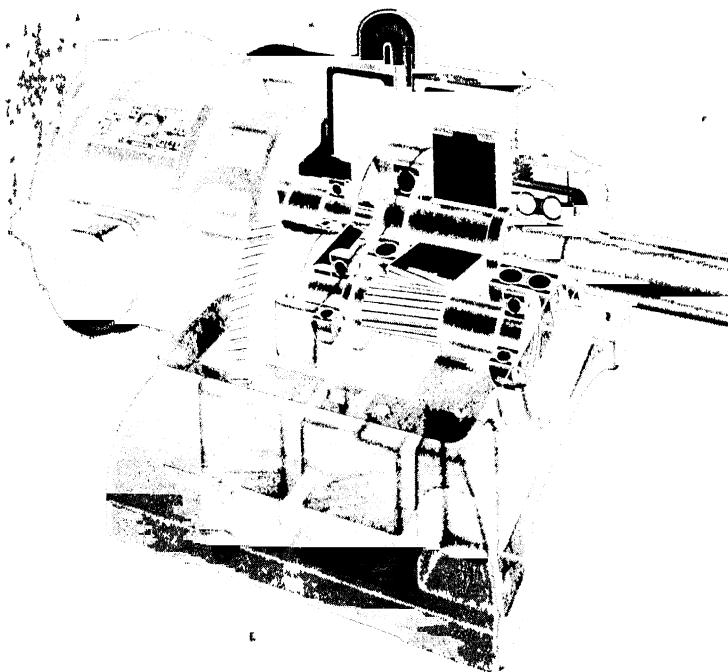


FIG. 49-6b. Double-reduction gear motor.

and low maintenance cost. The implication of these curves is that other things being equal the higher-speed motor should be chosen. In many cases it is possible and desirable to get lower speeds, when required, by gears or pulleys. In case of speeds below 700 rpm at low output, a gear motor (Fig. 49-6a or 49-6b) usually will be lighter in weight and less expensive than a regular low-speed motor. Fig. 49-7 shows a gear-motor application.

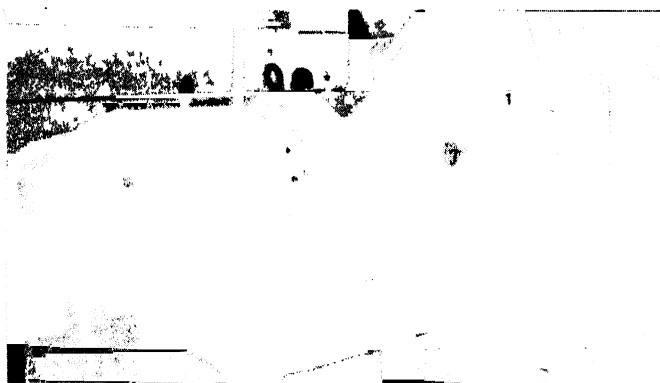


FIG. 49-7. Application of a gear motor to an agitator.

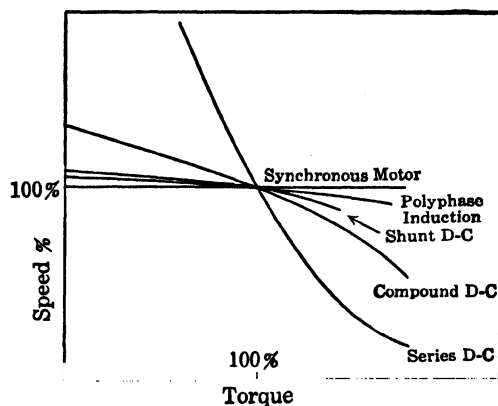


FIG. 49-8. Typical torque-speed curves of motors.

**49-3. Applications of Various Types of Motors.** Fig. 49-8 shows the typical speed-torque curves of the various types of industrial motors on the basis of the same full-load speed. Table 49-1 shows the general characteristics and typical applications of a-c motors. Standard ratings for polyphase and single-phase induction motors are given in Tables 49-4 and 49-6 incl. The *synchronous-motor* is the only one having *absolutely constant speed*, while the general-purpose (NEMA class A or B) *polyphase induction motor* and the *constant-speed d-c shunt motor* have *nearly constant speed*, the speed regulation usually being less than 10%.

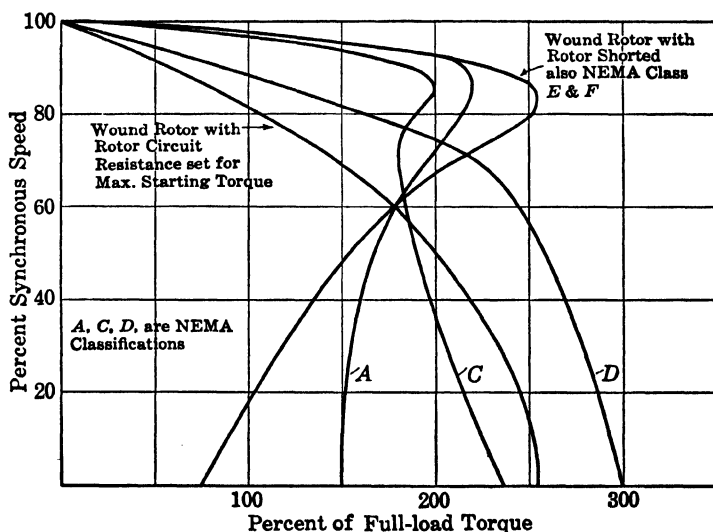


FIG. 49-9. Torque-speed curves of induction motors, NEMA classification.

Curves in Fig. 49-9 show the range of characteristics obtained in polyphase induction motors. There are six NEMA classified motors (see Art. 49-4). The variation in characteristics is obtained by the design of the rotor slots and the relation of the reactance to resistance. (See Art. 19-1.)

#### 49-4. NEMA Classifications of Induction Motors.

*NEMA Class A — General Purpose Squirrel-Cage Induction Motor.* This is the most widely used of all industrial power motors. As Table 49-1 and Fig. 49-9 show, the starting torque varies with the number of poles, but is between 115 and 150% for high-speed motors when started at full voltage. In order to meet power company restriction on starting current, it may be started at reduced voltage, if the starting-torque requirements can be met. The starting current at full voltage will be between 500 and 1000%, depending upon size and speed rating. This motor has a very high pull-out torque and therefore will operate through high-peak loads, but if they are sustained, overheating results. The characteristics of this motor are obtained by a low-resistance squirrel-cage rotor, with medium or deep slots, semi- or completely closed at the top. Wherever possible this motor is used because of its low first cost, low maintenance, high efficiency and power factor, and low slip. It is practically the equivalent of the d-c shunt motor in operating characteristics. Fig. 49-10 shows an 800-hp 3600-rpm induction motor directly connected to a centrifugal pump.



FIG. 49-10. Application of a squirrel-cage induction motor, 800 hp, 3600 rpm, driving a centrifugal boiler-feed pump.

TABLE 49-1  
CHARACTERISTICS AND APPLICATIONS OF POLYPHASE 60-CYCLE A-C MOTORS

Type Classification	Hp Range	Starting Torque (%)*	Pull-Out Torque (%)*	Starting Current (%)*	Slip (%)	Power Factor (%)	Efficiency (%)	Typical Applications
General-purpose, normal torque and starting current NEMA Class A	0.5 to 200	Poles — Torque 2 — 150 4 — 160 6 — 135 8 — 125 10 — 120 12 — 115 14 — 110 16 — 105	Up to 250 but not less than 200	500-1000	Low, 3-5	High, 87-89	High, 87-89	Constant-speed loads where excessive starting torque is not needed and where high starting current is tolerated. Fans, blowers, centrifugal pumps, most machine tools, woodworking tools, line shafting. Lowest in cost. May require reduced voltage starter. Not to be subjected to sustained overloads, because of heating. Has high pull-out torque.
General-purpose, normal torque low starting current, NEMA Class B	0.5 to 200	Same as above or larger.	About the same as Class A but may be less	About 500-550, less than average of Class A	3-5	A little lower than Class A	87-89	Same as Class A — advantage over Class A is lower starting current, but power factor slightly less.
High torque, low starting current, NEMA Class C	1 to 200	200 to 250	Usually a little less than Class A but not less than 200	About same as Class B	3-7	Less than Class A	82-84	Constant-speed loads requiring fairly high starting torque and lower starting current. Conveyors, compressors, crushers, agitators, reciprocating pumps. Maximum torque at standstill.

TABLE 49-1—(Continued)

High torque, medium and high slip, NEMA Class D	0.5 to 150	Medium slip 350 high slip 250-315	Usually same as standstill torque	Medium slip 400-800, high slip 300-500	Medium 7-11, high 12-16	Low	Low	Medium slip. Highest starting torque of all squirrel-cage motors. Used for high-inertia loads such as shears, punch presses, die stamping, bulldozers, boilers. Has very high average accelerating torque. High slip used for elevators, hoists, etc., on intermittent loads.
Low starting torque, either normal starting current, NEMA Class E, or low starting current, NEMA Class F	40 to 200	Low, not less than 50	Low but not less than 150	Normal 500-1000, low 350-500	1 to $3\frac{1}{2}$	About same as Class A or Class B	About same as Class A or Class B	Direct-connected loads of low inertia requiring low starting torque, such as fans and centrifugal pumps. Has high efficiency and low slip.
Wound-rotor	0.5 to 5000	Up to 300	200-250	Depends upon external rotor resistance but may be as low as 150	3-50	High, with rotor shorted same as Class A	High with rotor shorted same as Class A, but low when used with rotor resistor for speed control	For high-starting-torque loads where very low starting current is required or where torque must be applied very gradually and where some speed control (50%) is needed. Fans, pumps, conveyors, hoists, cranes, compressors. Motor with speed control more expensive and may require more maintenance.

\* Figures are given in per cent of rated full-load values.

TABLE 49-1 — (Continued)

Type Classification	Hp Range	Starting Torque (%)*	Pull-out Torque (%)*	Starting Current (%)*	Slip (%)	Power Factor (%)	Efficiency (%)	Typical Applications
Synchro-nous high speed, above 500 rpm	25 to several thou-sand	Up to 120	Up to 200	500-700	Zero	High, but varies with load and with excitation	Highest of all motors, 92-96	Fans, blowers, d-c generators, line shafts, centrifugal pumps and compressors, reciprocating pumps and compressors. Useful for power-factor correction. Constant speed. Frequency changers.
Synchro-nous, low speed, be-low 500 rpm	Usually above 20 to several thou-sand	Low 40	Up to 180	200-350	Zero	High but varies with excitation	Highest of all motors, 92-96	Lower-speed direct-connected loads such as reciprocating compressors when started unloaded, d-c generators, rolling mills, band mills, ball mills, pumps. Useful for power-factor control. Constant speed. Flywheel used for pulsating loads.

\* Figures are given in per cent of rated full-load values.

*NEMA Class B — Normal-Starting-Torque, Low-Starting-Current Motor.* The designated characteristics of this motor are obtained by putting the rotor bars in deeper slots and usually by having a double rotor winding, the high-resistance bars for starting being at the top near the gap. (See Fig. 22-4.) This construction produces a motor having about the same or slightly larger starting torque as Class A, with about 75% of the starting current of Class A, about the same slip, but slightly lower pull-out torque, and somewhat lower power factor (see Table 49-1). It is used where line starting is desired and when the higher starting current of Class A limits its use. The cost of this motor is but slightly greater than that of Class A motors.

*NEMA Class C — High-Starting Torque, Low-Starting-Current Motor.* This motor also has a double-cage rotor, and has a slightly lower starting current than Class B, but the starting torque is much higher, up to 240%, and the pull-out torque is less than Class A (see Art. 19-1). In Class A and Class B motors the pull-out torque exceeds the starting torque, while the Class C motor produces its maximum torque at starting (see Fig. 49-9). This may be important in accelerating a load, and this motor is especially useful in handling a load with excessive starting friction, such as conveyors and compressors in cold weather. The overload capacity is less than Class A. This motor, started at reduced voltage, often may be used instead of a wound-rotor type, in order to reduce starting-current demands and produce smooth acceleration. The efficiency is lower and the slip higher than in Class A motors.

*NEMA Class D — High-Slip Motor.* These motors often are subdivided by manufacturers into high-slip intermittent rating and medium-slip continuous rating. Curve D, Fig. 49-9, is for medium-slip, the full-load slip being about 7 to 11%. The medium-slip motor is applied to punch presses, shears, etc., having flywheels to give energy to the load during the working stroke. This motor has the highest starting torque of all polyphase motors, and the greatest accelerating ability. The greater the area between the speed-torque curves of the motor and of the load, the greater the average accelerating torque. The use of a fairly high slip, in connection with the inertia of the flywheel, makes this motor especially useful in such loads as a punch press where the slowing down during the working stroke enables the stored energy in the flywheel to be released to the load, and the motor to restore it quickly to the flywheel when the working stroke is completed. This smooths out the peaks in power demanded from the power lines, whereas if a Class A motor were used the power peaks in the lines would be much larger. These characteristics are obtained in the design of rotor by using high-resistance bars. This results in higher slip and lower efficiency. The flux densities usually are higher, and the power factor lower than in the motors previously mentioned. The motors having high instead of medium slip, are applied to cranes and hoists, and sometimes to elevators, where the starting torque required usually is about 250%. The full-load slip is between 12 and 16%, and these

motors, as previously mentioned, usually are used on intermittent loads, and are rated on the *intermittent* basis.

**NEMA Class E and Class F — High-Speed Motors.** These motors usually are high-speed motors used for direct connection to fans and centrifugal pumps where low starting torque is satisfactory. They have low slip and high efficiency. The same results can be obtained by using a Class A motor at reduced voltage starting, so that these classes are not applied widely.

**49-5. Wound-Rotor Induction Motor Application.** The use of wound-rotor motors is much less than it was before the NEMA Classes C, D, E, and F were developed to produce the necessary high starting torque and low starting current. The wound-rotor motor with secondary rheostat does provide the most efficient starting conditions, namely, highest starting torque and lowest starting current, when properly applied. It also offers the possibility of speed control, although at reduced speeds the efficiency is affected adversely. At 50% speed the efficiency is about half its value with the rotor shorted. Its use for speed variation is limited to about 50% reduction, due to poor speed regulation and low efficiency. The main applications are where a *high starting torque, low starting current, and smooth acceleration* are required, especially when some speed regulation may be desired. In any case the rheostat in the rotor must be designed carefully for the type of duty required.

Two general types of application may be considered: (1) constant speed, and (2) varying speed. The constant-speed application simply uses the characteristics of the wound rotor to produce the desired starting conditions of high and controlled torque at low current. Only a few starting steps are required, and the control may be manual or automatic as suggested in Art. 49-10. Typical of these applications are conveyors, crushers, ice machines, air compressors, steel-mill machinery, locomotives. In the varying-speed applications are included hoists, cranes, elevators, shovels, coal and ore unloaders, fans, blowers.

The starting and operation of the wound-rotor motor is studied easily with the use of Fig. 49-11 (see Art. 23-2). Shown in this figure are also typical speed-torque characteristics of (A) loaded centrifugal pumps, (B) fan or blower, (C) conveyor (typical of large friction loads). The primary current also is shown. Assuming the motor is to operate the load (C) and a starting torque of 150% is chosen, this requires about 150% starting current, shown at point X. The motor starts at point (a) and accelerates along curve 50. The current and the torque drop, as the motor accelerates along curve 50. At 100% torque the current will be 100%. If the first step of starting resistor is now cut out, to shift the operation to curve 40, the current and torque will rise to about 150% and the motor accelerates again to point d, at which time more resistance is cut out. Acceleration thus proceeds as resistance is cut out, and with the rotor shorted the operating point is N. Note that, in shifting from curve 10 to shorted rotor, there is a high current peak, up to



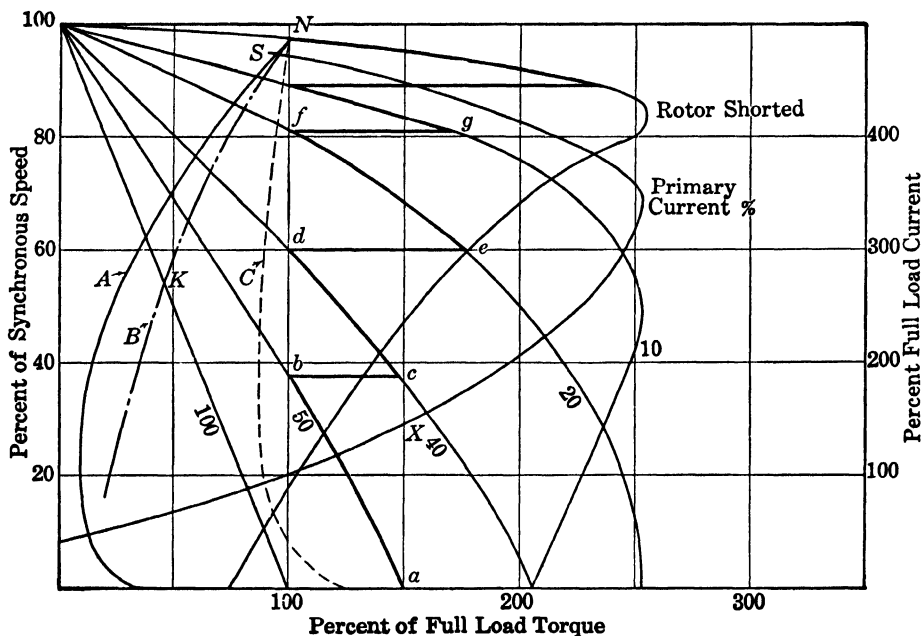


FIG. 49-11. Torque-speed characteristics of a wound-rotor induction motor. A, B, C are characteristics of loads.

240%. This could be reduced by a different resistor design if necessary. The starter shown here would have 4 sections in the resistor, or 5 points on the control. On the other hand, if the motor were started at 250% torque, curve 20, only 3 points are needed, and the starting-current peak would be limited to 350% at the first moment of starting.

If this motor were used as a variable-speed motor for operating the fan (B) and started on 100% torque (curve 100), the motor would speed up to point K, about 55% speed, and run here. If it were then shifted to curve 40, the speed would rise to about 75%.

It is to be noted that for a *given torque the current always is the same*, but the *speed* will depend upon the value of *rotor resistance*. Also, the wound-rotor motor is never started with rotor shorted, as the starting torque is very low and the starting current high (latter shown at point S to be about 450%), while starting torque is only 75%. The acceleration of the load always demands a motor torque in excess of the load requirements. The weight of the wound-rotor motor will be from 120 to 150% of that of the squirrel-cage motor of the same rating, and the cost considerably higher.

In applying induction motors it is important *not to over-motor*, i.e., to use a motor too large for the purpose, as both power factor and efficiency drop off rapidly below 60% load (see Figs. 22-9 and 22-10). Momentary overloads usually are taken care of by the inherent overload capacity of the motor.

It also is to be noted that the higher-speed motors have higher power factor, better starting characteristics, and usually higher efficiency, and are lower in first cost, as shown in Fig. 49-5.

**49-6. Polyphase Induction Motors as Multi-Speed Motors.** Some industrial applications require that the load be operated at more than one constant speed, among such applications being machine tools, pumps, blowers, elevators, dough mixers, laundry machinery, etc. Such loads usually are classified in the same way as for variable-speed loads (see Art. 49-1), namely, as either (1) constant-torque, (2) constant horsepower, (3) variable-torque loads. The type of motor will depend upon the use within these classifications. Typical of constant-torque loads are air compressors, reciprocating pumps, mixers, conveyors, stokers, printing presses, ironing machines. To drive such a load the motor must develop the same torque at each speed. Its output therefore varies directly with the speed. The number of speeds depends upon the load requirements, but may be 2, 3, or 4 speeds. The speeds are obtained in polyphase motors by arranging a special 2-speed winding or 2 such windings on the stator and by suitable switching of the coil groups. Thus a 60-cycle motor could have synchronous speeds of 1800, 1200, 900, 600.

Typical of constant horsepower loads are lathes, millers, and other machine tools, and some woodworking tools. In this type of application the torque varies inversely with the speed, so the output remains constant.



FIG. 49-12. Four-speed induction motor, 125 hp, driving an induced draft fan.

Typical of multi-speed, variable torque application are fans and blowers. Here the torque varies about as the square of the speed. Multi-speed motors are well adapted to such drives, where several constant speeds of operation are needed, according to the load demands of the fan. The operation of multi-speed motors is more efficient than that of a wound-rotor motor with a resistor in the rotor circuit. Fig. 49-12 shows a 4-speed, 125-hp motor driving an induced-draft fan in a steam-power plant.

**49-7. Synchronous Motor Characteristics and Application.** Synchronous motors offer the following important advantages over induction motors: (1) Speed is constant. (2) Power factor is controlled readily by the field excitation and it may be made leading in order to correct for other lagging loads. (3) Efficiencies usually are from 1 to 2% higher than Class A induction motors. (4) Initial cost is lower for the low-speed ratings, i.e., for 500 rpm, or less, and in large output ratings, i.e., for 500 hp, and above. On the other hand, there are certain disadvantages of the synchronous motor: (1) It is not economical in smaller sizes, usually not being applied below 50 hp, and even here the cost is considerably greater than for induction motors. (2) It requires a separate source of direct current for excitation. (3) The starting characteristics usually are not quite as favorable as those of induction motors of Class C or Class D, although they are nearly the same as those of Class A motors for speeds of 900 rpm, or lower. (4) The inertia of the load affects the pull-in characteristics when starting. (5) It does not lend itself to speed control as readily as the wound-rotor motor. (6) Starting and control devices usually are more expensive, especially for automatic control.

From the standpoint of the design and operating characteristics, synchronous motors usually are divided into two general classes, (1) high-speed, above 514 rpm, and (2) low-speed, below 514 rpm. These classes cover motors for general purposes, and there might be, in addition, a class for special purposes, namely for high-starting torque, or low-starting-current motors. Within these groups motors are classified also as unity-power-factor or 0.8-power-factor motors as well as lower-power-factor motors in some cases. Motors designed for unity power factor have a somewhat smaller field structure, are less expensive, require less field exciting power, are more efficient, although they have somewhat poorer starting, pull-out, and pull-in torque. The 0.8-power-factor motors are designed to operate with leading current, to correct for other lagging-power-factor loads on the system, and thus improve the efficiency, the voltage regulation, and the capacity of the power system. These motors require greater exciting current and are somewhat larger in size than the unity-power-factor motors. Table 49-2 shows the relative torque characteristics for the various classifications as specified by NEMA. Fig. 49-13 shows characteristics during the starting period at full voltage for low- and high-speed unity-power-factor synchronous motors.

The synchronous motor always is supplied with a *starting* (damper)

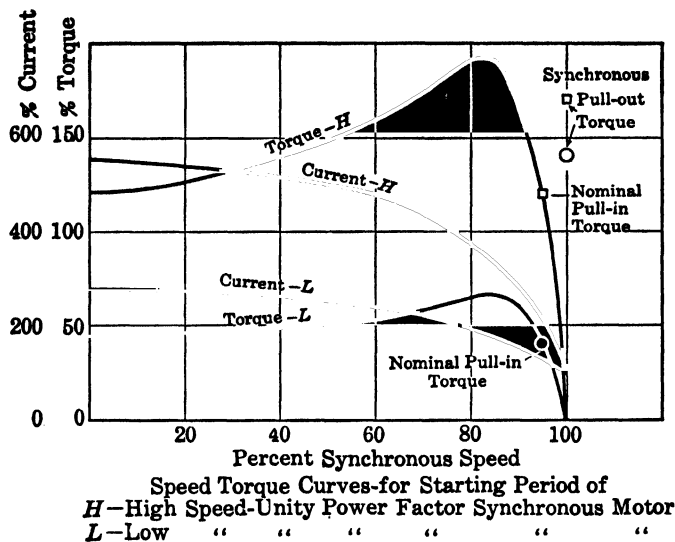


FIG. 49-13. Typical torque-speed and current curves of synchronous motors during starting period.

winding to start the motor as an induction motor (see Art. 38-4). While coming up to speed the characteristics are similar to those of an induction motor, and are shown in Fig. 49-13. During starting the d-c field winding usually is closed through a resistor. (See Fig. 49-29.) However, at the proper time, the d-c field current must be applied and the motor must synchronize or pull into step, and then operate as a synchronous motor. The *pull-in torque* is the torque developed by the motor operating as an induction motor at the speed from which it will pull into synchronism, when rated field current is applied. The slip at which it will pull in against the load torque depends upon the inertia of the load, the applied voltage, and the field excitation. (See Chap. 61.) It varies inversely with the square root of the inertia. For this reason NEMA has defined normal  $WR^2$  (moment of inertia in lb. ft.<sup>2</sup>) of loads (see NEMA Section MG 10 of Motor and Generator Standards). Special care must be given to the starting ability of synchronous motors when applying them. Table 49-2 gives the pull-in torque for normal  $WR^2$ . The pull-in torque varies with the square of the terminal voltage, and so usually full voltage is applied before supplying the d-c current to the field winding. The pull-in torques shown in Table 49-2 are those which will be developed at a slip of about 5%. If the  $WR^2$  is greater than normal, the slip from which the motor is able to pull into step will be less than 5%. In this case the motor damper winding would be designed to bring the motor up to a higher speed than 95%, before d-c field is applied. Some high-speed fans are typical of this difficulty.

The synchronous pull-out torque is very important in synchronous-motor

**TABLE 49-2**  
**STARTING, PULL-IN, AND PULL-OUT TORQUES, AND STARTING CURRENTS**  
**OF NEMA STANDARD SYNCHRONOUS MOTORS**

Type	Rpm	Starting Torque	Pull-In Torque	Pull-Out Torque	Starting Current Full-voltage
<b>General-purpose motors</b>					
Unity pf	1800	110	110	150	550-750
(Up to 200 hp)	514-1200	110	110	175	550-750
0.8 pf	1800	125	125	200	500-700
(Up to 150 hp)	514-1200	125	125	250	500-700
<b>Large high-speed motors</b>					
Unity pf					
250 to 500 hp	514-1800	110	110	150	550-700
600 hp and above	514-1800	85	85	150	550-700
0.8 pf					
200 to 500 hp	514-1800	125	125	200	500-700
600 hp and above	514-1800	100	100	200	500-700
<b>Low-speed motors</b>					
Unity pf	less than 514	40	30	140	300-500
0.8 pf	514	40	30	200	250-400

Torques and currents are expressed in percent of rated full-load values.

Pull-in torque is based on NEMA standards for normal  $WR^2$  of the load.

operation, especially when the motor is subject to high-peak loads. This torque must be high for loads such as crushers, ball and rod mills, banbury mixers (used in rubber mills). Pull-out torque varies directly with the terminal voltage and directly with the field excitation. Therefore, 0.8-power-factor motors have higher pull-out and pull-in torques than 1.0-power-factor motors.

The exciting direct current is usually obtained from a direct-connected exciter in the high-speed machines. Fig. 49-14, which shows a 50-hp 900-rpm motor driving a compressor, is a typical application. The low-speed motors usually have a separate motor-generator set to supply the direct current. In a plant using several synchronous motors, at least two such motor-generator sets would be used. Fig. 49-15, showing a 225-hp 277-rpm motor driving a compressor, is a typical low-speed application.

Typical of the low-speed applications are reciprocating compressors, line shafts, centrifugal and screw pumps, rubber mills, Jordans (used in paper mills to separate the fibers of paper pulp), electroplating generators. Fig. 49-16 shows 350 hp 400-rpm synchronous motors, driving Jordans. These usually are started unloaded and hence the low starting torque of these motors is satisfactory. Typical of high-speed applications are d-c generators, fans, blowers, belt-driven compressors, line shafts, centrifugal pumps.

In many cases the ability of the synchronous motor to operate at *leading power factor* is made use of to improve the over-all power factor of a plant,



FIG. 49-14. Synchronous motor, 50 HP, 900 rpm, with directly coupled exciter, driving a compressor.

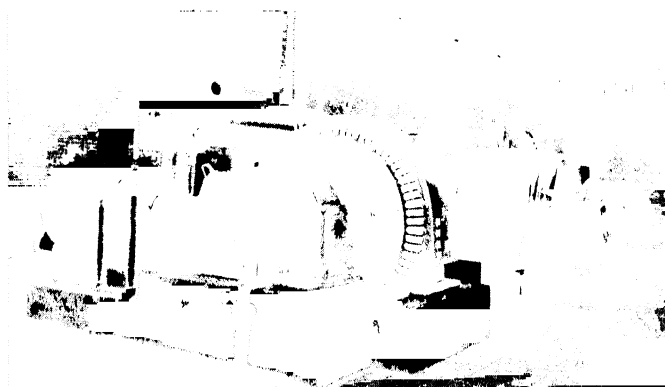


FIG. 49-15. Typical low-speed synchronous motor application: 225-HP, 227-rpm motor, driving compressors.

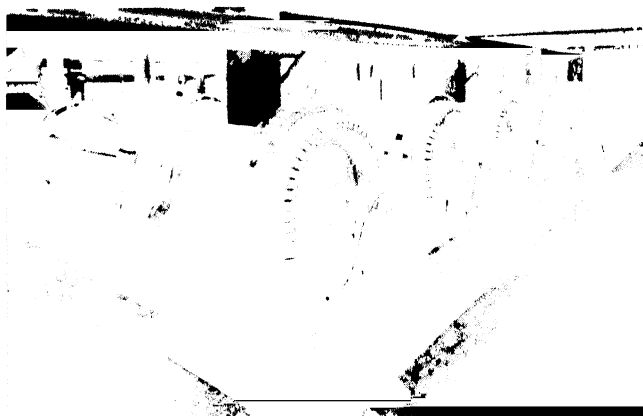


FIG. 49-16. Synchronous motors, 350 HP, 400 rpm, driving paper-mill Jordans.

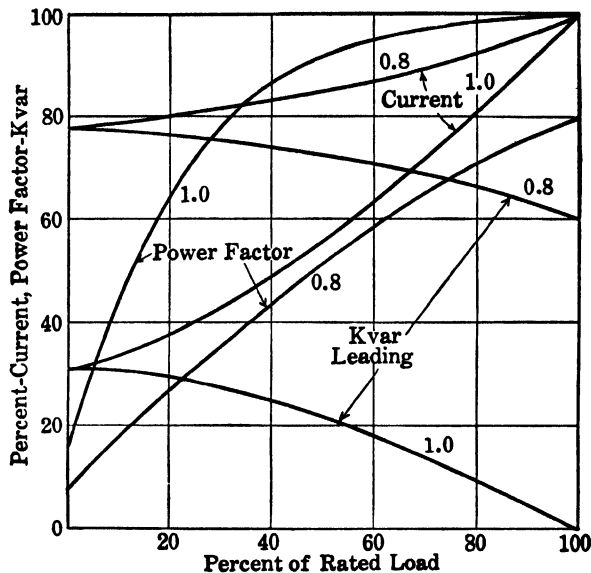


FIG. 49-17. Characteristics of unity and 0.8-power-factor synchronous motors.

in order to give better power system operation. Synchronous motors ordinarily are rated at unity power factor or 0.8 leading power factor at full-load. The 0.8-power-factor motor is larger in size than the unity-power-factor motor. The characteristic curves for these two types of motors are shown in Fig. 49-17. The increase in power factor with increase in load is to be noted, and also the decrease in leading kvar with increase in load, the decrease being much less for the 0.8-power-factor motor. It is to be observed in comparing the current curves for the two motors, that 100% current at 100% load for the 0.8-power-factor motor is actually 125% of the current in the 1.0-power-factor motor. Illustrative of the use of a synchronous motor to improve power factor are the following problems.

1. A plant operates with an average load of 1200 kw at 0.65 power factor lagging. If a 500-hp 0.8-power-factor synchronous motor is added, what will be the over-all power factor when the motor operates at full-load? Assume efficiency = 94.5%; motor input =  $(500 \times 0.746)/0.945 = 394$  kw;  $394/0.8 = 493$  kva;  $394 \times 0.75 = 296$  kvar;  $1200 \times 1.168 = 1400$  kvar of original lagging load; total kw =  $1200 + 394 = 1594$ ; total kvar =  $1400 - 296 = 1104$ ;  $\tan \phi = 1104/1594 = 0.697$ ;  $\cos \phi = 0.82$ .

2. If the synchronous motor operates at  $\frac{1}{2}$  load with excitation unchanged, what will be the plant power factor? From Fig. 49-17 it is seen that the motor kva =  $493 \times 0.85 = 418$ , kvar =  $493 \times 0.73 = 360$ , power factor = 0.51, so kw =  $418 \times 0.51 = 214$ ; total kw =  $1200 + 214 = 1414$ ; total kvar =  $1400 - 360 = 1040$ ;  $\tan \phi = 1040/1414 = 0.734$ ,  $\cos \phi = 0.806$ , or practically the same as before.

3. How much additional kw can be carried by a synchronous motor added to the

original plant, so as to raise the plant power factor to 0.95 but not to exceed the original kva of the feeders? What would be the power factor of the synchronous motor and about what would be its hp rating? Original load 1200 kw,  $1200/0.65 = 1845$  kva (this is the original feeder capacity),  $1200 \times 1.168 = 1400$  kvar. At 0.95 pf,  $1845 \times 0.95 = 1750$  kw; motor kw =  $1750 - 1200 = 550$ . Resulting kvar =  $1845 \times 0.312 = 575$ ; leading kvar =  $1400 - 575 = 825$  for motor. Hp input of motor =  $550/0.746 = 736$ . Thus a synchronous motor rated 700 hp would be suitable, operating at about 0.65 pf at full-load.

**49-8. Fractional-Horsepower Motors.** Fractional-horsepower motors have a wider application than any other class of motors. The important uses are in domestic appliances such as refrigerators, oil burners, vacuum cleaners, office and commercial appliances, small air-compressors, fans, blowers, machine tools, woodworking tools. These services usually require constant speed, although some may require adjustable speed control. For the former, the single-phase motors are almost universally applied, due to the wide availability of a-c power. When speed control over a wide range is required, the d-c shunt motor is applied; where only a-c power is available it is necessary to use a converter of some sort, and several very satisfactory electronic converters or rectifiers are available which make possible a wide range of speed control. Table 49-3 shows the general types, characteristics and applications of the various fractional-horsepower motors, and Table 49-4 shows the standard ratings.

## 49-9. DEFINITIONS

### 1. Duty.

a. *Continuous Duty.* A requirement of service that demands operation at a substantially constant load for an indefinitely long time. (MG50-50.)

b. *Intermittent Duty.* A requirement of service that demands operation for alternate periods of either (1) load and no-load; (2) load and rest; (3) load, no-load, and rest. (MG50-51.)

c. *Periodic Duty.* A type of intermittent duty in which the load conditions are regularly recurrent. (MG50-52.)

d. *Varying Duty.* A requirement of service that demands operation at loads and for periods of time both of which may be subject to wide variation. (MG50-63.)

### 2. Motors.

a. *General-Purpose Motor.* (1) A general-purpose motor is any motor of 200 hp or less and 450 rpm or more, having a continuous rating, and designed, listed, or offered in standard ratings for use without restriction to a particular application. (NEMA number MG50-110.) (2) A general-purpose synchronous motor is any motor rated 200 hp or less at 1.0 power factor, or 150 hp or less at 0.8 power factor, and speeds higher than 450 rpm, having a continuous time rating, and designed listed, or offered in standard ratings for use without restriction to a particular application. (See MG4-11 for the basis of rating general-purpose motors.)



TABLE 49-3

Type Designation	Starting Torque (% of Normal)	Pull-Up Torque (% of Normal)	Pull-Out Torque (% of Normal)	Starting Current at 115 V	Power Factor	Efficiency (%)	hp Range	Application and General Remarks
General-purpose split-phase motor	90-200 Medium normal	200-250	185-250 Medium	23 $\frac{1}{4}$ hp	56-65	62-67	$\frac{1}{16}$ to $\frac{3}{4}$	Fans, blowers, office appliances, food-preparation machines. Low- or medium-starting-torque, low-inertia loads. Continuous operation loads. May be reversed.
High-torque split-phase motor	200-275 High	160-350 High	Up to 350	32 High $\frac{1}{4}$ hp	50-62	46-61	$\frac{1}{8}$ to $\frac{1}{3}$	Washing machines, sump pumps, home workshops, oil burners. Medium- to high-starting-torque loads. May be reversed.
Permanent-split-capacitor motor	60-75 Low	60-75 Low	Up to 225	Medium	80-95	55-65	$\frac{1}{16}$ to $\frac{3}{4}$	Direct-connected fans, blowers, centrifugal pumps. Low-starting-torque loads. Not for belt drives. May be reversed.
Permanent-split-capacitor motor	Up to 200 Normal	200	260		80-95	55-65	$\frac{1}{8}$ to $\frac{3}{4}$	Belt-driven or direct-drive fans, blowers, centrifugal pumps, oil burners. Moderate-starting-torque loads. May be reversed.
Capacitor-start general-purpose motor	Up to 435 Very high	265 High	Up to 400		80-95	55-65	$\frac{1}{8}$ to $\frac{3}{4}$	Dual voltage. Compressors, stokers, conveyors, pumps. Belt-driven loads with high static friction. May be reversed.

TABLE 49-3 — (Continued)

Type Designation	Starting Torque (% of Normal)	Pull-Up Torque (% of Normal)	Pull-Out Torque (% of Normal)	Starting Current at 115 V	Power Factor	Efficiency (%)	hp Range	Application and General Remarks
Capacitor-start capacitor-run motor	380 High	260	Up to 260		80-95	55-65	$\frac{1}{8}$ to $\frac{3}{4}$	Compressors, stokers, conveyors, pumps. High-torque loads. High power factor. Speed may be regulated.
Repulsion-start induction-run motor	350-500 Very high	225	Up to 275	350%	70-80	55-65	Up to 10	Very-high-starting-torque loads. Pumps, compressors, conveyors, machine tools. Reversed by shifting brushes.
Shaded-pole motor	50	50	150			30-40	$\frac{1}{300}$ to $\frac{1}{20}$	Fans, toys, hair dryers, unit heaters. Low-starting-torque loads.
Series motor	400-500 Very high	High	400-500	Medium	85-95	40-60	$\frac{1}{100}$ to 1	Usually high speed, 3000 to 11,000. Hand tools, vacuum cleaners. Speed control possible with resistor or reactor. Larger sizes require compensating winding. Used on either alternating current or direct current — called "Universal" motor.
Shunt or compound d-c motor	400 Very high	400	400	Medium			$\frac{1}{20}$ to $\frac{3}{4}$	Same application as high-torque split-phase, or capacitor-start or repulsion-start motor. Speed control. May be reversed. More expensive than corresponding a-c motor.

TABLE 49-4

HORSEPOWER AND SPEED RATINGS OF FRACTIONAL HORSEPOWER  
SINGLE-PHASE MOTORS

Brake Hp Rating	60 Cycle		25 Cycle	
	Syn- chronous Rpm	Approx. Full Load Rpm	Syn- chronous Rpm	Approx. Full Load Rpm
1	3600	3450	...	...
	3600	3450		
	1800	1725		
$\frac{1}{2}$	3600	3450	1500	1425
	1800	1725		
	1200	1140		
$\frac{1}{3}$	3600	3450	1500	1425
	1800	1725		
	1200	1140		
$\frac{1}{4}$	900	860	1500	1425
	3600	3450		
	1800	1725		
$\frac{1}{6}$	1200	1140	1500	1425
	900	860		
	3600	3450		
$\frac{1}{8}$	1800	1725	1500	1425
	1200	1140		
	900	860		
$\frac{1}{12}$	3600	3450	1500	1425
	1800	1725		
	1200	1140		
$\frac{1}{20}$	900	860	1500	1425
	3600	3450		
	1800	1725		
	1200	1140		
	900	860		

TABLE 49-5

HORSEPOWER AND SYNCHRONOUS SPEED RATINGS FOR GENERAL PURPOSE  
POLYPHASE INDUCTION MOTORS

Standard horsepower and speed ratings for open and semi-closed continuous-duty constant speed motors shall be as given in this table.

Cycles	60	60	60	60	60	60	60	25	25	25
Hp	Rpm	Rpm	Rpm	Rpm	Rpm	Rpm	Rpm	Rpm	Rpm	Rpm
$\frac{1}{2}$	....	....	....	...	...	...	...	....	750	...
$\frac{3}{4}$	....	....	1200	...	...	...	...	....	750	...
1	....	1800	1200	...	...	...	...	*1500	750	...
$1\frac{1}{2}$	*3600	1800	1200	...	...	...	...	*1500	750	...
2	*3600	1800	1200	900	...	...	...	*1500	750	...
3	*3600	1800	1200	900	...	...	...	*1500	750	...
5	*3600	1800	1200	900	...	...	...	*1500	750	...
$7\frac{1}{2}$	*3600	1800	1200	900	...	...	...	*1500	750	...
10	*3600	1800	1200	900	...	600	...	*1500	750	500
15	*3600	1800	1200	900	...	600	...	*1500	750	500
20	*3600	1800	1200	900	...	600	...	*1500	750	500
25	....	1800	1200	900	...	600	...	*1500	750	500
30	....	1800	1200	900	...	600	...	*1500	750	500
40	....	1800	1200	900	...	600	...	*1500	750	500
50	....	....	1200	900	...	600	...	....	750	500
60	....	....	1200	900	...	600	...	....	750	500
75	....	....	1200	900	...	600	...	....	750	500
100	....	....	....	900	...	600	450	....	750	500
125	....	....	....	900	720	600	450	....	750	500
150	....	....	....	...	720	600	450	....	750	500
200	....	....	....	...	720	600	...	....	...	500

\* NOTE—The 3600 and 1500 rpm ratings apply to squirrel-cage motors only.  
(NEMA MG9-512)

TABLE 49-6

HORSEPOWER AND SPEED RATINGS OF OPEN AND SEMI-ENCLOSED CONTINUOUS-DUTY  
CONSTANT-SPEED INTEGRAL-HORSEPOWER SINGLE-PHASE INDUCTION MOTORS

60 Cycles		25 Cycles	
Hp	Rpm	Hp	Rpm
$\frac{3}{4}$	1200		
1	1800—1200	1	1500
$1\frac{1}{2}$	1800—1200	$1\frac{1}{2}$	1500
2	1800—1200	2	1500—750
3	1800—1200	3	1500—750
5	1800—1200—900	5	1500—750
$7\frac{1}{2}$	1800—1200—900	$7\frac{1}{2}$	1500—750
10	1800—1200—900	10	1500—750
15	1800—1200—900	15	1500—750
20	1800—1200—900	20	1500—750
25	1800—1200—900		

The speeds given are synchronous speeds.

(NEMA MG9-314)

**b. Special-Purpose Motor.** An industrial power motor specifically designated and listed for a particular power application where the load requirements and duty cycle definitely are known. (MG50-112.)

**c. Universal Motor.** A series-wound or a compensated series-wound motor which may be operated either on direct current or single-phase alternating current at approximately the same speed and output. These conditions must be met when the d-c and a-c voltages are approximately the same and the frequency of the alternating current is not greater than 60 cps. (MG50-118.)

**d. Squirrel-Cage Induction Motor.** A motor in which the secondary circuit consists of a squirrel-cage winding suitably disposed in slots in the secondary core. (MG50-119.) Squirrel-cage induction motors may be in one of the following classes:

(1) **Class A—Normal-Torque Normal-Starting-Current Squirrel-Cage Motor.** An induction motor with normal starting torque and low slip at the rated load. May have sufficiently high starting current to require in most cases a compensator or resistance starter for motors above  $7\frac{1}{2}$  hp.

(2) **Class B—Normal-Torque Low-Starting-Current Squirrel-Cage Motor.** An induction motor which develops normal starting torque at relatively low starting current and can be started at full voltage. The low starting current is obtained by design of motor to include inherently high reactance. The slip at rated load is relatively low.

(3) **Class C—High-Torque Low-Starting-Current Squirrel-Cage Motor.** An induction motor which develops relatively high starting torque at relatively low starting current and can be started at full voltage. The low starting current is obtained by design of motor to include inherently high reactance. The slip at rated load is relatively low.

(4) **Class D—High-Slip Squirrel-Cage Motor.** An induction motor in which starting current is limited by relatively high slip at rated load. Motors of this class used in elevator service are quiet in operation and have relatively low starting current.

(5) **Class E—Low-Starting-Torque Normal-Starting-Current Squirrel-Cage Motor.** An induction motor with low starting torque and low slip at the rated load. May have sufficiently high starting current to require in most cases a compensator or resistance starter for motors above  $7\frac{1}{2}$  hp.

(6) **Class F—Low-Starting-Torque Low-Starting Current Squirrel-Cage Motor.** An induction motor which develops low starting torque at relatively low starting current and can be started at full voltage. The low starting current is obtained by design of motors to include inherently high reactance. The slip at rated load is relatively low.

e. *Shunt-Wound Motor.* A d-c motor in which the field circuit and armature circuit are connected in parallel. (MG50-122.)

f. *Compound-Wound Motor.* A d-c motor which has two separate field windings—one, usually the predominating field, connected in parallel with the armature circuit, and the other connected in series with the armature circuit. (MG50-124.)

g. *General-Purpose Compound-Wound Motor.* A d-c motor employing both shunt and series windings and giving a speed regulation between no-load and full-load greater than is permissible for standard shunt-wound machines. (MG50-125.)

h. *Constant-Speed Motor.* A motor the speed of which at normal operation is constant or practically constant. For example, a synchronous motor, an induction motor with small slip, or an ordinary d-c shunt-wound motor. (MG50-141.)

i. *Varying-Speed Motor.* A motor the speed of which varies with the load, ordinarily decreasing when the load increases, such as a series motor, or an induction motor with large slip. (MG50-142.)

j. *Adjustable-Speed Motor.* A motor the speed of which can be varied gradually over a considerable range, but when once adjusted remains practically unaffected by the load, such as a shunt motor with field-resistance control designed for a considerable range of speed adjustment. (MG50-143.)

k. *Adjustable Varying-Speed Motor.* A motor the speed of which can be adjusted gradually, but when once adjusted for a given load will vary in considerable degree with change in load, such as compound-wound d-c motor adjusted by field control or a slip-ring induction motor with rheostatic speed control. (MG50-144.)

l. *Multi-Speed Motor.* A motor which can be operated at any one of two or more definite speeds, each being practically independent of the load. For example, a d-c motor with two armature windings, or an induction motor with windings capable of various pole groupings. (MG50-145.)

### 3. Rated Load.

Rated load means horsepower output for motors, kilowatt output for d-c generators, and kilovolt-ampere output for a-c generators. (MG50-64.)

### 4. Rated Speed.

The rated speed of an a-c general-purpose motor is defined as the full-load speed stamped on the name plate. (MG50-140.)

## 5. Rating.

Designated operating limit of a machine, based on definite conditions. (MG50-62.)

## 6. Service Factor—General-Purpose Motors.

A service factor of a general-purpose motor is a multiplier which, applied to the normal horsepower rating, indicates a permissible loading which may be carried under the conditions specified for the service factor. (MG50-63.)

## 7. Temperature.

*Ambient Temperature.* Temperature of the air or water which, coming into contact with the heated parts of a machine, carries off their heat. (MG50-60.)

Note: Ambient temperature is commonly known as room temperature in connection with air-cooled apparatus not provided with artificial ventilation.

## 8. Time Ratings and Duration of Tests.

a. Many machines are operated on a cycle of duty which repeats itself with more or less regularity. The heating of machines operating under such conditions is equivalent to a continuous run for a certain specified time. The standard duration of load tests, or time ratings, for machines operating on such duty cycles is as follows:

5 min, to and including 30 hp  
15 min, to and including 50 hp  
30 min, to and including 60 hp

b. Of the foregoing ratings, the first four are commonly known as short-time ratings. In every case the short-time load test shall commence only when the windings and other parts of the machine are within 5°C of the room temperature at the time of starting the test. (MG50-65.)

## 9. Torque.

a. *Full-Load Torque.* The torque necessary to produce rated horsepower of a motor at full-load speed. In pounds at 1 foot radius it is equal to the horsepower times 5250 divided by the full-load speed. (MG50-66.)

b. *Locked-Rotor or Static Torque—A-C Motor.* The minimum torque which a motor will develop at rest for all angular positions of the rotor, with rated voltage applied at rated frequency. (MG50-67.)

c. *Pull-Up Torque—A-C Motor.* The minimum torque developed by a motor during the period of acceleration from rest to full-speed with rated voltage at rated frequency. (MG50-68.)

d. *Breakdown Torque—A-C Motor.* The maximum torque which a motor will develop with rated voltage applied at rated frequency, without an abrupt drop in speed. (MG50-69.)

**49-10. Starting Induction Motors.** Many a-c motors may be started at full voltage, provided the power line is adequate to supply the large starting current, and provided the load will not be damaged by excessive torques.

However, when squirrel-cage motors require reduced voltage, either a resistance or reactance starter or autotransformer type starter may be used. Line starters simply apply full voltage, but over-current protection usually is incorporated within them.

(a) *Line Starters.* Practically all squirrel-cage induction motors now are designed so that they may be started with full voltage, as far as the motor is concerned. For 3-phase motors up to 3-hp 120 volts, 5 hp-220 volts, and  $7\frac{1}{2}$  hp-440 volts, a manual starter may be used, if the starter can be mounted where it is convenient for operation, and when the motor is started or stopped

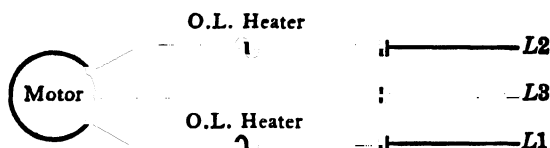


FIG. 49-18. Schematic wiring diagram of a 3-phase manual line starter.

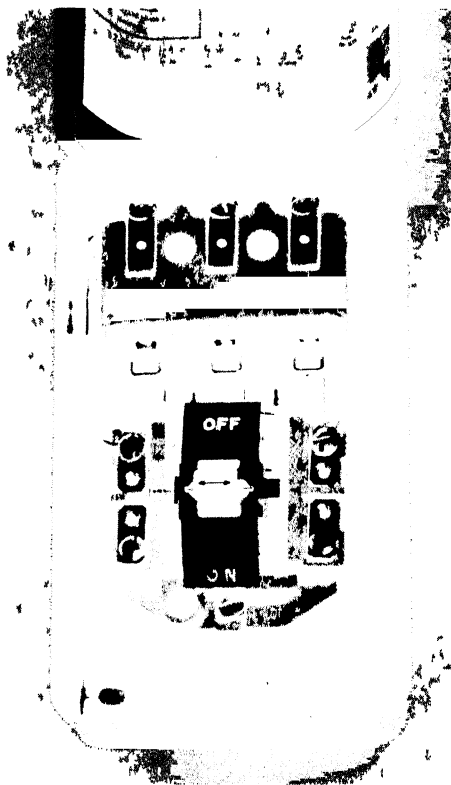


FIG. 49-19. Manual full-voltage starting switch with thermal protection.



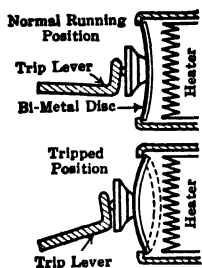


FIG. 49-19a. Bi-metallic thermal element for starting switch.

infrequently (less than 3 to 5 times an hour). The connections for such a starter are shown in Fig. 49-18, and the general appearance of a typical starter in Fig. 49-19. The overload protection is provided by the bimetallic element (Fig. 49-19a) which trips the toggle switch on sustained overload.

The general trend is definitely towards the use of *magnetic starters*. In these starters the main switching is done through magnetically operated contactors. Push-button and other relatively small pilot control devices then are used to operate the contactor coils. Fig. 49-20 shows a schematic diagram for a 3-phase magnetic non-reversing line starter available up to 750 hp. Momentarily pressing the start button energizes the main contactor coil  $M$ ; this closes the main contacts  $M$ . The control contacts  $Ma$  also close, shunting the

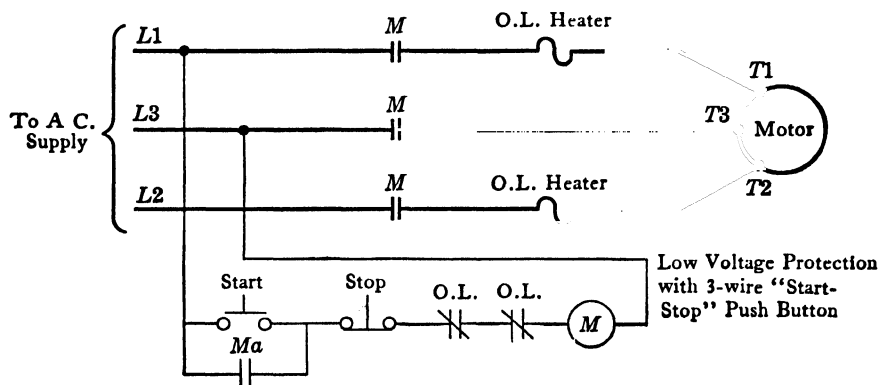


FIG. 49-20. Schematic wiring diagram of a 3-phase magnetic non-reversing line starter.



FIG. 49-20a. Magnetic line starter with clapper-type magnet.

start button and maintaining current through (M). The bimetallic overload device opens the circuit through (M) upon sustained overload. Fig. 49-20a shows the construction of such a magnetic starter. The arc at the main contacts is quenched by De-Ion arc quenchers, or by magnetic blow-out coils.

When it is necessary to provide for operating the motor in either direction of rotation a *reversing starter* is necessary. The construction is generally similar to the non-reversing type though somewhat more involved, requiring two sets of contactors, one for *forward* and one for *reverse*. Fig. 49-21 shows a schematic wiring diagram for a 3-phase reversing/magnetic starter, with overload and low-voltage protection. The coil (F) (Fig. 49-21) is the operating coil for the *forward* contactor *FWD*, and (R) for the *reverse* contactor *REV*. The heaters *OL* in the line operate on sustained overload to open

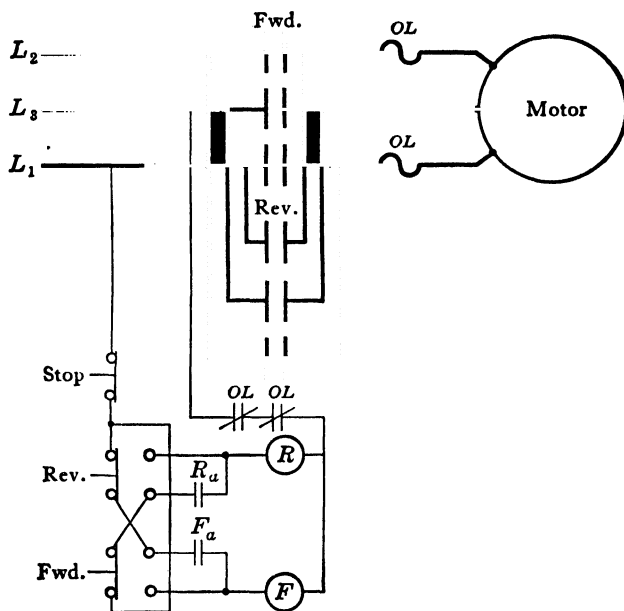


FIG. 49-21. Schematic wiring diagram for the 3-phase reversing magnetic line-starter.

contacts *OL* in the operating coil circuit. Pressing *FWD* button provides coil (F) with current, causing it to close the line contacts *FWD*, as well as control contacts *Fa* which shunt the *FWD* button contacts and maintain current in (F) upon release of *FWD* button. Pressing *REV* button first opens coil (F) and then the forward contactor *FWD*. Pressing button *REV* to its limit energizes coil (R), closing reverse contactor *REV*, and reversing the phase sequence of the voltage applied to the motor terminals.

(b) *Reduced Voltage Starters*. When it is necessary to provide reduced voltage to limit the starting current and torque, this may be accomplished by using an *autotransformer* (also called starting compensator or autostarter)

or by inserting resistance or reactance in series with the lines to the motor. Each type of starter has certain advantages and limitations. With the autotransformer both the *line current* and *starting torque* are reduced as the *square of the voltage at the motor terminals*, while with the resistance and reactance in series with the motor, the line current is reduced in direct proportion to the voltage and the torque as the square of the voltage at the motor terminals.

With the autotransformer type the voltage at the motor usually is reduced to 80%, or 65%, or 50% of line voltage by means of a single tap. When the motor has ceased to accelerate further, full voltage is applied. This switching is done manually or automatically by magnetic contactors. Fig. 49-22 shows the schematic diagram for a manual non-reversing autostarter, and Fig. 49-23 shows the appearance of such a starter. To start the motor the handle is pulled forward to *Start* position. This closes all contacts marked *S*, and opens all contacts *R*, as shown in Fig. 49-22. In this condition the open- $\Delta$  or V-connected autotransformer is connected to the line, and the motor is connected to tapped points on the transformer to give reduced voltage. After the motor has ceased to accelerate further, the handle is pushed back to the *Run* position. This first opens the starting contacts *S* and then closes the running contacts *R* to apply full voltage to the motor. The arm is held in the running position by the magnetic coil (*UV*). If line voltage fails, or becomes too low, the coil (*UV*) releases the arm, which returns to the *Off* position. Sustained overload in either of the heaters *OL* opens the contacts *OL* to release the arm which returns to *Off*. Autotransformer starters are available also in the magnetic type, with push-button control.

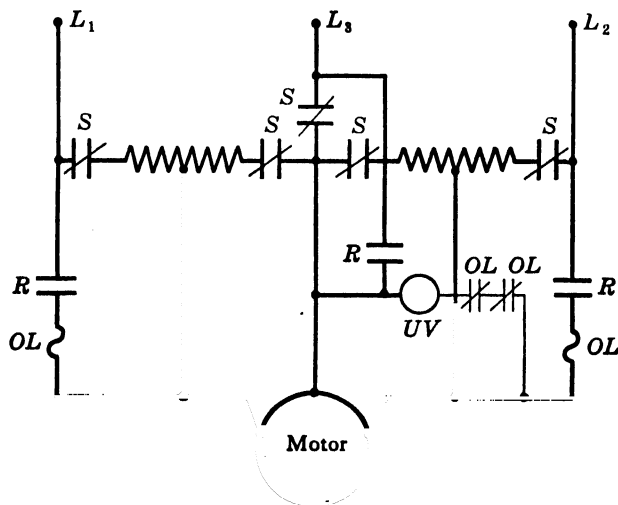


FIG. 49-22. Schematic connection diagram of a 3-phase autostarter for squirrel-cage motor.

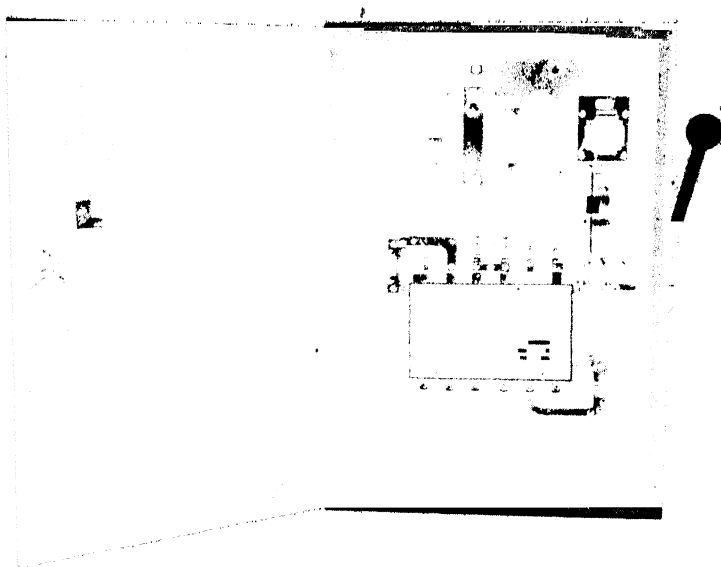


FIG. 49-23. Autostarter for squirrel-cage motors.

Where the characteristics of reduced voltage by series resistors or reactors is desired, this may be accomplished conveniently with the drum-type controller, or by the magnetic type. Fig. 49-24 shows a resistance starter with automatic control, operated by magnetic contactors, and Fig. 49-25 shows the schematic connection diagram. Pressing the start button energizes coil (M), closing the line contactor *M*, and setting in operation the timing mechanism, which after the definite predetermined time closes the contacts *T*, energizing the coil (A) which closes the accelerating contactor *A* and the contacts *Ma*. The starting resistor now is shorted and the motor receives full line voltage. Where the characteristics of a series reactor are desired, the same arrangement may be used as for the resistance starter. See Chap. 23 for part winding starting and Y-start,  $\Delta$ -Run connections.

(c) *Controllers for Wound-Rotor Motors.* Where low starting current or slow acceleration is desired, or where the speed-control possibilities of the wound rotor are needed, a controller to provide adjustable rotor resistance is required. For motors up to 20 or 25 hp this is obtained readily in a face-plate controller with a resistor connected in Y and arranged with taps. For motors of 1000 h.p. and larger, the resistor element is usually a liquid rheostat. The arm is manually operated and remains in any position when speed control is used, or is spring-returned to *Off* when starting duty is required. Fig. 49-26 shows the schematic wiring diagram for such a controller, incorporated with a line starter such as described in Art. 49-1a. This gives overload and low-voltage protection and provides that the motor always shall be



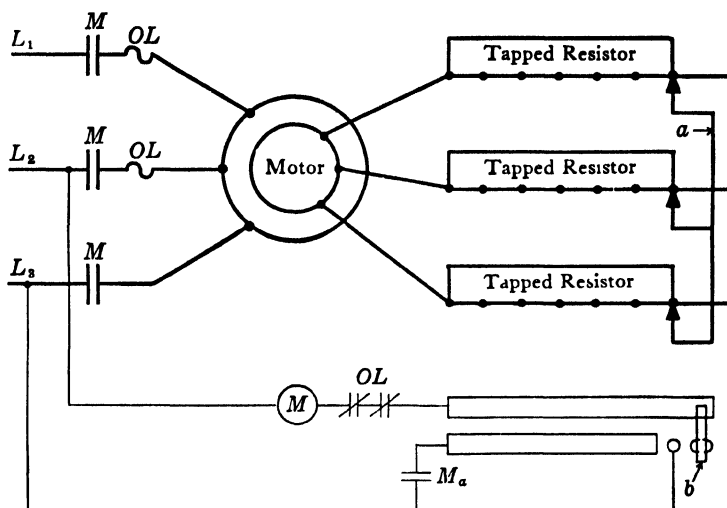


FIG. 49-26. Schematic connection diagram of a 3-phase wound-rotor controller for starting and speed control.

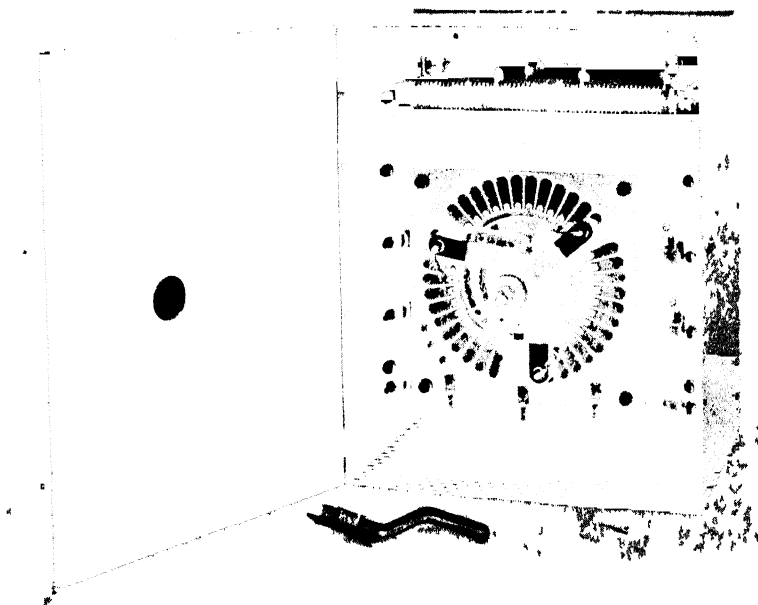


FIG. 49-27. Manual, faceplate-type controller for wound-rotor motor.

started with the maximum resistance in the rotor. Fig. 49-27 shows the general appearance of such a starter. In Fig. 49-26 the arm  $a$  represents the three arms of the starter, sliding over the contacts on the resistors, and  $b$

represents a sliding contact for control purposes. This can be seen in Fig. 49-27 contacts. These parts for the control are insulated from the arm. As shown in Fig. 49-26 the controller is *Off*, as the circuit through main contactor coil (M) is open, and contacts *M* are open. Moving the arm of the controller clockwise, the sliding contacts *a* and *b*, shown in Fig. 49-26, move to the left, and on the first contact a circuit through (M) is established and the main contactor closes. Control contacts *Ma* also close, so that as *b* moves further to the left the circuit through (M) is maintained. Should the line voltage fail, *M* will open and the arm must be returned to *Off* before the motor can be started. This assures that the rotor always shall start with all resistance in. An overload also will de-energize coil (M) and shut down the motor. If the controller is designed for starting duty only, then the auxiliary control contacts are arranged so that the circuit through *Ma* is not complete through slider *b* until it reaches the end position, when all resistance is shorted out. If desired, the automatic features of the controller do not have to be used.

The functions carried out by the face-plate controller may be done by a drum type. For motors between 25 and 500 hp, where manual control is suitable, a drum type is used. Starting duty may be obtained also by means of a definite time magnetic starter.

(d) *Starters for Fractional Horsepower and Small-Horsepower Motors.* These motors practically always are started at full voltage, by an "across the line starter" or switch, which usually has thermal overload protection incorporated within the switch mechanism. The switch may be either manual or magnetic with push-button control. There are many types of each. Fig. 49-28 shows a single-pole snap switch for starting and protecting a single-phase motor. It is of the solder-film type. The heater coil through which the



FIG. 49-28. Starting switch, with thermal protection, for small single-phase motors.

motor current flows is shown in the upper right. It surrounds a shaft over which is mounted a hollow sleeve and in which the shaft may rotate. It normally is prevented from rotating by a thin solder film between it and the shaft. Prolonged overload current through the heater melts the solder and releases the shaft to rotate. A spring then rotates the shaft and another spring opens the contacts to shut down the motor. Upon cooling, the mechanism may be reset by operating the switch handle. It then is ready to operate again. Other types of thermal switches (Fig. 49-19) use a bimetallic strip, arranged to snap open a set of contacts when the heater current is excessive. Heaters are chosen according to the current rating of the motor, and the same size switch may be used for various size motors.

The same type of switch is available also for 3-phase motors up to 3 hp-115 volts, 5 hp-230 volts, and  $7\frac{1}{2}$  hp-440 volts. Of course magnetic starters with push-button control are used also where required on fractional- and small-horsepower motors.

**49-11. Starting Synchronous Motors.** (See also Art. 38-4 and Chap. 61.) Practically all synchronous motors are 3-phase and have a *starting winding*. The starting winding acts like a squirrel-cage winding, and *provides torque to start the motor*. The motor may be started at reduced voltage if the current demands of full voltage are too great, or if the required starting torque is low, as is the case with certain types of load. Reduced voltage usually is obtained by autotransformer or reactor. In cases where large current inrush is allowable, and where the load requires large torque, full-voltage starting is used.

The motor of course would not reach synchronism as an induction motor. However, when the slip is small, d-c excitation may be applied and the motor will pull into synchronism. Before the direct current is put on, the asynchronous torque of the damper winding balances the load torque. As soon as the d-c excitation is applied, a synchronous torque appears which tends to decrease or increase the slip, depending upon the position of the field poles with respect to the armature mmf wave. There is a most favorable position of the field poles at which the pulling-into-step occurs with a minimum direct current and minimum disturbance in the a-c line. Several methods are used to apply the direct current automatically at the most favorable position of the field poles. Only one of them will be discussed.

During the starting period, a high voltage is induced in the d-c field winding. To prevent damage by this voltage, the field usually is shorted through a discharge resistor. This also helps the production of pull-in torque (see Art. 38-4). In order to connect the field at the proper time a synchronizing relay is used. This relay operates so as to apply d-c excitation at the best instant of time within the slip cycle of the motor. Fig. 49-29 shows a schematic connection diagram for such a starter, with the synchronizing relay. At the proper time in the slip-cycle the synchronizing relay energizes the coil (MF) which in turn opens the normally closed field contacts  $MF \parallel$  and closes the normally open field contacts  $\parallel MF$ , thus energizing the d-c field. In one type of synchronizer the timing relay is sensitive to the varying frequency of the voltage induced in the field winding. When this frequency is sufficiently small, the d-c excitation is applied. The operation during starting as an induction motor is controlled by the conventional starter, either at full or reduced voltage. The overload heaters open the main coil (M) in case of overload. In case of voltage failure the coil (M) is de-energized and main contacts  $M$  open and shut down the motor.

The damper winding relay is an a-c relay, sensitive only to alternating current induced in the d-c field winding at nonsynchronous speeds. If this



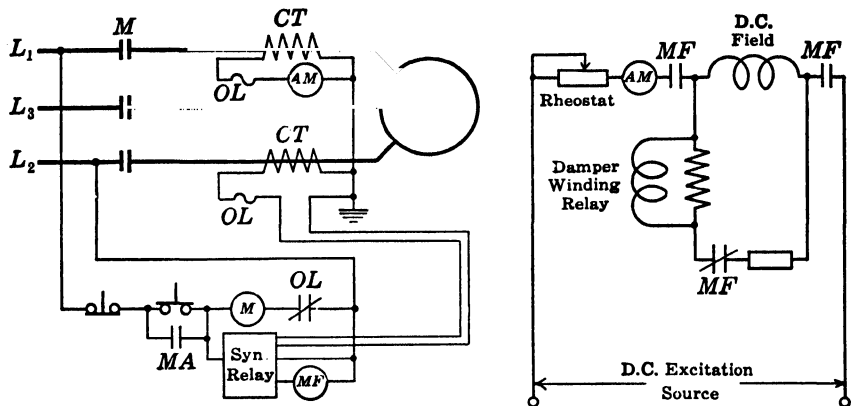


FIG. 49-29. Schematic wiring diagram for full-voltage starter and automatic synchronizer for synchronous motors.

alternating current continues too long it will open coil (M) and shut down the motor, thereby preventing overheating caused by current flowing in the damper winding due to nonsynchronous operation.

**49-12. Factors governing the Type of Controller or Starter To Be Used—Manual or Magnetic.** In deciding between manual and magnetic controls, some of the factors to consider are as follows: Manual controls are available generally only in the smaller sizes, namely, for full-voltage direct current or alternating current only up to  $1\frac{1}{2}$  or 2 hp, for d-c and a-c resistance starters up to 50 hp, for autotransformer starters from 5 to 50 hp. For infrequent operation (less than 5 to 7 operations an hour) the manual type is satisfactory; for more frequent operation, especially under heavy loads, the magnetic type usually is chosen as it is able to stand up better under more severe operation. Repairs usually are made more easily on the magnetic type. The manual type must be mounted near the operator for convenience of operation, but space may not be available; then the magnetic type is used, because it may be mounted in a less convenient place where space is available, and push-button control may be used. The magnetic type is entirely automatic after pressing the control button, and hence careless operation of the controller with its possible attendant damage to machinery does not result. If control must be remote, such as by a limit switch, float switch, pressure switch, etc., there is no choice except the magnetic type. The manual control usually is less expensive in first cost, but may be more expensive to maintain especially under severe service, and there is a definite trend favoring magnetic control.

A further advantage of the magnetic control is that there may be several control points, suitably interlocked and with indicating pilot lamps. Push-button stations may be installed at several points. Push buttons are either

of the momentary-contact type or of the maintained-contact type. The former ordinarily is used, as it provides undervoltage protection in connection with a set of control contacts on the main contactor, which are in parallel with the momentary-contact start button, and normally are open, but they close when the main contactor closes, thus maintaining current in the magnetic contactor coil when the *start* button is released. (To illustrate this point see any of the figures showing the magnetic controller.) Float switches, pressure switches, temperature relays, and other types of controls may be used in connection with magnetic controls, to start and stop the motor. Sometimes the mechanical motion of some part of the driven machine must be limited, as in a material-testing machine, a hoist, a planer, etc., in which case the contacts of a limit switch are placed in series with the stop button to shut down the motor.

In choosing between full-voltage, autotransformer, resistance, or reactance starting for polyphase induction motors, the following factors must be considered. Full-voltage starting is the least expensive and most simple in application. It is used when the starting current is not too severe on the power line, or when the sudden application of large torque will not damage the load. Direct-connected loads such as fans, blowers, etc., usually may be started with full voltage without difficulty. Whether or not full-voltage starting is permissible depends upon the ratio of starting kva to available line-kva and is usually decided upon by the utilities.

The *starting torque of polyphase induction motors varies with the square of the current*, i.e., with the square of the applied voltage. In the autotransformer starter the motor current at starting varies directly with the voltage at the motor terminal voltage. Thus an autotransformer starter designed to reduce the motor terminal voltage to 80% of line voltage will produce a motor torque of 64% and require a line current of 64% of that which would be taken at full voltage (Fig. 49-30). The comparison between full voltage autotransformers at 80% voltage and resistor at 65% standstill voltage is shown in Fig. 49-31, for a squirrel-cage motor starting a loaded centrifugal pump. Full voltage requires an initial current of 600%, but the accelerating time is small. The initial line current for the autotransformer starter varies as the square of the tap voltage. In autotransformer starting there is a short *off* time when changing from tap voltage to line voltage, which produces a higher peak at change-over than in resistor starting at the same starting voltage, and results in greater line disturbance. Resistor starting at the same starting voltage at the motor terminals as autotransformer starting takes about the same accelerating time, but the initial starting currents taken from the line are greater for resistor starting. For 65% starting voltage the percent currents are 42% for autotransformer and 65% for resistor, while the respective starting torques are each 42%. If the line currents are to be made equal the 80% tap is used, or 65% starting voltage with resistor is used. In this case acceleration time is shorter for the

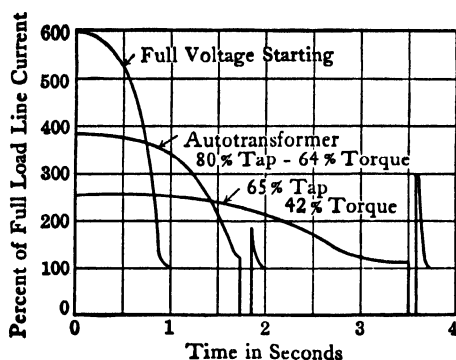


FIG. 49-30. Starting current *vs.* time for a squirrel-cage motor driving a loaded centrifugal pump. Starting with full voltage and with autotransformer.

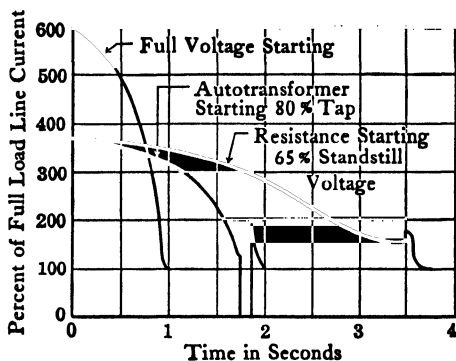


FIG. 49-31. Comparison of starting characteristics for a squirrel-cage motor driving a loaded centrifugal pump: full-voltage starting, autotransformer starting, and resistance starting.

autotransformer starting, due to greater torque. Generally the autotransformer type is more efficient, while the resistor type gives smoother acceleration. Reactor acceleration likewise is very smooth. When very low starting current with high starting torque is required, with smooth acceleration, a wound rotor with a secondary rheostat is used.

**49-13. Motor Protection.** Electric machines generally are not self-protecting, i.e., overloads, overvoltage, overspeed, etc., may damage the machines, unless externally applied protective devices are used. The various types of protection for motors are undervoltage, overvoltage, overload, phase failure, phase reversal. See definitions Art. 49-14.

Undervoltage may cause a motor to carry excessive current, or to run at low speed. If the voltage fails altogether, and is restored with the machine still connected to the line, it may damage the equipment or injure the operator. On some installations such as fans, pumps, etc., it might do no damage. Undervoltage protection generally is desired in industrial motor applications and is incorporated in the starting device, by a coil which releases the main line contacts upon low voltage or voltage failure, and these contacts remain open until the operator starts the motor again. All automatic starters inherently have undervoltage protection. Fig. 49-20 illustrates how undervoltage protection is provided. If the line voltage fails the coil (M) will become de-energized and the main contacts *M* open. The motor will not start again until the start button is closed.

The most common type of protection required is for overload. The general effect of overload is excessive heating of the motor insulation, greatly lessening its life, or in the case of very excessive overloads quickly burning out the insulation, causing a short, with its attendant severe damage.

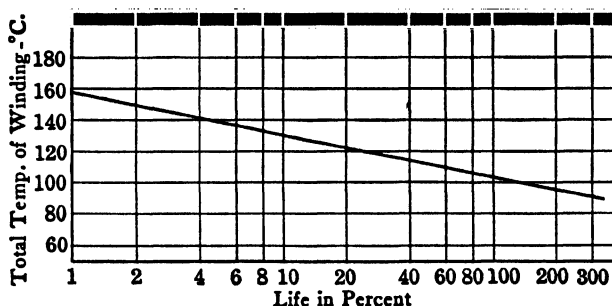


FIG. 49-32. Effect of winding temperature on the life of class A insulation.

The effects on insulation life caused by continuous operation at different temperatures are illustrated in Fig. 49-32, which shows the relation between expected life in percent and the temperature of the winding. The general effect of overload is manifest in overheating, but due to the heat capacity of the machine, it takes time for the temperature of the windings to rise, the time depending upon the degree of overload (Fig. 49-33), the ambient temperature, the previous load history, and the heat capacity of the machine. The effect of load on the time required for a motor to reach normal limiting temperature for Class A motor insulation is shown in Fig. 49-33. An overload

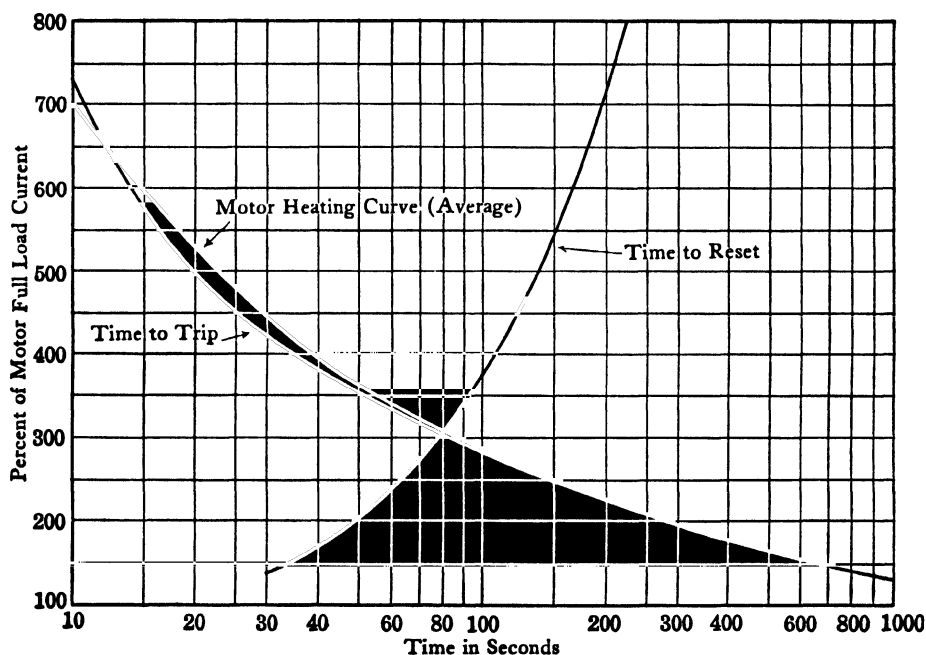


FIG. 49-33. Characteristics of thermal protection for motors. Ambient 40° C.

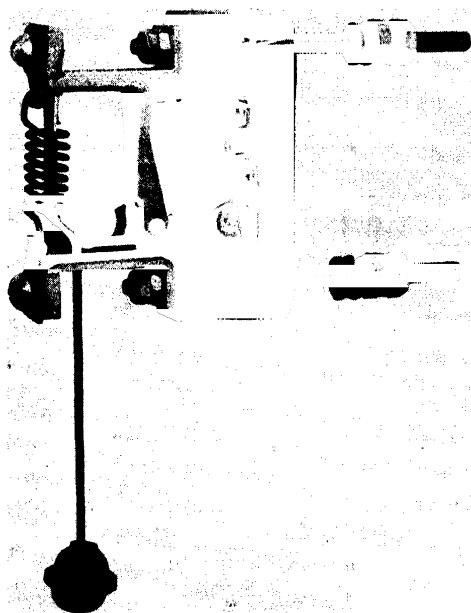


FIG. 49-34. Thermal overload relay.

device to protect such a motor should have its delay characteristic coordinated with the heating time of the motor. With rotor locked the average poly-phase induction motor takes a current of about 600%, which according to Fig. 49-33 would cause the safe limiting temperature to be reached in about 15 seconds. The overload device should open the line in less than 15 seconds on 600% load current and in less than 5 minutes on 200% load. If the overload protective device operates too quickly the motor will be shut down unnecessarily. Thermal overload devices, using a heater coil surrounding a bimetallic strip, or solder film device, or an induction type thermal relay may be designed to duplicate closely the thermal properties of the motor. Fig. 49-33 shows the tripping time and reset time (time for element to cool before it can be reset) for a typical thermal device, showing how closely it can be coordinated with the heating curve of the motor. Fig. 49-34 shows the construction of a typical bimetallic type of overload relay for use with a magnetic contactor. The main motor current flows through the spiral heater coil surrounding a vertical bimetallic strip. The control contacts shown in the rear center of Fig. 49-34 normally are closed. Overload currents cause the heating of the bimetallic strip, and it moves to the left, releasing the horizontal arm just beneath the reset and in turn opening the control contacts in the rear. This opens the main contactor coil and shuts down the motor. When the strip has cooled, the device is reset by pulling down on the reset string. In some cases where the ambient temperatures at the starter are likely to be

very different than at the motor, the thermal elements are placed directly on the motor or windings. In small motors using manual starters, the thermal device operates on the main switch directly as shown in Fig. 49-28.

The fundamental purpose of the motor-running overload device is to protect the motor from overheating. The contactors on the starters usually are not designed to open on short circuits, as this would cause currents to flow in excess of the interrupting capacity of the contactor or switch. Therefore a protective device effective for short circuits is required, unless the starter is specifically designed for this duty also. Fig. 49-35, taken from the National Electrical Code 1956, shows the scheme of connection required by the National Board of the Fire Underwriters, for protecting the feeder, branch circuit, and motor. In many installations the disconnect switch, the motor-running overcurrent device and the motor controller (Fig. 49-35) are made as a unit and mounted in the same case. Fuses commonly are used in the feeder and motor branch circuit for overcurrent protection because when they are applied correctly they will operate to open a short circuit satisfactorily. The fuses usually are integral with the disconnect switch. Certain types of magnetic circuit breakers also are used, though they are more expensive and generally are used only on large power motors. The overcurrent protection for the feeder is chosen according to the following rule of NEC-1956 (National Electrical Code). Section 4362 reads: "A feeder which supplies motors shall be provided with overcurrent protection which shall not be greater than the largest rating or setting of the branch-circuit protective device, for any motor of the group (see NEC Tables 20, 26, 27) plus the sum of the full-load currents of the other motors of the group." For the rating or setting of the overcurrent device for the motor branch circuit see NEC Table 20 and refer to Section 4342 of the NEC. For the running or overload protection of the motor see NEC, Sections 4321-4331, NEC Table 20. (In general the size of wire for a motor branch circuit is not to be less than 125% of the motor full-load current.) In general, continuous-duty motors of more than 1 hp shall have

running overcurrent protection of not greater than 125% of full-load current. In some cases it may be 140%. The rating of the motor-running overcurrent protective device shall not be greater than 150% of full-load current.

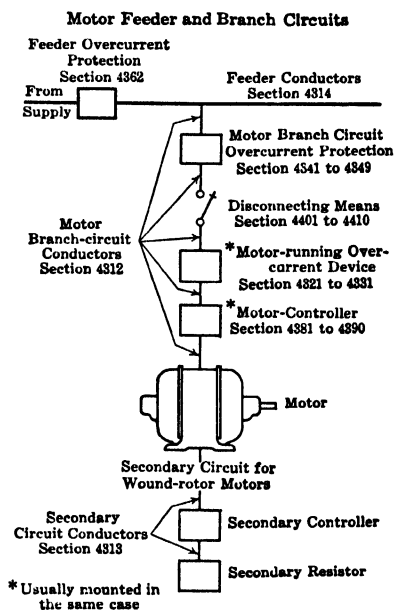


FIG. 49-35. Connection diagram for protective devices in motor feeder and branch circuits.

Certain modifications from these requirements are applicable for fractional-horsepower motors, and the NEC always should be consulted before applying protective devices, or laying out feeder and branch circuits for motors.

#### 49-14. DEFINITIONS

1. *Undervoltage Protection.* The effect of a device operative on the reduction or failure of voltage to cause and maintain the interruption of power to the main circuit. (NEMA IC50-230.)

2. *Undervoltage Release.* The effect of a device operative on the reduction or failure of voltage to cause the interruption of power to the main circuit but not to prevent the re-establishment of the main circuit on return of voltage. (IC50-232.)

3. *Phase-Failure Protection.* The effect of a device operative upon the failure of power in one wire of a polyphase circuit, to cause and maintain the interruption of power in all the wires of the circuit. (IC50-234.)

4. *Phase-Reversal Protection.* The effect of a device operative on the reversal of the phase-rotation in a polyphase circuit, to cause and maintain the interruption of power in all the wires of the circuit. (IC50-236.)

5. *Overload Protection.* The effect of a device operative on excessive current, but not necessarily on short-circuit, to cause and maintain the interruption of current flow to the device governed.

NOTE: By operating overload is meant a current not in excess of 4 times the rated current for a-c motors, nor in excess of 4 times the rated current for d-c motors. (IC50-238.)

6. *Resistor.* A device used primarily because it possesses the property of electrical resistance. A resistor as used in electric circuits for purposes of operation, protection or control, commonly consists of an aggregation of units. (IC50-248.)

7. *Constant Torque Resistor.* A resistor for use in the armature or rotor circuit of a motor in which the current remains practically constant throughout the entire speed range. (IC50-254.)

8. *Fan Duty Resistor.* A resistor for use in the armature or rotor circuit of a motor in which the current is approximately proportional to the speed of the motor. (IC50-256.)

9. *Relay.* A device that is operative by a variation in the conditions of one electric circuit to effect the operation of other devices in the same or another electric circuit.

NOTE: Where relays operate in response to changes in more than one condition, all functions should be mentioned. (IC50-275.)

10. *Notching.* A qualifying term indicating that a predetermined number of separate impulses are required to complete operation. (IC50-300.)

11. *Inverse Time.* A qualifying term indicating that there is purposely introduced a delayed action, which delay decreases as the operating force increases. (IC50-302.)

**12. *Definite Time.*** A qualifying term indicating that there is purposely introduced a delay in action, which delay remains substantially constant regardless of the magnitude of the quantity that causes the action. (IC50-304.)

**13. *Instantaneous.*** A qualifying term indicating that no delay is purposely introduced in the action of the device. (IC50-306.)

**14. *Magnetic Contactor.*** A contactor actuated by electromagnetic means. (IC50-322.)

**15. *Electric Controller.*** A device, or group of devices, which serves to govern, in some predetermined manner, the electric power delivered to the apparatus to which it is connected. (IC50-324.)

**16. *Manual Controller.*** A controller operated by hand. (IC50-332.)

**17. *Drum Controller.*** A controller which utilizes a drum switch as the main switching element.

**NOTE:** A drum controller usually consists of a drum switch and a resistor. (IC50-334.)

**18. *Starter.*** A controller designed for accelerating a motor to normal speed in one direction of rotation.

**NOTE:** A device designed for starting a motor in either direction of rotation includes the additional function of reversing and should be designated a controller.

**NOTE:** By basic functions is usually meant acceleration, retardation, line closing, reversing, etc. (IC50-336.)

**19. *Automatic.*** Automatic means self-acting, operating by its own mechanism when actuated by some impersonal influence, as, for example, a change in current strength; not manual, without personal intervention. Remote control that requires personal intervention is not automatic, but manual. (IC50-338.)

**20. *Automatic Starter.*** A starter designed to control automatically the acceleration of a motor during the acceleration period. (IC50-340.)

**21. *Autotransformer Starter.*** A starter having an autotransformer to furnish a reduced voltage for starting. The device includes the necessary switching mechanism and frequently is called a compensator or autostarter. (IC50-342.)

**22. *Control Cutout Switch.*** A switch that isolates the control circuit of a motor controller. (IC50-344.)

**23. *Magnet Brake.*** A friction brake controlled by electromagnetic means. (IC50-350.)

**24. *Sealing Gap.*** The distance between the armature and center of the core of a magnetic contactor when the contacts first touch each other. (IC50-352.)

**25. *Sealing Voltage (or Current).*** The voltage (or current) necessary to seat the armature of a magnetic contactor from the position at which the contacts first touch each other. (IC50-354.)

**26. *Pick-Up Voltage (or Current).*** The voltage (or current) at which a magnetic contactor starts to close. (IC50-356.)



27. *Drop-Out Voltage (or Current).* The voltage (or current) at which a magnetic contactor will release to its de-energized position. (IC50-358.)

28. *Normally Open and Normally Closed.* The terms *normally open* and *normally closed* when applied to a magnet-operated switching device, such as a contactor or relay, or to the contacts thereof, signify the position taken when the operating magnet is de-energized. These terms apply only to non-latching types of devices. (IC50-360.)

29. *Jogging.* *Jogging* or *inching* is the quickly repeated closure of the circuit to start a motor from rest for the purpose of accomplishing small movements of the driven machine. (IC50-374.)

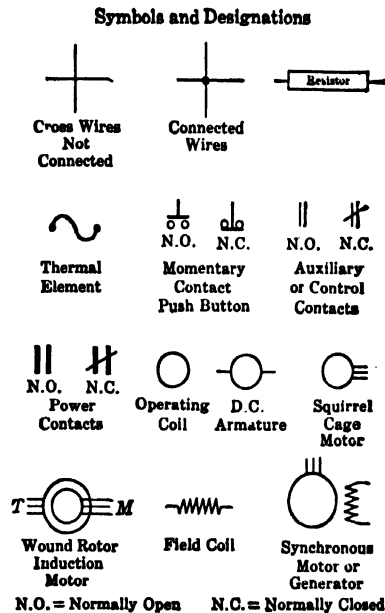


FIG. 49-36. Symbols and Designations.

## PART TWO



## Chapter 50

### DETERMINATION OF THE NO-LOAD MMF

**50-1. The Five Parts of the Magnetic Circuit.** In the induction motor, turbine generator, and a-c commutator motor, the magnetic path traverses the stator core, the stator teeth twice, the air gap twice, the rotor teeth twice, and the rotor core. In the salient pole synchronous machine, two poles and the rotor yoke appear in place of the two rotor teeth and the rotor core.

The emf to be induced in the armature winding is given for the induction motor and the polyphase a-c commutator motor by the terminal voltage and the small voltage drop in the primary winding. For the other machine types where the armature reaction has to be taken into account, the no-load characteristic must be computed, i.e., computations must be made for several values of the induced emf. If the magnitude of the induced emf is given, the flux is also given. Magnitude is determined by the equation (see Art. 39-1)

$$E = 4f_B f N k_{ap} \Phi 10^{-8} \quad \text{volt} \quad (50-1)$$

The mmf curve of an induction motor is sinusoidal (since only the fundamental of the mmf curve is considered here). However, its flux distribution curve is flattened, because of the saturation of the iron. It is found that there is a pronounced 3rd harmonic. The other harmonics are small. These saturation harmonics have little influence on the starting performance or the pull-out torque, since at these conditions of operation the main flux is reduced. At rated load the fundamental of the flux distribution curve is also of main importance. Therefore, for the induction motor  $f_B = 1.11$ .

In the salient-pole machine,  $f_B$  is a function of the ratio  $b_p/\tau$  ( $b_p$  is the pole arc). Approximately

$b_p/\tau = 0.50$	0.55	0.60	0.65	0.7	0.75
$f_B = 1.18$	1.168	1.15	1.128	1.104	1.074

These values of  $f_B$  were obtained by evaluating a large number of actual flux distribution curves. For each individual case, the value of  $f_B$  can be obtained from a flux map.

A certain mmf is necessary to drive the flux through the machine structure. The magnitude of this mmf is determined by the basic law, Eq. 1-23; this is

the circuital law of the magnetic field. If this law is applied in the form of Eqs. 1-26 and 1-27, it is seen that the sum

$$\Phi \sum \frac{l}{\mu A} = 0.4\pi NI \quad (50-2)$$

has to be extended over five terms for which the permeability  $\mu$ , the length of the magnetic path  $l$ , and the cross-section  $A$  are each different. Thus, for the non-salient pole machines, Eq. 50-2 can be written in the form

$$\Phi \left( \frac{l_{c1}}{\mu_{c1}A_{c1}} + \frac{2l_{t1}}{\mu_{t1}A_{t1}} + \frac{2g}{A_g} + \frac{2l_{t2}}{\mu_{t2}A_{t2}} + \frac{l_{c2}}{\mu_{c2}A_{c2}} \right) = 0.4\pi NI \quad (50-3)$$

where the subscript 1 refers to the stator and subscript 2 to the rotor.  $g$  is the length of a single air-gap. For the salient-pole machines, the last two terms are  $2l_p/\mu_p A_p$  and  $l_r/\mu_r A_r$ .

It follows from Eqs. 1-25 and 50-3 that

$$\frac{B_{c1}}{0.4\pi\mu_{c1}} l_{c1} + 2 \frac{B_{t1}}{0.4\pi\mu_{t1}} l_{t1} + 2 \frac{B_g}{0.4\pi} g + 2 \frac{B_{t2}}{0.4\pi\mu_{t2}} l_{t2} + \frac{B_{c2}}{0.4\pi\mu_c} l_{c2} = NI \quad (50-4)$$

$$\text{or} \quad H_{c1}l_{c1} + 2H_{t1}l_{t1} + 2H_g g + 2H_{t2}l_{t2} + H_{c2}l_{c2} = NI \quad (50-5)$$

$H$  is the ampere-turns per unit length. Eq. 50-5 states that, in order to find the total ampere-turns  $NI$  necessary to force the flux through the structure, the ampere-turns of each of the five components are to be determined separately and then added up.

Eqs. 50-3 to 50-5 describe how to determine the five component ampere-turns. First divide the flux  $\Phi$  by each of the five cross-sections, i.e., determine the five values of  $B$  to be used in Eq. 50-4. Then determine from the saturation curves of the iron used for stator and rotor, the values of  $H = B/0.4\pi\mu$  which correspond to the values of  $B$  given by Eq. 50-4. Finally, multiply the values of  $H$  found from the saturation curves by their path lengths  $l$  and add the five components. This yields the mmf of one complete magnetic circuit. A 2-pole machine has only one magnetic circuit, and the  $NI$  ampere-turns are placed half on each pole. A multipole machine has  $p/2$  magnetic circuits, and the total number of necessary ampere-turns is  $p/2$  times the ampere-turns necessary for one circuit.

The term  $2(B_g/0.4\pi)g = 2H_g g$  which represents the ampere-turns necessary to drive the flux  $\Phi$  through two air gaps is the largest of the five terms. Its magnitude is 70 to 85 per cent of the total ampere-turns  $NI$ .

**50-2. The Air-gap mmf.** The cross-section of the air gap is

$$A_g = b_e l_e \quad (50-6)$$

$b_e$  is the width of a rectangle the height of which is the maximum value of the flux distribution curve (Fig. 50-1) and the area of which is the area under the

flux distribution curve.  $l_e$  is the *effective* core length the magnitude of which is determined in the following.

For a sinusoidal flux distribution,  $b_e = (2/\pi)\tau$ . Since only the fundamental of the flux distribution curve is of importance for the induction motor, for this machine  $b_e = (2/\pi)\tau$ .

For the salient-pole machine, approximately,

$b_p/\tau = 0.50$	0.55	0.60	0.65	0.70	0.75
$b_e = 0.58$	0.625	0.665	0.705	0.745	$0.785 \times \tau$

These values of  $b_e$  were obtained in the same manner as the values of  $f_B$ . For each individual case, the value of  $b_e$  can be obtained from a flux map.

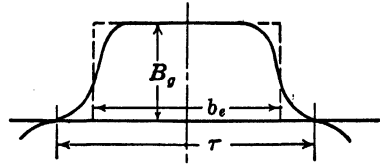


FIG. 50-1. Flux distribution curve of a salient-pole machine.

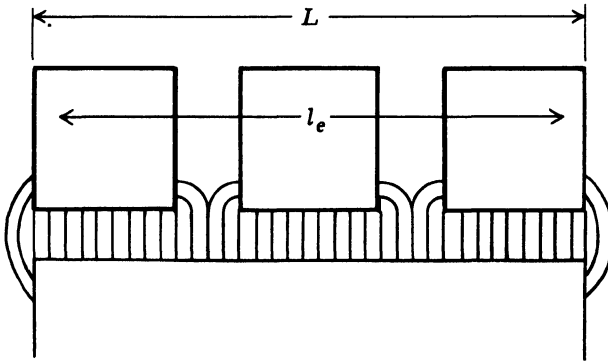


FIG. 50-2. Explanation of the effective core length.

The effective core length  $l_e$  is smaller than the core length  $L$  and larger than the iron length  $L - n_v b_v$  (Fig. 50-2).  $n_v$  is the number of radial vents and  $b_v$  the width of a vent.  $n_v b_v$  is approximately 15 per cent of the core length  $L$ . The effective core length takes into consideration the lines of force which enter the armature laterally and through the air vents.  $l_e$  is best determined by the method of conformal mapping or from flux maps. They show (Ref. A11) that the loss of  $L$  per vent ( $l'$ ) is

$$l' = \frac{b_v/g}{5 + b_v/g} b_v \quad (50-7)$$

If  $\tau_v$  is the width of one stack of laminations plus one vent

$$\tau_v = \frac{L + b_v}{n_v + 1} \quad (50-8)$$

then the effective width of this stack is  $\tau_v - l'$  and the ratio

$$k_v = \frac{\tau_v}{\tau_v - l'} = \frac{\tau_v(5g + b_v)}{\tau_v(5g - b_v) - b_v^2} \quad (50-9)$$

is the factor by which the length of a stack is to be divided in order to obtain its effective length. Therefore, the effective core length

$$l_e = \frac{L}{k_v} \quad (50-10)$$

Fig. 50-2 refers to a machine in which only one part has radial vents, as is the case in the salient-pole synchronous machine. When both machine parts have radial vents, as is the case in the induction motor, then  $k_v$  has to be computed for both parts and

$$l_e = \frac{L}{k_{v1} \times k_{v2}} \quad (50-11)$$

Fig. 50-3 shows the vent factor  $k_v$  as a function of  $b_v/g$  with  $b_v/\tau_v$  as parameter.

When the radial vents of both machine parts are opposite to each other, the total vent factor  $k_{vt} = k_{v1} \times k_{v2}$  can be determined from flux maps in the same manner as the factor  $k_v$  is determined when only one machine part has radial vents (Ref. A11). This yields

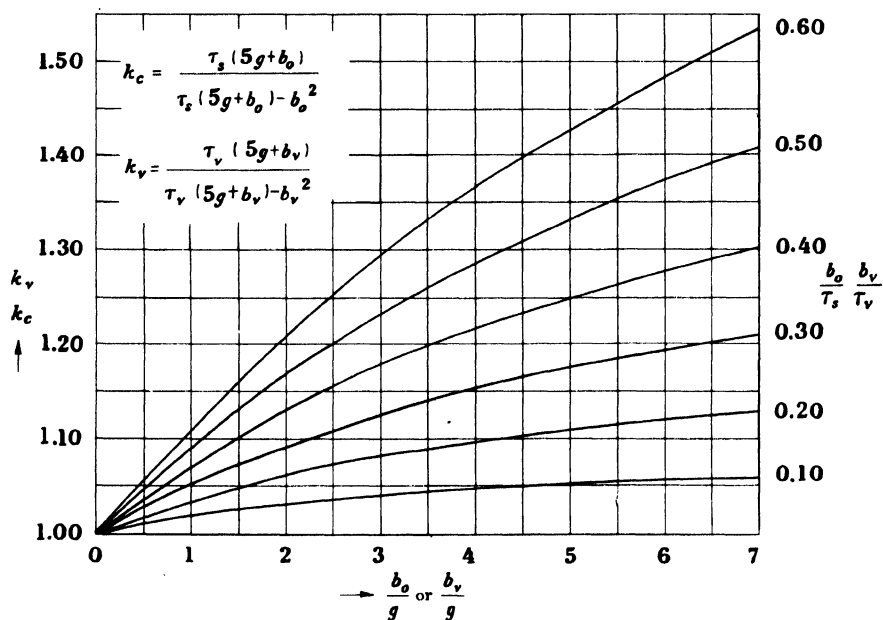


FIG. 50-3. Vent factor  $k_v$  and Carter factor  $k_c$ .

$$k_{vt} = \frac{\tau_v(5g + 2b_v)}{\tau_v(5g + 2b_v) - 2b_v^2}, \quad \text{and} \quad l_e = \frac{L}{k_{vt}} \quad (50-11a)$$

With  $b_e$  and  $l_e$  determined  $A_g$  is given by Eq. 50-6 and

$$B_g = \frac{\phi}{A_g} \quad (50-12)$$

The mmf for the two air-gaps is then (Eq. 50-4)

$$M_g = \frac{2}{0.4\pi} B_g g = 1.6 B_g g$$

However, this equation yields a correct value for the gap-mmf only when the armature has no slots. When the armature is slotted, the air-gap appears increased at the spots opposite the slots. This increase of the air-gap can be expressed by a factor  $k_c$  the derivation of which is the same as for the vent factor  $k_v$  (Ref. A11). In this factor the slot pitch  $\tau_s$  is substituted for the vent pitch  $\tau_v$  and the slot-opening  $b_o$  substituted for the vent width  $b_v$ , thus

$$k_c = \frac{\tau_s(5g + b_o)}{\tau_s(5g + b_o) - b_o^2} \quad (50-13)$$

and the effective air-gap is  $g \times k_c$ . If both machine parts are slotted, the factor  $k_c$  must be calculated for both parts separately and the effective air-gap is  $g \times k_{c1} \times k_{c2}$ . The factor  $k_c$  is called the *Carter factor* because it was derived first (analytically) by C. W. Carter. It is shown in Fig. 50-4 as function of  $b_o/g$  with  $b_o/\tau_s$  as parameter.

Taking into account the slot-openings, the mmf for the two air-gaps becomes

$$M_g = 1.6 B_g g k_c$$

In this equation  $B_g$  is expressed in Gauss and  $g$  in cm. If  $B_g$  is expressed in lines per square inch and  $g$  in inches

$$M_g = 0.63 B_g g k_c \quad (50-14)$$

**50-3. The Teeth Mmf.** With the value of  $B_g$  from Eq. 50-12 the tooth density can be determined as

$$B_t = \frac{\tau_{sg} l_e B_g}{b_t k_i l} \quad (50-15)$$

where  $\tau_{sg}$  is the slot pitch at the air gap,  $b_t$  the tooth width,  $l = L - n_v b_v$  the axial length of the armature iron, including the insulation between the laminations, and  $k_i$  the stacking factor which takes into account the insulation between laminations.  $k_i = 0.92$  for waterglass or lacquer insulation;  $k_i = 0.96$  for oxide-film insulation. The numerator of Eq. 50-15,  $\tau_{sg} l_e B_g$ , is the flux which enters the armature through a slot pitch. In induction motors,



saturation in the teeth will cause a redistribution of the flux resulting in a decrease in the peak tooth density. Therefore, the value of  $B_t$  given by Eq. 50-15 must be multiplied by 0.8.

The length of the magnetic path in the two teeth is  $2h_t$ , where  $h_t$  is the height of the tooth.

Eq. 50-15 assumes that the flux entering the armature through a slot pitch passes only through the iron (through the tooth). This is the case when  $B_t$  is equal to or smaller than about 118,000 lines/in.<sup>2</sup> When  $B_t$  is larger than this value, a part of the flux  $\tau_{sg}l_eB_g$  takes a path through the slot, i.e., parallel to the tooth iron. With respect to the flux  $\tau_{sg}l_eB_g$ , tooth and slot are magnetically in parallel. In the case of low saturation, the reluctance of the tooth is small in comparison to that of the slot so that practically no lines of force go through the slot. On the other hand, if the tooth is saturated, its permeability will be low, the reluctance will be comparatively large, and a part of the lines of force will go through the slot. In this latter case, Eq. 50-15 would yield too high a value for the tooth density.

For high tooth saturation, the value of  $B_t$  yielded by Eq. 50-15 will be called the fictitious tooth density  $B_t'$ . The *actual tooth density*  $B_t$  is determined as follows:

The flux through a slot pitch is

$$\tau_{sg}l_eB_g = \Phi' \quad (50-16)$$

For high tooth saturation, it divides into two parts:

$$\Phi' = \Phi_t + \Phi_s \quad (50-17)$$

The flux  $\Phi_t$  goes through the tooth and the flux  $\Phi_s$  through the slot. The ratio of the cross section of the slot,  $A_s$ , to the cross section of the tooth,  $A_t$ , is

$$k_t = \frac{A_s}{A_t} = \frac{\tau_s l_e - b_t k_t l}{b_t k_t l} \quad (50-18)$$

Dividing Eq. 50-17 by  $A_t$ ,

$$\frac{\Phi'}{A_t} = \frac{\Phi_t}{A_t} + \frac{\Phi_s}{A_s} k_t$$

or

$$B_t' = B_t + B_s k_t$$

Thus the actual tooth density is

$$B_t = B_t' - B_s k_t \quad (50-19)$$

$B_t'$ , the fictitious tooth density, is given by Eq. 50-15. Introducing  $B_s = 0.4\pi H$ ,

$$B_t = B_t' - 0.4\pi k_t H \quad (50-20)$$

Since  $H$  is the same along the slot as along the tooth,  $H$  and  $B_t$  in Eq. 50-20 are related to each other by the magnetization curve of the tooth iron.

The axis of abscissa of the magnetization curve is usually given in ampere-

turns per unit length ( $at = H$ ). Furthermore,  $B$  and  $at$  are drawn to different scales. If  $S_{at}$  is the number of ampere-turns per cm per unit length in the axis of  $at$  and  $S_B$  the number of lines per  $cm^2$  per unit length in the axis of  $B$ , then

$$B_t = B'_t - 0.4\pi k_t \frac{S_{at}}{S_B} \times at \quad (50-21)$$

If, further, the magnetization curve is given in the units

$$B/\text{in.}^2 = f(at = AT/\text{in.})$$

and  $S_{at}'$  is the number of ampere turns per inch per unit length in the axis of  $at$  and  $S_B'$  the number of lines per  $\text{in.}^2$  per unit length in the axis of  $B$ , then

$$B_t = B'_t - 0.4\pi k_t \frac{S_{at}'}{S_B'} \times at = B'_t - 3.19k_t \frac{S_{at}'}{S_B'} \times at \quad (50-22)$$

In order to determine the actual tooth density  $B_t$ , draw the quantity

$$3.19k_t(S_{at}'/S_B') \times at$$

as a function of  $at$  below the magnetization curve  $B = f(at)$ , as shown in Fig. 50-4. This is a straight line. If the fictitious tooth density  $B'_t$  (Eq. 50-15) is equal to  $DA$  and from  $A$  a line is drawn parallel to the line

$$3.19k_t(S_{at}'/S_B') \times at,$$

the distance  $BC$  is equal to the actual tooth density  $B_t$  and the distance  $OC$  is the corresponding value of  $H_t = at$ .

The tooth mmf is then

$$M_t = 2h_t H_t \quad (50-23)$$

Fig. 50-5 shows the corresponding values of the fictitious tooth density, the actual tooth density, and the field intensity  $H = at$  for USS Electrical Steel, Gauge 26.

When the width of the tooth at its top is different from that at its base, the tooth density varies along the tooth. In this case, it is often satisfactory to compute with the tooth density at  $\frac{1}{3}h_t$  measured from base of the tooth; i.e., for  $b_t$  in Eq. 50-15 and for  $\tau_s$  and  $b_t$  in Eq. 50-18 the values at this place are to be used. A more accurate value for  $M_t$  than the  $\frac{1}{3}h_t$ -computation yields is obtained by applying *Simpson's rule*. Here the values of tooth density and corresponding  $H_t$  are calculated for top, middle, and base of the tooth by substituting the value of  $b_t$  in Eq. 50-15 and the values  $\tau_s$  and  $b_t$  in Eq. 50-18 for each of these places. The tooth mmf is then

$$M_t = 2h_t \frac{(H_{t,\text{top}} + 4H_{t,\text{mi}} + H_{t,\text{base}})}{6} \quad (50-24)$$

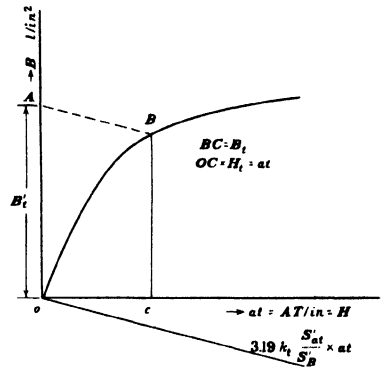


FIG. 50-4. Determination of the actual tooth density from the fictitious tooth density.

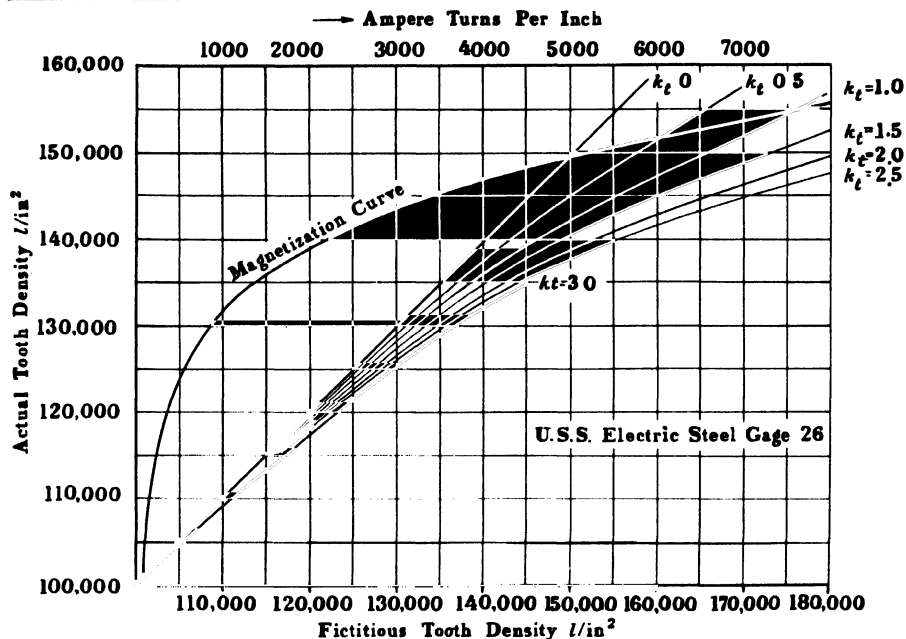


FIG. 50-5. Actual tooth density and field intensity  $H$  (at) vs. fictitious tooth density for USS Electrical Steel, gage 26.

**50-4. The Core Mmf.** The flux density in that core cross-section which divides the magnetic path into two symmetrical parts is equal to

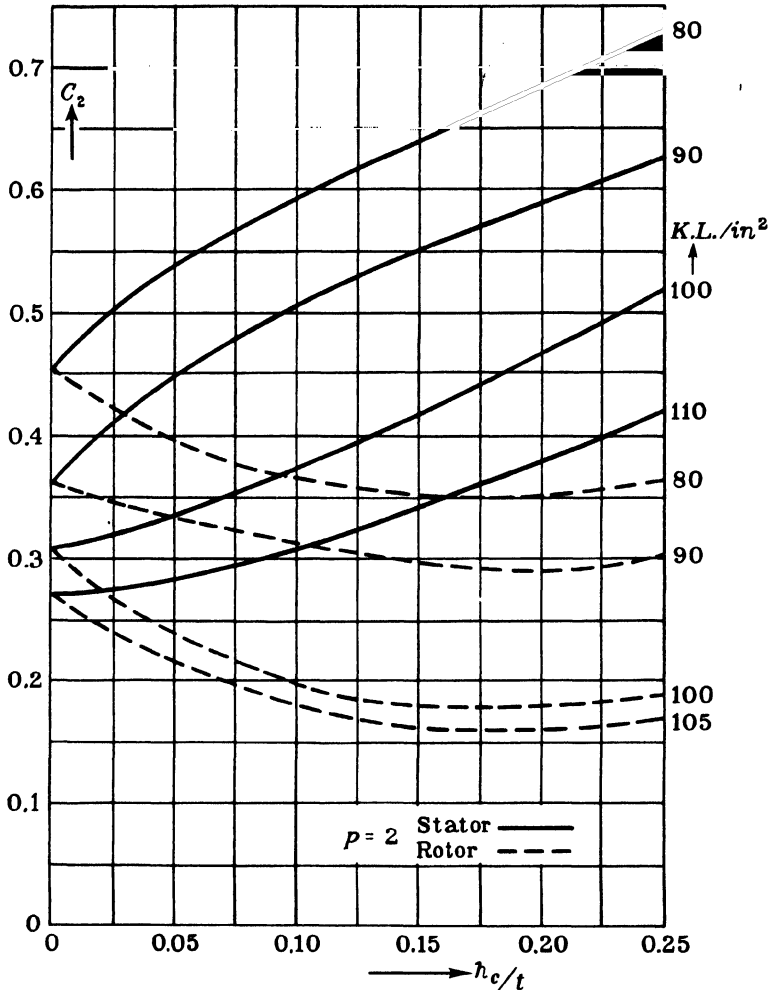
$$B_c = \frac{\Phi}{2h_c k_t l} \quad (50-25)$$

where  $h_c$  is the height of the core behind the teeth. In other core cross-sections the flux density is smaller than this value of  $B_c$ . The mmf of the air-gap and teeth is computed for the line of force which passes the center-line of the pole. Computing the core-mmf with the value of  $B_c$  given by Eq. 50-25 for the same line of force, which is the longest one, would yield a too large value for the core mmf because this value of  $B_c$  is a maximum value. Figures 50-6 and 50-7 show the factor ( $C_c$ ) by which the core mmf must be multiplied when Eq. 50-25 is used for computation of the core mmf. (Ref. A7). Fig. 50-6 refers to 2-pole machines, Fig. 50-7 to machines with the number of poles  $> 4$ . For four poles, an average value of Figures 50-6 and 50-7 can be taken. The length of the path in the core is to be taken as

$$l_c = \frac{\pi(D + 2h_t)}{p} \quad (50-26)$$

for stator cores and

$$l_c = \frac{\pi(D - 2h_t)}{p} \quad (50-27)$$

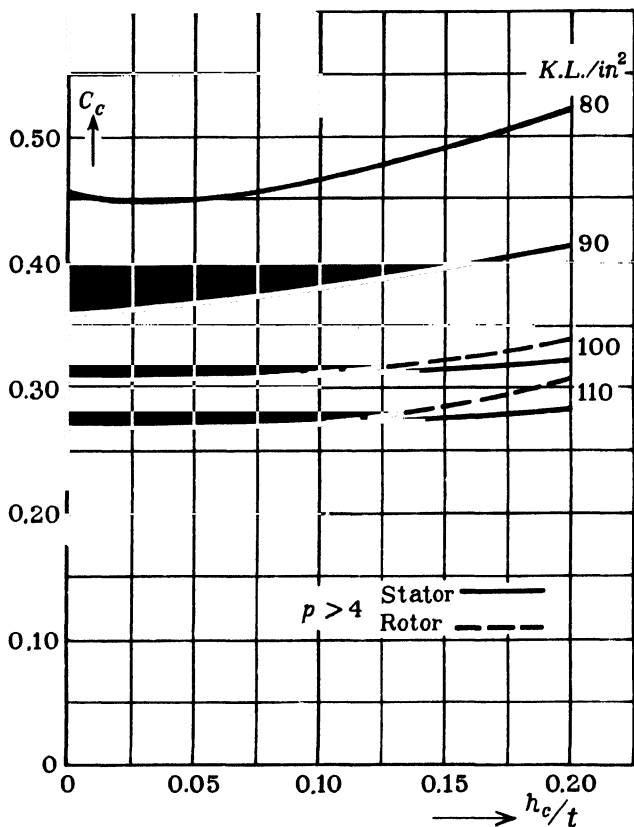
FIG. 50-6. Correction factor  $C_c$  for 2-pole machines.

for rotor cores. Thus the core mmf

$$M_c = 0.93 C_c l_c H_c \quad (50-28)$$

$H_c$  is the value which corresponds to  $B_c$  from Eq. (50-25). The Figures 50-6 and 50-7 refer to a sinusoidal flux distribution. The factor 0.93 in Eqs. 50-26 and 50-27 takes into account the flattening of the flux distribution curve (Fig. 50-1).

**50-5. The Pole and Yoke Mmf.** The flux which goes through the poles and yoke of a salient-pole machine is, due to leakage, larger than the flux  $\Phi$

FIG. 50-7. Correction factor  $C_c$  for  $p > 4$ .

determined by Eq. 50-1 and used in the previous equations. Some of the lines of force produced by the field winding go from pole tip to pole tip and from pole body to pole body, without passing the gap and armature. Although the reluctance of the interpolar space is large, the flux which takes a path through these regions is considerable: it is about 15 to 25 per cent of the armature flux  $\Phi$ . Since only the flux  $\Phi$  which enters the armature induces an emf in the armature winding, the flux which passes through the space between the poles is not a useful flux and is called the *pole-leakage flux*; it is a disadvantage in that it requires the flux in the pole and yoke to be greater than that in the armature. This requires a greater mmf to magnetize the yoke and poles than if no leakage whatever were present.

The leakage flux can be calculated with the aid of Ampere's law, Eq. 1-18. The same mmf which acts upon 2 air-gaps, 2 armature teeth, and armature

core, i.e.,  $(M_g + M_t + M_c)$ , is influential in determining the magnitude of the leakage flux between the pole shoes. This fact follows without further discussion from Eq. 5-4. If the line integral  $\oint H_l dl$  is set up, beginning at a pole surface adjacent to the air-gap and going through the pole, the pole yoke, a second pole, air-gap, armature teeth, armature core, armature teeth, and air-gap (see Fig. 30-3), the result will be exactly the same as for a path following through the first pole, pole yoke, second pole, and the distance in the air between the pole shoes; the contribution to this integral furnished by the air-gap and the armature must be the same as that furnished by the distance in the air between the pole shoes, for other terms in the summation are equal in both cases. By similar considerations, the mmf acting between the pole bodies decreases linearly from the pole shoe to the yoke and is equal to  $(M_g + M_t + M_c) = AB$  (Fig. 50-8) at the pole shoe and nearly zero at the yoke.

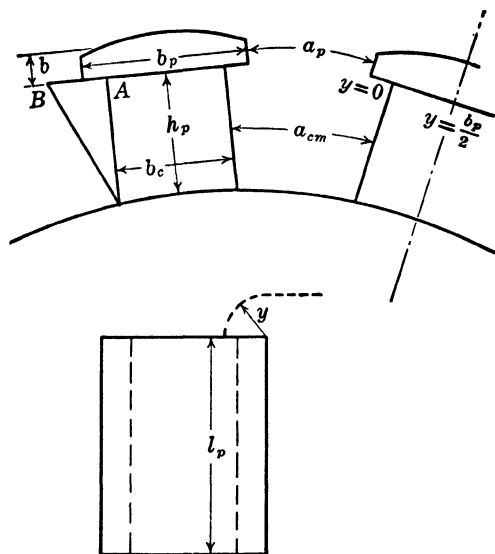


FIG. 50-8. Determination of the leakage flux of salient poles.

The leakage flux consists of the following four parts:

- Leakage flux between the inside surfaces of the pole shoes.
- Leakage flux between the end surfaces of the pole shoes.
- Leakage flux between the inside surfaces of the pole bodies.
- Leakage flux between the end surfaces of the pole bodies.

If

$$M_t = M_g + M_t + M_c \quad (50-29)$$

the flux between the internal surfaces of the pole shoes is (Fig. 50-8)

$$\Phi_a = \frac{0.4\pi M_l}{R_a} = \frac{0.4\pi M_l l_p b}{a_p} \times 2.54 \quad (50-30)$$

The significance of the individual quantities follows from Fig. 50-8. If it is assumed that the lines of force between the external surfaces of the pole shoes go part of the way in the arc of a circle of radius  $y$  (Fig. 50-8), and part of the way in a straight line (along the line  $a_p$ ), then

$$\begin{aligned} \Phi_b &= 2M_l \int_{y=0}^{y=b_p/2} \frac{0.4\pi b dy}{(a_p + \pi y)} \\ &= 2 \times 0.4\pi M_l b \times \frac{2.3}{\pi} \log \left( 1 + \frac{\pi b_p}{2 a_p} \right) \times 2.54 \\ &= 1.84 M_l b \log \left( 1 + \frac{\pi b_p}{2 a_p} \right) \times 2.54 \end{aligned} \quad (50-31)$$

$b$  = height of pole shoe at the pole shoe tip +  $\frac{2}{3}g_{\max}$ . The factor 2 takes into account both ends of the machine.

If the leakage flux between the pole bodies is calculated using the average value of the mmf which prevails between the bodies, that is, with

$$(M_l + 0)/2 = M_l/2,$$

then

$$\Phi_c = 0.4\pi \frac{M_l l_p h_p}{2 a_{cm}} \times 2.54. \quad (50-32)$$

With the same considerations as for  $\Phi_b$

$$\begin{aligned} \Phi_d &= \frac{2 \times 0.4\pi M_l}{2} h_p \times \frac{2.3}{\pi} \log \left( 1 + \frac{\pi b_c}{2 a_{cm}} \right) \times 2.54 \\ &= 0.92 M_l h_p \log \left( 1 + \frac{\pi b_c}{2 a_{cm}} \right) \times 2.54 \end{aligned} \quad (50-33)$$

The entire leakage flux  $\Phi_l$  for both pole halves is

$$\Phi_l = 2(\Phi_a + \Phi_b + \Phi_c + \Phi_d) \quad (50-34)$$

The flux in the pole body and yoke is

$$\Phi_p = \Phi + \Phi_l \quad (50-35)$$

The flux density in the pole body is

$$B_p = \frac{\Phi_p}{A_b} \quad (50-36)$$

and the pole mmf is

$$M_p = 2h_p H_p \quad (50-37)$$

The flux density in the yoke is

$$B_y = \frac{\Phi_p}{2A_y} \quad (50-38)$$

The length of the magnetic path in the yoke is

$$l_y = C_c \frac{\pi D''}{p} \quad (50-39)$$

where  $D''$  is the diameter in the middle of the yoke and  $C_c$  is given by Fig. 50-7. The yoke mmf is

$$M_y = l_y H_y \quad (50-40)$$

Thus, the calculation of the mmf necessary to produce the armature flux  $\Phi$  in the salient-pole machine is as follows: First, the air-gap flux density  $B_g$ , the tooth flux density  $B_t$ , and the armature-core flux density  $B_c$  are calculated, and from these the value of  $(M_g + M_t + M_c)$  is obtained. With this, the mmf  $M_l$  which produces the leakage flux is known, and the leakage flux  $\Phi_l$  and pole flux  $\Phi_p = \Phi_l + \Phi$  can be calculated. From this,  $B_g$  and  $B_y$  and the mmf necessary to magnetize the pole and yoke can be determined.



## Chapter 51

### THE ROTATING POLYPHASE INDUCTION MOTOR AS A STATIONARY TRANSFORMER · THE PRIMARY AND SECONDARY CURRENT · THE CIRCLE DIA- GRAM OF THE POLYPHASE INDUCTION MOTOR

**51-1. The rotating polyphase induction motor as a stationary transformer—Kirchhoff's equations.** It has been explained in Art. 17-2 that the rotating polyphase induction motor can be considered as a stationary transformer loaded with a pure resistance. The total resistance of the secondary circuit is equal to  $r_2'/s$ ,  $r_2'$  being the resistance of the secondary referred to the primary and  $s$  the slip of the motor. This will be proved here from a more general point of view than in Chap. 17.

It has been shown in Chap. 4 that the voltage equations of the transformer are

$$\begin{aligned}\dot{V}_1 &= (r_1 + jx_1)\dot{I}_1 + jx_m(\dot{I}_1 + \dot{I}_2') = (r_1 + jx_1)\dot{I}_1 - \dot{E}_1, \\ -\dot{V}_2' &= (r_2' + jx_2')\dot{I}_2' + jx_m(\dot{I}_1 + \dot{I}_2') = (r_2' + jx_2')\dot{I}_2' - \dot{E}_1.\end{aligned}\tag{51-1}$$

$-jx_m(I_1 + I_2')$  is the emf induced in the primary and secondary winding by the main flux which is produced by the resultant mmf  $(I_1 + I_2')$ . In the case of low saturation, it can be assumed that the main flux consists of two components, one produced by the stator current  $I_1$ , the other produced by the rotor current  $I_2'$ . The corresponding emf's then are  $-jx_m I_1$  and  $-jx_m I_2'$ .

Eq. (51-1) refers to two windings which have the same axis (Fig. 51-1a) as is the case in the transformer and also in the induction motor at standstill when the axes of the stator and rotor windings coincide. If the rotor winding is moved by an angle  $\alpha$  in the direction of rotation of the rotating field (Fig. 51-1b), the voltage equations of the induction motor at standstill are

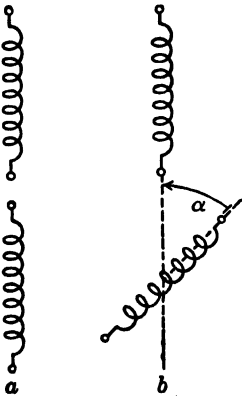


FIG. 51-1. Mutual position of stator and rotor windings.

$$\begin{aligned}\dot{V}_1 &= (r_1 + jx_1)\dot{I}_1 + jx_m(\dot{I}_1 + \dot{I}_2' \epsilon^{j\alpha}), \\ 0 &= (r_2' + jx_2')\dot{I}_2' + jx_m(\dot{I}_1 \epsilon^{-j\alpha} + \dot{I}_2').\end{aligned}\quad (51-2)$$

The emf induced in the stator by the main flux of the rotor is  $-jx_m I_2' \epsilon^{j\alpha}$  since it cuts the stator winding at the angle  $\alpha$  earlier than in the case when both axes coincide. For the same reason the rotor winding is cut by the main flux of the stator at the angle  $\alpha$  later than in the case when both axes coincide, and the emf induced by the main flux of the stator in the rotor winding is  $-jx_m I_1 \epsilon^{-j\alpha}$ .

When the rotor rotates, the angle  $\alpha$  is a function of time. If it is assumed that at the instant  $t=0$  the axes of both windings coincide ( $\alpha=0$ ), then

$$\alpha = (1-s)\omega t. \quad (51-3)$$

For  $\dot{V}_1$ ,  $\dot{I}_1$ , and  $\dot{I}_2'$  the following equations can be introduced:

$$\begin{aligned}\dot{V}_1 &= V_1 \epsilon^{j(\omega t + \beta_1)}, \\ \dot{I}_1 &= I_1 \epsilon^{j(\omega t + \gamma_1)}, \\ \dot{I}_2' &= I_{2s}' \epsilon^{j(s\omega t + \gamma_2)}.\end{aligned}\quad (51-4)$$

where  $\gamma_1 - \beta_1$  is the phase angle between  $\dot{V}_1$  and  $\dot{I}_1$ . Inserting these equations and Eq. (51-3) in Eq. (51-2),

$$\begin{aligned}V_1 \epsilon^{j(\omega t + \beta_1)} &= (r_1 + jx_1)I_1 \epsilon^{j(\omega t + \gamma_1)} + jx_m[I_1 \epsilon^{j(\omega t + \gamma_1)} + I_{2s}' \epsilon^{j(\omega t + \gamma_2)}], \\ 0 &= (r_2' + jsx_2')I_{2s}' \epsilon^{j(s\omega t + \gamma_2)} + jsx_m[I_1 \epsilon^{j(\omega t + \gamma_1)} + I_{2s}' \epsilon^{j(s\omega t + \gamma_2)}].\end{aligned}\quad (51-5)$$

In the latter equation the reactances at slip frequency ( $sx_2'$  and  $sx_m$ ) have to be introduced since in Eq. (51-4) the secondary current is considered at slip frequency. Multiplying the second Eq. (51-5) by  $\epsilon^{j(1-s)\omega t}$ ,

$$0 = (r_2' + jsx_2')I_{2s}' \epsilon^{j(\omega t + \gamma_2)} + jsx_m[I_1 \epsilon^{j(\omega t + \gamma_1)} + I_{2s}' \epsilon^{j(\omega t + \gamma_2)}] \quad (51-5a)$$

or

$$0 = [(r_2'/s) + jx_2']I_{2s}' \epsilon^{j(\omega t + \gamma_2)} + jx_m[I_1 \epsilon^{j(\omega t + \gamma_1)} + I_{2s}' \epsilon^{j(\omega t + \gamma_2)}]. \quad (51-5b)$$

In this equation the secondary current appears at line frequency. Introducing

$$I_{2s}' \epsilon^{j(\omega t + \gamma_2)} = \dot{I}_2', \quad (51-6)$$

where  $\dot{I}_2'$  is different from that in Eq. (51-4), the voltage equations of the rotating induction motor are (see Eqs. (51-4) and (51-5))

$$\dot{V}_1 = (r_1 + jx_1)\dot{I}_1 + jx_m(\dot{I}_1 + \dot{I}_2') = (r_1 + jx_1)\dot{I}_1 - \dot{E}_1 \quad (51-7)$$

$$0 = [(r_2'/s) + jx_2']\dot{I}_2' + jx_m(\dot{I}_1 + \dot{I}_2') = [(r_2'/s) + jx_2']\dot{I}_2' - \dot{E}_1$$

These are the same equations as for the stationary transformer (Eq. 51-1) the windings axes of which coincide except that  $r_2'/s$  appears instead of  $r_2'$ .

As for the transformer with  $g_m \neq 0$  (Art. 3-1) and Art. 4-3

$$\dot{I}_1 + \dot{I}_2' = \dot{I}_m, \quad (51-8)$$

$$\dot{I}_m = -\dot{E}_1 \dot{Y}_m = -\dot{E}_1 (g_m - jb_m) = -\dot{E}_1 \frac{1}{\dot{Z}_m} = -\dot{E}_1 \frac{1}{r_m + jx_m}. \quad (51-9)$$

$g_m$  is a measure of the iron losses due to the main flux,

$$g_m = \frac{P_{h+e}}{m_1 E_1^2} \quad (51-10)$$

where  $m_1$  is the number of phases.  $Y_m$ ,  $g_m$ , and  $b_m$  can be determined from the no-load condition of operation.

$$Y_m = \frac{I_m}{E_1} \approx \frac{I_0}{V_1 - I_0 x_1} \quad (51-11)$$

and

$$b_m \approx \sqrt{\left(\frac{I_0}{V_1 - I_0 x_1}\right)^2 - g_m^2}. \quad (51-12)$$

$g_m$  and  $b_m$  have the dimension of a conductivity. For normal machines  $g_m$  is small in comparison with  $b_m$  and therefore

$$\dot{I}_m \sim \frac{I_0}{V_1 - I_0 x_1} \sim \frac{1}{x_m}. \quad (51-12a)$$

## 51-2. Primary and secondary current—power factor. Let

$$\begin{aligned} r_1 + jx_1 &= \dot{Z}_1, \\ (r_2'/s) + jx_2' &= \dot{Z}_2'. \end{aligned}$$

Eqs. (51-7), (51-8), and (51-9) yield

$$\dot{I}_1 = \dot{V}_1 \frac{1 + \dot{Y}_m \dot{Z}_2'}{\dot{Z}_1 + \dot{Z}_2' + \dot{Z}_1 \dot{Z}_2' \dot{Y}_m}, \quad (51-13)$$

$$\dot{I}_2' = -\dot{V}_1 \frac{1}{\dot{Z}_1 + \dot{Z}_2' + \dot{Z}_1 \dot{Z}_2' \dot{Y}_m}, \quad (51-14)$$

where

$$\dot{Z}_1 \dot{Y}_m = (r_1 g_m + x_1 b_m) + j(x_1 g_m - r_1 b_m).$$

There will be no noticeable error if the assumption is made that

$$\dot{Z}_1 \dot{Y}_m \approx x_1 b_m [1 - j(r_1/x_1)] \quad (51-15)$$

Introducing the primary and secondary leakage coefficients

$$\tau_1 = (x_1/x_m) \quad \tau_2 = (x_2'/x_m), \quad (51-16)$$

and the abbreviations

$$\begin{aligned} r_t &= r_1 + (1 + \tau_1)r_2', & x_t &= x_1 + (1 + \tau_1)x_2', \\ f &= g_m(r_2'/s) + (1 + \tau_2), & h &= g_m x_2' - b_m(r_2'/s), \\ l &= (1 + \tau_2)r_1 + (1 + \tau_1)(r_2'/s), & m &= x_t - b_m r_1(r_2'/s), \end{aligned} \quad (51-17)$$

the primary and secondary currents become

$$I_1 = V_1 \frac{\sqrt{f^2 + h^2}}{\sqrt{l^2 + m^2}}, \quad (51-18)$$

$$I_2 = V_1 \frac{1}{\sqrt{l^2 + m^2}}, \quad (51-19)$$

and the phase angle between the primary current and primary voltage is

$$\varphi_1 = \tan^{-1}(h/f) - \tan^{-1}(m/l). \quad (51-20)$$

For medium-size and larger machines the term  $-j(r_1/x_1)$  can be neglected in Eq. (51-15). Then

$$l \approx r_1 + (1 + r_1)(r_2'/s), \quad m \approx x_i. \quad (51-21)$$

For larger values of  $s$  the main flux is small and  $g_m \approx 0$ . Thus the inrush (starting current) of the induction motor

$$I_{1(s=1)} \approx V_1 \frac{1 + \tau_2}{\sqrt{r_i^2 + x_i^2}}; \quad \tan \varphi_{1(s=1)} = \frac{x_i}{r_i}. \quad (51-22)$$

**51-3. Geometric loci.** (See Ref. H.) A geometric locus is a curve along which the end point of a vector, representing a certain quantity in an electric machine, travels when the machine continuously goes through all possible conditions of operation. For example, the end point of the primary current of an induction motor moves on a circle when the motor slip is changed continuously; the geometric locus of the primary current of the induction motor therefore is a circle the parameter of which is the slip.

(a) *Straight Line.* Let  $P$  be a variable phasor the end point of which runs through a geometric locus,  $A$  a constant complex number, and  $\lambda$  a real parameter between the value  $+\infty$  and  $-\infty$ . If

$$\dot{P} = \dot{A}\lambda. \quad (51-23a)$$

the geometric locus of the vector  $P$  is a straight line through the origin as shown in Fig. 51-2. It can be said also that Eq. (51-23a) is the equation of a straight line through the origin in parameter form.

Therefore, if  $\dot{A}$  and  $\dot{B}$  are two constant complex numbers, the equation

$$\dot{P} = \dot{A} + \dot{B}\lambda \quad (51-23b)$$

is the equation of a straight line which does not pass the origin. This can be seen readily from Fig. 51-3.

(b) *Circle.* Fig. 51-4 shows a straight line  $\dot{Q} = \dot{C} + \dot{D}\lambda$ . It can be shown by simple geometrical considerations that if along each vector  $\dot{Q}$  the quantity  $1/\dot{Q}$  is drawn from the origin  $O$ , the end points of all quantities  $1/\dot{Q}$  lie on a circle  $K_1$  through the origin.  $\lambda = \pm \infty$  corresponds to the origin. While the

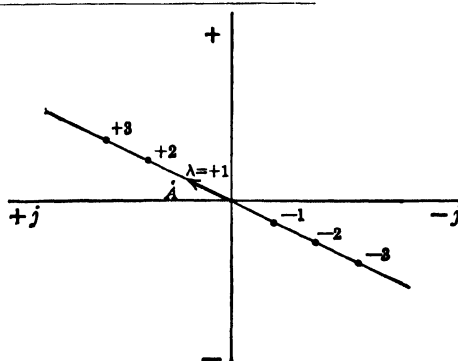


FIG. 51-2. Representation of a straight line through the origin in parameter form.

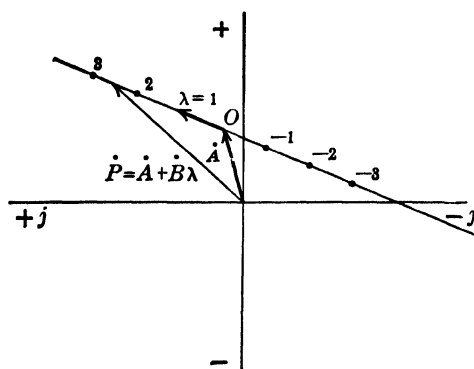


FIG. 51-3. Representation of a straight line in parameter form.

spacing of the parameter  $\lambda$  is equal on the straight line, it is not equal on the circle.

Consider the circle  $K_2$  which is a mirror image of the circle  $K_1$  with respect to the axis of abscissae. If  $OG = 1/Q$  in circle  $K_1$  makes an angle  $\varphi$  with the axis of abscissae, then  $OG'$  in circle  $K_2$  makes an angle  $-\varphi$  with the axis of abscissae, i.e.,

$$OG' = \frac{1}{Q} \epsilon^{-j\varphi}.$$

The vector  $\dot{Q} = \dot{C} + \dot{D}\lambda$  can be expressed also in the form

$$\dot{Q} = Q \epsilon^{j\varphi}.$$

Then

$$\frac{1}{\dot{Q}} = \frac{1}{\dot{C} + \dot{D}\lambda} = \frac{1}{Q} \epsilon^{-j\varphi}.$$

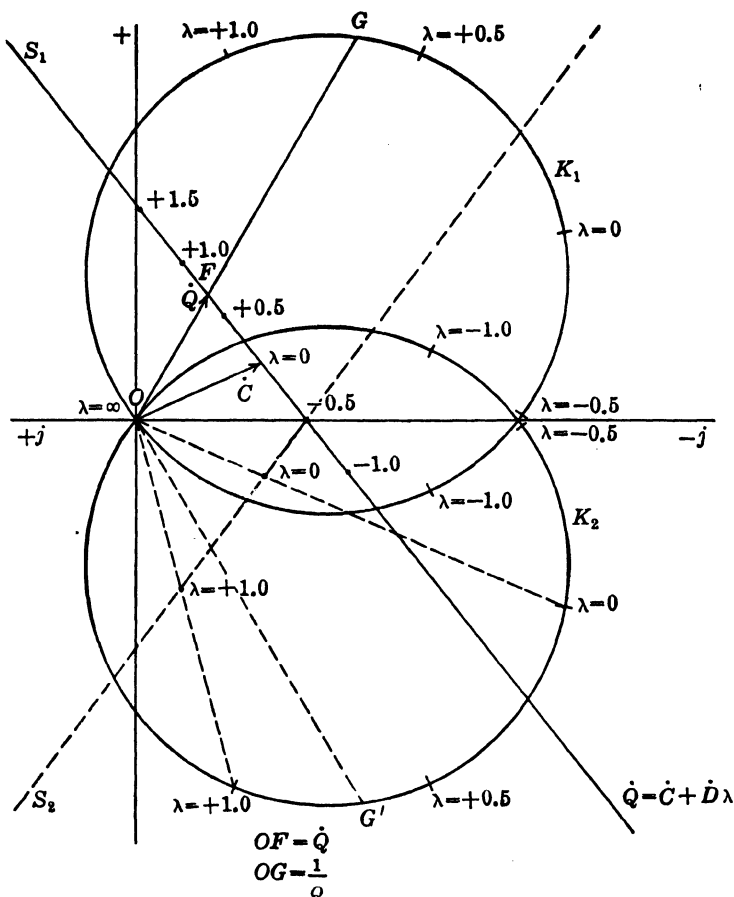


FIG. 51-4. Representation of a circle in parameter form.

Therefore the circle  $K_2$  is the geometric locus of the vector

$$\dot{P} = \frac{1}{\dot{C} + \dot{D}\lambda}, \quad (51-24)$$

i.e., this latter equation is the equation of a circle through the origin.

Thus the general equation of a circle in parameter form is

$$\dot{P} = \dot{E} + \frac{1}{\dot{C} + \dot{D}\lambda} = \frac{(\dot{C}\dot{E} + 1) + \dot{D}\dot{E}\lambda}{\dot{C} + \dot{D}\lambda} = \frac{\dot{A} + \dot{B}\lambda}{\dot{C} + \dot{D}\lambda}. \quad (51-25)$$

The addition of the vector  $\dot{E}$  to Eq. (51-24) corresponds to a shift of the origin in Fig. 51-4 by  $-\dot{E}$ .

There are three characteristic points on the geometric loci encountered in practice:  $\lambda = 0$ ,  $\lambda = 1$ , and  $\lambda = \infty$ .

$$\begin{aligned}
 \lambda = 0 & \quad \dot{P}_{\lambda=0} = \dot{A}/\dot{C}, \\
 \lambda = 1 & \quad P_{\lambda=1} = (\dot{A} + \dot{B})/(\dot{C} + \dot{D}), \\
 \lambda = \pm \infty & \quad P_{\lambda=\pm \infty} = \dot{B}/\dot{D}.
 \end{aligned} \tag{51-26}$$

When the circle diagram is given and the three characteristic points of the circle also are fixed, the parameter  $\lambda$  for any other point of the circle can be determined by the construction shown in the following.

Consider Fig. 51-4 again. The parameter  $\lambda$  has equal spacing on the straight line  $S_1$ . This applies not only to the straight line  $S_1$  but to any other straight line which is parallel to the tangent of the circle  $K_1$  through the point  $\lambda = \pm \infty$ . If the values of  $\lambda$  are known for two points of the straight line, the value of  $\lambda$  can be determined for any other point of the straight line and, therefore, also for any point of the circle  $K_1$ . If a mirror image  $S_2$  is drawn to the straight line  $S_1$ , then the same conditions apply to this straight line and circle  $K_2$  as to the line  $S_1$  and the circle  $K_1$ , i.e., the parameter  $\lambda$  has equal spacing on  $S_2$  or any straight line which is parallel to the tangent of the circle  $K_2$  through the point  $\lambda = \pm \infty$ . Further, if the values of  $\lambda$  are known for two points of the straight line  $S_2$ , the value of  $\lambda$  can be determined for any other point of the straight line and for any point of the circle  $K_2$ .

It can be seen from Fig. 51-4 that if the points  $\lambda = 0$ ,  $\lambda = 1$ , and  $\lambda = \pm \infty$  on the circle  $K_2$  are given, the points  $\lambda = 0$  and  $\lambda = 1$  can be found on the

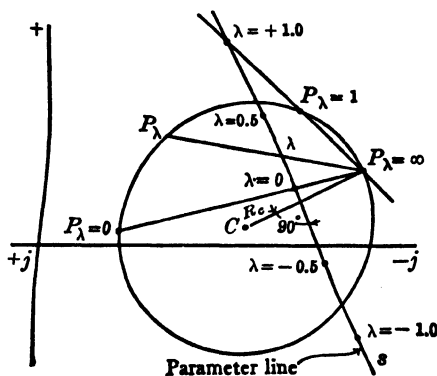


FIG. 51-5. Determination of the parameter for any arbitrary point on the circle.

straight line  $S_2$  by connecting the point  $P_{\lambda=\infty}$  with  $P_{\lambda=0}$  and  $P_{\lambda=1}$ , respectively. This leads to the construction of Fig. 51-5. The circle and the points  $\lambda = 0$ ,  $\lambda = +1$ , and  $\lambda = \pm \infty$  are given. The straight line  $s$  (parameter line) is parallel to the tangent to the circle through the point  $P_{\lambda=\pm \infty}$ , i.e., the perpendicular to the line  $CP_{\lambda=\infty}$ . The intersections of the parameter line  $s$  with the lines  $P_{\lambda=\infty}P_{\lambda=0}$  and  $P_{\lambda=\infty}P_{\lambda=1}$  yields the points  $\lambda = 0$  and  $\lambda = +1.0$ . Dividing the distance between  $\lambda = 0$  and  $\lambda = +1$  in equal parts, other values of  $\lambda$  on the parameter line  $s$  will be obtained. The value of  $\lambda$  for any arbitrary point  $P_{(\lambda)}$  on the circle will be found by connecting

the point  $P_{\lambda=\infty}$  with this point (Fig. 51-5). The intersection with the parameter line yields the value of  $\lambda$  which corresponds to the point  $P_{(\lambda)}$  of the circle.

#### 51-4. Circle diagram of the polyphase induction motor—slip line.

With the aid of Eqs. (51-12a), (51-15), (51-16), and (51-17), Eq. (51-13) for the primary current of the polyphase induction motor can be rewritten

$$\frac{\dot{I}_1}{\dot{V}_1} = \frac{r_2'(g_m - j b_m) + [(1 + \tau_2) + j g_m x_2'] s}{r_2'[(1 + \tau_1) - j r_1 b_m] + [r_1(1 + \tau_2) + j x_t] s}. \quad (51-27)$$

$V_1$  will be assumed in the real axis (axis of ordinates). Then  $\dot{V}_1 = V_1$ . With the abbreviations

$$\begin{aligned} r_2'(g_m - j b_m) &= \dot{A}, & (1 + \tau_2) + j g_m x_2' &= \dot{B}, \\ r_2'[(1 + \tau_1) - j r_1 b_m] &= \dot{C}, & r_1(1 + \tau_2) + j x_1 &= \dot{D}, \end{aligned} \quad (51-28)$$

Eq. (51-27) becomes

$$\frac{\dot{I}_1}{V_1} = \frac{\dot{A} + \dot{B}s}{\dot{C} + \dot{D}s}. \quad (51-28a)$$

Comparing this equation with Eq. (51-25) it follows that the *geometric locus of the end point of the primary current  $I_1$  is a circle with the slip  $s$  as the parameter.*

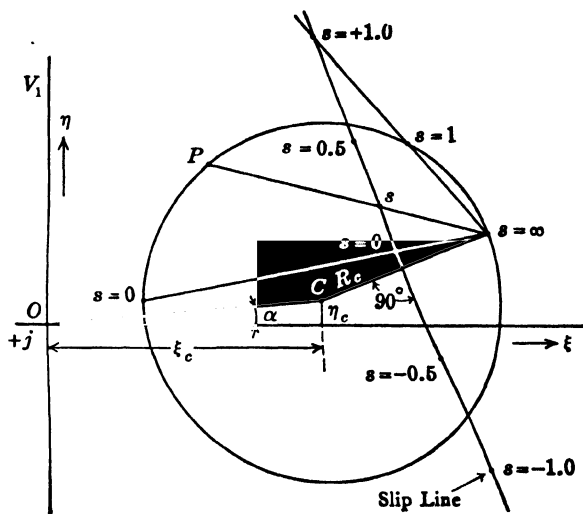


**FIG. 51-6. Determination of the slip line in the circle diagram of the induction motor.**

In order to determine the radius and the coordinates of the center of the circle, Cartesian coordinates  $\xi$  and  $\eta$  (Fig. 51-6) will be introduced. Thus

$$\begin{aligned} \dot{I}_1 &= \eta - j\xi, \\ \dot{V}_1 &= V_n = V_1. \end{aligned} \quad (51-29)$$

### Rewriting Eq. (51-28a)

$$(\dot{I}_1 \dot{C} - V_1 \dot{A}) = (V_1 \dot{B} - \dot{I}_1 \dot{D})_g. \quad (51-30)$$



From Eq. (51-28)

$$\begin{aligned} r_2'g_m = A_\eta, \quad (1 + \tau_2) = B_\eta, \quad r_2'(1 + \tau_1) = C_\eta, \quad r_1(1 + \tau_2) = D_\eta, \\ -r_2'b_m = A_\xi, \quad g_mx_2' = B_\xi, \quad -r_2'r_1b_m = C_\xi, \quad x_t = D_\xi. \end{aligned} \quad (51-31)$$

Inserting these equations and Eq. (51-29) in Eq. (51-30) and separating the real terms from the imaginary, two equations are obtained:

$$\begin{aligned} \eta C_\eta + \xi C_\xi - V_1 A_\eta &= (V_1 B_\eta - \eta D_\eta - \xi D_\xi)s, \\ \eta C_\xi - \xi C_\eta - V_1 A_\xi &= (V_1 B_\xi - \eta D_\xi + \xi D_\eta)s. \end{aligned} \quad (51-31a)$$

Elimination of the slip  $s$  from these equations yields the equation of a circle in Cartesian coordinates with the coordinates of the center  $(\xi_c, \eta_c)$  and the radius  $R_c$ :

$$\xi_c = \frac{V_1}{2} \frac{\alpha_3}{\alpha_2}, \quad \eta_c = \frac{V_1}{2} \frac{\alpha_4}{\alpha_2}, \quad (51-32)$$

$$R_c = \sqrt{|\xi_c^2 + \eta_c^2 + V_1^2(\alpha_1/\alpha_2)|}, \quad (51-33)$$

where

$$\begin{aligned} \alpha_1 &= A_\xi B_\eta - A_\eta B_\xi, \quad \alpha_3 = (B_\eta C_\eta + B_\xi C_\xi) - (A_\eta D_\eta + A_\xi D_\xi), \\ \alpha_2 &= C_\eta D_\xi - C_\xi D_\eta, \quad \alpha_4 = (A_\eta D_\xi - A_\xi D_\eta) - (B_\eta C_\xi - B_\xi C_\eta). \end{aligned} \quad (51-34)$$

For the point on the circle  $s=0$  (ideal no-load point), according to Eqs. (51-26), (51-28), and (51-28a),

$$\dot{I}_{1(s=0)} = V_1 \frac{\dot{A}}{C} = V_1 \frac{(A_\eta C_\eta + A_\xi C_\xi) - j(A_\eta C_\xi - A_\xi C_\eta)}{C_\xi^2 + C_\eta^2}. \quad (51-35)$$

Thus

$$\begin{aligned} \xi_{(s=0)} &= V_1 \frac{A_\eta C_\xi - A_\xi C_\eta}{C_\xi^2 + C_\eta^2}, \\ \eta_{(s=0)} &= V_1 \frac{A_\eta C_\eta + A_\xi C_\xi}{C_\xi^2 + C_\eta^2}. \end{aligned} \quad (51-36)$$

For the point on the circle  $s = \pm \infty$ ,

$$\dot{I}_{1(s=\infty)} = V_1 \frac{\dot{B}}{D} = V_1 \frac{(B_\eta D_\eta + B_\xi D_\xi) - j(B_\eta D_\xi - B_\xi D_\eta)}{D_\xi^2 + D_\eta^2}, \quad (51-37)$$

$$\xi_{(s=\infty)} = V_1 \frac{B_\eta D_\xi - B_\xi D_\eta}{D_\xi^2 + D_\eta^2}, \quad (51-38)$$

$$\eta_{(s=\infty)} = V_1 \frac{B_\eta D_\eta + B_\xi D_\xi}{D_\xi^2 + D_\eta^2}.$$

The point on the circle  $s = +1.0$  can be determined from Eq. (51-18) or (51-22).

The angle  $\alpha$  (Fig. 51-6) between the line  $OC$  and the axis of abscissae is, according to Eqs. (51-31), (51-32), and (51-34):

$$\tan \alpha = \frac{\eta_c}{\xi_c} \approx \frac{2r_1(1 + \tau_2)}{x_m + 2x_i} \approx \frac{2r_1}{x_m(1 + 2\tau_1 + \tau_2)}. \quad (51-39)$$

In the problems encountered in practice, two points of the circle, the no-load point and the point  $s = 1$ , are given, since they can be determined easily by tests. From the same tests  $\tan \alpha$  [Eq. (51-39)] also can be determined and therefore the circle,  $x_m$ ,  $\tau_1$ , and  $\tau_2$  are given by (see Arts. 22-1, and 19-2),

$$x_m \approx \frac{V_1 - I_0 x_i}{I_0}, \quad \tau_1 \approx \frac{X_L}{2x_m} \approx \tau_2. \quad (51-40)$$

In Fig. 51-6 the slip line (parameter line) is plotted in accordance with Fig. 51-5. This line is perpendicular to the radius connecting the center point  $C$  with the point on the circle  $s = \infty$ . The line which connects the points  $s = 0$  and  $s = \infty$  intersects the slip line in the point  $s = 0$ , and the line which connects the points  $s = 1$  and  $s = \infty$  intersects the slip line in the point  $s = 1$ . For any arbitrary point  $P$  of circle the slip is found by connecting this point with the point  $s = \infty$ .

**51-5. The torque line.** The ordinate of an arbitrary point  $P$  on the circle (Fig. 51-7) is the active component of the primary current which corresponds to this point. Since the primary voltage  $V_1$  is constant, the active component of the primary current represents the power input of the machine to another scale. The axis of abscissae intersects the circle at the zero-power-input points. This is the zero-power-input line or simply *power-input line*. The distances from points on the circle to this line give the power input.

It will be shown that a similar line also exists for the power of the rotating field, i.e., for the torque of the machine, since the power of the rotating field and the torque are directly proportional to each other (Eq. 19-9).

The Cartesian coordinates of the circle will be denoted by  $\xi$ ,  $\eta$  as before. The iron losses due to the main flux will be neglected. Then the power of the rotating field is

$$P_{r,f} \approx V_1 \eta - I_1^2 r_1 = V_1 \eta - (\xi^2 + \eta^2) r_1. \quad (51-41)$$

The equation of the circle is

$$(\xi - \xi_c)^2 + (\eta - \eta_c)^2 - R_c^2 = 0. \quad (51-42)$$

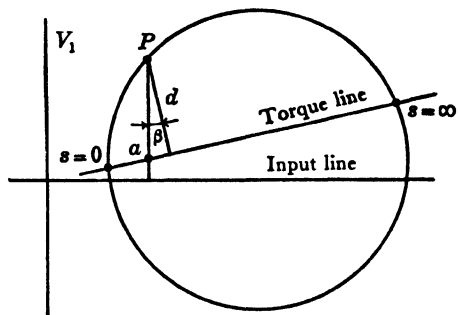


FIG. 51-7. Determination of the torque line in the circle diagram of the induction motor.

From this

$$\xi^2 + \eta^2 = 2(\xi\xi_c + \eta\eta_c) + R_c^2 - \xi_c^2 - \eta_c^2.$$

Inserting this equation in Eq. (51-41),

$$P_{r,f} = V_1\eta - 2r_1[\xi\xi_c + \eta\eta_c + \frac{1}{2}(R_c^2 - \xi_c^2 - \eta_c^2)]. \quad (51-43)$$

The points on the circle at which the power of the rotating field and the torque are zero thus satisfy the equation

$$\xi\xi_c + \eta[\eta_c - (V_1/2r_1)] + \frac{1}{2}(R_c^2 - \xi_c^2 - \eta_c^2) = 0. \quad (51-44)$$

This is a straight line, the zero-torque line or simply the *torque line*. It has been explained in Art. 21-3 that the torque line goes through the points  $s=0$  and  $s=\infty$ .

If the general equation of a straight line is given as

$$A\xi + B\eta + C = 0,$$

the distance from an arbitrary point of the plane  $(\xi_1, \eta_1)$  to this line is

$$d = \frac{1}{\sqrt{A^2 + B^2}} (A\xi_1 + B\eta_1 + C).$$

Applying this to Eq. (51-44), i.e., to the torque line, the distances from the points on the circle to the torque line are

$$d = \frac{1}{\sqrt{[\xi_c^2 + \{\eta_c - (V_1/2r_1)\}^2]}} [\xi_c\xi + \{\eta_c - (V_1/2r_1)\}\eta + \frac{1}{2}(R_c^2 - \xi_c^2 - \eta_c^2)], \quad (51-45')$$

or, inserting Eq. (51-43),

$$d = \frac{1}{\sqrt{[\xi_c^2 + \{\eta_c - (V_1/2r_1)\}^2]}} \frac{P_{r,f}}{2r_1}. \quad (51-46)$$

Thus

$$P_{r,f} = 2r_1\sqrt{[\xi_c^2 + \{\eta_c - (V_1/2r_1)\}^2]} \times d, \quad (51-46a)$$

i.e., the distances  $d$  from the points on the circle to the torque line give the torques. If  $\xi_c$ ,  $\eta_c$ , and  $d$  are inserted in amperes,  $V_1$  in volts, and  $r_1$  in ohms,  $P_{r,f}$  is obtained in watts. From this the torque

$$T_{\text{lb-ft}} = P_{r,f} \text{ (watts)} \times \frac{n_s}{7.04}. \quad (51-47)$$

In order to determine the torque corresponding to an arbitrary point of the circle  $P$  (Fig. 51-7), it is not necessary to plot the perpendicular  $d$  to the torque line. The distance  $Pa$  which is perpendicular to the axis of abscissae also represents the torque, since the angle  $\beta$  is a constant angle for all points of the circle. The scale for  $Pa$  is different from that for  $d$  by the factor  $\cos \beta$ .

**51-6. Influence of variation of leakage reactances and secondary resistance on the shape of the geometric locus of the primary current.** It has been shown in Art. 51-3 that the geometric locus of the primary current of a polyphase motor is a circle. This holds only when the reactances and resistances of the machine are constants independent of the slip.

In highly saturated induction motors the leakage reactances of stator and rotor depend upon the current, i.e., upon the slip (see Art. 22-6). The higher the current, the more the leakage paths are saturated and the lower the leakage reactances. In these cases Eq. (51-27) for the primary current cannot be applied and the geometric locus of the primary current is not a circle.

In squirrel-cage motors with deep bars and in double-cage motors the rotor resistance and rotor reactance vary with the slip due to the skin effect (Art. 22-5). They consist of a constant term (the resistance and reactance of the end winding) and of a variable term (the resistance and reactance of the embedded bars). If both terms are introduced into Eq. (51-13), the geometric locus of the end point of the primary current will be given by an equation of the form

$$\frac{\dot{I}_1}{V_1} = \frac{\dot{A} + \dot{B}s + \dot{C}s^2}{\dot{D} + \dot{F}s + \dot{G}s^2}. \quad (51-48)$$

This is the equation of a *bicircular quartic* (see Fig. 22-7 and 22-8).

## Chapter 52

### DERIVATION OF THE TORQUE OF THE POLY-PHASE INDUCTION MOTOR FROM THE LAW OF FORCE ON A CONDUCTOR IN A MAGNETIC FIELD (BIOT-SAVART'S LAW)

In Art. 19-1, the torque of the polyphase induction motor was derived from the power of the rotating field of the motor as,

$$P_{\text{rot.f.}} = m_1 I_2'^2 (r_2'/s) = m_1 E_2' I_2' \cos \psi_{2s} = m_2 E_2 I_2 \cos \psi_{2s} \quad (52-1)$$

$$T = \frac{7.04}{n_s} P_{\text{rot.f.}} \quad (52-2)$$

In this chapter, the torque will be derived from Biot-Savart's law and only for the main wave ( $\nu=1, \nu'=p/2$ ) of a 3-phase machine. A general derivation of the torque for the main wave and harmonics on the basis of Biot-Savart's law, is given in Chap. 57.

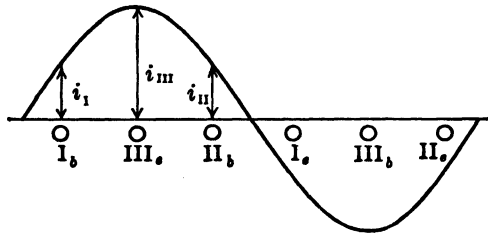


FIG. 52-1. Determination of the torque for an elementary 3-phase motor from Biot-Savart's law.

Consider Fig. 52-1 in which an elementary 3-phase system consisting of 3 full-pitch coils is shown. Assume small slip, i.e.,  $\psi_{2s} \approx 0$ ; the current and flux density then are in-phase. For the instant chosen, the conductors of phase III lie in maximum flux density ( $B_{om}$ ), while for the conductors of phases I and II the flux density is one-half of the maximum. Therefore the current in phase III will be a maximum ( $I_{2m}$ ) and the currents in phases I and II one-half of the maximum value. Corresponding to the fundamental law (see Eq. 1-28b), the force per pole is

$$F = 8.85 \times 10^{-8} l_e n_{c2} \left[ \frac{B_{gm} I_{2m}}{2} + B_{gm} I_{2m} + \frac{B_{gm} I_{2m}}{2} \right]$$

$$= 18.75 \times 10^{-8} l_e n_{c2} B_{gm} I_2 \quad \text{lb.} \quad (52-3)$$

$l_e$  is the effective length of the core (see Art. 1-2d) and  $n_{c2}$  the number of turns per rotor coil. If each phase has  $q_2$  slots per pole and the coils are chorded (fractional-pitch winding), the value of  $F$  obtained from Fig. 52-1 has to be multiplied by  $q_2$  and by the winding factor of the rotor for the fundamental  $k_{dp2}$ . This yields for all  $p$  poles,

$$F = 6.25 \times 10^{-8} l_e Z_2 k_{dp2} B_{gm} I_2 \quad \text{lb.} \quad (52-4)$$

where  $Z_2 = 3n_{c2}q_2p$  is the total number of conductors of the rotor. Introducing Eqs. (1-5) and (1-32)

$$\Phi = \frac{2}{\pi} \tau l_e B_{gm}, \quad \tau = \frac{\pi D}{p}, \quad R = \frac{D}{2} \times \frac{1}{12} \quad \text{feet,}$$

the torque becomes

$$T = 0.1303 \times 10^{-8} p \Phi I_2 Z_2 k_{dp2} \quad \text{lb. ft.} \quad (52-5)$$

This equation has been derived under the assumption that the rotor current is in phase with its emf (Fig. 52-1). If this is not the case, the cosine of the angle between them ( $\cos \psi_{2s}$ ) has to be introduced into the torque equation. The considerations are the same as for the determination of the power of a circuit where voltage and current are in-phase or out-of-phase (see Art. 1-2d). Thus, in general,

$$T = 0.1303 \times 10^{-8} p \Phi I_2 Z_2 k_{dp2} \cos \psi_{2s} \quad \text{lb-ft.} \quad (52-6)$$

Introducing into Eqs. 52-1  $m_2 = 3$  and

$$E_2 = 4.44 \frac{pn_s}{120} \frac{Z_2}{2 \times 3} k_{dp2} \Phi \times 10^{-8}$$

there results from Eqs. (52-1) and (52-2)

$$T = 0.1303 \times 10^{-8} p \Phi I_2 Z_2 k_{dp2} \cos \psi_{2s} \quad \text{lb-ft.}$$

This equation is the same as Eq. 52-6.

## Chapter 53

### THE UNSYMMETRICAL TWO-PHASE INDUCTION MOTOR

In this chapter the unsymmetrical two-phase motor will be treated, i.e., it is assumed that the two stator windings are shifted from each other in space by an angle different from 90 electrical degrees and that voltages are applied to these two windings which are different in magnitude and are shifted in time by an angle different from 90°. The results obtained apply to all types of single-phase motors during starting and running and to the 2-phase servomotor. The symmetrical 2-phase induction motor appears as a special case of the results obtained for the unsymmetrical motor.

It is assumed that the machine is not saturated, so that superposition of fluxes becomes permissible.

One of the two stator windings will be called *main winding* (subscript  $M$ ) and the other *starting winding* (subscript  $S$ ).

**53-1. Current in the main winding only.** This is the case of the split-phase and capacitor-start single-phase motor during running. Referring to Art. 26-6, the equivalent circuit for this case is given by Fig. 53-1. Denoting by  $Z_f$  and  $Z_b$  the impedance of the forward and backward branch, respectively,

$$\dot{Z}_f = R_f + jX_f \quad (53-1)$$

$$R_f = \frac{a(r_m + r_2'/s) + bk_2x_m}{(r_m + r_2'/s)^2 + (k_2x_m)^2} \quad (53-2)$$

$$X_f = \frac{b(r_m + r_2'/s) - ak_2x_m}{(r_m + r_2'/s)^2 + (k_2x_m)^2} \quad (53-3)$$

$$k_2 = 1 + (x_2'/x_m) = 1 + \tau_2 \quad a = r_m(r_2'/s) - x_2'x_m \quad b = (r_2'/s)x_m + x_2'r_m \quad (53-4)$$

$$\dot{Z}_b = R_b + jX_b \quad (53-5)$$

The values of  $R_b$  and  $X_b$  are obtained from those for  $R_f$  and  $X_f$  by substituting  $(2-s)$  for  $s$ .  $x_m$  is the reactance of each of the two rotating fluxes. Its value is

$$x_m = 3.2f_1 \frac{\tau l_e}{pgk_c k_s} (N_M k_{apM})^2 \times 2.54 \times 10^{-8} \text{ ohm} \quad (53-6)$$

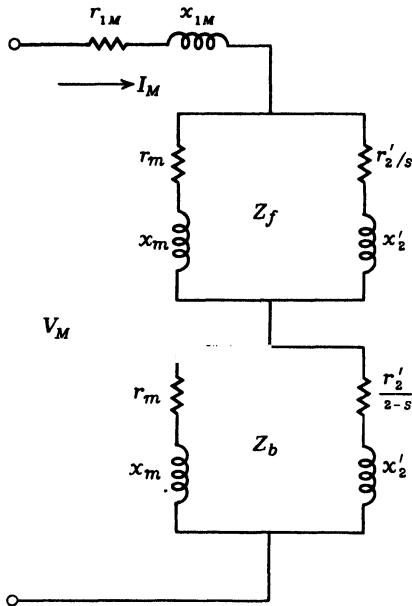


FIG. 53-1. Equivalent circuit of the M-winding.

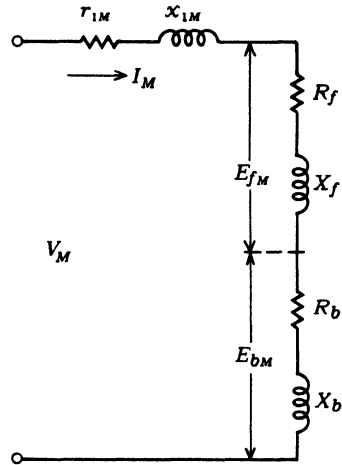


FIG. 53-2. Equivalent circuit of the M-winding.

(see Art. 57-8).  $k_c$  is the Carter factor and

$$k_s = \frac{M_g + M_{Fe}}{M_g}$$

is the saturation factor, i.e., the ratio of the total mmf needed to produce the rotating flux, to the gap mmf.

Further, with the subscript 2 for the secondary (Art. 26-4)

$$r'_2 = r_2 \left( \frac{N_{M,\text{eff}}}{N_{2,\text{eff}}} \right)^2 \frac{1}{m_2} \quad x'_2 = x_2 \left( \frac{N_{M,\text{eff}}}{N_{2,\text{eff}}} \right)^2 \frac{1}{m_2} \quad (53-7)$$

$N_{\text{eff}}$  means  $Nk_{dp}$  or  $Nk_w$  ( $k_w$  = winding factor of a single phase winding). For the squirrel-cage rotor (Art. 26-4)

$$m_2 = Q_2, \quad N_{2,\text{eff}} = \frac{1}{2} K_{sk}. \quad (53-8)$$

$r_2$  and  $x_2$  per bar are to be used in Eq. (53-7).  $K_{sk}$  is the skew factor (Art. 56-6).

With the impedances  $Z_f$  and  $Z_b$ , the equivalent circuit Fig. 53-1 can be represented as shown in Fig. 53-2.  $E_{fM}$  and  $E_{bM}$  in this figure are the components of  $V_M$  necessary to overcome the impedances of  $Z_f$  and  $Z_b$ . The corre-



sponding induced emf's are

$$\begin{aligned} -\dot{E}_{fM} &= -\dot{I}_M(R_f + jX_f) \\ -\dot{E}_{bM} &= -\dot{I}_M(R_b + jX_b) \end{aligned} \quad (53-9)$$

Each of these two emf's consists of two components, one in phase with  $I_M$ , the other  $90^\circ$  ahead of  $I_M$ . Therefore, with

$$i_M = \sqrt{2} I_M \sin \omega t \quad (53-10)$$

the instantaneous values of  $-E_{fM}$  and  $-E_{bM}$  are

$$\begin{aligned} -e_{fM} &= -\sqrt{2} I_M [R_f \sin \omega t + X_f \sin (\omega t + \tfrac{1}{2}\pi)] \\ &= -\sqrt{2} I_M (R_f \sin \omega t + X_f \cos \omega t) \\ -e_{bM} &= -\sqrt{2} I_M (R_b \sin \omega t + X_b \cos \omega t) \end{aligned} \quad (53-11)$$

**53-2. Current in the starting winding only.** It is assumed that this winding is placed  $\alpha$  electrical degrees *ahead* of the main winding with respect to a *forward* rotating flux, i.e., with respect to the direction of rotation of the rotor. It has  $N_{S,\text{eff}}$  turns

$$N_{S,\text{eff}} = a N_{M,\text{eff}} \quad (53-12)$$

A Voltage  $V_S$  is impressed on the winding and it carries the current

$$i_S = \sqrt{2} I_S \sin (\omega t + \varphi) \quad (53-13)$$

The equivalent circuit of this winding is shown in Fig. 55-3.  $r_m$ ,  $x_m$ ,  $r_2'$ , and  $x_2'$  all refer to the main winding. Since the starting winding has  $a N_{M,\text{eff}}$  turns, these quantities appear in its equivalent circuit multiplied by  $a^2$ .  $r_{1S}$  and  $x_{1S}$  are *not the actual values* of resistance and leakage reactance of the starting winding but the actual values times  $1/a^2$ , so that  $a^2 r_{1S}$  and  $a^2 x_{1S}$  are the actual values.  $r_c$  and  $x_c$  take into account the fact that a capacitor may be inserted into the circuit of the starting winding, as is the case with the capacitor motors.

The equivalent circuit Fig. 53-3 can be replaced by that shown in Fig. 43-4. Similar to Eqs. (53-9) and 53-11)

$$\begin{aligned} -\dot{E}_{fS} &= -\dot{I}_S a^2 (R_f + jX_f) \\ -\dot{E}_{bS} &= -\dot{I}_S a^2 (R_b + jX_b) \end{aligned} \quad (53-14)$$

$$\begin{aligned} -e_{fS} &= -\sqrt{2} I_S a^2 [R_f \sin (\omega t + \varphi) + X_f \cos (\omega t + \varphi)] \\ -e_{bS} &= -\sqrt{2} I_S a^2 [R_b \sin (\omega t + \varphi) + X_b \cos (\omega t + \varphi)] \end{aligned} \quad (53-15)$$

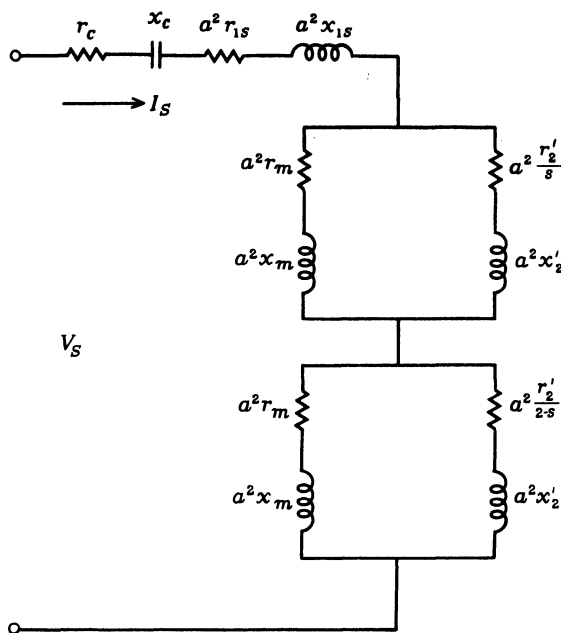


FIG. 53-3. Equivalent circuit of the S-winding.

**53-3. Both windings carry current.** Since each of the two windings produces a forward and backward rotating flux, the two fluxes of the main winding will induce two emf's in the starting winding and, vice versa, the two fluxes of the starting winding will induce two emf's in the main winding. The four fluxes and the emf's induced by them are tabulated below:

Fluxes	Emf's in the M-winding	Emf's in the S-winding
$\Phi_{fM}$	$-E_{fM}$ (Eq. (53-9))	$-E_{S,fM}$ (Eq. (53-16))
$\Phi_{bM}$	$-E_{bM}$ (Eq. (53-9))	$-E_{S,bM}$ (Eq. (53-17))
$\Phi_{fS}$	$-E_{S,fM}$ (Eq. (53-18))	$-E_{fS}$ (Eq. (53-14))
$\Phi_{bS}$	$-E_{S,bM}$ (Eq. (53-19))	$-E_{bS}$ (Eq. (53-14))

The emf's  $-E_{fM}$  and  $-E_{bM}$  induced in the main winding by its fluxes  $\Phi_{fM}$  and  $\Phi_{bM}$  are given by Eqs. (53-9) and (53-11). The emf's  $-E_{fS}$  and  $-E_{bS}$  induced in the starting winding by its fluxes  $\Phi_{fS}$  and  $\Phi_{bS}$  are given by Eqs. (53-14) and (53-15).

With respect to the emf induced by the forward flux of the main winding ( $\Phi_{fM}$ ) in the starting winding,  $E_{S,fM}$ , it should be remembered that the latter winding has  $aN_{M,\text{eff}}$  turns and that it lies  $\alpha^\circ$  ahead of the main winding with respect to a forward rotating flux. Thus

$$-\dot{E}_{S,fM} = -a\dot{E}_{fM}\epsilon^{j\alpha} \quad (53-16)$$

With respect to the backward rotating flux of the main winding, the starting winding lies  $\alpha^\circ$  behind the main winding. Therefore,

$$-\dot{E}_{S,bM} = -a\dot{E}_{bM}\epsilon^{-j\alpha} \quad (53-17)$$

With the same consideration, the two emf's induced in the main winding by the two rotating fluxes of the starting winding are

$$-\dot{E}_{M,fS} = -(1/a)\dot{E}_{fM}\epsilon^{-j\alpha} \quad (53-18)$$

and

$$-\dot{E}_{M,bS} = -(1/a)\dot{E}_{bS}\epsilon^{j\alpha} \quad (53-19)$$

Inserting into Eqs. 53-16 to 19 the values of Eqs. (53-9) and (53-14),

$$\begin{aligned} -\dot{E}_{S,fM} &= -a\dot{I}_M(R_f + jX_f)\epsilon^{j\alpha} \\ &= -a\dot{I}_M[(R_f \cos \alpha - X_f \sin \alpha) + j(X_f \cos \alpha + R_f \sin \alpha)] \end{aligned} \quad (53-20)$$

$$\begin{aligned} -\dot{E}_{S,bM} &= -a\dot{I}_M(R_b + jX_b)\epsilon^{-j\alpha} \\ &= -a\dot{I}_M[(R_b \cos \alpha + X_b \sin \alpha) + j(X_b \cos \alpha - R_b \sin \alpha)] \end{aligned} \quad (53-21)$$

$$\begin{aligned} -\dot{E}_{M,fS} &= -a\dot{I}_S(R_f + jX_f)\epsilon^{-j\alpha} \\ &= -a\dot{I}_S[(R_f \cos \alpha + X_f \sin \alpha) + j(X_f \cos \alpha - R_f \sin \alpha)] \end{aligned} \quad (53-22)$$

$$\begin{aligned} -\dot{E}_{M,bS} &= -a\dot{I}_S(R_b + jX_b)\epsilon^{j\alpha} \\ &= -a\dot{I}_S[(R_b \cos \alpha - X_b \sin \alpha) + j(X_b \cos \alpha + R_b \sin \alpha)] \end{aligned} \quad (53-23)$$

The instantaneous values of these emf's are (see Eqs. 53-11 and 53-15)

$$\begin{aligned} -e_{S,fM} &= -\sqrt{2}aI_M \\ &\times [(R_f \cos \alpha - X_f \sin \alpha) \sin \omega t + (X_f \cos \alpha + R_f \sin \alpha) \cos \omega t] \end{aligned} \quad (53-24)$$

$$\begin{aligned} -e_{S,bM} &= -\sqrt{2}aI_M \\ &\times [(R_b \cos \alpha + X_b \sin \alpha) \sin \omega t + (X_b \cos \alpha - R_b \sin \alpha) \cos \omega t] \end{aligned} \quad (53-25)$$

$$\begin{aligned} -e_{M,fS} &= -\sqrt{2}aI_S \\ &\times [(R_f \cos \alpha + X_f \sin \alpha) \sin (\omega t + \varphi) + (X_f \cos \alpha - R_f \sin \alpha) \cos (\omega t + \varphi)] \end{aligned} \quad (53-26)$$

$$\begin{aligned} -e_{M,bS} &= -\sqrt{2}aI_S \\ &\times [(R_b \cos \alpha - X_b \sin \alpha) \sin (\omega t + \varphi) + (X_b \cos \alpha + R_b \sin \alpha) \cos (\omega t + \varphi)] \end{aligned} \quad (53-27)$$

With the emf's induced in both windings determined, Kirchhoff's equations of both stator circuits can be set up.

**55-4. Kirchhoff's equations of the stator circuits and the currents in the stator windings.** For the main winding,

$$\dot{V}_M - \dot{E}_{fM} - \dot{E}_{bM} - \dot{E}_{M,fS} - \dot{E}_{M,bS} - j\dot{I}_M x_{1M} \pm j\omega M_{MS} \dot{I}_S = \dot{I}_M r_{1M} \quad (53-28)$$

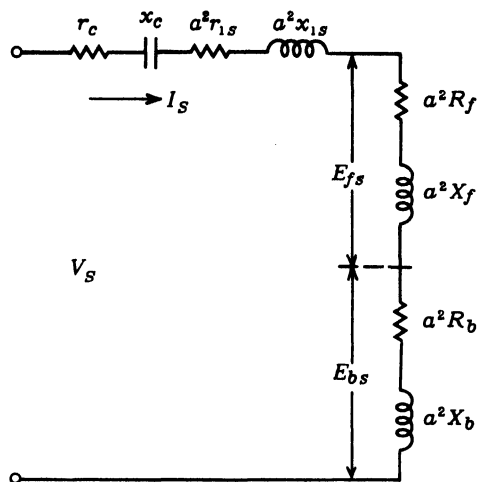


FIG. 53-4. Equivalent circuit of the S-winding.

and for the starting winding (see Fig. 53-4)

$$\dot{V}_S - \dot{E}_{fS} - \dot{E}_{bS} - \dot{E}_{S,IM} - \dot{E}_{S,bM} - j\dot{I}_S(x_c + a^2x_{1s}) \pm j\omega M_{MS}\dot{I}_M = \dot{I}_S(r_c + a^2r_{1s}) \quad (53-29)$$

The terms  $\pm j\omega M_{MS}I_S$  and  $\pm j\omega M_{MS}I_M$  take into account the mutual induction of both windings by their slot-leakage and harmonic fluxes. Inserting into Eqs. (53-28) and (53-29) Eqs. (53-9), (53-14) and (53-20) to (53-23).

$$\begin{aligned} \dot{V}_M = \dot{I}_M[(r_{1M} + jx_{1M}) + (R_f + jX_f) + (R_b + jX_b)] \\ + \dot{I}_S[a[(R_f \cos \alpha + X_f \sin \alpha) + j(X_f \cos \alpha - R_f \sin \alpha)] \\ + a[(R_b \cos \alpha - X_b \sin \alpha) + j(X_b \cos \alpha + R_b \sin \alpha)] \pm j\omega M_{MS}] \end{aligned} \quad (53-30)$$

$$\begin{aligned} \dot{V}_S = \dot{I}_S\{[(r_c + a^2r_{1s}) + j(x_c + a^2x_{1s})] + a^2(R_f + jX_f) + a^2(R_b + jX_b)\} \\ + \dot{I}_M[a[(R_f \cos \alpha - X_f \sin \alpha) + j(X_f \cos \alpha + R_f \sin \alpha)] \\ + a[(R_b \cos \alpha + X_b \sin \alpha) + j(X_b \cos \alpha - R_b \sin \alpha)] \pm j\omega M_{MS}] \end{aligned} \quad (53-31)$$

The emf's  $\pm j\omega M_{MS}I_S$  and  $\pm j\omega M_{MS}I_M$  can be best taken care of as parts of the slot and differential leakage, i.e., as parts of  $jI_Mx_{1M}$  and  $jI_Sx_{1s}$ .

With the abbreviations

$$\begin{aligned} l_M = r_{1M} + R_f + R_b & \quad l_S = r_c + a^2(r_{1s} + R_f + R_b) \\ m_M = X_{1M} + X_f + X_b & \quad m_S = x_c + a^2(x_{1s} + X_f + X_b) \\ l_M = jm_M = \dot{Z}_M & \quad l_S + jm_S = \dot{Z}_S \end{aligned} \quad (53-32)$$

$$\begin{aligned}
 a[(R_f + R_b) \cos \alpha + (X_f - X_b) \sin \alpha] &= q_1 \\
 a[(X_f + X_b) \cos \alpha - (R_f - R_b) \sin \alpha] &= q_2 \\
 a[(R_f + R_b) \cos \alpha - (X_f - X_b) \sin \alpha] &= t_1 \\
 a[(X_f + X_b) \cos \alpha + (R_f - R_b) \sin \alpha] &= t_2
 \end{aligned} \tag{53-33}$$

$$\dot{Z}_q = q_1 + jq_2 \quad \dot{Z}_t = t_1 + jt_2 \tag{53-34}$$

$$\dot{V}_M = \dot{I}_M \dot{Z}_M + \dot{I}_S \dot{Z}_q \tag{53-35}$$

$$\dot{V}_S = \dot{I}_S \dot{Z}_S + \dot{I}_M \dot{Z}_t \tag{53-36}$$

$$\dot{I}_M = \frac{\dot{V}_M \dot{Z}_S - \dot{V}_S \dot{Z}_q}{\dot{Z}_M \dot{Z}_S - \dot{Z}_q \dot{Z}_t} \tag{53-37}$$

$$\dot{I}_S = \frac{\dot{V}_S \dot{Z}_M - \dot{V}_M \dot{Z}_t}{\dot{Z}_M \dot{Z}_S - \dot{Z}_q \dot{Z}_t} \tag{53-38}$$

Eqs. (53-37) and (53-38) determine the magnitude and phase of the currents in both stator windings.

(a) *Split-phase and capacitor-start motor during starting and permanent-split capacitor motor during starting and running.* In these cases

$$\begin{aligned}
 \alpha &= (\pi/2) & V_M &= V_S = V \\
 q_1 &= a(X_f - X_b) = n_X & t_1 &= -a(X_f - X_b) = -n_X \\
 q_2 &= -a(R_f - R_b) = -n_R & t_2 &= a(R_f - R_b) = n_R
 \end{aligned} \tag{53-33a}$$

and with the abbreviations

$$l_S l_M - m_S m_M - n_R^2 + n_X^2 = c \tag{53-39}$$

$$\begin{aligned}
 l_M m_S + l_S m_M - 2n_R n_X &= d \\
 \frac{(l_S - n_X)c + (m_S + n_R)d}{c^2 + d^2} &= p_1 \\
 \frac{-(l_S - n_X)d + (m_S + n_R)c}{c^2 + d^2} &= p_2
 \end{aligned} \tag{53-40}$$

$$\begin{aligned}
 \frac{(l_M + n_X)c + (m_M - n_R)d}{c^2 + d^2} &= s_1 \\
 \frac{-(l_M + n_X)d + (m_M - n_R)c}{c^2 + d^2} &= s_2
 \end{aligned} \tag{53-41}$$

$$\dot{I}_M = \dot{V}(p_1 + jp_2) \quad \tan \varphi_M = p_2/p_1 \tag{53-42}$$

$$\dot{I}_S = \dot{V}(s_1 + js_2) \quad \tan \varphi_S = s_2/s_1 \tag{53-43}$$

(b) *Split-phase and capacitor-start motor during running.* In these cases  $I_s = 0$  and Eq. (53-30) yields

$$\dot{I}_M = \frac{\dot{V}_M}{(r_{1M} + R_f + R_b) + j(x_{1M} + X_f + X_b)} \quad (53-44)$$

where  $R_f$ ,  $R_b$ ,  $X_f$ ,  $X_b$  are functions of the slip  $s$  (see Eqs. (53-2) and (53-3) and the remarks with respect to  $R_b$  and  $X_b$ ).

(c) *Symmetrical two-phase motor.* In this case

$$\begin{aligned} \dot{V}_s &= j \dot{V}_M & a &= 1 & \alpha &= \pi/2 & \varphi &= \pi/2 \\ r_{1M} &= r_{1S} = r_1 \\ x_{1M} &= x_{1S} = x_1 \end{aligned} \quad (53-45)$$

Eqs. (53-37) and (53-38) yield with Eq. (53-45)

$$I_M = \frac{V_M}{(r_1 + 2R_f) + j(x_1 + 2X_f)} \quad (53-46)$$

$$I_s = \frac{V_s}{(r_1 + 2R_f) + j(x_1 + 2X_f)} \quad (53-47)$$

$R_b$  and  $X_b$  dropped out, as could be expected, since there is no backward rotating flux.

**53-5. The power of the rotating field and the torque.** The power of the rotating field is determined by the product of emf (due to the main flux) and current. Considering Figs. 53-2 and 53-4 and Eqs. (53-28) and (53-29), the instantaneous power of the rotating field is

$$\begin{aligned} p_{\text{rot.f.}} &= [(e_{fM} - e_{bM}) + (e_{M,fs} - e_{M,bs})] \sqrt{2} I_M \sin \omega t \\ &\quad + [(e_{fs} - e_{bs}) + (e_{S,fM} - e_{S,bM})] \sqrt{2} \sin (\omega t + \varphi) \end{aligned} \quad (53-48)$$

The negative signs of  $e_{bM}$ ,  $e_{M,bs}$ ,  $e_{bs}$ , and  $e_{S,bM}$  are in accordance with the considerations of Art. 26-4.

Inserting into Eq. (53-48) Eqs. (53-24) to (53-27), two terms for the instantaneous power are obtained: one term is independent of time and represents the *average value* of the power of the rotating field; the other term depends upon  $2\omega t$  and represents a power which alternates with twice the line-frequency.

The first term is

$$\begin{aligned} P_{\text{rot.f.,ave}} &= (I_M^2 + a^2 I_s^2)(R_f - R_b) \\ &\quad + 2I_M I_s a [R_f \cos (\alpha - \varphi) - (R_b \cos (\alpha + \varphi))] \quad \text{watts} \end{aligned} \quad (53-49)$$

and the second term

$$\begin{aligned} P_{\text{rot.f.,alt}} &= I_M^2 [-(R_f - R_b) \cos 2\omega t + (X_f - X_b) \sin 2\omega t] \\ &\quad + a^2 I_s^2 [-(R_f - R_b) \cos 2(\omega t + \varphi) + (X_f - X_b) \sin 2(\omega t + \varphi)] \\ &\quad + 2I_M I_s a \cos \alpha [-(R_f - R_b) \cos (2\omega t + \varphi) \\ &\quad \quad + (X_f - X_b) \sin (2\omega t + \varphi)] \quad \text{watts} \end{aligned} \quad (53-50)$$

The average torque is

$$T_{\text{ave}} = \frac{7.04}{n_s} P_{\text{rot.f.,ave}} \text{ lb-ft.} \quad (53-51)$$

(a) *Split-phase and capacitor-start motor during starting and permanent-split capacitor motor during starting and running.* In these cases  $\alpha = \pi/2$  and Eqs. (53-49) and (53-50) yield

$$P_{\text{rot.f.,ave}} = (I_M^2 + a^2 I_S^2)(R_f - R_b) + 2I_M I_S a (R_f + R_b) \sin \varphi \text{ watts} \quad (53-52)$$

$$P_{\text{rot.f.,alt}} = I_M^2 [ - (R_f - R_b) \cos 2\omega t + (X_f - X_b) \sin 2\omega t ] \\ + a^2 I_S^2 [ - (R_f - R_b) \cos 2(\omega t + \varphi) \\ + (X_f - X_b) \sin 2(\omega t + \varphi) ] \text{ watts} \quad (53-53)$$

At  $s = 1$  (standstill),  $R_f = R_b$  and  $X_f = X_b$ . Therefore, at  $s = 1$

$$P_{\text{rot.f.,ave}} = 4I_M I_S a R_f \sin \varphi \text{ watts} \quad (53-54)$$

and the starting torque

$$T_{s=1} = \frac{7.04}{n_s} 4I_M I_S a R_f \sin \varphi \text{ lb-ft.} \quad (53-55)$$

At  $s = 1$ ,  $P_{\text{rot.f.,alt}} = 0$ , i.e., there is no alternating torque at standstill.

(b) *Split-phase and capacitor-start motor during running.* Since  $I_S = 0$ , Eqs. (53-49) and (53-50) yield

$$P_{\text{rot.f.,ave}} = I_M^2 (R_f - R_b) \text{ watts} \quad (53-56)$$

$$T_{\text{ave}} = \frac{7.04}{n_s} I_M^2 (R_f - R_b) \text{ lb-ft.} \quad (53-57)$$

$$P_{\text{rot.f.,alt}} = I_M^2 [ - (R_f - R_b) \cos 2\omega t + (X_f - X_b) \sin 2\omega t ] \text{ watts} \quad (53-58)$$

(c) *Symmetrical two-phase motor.* In this case

$$I_M = I_S, \quad \alpha = \pi/2, \quad \varphi = \pi/2, \quad a = 1$$

and Eqs. (53-49) and (53-50) yield

$$P_{\text{rot.f.,ave}} = 4I_M^2 R_f \text{ watts} \quad (53-49)$$

$$T_{\text{ave}} = \frac{7.04}{n_s} 4I_M^2 R_f \text{ lb-ft.} \quad (53-60)$$

$$P_{\text{rot.f.,alt}} = 0$$

The torques given in the previous equations are developed torques. The delivered torques are obtained by subtracting the loss torque corresponding to  $P_{F+W} + P_{\text{ir.,rot}}$ .

## Chapter 54

### THE PERMANENT-SPLIT CAPACITOR MOTOR UNDER BALANCED AND UNBALANCED CONDITIONS

**54-1. Balanced conditions.** The connection diagram of the permanent split capacitor motor (for running condition) is shown schematically in Fig. 54-1. Its main winding  $M$  is connected directly to the line; its auxiliary winding  $S$  is in series with a capacitor  $C$ . Main and auxiliary windings have different numbers of turns. The rotor has a squirrel-cage winding.

It is desirable that the motor operate *balanced at full-load*, i.e., that main winding and auxiliary winding operate as a symmetrical 2-phase winding. In order to achieve this, two conditions must be satisfied. First, the mmf's of both windings must be equal and displaced by  $90^\circ$  at full-load. Secondly, the constants of the auxiliary winding when referred to the main winding must be equal to the constants of the main winding.

The main winding will be denoted by the subscript  $M$ , the auxiliary (starting) winding by the subscript  $S$ . The first condition is satisfied when

$$N_S k_{apS} \dot{I}_S = j N_M k_{apM} \dot{I}_M \quad (54-1)$$

or with

$$\frac{N_M k_{apM}}{N_S k_{apS}} = a \quad (54-2)$$

when

$$\frac{\dot{I}_S}{a} = j \dot{I}_M. \quad (54-1a)$$

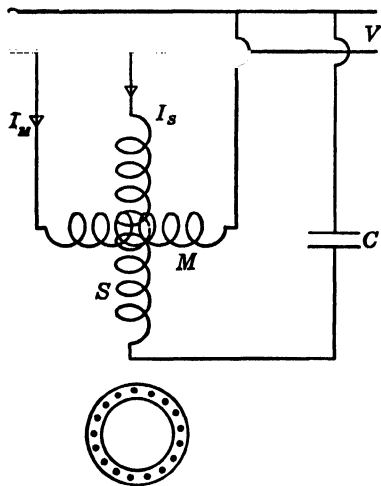


FIG. 54-1. Stator and rotor windings of the capacitor motor.



When Eq. (54-1) holds, the emfs of both windings are proportional to the numbers of their effective turns and are also displaced by  $90^\circ$ , i.e.,

$$\frac{E_M}{E_S} = \frac{N_M k_{apM}}{N_S k_{apS}} = a, \quad aE_S = jE_M. \quad (54-3)$$

For the same distribution of both windings, the second condition is satisfied with respect to the leakage reactances and is

$$x_S' = a^2 x_S = x_M. \quad (54-4)$$

However, this condition is satisfied with respect to the resistances only when the ratio of the area of the conductor of the auxiliary winding to the area of the conductor of the main winding is equal to  $a$  (Eq. 54-2). If the ratio of the areas of both conductors is denoted by  $K_a$ , it should be

$$K_a = a. \quad (54-5)$$

Then

$$r_S' = a^2 r_S = r_M, \quad (54-6)$$

and the weights of copper and current densities of both windings are equal.

Fig. 54-2 shows the phasor diagram for balanced operation.  $r_C$  and  $x_C = 1/\omega C$  are the resistance and reactance respectively of the capacitor.  $I_S$  and  $-E_S$  are displaced  $90^\circ$  with respect to  $I_M$  and  $-E_M$  respectively.

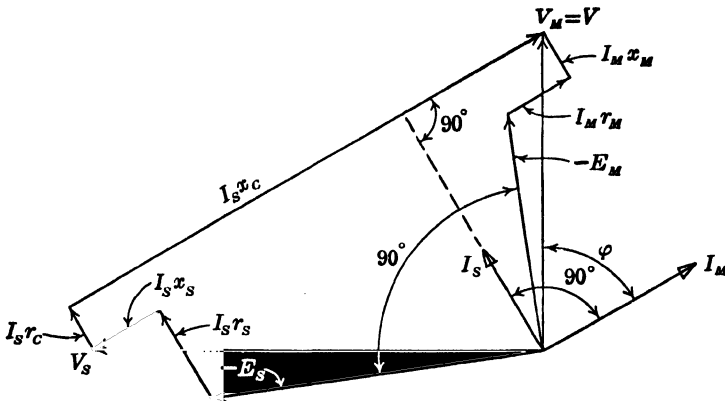


FIG. 54-2. Voltage and current diagram of the capacitor motor for balanced operation.

The phasor diagram of Fig. 54-2 can be used in order to determine the turn ratio  $a$  and the capacitance  $C$  of the capacitor for balanced operation, if the constants of the main winding are given. For this purpose calculate the primary current  $I_M$  and the primary phase angle  $\varphi$  between current  $I_M$  and line voltage  $V$  for a 2-phase motor having both phases the same as the main winding. This determines the part of the phasor diagram which refers to the

main winding and also the directions and positions of  $-E_s$ ,  $I_s$ , and  $I_s x_C$ , the last two phasors being perpendicular to each other. From Eqs. (54-1a), (54-4), and (54-6)

$$I_s r_s = (1/a) I_M r_M, \quad I_s r_C = a I_M r_C, \quad I_s x_s = (1/a) I_M x_M. \quad (54-7)$$

Now assume a value for the turn ratio  $a$ , then determine the three phasors of Eq. (54-7) and check whether these phasors fit between  $-E_s$  and  $I_s x_C$ . If they do not close the diagram, another value for  $a$  has to be assumed. The phasor  $V_s$  is found as the last phasor of the diagram.

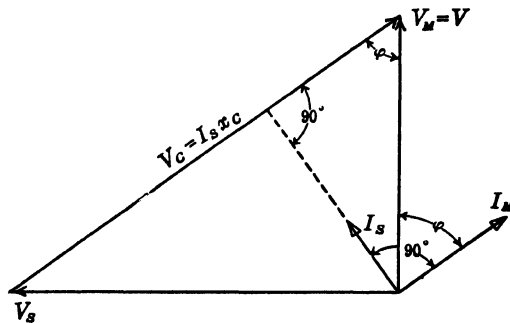


FIG. 54-3. Simplified voltage diagram of the capacitor motor for balanced operation.

The turn ratio  $a$  and the capacitance  $C$  for balanced operation can be found approximately from the phasor diagram of Fig. 54-3 in which it is assumed that  $V_s$  is displaced  $90^\circ$  with respect to  $V_M = V$  and  $r_C$  is neglected.  $\varphi$  is the same angle as in Fig. 54-2, i.e., the phase angle between primary current and line voltage of a symmetrical 2-phase motor having both windings the same as the main winding. It follows from Fig. 54-3 that

$$a \approx \frac{V_M}{V_s} \approx \cot \varphi \quad (54-8)$$

Furthermore, since

$$I_s x_C \cos \varphi \approx a I_M x_C \cos \varphi \approx V, \quad x_C = \frac{1}{\omega C} \approx \frac{V}{a I_M \cos \varphi} \quad (54-9)$$

The  $VA$  of the capacitor are

$$P_C \approx \frac{V}{\cos \varphi} I_s \approx \frac{V}{\cos \varphi} a I_M \quad (54-10)$$

The ratio of the capacitor  $VA$  to the  $VA$  of the symmetrical 2-phase machine is approximately (by Eqs. (54-8) and (54-10))

$$\frac{P_C}{2 V I_M} \approx \frac{a}{2 \cos \varphi} \approx \frac{1}{2 \sin \varphi} \quad (54-11)$$

The current delivered by the line is

$$\begin{aligned} \dot{I}_L &= \dot{I}_M + \dot{I}_S = \dot{I}_M(1 + ja), \\ I_L &= I_M \sqrt{1^2 + a^2} = I_M \frac{1}{\sin \varphi} \end{aligned} \quad (54-12)$$

and the line power factor, including capacitor,

$$\cos \varphi_L \approx \frac{I_M \cos \varphi + I_S \sin \varphi}{I_M} \sin \varphi = 2 \sin \varphi \cos \varphi = \sin 2\varphi. \quad (54-13)$$

The simplified diagram, Fig. 54-3, makes it possible to determine approximately the turn ratio  $a$ , the  $VA$  of the capacitor, and the line power factor  $\cos \varphi_L$  as a function of the phase angle ( $\varphi$ ) between the line voltage and the motor current which would appear if a 2-phase motor, having both windings the same as the main winding of the capacitor motor, were connected to a symmetrical 2-phase power supply (Ref. D15).

**54-2. Unbalanced conditions.** If the turn ratio  $a$  and the capacitor are chosen to give balanced operation at a certain load and slip, the capacitor motor will be *unbalanced* at other loads and slips. In order to determine the currents in both windings, the torque, etc., at other loads, the two-rotating-field theory can be applied as shown in Chap. 53. These quantities can also be determined by the method of symmetrical components, i.e., the unsymmetrical 2-phase current system of the machine will be resolved into two symmetrical 2-phase current systems having different phase sequences. Each of the two symmetrical systems then can be treated as in the polyphase motor (Chap. 51) and the effects of both symmetrical systems superimposed. (See Ref. A13.)

It is a simple matter to determine the symmetrical components for a 2-phase system. The assumption will be made that both stator windings have the same weight of copper, i.e., that  $K_a = a$ , and the same distribution. With this assumption the resistance and leakage reactance of the auxiliary winding referred to the main winding are the same as those of the main winding. All constants of the auxiliary winding and of the rotor are referred to the main winding. The reduction factor is  $1/a$  for the current  $I_s$ ,  $a$  for the voltage of the auxiliary winding, and  $a^2$  for resistances and reactances in the circuit of the auxiliary winding. Thus

$$r_s' = a^2 r_s = r_M, \quad x_s' = a^2 x_s = x_M, \quad r_c' = a^2 r_c, \quad x_c' = a^2 x_c. \quad (54-14)$$

The reduction factors for the rotor are the same as for a symmetrical 2-phase machine both stator windings of which are the same as the main winding.

The identities

$$\begin{aligned} \dot{I}_M &= \frac{1}{2}(\dot{I}_M - j\dot{I}_S') + \frac{1}{2}(\dot{I}_M + j\dot{I}_S') = \dot{I}_f + \dot{I}_b, \\ \dot{I}_S' &= \frac{1}{2}(j\dot{I}_M + \dot{I}_S') + \frac{1}{2}(-j\dot{I}_M + \dot{I}_S') = j\dot{I}_f - j\dot{I}_b, \end{aligned} \quad (54-15)$$

yield for the unsymmetrical 2-phase current system,  $I_M$  and  $I_S'$ , two symmetrical 2-phase current systems with different phase sequences, one  $I_f$ ,  $+jI_f$ , and the other  $I_b$ ,  $-jI_b$ . These two current systems produce rotating fields traveling in opposite directions. The unbalanced capacitor motor thus is replaced by two balanced 2-phase machines, one having in its stator windings the currents  $I_f$  and  $+jI_f$ , the other having in its stator windings the currents  $I_b$  and  $-jI_b$ , where

$$\begin{aligned} I_f &= \frac{1}{2}(\dot{I}_M - j\dot{I}_S'), \\ I_b &= \frac{1}{2}(\dot{I}_M + j\dot{I}_S'). \end{aligned} \quad (54-16)$$

If the rotor rotates in the direction of the rotating field produced by the current system  $I_f$ ,  $jI_f$ , its impedance with respect to this (forward) rotating field is different from that with respect to the rotating field produced by the backward current system  $I_b$ ,  $-jI_b$ , since the rotor has different speeds relative to both rotating fields. If the slip is  $s$  with respect to the forward rotating field, it is  $(2-s)$  with respect to the backward rotating field.

The total impedances of the machine with respect to both systems will be denoted by  $\dot{Z}_f$  and  $\dot{Z}_b$  respectively.  $\dot{Z}_f$  then is the impedance for the slip  $s$  of a symmetrical 2-phase machine having both stator windings the same as the main winding. The impedance  $\dot{Z}_b$  is obtained by substituting  $(2-s)$  for  $s$  in the equation for  $\dot{Z}_f$ . It is (see (Eq. 51-13))

$$\dot{Z}_f = \frac{\dot{Z}_1 + \dot{Z}_1 \dot{Z}_{2s}' \dot{Y}_m + \dot{Z}_{2s}'}{1 + \dot{Y}_m \dot{Z}_{1s}'} \quad (54-17)$$

where (see Art. 51-2)

$$\dot{Z}_1 = r_1 + jx_1, \quad \dot{Z}_{2s}' = (r_2'/s) + jx_2', \quad \dot{Y}_m = g_m - jb_m, \quad (54-18)$$

$$r_1 = r_2' = r_M, \quad x_1 = x_2' = x_M, \quad g_m = \frac{P_{h+e}}{2E_1^2}, \quad b_m = \sqrt{(I_m/E_1)^2 - g_m^2},$$

$$E_1 \approx V - I_m x_1 \approx V - I_0 x_1. \quad (54-19)$$

Eq. (54-17), can be written with very close approximation as

$$\dot{Z}_f \approx \frac{l + jm}{f + jh} \quad (54-20)$$

where (see Art. 51-2)

$$\begin{aligned} l &= (1 + \tau_2)r_1 + (1 + \tau_1)\frac{r_2'}{s}, & f &= (1 + \tau_2) + g_m \frac{r_2'}{s} \\ m &= x_1 + (1 + \tau_1)x_2' - \frac{r_1}{x_m} \frac{r_2'}{s}, & h &= g_m x_2' - b_m \frac{r_2'}{s}, \\ b_m &\approx \frac{1}{x_m}, & \tau_1 &= x_1 b_m = \frac{x_1}{x_m}, & \tau_2 &= x_2' b_m = \frac{x_2'}{x_m}. \end{aligned} \quad (54-21)$$

With

$$Z_C' = r_C' - jx_C' \approx -jx_C' \quad (54-22)$$

The voltage equations of both stator windings are

$$\dot{V} = \dot{I}_f \dot{Z}_f + \dot{I}_b \dot{Z}_b \quad \text{for the main winding.} \quad (54-23)$$

$$\dot{V}_S' = a\dot{V} = j\dot{I}_f(\dot{Z}_f + \dot{Z}_C') - j\dot{I}_b(\dot{Z}_b + \dot{Z}_C') \quad \text{for the auxiliary winding.} \quad (54-24)$$

In both equations, the first term on the right side represents the voltage drop in the winding due to the forward rotating field produced by the current system,  $\dot{I}_f$ ,  $+j\dot{I}_f$ , and the second term the voltage drop due to the backward rotating field produced by the current system  $\dot{I}_b$ ,  $-j\dot{I}_b$ .

Since all values of the auxiliary winding are referred to the main winding, the quantity  $aV_M = aV$  has to be introduced for  $V_S$ .

From Eqs. (54-23) and (54-24) the currents of the forward and backward systems are:

$$\dot{I}_f = \frac{\dot{V}}{2} \frac{(1 - ja)\dot{Z}_b + \dot{Z}_C'}{\dot{Z}_f \dot{Z}_b + \frac{1}{2}\dot{Z}_C'(\dot{Z}_f + \dot{Z}_b)}, \quad (54-25)$$

$$\dot{I}_b = \frac{\dot{V}}{2} \frac{(1 + ja)\dot{Z}_f + \dot{Z}_C'}{\dot{Z}_f \dot{Z}_b + \frac{1}{2}\dot{Z}_C'(\dot{Z}_f + \dot{Z}_b)} \quad (54-26)$$

The geometric loci of the end points of these currents are not circles but bicircular quartics (see Eq. (51-48)).

With the aid of Eq. (54-15), the currents  $\dot{I}_M$  and  $\dot{I}_S$  of both stator windings now can be determined. The geometric loci of the end points of these currents also are bicircular quartics, while the geometric locus of the end point of the stator current of the single-phase motor is a circle with the parameter  $s(2 - s)$ .\*

The current delivered by the line is

$$\dot{I}_L = \dot{I}_M + \dot{I}_S = \dot{I}_M + a\dot{I}_S'. \quad (54-27)$$

The geometric locus of the end point of the line current  $\dot{I}_L$  is a part of a circle with the parameter  $s(2 - s)$ . This circle can be determined best from the three points which correspond to the slip  $s = 0$ ,  $s = 1$ , and  $s = \infty$ . Eq. (54-27) also determines the power factor of the line.

The currents induced in the rotor by both rotating fields, i.e., the rotor currents which correspond to the stator currents  $\dot{I}_f$  and  $\dot{I}_b$ , can be found from the equations derived for the polyphase machine. From Eqs. (51-13) and (51-14) for the ratio of secondary to primary current of the polyphase motor

$$\frac{\dot{I}_2'}{\dot{I}_1} = -\frac{1}{\dot{Y}_m \dot{Z}_{2s}' + 1} \approx -\frac{jx_m}{(r_2'/s) + j(1 + \tau_2)x_m} \quad (54-28)$$

Thus the forward-rotating field induces in the rotor

\* Eq. (26-22) has the form

$$\frac{\dot{I}}{\dot{V}_1} = \frac{\dot{A} + \dot{B}s(2 - s)}{\dot{C} + \dot{D}s(2 - s)}$$

$$\dot{I}_{2f}' = -\dot{I}_f \frac{jx_m}{(r_2'/s) + j(1 + \tau_2)x_m} \quad (54-29)$$

and the backward-rotating field

$$\dot{I}_{2b}' = -\dot{I}_b \frac{jx_m}{[r_2'/(2-s)] + j(1 + \tau_2)x_m} \quad (57-30)$$

From Eqs. (54-29) and (54-30) the torques produced by the forward- and backward-rotating fields can be determined:

$$T_f = 2 \frac{112.7}{n_s} I_{2f}'^2 \frac{r_2'}{s} \quad \text{oz-ft.}, \quad (54-31)$$

$$T_b = -2 \frac{112.7}{n_s} I_{2b}'^2 \frac{r_2'}{2-s} \quad \text{oz-ft.}, \quad (54-32)$$

and the resultant torque

$$T = T_f + T_b. \quad (54-33)$$

The torques yielded by Eqs. (54-31) to (54-33) are developed torques.

## Chapter 55

### FRACTIONAL-SLOT WINDINGS

**55-1. General considerations.** In low-speed machines with many poles, the number of slots per pole per phase may become two or less. In these cases the fractional-slot winding is used. The use of  $q=1$  is avoided since it has a high harmonic content. When there is a possibility that harmonic currents may cause interference with telephone lines, a fractional value of  $q$  is used even in cases where it could be made an integer.

An example is helpful for the introduction into fractional-slot windings. Consider a 3-phase stator with 20 poles and  $Q=135$ . The *average* number of slots per pole per phase is

$$q = \frac{135}{3 \times 20} = \frac{9}{4} = 2 + \frac{1}{4}$$

Since each coil group must have an integral number of single coils (2 or 3 or 4, etc.),  $q=2\frac{1}{4}$  can be realized if each phase has in four (= denominator of  $q$ ) poles, three coil groups with two single coils and one coil group with three single coils, making the average value of  $q = (3 \times 2 + 1 \times 3)/4 = \frac{9}{4} = 2 + \frac{1}{4}$ . Each phase has in four poles 9 (= numerator of  $q$ ) slots. All three phases have in four poles  $3 \times 9 = 27$  slots. Four poles make the *basic unit* of this winding. The four coil groups of each phase, within this basic unit, must be connected in series. Since the stator has 20 poles, the maximum number of parallel circuits is  $20/4 = 5$ , whereas a 20-pole machine with  $q = \text{an integer}$  may have 20 parallel circuits.

Thus considering  $q$  in the form  $\frac{9}{4}$  (numerator and denominator must have no common divisor) reveals that four poles make the basic unit of this winding and that each phase has nine slots in the four poles. Considering  $q$  in the form  $2 + \frac{1}{4}$  reveals that there are in the basic unit (= 4 poles)  $4 - 1 = 3$  coil groups with 2 (= integral part of  $q$ ) single coils and 1 (= numerator of fractional part of  $q$ ) coil group with  $2 + 1 = 3$  single coils.

Expressed in general terms,

$$q = \frac{Q}{m \times p} = \frac{N}{\beta} = a + \frac{b}{\beta} \quad (55-1)$$

where  $N$  and  $\beta$  have no common divisor, it means that

(a)  $\beta$  poles make the basic unit of the winding

- (b) each phase has within  $\beta$  poles  $N = q\beta$  slots
- (c) all  $m$  phases have within  $\beta$  poles,  $mN$  slots
- (d) each phase has within  $\beta$  poles  $\beta - b$  coil groups with  $a$  single coils and  $b$  coil groups with  $(a + 1)$  single coils
- (e) the maximum possible number of parallel circuits is  $p/\beta$ .

**55-2. The slot star.** The star which shows the position of the coil sides in the magnetic field is useful for the investigation of the fractional-slot windings.

Two-layer windings are considered. Both layers are entirely symmetrical; for example, the current distribution around the armature is the same in both layers. However, the current distributions (and also the induced emf's of both layers) are not in phase; they are shifted with respect to each other by the chording angle, i.e., by the angle which corresponds to the difference between pole pitch and coil span. The stars of the coil sides of both layers are, therefore, identical though shifted with respect to each other by the chording angle and it suffices to consider *any one of the two layers*. The coil-side star then becomes also a *slot star*.

Fig. 55-1 shows the slot star of a 2-pole, 3-phase *integral-slot* winding with  $q = 2$ . The angle between two adjacent slots is, in general,

$$\alpha_s = \frac{180p}{Q} = \frac{180}{mq} \quad (55-2)$$

In this case  $\alpha_s = 180/6 = 30$  electrical degrees. Two adjacent phasors correspond to two adjacent slots.

If the top layer is considered, slots 1, 2, 7, and 8 belong to phase *A*, slots 3, 4, 9, and 10 to phase *C*, and so forth. Phasor 7 with which the second pole starts is shifted  $180^\circ$  with respect to phasor 1; phasor 8 is shifted  $180^\circ$  with respect to phasor 2, and so on. Slots 1 and 7 lie in fields of *same strength* but of different polarity; this explains the shift of  $180^\circ$ . The same applies to slots 2 and 8, 3 and 9, and so forth. The external connections (the end-windings) are made so that the emf's of the coil-side pairs 1 and 7, 2 and 8, and so on, add up. Therefore, the shift of  $180^\circ$  can be disregarded and phasor 7 can be shown to coincide with phasor 1, phasor 8 to coincide with phasor 2, and so forth. The slot star of the 2-pole integral-slot winding is then completely represented by half of a circle.

The following presentation of the slot star can be used instead of the graphical (*slot 1 is used as reference*).

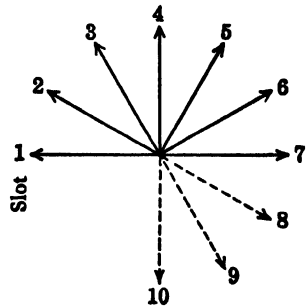


FIG. 55-1. Slot star of a 3-phase integral-slot winding with two slots per pole per phase.



Slot	1	2	3	4	5	6	7	8	9	10	11	12
Angle between the slots	0	30	60	90	120	150	180	210	240	270	300	330°

and disregarding (subtracting) the 180° shift

Slot	1	2	3	4	5	6
Angle between the slots	0	30	60	90	120	150°
Slot	7	8	9	10	11	12

The sequence of the phasors in the slot star, i.e., the sequence of the slots *in the magnetic field*, is the *same as* the sequence of the slots *in the machine*.

A fractional-slot winding will be considered now and the slot star of this winding will be determined. It is assumed that:  $m=3$ ,  $p=20$ ,  $Q=75$ . Thus

$$q = \frac{75}{3 \times 20} = \frac{5}{4} = 1 + \frac{1}{4} = \frac{N}{\beta} = a + \frac{b}{\beta}$$

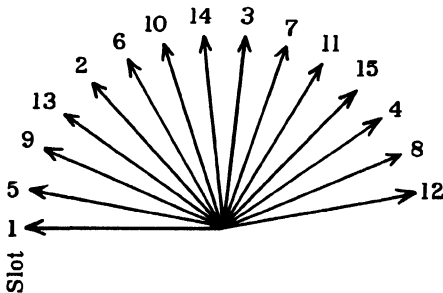


FIG. 55-2. Slot star of a 3-phase, 20-pole fractional-slot winding with  $1 \frac{1}{4}$  slots per pole per phase.

$\beta=4$  poles make the basic unit of this winding. Each phase has in the  $\beta=4$  poles  $N=5$  slots. All three phases have in the  $\beta=4$  poles  $m \times N = 3 \times 5 = 15$  slots. Each phase has in the  $\beta=4$  poles  $\beta - b = 4 - 1 = 3$  coil groups with  $a=1$  coil and  $b=1$  coil group with  $(a+1)=2$  single coils.

The angle between two consecutive slots of the stator is

$$\alpha_s = \frac{180 \times 20}{75} = \frac{180 \times 4}{3 \times 5} = 48^\circ$$

The *basic unit* of the *integral-slot* winding is represented by two poles. The *basic unit* of the *fractional-slot* winding is represented by  $\beta$  poles and the slot star of  $\beta$  poles has to be considered. In this case,  $\beta=4$ . The total number of slots in four poles is  $mN = 3 \times 5 = 15$  and 15 phasors must appear in the slot star. The slot star is (see also Fig. 55-2)

Slot	1	2	3	4	5	6	7	8	9	10	11	12	13	14	15
Angle between the slots	0	48	96	144	192	240	288	336	384	432	480	528	576	624	672

Subtracting again  $180^\circ$ , or a multiple of it, the slot star becomes

Slot	1	2	3	4	5	6	7	8	9	10	11	12	13	14	15
Angle between the slots	0	48	96	144	12	60	108	156	24	72	120	168	36	84	132

It is seen that, contrary to the integral-slot winding, the sequence of the phasors in the slot star, i.e., the sequence of the slots *in the magnetic field*, is *not the same* as the sequence of the slots in the machine. The sequence of the slots in the magnetic field is

Slot 1 5 9 13 2 6 10 14 3 7 11 15 4 8 12

the angle between *two consecutive phasors* of the slot star being  $12^\circ$ . Between two phasors which correspond to two consecutive slots in the machine lies three (in general,  $\beta - 1$ ) other phasors. For example, between the phasors which correspond to slots 1 and 2 lie the phasors 5, 9, and 13. *The winding creeps in the magnetic field.*

It becomes necessary to distinguish between the *angle between two consecutive slots in the machine*,  $\alpha_s$ , and the *angle between two consecutive phasors of the slot star*,  $\alpha_m$ . This latter angle is the *magnetic field angle* of the winding. It is important with respect to the emf and the mmf of the winding, because it determines the distribution factor of the winding.

The magnetic field angle is (Fig. 55-2)

$$\alpha_m = \frac{180}{mN} \quad (55-3)$$

For the winding under consideration,  $\alpha_m = 180/15 = 12^\circ$ .

In the integral slot winding,  $\alpha_m = \alpha_s$ . In the fractional slot winding  $\alpha_m < \alpha_s$ ; the ratio of the two angles is (Eqs. (55-2) and (55-3))

$$\frac{\alpha_s}{\alpha_m} = \beta \quad (55-4)$$

The *largest distribution factor of the main* (synchronous) *wave* is obtained when the first five phasors of the slot star (Fig. 55-2) are assigned to phase *A*, the following five phasors to phase *C*, and the last five phasors to phase *B*, because the closer together that the slots belonging to the phase lie, the larger is the distribution factor of the winding (Art. 14-1). Thus, in each basic unit ( $=\beta=4$  poles), phase *A* will occupy the slots 1, 5, 9, 13 and 2; phase *C* will occupy the slots 6, 10, 14, 3, and 7; and phase *B* the slots 11, 15, 4, 8, and 12.

Consider the sequence of the *slots* in the slot star (Fig. 55-2). Starting with slot 1, the sequence of the slots follows the series

$$1, \quad 1+4, \quad 1+2 \times 4, \quad 1+3 \times 4, \quad 1+(4 \times 4 - mN), \quad 1+(5 \times 4 - mN), \dots$$

Since the total number of slots in the basic unit of the winding is  $mN$ , this value (or a multiple of it) has to be subtracted from the terms of the series if they become larger than  $mN$ .

In general, the series is

$$1, 1+d, 1+2d, 1+3d, \dots, 1+[(mN-1)d - \text{integer} \times mN] \quad (55-5)$$

where  $d$  is the difference between two slots which correspond to two consecutive phasors of the slot star. For the winding under consideration,  $d=4$ .

This difference  $d$  can be found from the following consideration. If  $P$  denotes the number of full pole pitches between two slots which correspond to two consecutive phasors of the slot star, then

$$d \times \alpha_s = \alpha_m + 180P \quad (55-6)$$

Checking on the winding under consideration and considering, for example, slots 1 and 5,  $P=1$ , because slot 5 is shifted in the stator  $192^\circ$  from slot 1. Then, for this winding  $d \times \alpha_s = 4 \times 48 = 192^\circ$  and also  $\alpha_m + 1 \times 180 = 12 + 180 = 192^\circ$ .

Inserting into Eq. (55-6) the values of  $\alpha_s$  and  $\alpha_m$  from Eqs. (55-2) and (55-3) there results

$$d = \frac{mNP + 1}{\beta} \quad (55-7)$$

For  $P$  there must be used the *smallest integer* that makes  $d$  an integer.  $P$  is equal to or larger than 1.

Having the value of  $d$ , the layout of the winding is readily made.

**55-3. The layout of a fractional-slot winding with respect to the main wave. The coil grouping.** The layout of a fractional-slot winding and the determination of the coil grouping, i.e., the sequence of the larger and smaller coil groups in the machine, will be demonstrated by an example of a 3-phase, 10-pole winding in  $Q=48$  slots. Thus

$$q = \frac{48}{30} = \frac{8}{5} = 1 + \frac{3}{5} \quad \beta = 5 \quad N = 8 \quad a = 1 \quad b = 3$$

5 poles make the basic unit of this winding. There will be within 5 poles  $3 \times N = 24$  slots,  $N=8$  for each phase. Each phase will have, per basic unit,  $b=3$  coil groups with  $1+1=2$  single coils and  $\beta-b=5-3=2$  coil groups with 1 coil. It follows from Eq. (55-7)

$$d = \frac{3 \times 8 \times P + 1}{5} = 5 \quad P = 1$$

The  $N=8$  slots assigned to phase  $A$  are, therefore,

1	$1+d$	$1+2d$	$1+3d$	$1+4d$	$1+5d-3N$	$1+6d-3N$	$1+7d-3N$
1	6	11	16	21	2	7	12

or, arranged corresponding to the sequence of the slots in the machine,

1 2      6 7      11 12      16      21

The 8 slots assigned to phase *C* are

$1 + 8d - 3N,$	$1 + 9d - 3N,$	$1 + 10d - 6N,$	$1 + 11d - 6N,$
17	22	3	8
$1 + 12d - 6N,$	$1 + 13d - 6N,$	$1 + 14d - 6N,$	$1 + 15d - 9N$
13	18	23	4

or, arranged corresponding to the sequence of the slots in the machine,

3 4      8      13      17 18      22 23

and the 8 slots assigned to phase *B* are

5      9 10      14 15      19 20      24

Starting with slot 1 and considering the slots assigned to the 3 phases, the first pole-phase group consists of slots 1 and 2 and belongs to phase *A*. The second pole-phase group consists of slots 3 and 4 and belongs to phase *C*. The third pole-phase group consists of slot 5 and belongs to phase *B*, and so forth. The sequence of the *coil groups* in a basic unit of the winding is

2	2	1	2	1	2	2	1	2	1	2	2	1	2	1
<i>A</i>	<i>C</i>	<i>B</i>	<i>A</i>	<i>C</i>	<i>B</i>	<i>A</i>	<i>C</i>	<i>B</i>	<i>A</i>	<i>C</i>	<i>B</i>	<i>A</i>	<i>C</i>	<i>B</i>

In the example considered,  $p = 10$ . Thus, the number of basic units is  $p/\beta = 10/5 = 2$  and the sequence of the coil groups around the total stator is twice the sequence found for one unit.

Note that the grouping found for the unit consists of three repetitions of the grouping

2 2 1 2 1

Therefore, it suffices to know the coil grouping for only *a third of one basic unit* and to repeat this grouping six times. (An explanation for this is given in the following.)

The number of coil groups in one basic unit, i.e., in  $\beta$  poles, is  $m \times \beta = 3 \times 5 = 15$  and a third of this number is  $\beta = 5$ . Hence, *in general*, it is necessary to determine the sequence of *only  $\beta$  consecutive coil groups*, in order to know the sequence of all coil groups around the winding. The grouping of the  $\beta$  pole-

phase groups repeats in 3-phase windings  $3 \times (p/\beta)$  times and in 2-phase windings  $2 \times (p/\beta)$  times.

The determination of the  $\beta$  consecutive coil groups can be made on the basis of the  $d$ -series (Eq. (55-7)), as has been shown in the example. There is also a shorter way to find these coil groups.

**55-4. Simplification of the determination of the coil grouping.** (Ref. I6). Considering at first the 3-phase windings, the first  $60^\circ$  of the slot star are assigned to phase  $A$ , the next  $60^\circ$  to phase  $C$ , and so on. Indicating by two vertical lines the *integral part* of the fraction  $60/\alpha_s$ , the first coil group of phase  $A$  will consist of the first  $(\lfloor 60/\alpha_s \rfloor + 1)$  consecutive slots, since  $\lfloor 60/\alpha_s \rfloor$  angles  $\alpha_s$  are contained in the angle assigned to phase  $A$ . 1 has to be added to  $\lfloor 60/\alpha_s \rfloor$ , because the angle 0 is assigned to the slot number 1 of the star and this slot belongs to phase  $A$ . The first coil group of phase  $C$  consists of the

$$(\lfloor 120/\alpha_s \rfloor + 1) - (\lfloor 60/\alpha_s \rfloor + 1)$$

next following consecutive slots. The first coil group of phase  $B$  consists of the

$$(\lfloor 180/\alpha_s \rfloor + 1) - (\lfloor 120/\alpha_s \rfloor + 1)$$

following consecutive slots. The second pole-phase group of phase  $A$  consists of the

$$(\lfloor 240/\alpha_s \rfloor + 1) - (\lfloor 180/\alpha_s \rfloor + 1)$$

following consecutive slots and so on. Since  $\alpha_s = 180/mq$  (Eq. 55-3)

$$\frac{60}{\alpha_s} = \frac{60}{180} mq = q$$

$$\frac{2 \times 60}{\alpha_s} = 2q$$

$$\frac{3 \times 60}{\alpha_s} = 3q$$

and so forth. Thus, the first coil group of phase  $A$  consists of the first  $|q| + 1$  single coils. The first coil group of phase  $C$  of the following

$$(\lfloor 2q \rfloor + 1) - (\lfloor q \rfloor + 1)$$

single coils; the first coil group of phase  $B$  of the further following

$$(\lfloor 3q \rfloor + 1) - (\lfloor 2q \rfloor + 1)$$

single coils, and so on. Consider the same winding as before, namely,  $q = 1\frac{2}{3}$ . In order to determine the number of single coils, for example in the first three coil groups, write

	$q$	$2q$	$3q$
0	$ q  + 1$	$ 2q  + 1$	$ 3q  + 1$

The differences between the consecutive quantities must yield the number of single coils of the first three coil groups:

	$1\frac{3}{5}$	$3\frac{1}{5}$	$4\frac{4}{5}$
0	2	4	5
	2	2	1
	A	C	B

This is the same as has been determined from the  $d$ -series.

Consider now the  $\beta$ -th *pole-phase group*. Since  $q = N/\beta$ , for this coil group,

$$\frac{\beta \times 60}{\alpha_s} = \frac{\beta \times 60}{180} m q = N$$

i.e., the total angle  $\beta \times 60$  which corresponds to the  $\beta$ -th coil group comprises *an integral number of angles*  $\alpha_s$  and, therefore, ends in the slot which begins the following phase. This latter slot is to be subtracted from the number of slots contained in  $\beta \times 60^\circ$ . Thus, the number of single coils in the  $\beta$ -th coil group is

$$(N - 1 + 1) - [(\beta - 1)60/\alpha_s + 1] = N - [(\beta - 1)60/\alpha_s + 1]$$

Consider now the  $(\beta + 1)$ -th *pole-phase group*. To this coil group there corresponds the angle  $(\beta + 1) \times 60^\circ$  and the number of single coils of this coil group is

$$[(\beta + 1)60/\alpha_s + 1] - N = N + (|60/\alpha_s| + 1) - N = |60/\alpha_s| + 1$$

The number of single coils of the  $(\beta + 2)$ -th coil group is

$$[(\beta + 2)60/\alpha_s + 1] - [(\beta + 1)60/\alpha_s + 1] = N + (|2 \times 60/\alpha_s| + 1) - (N + |60/\alpha_s| + 1) \\ = (|2 \times 60/\alpha_s| + 1) - (|60/\alpha_s| + 1)$$

i.e., the  $(\beta + 1)$ -th coil group has the same number of single coils as the first coil group, the  $(\beta + 2)$ -th pole-phase has the same number of single coils as the second coil group, and so on. It follows from this that the coil grouping *starts repeating after the  $\beta$ -th coil group*. This explains why the *grouping for only  $\beta$  coil groups has to be determined*. Thus, it is necessary to write

$$\begin{array}{ccccccc} q & 2q & 3q & \dots & \beta q (= N) \\ 0 & |q| + 1 & |2q| + 1 & |3q| + 1 & \dots & \beta q = N & (55-8) \end{array}$$

The differences represent the coil grouping for  $N$  slots. Since the slot star contains  $m \times N$  slots, the grouping obtained is to be repeated  $(m - 1)$  times more, in order to obtain the grouping of one basic unit. Since there are  $(p/\beta)$  basic units, *the grouping obtained for  $\beta$  coil groups must be repeated  $[m(p/\beta) - 1]$  times more*, in order to obtain the coil grouping for the whole winding.

Applying to the example with  $m = 3$ ,  $q = 1\frac{3}{5}$ ,  $N = 8$ ,  $\beta = 5$

	$q$	$2q$	$3q$	$4q$	$5q = N$
	$1\frac{3}{5}$	$3\frac{1}{5}$	$4\frac{4}{5}$	$6\frac{2}{5}$	8
0	2	4	5	7	8
	2	2	1	2	1

This is the same grouping as obtained before from the  $d$ -series. For  $p = 10$ , repeat  $[3 \times (10/5) - 1] = 5$  times more.

The considerations applied to the 3-phase windings apply also to the 2-phase windings. The first pole-phase group of the 2-phase winding consists of the first  $|90/\alpha_s| + 1$  consecutive slots. The second pole-phase group consists of the next following  $(|180/\alpha_s| + 1) - (|90/\alpha_s| + 1)$  consecutive slots, and so on.

Since  $\alpha_s = 190/mq$

$$\begin{aligned}\frac{90}{\alpha_s} &= \frac{90}{180} mq = q \\ \frac{2 \times 90}{\alpha_s} &= 2q \\ \frac{3 \times 90}{\alpha_s} &= 3q\end{aligned}$$

and so on. This is the same as for the 3-phase windings. Furthermore

$$\frac{\beta \times 90}{\alpha_s} = \frac{\beta \times 90}{180} mq = N$$

Therefore, the same scheme is to be applied as for  $m = 3$ , in order to determine the number of single coils in the  $\beta$  coil groups.

A further simplification in the layout of the fractional-slot windings with maximum distribution factor of the main wave is based on the following considerations (Ref. I7).

Consider a 3-phase winding with  $q = 2\frac{3}{5}$ ,  $N = 13$ ,  $\beta = 5$ . The grouping of this winding is

	$2\frac{3}{5}$	$5\frac{1}{5}$	$7\frac{4}{5}$	$10\frac{2}{5}$	$13 = N$
0	3	6	8	11	13
	3	3	2	3	2

Comparing this grouping with that determined for  $q = 1\frac{3}{5}$

2	2	1	2	1
---	---	---	---	---

it is found that the sequence of the larger and smaller pole-phase groups is the same.

In general, if the number of slots per pole per phase is written as  $q = I + (b/\beta)$ , the sequence of the larger and smaller groups does not depend on the value of

the integral part of  $q$ ,  $I$ , but it depends only upon the values of  $b$  and  $\beta$ . If the distribution has been determined for a certain value of  $I$ , say for  $I=1$ , the distribution for  $I=3$  is found by adding to all numbers of the ( $I=1$ )-distribution  $(3-1)=2$ .

Thus, the sequence of the larger and smaller pole-phase groups can be determined for  $I=0$  and then the same sequence applies to  $I=1, 2, 3, 4 \dots$ . The value of  $I$  determines then the number of single coils in the coil groups. The distribution found for  $I=0$  yields coil groups with 1 and 0 single coils. Adding to *all figures* of the ( $I=0$ )-distribution 1, the distribution for  $I=1$  is found; adding to all figures of the ( $I=0$ )-distribution 2, the distribution for  $I=2$ , is found, and so on.

In order to determine the distribution for  $I=0$ ,

- write the series  $(b/\beta), 2(b/\beta), 3(b/\beta) \dots \beta(b/\beta)=b$
- add to all numbers of the (a) series 1 except the last number  $b$
- write to the left of the (b) series 0 and determine the differences between adjacent numbers
- add to all numbers of the (c) series the value of  $I$ .

The last series represents the coil grouping of a  $(1/m)$ -th part of a basic unit. Repeat  $[m(p/\beta) - 1]$  times, in order to get the coil-group distribution for the whole winding.

Taking, as examples again,  $q=1\frac{3}{5}$  and  $q=2\frac{3}{5}$

	$\frac{3}{5}$	$1\frac{1}{5}$	$1\frac{4}{5}$	$2\frac{3}{5}$	$3=b$
	0	1	2	3	3
Sequence of large and small coil groups	1	1	0	1	0
$q=1\frac{3}{5}$	2	2	1	2	1
$q=2\frac{3}{5}$	3	3	2	3	2

**55-5. Conditions for balance.** Consider Fig. 55-2. The first five phasors 1, 5, 9, 13, and 2 are assigned to phase  $A$ , the next five phasors 6, 10, 14, 3, and 7 to phase  $C$  and the last five phasors 11, 15, 4, 8, and 12 to phase  $B$ . The *resultant* phasor of phase  $C$  is shifted  $60^\circ$  from the resultant phasor of phase  $A$  and the resultant phasor of phase  $B$  is shifted  $120^\circ$  from the resultant phasor of phase  $A$ . Reversing the connections of phase  $C$ , the three resultant phasors are shifted  $120^\circ$  and  $240^\circ$  from each other. Since they are also equal in magnitude, the winding is perfectly balanced: the emf's (and mmf's) of this winding will make a symmetrical 3-phase (polyphase) system.

Consider now a 3-phase, 6-pole winding in 24 slots:

$$q = \frac{24}{3 \times 6} = \frac{4}{3} \quad \beta = 3 \quad N = 4$$



Applying Eq. (55-7)

$$d = \frac{3 \times 4 \times P + 1}{3} = \frac{12P + 1}{3}$$

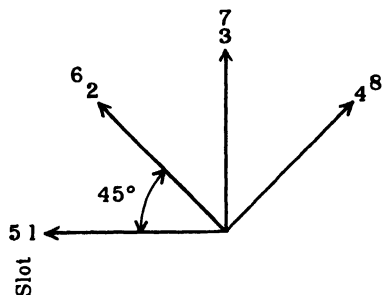


FIG. 55-3. Slot star of a 3-phase, 6-pole winding with  $1 \frac{1}{3}$  slots per pole per phase.

where  $P$  is the smallest integer which makes  $d$  an integer, it is seen that there is no integral value for  $P$  which can make  $d$  an integer.  $\alpha_s$  of this winding is  $45^\circ$ ; its slot star is shown in Fig. 55-3. The sequence of the phasors in the slot star is the same as the sequence of the slots in the machine, i.e., the winding does not creep in the magnetic field. It is not balanced. The same with respect to  $d$  and to the slot star will be observed

for all other windings in which the denominator of  $q$ ,  $\beta$ , is divisible by the number of phases,  $m$ .

$$(\beta/m) \neq \text{integer} \quad (55-9)$$

is a condition for balance of a fractional-slot winding. Another condition for balance is

$$(p/\beta) = \text{integer} \quad (55-10)$$

i.e., the winding must have an integral number of basic units.

**55-6. Beginnings of phases.** Consider Fig. 55-2 which represents the slot star of a 3-phase winding with  $q = 1\frac{1}{4}$ . The first  $N = 5$  slots (phasors) of the slot star are assigned to phase  $A$ , the following five slots (phasors) to phase  $C$ , and the last five slots (phasors) to phase  $B$ . Since the sequence of geometric addition of several phasors is of no influence on the resultant phasor, *any of the five slots of a phase can be taken as the beginning of the phase*. However, care must be taken that no phase is reversed, i.e., the beginnings of the phases must lie *approximately*  $120^\circ$  and  $240^\circ$  apart and not approximately  $60^\circ$  and  $120^\circ$  apart. So the beginnings of the phases can be placed in the slots 1, 4, and 6, each of which belongs to a different phase. The angle between two slots is (Eq. (55-2))

$$\alpha_s = \frac{180 \times 4}{3 \times 5} = 48^\circ$$

and thus the angles between the beginnings of the three phases are  $(4 - 1) \times 48 = 144^\circ$  and  $(6 - 1) \times 48 = 240^\circ$ . In the 3-phase winding with  $q = 1\frac{2}{3}$ , the beginnings of the phases can be placed in the slots 1, 5, and 8, which are  $150^\circ$  and  $262.5^\circ$  apart. These windings are balanced, i.e., their three emf's

and mmf's are equal and the angles between them are  $120^\circ$  and  $240^\circ$  despite the fact that the angles between the beginnings of the phases are not equal to  $120^\circ$  and  $240^\circ$ .

In 2-phase windings, the beginnings of the phases must lie approximately  $90^\circ$  apart, i.e., the beginnings of any two consecutive pole-phase groups can be chosen as phase beginnings.

### **55-7. Layout of a fractional-slot winding with respect to harmonics.**

As has been pointed out in the previous articles, the method of laying out a fractional-slot winding treated there refers to the main wave, i.e., it aims at the maximum distribution factor of this wave. Once the winding is laid out in this manner, the distribution factors of the harmonics are fixed. With respect to magnetic noise or telephone interference, it may be desirable in some cases to reduce the distribution factor of a certain harmonic. This can be done, at the expense of the distribution factor of the main wave, by a *cyclic shift* of slots from one phase to another. For example, if in the slot star Fig. 55-2 slot 5 of phase *A* is shifted to the place of slot 10 of phase *C*, slot 10 of phase *C* is shifted to the place of slot 15 of phase *B*, and slot 15 of phase *B* is shifted to the place of slot 5 of phase *A*, this cyclic shift will not only reduce the distribution factors of some harmonics but also that of the main wave (see Ref. I6).

## Chapter 56

### HARMONIC MMF's AND FLUXES OF THE INDUCTION MOTOR

**56-1. Stator windings with an integral number of slots per pole per phase ( $q = \text{integer}$ ).** It has been shown in Art. 24-1 (Eq. (24-2)) that the  $\nu$ -th harmonic mmf of a single stator phase is

$$f_{sv} = F_{sv} \sin \omega t \cos \nu \frac{x_1}{\tau} \pi \quad (56-1)$$

The subscript  $s$  indicates that the quantity refers to a single phase and the subscript 1 indicates that the primary part of the machine is considered.  $\nu = 1$  is the fundamental of the Fourier series and also the main (synchronous) mmf wave. The length of the main wave is  $2\tau$ , and the length of the  $\nu$ -th harmonic  $2\tau/\nu$ .  $f_{sv}$  is a standing wave, or alternating wave.

The amplitude  $F_{sv}$  of the fundamental wave ( $\nu = 1$ ) is given by Eq. (15-10)

$$F_{s(\nu=1)} = 1.8 \frac{N_1 k_{d\phi 1(\nu=1)}}{p} I_1 \quad (56-2)$$

Eq. (56-1) refers to a definite phase which will be called phase zero. Considering the phase adjacent to this zero phase (phase 1), the time angle between the two phases will be the same for all harmonics, namely,  $2\pi/m_1$ : this is the time angle between the currents of two adjacent phases of an  $m_1$  phase system. It is necessary to keep in mind that the harmonics in consideration are *space harmonics* and that in each phase all space harmonics are produced by the same current.

The space angle between two adjacent phases of the winding is equal to  $2\pi/m_1$  for the fundamental wave, and therefore to  $\nu(2\pi/m_1)$  for the  $\nu$ -th harmonic, since the wave length of the  $\nu$ -th harmonic is  $1/\nu$  times the wave length of the fundamental. Thus the mmf of the  $\nu$ -th-harmonic of the neighboring phase is

$$f_{sv1} = F_{sv} \sin [\omega t - (2\pi/m_1)] \cos [\nu (x_1/\tau) \pi - \nu (2\pi/m_1)], \quad (56-3)$$

and the mmf of the  $\nu$ -th harmonic of the  $c$ -th phase

$$f_{svc} = F_{sv} \sin [\omega t - c (2\pi/m_1)] \cos [\nu (x_1/\tau) \pi - \nu (2\pi/m_1)] \quad (56-4)$$

Introducing the relation  $\sin \alpha \cos \beta = \frac{1}{2} [\sin (\alpha - \beta) + \sin (\alpha + \beta)]$ ,

$$f_{\nu c} = \frac{1}{2} F_{\nu} \sin [\{\omega t - \nu (x_1/\tau)\} + (\nu - 1) c (2\pi/m_1)] \\ + \sin [\{\omega t + \nu (x_1/\tau) \pi\} - (\nu + 1) c (2\pi/m_1)] \quad (56-5)$$

The first right-hand term of this equation yields for negative  $\nu$  the value of the second term. Therefore, if  $\nu$  is assumed to be positive as well as negative, the second term can be omitted and the resultant mmf of the  $\nu$ -th harmonic for all  $m_1$  phases is

$$f_{\nu} = \frac{1}{2} F_{\nu} \left[ \sin \{\omega t - \nu (x_1/\tau) \pi\} \sum_{c=0}^{c=m_1-1} \cos (\nu - 1) c (2\pi/m_1) \right. \\ \left. + \cos \{\omega t - \nu (x_1/\tau) \pi\} \sum_{c=0}^{c=m_1-1} \sin (\nu - 1) c (2\pi/m_1) \right] \quad (56-6)$$

Since  $\nu$  is an integer, the sums of Eq. (56-6) become zero, except when

$$(\nu - 1)(2\pi/m_1) = k_1 \times 2\pi$$

or

$$\nu = k_1 m_1 + 1 \quad (56-7)$$

where  $k_1$  is any positive or negative integer including 0. Eq. (56-7) is the *criterion for the existence of the  $\nu$ -th harmonic*. Consider, as an example, a 3-phase winding ( $m_1 = 3$ ). Eq. (56-7) yields the harmonics

$$\begin{array}{cccccccc} k_1 = 0 & k_1 = -1 & k_1 = +1 & k_1 = -2 & k_1 = +2 & k_1 = -3 & k_1 = +3 & \dots \\ \nu = +1 & -2 & +4 & -5 & +7 & -8 & +10 & \dots \end{array}$$

The harmonics of the order 3 or a multiple of 3 do not appear, as could be expected (see Eq. (24-8)).

The *sign of  $\nu$  indicates the direction of rotation of the harmonic*. The harmonics with positive sign travel with the main (fundamental) wave, and those with negative sign travel in the opposite direction.

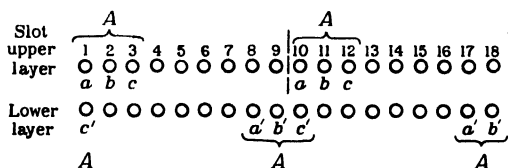


FIG. 56-1. 2-pole, 3-phase winding with two slots per pole per phase.

Eq. (56-7) yields odd and even harmonics, as demonstrated by the example. A full pitch, i.e., a non-chorded winding produces only odd harmonics (see Art. 24-1). The fractional pitch winding produces odd and even harmonics. However, the most commonly used fractional-pitch winding (2-layer, 6-zone,

60° phase-belt) does not produce even harmonics, because it can be made up of full pitch coils. Fig. 56-1 shows a 2-pole, 3-phase winding with  $q=3$ . The coil width ( $W$ ) is 7 slot pitches ( $W/\tau=7/9$ ). The top layer of phase  $A$  lies in slots 1, 2, 3 and 10, 11, 12; its bottom layer lies in slots 8, 9, 10 and 17, 18, 1.  $a$  and  $a'$  represent one coil,  $b$  and  $b'$  the next coil, etc. From Fig. 56-1 it is evident that the winding could be arranged differently, i.e., in the top layer  $a$  connected to  $a$ ,  $b$  to  $b$ , and  $c$  to  $c$ , in the bottom layer  $a'$  to  $a'$ ,  $b$  to  $b'$ ,  $c'$  to  $c'$ , and then both layers connected in series. This type of winding is not practical for larger machines but is used in small machines. It consists of full pitch coils and consequently does not develop even harmonics. Contrary to the 2-layer, 6-zone winding, the 2-layer, 3-zone which is used in 2-speed (or multi-speed) motors develops even harmonics when chorded.

There are among the harmonics those which have the same distribution and pitch factor as the main wave ( $\nu=1$ ). These harmonics, called *slot harmonics*, have the orders

$$\nu_{s1} = \mp c \frac{Q_1}{(p/2)} + 1 \quad c = 1, \quad 2, \quad 3 \dots \quad (56-8)$$

$c=1$  yields the slot harmonics of first order,  $c=2$  yields the slot harmonics of second order, and so forth.

Denoting in Eq. (56-6) the  $\sum \cos$  by  $a$  and the  $\sum \sin$  by  $b$ , then

$$f_\nu = \frac{1}{2} F_{s\nu} \sqrt{a^2 + b^2} \sin [\omega t - \nu (x_1/\tau) \pi + \gamma_\nu] \quad (56-9)$$

$$\gamma_\nu = \tan^{-1} (b/a)$$

For the values of  $\nu$  which satisfy Eq. (56-7), the quantity  $\sqrt{a^2 + b^2}$  becomes equal to  $m_1$  and  $\gamma_\nu$  becomes equal to 0, so that Eq. (56-9) represents a traveling mmf wave with the amplitude of the fundamental (see Eq. (56-2))

$$F_{(\nu=1)} = 0.9m_1 \frac{N_1 k_{d\pi 1(\nu=1)}}{p} I_1 \quad (56-10)$$

This is in accordance with Eq. (15-11). From Eq. (24-13), the amplitude of the  $\nu$ -th harmonic mmf

$$F_\nu = 0.9m_1 \frac{1}{\nu} \frac{N_1 k_{d\pi 1\nu}}{p} I_1 \quad (56-11)$$

To the sinusoidal mmf

$$f_\nu = F_\nu \sin [\omega t - \nu (x_1/\tau) \pi] \quad (56-12)$$

corresponds a sinusoidal flux distribution

$$b_\nu = B_\nu \sin [\omega t - \nu (x_1/\tau) \pi] \quad (56-13)$$

the amplitude of which is obtained from Eq. (56-11) and Ohm's law of the magnetic circuit as

$$B_v = 0.4\pi F_v \frac{1}{gk_c k_s} \frac{2.54^2}{2.54} = 0.9m_1 \frac{1}{\nu} \frac{N_1 k_{d21\nu}}{p} \frac{3.19}{gk_c k_s} I_1 \quad \text{lines/sq.in.} \quad (56-14)$$

The saturation factor  $k_s$  (see Art. 53-1) can be assumed equal to 1 for the harmonics.  $g$  is measured in inches.

The velocity of propagation of the  $\nu$ -th mmf harmonic and the corresponding  $b_v$ -th harmonic with respect to the stator can be found by the consideration applied in Arts. 15-2 (Eq. (15-4)) and 24-1

$$v_{1\nu} = \frac{dx_1}{dt} = \frac{\omega}{\pi} \tau \frac{1}{\nu} = v_{1(\nu=1)} \times \frac{1}{\nu} \quad (56-15)$$

where

$$v_{1(\nu=1)} = (\omega/\pi) \tau = 2\tau f_1 \quad (56-16)$$

is the velocity of propagation of the main wave with respect to the stator.  $2\tau$  is the length of the main wave  $\nu = 1$ .  $2\tau/\nu$  is the wave length of the  $\nu$ -th harmonic.  $f_1$  is the number of cycles per second of the primary current. It is seen that each harmonic travels with respect to the stator *its own wave length* during *one cycle* of the current. The reduction factor from the velocity of propagation to rpm is  $60/p\tau$  (see Eq. (15-5)).

**56-2. Rotor windings.** According to the definition of the slip of the rotor with respect to the main wave

$$s = \frac{n_s - n}{n_s} \quad (56-17)$$

with 
$$n_s = \frac{120f_1}{p} \quad (56-18)$$

the slip of the rotor with respect to the  $\nu$ -th harmonic is

$$s_\nu = \frac{n_{s\nu} - n}{n_{s\nu}} = \frac{n_{s/\nu} - n}{n_{s/\nu}} = 1 - \nu(1 - s) \quad (56-19)$$

This equation gives a relation between the slip of the rotor with respect to the main wave and the slip of the rotor with respect to the  $\nu$ -th harmonic.

The frequency of the rotor currents produced by the main wave is (see Eq. (17-21))  $f_2 = sf_1$ . Likewise, the frequency of the rotor currents produced by the  $\nu$ -th stator harmonic is

$$f_{2\nu} = s_\nu f_1 \quad (56-20)$$

For example, the frequency of the rotor currents due to the 5th stator harmonic ( $\nu = -5$ ) at  $s = 0.01$  is  $(1 + 5 \times 0.99)60 = 357$  c/s.

Thus, in general, the  $\nu$ -th stator harmonic induces in the rotor the current

$$i_{2\nu} = \sqrt{2} I_{2\nu} \sin s_\nu \omega t \quad (56-21)$$

with  $\omega = 2\pi f_1$ . This current produces a rotor mmf which contains a series of

harmonics. Consider the  $\mu$ -th of these harmonics. Its mmf is (see Eq. (56-1))

$$f_{s\mu} = F_{s\mu} \sin s_v \omega t \cos \mu (x_2/\tau) \pi \quad (56-22)$$

$x_2$  is a coordinate fixed to the rotor.

(a) *Wound rotor.* The amplitude  $F_{s\mu}$  of one phase of a wound rotor with  $N_2$  turns per phase is (see Eq. (56-2))

$$F_{s\mu} = 1.8 \frac{1}{\mu} \frac{N_2 k_{d\mu} I_{2\mu}}{p} \quad (56-23)$$

If the mmf of the zero phase is represented by Eq. (56-22) the mmf of the neighboring phase will be obtained by inserting in Eq. (56-22) its time and phase angle. *The time angle is determined by the  $\nu$ -th harmonic of the stator which produces the harmonic in consideration and is  $\nu(2\pi/m_2)$ . The space angle is  $\mu(2\pi/m_2)$ , similar to that of the stator. Therefore, the mmf of the  $\mu$ -th harmonic of the  $c$ -th phase is*

$$f_{s\mu c} = F_{s\mu} \sin [s_v \omega t - \nu (2\pi/m_2)c] \cos [\mu(x_2/\tau) \pi - \mu (2\pi/m_2) c] \quad (56-24)$$

or

$$\begin{aligned} f_{s\mu c} = \frac{1}{2} F_{s\mu} \left[ \sin \left\{ \left( s_v \omega t - \mu \frac{x_2}{\tau} \pi \right) + (\mu - \nu) \frac{2\pi}{m_2} c \right\} \right. \\ \left. + \sin \left\{ \left( s_v \omega t + \mu \frac{x_2}{\tau} \pi \right) - (\mu + \nu) \frac{2\pi}{m_2} c \right\} \right] \quad (56-25) \end{aligned}$$

Introducing for  $\mu$  positive as well as negative values, as before for Eq. (56-5), the second term of Eq. (56-25) can be omitted. Furthermore, applying the same considerations as before in order to determine the resultant mmf of the  $\mu$ -th harmonic for all  $m_2$  phases, it is found that the *criterion for the existence of the  $\mu$ -th harmonic is*

$$(\mu - \nu) \frac{2\pi}{m_2} = k_2 \times 2\pi$$

or

$$\mu = k_2 m_2 + \nu \quad (56-26)$$

where  $k_2$  is any positive or negative integer including 0 (compare Eq. (56-26) with Eq. (56-7)). For the 3-phase, 2-layer,  $60^\circ$  phase-belt winding,  $k_2$  is any positive or negative *even* integer including 0. Notice that the harmonic  $\nu$  has to be introduced in Eq. (56-26) with the right sign, i.e., *the harmonics which travel opposite to the fundamental  $\nu=1$  have to be introduced with a negative sign.*

The amplitude of the resultant  $\mu$ -th harmonic is obtained as (see Eq. (56-11))

$$F_\mu = 0.9 m_2 \frac{1}{\mu} \frac{N_2 k_{d\mu} I_{2\mu}}{p} \quad (56-27)$$

and the resultant  $\mu$ -th harmonic is (see Eq. (56-12))

$$f_\mu = F_\mu \sin [s_r \omega t - \mu (x_2/\tau) \pi] \quad (56-28)$$

The corresponding flux distribution is (see Eq. (56-13))

$$b_\mu = B_\mu \sin [s_r \omega t - \mu (x_2/\tau) \pi] \quad (56-29)$$

with the amplitude (see Eq. (56-14))

$$B_\mu = 0.9 m_2 \frac{1}{\mu} \frac{N_2 k_{d\mu} 3.19}{p g k_c k_s} I_{2r} \quad (56-30)$$

As will be seen later, it is important to know the velocity of propagation of the wave  $f_\mu$  (or  $b_\mu$ ) with respect to the stator.  $x_1$  is a co-ordinate fixed to the stator;  $x_2$  is a co-ordinate fixed to the rotor. It will be assumed that, at  $t=0$  the origins of the co-ordinates  $x_1$  and  $x_2$  coincide (Fig. 56-2), i.e.,  $x_2 = x_1$ . Since the rotor has the speed (in rpm)

$$n = (1-s)n_s$$

or the peripheral speed (in in/s)

$$v_r = (1-s)(n_s/60) p \tau = (1-s) 2\pi f_1 = (1-s)(\tau/\pi) \omega \quad (56-31)$$

at any instant of time  $t \neq 0$

$$x_2 = x_1 - v_r t = x_1 - (1-s)(\tau/\pi) \omega t \quad (56-32)$$

Inserting this equation and Eq. (56-19) into Eq. (56-29), there results

$$b_\mu = B_\mu \sin \{ [1 + (\mu - \nu)(1-s)] \omega t - \mu (x_1/\tau) \pi \} \quad (56-33)$$

$b_\mu$  is now expressed as a function of  $t$  and the stator co-ordinate  $x_1$ . Differentiating the quantity in [ ] brackets, the velocity of propagation of the  $\mu$ -th harmonic with respect to the stator is

$$v_{1\mu} = \frac{dx_1}{dt} = [1 + (\mu - \nu)(1-s)] \frac{1}{\mu} \frac{\tau}{\pi} \omega \quad (56-34)$$

Since  $(\tau/\pi)\omega$  is the velocity of propagation of the main stator wave ( $\nu=1$ ) with respect to the stator,  $v_{1\nu}$ , (Eq. (56-16))

$$v_{1\mu} = [1 + (\mu - \nu)(1-s)] (1/\mu) v_{1(\nu=1)} \quad (56-35)$$

(b) *Squirrel-cage rotor.* Eq. 56-26 (just as Eq. 56-7) was obtained by the summation of the mmf's of the phases lying within  $2\pi$  radians. For the squirrel-cage rotor, this corresponds to the number of bars in a pole pair:

$$\text{Bars/pole pair} = Q_s / \frac{1}{2} p \quad (56-36)$$

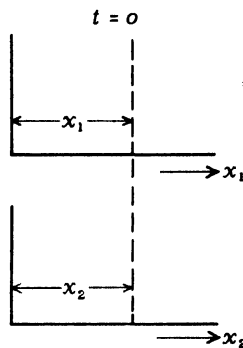


FIG. 56-2. Relative position of the origins of the coordinates  $x_1$  and  $x_2$  at  $t=0$ .



and, therefore, the criterion for the existence of the  $\mu$ -th harmonic for the squirrel-cage rotor (Eq. (56-26)) is

$$\mu = k_2(Q_2/\frac{1}{2}p) + \nu \quad (56-37)$$

As in Eq. (56-26),  $\nu$  has to be introduced with the right sign into Eq. (56-37). For the squirrel-cage rotor,

$$m_2 = Q_2, \quad N_2 = \frac{1}{2}, \quad k_{ap\mu} = 1 \quad (56-38)$$

must be introduced into Eqs. (56-27) and (56-30).  $I_{\omega}$  is then the current per rotor bar. If the rotor is skewed, the latter two equations must be multiplied by the skew factor (see Art. 56-6).

The slot-harmonics of the rotor, both wound and squirrel-cage, are given by the equation (see Eq. (56-8))

$$\mu_{s1} = \pm c(Q_2/\frac{1}{2}p) + 1 \quad c = 1, 2, 3, \dots \quad (56-39)$$

As an example, a 4-pole squirrel-cage motor with  $Q_2 = 57$  will be assumed, although an odd number of slots in the rotor is usually avoided because of the noise that it may cause (see Art. 59-2). Eq. (56-39) yields for  $c = 1$  (slot harmonics of first order)

$$\mu_{s1} = -27.5 \quad \text{and} \quad +28.5$$

These are harmonics of fractional order. Harmonics of fractional order appear also in the fractional slot windings (see Art. 56-4). This is inconvenient and can be avoided by introducing another fundamental as shown in the following article.

**56-3. Introduction of a fundamental with the wave length equal to  $p\tau = \pi D$ .** In the previous articles of this chapter, the main (synchronous) wave is the fundamental wave. Its order is  $\nu = 1$  and its wave length is  $2\tau = \pi D/(\frac{1}{2}p)$ . As we have seen at the end of the last article, this may lead to harmonics of fractional order. In order to avoid such harmonic orders, it is expedient to introduce a *new fundamental*, namely one the *wave length* of which is *equal to the circumference of the armature*  $\pi D = p\tau$ , and to refer the actual harmonics to this fundamental. With this fundamental the main wave itself becomes a harmonic the order of which is equal to

$$\frac{\text{wave length of the new fundamental} = p\tau}{\text{wave length of the main wave} = 2\tau} = \frac{1}{2}p \quad (56-40)$$

Since the wave length of the new fundamental is  $p\tau$ , it is a 2-pole wave. Consider, as an example, a 6-pole motor. The main wave has three pole pairs around the armature circumference, while the new fundamental has only one pole pair around the armature (Fig. 56-3), and the main wave appears as a harmonic of the 3rd ( $=p/2=6/2$ ) order. The harmonic  $\nu = 7$  which has seven times the number of pole pairs of the main wave will appear in Fig. (56-3) as a harmonic of the order  $21 (=3 \times 7)$ .

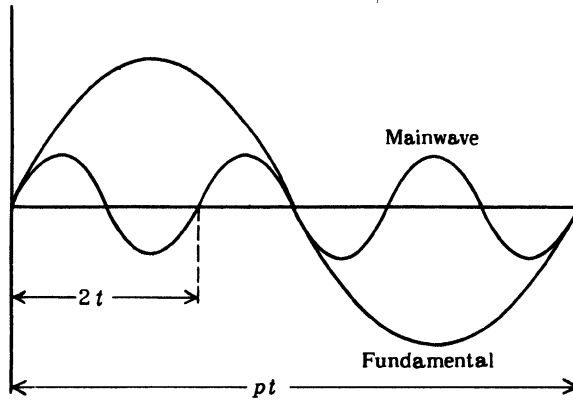


FIG. 56-3. Explanation of a fundamental wave with a wave length  $p\tau$ .

The orders of the harmonics with respect to the new 2-pole fundamental wave will be indicated by a primed symbol. Thus

$$\nu' = (p/2)\nu \quad \mu' = (p/2)\mu \quad (56-41)$$

In order to introduce the new orders of the harmonics into the previous equations,  $\nu'/(1/2)p$  simply has to be substituted for  $\nu$  and  $\mu'/(1/2)p$  for  $\mu$  (Eq. 56-41). The equations for the orders of the harmonics, for the harmonic flux distributions, and for the velocities of propagation of the harmonics become then as follows:

(a) *Stator*

$$\nu' = (k_1 m_1 + 1)p/2 \quad (56-42)$$

$$\nu_{s1}' = \pm cQ_1 + p/2 \quad c = 1, 2, 3 \dots \quad (56-43)$$

$$b_{\nu}' = B_{\nu}' \sin [\omega t - (\nu'/\frac{1}{2}p)(x_1/\tau) \pi] \quad (56-44)$$

$$B_{\nu}' = 0.45 m_1 \frac{1}{\nu'} N_1 k_{d p 1 \nu'} \frac{3.19}{g k_c k_s} I_1 \text{ lines/sq.in.} \quad (56-45)$$

$$v_{1\nu'} = v_{1(\nu'=1p)} (p/2\nu') \quad (56-46)$$

$$v_{1(\nu'=1p)} = (\omega/\pi) \tau = 2\tau f_1 \quad (56-47)$$

(b) *Rotor*

$$s_{\nu'} = 1 - (\nu'/\frac{1}{2}p) (1 - s) \quad (56-48)$$

$$f_{2\nu'} = s_{\nu'} f_1 \quad (56-49)$$

$$\mu' = k_2 m_2 (p/2) + \nu' \quad \text{wound rotor} \quad (56-50)$$

$$\mu' = k_2 Q_2 + \nu' \quad \text{squirrel-cage rotor} \quad (56-51)$$

$$\mu_{s1}' = \pm cQ_2 + (p/2) \quad c = 1, 2, 3 \dots \quad (56-52)$$

$$b_{\mu'} = B_{\mu'} \sin [s_{\nu'} \omega t - (\mu'/\frac{1}{2}p) (x_2/\tau) \pi] \quad (56-53)$$

$$B_{\mu'} = 0.45 m_2 \frac{1}{\mu'} N_2 k_{d_{p2\mu'}} \frac{3.19}{g k_c k_s} I_{2\nu'} \quad \text{wound rotor} \quad (56-54)$$

$$B_{\mu'} = 0.45 \frac{Q_2}{2} \frac{1}{\mu'} \frac{3.19}{g k_c k_s} I_{2\nu'} \quad \text{squirrel-cage rotor} \quad (56-55)$$

$I_{2\nu'}$  is the current per bar.

$$v_{1\mu'} = [1 + \{(\mu' - \nu')/\frac{1}{2}p\} (1 - s)] (\frac{1}{2}p/\mu') v_{1(\nu'=\frac{1}{2}p)} \quad (56-56)$$

The equations which are not referred to a specific rotor type apply to both rotor types.

It follows from Eqs. (56-50) and (56-51)

$$\begin{aligned} \mu' - \nu' &= k_2 m_2 p/2 && \text{wound rotor} \\ \mu' - \nu' &= k_2 Q_2 && \text{squirrel-cage rotor} \end{aligned} \quad (56-57)$$

Inserting these equations into Eq. (56-56)

$$v_{i\mu'} = (\frac{1}{2}p/\mu') [1 + k_2 m_2 (1 - s)] v_{1(\nu'=\frac{1}{2}p)} \quad \text{wound rotor} \quad (56-58)$$

$$v_{1\mu'} = (\frac{1}{2}p/\mu') [1 + k_2 (Q_2/\frac{1}{2}p) (1 - s)] v_{1(\nu'=\frac{1}{2}p)} \quad \text{squirrel-cage rotor} \quad (56-59)$$

As before (see Eq. (56-16) or Eq. (56-47))

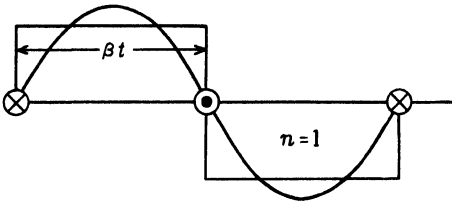
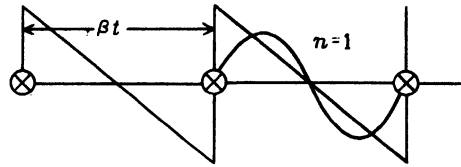
$$v_{1(\nu'=\frac{1}{2}p)} = (\omega/\pi) \tau = 2\tau f_1$$

is the speed of the main wave ( $\nu' = p/2$ ) with respect to the stator (subscript 1).

The introduction of a new fundamental with two poles was motivated by the desire to avoid harmonics of fractional order. In integral-slot windings a 2-pole wave is realized only in 2-pole machines; for other numbers of poles, the fundamental 2-pole wave is a fictitious one. It will be shown in the next article that, in fractional-slot windings, a 2-pole wave may exist also in a multi-pole machine. In such a case, it is reasonable to use the 2-pole wave as the fundamental. Furthermore, in the investigation of the magnetic noise produced by the harmonic fluxes, it is necessary to use a 2-pole wave as the fundamental.

**56-4. Balanced fractional slot-stator windings.** In the fractional-slot windings,  $\beta$  poles make the basic unit of the winding, where  $\beta$  is the denominator of the fraction  $q = (N/\beta)$  (see Art. 55-1).

(a)  $\beta = \text{odd number}$ . In this case the simplified shape of the mmf curve is given by Fig. 56-4. This figure compares with Fig. 55-3 which relates to the integral-slot winding, yet with the important difference that the wave length here is  $2\beta\tau$  while it is  $2\tau$  in Fig. 55-3. Applying the Fourier series to Fig.

FIG. 56-4. The mmf curve of a fractional slot winding with  $\beta$ =an odd number.FIG. 56-5. The mmf curve of a fractional slot winding with  $\beta$ =an even number.

56-4, only odd harmonics are obtained. Denoting the order of these harmonics by  $n$

$$n = 1 \quad 3 \quad 5 \quad 7 \quad 9 \quad 11 \quad \dots \quad (56-60)$$

$n = 1$  has the wave length  $2\beta\tau$ . The wave length of a harmonic of higher order ( $n > 1$ ) is inversely proportional to the order of the harmonic.

A 2-pole wave has been fixed as the fundamental ( $\nu' = 1$ ) for harmonic waves. In order to refer the  $n$ -series (Eq. (56-60)) to the  $\nu'$ -series, the  $n$ -series must be multiplied by the ratio of the wave length of the fundamental of the  $\nu'$ -series,  $p\tau$ , to the wave length of the fundamental of the  $n$ -series,  $2\beta\tau$  (see Eq. (56-40)). This ratio is  $p/2\beta$ , therefore for  $\beta$ =odd number

$$\nu' = (p/2\beta) n \quad n = 1 \quad 3 \quad 5 \quad 7 \quad 9 \quad 11 \quad \dots \quad (56-61)$$

**Example:**  $Q_1 = 48$ ,  $p = 10$ ,  $m_1 = 3$ .

$$q = \frac{48}{3 \times 10} = \frac{8}{5} \quad \beta = 5 = \text{odd number}$$

$$\nu' = (10/10) n = 1 \quad 3 \quad \underline{5} \quad 7 \quad 9 \quad \dots$$

The main wave has the order  $\nu' = p/2 = 5$  and is underlined. It is seen that the winding under consideration develops in addition to the harmonics of higher order than the main wave harmonics of lower order than the main wave (sub-harmonics). The sub-harmonic of the order  $\nu' = 1$  has two poles. At a line current of 60 cycles, it rotates at 3600 rpm, while the main wave rotates at 720 rpm.

(b)  $\beta$ =even number. In this case the simplified shape of the mmf-curve is given by Fig. 56-5. Since  $\beta$  is even here, a cross follows a cross, while in Fig. 56-4 a cross is followed by a dot. Applying the Fourier series to Fig. 56-4, there follows:

$$n = 1 \quad 2 \quad 3 \quad 4 \quad 5 \quad 6 \quad 7 \quad \dots \quad (56-62)$$

Contrary to the case  $\beta$ =odd number, the windings with  $\beta$ =even number develop odd and even harmonics.  $n = 1$  of the series has the wave length  $\beta\tau$ . Multiplying the  $n$ -series by the ratio  $p\tau/\beta\tau = p/\beta$ , the harmonics developed by the fractional-slot winding with  $\beta$ =even number becomes

$$\nu' = (p/\beta)n \quad n = 1 \quad 2 \quad 3 \quad 4 \quad 5 \quad 6 \quad 7 \quad \dots \quad (56-63)$$

**Example:**  $Q_1 = 30$ ,  $p = 8$ ,  $m_1 = 3$ .

$$q = \frac{30}{3 \times 8} = \frac{5}{4} \quad \beta = 4 = \text{even number}$$

$$\nu' = (8/4)n = 2 \quad 4 \quad 6 \quad 8 \quad 10 \quad 12 \quad \dots$$

The main wave has the order  $\nu' = p/2 = 4$ . Also this winding develops a sub-harmonic (with four poles).

The sub-harmonics travel with high speed and are normally damped by eddy currents which they produce on the iron surface.

It should be noted that Eqs. (56-43) to (56-47) for  $\nu_{s1}'$ ,  $b_{\nu'}$ ,  $B_{\nu'}$ ,  $v_{1\nu'}$ , and  $v_{1(\nu'=\frac{1}{2}p)}$  derived for the integral-slot windings also apply to the fractional-slot windings.

Notice that in the  $n$ -series of Eqs. (56-60) and (56-62) harmonics of the order  $n = 3$  or  $n = \text{a multiple of } 3$  do not exist in 3-phase windings, except when zero-sequence currents flow in the winding.

In order to determine the sign, i.e., the direction of rotation of the  $\nu'$ -th harmonic, assign to the main wave the plus sign and alternate the signs of the preceding and following harmonics. The signs of the harmonics in the two examples considered are then

$$q = 8/5 \quad \nu' = -1 \quad +\underline{5} \quad -7 \quad +11 \quad -13 \quad +17 \quad -19 \quad \dots$$

$$q = 5/4 \quad \nu' = -2 \quad +\underline{4} \quad -8 \quad +10 \quad -14 \quad +16 \quad -20 \quad \dots$$

In general, for 3-phase windings, the harmonics  $\nu'$  which correspond to the values of

$$n = 1 + 3C = 1 \quad 4 \quad 7 \quad 10 \quad 13 \quad 16 \quad 19 \quad \dots \quad (56-64)$$

( $C = \text{positive integer} = 0, 1, 2, 3 \dots$ ) have the same signs. The harmonics  $\nu'$  which correspond to the values of

$$n = (2 + 3C) = 2 \quad 5 \quad 8 \quad 11 \quad 14 \quad 17 \quad 20 \quad \dots \quad (56-65)$$

also have the same sign but opposite to that of the previous series. When  $\beta = \text{odd number}$ , the even values of Eqs. (56-64) and (56-65) do not exist.

If a plus sign is assigned to the main wave, a harmonic  $\nu'$  with a minus sign rotates in opposite direction to the main wave and a harmonic with a plus sign rotates in the same direction as the main wave.

**56-5. The distribution and pitch factors.** (a) *Integral slot windings.* For these windings the distribution factor of the  $\nu'$ -th harmonic is given by Eq. (24-11)

$$k_{d\nu'} = \frac{\sin \frac{\nu'}{p/2} \times q \times \frac{\alpha_s}{2}}{q \sin \nu' \times \frac{p}{2} \times \frac{\alpha_s}{2}} \quad (56-66)$$

where  $\alpha_s = 180p/Q = 180/mq$ , and the pitch factor by Eq. (24-12)

$$k_{p\nu'} = \sin(\nu'/\frac{1}{2}p)(W/\tau)(\pi/2) \quad (56-67)$$

This applies to stator as well as rotor integral-slot windings. (Literature on harmonics, see Ref. A7 and papers under J.)

(b) *Balanced fractional-slot windings.* (Ref. I5.) The magnetic field angle (Eq. (55-3))

$$\alpha_m = \frac{180}{mN} \quad (56-68)$$

is of importance here. The distribution factor of the main wave ( $\nu' = p/2$ ) is (Ref. I5)

$$k_{d(\nu'=\frac{1}{2}p)} = \frac{\sin N\alpha_m/2}{N \sin \alpha_m/2} \quad (56-69)$$

This can be seen directly from the slot star of the main wave (Fig. 55-2). Since  $N$  is normally larger than 4,  $k_{d(\nu'=\frac{1}{2}p)} = 0.9555$ .

The distribution factors of the harmonics depend upon  $\beta$  and  $P$  (see Eq. 55-7) i.e., whether these quantities are odd or even (Ref. I5). For 3-phase windings:

$$k_{d\nu'} = \frac{0.5}{N \cos [(d/N) 60^\circ n]} \quad \beta = \text{even number} \quad (56-70)$$

$$k_{d\nu'} = \frac{0.5}{N \sin [(d/N) 30^\circ n]} \quad \begin{array}{l} \beta = \text{odd number} \\ p = \text{even number} \end{array} \quad (56-71)$$

$$k_{d\nu'} = \frac{0.5}{N \cos [(d/N) 30^\circ n]} \quad \begin{array}{l} \beta = \text{odd number} \\ p = \text{odd number} \end{array} \quad (56-72)$$

The value of  $d$  is given by Eq. (55-7).  $n$  is the value of Eq. (56-61) or Eq. (56-63) which corresponds to  $\nu'$ . Eqs. (56-70) to (56-72) yield only the absolute value of  $k_{d\nu'}$ , but not the sign. This suffices for the force computations made in the following chapters.

The pitch factor of the  $\nu'$ -th harmonic of a fractional-slot winding is given by the same equation as for the integral-slot winding, i.e., by Eq. (56-67).

(c) *Concentric windings with different numbers of turns in the coils, as used in the unsymmetrical 2-phase motor and in the single-phase motor (Chaps. 26 and 53).* The winding factor (= product of distribution and pitch factor) of the main wave is (see Fig. 56-6)

$$k_w = \frac{N_{c1} \sin \alpha_1 + N_{c2} \sin \alpha_2 + N_{c3} \sin \alpha_3 + \dots}{N_{c1} + N_{c2} + N_{c3} + \dots} \quad (56-73a)$$

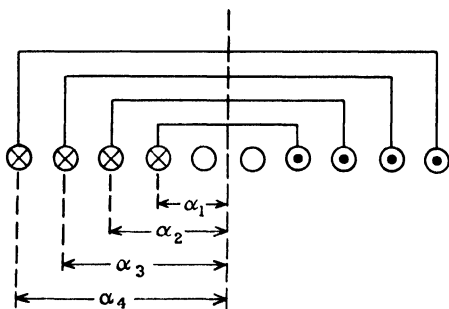


FIG. 56-6. Derivation of the winding factor of a concentric (single-phase) winding.

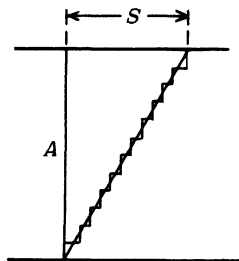


FIG. 56-7. Derivation of the skew factor.

**56-6. The skew factor.** Skewing of the rotor slots or stator slots is applied in order to reduce the magnitude of parasitic torques produced by harmonics. Skewing reduces the emf induced in the secondary winding. The skew factor is a distribution factor and has to be used in connection with the factor  $k_{ap\mu'}$  ( $k_{ap\mu'} \times K_{skv}$ ). Fig. 56-7 shows a straight bar ( $A$ ) and a skewed bar. The magnitude of the skew is  $S$  inches. The angle in radians which corresponds to  $S$  is

$$\gamma_s = \frac{S}{\tau_{2s}} \alpha_{2s} = \frac{S}{\tau_{2s}} \frac{p\pi}{Q_2} \quad (56-73b)$$

$\alpha_{2s}$  is the angle between two rotor slots. The skewed bar can be replaced by a large number ( $c$ ) of vertical and horizontal elements, as shown in Fig. 56-7. In order to determine the skew factor, the emf's  $E$  and  $E_{sk}$  induced in the straight and skewed bar, respectively, will be considered. Then

$$K_{sk} = \frac{E_{sk}}{E}$$

The horizontal elements of the skewed bar in Fig. 56-7 do not contribute to the induced emf and only the vertical elements are to be considered. The first element (that at the bottom of the figure) coincides with the straight bar and has the induced emf  $E/c$ . The next following vertical element has the induced emf  $(E/c)e^{j\beta}$ , where

$$\beta = \gamma_s / c \quad (56-74)$$

The third element has the induced emf  $(E/c)e^{j2\beta}$ , and so forth. Thus

$$E_{sk} = (E/c) (1 + e^{j\beta} + e^{j2\beta} + \dots + e^{j(c-1)\beta}) = \frac{E e^{jc\beta} - 1}{c e^{j\beta} - 1} = \frac{E \cos c\beta - 1 + j \sin c\beta}{c \cos \beta - 1 + j \sin \beta}$$

Taking the ratio of the absolute values

$$K_{sk} = E_{sk}/E = \frac{1}{c} \sqrt{\frac{(\cos c\beta - 1)^2 + \sin^2 c\beta}{(\cos \beta - 1)^2 + \sin^2 \beta}} = \frac{1 \sin c(\beta/2)}{c \sin (\beta/2)}$$

Limiting the numerator and denominator separately

$$K_{sk} = \lim_{\substack{c \rightarrow \infty \\ \beta \rightarrow 0}} \frac{\sin c(\beta/2)}{c \sin(\beta/2)} = \frac{\sin c(\beta/2)}{c(\beta/2)}$$

Inserting Eqs. (56-74) and (56-73)

$$K_{sk(\nu' = \frac{1}{2}p)} = \frac{\sin(S/\tau_{2s})(p\pi/Q_2)^{\frac{1}{2}}}{(S/\tau_{2s})(p\pi/Q_2)^{\frac{1}{2}}} \quad (56-75)$$

This value of  $K_{sk}$  apparently applies to the main wave ( $\nu' = p/2$ ), because only for this wave  $\pi$  radians correspond to a pole pitch (see Eq. (56-73a)). For the  $\mu'$ -th harmonic

$$K_{sk,\mu'} = \frac{\sin(\nu'/\frac{1}{2}p)(S/\tau_{2s})(p\pi/Q_2)^{\frac{1}{2}}}{(\nu'/\frac{1}{2}p)(S/\tau_{2s})(p\pi/Q_2)^{\frac{1}{2}}} = \frac{\sin \nu' [(S/\tau_{2s})(\pi/Q_2)]}{\nu' (S/\tau_{2s})(\pi/Q_2)} \quad (56-76)$$

The skew factor decreases with the increasing order of the harmonic. It is practically equal to 1 for the main waves ( $\nu' = p/2$ ).

It should be noted that  $S$  is the skew of the rotor slots with respect to the stator slots independent of whether rotor or stator is skewed. If the slots of both machine parts are skewed,  $S$  is the resultant skew.

**56-7. The rotor current  $I_{2\nu'}$ .** The current  $I_{2\nu'}$  in Eqs. (58-54) and (58-55) is the actual rotor current (not referred to the primary). The stator currents at which the parasitic torques and the magnetic noise occur are given. Therefore, it suffices to express  $I_{2\nu'}$  in terms of the primary current  $I_1$  and the parameters of the machine.

For the main wave,  $\nu' = p/2$ , the relation between rotor and stator current is determined by Kirchhoff's equation for the rotor, i.e., by Eqs. (18-2) and (18-3.) Apparently, the current  $I_{2\nu'}$  induced in the rotor by the  $\nu'$ -th stator harmonic will have to be determined from Kirchhoff's equation for the rotor, set up for this harmonic. In Chaps. 17 and 18, the secondary quantities are referred to the primary. In order to get the actual value of the rotor current,  $I_{2\nu'}$ , the *primary quantities will be referred to the secondary*.

The amplitude of the mmf of the  $\nu'$ -th stator harmonic is (see Eqs. (56-11) and (56-41))

$$F_{\nu'} = 0.45m_1 (1/\nu') N_1 k_{d p 1 \nu'} I_1$$

Expressed in terms of the secondary winding, this mmf is

$$F_{\nu'} = 0.45m_2 (1/\nu') N_2 k_{d p 2 \nu'} K_{sk \nu'} I_{1\nu'}$$

where  $I_{1\nu'}$  is the primary current referred to the secondary, with respect to the  $\nu'$ -th harmonic. Thus

$$I_{1\nu'} = \frac{m_1 N_1 k_{d p 1 \nu'}}{m_2 N_2 k_{d p 2 \nu'} K_{sk \nu'}} I_1 \quad (56-77)$$



For the squirrel-cage rotor,

$$m_2 = Q_2 \quad N_2 = \frac{1}{2} \quad k_{ap2\nu'} = 1$$

and

$$I_{1\nu'} = \frac{2m_1 N_1 k_{ap1\nu'}}{Q_2 K_{sk\nu'}} I_1 \quad (56-77a)$$

Kirchhoff's equation for the secondary, with respect to the harmonic current  $I_{2\nu'}$ , per bar, is

$$0 - j(\dot{I}'_{1\nu'} + \dot{I}_{2\nu'})s_{\nu'}x_{m2\nu'} - j\dot{I}_{2\nu'}s_{\nu'}x_{2\nu'} = \dot{I}_{2\nu'}r_{2\nu'} \quad (56-77b)$$

$s_{\nu'}$  is the slip of the rotor with respect to the  $\nu'$ -th stator harmonic; it is given by Eq. (56-48).  $x_{m2\nu'}$  is the secondary main flux reactance of the  $\nu'$ -th harmonic.  $x_{2\nu'}$  is the leakage reactance of the rotor for the  $\nu'$ -th harmonic.

From Eq. (56-77b), per phase for the wound rotor, per bar for the squirrel-cage rotor

$$\dot{I}_{2\nu'} = - \frac{1}{(1 + \tau_{2\nu'}) - j(r_{2\nu'}/s_{\nu'})x_{m2\nu'}} I_{1\nu'} \quad (56-78)$$

where

$$\tau_{2\nu'} = x_{2\nu'}/x_{m2\nu'} \quad (56-79)$$

Eqs. (56-78) and (56-77) express  $I_{2\nu'}$  in terms of  $I_1$  and the secondary parameters. It follows from Eq. (56-78) that  $I_{2\nu'}$  lags  $I_{1\nu'}$  by the angle

$$\psi_{2\nu'} = \pi - \alpha_{\nu'} \quad \tan \alpha_{\nu'} = \frac{r_{2\nu'}}{(1 + \tau_{2\nu'})s_{\nu'}x_{m2\nu'}} \quad (56-80)$$

Notice that, for the squirrel-cage rotor the number of phases was assumed equal to  $Q_2$ . Therefore, its rotor parameters are those of a single bar.

The reactances  $x_{m2\nu'}$  and  $x_{2\nu'}$  are treated in Chap. 57. With respect to  $r_{2\nu'}$  of the squirrel-cage rotor, the following has to be considered. The sinusoidally distributed fluxes induce sinusoidal currents in the rotor bars, the rms values of which can be represented by phasors. The phasors of two adjacent bars are not in phase but displaced by the slot angle

$$\alpha_{s2} = \pi p / Q_2 \quad (58-81)$$

with respect to the main wave ( $\nu' = p/2$ ). The end-ring segments between the bars make, with respect to the bars, a polygonal mesh impedance the external line currents of which are the bar currents. Due to the symmetry of the cage, the current distribution in the ring is also sinusoidal and the current in each single segment can be represented by a phasor; the phasors of adjacent segments are displaced by the same angle  $\alpha_{s2}$  as the phasors representing the bar currents. Fig. 56-8a shows a few bars and ring segments; Fig. 56-8b shows the phasor diagram for the currents in the bars and segments. If the bar current is denoted in general by  $I_b$  and the ring current by  $I_r$ , it follows from Fig. 56-8c that

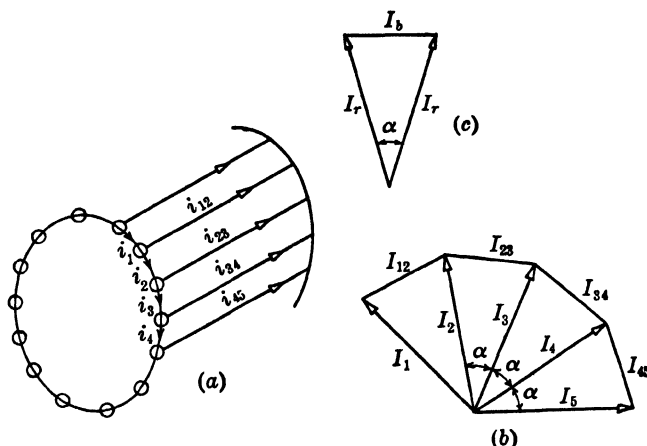


FIG. 56-8. Determination of the ring current in a squirrel-cage rotor ( $\alpha = \alpha_{s2}$ ).

$$I_b = I_r 2 \sin (\alpha_{s2}/2) \quad (56-81a)$$

The angle  $\alpha_{s2}$  is usually small for the main wave and, therefore, for this wave

$$I_r = \frac{I_b}{2 \sin (\alpha_{s2}/2)} = 2 \sin (\pi p/2Q_2) \approx \frac{I_b}{\pi p/Q_2} \quad (56-82)$$

The copper losses in the cage are

$$P_{co} = Q_2 (I_b^2 r_b + 2 I_r^2 r_r). \quad (56-83)$$

$r_b$  and  $r_r$  are the resistances of a single bar and of a single ring segment, respectively. The factor 2 takes into account the fact that there are two rings. Introducing the value of  $I_r$  from Eq. (56-82)

$$P_{co} = Q_2 I_b^2 \left[ r_b + \frac{2}{\pi^2} \frac{r_r}{\sin^2 (\alpha_{s2}/2)} \right] = Q_2 I_b^2 r_{be}, \quad (56-84)$$

$$r_{be} = r_b + \frac{2}{\pi^2} \frac{r_r}{\sin^2 (\alpha_{s2}/2)} \quad (56-85)$$

$r_{be}$  is the *equivalent* bar resistance which also takes into account the ring segments. Eq. (56-85) applies to the main wave. Considering the  $\nu'$ -harmonic, the skin effect has to be taken into account in the term  $r_b$ . For the  $\nu'$ -harmonic the angle  $\alpha_{s2\nu'}$  becomes

$$\alpha_{s2\nu'} = (\nu'/\frac{1}{2}p) \alpha_{s2} \quad (56-86)$$

and, therefore,

$$r_{be\nu'} = r_{b\nu'} + \frac{r_r}{2 \sin^2 (\alpha_{s2\nu'}/2)} \quad (56-87)$$

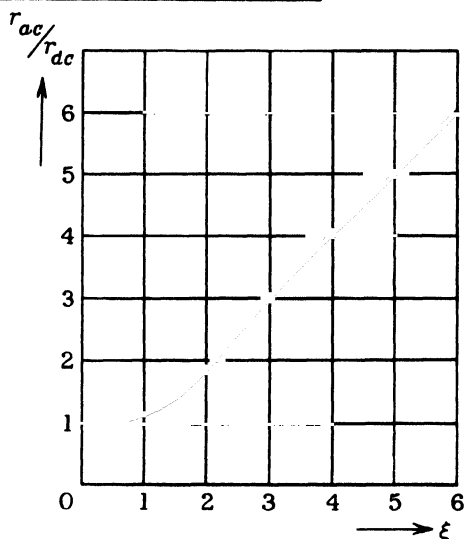


FIG. 56-9. Increase of the resistance of the embedded part of the rotor bar due to skin effect.

Fig. 56-9 shows the increase of  $r_b$  due to skin effect for a rectangular bar. The quantity

$$\xi = 0.316 h_b \sqrt{(\bar{b}_b / \bar{b}_s)(f_2 / \zeta)} \quad (56-88)$$

is drawn in the axis of abscissae.  $b_b$  and  $b_s$  are the widths of bar and slot, respectively.  $h_b$  is the height of the bar.  $f_2 = s_v f_1$  is the frequency of the secondary current.  $\zeta$  is the bar resistivity in microohms/in.<sup>2</sup> (For copper,  $\zeta = 0.825$  at 75° C and  $\zeta = 0.91$  at 100° C). The ordinates of Fig. 56-9 show the ratio of a-c to d-c resistance due to skin effect. Notice that the increase of resistance applies only to the part of the bar which lies in the slot leakage flux (to its length  $l_s$ , see Eqs. (57-18) and (57-19)).

## Chapter 57

### THE LEAKAGE REACTANCES AND MAIN FLUX REACTANCES OF WINDINGS EMBEDDED IN SLOTS

**57-1. General formulae for the coefficients of self- and mutual-inductance.** It has been mentioned in Art. 17-1 that a-c windings embedded in slots produce four kinds of leakage fluxes: (1) the slot leakage flux (Fig. 17-2); (2) the tooth-top leakage flux (Fig. 17-2); (3) the end-winding leakage flux (Fig. 17-3); (4) the harmonic (or differential) leakage flux. The magnetic paths of these fluxes are different and, therefore, their reluctances are different. The magnetic paths lie mainly in air but partially in iron. The leakage fluxes are *directly proportional* to the current which produces them, if the iron which lies in the path of the leakage flux is not saturated. This is usually the case when the machine operates under normal conditions. For example, the saturation of the leakage paths is negligible in an induction motor operating with rated load. However, the saturation of the leakage paths is considerable at high currents, as, for example, during the starting of an induction motor (see Art. 22-6). It will be assumed in the following derivations that the saturation of the leakage paths is negligible. The effect of saturation at high currents will be taken care of by an experimental factor, since a reliable method for the consideration of the saturation of the leakage paths is not available.

The leakage fluxes induce in the windings producing them emf's of self-induction ( $I\omega L$ ) and in adjoining windings emf's of mutual induction.

According to Eq. (1-13), in general

$$L = \frac{\sum (N_x \Phi_x)}{i} \quad (57-1)$$

This equation assumes that not all turns are interlinked with the same flux, and, therefore, the total flux interlinkage has to be determined as the sum of the partial flux interlinkages.

Since  $\Phi_x$  is produced by the mmf  $iN_x$ , it follows from Eq. (1-26) that

$$\Phi_x = 0.4\pi i N_x / R_x \quad \text{and} \quad R_x = l_x / \mu_x a_x \quad (57-2)$$

where  $R_x$  is the reluctance applying to the path of the flux  $\Phi_x$ . Thus,

$$L = 0.4\pi \sum (N_x^2 / R_x) = 0.4\pi \sum N_x^2 \Lambda_x \quad (57-3)$$

$\Lambda_x$  is the permeance of the flux  $\Phi_x$ .

Corresponding to Eq. (1-15), in general,

$$M_{12} = M_{21} = \frac{\sum (n_{x1} \Phi_{x2})}{i_2} = \frac{\sum (n_{x2} \Phi_{x1})}{i_1} \quad (57-4)$$

$\sum (n_{x1} \Phi_{x2})$  is the sum of all flux interlinkages with the circuit 1 due to a current  $i_2$  in circuit 2; vice versa,  $\sum (n_{x2} \Phi_{x1})$  is the sum of all flux interlinkages with the circuit 2 due to a current  $i_1$  in circuit 1. In order to determine  $M_{12} = M_{21}$ , either a current of one ampere is assumed to flow in circuit 1 and the sum of flux interlinkages with circuit 2 is computed or a current of one ampere is assumed to flow in circuit 2 and the sum of flux interlinkages with circuit 1 is computed.

The following Arts. 57-2 to 57-5 refer to the main wave. The harmonics are considered in Art. 57-6.

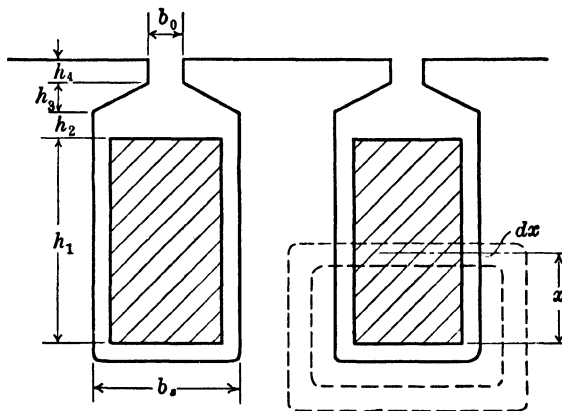


FIG. 57-1. Determination of the slot leakage permeance of a semi-open slot.

**57-2. Slot leakage. Single-layer windings.** First a semi-closed slot (Fig. 57-1) with a single coil of  $n_s$  turns will be treated. The slot is divided into four parts with the heights  $h_1$ ,  $h_2$ ,  $h_3$ , and  $h_4$ . Consider a tube of force crossing part 1 at the distance  $x$  from the bottom of the coil; the height of the tube of force is  $dx$ . Then for this tube of force (Eq. (57-3))

$$N_x = (x/h_1) n_s \quad \text{and} \quad \Lambda_x = dx (l_s/b_s) \quad (57-5)$$

$l_s$  is the length of the iron effective for the slot-leakage flux; its value will be determined in the following.

The sum  $\sum N_x^2 \Lambda_x$  for part 1 is found by integrating  $N_x^2 \Lambda_x$  in Eq. (57-5) from  $x = 0$  to  $x = h_1$ . Thus, for part 1,

$$L_1 = 0.4\pi n_s^2 l_s \frac{1}{b_s h_1^2} \int_{x=0}^{x=h_1} x^2 dx = 0.4\pi n_s^2 l_s \frac{h_1}{3b_s} \quad (57-6)$$

For part 2

$$N_x = n_s, \quad A_x = dx(l_s/b_s)$$

For part 3

$$N_x = n_s, \quad A_x = dx[l_s/\frac{1}{2}(b_s + b_0)]$$

For part 4

$$N_x = n_s, \quad A_x = dx(l_s/b_0)$$

Thus

$$L_2 = 0.4\pi n_s^2 l_s (h_2/b_s) \quad (57-7)$$

$$L_3 = 0.4\pi n_s^2 l_s [2h_3/(b_s + b_0)] \quad (57-8)$$

$$L_4 = 0.4\pi n_s^2 l_s (h_4/b_0) \quad (57-9)$$

and the total slot-leakage inductance for *one coil side* is

$$L_s = L_1 + L_2 + L_3 + L_4 = 0.4\pi n_s^2 l_s \left[ \frac{h_1}{3b_s} + \frac{h_2}{b_s} + \frac{2h_3}{b_s + b_0} + \frac{h_4}{b_0} \right] \times 2.54 \times 10^{-8} \text{ henry} \quad (57-10)$$

$l_s$  is measured in inches. The quantity in brackets is called the *permeance per unit length* of the slot-leakage flux and is denoted by  $\lambda_s$ . Eq. (57-10) is usually written in the form

$$L_s = 0.4\pi n_s^2 l_s \lambda_s \times 2.54 \times 10^{-8} \text{ henry} \quad (57-11)$$

Hence for a semi-open slot

$$\lambda_s = \frac{h_1}{3b_s} + \frac{h_2}{b_s} + \frac{2h_3}{b_s + b_0} + \frac{h_4}{b_0} \quad (57-12)$$

For the open slot shown in Fig. 57-2 the parts 2 and 4 can be combined, so that, for this slot

$$\lambda_s = \frac{h_1}{3b_s} + \frac{h_2 + h_4}{b_s} + \frac{2h_3}{b + b_s} \quad (57-13)$$

For the open slot shown in Fig. 57-3

$$\lambda_s = \frac{h_1}{3b_s} + \frac{h_2}{b_s} \quad (57-14)$$

For the slot shown in Fig. 57-4

$$\lambda_s = \frac{h_1}{3b'} + \frac{2h_2}{b' + b_1} + \frac{2h_3}{b_1 + b_2} + \frac{h_4}{b_0} \quad (57-15)$$

and for the round slot of Fig. 57-5

$$\lambda_s = 0.66 + (h_4/b_0) \quad (57-16)$$

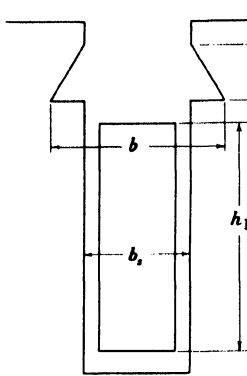


FIG. 57-2. Determination of the slot leakage permeance of an open slot.

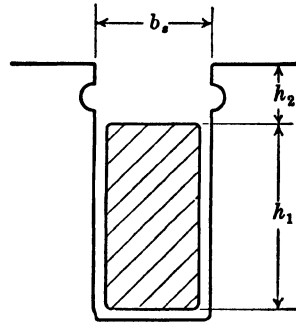


FIG. 57-3. Determination of the slot leakage permeance of an open slot.

The quantity  $l_s \lambda_s = \Lambda_s$  is the *total permeance* of the slot-leakage flux.

Eq. (57-11) yields for *one bar of the squirrel cage rotor* ( $n_s = 1$ )

$$L_s = 0.4\pi l_s \lambda_s \times 2.54 \times 10^{-8} \quad \text{henry} \quad (57-17)$$

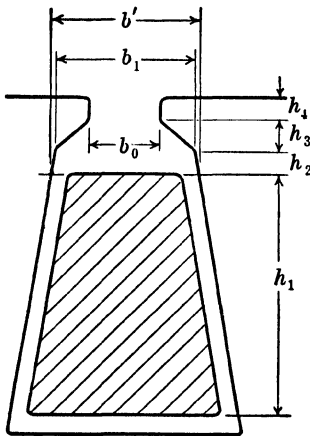


FIG. 57-4. Determination of the slot leakage permeance of a trapezoidal slot.

The coefficient of self-inductance is proportional to the square of the number of turns  $n_s$ , because the flux  $\Phi_x$  in the product  $N_x \Phi_x$  is proportional to the number of turns  $N_x$  (Eq. (57-2)).

Consider Fig. 57-6 which shows a coil in a slot. The core consists of three stacks separated by two radial vents of the width  $b_v$ . It is seen that, due to the vents, the effective length for the slot-leakage flux is smaller than the gross length of the armature  $L$ , but it is larger than the iron length  $L - n_v b_v$  ( $n_v$  = number of vents) due to the fringing within the vents. Apparently, flux mapping will yield the same result for  $l_s$  as for the effective core length  $l_e$  (Art. 50-2), when the radial vents of both machine parts are opposite to each other, i.e.,

$$l_s = L/k_s \quad (57-18)$$

where the slot-leakage factor  $k_s$  is obtained from Eq. (50-11a) by substituting  $b_s$  for  $g$ :

$$k_s = \frac{\tau_v(5b_s + 2b_v)}{\tau_v(5b_s + 2b_v) - 2b_v^2} \quad (57-19)$$

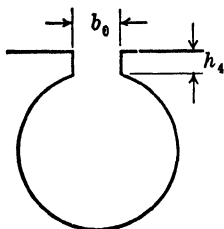


FIG. 57-5. Determination of the slot leakage permeance of a round slot.

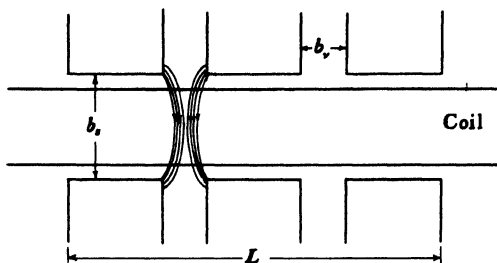


FIG. 57-6. Explanation of the slot-leakage factor  $k_s$ .

**57-3. Slot leakage. Two-layer windings.** Polyphase windings are normally two-layer (Fig. 57-7) and mostly fractional pitch. In the latter case, the two coil sides lying in a slot belong to different phases: in a part of the slots if  $w/\tau > 2/3$  and in all slots if  $w/\tau \leq 2/3$ . Since the currents of the different phases are time-shifted with respect to each other, the leakage flux of a slot with coil sides belonging to different phases will be less than in a slot with coil sides belonging to the same phase.

The coefficients of self-inductance are different for each coil side and mutual inductance exists between them. The number of conductors per coil side is  $n_c$ . Consider Fig. 57-7.

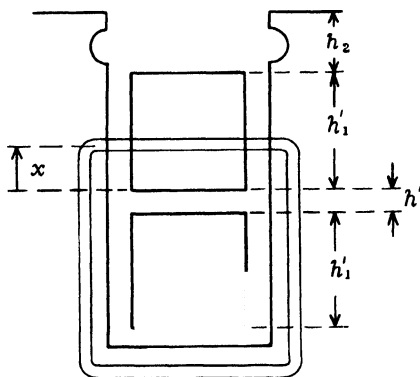


FIG. 57-7. Two-layer winding.

The permeance per unit-length for the *top* coil side is (Eq. (57-14))

$$\lambda_{st} = \frac{h_1'}{3b_s} + \frac{h_2}{b_s} \quad (57-20)$$

Therefore, the slot-leakage inductance of the *top* coil side is

$$L_{st} = 0.4\pi n_c^2 l_s \lambda_{st} \times 2.54 \times 10^{-8} \text{ henry} \quad (57-21)$$

For the permeance of the *bottom* coil side the space taken by the upper coil side has to be considered as air space. Neglecting the small distance  $h'$ ,

$$\lambda_{sb} = \frac{h_1'}{3b_s} + \frac{h_1' + h_2}{b_s} = \frac{4h_1'}{3b_s} + \frac{h_2}{b_s} \quad (57-22)$$

and

$$L_{sb} = 0.4\pi n_c^2 l_s \lambda_{sb} \times 2.54 \times 10^{-8} \text{ henry} \quad (57-23)$$

It is seen that  $L_{sb}$  is much larger than  $L_{st}$ .



The coefficient of mutual inductance between both coil sides is, according to Eq. (57-4),

$$M_{tb} = M_{bt} = \frac{\sum(n_{xt}\Phi_{xb})}{i_b} = \frac{\sum(n_{xb}\Phi_{xt})}{i_t} \quad (57-24)$$

It will be assumed that one ampere flows in the top coil side and the sum of all flux interlinkages  $\sum(n_{xb}\Phi_{xt})$  with the bottom coil side will be determined. Since current flows only in the top coil side, there are no tubes of force below this coil side and, therefore, for all tubes of force interlinked with the bottom coil side,  $n_{xb} = n_c$ . Further, for a tube of force crossing the top coil side at the distance  $x$  from the bottom of this coil side

$$\Phi_{xt} = \frac{0.4\pi n_{xt} \times 1}{(b_s/l_s) dx} \quad n_{xt} = (x/h_1') n_c \quad (57-25)$$

Inserting into Eq. (57-24),  $n_{xb} = n_c$ ,  $\Phi_{xt}$  from Eq. (57-25) and integrating from  $x = 0$  to  $x = h_1'$ , there results for all tubes of force crossing the top coil side,

$$0.4\pi n_c^2 l_s (h_1'/2b_s)$$

The tubes of force which are produced by the current of one ampere in the top coil side and which lie above this coil side yield the flux interlinkage with the *bottom coil side*

$$0.4\pi n_c^2 l_s (h_2/b_s)$$

so that

$$M_{tb} = M_{bt} = 0.4\pi n_c^2 l_s \lambda_{bt} \times 2.54 \times 10^{-8} \quad \text{henry} \quad (57-26)$$

where

$$\lambda_{bt} = \lambda_{tb} = (h_1'/2b_s) + (h_2/b_s) \quad (57-27)$$

$\lambda_{bt} = \lambda_{tb}$  is the permeance per unit length for mutual induction. The total coefficient of self- and mutual-inductance for the slot is

$$L_s = L_{sb} + L_{st} + 2M_{bt} \quad (57-28)$$

In the previous considerations, the time shift of the currents in the two coil sides of the slot has not been taken into account. Therefore, Eq. (57-28) applies to the full-pitch winding and must apply also to the single-layer winding because in both cases all conductors carry currents of the same phase. Indeed, if Eqs. (57-20) to (57-23) and Eqs. (57-26) and (57-27) are inserted into Eq. (57-28), with  $n_c = n_s/2$ , Eq. (57-11) with  $\lambda_s$  according to Eq. (57-14) will be obtained.

In order to take into account the time shift of the currents of the two coil sides of the slot, Eq. (57-28) must be written as

$$L_s = L_{sb} + L_{st} + 2k_r M_{bt} \quad (57-29)$$

The correction factor  $k_r$  is smaller than 1 for fractional-pitch windings; it is equal to 1 for full pitch and single-layer windings.

Inserting into Eq. (57-29) Eqs. (57-21), (57-23), and (57-26)

$$L_s = 0.4\pi n_c^2 l_s (\lambda_{sb} + \lambda_{st} + \lambda_{st} + 2k_r \lambda_{bt}) \times 2.54 \times 10^{-8} \text{ henry} \quad (57-29)$$

This refers to 1 slot and also to 1 *coil* because a coil consists of a top and a bottom coil side.

Consider an integral-slot winding. If there are  $q$  slots in the coil group and  $N_g$  coil groups of the phase are connected in series, Eq. (57-29) must be multiplied by  $q \times N_g$ , in order to get the inductance per phase. The slot-leakage emf per phase is then  $-j\omega L_s q N_g I_c$ , where  $L_s$  is given by Eq. (57-29) and  $I_c$  is the current in the conductor. The slot-leakage emf is normally computed with *phase* current. An integral-slot winding has a maximum of  $p$  parallel paths, i.e., as many as there are coil groups per phase. If  $N_g$  coil groups are connected in series,  $p/N_g$  coil groups are connected in parallel and, therefore, the ratio of the phase current  $I$  to the current in the conductor  $I_c$  is  $p/N_g$ , i.e.,  $I/I_c = p/N_g$ . Thus the slot-leakage emf per phase, with  $I$  = phase current, is  $-j\omega L_s q N_g (N_g/p) I$  and the inductance for the total phase is  $L_s q N_g^2/p$ . Denoting the *series turns per phase* by  $N$ ,

$$N = n_c q N_g \quad (57-30)$$

and the inductance *per phase* is  $L_s q (N^2/n_c^2 q^2) (1/p)$ , i.e.,

$$L_s = 1.6\pi (N^2/pq) l_s \frac{1}{4} (\lambda_{sb} + \lambda_{st} + 2k_r \lambda_{bt}) \times 2.54 \times 10^{-8} \text{ henry per phase} \quad (57-31)$$

Eq. (57-31) also applies to fractional-slot windings. There are  $q\beta$  coil groups per basic unit in this winding.  $q\beta N_g$  turns in series per phase, and  $I/I_c = p/\beta N_g$ .

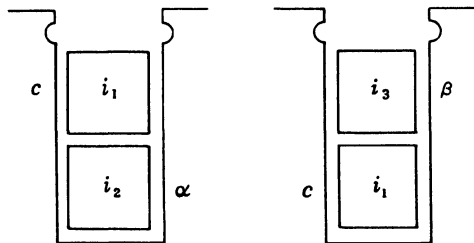


FIG. 57-8. Explanation of the correction factor  $k_r$ .

**Correction Factor  $k_r$ .** The correction factor  $k_r$  can be determined from the following consideration. Fig. 57-8 shows a coil  $cc$  carrying the instantaneous current  $i_1$ . In slot 1 the bottom coil side which may belong to another phase carries the current  $i_2$ , in slot 2 the top coil which may belong to another phase carries the current  $i_3$ . The coefficient of self-inductance of the top coil side of the coil  $cc$  is given by Eq. (57-21), and the coefficient of self-inductance of its bottom coil side by Eq. (57-23). The coefficient of mutual-inductance between bottom and top coil sides of either of the slots 1 and 2 is given by Eq. (57-26). The emf induced in the top coil side is

$$e_t = -L_{st}(di_1/dt) - M_{bt}(di_2/dt)$$

and the emf induced in the bottom coil side

$$e_b = -L_{sb}(di_1/dt) - M_{bt}(di_3/dt)$$

The total emf of the coil

$$e_c = -(L_{st} + L_{sb})(di_1/dt) - M_{bt}[(di_2/dt) + (di_3/dt)]$$

Introducing

$$i_1 = \sqrt{2}I\epsilon^{j\omega t}$$

$$i_2 = \sqrt{2}I\epsilon^{j(\omega t + \alpha)}$$

$$i_3 = \sqrt{2}I\epsilon^{j(\omega t + \beta)}$$

and inserting these equations into the equation for  $e_c$ , the rms value of the emf induced in the coil becomes

$$\dot{E}_c = -j\dot{I}\omega[(L_{st} + L_{sb}) + M_{bt}(\epsilon^{j\alpha} + \epsilon^{j\beta})]$$

and, correspondingly,

$$\begin{aligned} L_c &= L_{st} + L_{sb} + M_{tb}(\epsilon^{j\alpha} + \epsilon^{j\beta}) \\ &= L_{st} + L_{sb} + M_{tb}[(\cos \alpha + \cos \beta) + j(\sin \alpha + \sin \beta)] \end{aligned}$$

There are  $q$  single coils in a coil group. Denoting the angles of coil 1 by  $\alpha_1$  and  $\beta_1$ , of coil 2 by  $\alpha_2$  and  $\beta_2$ , and so forth, the coefficient of self-inductance of the total group is

$$\begin{aligned} L_g &= qL_{st} + qL_{sb} + M_{tb}[(\cos \alpha_1 + \cos \beta_1) + (\cos \alpha_2 + \cos \beta_2) + \dots \\ &\quad + (\cos \alpha_q + \cos \beta_q) + j(\sin \alpha_1 + \sin \beta_1) + j(\sin \alpha_2 + \sin \beta_2) + \dots \\ &\quad + j(\sin \alpha_q + \sin \beta_q)] \end{aligned}$$

The average value of  $L$  per coil is

$$L_{c,ave} = L_{st} + L_{sb} + (1/q)M_{tb}(\sum_{2q} \cos + j\sum_{2q} \sin) \quad (57-32)$$

Comparing this equation with Eq. (57-29) which also applies to a single coil,

$$k_r = (1/2q)[\sum_{2q} \cos + j\sum_{2q} \sin] \quad (57-33)$$

**Example.**  $q=2$ ,  $W/\tau=5/6$ . This winding is schematically shown in Fig. 57-9. Coils  $aa$  and  $bb$  making a coil group will be considered in turn. Notice that in previous equations  $\alpha$  is the angle by which the current in the top coil side of a coil (for example, of coil  $aa$ ) lags the current of the bottom coil side lying in the same slot and  $\beta$  is the angle by which the current of the bottom coil side of the same coil (coil  $aa$ ) lags the current of the top coil side lying in the same slot. Consider in slot 1 the top coil side of coil  $aa$  which belongs to the beginning of phase  $A$ . The bottom coil side of this slot also belongs to phase  $A$ , therefore,  $\alpha_1=0$ . The bottom coil side of coil  $aa$  lies in slot 6. The top coil side of this slot belongs to the beginning of

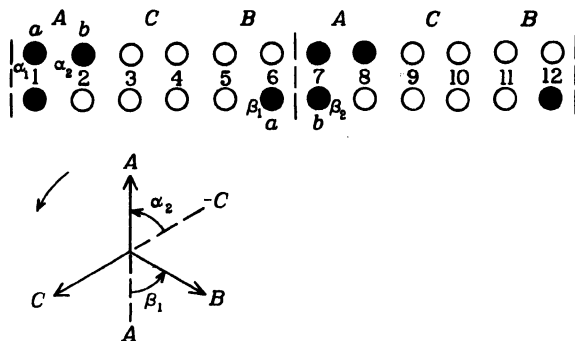


FIG. 57-9. Determination of the correction factor— $k_r$ —for a 3-phase winding, with two slots per pole per phase and  $W/\tau = 5/6$ .

phase  $B$ . The emf of the bottom coil side of coil  $aa$  is opposite to that of the top coil side of this coil. Therefore, the angle  $\beta_1$  between the top coil side and the bottom coil side of slot 6 is  $+60^\circ$  (this is the angle between  $\beta$  and  $-A$  in Fig. 57-9). Considering the coil  $bb$  which makes with the coil  $aa$  a coil group, it is found:  $\alpha_2 = -60^\circ$  (= angle between  $-C$  and  $A$  in Fig. 57-9) and  $\beta_2 = 0$ . Thus (Eq. (57-33))

$$k_q = \frac{1}{4}[(1 + 0.5 + 0.5 + 1) + j(0 + 0.866 - 0.866 + 0)] = \frac{3}{4}$$

It will be found that  $\sum_{2q} \sin = 0$  for any value of  $W/\tau$  and, therefore,

$$k_q = (1/2q) \sum_{2q} \cos$$

Three cases will be considered. The chording  $\epsilon$  will be measured in slot pitches. Then

$$W/\tau = (mq - \epsilon)/mq \quad \epsilon = mq[1 - (W/\tau)] \quad (57-35)$$

(a)  $m=3$ ,  $2/3 \leq W/\tau \leq 1$ . In this case  $2(q - \epsilon)$  coil sides are not influenced by other phases and  $2\epsilon$  coil sides are influenced by other phases with a time-phase shift between currents of  $\pm 60^\circ$  (see Fig. 57-9). Therefore,

$$k_r = (1/2q) \sum \cos = (1/2q)[2(q - \epsilon) \cos 0 + 2\epsilon \cos 60^\circ]$$

Inserting the value of  $\epsilon$  from Eq. (57-35),

$$k_r = \frac{1}{2}[3(W/\tau) - 1] \quad (57-36)$$

(b)  $m=3$ ,  $1/2 \leq W/\tau \leq 2/3$ . In this case  $[2q - 2(\epsilon - q)]$  coil sides are influenced by other phases with a time-phase shift between currents of  $\pm 60^\circ$  and  $2(\epsilon - q)$  coil sides are influenced by other phases with a time-phase shift between currents of  $\pm 120^\circ$ . Therefore,

$$k_r = (1/2q) \sum \cos = (1/2q)[\{2q - 2(\epsilon - q)\} \cos 60^\circ + 2(\epsilon - q) \cos 120^\circ]$$

Inserting the value of  $\epsilon$  from Eq. (57-35)

$$k_r = 3(W/\tau - \frac{1}{2}) \quad (57-37)$$

(c)  $m = 2$ . In this case  $2(q - \epsilon)$  coil sides are not influenced by the other phase and  $2\epsilon$  coil sides are influenced by the other phase with a time-phase shift of  $90^\circ$ . Therefore

$$k_r = (1/2q) \sum \cos = (1/2q)[2(q - \epsilon) \cos 0 + 2\epsilon \cos 90^\circ]$$

Inserting the value of  $\epsilon$  from Eq. (57-35),

$$k_r = (2W/\tau) - 1 \quad (57-38)$$

It is seen from Eqs. (57-36) to (57-38), that the correction factor  $k_r$  depends only upon the coil span; it is independent of the number of slots per pole per phase,  $q$ .

With the value of  $k_r$  fixed by Eqs. (57-36) to (57-38), it is possible to compute  $L_s$  per phase using Eq. (57-31) and inserting the proper values for  $\lambda_{sb}$ ,  $\lambda_{st}$ , and  $\lambda_{bt}$ . This will be made for the open slot Fig. 57-7. Case (a) will be assumed, i.e.,  $m = 3$  and  $2/3 \leq W/\tau \leq 1$ . Thus

$$k_r = \frac{1}{2}[3(W/\tau) - 1]$$

For the slot selected, from Eqs. (57-20), (57-22), and (57-27)

$$\lambda_{st} = \frac{h_1'}{3b_s} + \frac{h_2}{b_s} \quad \lambda_{sb} = \frac{4h_1'}{3b_s} + \frac{h_2}{b_s} \quad \lambda_{bt} = \frac{h_1'}{2b_s} + \frac{h_2}{b_s}$$

Inserting into Eq. (57-31) and assuming  $h_1' = (h_1/2)$ , where  $h_1$  is the total height of the conductors

$$L_s = 1.6\pi \frac{N^2}{pq} l_s \left[ \frac{h_1}{3b_s} \times \frac{1}{16} \left( 9 \frac{W}{\tau} + 7 \right) + \frac{h_2}{b_s} \times \frac{1}{4} \left( 3 \frac{W}{\tau} + 1 \right) \right] \times 2.54 \times 10^{-8} \lambda$$

henry per phase

For the full-pitch winding and single-layer winding ( $k_r = 1$ ) the result is

$$L_s = 1.6 \frac{N^2}{pq} l_s \left( \frac{h_1}{3b_s} + \frac{h_2}{b_s} \right) \times 2.54 \times 10^{-8} \quad \text{henry per phase}$$

Comparing the two values of  $L_s$ , it is seen that  $L_s$  for the fractional-pitch winding can be calculated from the value of  $L_s$  for the single-layer winding if *two correction factors* are used, one

$$k_{xco} = \frac{1}{16}[9(W/\tau) + 7] \quad (57-39)$$

for the part of the slot in which the conductors lie, and the other

$$k_{xt} = \frac{1}{4}[3(W/\tau) + 1] \quad (57-40)$$

for the part of the slot above the conductors.

Case (a) was assumed. If case (b) is computed, i.e.,  $m = 3$ ,  $1/2 \leq W/\tau \leq 2/3$ , the factors  $k_{xco}$  and  $k_{xt}$  become

$$k_{xco} = \frac{1}{16}[18(W/\tau) + 1] \quad k_{xt} = \frac{1}{4}[6(W/\tau) - 1] \quad (57-41)$$

and for the 2-phase windings

$$k_{xco} = \frac{1}{4}[3(W/\tau) + 1] \quad k_{xt} = W/\tau \quad (57-42)$$

Fig. 57-10 shows the factors  $k_{xco}$  and  $k_{xt}$  for 3-phase windings corresponding to Eqs. (57-39) to (57-41).

Summarizing, compute  $L_s$  using the formula

$$L_s = 1.6(N^2/pq)l_s\lambda_s \times 2.54 \times 10^{-8} \quad \text{henry per phase} \quad (57-43)$$

with the value of  $\lambda_s$  from Eqs. (57-12) to (57-16) which apply to the single-layer and full-pitch windings. Multiply the term of  $\lambda_s$  which relates to the part of the slot where the conductors lie by  $k_{xco}$  and the terms of  $\lambda_s$  which relate to the part of the slot above the conductors by  $k_{xt}$ .

The slot-leakage reactance is

$$x_s = 2\pi f L_s \quad \text{ohm per phase.} \quad (57-44)$$

**57-4. Tooth-top leakage.** The tooth-top leakage comprises the leakage lines that go from tooth-top to tooth-top through the air. In induction machines the air-gap is small and the tooth-top leakage can be neglected. The permeance of the tooth-top leakage of the stator of the synchronous machine is found by the method of conformal mapping (Ref. A7).

$$\lambda_{tt} = \frac{5(g/b_0)}{5 + 4(q/b)} \quad (57-45)$$

Therefore, the tooth-top leakage inductance of *one coil side* is

$$L_{tt} = 0.4\pi n_s^2 l_s \lambda_{tt} k_{xt} \times 2.54 \times 10^{-8} \quad \text{henry} \quad (57-46)$$

For salient-pole synchronous machines,  $L_{tt}$  as given by this equation is to be multiplied by  $b_p/\tau$ , where  $b_p$  is the pole arc and  $\tau$  the pole pitch.

Corresponding to Eq. (57-43), the tooth-top leakage inductance per phase is

$$L_{tt} = 1.6\pi(N^2/pq)l_s\lambda_{tt}k_{xt} \times 2.54 \times 10^{-8} \quad \text{henry per phase} \quad (57-47)$$

The tooth-top leakage reactance is

$$x_{tt} = 2\pi f L_{tt} \quad \text{ohm} \quad (57-48)$$

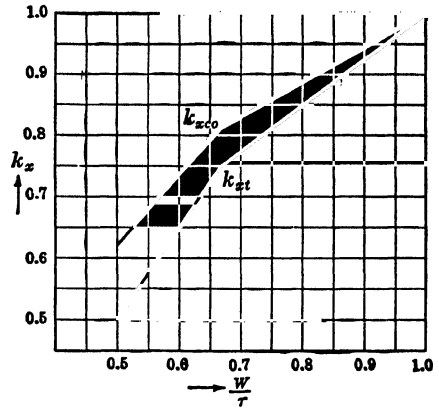


FIG. 57-10. Reduction factors for slot leakage permeance of fractional-pitch 3-phase windings.

**57-5. End-winding leakage.** The exact calculation of the end-winding leakage is very difficult since the effect of adjacent coils and adjacent phases on each other as well as the effect of the rotor and stator on each other must be considered. The formula given below for end-winding leakage is partly the result of theoretical derivations and partly of experience.

For the end-winding leakage inductance *per coil side*, the following holds:

$$L_e = 0.4\pi n_s^2 q [1.20k_{dp}^2 (l_{e2} + \frac{1}{2}l_{e1})] 2.54 \times 10^{-8} \text{ henry.} \quad (57-49)$$

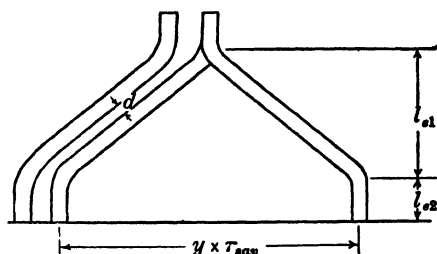


FIG. 57-11. Determination of the end-winding leakage.

The significance of  $l_{e2}$  and  $l_{e1}$  is seen from Fig. 57-11

$$l_{e1} = \frac{y\tau_{s,av}a}{2\sqrt{\tau_{s,av}^2 - a^2}}, \quad (57-50)$$

where  $y$  is the coil width in slot pitches and  $a$  is the distance in inches between the mid-points of two adjacent coil ends.

$$a = b_s + d \text{ inches,} \quad (57-51)$$

where  $d$  is the air space between two insulated coil ends.  $\tau_{s,av}$  is the average slot pitch, i.e., the slot pitch in the middle of the tooth.

The magnitude of  $l_{e2}$  depends upon the voltage. It can be taken as:

$$\begin{aligned} l_{e2} &= 0.25 \text{ to } 0.5 \text{ inch for } 120 \text{ to } 440 \text{ volts,} \\ &= 0.75 \text{ inch for } 600 \text{ volts,} \\ &= 1.25 \text{ inches for } 2300 \text{ volts,} \\ &= 2.5 \text{ inches for } 6600 \text{ volts,} \\ &= 3.5 \text{ inches for } 11,000 \text{ volts,} \\ &= 4.0 \text{ inches for } 13,200 \text{ volts} \end{aligned}$$

Eq. (57-50) applies to the stator windings of induction motors and synchronous machines and also to the rotor winding of the wound-rotor induction motor.

Corresponding to Eq. (57-43), the end-winding leakage inductance *per phase* is

$$L_e = 1.6\pi (N^2/p) [1.2k_{dp}^2 (l_{e2} + \frac{1}{2}l_{e1})] \times 2.54 \times 10^{-8} \text{ henry per phase} \quad (57-52)$$

The end-winding leakage inductance *per bar* of a squirrel-cage winding is (see Fig. 57-11a)

$$L_e = 0.4\pi (Q_2/m_l p) [\frac{2}{3}(L_b - L) + k\tau'] 2.54 \times 10^{-2} \text{ henry} \quad (57-53)$$

where

$L_b$  = length of bar between rings,

$L$  = gross core length,

$\tau' = (\pi D'/p) =$  pole pitch in the middle of the ring,

$k = 0.36$  for  $p = 2$ ,  $k = 0.18$  for  $p > 2$

The end-winding leakage reactance is

$$x_e = 2\pi f L_e \quad \text{ohms} \quad (57-54)$$

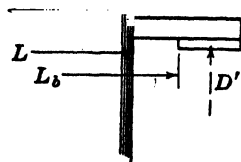


FIG. 57-11a. Determination of the end-winding leakage of a squirrel-cage winding.

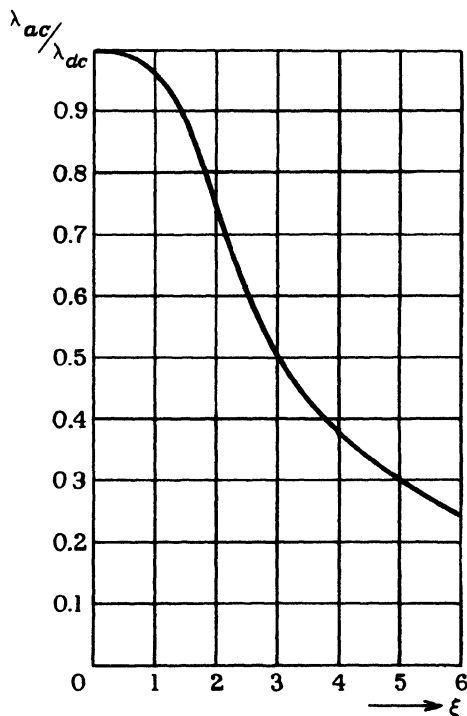


FIG. 57-12. Ratio of a-c to d-c slot permeance for rotor bars (influence of skin effect).

**57-6. Slot leakage tooth-top leakage, and end-winding leakage with respect to harmonics.** The stator slot-leakage reactance, the tooth-top leakage reactance, the end-winding leakage reactance can be assumed the same for  $\nu'$ -th harmonic as for the main wave  $\nu' = p/2$ . For the squirrel-cage rotor, the slot permeance  $\lambda_s$  (Eq. (57-17)) can be considerably smaller for the  $\nu'$ -th harmonic than for the main wave due to skin effect. Fig. 57-12 shows the ratio  $\lambda_{s,ac}/\lambda_{s,dc}$  as a function of  $\xi$  (Eq. (56-88)) for a rectangular bar. As for



$r_{ac}/r_{dc}$ , this ratio must be applied to the part of the bar  $l$ , (Eqs. (57-18)) and (57-19)).

For the end-winding leakage of the squirrel-cage rotor with respect to the  $\nu'$ -th harmonic, Eq. (57-53) multiplied by the ratio

$$\frac{\sin^2 (\alpha_{s2}/2)}{\sin^2 (\alpha_{s2\nu'}/2)}$$

can be used (see Eqs. (56-81) and (56-86)).

**57-7. Harmonic leakage of an integral-slot winding (Ref. K1).** The harmonic leakage is also called differential leakage. This name is justified by the fact that the sum of all harmonics is equal to the total function minus fundamental.

The following harmonic chart refers to a 4-pole, 3-phase squirrel-cage induction motor, with 72 slots ( $q_1=6$ ) and a normal  $60^\circ$  phase-belt winding in the stator and 60 slots in the rotor. Eqs. (56-42) and (56-51) yield this chart.

Stator Harmonics		Rotor Harmonics		
$\nu'$		$\mu' = k_2 Q_2 + \nu'$		
		$k_2 = 0$	$k_2 = +1$	$k_2 = -1$
$+$ (2)		$+$ (2)	$+$ 62	$-$ 58
$-$ 10		$-$ 10	$+$ 50	$-$ 70
$+$ 14		$+$ 14	$+$ 74	$-$ 46
$-$ 22		$-$ 22	$+$ 38	$-$ 82
$+$ 26		$+$ 26	$+$ 86	$-$ 34
$-$ 34		$-$ 34	$+$ 26	$-$ 94
$+$ 38		$+$ 38	$+$ 98	$-$ 22
$-$ 46		$-$ 46	$+$ 14	$-$ 106
$+$ 50		$+$ 50	$+$ 110	$-$ 10
$-$ 58		$-$ 58	$+$ 2	$-$ 118
$+$ 62		$+$ 62	$+$ 122	$+$ 2
$-$ 70		$-$ 70	$-$ 10	$-$ 130
$+$ 74		$+$ 74	$+$ 134	$+$ 14

The first column represents the stator harmonics. Since the stator winding is a  $60^\circ$ -phase-belt 2-layer winding it does not produce even harmonics. Each stator harmonic produces a series of rotor harmonics; these are the horizontal rows corresponding to the stator harmonics. The first vertical column of the rotor harmonics has the same orders as the stator harmonics producing them. The slot harmonics are marked by a square. These harmonics are given by Eqs. (56-43) and (56-52). The main (synchronous) waves,  $\nu' = p/2$ , are marked by a circle.

In the normal design of an induction motor, only the torque produced by the main waves is computed. In this case all stator harmonic fluxes of the order  $\nu' > p/2$  are considered as leakage fluxes, and, of the rotor harmonics, only the *first* horizontal row produced by the currents of the frequency  $sf_1$  is taken into account. The harmonic fluxes of the order  $\mu' > p/2$  of this row constitute the rotor leakage.

It should be noted that the harmonic fluxes of the stator and the emf's induced by them in the stator winding are all in-phase, because they are produced by the same current. The same applies to the harmonic fluxes of the rotor.

The harmonic leakage reactance of the stator winding is determined as follows: From Eq. (56-45), the amplitude of the flux distribution produced by the  $\nu'$ -th mmf harmonic is

$$B_{\nu'} = 0.45m_1 \frac{N_1 k_{dp1\nu'}}{\nu'} \frac{3.19}{gk_c k_s} I_1 \quad (57-55)$$

The corresponding flux distribution is

$$\Phi_{\nu'} = \frac{2}{\pi} \frac{\tau(p/2)}{\nu'} l_e B_{\nu'} \quad (57-56)$$

and the flux interlinkages with the stator winding due to the flux  $\Phi_{\nu'}$  are

$$\psi_{\nu'} = \Phi_{\nu'} N_1 k_{dp1\nu'} \quad (57-57)$$

Since  $L_{\nu'} = \psi_{\nu'} / \sqrt{2} I_1$ , the harmonic leakage reactance of the stator winding is

$$x_{h1} = 2\pi f_1 \frac{1}{\sqrt{2} I_1} \sum_{\nu' \neq p/2} \psi_{\nu'} \times 10^{-8} \quad \text{ohm per phase} \quad (57-58)$$

Inserting Eqs. (57-55) to (57-57)

$$x_{h1} = 0.80m_1 f_1 N_1^2 \frac{\tau l_e}{pgk_c k_s} \times 2.54 \times 10^{-8} \sum_{\nu' \neq p/2} \left( \frac{k_{dp1\nu'}}{\nu'} \right)^2 \quad \text{ohm per phase} \quad (57-59)$$

or

$$x_{h1} = 3.2m_1 f_1 N_1^2 \frac{\tau l_e}{pgk_c k_s} \times 2.54 \times 10^{-8} \sum_{\nu \neq 1} \left( \frac{k_{dp1\nu}}{\nu} \right)^2 \quad \text{ohm per phase} \quad (57-60)$$

For the integral-slot, 2-layer,  $60^\circ$  phase belt winding, the summation must be extended over the harmonics  $\nu' = 5(p/2), 7(p/2), 11(p/2) \dots$  or  $\nu = 5, 7, 11 \dots$

It is possible to derive a formula for the sum

$$\sum_{\nu \neq 1} \left( \frac{k_{dp1\nu}}{\nu} \right)^2$$

through the consideration of the magnetic energy in the gap of the machine (Ref. A7). For the 3-phase, integral-slot, 2-layer, 60° phase belt winding, the sum is

$$\sum_{\nu \neq 1} \left( \frac{k_{dp\nu}}{\nu} \right)^2 = \frac{\pi^2 (5q^2 + 1) - [\frac{1}{4}(\epsilon/q) + \frac{3}{2}\epsilon^2 - \frac{1}{4}(\epsilon^3/q)]}{3q^2} - k_{dp1(\nu=1)}^2 \quad (57-61)$$

if  $\frac{2}{3} \leq (W/\tau) \leq 1$ . If  $\frac{1}{3} \leq (W/\tau) \leq \frac{2}{3}$

$$\begin{aligned} \sum_{\nu \neq 1} \left( \frac{k_{dp\nu}}{\nu} \right)^2 \\ = \frac{\pi^2 (5q^2 + 1) - [3q(\epsilon - q) + \frac{2}{3}\{(\epsilon - q)/q\} + (\epsilon - q)^2 - \frac{2}{3}\{(\epsilon - q)^2/q\}]}{4q^2} - k_{dp1(\nu=1)}^2 \end{aligned} \quad (57-62)$$

For two-phase windings

$$\sum_{\nu \neq 1} \left( \frac{k_{dp\nu}}{\nu} \right)^2 = \frac{\pi^2 (4q^2 + 2) - [(\epsilon/q) + 3\epsilon^2 - (\epsilon^3/q)]}{3q^2} - k_{dp1(\nu=1)}^2 \quad (57-63)$$

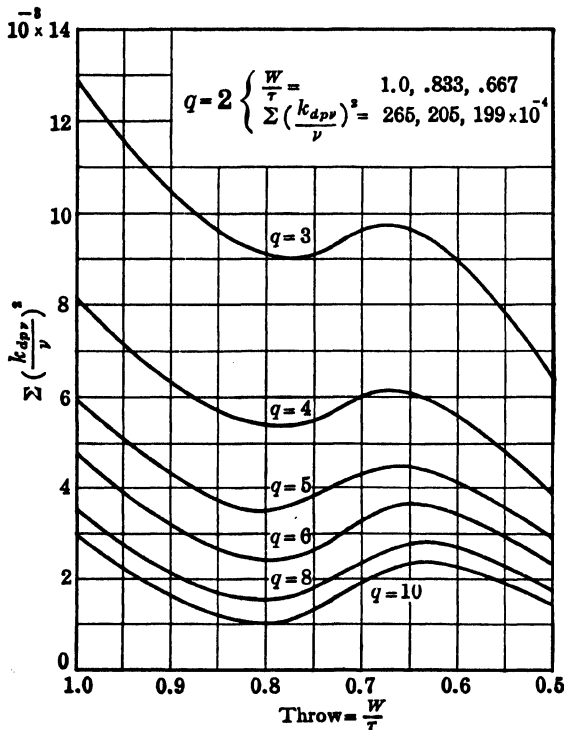


FIG. 57-13. Harmonic (differential) leakage curves for integral-slot windings.

The sums for  $m = 3$  (Eqs. (57-61) and (57-62)) are represented in Fig. 57-13. They depend upon the number of slots per pole per phase,  $q$ , and upon the chording  $\epsilon$  or, what is the same, upon the coil span  $W/\tau$ . In the figure  $W/\tau$  is used as abscissa and  $q$  as parameter. Since the distribution factors  $k_{dp}$  decrease with increasing  $q$ , the sums also decrease with increasing  $q$ , approximately with the square of  $q$ . Under the influence of the coil span, the curves show a minimum at  $W/\tau \approx 0.80$ .

**57-8. Harmonic leakage of a fractional slot-winding.** Consider Fig. 56-4. The amplitude of the first mmf harmonic ( $n = 1$ , see Eq. (56-60)) which has the wave length  $2\beta\tau$  is (Eq. (15-8))

$$F_\beta = 0.45m_1N'n_s k_{dp1\beta} I_1 \quad (57-64)$$

$N'$ , the numerator of  $q = N'/\beta$ , is the number of slots assigned to each phase in  $\beta$  poles.  $n_s$  is the number of series conductors per slot. The amplitude of the fundamental wave ( $\nu' = 1$ ) with the wave length  $p\tau$  is accordingly

$$F_f = 0.45m_1N'n_s k_{dp1f} I_1 \times (p/2\beta) \quad (57-65)$$

$p/2\beta$  is the ratio of the wave lengths. The amplitude of  $\nu'$ -th harmonic of the mmf is then

$$F_{\nu'} = \frac{F_f}{\nu'} \frac{k_{dp1\nu'}}{k_{dp1f}} = 0.45m_1N'n_s \frac{p}{2\beta} \frac{k_{dp1\nu'}}{\nu'} I_1 \quad (57-66)$$

From Eq. (56-14), the amplitude of the  $\nu'$ -th harmonic of the flux distribution

$$B_{\nu'} = 0.4\pi F_{\nu'} \frac{1}{gk_c k_s} \times 2.54 \quad \text{lines/square inch}$$

With  $N' = q\beta$  and  $N_1 = qn_s(p/2)$  ( $N_1$  = number of series turns per phase), Eqs. (57-56) to (57-58) yield

$$x_{h1} = 0.80m_1f_1N_1^2 \frac{p\tau l_e}{gk_c k_s} \times 2.54 \times 10^{-8} \sum_{\nu' \neq p/2} \left( \frac{k_{dp1\nu'}}{\nu_1} \right)^2 \quad \text{ohm per phase} \quad (57-67)$$

This is the same equation as that derived for the integral-slot winding (Eq. (57-59)). This could be expected. For the calculation of the harmonic leakage of an integral-slot winding, Eq. (57-60) in connection with Fig. 57-13 is used. In order to make the same equation, i.e., Eq. (57-60), applicable to both integral-slot and fractional-slot windings, Eq. (57-67) is multiplied by  $p^2/p^2$  and  $\nu'$  expressed in turn by Eq. (56-61) and Eq. (56-63). The harmonic leakage reactance then becomes

$$x_{h1} = 3.2m_1f_1N_1^2 \frac{\tau l_e}{pgk_c k_s} \times 2.54 \times 10^{-8} \times A \quad (57-68)$$

where

$$A = \beta^2 \sum_{n \neq \beta} \left( \frac{k_{dp1v'}}{n} \right)^2 \quad n = 1, 5, 7 \dots \quad \text{when } \beta = \text{odd number} \quad (57-69)$$

and

$$A = \frac{\beta^2}{4} \sum_{n \neq \beta/2} \left( \frac{k_{dp1v'}}{n} \right)^2 \quad n = 1, 2, 4, 5, 7 \dots \quad \text{when } \beta = \text{even number} \quad (57-70)$$

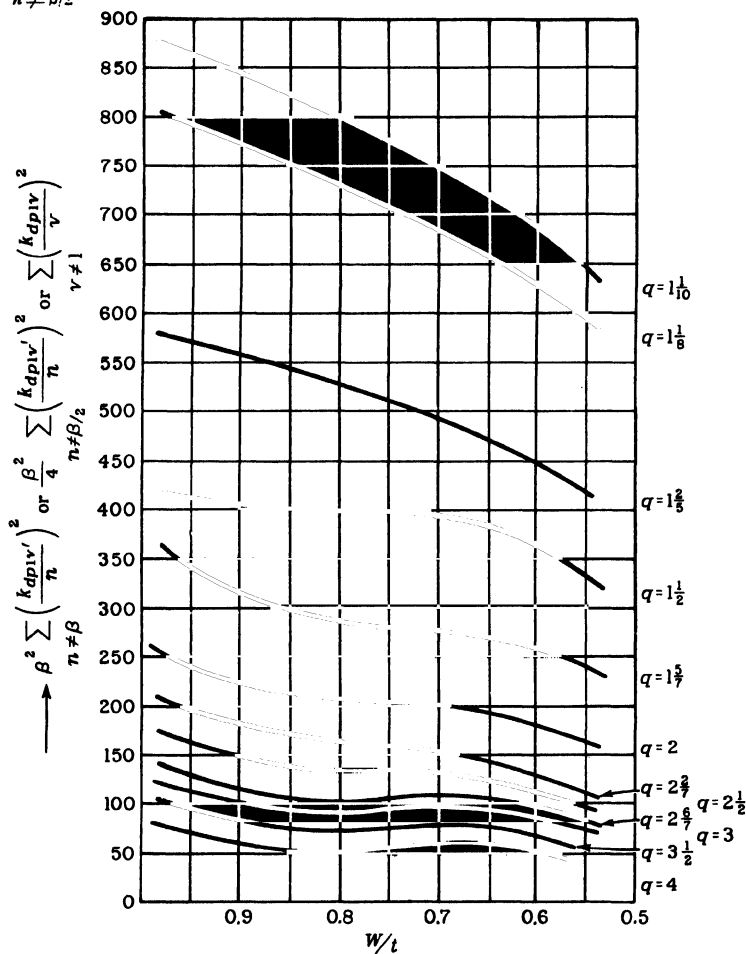


FIG. 57-14. Harmonic (differential) leakage curves for fractional-slot windings.

The quantity  $A$  which is a function of  $q$  and  $W/\tau$  is represented in Fig. 57-14. Some curves from Fig. 57-13 (for  $q=2, 3$ , and  $4$ ) are also shown in Fig. 57-14. For these latter curves the ordinate is equal to

$$\sum_{\nu \neq 1} \left( \frac{k_{d p 1 \nu}}{\nu} \right)^2$$

corresponding to Eq. (57-60).

**57-9. Influence of the rotor winding on the harmonic leakage reactance of the stator winding.** From Eq. (16-3) and also Fig. 16-1 which both refer to the main (synchronous) wave,  $\nu' = p/2$ , it is seen that the main flux is produced by the resultant of stator and rotor mmf's,  $N_1 I_1 + N_1 I_2' = N_1 I_m$ . For the main wave, the resultant mmf is 20 to 30 per cent (in low speed machines larger than this value) of the stator mmf. This is due to the armature reaction of the rotor: Its current is shifted by an angle larger than  $90^\circ$  from the stator current (Fig. 18-1). The same conditions apply to the harmonic mmf's. Consider the harmonic chart of Art. 57-6. What applies to the main waves  $\nu' = 2$  and  $\mu' = 2$ , applies to any harmonic pair of the columns to which  $\nu' = 2$  and  $\mu' = 2$  belong. For example,  $\nu' = -10$  and  $\mu' = -10$  produce a resultant mmf which is smaller than the stator mmf of the  $\nu' = -10$  harmonic. It can be said that each rotor harmonic of the column  $k_2 = 0$  *damps* the stator harmonic of the same order. It will be shown in Chap. 58 that each such pair of harmonics operate in the same manner as the main waves and produce a torque-slip characteristic of the same shape as that of the main waves.

In the previous considerations of the harmonic leakage reactance of the stator, the damping of the stator harmonics by the rotor harmonics has not been taken into account. For example, in Eq. (57-55)  $B_{\nu'}$  is computed with the stator mmf  $F_{\nu'}$  but not with the resultant of stator and rotor mmf's of the  $\nu'$ -th harmonic. The damping factor ( $D_{\nu'}$ ) by which  $B_{\nu'}$  is to be multiplied is given by

$$D_{\nu'} = \frac{I_{m\nu'}}{I_1} = \frac{I_1 + I_{2\nu'}}{I_1}$$

or, if the stator current is referred to the secondary,

$$D_{\nu'} = \frac{I'_{1\nu'} + I_{2\nu'}}{I'_{1\nu'}}$$

Inserting  $I_{2\nu'}$  from Eq. 56-78

$$D_{\nu'} = 1 - \frac{1}{(1 + \tau_{2\nu'}) - j r_{2\nu'} / (s_{\nu'} x_{m2\nu'})} \quad (57-71)$$

The absolute value of  $D_{\nu'}$  is 0.2 to 0.3 ( $I_m/I_1 = 0.2$  to 0.3) for the main wave,  $\nu' = p/2$ . It is approximately 0.5 for the 5th harmonic  $\nu' = 5(p/2)$ , 0.3 for the 7th harmonic, and decreases with increasing order of the harmonic. The damping factor  $D_{\nu'}$  also produces a shift between the individual harmonic

fluxes. It is tedious to compute the harmonic leakage reactance of the stator taking into account the damping factors of the individual harmonics. For this reason Eqs. (57-60) and (57-68) which assume that the harmonic fluxes of the stator are proportional to  $I$  are used in the customary design. The actual value of  $x_{h1}$  may be 10 to 15 per cent lower than that computed from Eqs. (57-60) and (57-68). This applies to the squirrel-cage rotor. The damping of the stator harmonics by a wound rotor is small because of its small number of phases.

Skewing reduces the rotor currents,  $I_{2\nu'}$ , of the higher harmonics  $\nu'$ . This reduces the damping (increases  $D_{\nu'}$ ) of the higher stator harmonics by the higher rotor harmonics, making the error in the computation with Eqs. (57-60) and (57-68) smaller.

*The Main Flux Reactance.* The value of the main flux reactance  $x_m$  of the fundamental  $\nu' = p/2$  which is used in Kirchhoff's equations of the polyphase induction motor (Eq. (17-23a)) can be derived from the previous considerations. If in Eq. (57-55)  $I_m$  is introduced for  $I_1$ ,  $B_{(\nu'=p/2)}$  is obtained. If further in Eqs. (57-56) and (57-57)  $p/2$  is substituted for  $\nu'$  and it is observed that  $L_{(\nu'=p/2)} = \psi_{(\nu'=p/2)} / \sqrt{2} I_m$ , there results

$$x_{m1(\nu'=p/2)} = 3.2m_1 f_1 (N_1 k_{d p 1(\nu'=p/2)})^2 \frac{\tau l_e}{p g k_c k_s} \times 2.54 \times 10^{-8} \text{ ohm per phase} \quad (57-72)$$

This equation also applies to fractional-slot windings. It can be derived directly from Eqs. (57-60) and (57-67) by setting  $\nu = 1$  and  $\nu' = p/2$ , respectively. Eq. (57-72) refers to  $\nu' = p/2$ .

It follows from Eqs. (57-59), (57-67), and (57-72) for the *main flux reactance of the  $\nu'$ -th harmonic* ( $k_s = 1$  for harmonics) that

$$\begin{aligned} x_{m1\nu'} &= 0.8m_1 f_1 N_1^2 \frac{p \tau l_e}{g k_c} 10^{-8} \left( \frac{k_{d p 1\nu'}}{\nu'} \right)^2 \\ &= x_{m1(\nu'=p/2)} \left( \frac{p}{2 \nu'} \right)^2 \left( \frac{k_{d p 1\nu'}}{k_{d p 1(\nu'=p/2)}} \right)^2 k_s \end{aligned} \quad (57-73)$$

Corresponding to Eq. (57-72) the main flux reactance of the *single-phase winding* (compare Eq. (15-10) with Eq. (15-11))

$$x_{m1(\nu'=p/2)} = 6.4 f_1 (N_1 k_{d p 1(\nu'=p/2)})^2 \frac{\tau l_e}{p g k_c k_s} \times 2.54 \times 10^{-8} \text{ ohm} \quad (57-74)$$

**57-10. Harmonic leakage of the rotor winding with respect to the main wave.** (a) *Wound rotor.* Using Eq. (56-50), it is found that the winding of a wound rotor with  $q = \text{integer}$ , what is normal for this rotor type, produces the same harmonics as the stator winding with  $q = \text{integer}$ . Therefore, Eq. 57-60 must apply also to the wound rotor winding and the harmonic leakage reactance of a wound rotor with respect to  $\nu' = p/2$  is

$$x_{h2(\nu'=p/2)} = 3.2m_2f_1N_1^2 \frac{\tau l_e}{pgk_c k_s} \times 2.54 \times 10^{-8} \sum_{\mu \neq 1} \left( \frac{k_{d22\mu}}{\mu} \right)^2 \text{ ohm per phase} \quad (57-75)$$

The sum is given in Fig. 57-13 for 3-phase, 2-layer, 60° phase-belt winding. Eq. (57-75) and Fig. 57-13 apply to the non-skewed rotor. The influence of skewing is discussed under (b). Corresponding to Eq. (57-72), the *main flux* ( $\mu' = p/2$ ) reactance is

$$x_{m2(\nu'=p/2)} = 3.2m_2f_1(N_2k_{d22(\mu'=p/2)})^2 \frac{\tau l_e}{pgk_c k_s} \times 2.54 \times 10^{-8} \text{ ohm per phase} \quad (57-76)$$

(b) *Squirrel-cage rotor.* Eq. 57-75 can be applied to the squirrel-cage. In order to determine the harmonic leakage reactance *per bar*, there must be introduced

$$m_2 = Q_2, \quad N_2 = \frac{1}{2}, \quad k_{d22\mu} = 1$$

and  $\mu = k_2Q_2/(\frac{1}{2}p) + 1$ , since the first horizontal row of the rotor harmonics for which  $\nu = 1$  is considered.

$$x_{h2(\nu'=p/2)} = 0.8Q_2f_1 \frac{\tau l_e}{pgk_c k_s} K_{sk(\nu'=p/2)}^2 \times 2.54 \times 10^{-8} \sum_{k_2 \neq 0} \left( \frac{1}{(k_2Q_2/(\frac{1}{2}p) + 1)} \right)^2 \text{ ohm per bar} \quad (57-77)$$

Again the consideration of the magnetic energy in the gap yields a simple expression for the sum, namely (Ref. A7)

$$\sum_{k_2 \neq 0} \left( \frac{1}{(k_2Q_2/(\frac{1}{2}p) + 1)} \right)^2 = \frac{1}{\xi_{2(\nu'=p/2)}^2 K_{sk(\nu'=p/2)}^2} 1 \quad (57-78)$$

where

$$\xi_{2(\nu'=p/2)} = \frac{\sin(\frac{1}{2}p)\pi/Q_2}{(\frac{1}{2}p)\pi/Q_2} \quad (57-79)$$

Fig. 57-15 shows the sum for three different values of skew. The value of the sum decreases rapidly with increasing number of slots per pole,  $Q_2/p$ . For small angles ( $\frac{1}{2}p/Q_2 \leq \frac{1}{10}$ ,  $[\frac{1}{2}p/Q_2][S/\tau_{2s}] \leq \frac{1}{10}$ ) the accuracy of the slide rule is not sufficient for determining the sum from Eq. (57-78). The following approximation holds

$$\sum_{k_2 \neq 0} \left( \frac{1}{(k_2Q_2/(\frac{1}{2}p) + 1)} \right)^2 \approx \frac{1}{3} \left( \frac{(p/2)\pi}{Q_2} \right)^2 \left[ 1 + \left( \frac{S}{\tau_{2s}} \right)^2 \right] \quad (57-80)$$

It is seen from this equation and also from the curves that skewing the rotor one rotor slot pitch doubles the harmonic leakage reactance of the rotor winding.



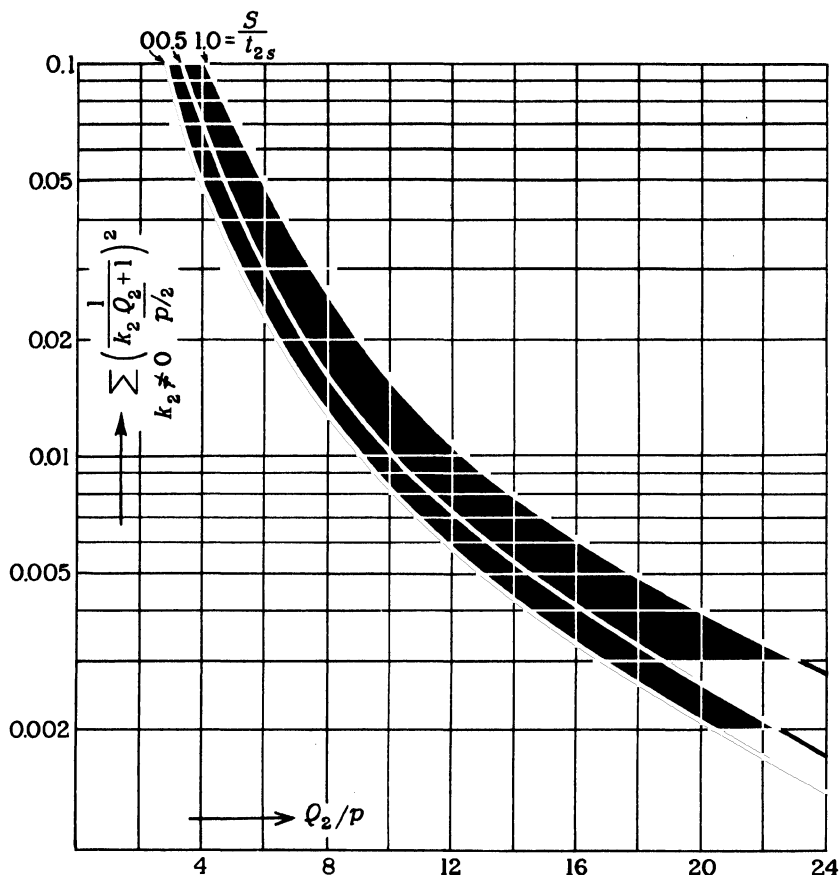


FIG. 57-15. Harmonic (differential) leakage curve of a squirrel-cage winding.

There are many factors involved in the computation of the harmonic leakage in addition to those mentioned, for example, the shape of the mmf curve (Ref. K2). All foregoing considerations are based on the assumption that the mmf of a single coil is a rectangle (Fig. 15-3), i.e., that the mmf changes abruptly in the center of the slot. The actual shape is closer to a trapezoid. Further, it is assumed in the previous considerations that the influence of the slot openings on the harmonic fluxes is the same as on the main wave: the same permeance of the air gap,  $1/gk_c$ , has been used for the main wave and the harmonics. This is not entirely correct (see Art. 57-13). Furthermore, the previous considerations assume that the rotor bars are insulated. This is normally not the case. When the bars are not insulated and especially when the non-insulated bars are skewed (skewing produces a phase-shift of the induced emf along the bar), the stator harmonics of low

order produce currents which flow between the bars through the iron. Experience shows that about half of the theoretical value of the increase of the harmonic leakage due to skewing should be used, i.e., that the factor  $(S/\tau_{2s})^2$  in Eq. (57-80) should be multiplied by 1/2. The same increase of the harmonic leakage can be applied to the skewed wound rotor.

It follows from Eq. (57-77) for the *main flux reactance* ( $k_2 = 0$ ), per bar,

$$x_{m2(\nu' = p/2)} = 0.8Q_2f_1 \frac{\tau l_e}{pgk_c k_s} K_{s k(\nu' = p/2)}^2 \times 2.54 \times 10^{-8} \text{ ohm per bar,} \quad (57-81)$$

**57-11. Harmonic leakage of a squirrel-cage winding with respect to the harmonic  $\mu' = \nu'$ .** Consider the harmonic chart of Art. 57-7. The  $\nu'$ -th stator harmonic, for example,  $\nu' = +14$ , produces a horizontal row of rotor harmonics  $\mu' = +14, +74, -46 \dots$ . The rotor harmonic  $\mu' = +14$  is the main wave with respect to  $\nu' = +14$ , just as  $\mu' = +2$  is the main wave with respect to  $\nu' = +2$ . It will be shown in the next chapter that any harmonic  $\nu'$  produces with the corresponding harmonic  $\mu'$  of the column  $k_2 = 0$  a torque characteristic of the same shape as the main wave. With respect to this harmonic pair, all other rotor harmonics of the same horizontal row constitute the harmonic leakage. Using the same example, the harmonics  $\mu' = +74, -46 \dots$  are leakage fluxes with respect to the pair  $\nu' = +14$  and  $\mu' = +14$ . This is exactly the same as with the main waves: there the harmonics  $\mu' = +62, -58 \dots$  are leakage fluxes.

The harmonic leakage reactance of the rotor with respect to the  $\nu'$ -th harmonic, per bar, is found from Eq. (57-77) by inserting into the sum  $(\nu'/\frac{1}{2}p)$  for 1, because for the  $\nu'$ -th harmonic  $\mu = (k_2Q_2/\frac{1}{2}p) + (\nu'/\frac{1}{2}p)$ . Thus

$$x_{h2\nu'} = 0.8Q_2f_1 \frac{\tau l_e}{pgk_c} K_{s k\nu'}^2 \times 2.54 \times 10^{-8} \sum_{k_2 \neq 0} \left( \frac{1}{(k_2Q_2/\frac{1}{2}p) + (\nu'/\frac{1}{2}p)} \right)^2 \text{ ohm per bar} \quad (57-82)$$

or

$$x_{h2\nu'} = 0.2Q_2f_1 \frac{p\tau l_e}{gk_c} K_{s k\nu'}^2 \times 2.54 \times 10^{-8} \sum_{k_2 \neq 0} \left( \frac{1}{k_2Q_2 + \nu'} \right)^2 \text{ ohm per bar} \quad (57-83)$$

Again, through the consideration of the magnetic energy of the gap, it is found that

$$\sum_{k_2 \neq 0} \left( \frac{1}{k_2Q_2 + \nu'} \right)^2 = \frac{1}{\nu'^2} \left( \frac{1}{\xi_{2\nu'}^2 K_{s k\nu'}^2} - 1 \right) \quad (57-84)$$

where

$$\xi_{2\nu'} = \frac{\sin(\nu'\pi/Q_2)}{\nu'\pi/Q_2} \quad (57-85)$$

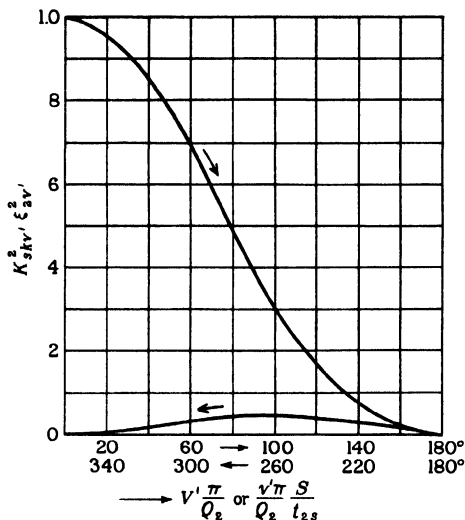


FIG. 57-16. The factors  $\xi_{2v'}^2$ , and  $K_{skv'}^2$  as a function of  $v' \frac{\pi}{Q_2}$  and  $v' \frac{\pi S}{Q_2 \tau_{2s}}$ .

The quantities  $\xi_{2v'}^2$  and  $K_{skv'}^2$  as functions of  $v' \pi / Q_2$  and  $(v' \pi / Q_2) \times (S / \tau_{2s})$  (see Eq. (56-76)), respectively, are given in Fig. 57-16.

The main flux reactance, per bar, follows from Eq. (57-82) with  $k_2 = 0$ .

$$x_{m2v'} = 0.2 Q_2 f_1 \frac{p \tau l_e}{g k_c} K_{skv'}^2 \frac{1}{v'^2} \times 2.54 \times 10^{-8} \quad \text{ohm per bar} \quad (57-86)$$

**57-12. Summary of main flux reactances and harmonic (differential) leakage reactances.** (a) *Stator windings.* The main flux reactance for  $v' = p/2$ ,  $x_{m1}(v' = p/2)$ , is given by Eq. (57-72) which applies to  $q = \text{integer}$  and  $q = \text{fractional number}$ . The main flux reactance with respect to any harmonic  $v'$  is given by Eq. (57-73) which also applies to  $q = \text{integer}$  and  $q = \text{fractional number}$ . From Eqs. (57-59) and (57-72), the harmonic leakage reactance is given for  $q = \text{integer}$  by the equation

$$x_{h1} = x_{m1}(v' = p/2) \left[ \sum_{v \neq 1} \left( \frac{k_{dp1v}}{v} \right)^2 / k_{dp1}(v' = p/2) \right] \quad \text{ohm per phase} \quad (57-87)$$

The value of  $\Sigma$  is given in Fig. 57-13. For  $q = \text{fractional number}$ , from Eqs. (57-68) to (57-70) and Eq. (57-72)

$$x_{h1} = x_{m1}(v' = p/2) [A / k_{dp1}(v' = p/2)] \quad \text{ohm per phase} \quad (57-88)$$

The values of  $A$  for  $\beta = \text{odd number}$  and  $\beta = \text{even number}$  are given in Fig. 57-14.

(b) *Rotor Windings.* For the wound rotor with  $q$ =integer and without skew, the main flux reactance for  $\nu' = p/2$ ,  $x_{m2(\nu'=p/2)}$ , is given by Eq. (57-76). From this equation and Eq. (57-75), the *harmonic* leakage reactance with respect to  $\nu' = p/2$  is given by the equation

$$x_{h2} = x_{m2(\nu'=p/2)} \left[ \sum_{\mu \neq 1} \left( \frac{k_{d p 2 \mu}}{\mu} \right)^2 / k_{d p 2(\mu=p/2)}^2 \right] \text{ ohm per phase} \quad (57-89)$$

For the influence of skewing see Art. 57-10. The value of  $\Sigma$  is given in Fig. 57-13.

The main flux reactance of a squirrel-cage winding for  $\nu_1 = p/2$ ,  $x_{m2(\nu'=p/2)}$ , is given by Eq. (57-81). The harmonic leakage reactance with respect to  $\nu' = p/2$ , which is given by the first horizontal row of the harmonic chart, is according to Eqs. (57-77) and (57-81)

$$x_{h2(\nu'=p/2)} = x_{m2(\nu'=p/2)} \times \sum_{k_2 \neq 0} \left( \frac{1}{(k_2 Q_2 / \frac{1}{2}) p + 1} \right)^2 \text{ ohm per bar} \quad (57-90)$$

The values of  $\Sigma$  for different values of  $S/\tau_{2s}$  are given in Fig. 57-15. The main flux reactance of a squirrel-cage winding with respect to any harmonic  $\nu' > p/2$ ,  $x_{m2\nu'}$ , is given by Eq. (57-86). The *harmonic* leakage reactance of a squirrel-cage winding with respect to the harmonic  $\nu' > p/2$  is determined by the corresponding horizontal row of the harmonic chart and is, according to Eqs. 57-83, 57-84 and 57-86

$$x_{h2\nu'} = x_{m2\nu'} \left( \frac{1}{\xi_{2\nu'}^2 K_{sk\nu'}^2} - 1 \right) \text{ ohm per bar} \quad (57-91)$$

The values of  $\xi_{2\nu'}^2$ , and  $K_{sk\nu'}^2$  are given in Fig. 57-16.

*Reduction factors to the primary.* The reduction factors of the secondary reactances and resistances to the primary are:

(a) Wound rotor, with respect to the wave  $\nu' = p/2$ ,

$$RF = \frac{m_1}{m_2} \left( \frac{N_1 k_{d p 1(\nu'=p/2)}}{N_2 k_{d p 2(\nu'=p/2)}} \right)^2 \quad (57-92)$$

(b) Squirrel-cage rotor, with respect to the wave  $\nu' = p/2$ ,

$$RF = \frac{4m_1(N_1 k_{d p 1(\nu'=p/2)})^2}{Q_2 K_{sk(\nu'=p/2)}^2} \quad (57-93)$$

and squirrel-cage rotor with respect to any wave  $\nu'$

$$RF = \frac{4m_1(N_1 k_{d p 1\nu'})^2}{Q_2 K_{sk\nu'}^2} \quad (57-94)$$

**57-13. Influence of the slot openings (Ref. K2).** The previous considerations are based on the assumption that the slot openings reduce all harmonics, stator as well as rotor harmonics, in the ratio  $1/k_c$ , where  $k_c = k_{c1} \times k_{c2}$ . For

example, Eq. 56-14 has been derived from Eq. 56-11 by multiplying the mmf by the factor  $0.4\pi[3.19/(gk_c k_s)]$ .  $gk_c$  represents the *average* gap. Considering the *stator*, the variation of the gap, due to the slot-openings above and below the average value, can be represented in the form

$$\frac{1}{g} = \frac{1}{gk_c} \left[ 1 + \epsilon_1 \cos Q_1 \frac{\pi}{(p/2)\tau} x_1 + \epsilon_2 2Q_1 \frac{\pi}{(p/2)\tau} x_1 + \dots \right] \quad (57-95)$$

This equation assumes, as before, a fundamental with the wave length equal to  $2p\tau$  ( $\pi$  is assigned to  $p/\tau$ ). With respect to this fundamental, the stator slot openings represent harmonics of the order  $Q_1, 2Q_1, \dots$ . Introducing Eq. 57-95 into Eq. 56-45 which applies to integral as well as to fractional-slot windings, Eq. 56-44 yields

$$b_{\nu'} = 0.45m_1 \frac{1}{\nu'} N_1 k_{ap1\nu'} \frac{3.19}{gk_c} I_1 D_{\nu'} \sin \left( \omega t - \frac{\nu'}{p/2} \frac{x_1}{\tau} \pi \right) \\ \times \left[ \epsilon_1 \cos Q_1 \frac{\pi}{(p/2)\tau} x_1 + \epsilon_2 \cos 2Q_1 \frac{\pi}{(p/2)\tau} x_1 + \dots \right] \quad (57-96)$$

$D_{\nu'}$  is the damping factor of the  $\nu'$ -th harmonic (see Art. 57-8). With the abbreviation

$$0.45m_1 \frac{1}{\nu'} N_1 k_{ap1\nu'} \frac{3.19}{gk_c} I_1 = A_{\nu'} \quad (57-97)$$

$$b_{\nu'} = A_{\nu'} D_{\nu'} \sin \left( \omega t - \frac{\nu'}{p/2} \frac{x_1}{\tau} \pi \right) \\ + A_{\nu'} D_{\nu'} \sum_{\lambda=1, 2, 3, \dots} \epsilon_{\lambda} \cos \left( 2Q_1 \frac{\pi}{(p/2)\tau} x_1 \right) \times \sin \left( \omega t - \frac{\nu'}{p/2} \frac{x_1}{\tau} \pi \right)$$

or

$$b_{\nu'} = A_{\nu'} D_{\nu'} \sin \left( \omega t - \frac{\nu'}{p/2} \frac{x_1}{\tau} \pi \right) \\ + A_{\nu'} D_{\nu'} \sum_{\lambda=1, 2, 3, \dots} \frac{\epsilon_{\lambda}}{2} \left[ \sin \left\{ \omega t - (-\lambda Q_1 + \nu') \frac{\pi}{(p/2)\tau} x_1 \right\} \right. \\ \left. + \sin \left\{ \omega t - (\lambda Q_1 + \nu') \frac{\pi}{(p/2)\tau} x_1 \right\} \right] \quad (57-98)$$

The first term is identical with Eq. 56-44. The second term is the result of the variation of the gap above and below the average value, produced by the slot openings. It represents a series of pairs of traveling waves with the orders

$$\nu'_{s2} = -\lambda Q_1 + \nu' \quad \text{and} \quad \nu'_{s0} = +\lambda Q_1 + \nu'. \quad (57-99)$$

Their respective velocities with respect to the stator are (see Art. 56-1)

$$v_{1\nu''} = \frac{p/2}{-\lambda Q_1 + \nu'} \frac{\tau}{\pi} \omega \quad \text{and} \quad v_{1\nu''} = \frac{p/2}{+\lambda Q_1 + \nu'} \frac{\tau}{\pi} \omega \quad \lambda = 1, 2, 3 \dots \quad (57-100)$$

These *slot-opening* waves will influence the magnitude of those  $b_{\nu'}$  harmonics with respect to which they are at standstill. These are the stator slot-harmonics. To each stator harmonic  $b_{\nu'}$  there corresponds a series of slot-opening waves. Consider the orders and the velocities of the slot-opening waves which correspond to the *main wave*  $\nu' = p/2$ . The orders are (Eq. 57-99)

$$\nu'_{so} = -\lambda Q_1 + p/2 \quad \text{and} \quad \nu'_{so} = +\lambda Q_1 + p/2 \quad \lambda = 1, 2, 3 \dots \quad (57-101)$$

and the velocities with respect to the stator are (Eq. 57-100)

$$v_{1\nu''} = \frac{p/2}{-\lambda Q_1 + p/2} \frac{\tau}{\pi} \omega \quad \text{and} \quad v_{1\nu''} = \frac{p/2}{+\lambda Q_1 + p/2} \frac{\tau}{\pi} \omega \quad \lambda = 1, 2, 3 \dots \quad (57-102)$$

The orders of the slot harmonics of the stator are (Eq. 56-43)

$$\nu'_{sl} = -cQ_1 + p/2 \quad \text{and} \quad \nu'_{sl} = +cQ_1 + p/2 \quad c = 1, 2, 3 \dots \quad (57-103)$$

and their velocities with respect to the stator are (Eqs. 56-46 and 56-47)

$$v_{1\nu''} = \frac{p/2}{-cQ_1 + p/2} \frac{\tau}{\pi} \omega \quad \text{and} \quad v_{1\nu''} = \frac{p/2}{+cQ_1 + p/2} \frac{\tau}{\pi} \omega \quad c = 1, 2, 3 \dots \quad (57-104)$$

Comparing Eqs. 57-101 and 57-102 with Eqs. 57-103 and 57-104, it is seen that the slot-opening waves of first order ( $\lambda = 1$ ) are at standstill with respect to the slot-harmonics of first-order ( $c = 1$ ), that the slot-opening waves of second order ( $\lambda = 2$ ) are at standstill with respect to the slot-harmonics of second order ( $c = 2$ ), and so forth. Normally, only  $\lambda = 1$  and  $\lambda = 2$  of the slot-opening waves which correspond to the main wave ( $\nu' = p/2$ ) have to be considered.

The damping factor of the main wave is  $D_{(\nu'=p/2)} = I_m/I_1$  (Art. 57-8). It follows from Eq. 57-98 for the slot-opening waves which correspond to the main wave  $\nu' = p/2$  (Eq. 57-101)

$$b_{so} = A_{(\nu'=p/2)} \frac{I_m \epsilon_\lambda}{I_1} \frac{1}{2} \sin \left[ \omega t - (\mp \lambda Q_1 + p/2) \frac{\pi}{(p/2)\tau} x_1 - \varphi_m \right] \quad (57-105)$$

where the terminal voltage  $V_1$  is used as the reference phasor for the current  $I_m$ .

For the slot harmonics (Eq. 57-103),  $D_{\nu'} \approx 1$  and from Eqs. 56-45 and 57-97

$$b_{sl} = A_{\nu''} \sin \left[ \omega t - (\mp cQ_1 + p/2) \frac{\pi}{(p/2)\tau} x_1 - \varphi_1 \right] \quad (57-106)$$

where again the terminal voltage  $V_1$  is used as reference for the current  $I_1$ .

The slot-opening waves  $b_{so}$  (Eq. 57-105) and the slot-harmonics  $b_{sl}$  (Eq. 57-106) which for equal values of  $\lambda$  and  $c$  are at standstill with respect to each other, are out of phase by the angle  $\varphi_m - \varphi_1$ . The magnitude of the harmonics is important either at large slip, where the parasitic torques occur (see Chap. 58) or at the rated slip, where the magnetic noise occurs (see Chap. 59). At large slips the magnetizing current  $I_m$  is small and the influence of the slot-openings can be neglected. At the rated slip the angle  $\varphi_m - \varphi_1$  is about  $65^\circ$  and it can be assumed, with satisfactory accuracy with respect to the noise level, that the amplitudes of  $b_{so}$  and  $b_{sl}$  add up under  $90^\circ$ . Thus,

$$B_{res} = \sqrt{B_{so}^2 + B_{sl}^2} \quad (57-107)$$

The amplitudes  $B_{so}$  and  $B_{sl}$  are given by Eqs. 57-105, 57-106, and 57-97. The value of  $\epsilon_\lambda$  for  $\lambda = 1$  and 2 is given at the end of this article.

The influence of the stator slot-openings has not been investigated till now and it has been found that the slot-opening waves which correspond to the main wave  $\nu' = p/2$  increase the stator slot-harmonics (Eq. 57-107). With the same considerations as before, i.e., introducing  $Q_2$  instead of  $Q_1$  into Eq. 57-95, it will be found that the slot-openings of the rotor produce waves which increase the rotor slot-harmonics. From Eqs. 56-33, 56-60, 56-51, 56-54, and 56-55

$$b_{\mu'} = B_{\mu'} \sin \left[ \left\{ 1 + \left( \frac{\mu' - \nu'}{p/2} \right) (1 - s) \right\} \omega t - \frac{\mu'}{p/2} \frac{x_1}{\tau} \pi \right] \quad (57-108)$$

where

$$\mu' - \nu' = k_2 m_2 (p/2) \quad \text{for the wound rotor} \quad (57-109)$$

$$\mu' - \nu' = k_2 Q_2 \quad \text{for the squirrel-cage rotor} \quad (57-110)$$

and

$$B_{\mu'} = 0.45 m_2 \frac{1}{\mu'} N_2 k_{a p 2 \mu'} \frac{3.19}{g k_c k_s} I_{2\nu'} \quad \text{wound rotor} \quad (57-111)$$

$$B_{\mu'} = 0.45 \frac{Q_2}{2} \frac{1}{\mu'} \frac{3.19}{g k_c k_s} I_{2\nu'} \quad \text{squirrel-cage rotor} \quad (57-112)$$

$k_s = 1$  for the harmonics. The current  $I_{2\nu'}$  is given by Eq. 56-78. For the slot-harmonics, the quantity  $r_{2\nu'}/s_\nu x_{m 2\nu'}$  can be neglected.

Then

$$I_{2\nu'} = - \frac{1}{1 + \tau_{2\nu'}} I'_{1\nu'} \quad (57-113)$$

In this equation  $I_{2\nu'}$  appears to be in-phase with  $I_1$  (see Eqs. 56-77 and 56-77a). Since  $I_{2\nu'}$  lags  $I_1$  by the angle  $\psi_\nu$  (Eq. 56-80), this angle must be introduced into Eq. 57-108.

Thus

$$b_{\mu'} = B_{\mu'} \sin \left[ \{ 1 + k_2 m_2 (1 - s) \} \omega t - \frac{\mu'}{p/2} \frac{x_1}{\tau} \pi + \psi_{\nu'} - \varphi_1 \right] \quad (57-114)$$

for the wound rotor and

$$b_{\mu'} = B_{\mu'} \sin \left[ \left\{ 1 + \frac{k_2 Q_2}{p/2} (1-s) \right\} \omega t - \frac{\mu'}{p/2} \frac{x_1}{\tau} \pi + \psi_{\nu'} - \varphi_1 \right] \quad (57-115)$$

for the squirrel-cage rotor. In these equations  $B_{\mu'}$  is in-phase with  $I_1$  and the angle  $\varphi_1$  is introduced for the same reason as before (Eq. 57-106). Since the slot-harmonics are under consideration, for  $\mu'$  the quantity

$$\mu_{s1}' = \mp cQ_2 + p/2$$

has to be introduced in Eqs. 57-111, 57-112, 57-114 and 57-115. With  $r_{2\nu'}$  neglected,  $\psi_{\nu'} = \pi$  (Eq. 56-80).

The amplitude of the slot-opening waves which corresponds to the main wave is given by the same factors as in the previous consideration, namely, by  $A_{(\nu'=p/2)} (I_m/I_1) (\epsilon_\lambda/2)$ .  $\epsilon_\lambda$  is different from that of the stator. With this amplitude, there follows from Eqs. 57-108 to 57-110

$$b_{so} = A_{(\nu'=p/2)} \frac{I_m \epsilon_\lambda}{I_1} \frac{1}{2} \sin \left[ \{1 + k_2 m_2 (1-s)\} \omega t - (\mp \lambda Q_2 + p/2) \frac{\pi}{p/2} \frac{x_1}{\tau} - \varphi_m \right] \quad (57-116)$$

for the wound rotor and

$$b_{so} = A_{(\nu'=p/2)} \frac{I_m \epsilon_\lambda}{I_1} \frac{1}{2} \sin \left[ \left\{ 1 + \frac{k_2 Q_2}{p/2} (1-s) \right\} \omega t - (\mp \lambda Q_2 + p/2) \frac{\pi}{p/2} \frac{x_1}{\tau} - \varphi_m \right] \quad (57-117)$$

for the squirrel-cage rotor. The angle  $\pi - \varphi_1 - \varphi_m$  is approximately equal to  $65^\circ$  so that again with satisfactory accuracy with respect to the noise level

$$B_{res} = \sqrt{B_{so}^2 + B_{s1}^2} \quad (57-118)$$

$B_{so}$  is given by Eq. 57-116 or 57-117.  $B_{s1}$  is given by Eq. 57-111 for the wound rotor and by Eq. 57-112 for the squirrel-cage rotor with

$$\mu' = \mu_{1'} = \mp cQ_2 + p/2.$$

The magnitude of  $\epsilon_\lambda$  depends upon the ratio of slot-opening and slot-pitch and upon the ratio of slot-opening and gap. There is (Ref. K2)

$$\epsilon_1 = k_{(\lambda=1)} \delta k_c \quad (57-119)$$

$$\epsilon_2 = k_{(\lambda=2)} \delta k_c.$$

$\delta$ , determined by the method of conformal mapping, gives the depth of the flux ripple.  $k_{(\lambda=1)}$  and  $k_{(\lambda=2)}$  were determined by resolving the flux ripple into a Fourier series.  $k_c = k_{c1} \times k_{c2}$  is the Carter factor. Fig. 57-17 shows  $\delta$  as a function of the ratio of slot-opening and air gap ( $b_o/g$ ). Fig. 57-18 shows  $k_{(\lambda=1)}$  and  $k_{(\lambda=2)}$  as a function of slot-opening and slot-pitch ( $b_o/\tau_s$ ).



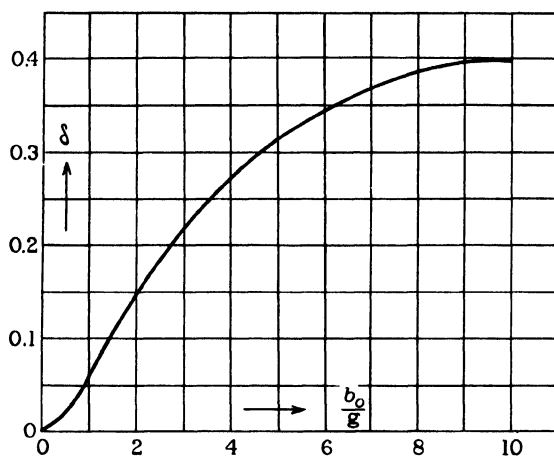


FIG. 57-17.  $\delta$  as a function of the ratio of slot-opening and air gap ( $b_o/g$ ).

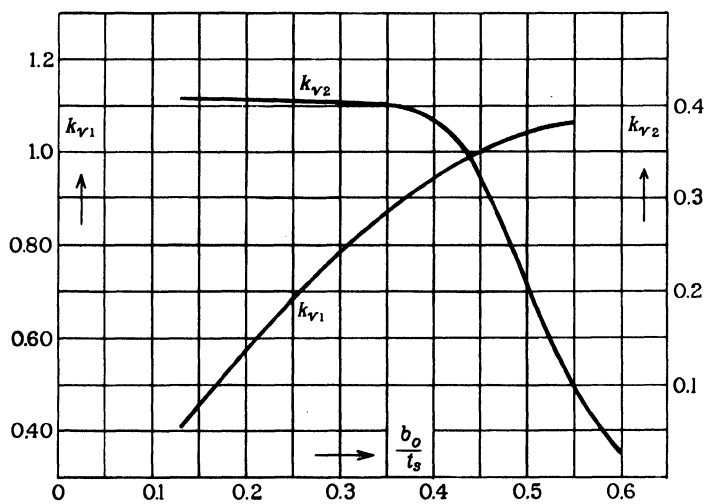


FIG. 57-18. Factors  $k_{\lambda=1}$  and  $k_{\lambda=2}$  as a function of the ratio of slot-opening and slot-pitch ( $b_o/\tau_s$ ).

## Chapter 58

### PARASITIC TORQUES OF THE POLYPHASE INDUCTION MOTOR

**58-1. Parasitic tangential forces and parasitic torques.** It was explained in Art. 1-2d, that the magnetic field in conjunction with current-carrying conductors produces tangential forces and torques. Resolving the magnetic field of the induction motor into a Fourier series, only the main (synchronous) wave will produce the useful tangential force and torque while *the harmonics will produce parasitic tangential forces and parasitic torques*. It has been shown in Chap. 24 that these parasitic torques may cause considerable distortion of the speed-torque curve produced by the main wave.

In the induction motor, the rotor is not connected to the line. The main (synchronous) mmf wave of the stator produces an mmf wave in the rotor which has the *same number of poles* as the stator wave and which is at standstill with respect to the stator wave at *any speed* of the rotor (see Chap. 17). This produces the useful torque of the motor. A torque of this kind is called an *asynchronous torque*.

In the synchronous machine, the stator as well as the rotor are connected to sources of current. As in the induction motor, both machine parts must have the *same number of poles* in order for a uniform useful torque to be produced by the machine. However, due to the fact that both machine parts are connected to different sources of power, a uniform torque is possible only at a *single speed* of the rotor. A torque produced in this manner is called a *synchronous torque*.

The harmonics produce asynchronous as well as synchronous torques in the induction motor. An asynchronous torque will occur when a stator harmonic produces a rotor harmonic of the same order, i.e., of the same number of poles as the stator harmonic, and which is at standstill with respect to the stator harmonic at *all* rotor speeds. A synchronous torque will occur when a stator harmonic  $\nu'_a$  produces a rotor harmonic  $\mu'_a$  which has the same order as *another* stator harmonic  $\nu'_b$  (i.e.,  $\mu'_a = \pm \nu'_b$ ), and which at a *single* rotor speed is at standstill with respect to this second harmonic  $\nu'_b$ .  $\nu'_a$  is the source of excitation of the rotor,  $\nu'_b$  the source of power of the stator. If the harmonic  $\mu'_a$  is at standstill with respect to the harmonic  $\nu'_b$  when the motor speed is

zero ( $n=0, s=1$ ) the synchronous torque is called a *locking torque* or *dead point*.

(a) It can be seen from the harmonic chart in Art. 57-7 that the rotor harmonics which correspond to  $k_2=0$ , i.e., the first column of the rotor harmonics, have the same orders as the stator harmonics producing them. If these rotor harmonics are at standstill with regard to the stator harmonics producing them at any value of  $s$ , the torques produced by the  $k_2=0$  rotor harmonics are asynchronous torques. Consider the  $\nu'_a$ -th stator harmonic, and the  $\mu'_a$ -th rotor harmonic produced the  $\nu'_a$ -th stator harmonic ( $\mu'_a=\nu'_a$ ). The speed of the  $\nu'_a$ -th stator harmonic with respect to the stator is Eq. 56-46

$$v_{1\nu'_a} = \frac{p/2}{\nu'_a} v_{1(\nu'=p/2)}$$

The speed of the  $\mu'_a$ -th rotor harmonic with respect to the stator is (Eq. 56-56)

$$v_{1\mu'_a} = \frac{p/2}{\mu'_a} \left[ 1 + \frac{\mu'_a - \nu'_a}{p/2} (1-s) \right] v_{1(\nu'=p/2)}$$

In order that  $v_{\mu'_a} = v_{1\nu'_a}$ , the condition to be satisfied is

$$\frac{\mu'_a - \nu'_a}{p/2} (1-s) = 0, \quad (58-1)$$

and since  $\mu'_a = \nu'_a$  this equation is satisfied for all values of  $s$ . Thus the first column of the rotor harmonics, i.e., the column which corresponds to  $k_2=0$ , produces asynchronous torques.

(b) In order that a synchronous torque occur, there must be

$$\mu'_a = \pm \nu'_b \quad \text{and} \quad v_{\mu'_a} = v_{\nu'_b}.$$

From Eq. 56-56 again

$$v_{1\mu'_a} = \frac{p/2}{\mu'_a} \left[ 1 + \frac{\mu'_a - \nu'_a}{p/2} (1-s) \right] v_{1(\nu'=p/2)},$$

and from Eq. (56-46)

$$v_{1\nu'_b} = \frac{p/2}{\nu'_b} v_{1(\nu'=p/2)}$$

When  $\mu'_a = +\nu'_b$ , the condition  $v_{1\mu'_a} = v_{1\nu'_b}$  is satisfied when

$$1 = 1 + \frac{\mu'_a - \nu'_a}{p/2} (1-s) \quad \text{or} \quad \frac{\mu'_a - \nu'_a}{p/2} (1-s) = 0. \quad (58-2)$$

Since  $k_2 \neq 0$ ,  $\mu'_a \neq \nu'_a$ . Hence a synchronous torque will occur at  $\mu'_a = +\nu'_b$  only when  $s=1$ . Therefore, if a stator harmonic  $\nu'_a$  produces a rotor har-

monic  $\mu'_a \neq \nu'_a$  and there exists another stator harmonic  $\nu'_b = +\mu'_a$ , the harmonics  $\mu'_a$  and  $\nu'_b$  will produce a synchronous torque at standstill, i.e., a locking torque.

(c) When  $\mu'_a = -\nu'_b$ , the condition  $v_{1\mu'_a} = v_{1\nu'_b}$  is satisfied when

$$-1 = 1 + \frac{\mu'_a - \nu'_a}{p/2} (1-s) \quad (58-3)$$

Since  $\mu'_a \neq \nu'_a$ , a synchronous torque will occur at  $\mu'_a = -\nu'_b$  only when

$$s = 1 + \frac{p}{\mu'_a - \nu'_a} \quad (58-4)$$

Introducing the speed  $n$  instead of the slip and also Eq. 56-57, there results

$$n = -\frac{240f_1}{k_{2a}m_2p} \quad \text{for the wound rotor,} \quad (58-5)$$

$$n = -\frac{120f_1}{k_{2a}Q_2} \quad \text{for the squirrel-cage rotor}$$

Thus, if a stator harmonic  $\nu'_a$  produces a rotor harmonic  $\mu'_a = \nu'_a$  and there exists another stator harmonic  $\nu'_b = -\mu'_a$ , the harmonics  $\mu'_a$  and  $\nu'_b$  will produce a synchronous torque at the fixed speed given by Eq. (58-5). If the harmonic  $\mu'_a$  corresponds to a negative  $k_{2a}$ , the synchronous cusp will occur at positive  $n$  ( $s < 1$ ); if the harmonic  $\mu'_a$  corresponds to a positive  $k_{2a}$ , the synchronous cusp will occur at a negative  $n$  ( $s > 1$ ).

The asynchronous parasitic torques have a torque-slip characteristic of the same shape as that of the main wave (Fig. 24-1). The pull-out torque occurs at a slip different from that of the main wave. The asynchronous parasitic torques appear as dips in the torque-slip characteristic of the motor; the synchronous parasitic torques appear as cusps (Fig. 24-2). The dips and cusps occur at high slips. Consider the harmonic chart of Art. 57-7. As stated under (a) the first column of the rotor harmonics, i.e., all harmonics obtained for  $k_2 = 0$ , will produce asynchronous torques with the corresponding stator harmonics. The main wave  $\nu'_a = +2$  produces the rotor slot harmonic  $\mu'_a = -58$  and another stator harmonic exists which has the same order as  $\mu'_a$ , namely,  $\nu'_b = -58$ . Since  $\nu'_b$  and  $\mu'_a$  have the same signs, they will produce a synchronous torque at standstill, i.e., a locking torque. The harmonic chart shows many combinations which will give locking torques. Thus the slot combination 72/60 in a 4-pole machine should be avoided.

The slot combinations 72/58 and 72/56 in the same 4-pole machine yield the harmonic charts following:

Stator harmonics	$Q_2 = 58$			$Q_2 = 56$		
	$k_2 = 0$	$k_2 = +1$	$k_2 = -1$	$k_2 = 0$	$k_2 = +1$	$k_2 = -1$
$\nu' = +2$	+2	+60	-56	+2	+58	-54
-10	-10	+48	-68	-10	+46	-66
+14	+14	+72	-44	+14	+70	-42
-22	-22	+36	-80	-22	+34	-78
+26	+26	+84	-32	+26	+82	-30
-34	-34	+24	-92	-34	+22	-90
+38	+38	+96	-20	+38	+94	-18
-46	-46	+12	-104	-46	+10	-102
+50	+50	+108	-8	+50	+106	-6
-58	-58	0	-116	-58	-2	-114
+62	+62	+120	+4	+62	+118	+6
-70	-70	-12	-128	-70	-14	-126
+74	+74	+132	+16	+74	+130	+18

Since  $k_2=0$  yields rotor harmonics of the same order as the stator harmonics for any slot combination, the asynchronous torques cannot be avoided. The slot combination 72/58 does not show any kind of synchronous torques, while the slot combination 72/56 shows synchronous torques during braking ( $s > 1$ ). For example, the main wave  $\nu'_a = +2$  produces the rotor slot harmonic  $\mu'_a = +58$  with  $k_{2a} = +1$ . The latter harmonic will produce a synchronous torque with the stator harmonic  $\nu'_b = -58$ . Since  $\mu'_a = -\nu'_b$  this torque, with  $f_1 = 60$ , will occur at the speed (Eq. 58-5)

$$n = - \frac{120 \times 60}{(+1) \times 56} = -128.5 \text{ rpm}$$

The slot-combination 72/64 in a 4-pole machine produces synchronous cusps at  $s < 1$ .

The three harmonic charts all refer to the squirrel-cage rotor. The parasitic torques are of importance only for this rotor type. The wound rotor motor can be started with its pull-out torque and is able to overcome the detrimental effect of the parasitic torques.

It is seen that the synchronous parasitic torques can be avoided entirely by a proper slot-combination. The asynchronous parasitic torques cannot be avoided but they can be reduced. They are produced mainly by the harmonics of low order (in integral-slot windings by the 5th and 7th harmonics, i.e., by  $\nu' = 5(p/2)$  and  $\nu' = 7(p/2)$  and by the slot harmonics. The magnitude of the harmonics of low order can be reduced by a proper coil span ( $W/\tau$ ) and the influence of the slot harmonics can be reduced by skewing.

When, for manufacturing reasons, the slot combination cannot be chosen

in such a manner that the synchronous parasitic torques are avoided, skewing will reduce the magnitude of the torques.

**58-2. The asynchronous parasitic torques (dips in the torque-slip characteristic).** The torque produced by the main wave has been found to be (Eq. 19-8a)

$$\begin{aligned} T_{(\nu'=p/2)} &= \frac{7.04}{n_s} m_1 I_2'^2 (\nu'=p/2) \frac{r_{2\nu'=p/2}}{s} \\ &= \frac{7.04}{n_s} Q_2 I_2'^2 (\nu'=p/2) \frac{r_{2\nu'=p/2}}{s} \quad \text{lb-ft.} \end{aligned} \quad (58-6)$$

The squirrel-cage rotor does not distinguish between the main wave and the harmonics. Therefore, Eq. 58-6 must also apply to the harmonic torques, if  $\nu'$  is substituted for  $\nu'=p/2$ ,  $s_{\nu'}$  is substituted for  $s$ , and  $n_{s\nu'}$  for  $n_s$ . Thus

$$T_{\nu'} = \frac{7.04}{n_{s\nu'}} Q_2 I_2'^2 \frac{r_{2\nu'}}{s_{\nu'}} \quad \text{lb-ft.} \quad (58-7)$$

The fundamental wave ( $\nu'=1$ ) has the synchronous speed  $n_{s(\nu'=1)} = 120f_1/2$ . Therefore,  $n_{s\nu'} = 120f_1/\nu'$ .  $I_{2\nu'}$  is given by Eq. 56-78. Introducing these equations and  $\omega = 2\pi f_1$  into Eq. 58-7, there results

$$T_{\nu'} = 0.738 \frac{\nu'}{\omega} Q_2 r_{2\nu'} \frac{s_{\nu'} x_{m2\nu'}^2}{r_{2\nu'}^2 + s_{\nu'}^2 (1 + \tau_{2\nu'})^2 x_{m2\nu'}^2} I_1'^2 \quad \text{lb-ft.} \quad (58-8)$$

$I_{1\nu'}$  is given by Eq. 56-77a. It is proportional to  $I_1$ .  $r_{2\nu'}$  is given by Eq. 56-87.

In order to find the maximum torque (pull-out torque) produced by the  $\nu'$ -th harmonic, Eq. 58-8 must be differentiated with respect to  $s_{\nu'}$ .  $I_{1\nu'}$  is a complicated function of  $s_{\nu'}$ . However, since the parasitic torques occur at high slips and the primary current changes little at high slips (see Fig. 20-2), it can be assumed for the differentiation that  $I_{1\nu'}$  is a constant. This yields the slip at which  $T_{\nu'\text{max}}$  occurs, i.e., the pull-out slip of the  $\nu'$ -th harmonic as

$$s_{\nu', \text{p.o.}} \approx \frac{r_{2\nu'}}{(1 + \tau_{2\nu'}) x_{m2\nu'}} \quad (58-9)$$

and the maximum asynchronous torque

$$T_{\nu'\text{max}} = 0.369 \frac{\nu'}{\omega} Q_2 \frac{x_{m2\nu'}}{1 + \tau_{2\nu'}} I_1'^2 \quad \text{lb-ft.} \quad (58-10)$$

$s_{\nu'}$  is the slip of the rotor with respect to the  $\nu'$ -th harmonic. Using Eq. 56-48,  $s_{\nu'}$  can be replaced by  $s$ , the slip of the rotor with respect to the main wave. This yields for the slip of the rotor with respect to the main wave at which  $T_{\nu'\text{max}}$  occurs as

$$s_{\nu', \text{p.o.}} \approx \frac{((\nu'/\frac{1}{2}p) - 1)(1 + \tau_{2\nu'})x_{m2\nu'} + r_{2\nu'}}{(\nu'/\frac{1}{2}p)(1 + \tau_{2\nu'})x_{m2\nu'}} \quad (58-11)$$

When  $r_{s'}$  can be neglected in comparison with the first term of the numerator,

$$s_{\nu', \text{p.o.}} \approx 1 - \frac{p/2}{\nu'} \quad (58-12)$$

Thus the 5th harmonic ( $\nu' = -5p/2$ ) has its pull-out slip at  $s \approx 1.2$  (in the range of operation as a brake) and the 7th harmonic ( $\nu' = +7p/2$ ) has its pull-out slip at  $s \approx 0.86$ .

Figs. 58-1 and 58-2 show examples of asynchronous parasitic torques. Fig. 58-1 represents the results of tests on a 2-speed, 150-hp, 3-phase, 60-

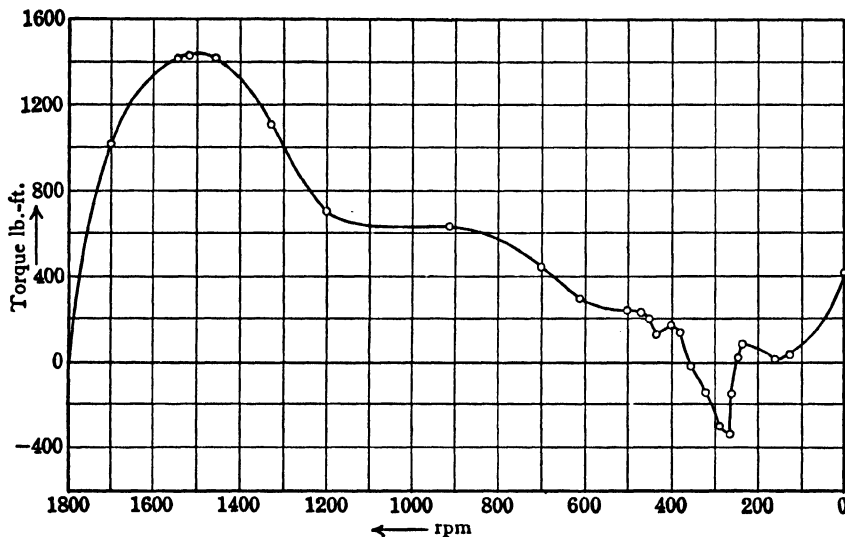


FIG. 58-1. Speed-torque curve of a 2-speed 150-hp 3-phase 60-cycle squirrel-cage motor for 4 and 6 poles. Slot combination 72/87. The torque-speed curve applies to the 4-pole connection.

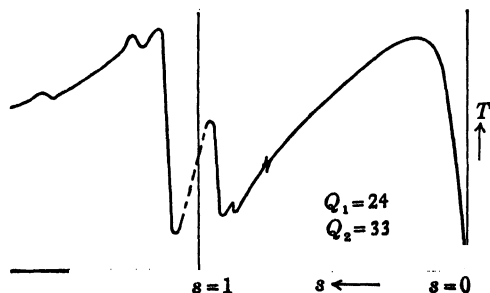


FIG. 58-2. Speed-torque curve of a 3-phase 1.5-hp 4-pole 50-cycle squirrel-cage motor. 24 slots in the stator, 33 slots in the rotor. Rotor not skewed.

cycle squirrel-cage motor with two windings for four and six poles. Slot combination 72/87. The two windings are placed in alternate slots, each winding having 36 coils. The torque-speed curve applies to the 4-pole winding. As can be seen, the motor develops a negative torque at about 265 rpm and is not able to start with the 4-pole connection. Fig. 58-2 represents the test results of a 1.5 hp, 3-phase, 4-pole, 50-cycle squirrel-cage motor. The stator winding is full-pitch, the rotor is not skewed. Slot combination 24/33.

**58-3. The synchronous parasitic torques (cusps in the torque-slip characteristic).** The magnitude of these torques will be determined by means of the law of the force on a current carrying conductor in a magnetic field (Biot-Savart's law). According to this law, the force on a single conductor is (see Eq. 1-28a)

$$f_t = 8.85 \times 10^{-8} B I \sin \alpha \quad \text{lb.} \quad (58-13)$$

In the production of a synchronous torque, the exciter is a  $\nu'_a$ -th harmonic of the stator. This harmonic produces a  $\mu'_a$ -th rotor harmonic which together with another stator harmonic of the order  $\nu'_b = \pm \mu'_a$  causes tangential forces and torque. In accordance with this, in Eq. 58-13 the flux distribution of the  $\mu'_a$ -th rotor harmonic has to be substituted for  $B$  and the ampere-conductor distribution of the  $\nu'_b$ -th stator harmonic for  $I$ .

When the rotor is not skewed,  $\sin \alpha = 1$ . When the rotor is skewed,  $\sin \alpha$  is equal to  $K_{sk\mu'_a}$  (see Art. 56-6).

In order to find the *total* tangential force, an integration over the total circumference of the armature,  $p\tau$ , is necessary. The total force times the armature radius  $p\tau/2\pi$  yields the torque. Thus,

$$T_{sv} = 0.369 \times 10^{-8} \frac{p\tau l_e}{\pi} \int_0^{p\tau} b_{\mu'_a} a_{\nu'_b} dx_1 \quad \text{lb-ft.} \quad (58-14)$$

$a_{\nu'_b}$  is the ampere-conductor distribution of the  $\nu'_b$ -th stator harmonic.

According to Eq. 57-107 and Eqs. 57-104, 56-78 and 56-77a

$$b_{\mu'_a} = B_{\mu'_a} \sin \left[ \left\{ 1 + \frac{k_2 Q_2}{p/2} (1-s) \right\} \omega t - \frac{\mu_a}{p/2} \frac{x_1}{\tau} \pi + \psi_{\nu'_a} \right] \quad (58-15)$$

$$B_{\mu'_a} = 0.45 \frac{1}{\mu'_a} \frac{3.19 m_1 N_1 k_{ap1\nu'_a}}{g k_c} G I_1 \quad (58-16)$$

$$G = \frac{s_{\nu'_a} x_{m2\nu'_a}}{\sqrt{r_{2\nu'_a}^2 + s_{\nu'_a}^2 (1 + \tau_{2\nu'_a})^2 x_{m2\nu'_a}^2}} \quad (58-17)$$

As has been explained in Art. 56-7, the introduction of the angle  $\psi_{\nu'_a}$  into the equation of  $b_{\mu'_a}$  is necessary, if  $B_{\mu'_a}$  is expressed in terms of the primary



current  $I_1$ , because  $B_{\mu'_a}$  is proportional to  $I_{2\nu'_a}$  and  $I_{2\nu'_a}$  lags  $I_1$  by the angle  $\psi_{\nu'_a} = \pi - \alpha_{\nu'_a}$ , where

$$\tan \alpha_{\nu'_a} = \frac{r_{2\nu'_a}}{(1 + \tau_{2\nu'_a})g_{\nu'_a}x_{m2\nu'_a}} \quad (58-18)$$

It is not necessary to introduce in Eq. 58-15 the angle  $\phi_1$ , i.e., to fix the primary current with respect to the primary voltage, as has been done in Eq. 57-107. On the other hand, Eq. 58-15 is not general enough for the computation of synchronous torques. The magnitude of a synchronous torque depends upon the relative position of stator and rotor mmf's. The basis for Eq. 58-15 which is expressed in  $t$  and  $x_1$  is Eq. 56-33 and this latter equation has been derived under the *limiting* assumption that at  $t=0$ ,  $x_2=x_1$  (see Art. 56-2, Fig. 56-2). This assumption which fixes the position of the rotor with respect to the stator must be dropped and Eq. 58-15 generalized. For this purpose it will be assumed that, at  $t=0$ , the system of rotor co-ordinates is shifted with respect to the system of stator co-ordinates by an unspecified arc  $x'_2$  in the direction opposite to that of rotation. Corresponding to this arc for the  $\mu'_a$ -th harmonic is angle  $\mu'_a [\pi/(p/2)] x'_2$  which must be introduced with positive sign into Eq. 58-15. This follows from Eq. 56-32 in which  $x_2$  becomes equal to  $x_2 = x_1 - v_t t - x'_2$  (see also Fig. 56-2).

Since the rotor is shifted in negative direction, the current which the harmonic  $\nu'_a$  induces in the rotor will be advanced by the time angle

$$\nu'_a \frac{\pi}{(p/2)\tau} x'_2.$$

This angle must be introduced in Eq. 58-15 with negative sign. Thus, Eq. 58-15 becomes

$$b_{\mu'_a} = B_{\mu'_a} \sin \left[ \left\{ 1 + \frac{k_2 Q_2}{p/2} (1-s) \right\} \omega t - \frac{\mu'_a x_1}{p/2 \tau} \pi + (\mu'_a - \nu'_a) \frac{\pi}{(p/2)\tau} x'_2 + \psi_{\nu'_a} \right] \quad (58-19)$$

The value of  $B_{\mu'_a}$  is not influenced by the shift of the rotor.

It remains to determine the ampere-conductor distribution  $a_{\nu'_b}$  of the  $\nu'_b$ -th harmonic, in order to be able to evaluate the integral of Eq. 58-14.

The following *rule* applies to any kind of winding, in order to *obtain* its *mmf-curve*: First determine the currents of the different winding groups, then superimpose the currents of the winding groups and obtain the ampere-conductor distribution of the winding; finally, integrate the ampere-conductor distribution. This yields the mmf-curve of the winding. (See Chap. 15, Figs. 15-7 and 15-8.)

It follows from the foregoing that the *mmf-curve* is the *integral curve* of the *ampere-conductor curve*, i.e.,

$$f_x = \int_0^x a_x dx \quad (58-20)$$

Conversely, the ampere-conductor curve can be obtained by differentiation of the mmf-curve. From Eqs. 56-11 and 56-12

$$f_{\nu'} = F_{\nu'} \sin \left( \omega t - \frac{\nu'}{p/2} \frac{x_1}{\tau} \pi \right) \quad (58-21)$$

$$F_{\nu'} = 0.45 m_1 (1/\nu') N_1 k_{dp1\nu'} I_1 \quad (58-22)$$

Therefore,

$$a_{\nu'} = -A_{\nu'} \cos \left( \omega t - \frac{\nu'}{p/2} \frac{x_1}{\tau} \pi \right) \quad (58-23)$$

$$A_{\nu'} = 2\sqrt{2} (1/p\tau) m_1 N_1 k_{dp1\nu'} I_1$$

If the stator slots are skewed with respect to the rotor slots (Art. 56-6), the right side of the last equation must be multiplied by  $K_{sk\mu'}$ . Thus, in general,

$$A_{\nu'} = 2\sqrt{2} (1/p\tau) m_1 N_1 k_{dp1\nu'} K_{sk\mu'} I_1 \quad (58-24)$$

With Eqs. 58-19 and 58-23 and the abbreviations

$$\frac{\pi}{p/2} \frac{x_1}{\tau} = \alpha, \quad \left[ 2 + k_{2a} \frac{Q_2}{p/2} (1-s) \right] \omega t + (\mu'_a - \nu'_a) \frac{\pi}{p/2} \frac{x'_2}{\tau} + \psi_{\nu'_a} = \delta_1 \quad (58-25)$$

$$k_{2a} \frac{Q_2}{p/2} (1-s) \omega t + (\mu'_a - \nu'_a) \frac{\pi}{p/2} \frac{x'_2}{\tau} + \psi_{\nu'_a} = \delta_2$$

Eq. 58-14 for the synchronous torque becomes

$$T_{sv} = -C \int_0^{2\pi} \sin [\delta_1 - (\mu'_a + \nu'_b)] d\alpha - C \int_0^{2\pi} \sin [\delta_2 - (\mu'_a - \nu'_b)] d\alpha \quad (58-26)$$

$$C = \frac{0.369}{4\pi^2} 10^{-8} (p\tau)^2 l_e B_{\mu'_a} A_{\nu'_b} \quad (58-27)$$

When  $\mu'_a = +\nu'_b$ , i.e., the synchronous torque occurs at  $s=1$ , the first integral of Eq. 58-26 becomes equal to 0 and the second integral becomes equal to  $2\pi \sin \delta_2$ . Thus

$$T_{sv(s=1)} = 2\pi C \sin \delta_2 \quad (58-28)$$

When  $\mu'_a = -\nu'_b$ , i.e., the synchronous torque occurs at  $s=1 + (p/k_{2a}Q_2)$  (Eq. 58-4), the first integral becomes equal to  $2\pi \sin \delta_1$  and the second integral to 0. Therefore,

$$T_{sv(s \neq 1)} = 2\pi C \sin \delta_1 \quad (58-29)$$

Introducing into Eq. 58-28 the value of  $\delta_2$  with  $s=1$  from Eq. 58-25, the value of  $\mu'_a - \nu'_a$  from Eq. 56-51, and the value of  $\psi_{\nu'_a}$  from Eq. 56-80

$$T_{sv(s=1)} = 2\pi C \sin \left( k_{2a} \frac{Q_2}{p/2} \frac{\pi}{\tau} x'_2 - \alpha_{\nu'} \right)$$

Introducing into Eq. 58-29 the value of  $\delta_1$  with  $s = 1 + (p/k_{2a}Q_2)$  from Eq. 58-25 and the values of  $\mu'_{a'} - \nu'_{a'}$  and  $\psi_{\nu'_{a'}}$  from the same equations as before, the same equation is obtained for  $T_{syn(s \neq 1)}$  as for  $I_{syn(s=1)}$ . Thus, in general,

$$T_{syn} = 2\pi C \sin \left( k_{2a} \frac{Q_2}{p/2} \frac{\pi}{\tau} x'_2 - \alpha_{\nu'} \right) \quad (58-30)$$

As could be expected, the synchronous torque is independent of the time and depends upon the relative position of stator and rotor mmf's (upon the magnitude of  $x'_2$ ). The maximum value of the synchronous torque is

$$T_{syn, \max} = 2\pi C \quad (58-31)$$

The value of  $C$  is given by Eq. 58-27, the value of  $B_{\nu'_{a'}}$  by Eqs. 58-16 and 58-17, and the value of  $A_{\nu'_{a'}}$  by Eq. 58-24. If in Eq. 58-17  $r^2_{2\nu'_{a'}}$  can be neglected against  $s^2_{\nu'_{a'}}(1 + \tau_{2\nu'_{a'}})^2 x^2_{m2\nu'_{a'}}$ , the value of  $G$  becomes

$$G \approx \frac{1}{1 + \tau_{2\nu'_{a'}}} \quad (58-32)$$

For harmonics of high order, the slot and end-winding leakage reactances may become small in comparison with the harmonic leakage reactance. Then

$$\tau_{2\nu'_{a'}} = \frac{(x_{2s} + x_{2e} + x_{2\lambda})_{\nu'_{a'}}}{x_{m2\nu'_{a'}}} \approx \frac{x_{2h\nu'_{a'}}}{x_{m2\nu'_{a'}}} = \tau_{2h\nu'_{a'}} \quad (58-33)$$

This latter ratio follows from Eqs. 57-83, 57-84, and 57-86 as

$$\tau_{2h\nu'_{a'}} = \frac{1}{\xi^2_{2\nu'_{a'}} K^2_{sk\nu'_{a'}}} - 1 \quad (58-34)$$

and

$$G \approx \xi^2_{2\nu'_{a'}} K^2_{sk\nu'_{a'}} \quad (58-35)$$

The equation for asynchronous parasitic torques was derived in Art. 58-2 from the power of the rotating field. It can also be derived from Eq. 58-14 and the following equations,  $k_{2a} = 0$ ,  $\mu'_{a'} = \nu'_{a'} = \nu'_{b'} = \nu'$ , and the value of  $\alpha_{\nu'}$  is introduced from Eq. 56-80.

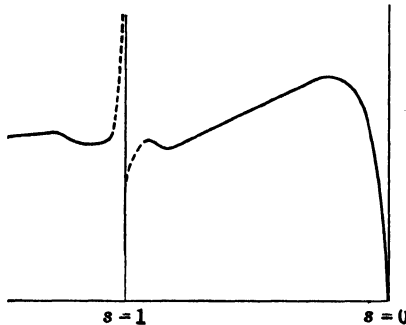


FIG. 58-3. Speed-torque curve of the same motor as in Fig. 58-2. High synchronous cusp (locking torque) at standstill.  $Q_1 = 36$ ;  $Q_2 = 24$ .

Figs. 58-3 to 58-5 represent test results on a 1.5 hp, 3-phase, 4-pole, 50-cycle induction motor with squirrel-cage rotor. The stator winding is full-pitch. The rotor is not skewed. The slot-combination of Fig. 58-3 is 36/24; it produces a synchronous cusp at standstill. The slot-combination of Fig. 58-4 is 36/28; it produces a synchronous cusp at  $s < 1$ . The slot combination of

Fig. 58-5 is 48/44; at  $s > 1$  it produces a very large cusp making the resultant torque negative.

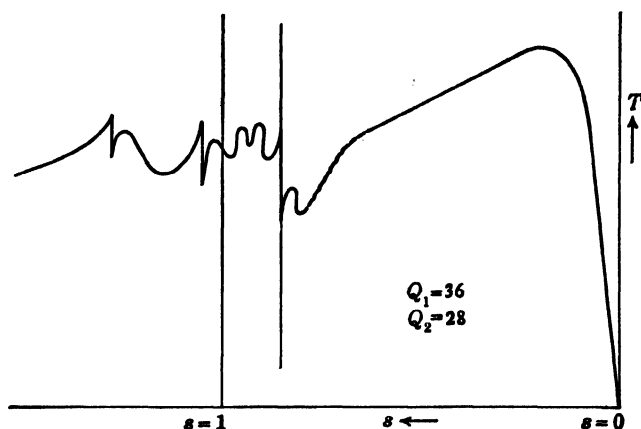


FIG. 58-4. Speed-torque curve of the same motor as in Fig. 58-2. Slot combination 36/28. Large synchronous cusp at  $s < 1$ .

*Influence of Skewing.* It should be pointed out again (see Art. 57-10b) that skewing is fully effective only when the bars are insulated. When the bars are not insulated, the skewing is not fully effective and the asynchronous and synchronous torques due to the slot harmonics are not entirely avoided. A skewed rotor with insulated bars shows a smoother torque-speed characteristic than one with non-insulated bars.

When the bars are not insulated, and especially when they are skewed currents flow between the bars (see Art. 57-10b) which produce additional losses. These losses can be reduced to about  $\frac{1}{2}$  of a per cent of the output by proper chording of the stator winding (Ref. M11a).

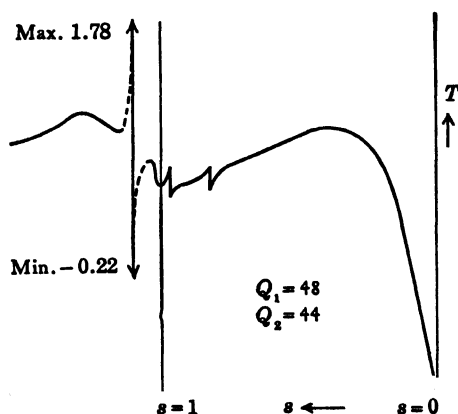


FIG. 58-5. Speed-torque curve of the same motor as in Fig. 58-2. Slot combination 48/44. Synchronous cusp at  $s > 1$ .

## Chapter 59

### RADIAL FORCES, VIBRATION, AND MAGNETIC NOISE IN POLYPHASE INDUCTION MOTORS

**59-1. General considerations.** The driving force of the electrical machine is a tangential force produced by the main flux wave and the main wave of the ampere-conductor distribution. The flux harmonics and the ampere-conductor distribution harmonics produce parasitic tangential forces which distort the torque-speed curve. There are other parasitic forces present in the electric machine, namely *parasitic radial forces*, which under certain circumstances may produce undesirable mechanical vibration and noise (Ref. M13 to 18).

If the induction at a fixed point in the air-gap is  $b$  lines per square inch, the radial force at this point is equal to

$$f_r = 1.385b^2 \times 10^{-8} \text{ lb-in.}^2 \quad (59-1)$$

The induction  $b$  is the sum of all stator and rotor harmonics. Hence  $b^2$  is the sum of the squares of all stator and rotor harmonics, plus twice the product of each stator harmonic with each other stator harmonic, of each rotor harmonic with each other rotor harmonic, and of each stator harmonic with each rotor harmonic.

Let  $n'$  and  $m'$  be the orders of any two harmonic fluxes the general equations of which are given as

$$b_{n'} = B_{n'} \sin \left( \omega_{n'} t - n' \frac{\pi}{(p/2)\tau} x_1 \right) \quad (59-2)$$

$$b_{m'} = B_{m'} \sin \left( \omega_{m'} t - m' \frac{\pi}{(p/2)\tau} x_1 \right) \quad (59-3)$$

According to Eq. (59-1), the radial force produced by these two harmonics is

$$f_r = \text{const} \times \frac{1}{2} B_{n'} B_{m'} \left[ \cos \left\{ (\omega_{n'} - \omega_{m'}) t - (n' - m') \frac{\pi}{(p/2)\tau} x_1 \right\} - \cos \left\{ (\omega_{n'} + \omega_{m'}) t - (n' + m') \frac{\pi}{(p/2)\tau} x_1 \right\} \right] \quad (59-4)$$

i.e., the radial force produced by any two harmonic fluxes consists of two traveling force waves. Comparing Eq. 59-4 with Eq. 56-44, it is seen that one of the two force waves has the angular velocity  $(\omega_n - \omega_m)$  and the order, with respect to a 2-pole fundamental,  $(n' - m')$ ; the other force wave has the angular velocity  $(\omega_n + \omega_m)$  and the order, with respect to the same fundamental,  $(n' + m')$ .

Consider Eq. 56-46 which determines the velocity of propagation of the wave given by Eq. 56-44. Writing Eq. 56-46 in the form

$$v_{1v} = \left( \frac{p\tau}{v'} \right) \frac{\omega}{2\pi},$$

the quantity in the parenthesis is the wave length of the harmonic  $v'(\tau_v)$  and  $\omega/2\pi$  is the number of wave lengths the harmonic travels per second. In the case of the traveling force waves,  $(\omega_n - \omega_m)/2\pi$  and  $(\omega_n + \omega_m)/2\pi$  are the numbers of force-wave lengths the two force waves travel per second. Since the force waves produce vibrations of the stator,  $(\omega_n - \omega_m)/2\pi$  and  $(\omega_n + \omega_m)/2\pi$  are called the *frequencies of the vibrations* (in accordance with  $\omega/2\pi = \text{frequency}$  in Eq. 56-44).

$(n' - m')$  and  $(n' + m')$  are the numbers of the force pole pairs with respect to the two-pole fundamental.

The symbol  $p'$  will be used for the *number of force pole pairs*. In Eq. 59-4, there are two values of  $p'$ , namely,  $p' = n' - m'$  and  $p' = n' + m'$ . As has been shown previously, the harmonics of stator and rotor may have positive as well as negative signs. Therefore, it depends upon the signs of  $n'$  and  $m'$ , which of the two waves has the smaller and which has the larger number of force pole pairs (the smaller or the larger  $p'$ ).

The larger the value of  $p'$ , the shorter is the wave length for a given armature diameter. In general, the stator is stiffer to short-wave distortion ( $p'$  large) than to long-wave distortion ( $p'$  small). Therefore *small values of  $p'$  are to be avoided*. However, vibration and noise depend not only on the value of  $p'$  but also on the mechanical construction and the dimensions of the machine and on the number of poles of the machine, which latter factor determines the depth of the stator core. In a small machine, a value of  $p' = 6$  may be satisfactory. In large machines with fabricated frames, a value of  $p'$  as high as 20 may not be permissible. The fabricated frame behaves like a membrane with many natural frequencies. A cast-iron frame is less sensitive to vibration than a fabricated frame.

Fig. 59-1 shows the distortion of the stator core which corresponds to  $p' = 0, 1, 2$ , and 3. It follows from Eq. 59-4 that, when  $p' = 0$  ( $n' - m' = 0$  or  $n' + m' = 0$ ), the corresponding force is not a traveling wave but a stationary pulsating wave. The stationary force makes the stator diameter all around the machine smaller and larger. This case is seldom disturbing and then only in large machines. The distortion shown in Fig. 59-1 for  $p' > 0$  travels around the machine with the force wave and produces vibrations from which magnetic noise may result. It is seen from this that the frequency

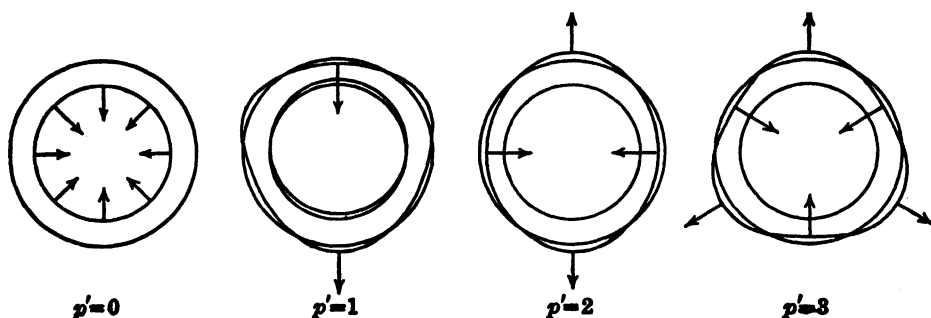


FIG. 59-1. Distortion of stator core for different numbers of force-pole pairs.

of vibration is the frequency of the distortion experienced at a fixed point of the stator.

Eq. 59-4 has been derived for *any* two harmonic fluxes. It, therefore, applies to any two stator harmonic fluxes, to any two rotor harmonic fluxes, and to any combination of a stator harmonic flux with a rotor harmonic flux. These three cases will be considered in turn with respect to the number of force pole pairs ( $p'$ ) and the frequency of vibration.

(a) *Stator harmonics only.* This case is obtained from Eq. 59-4 with  $\omega_n = \omega_m = \omega = 2\pi f_1$  and  $n' = \nu'_a$  and  $m_1 = \nu'_b$ . Thus

$$\begin{aligned} p' &= \nu'_a - \nu'_b & f'_- &= 0 \\ p' &= \nu'_a + \nu'_b & f'_+ &= 2f_1 \end{aligned} \quad (59-5)$$

$f'$  is the frequency of vibration.  $f'_-$  and  $f'_+$  are the frequencies of vibration corresponding to the difference and the sum of  $\nu'_a$  and  $\nu'_b$ , respectively. It is seen from Eq. 59-4 that  $f' = 0$  means a standing wave which does not produce vibrations.

Also, a *single* traveling flux wave of the stator produces a force wave. This case is obtained from Eq. 59-5 with  $\nu'_a = \nu'_b = \nu'$ . Therefore, each traveling flux wave of the stator produces a force wave with

$$p' = 2\nu' \quad f' = 2f_1 \quad (59-6)$$

This applies also to the main flux wave.

Eqs. 59-5 and 59-6 show that stator flux harmonics alone produce force waves of double line frequency. These force waves are seldom disturbing with respect to magnetic noise.

(b) *Rotor harmonics only.* This case is obtained from Eq. 59-4 with  $n' = \mu'_a$ ,  $m' = \mu'_b$  and Eq. 56-33

$$\begin{aligned} \omega_{\mu'_a} - \omega_{\mu'_b} &= \frac{(\mu'_a - \nu'_a) - (\mu'_b - \nu'_b)}{p/2} (1-s) 2\pi f_1 \\ \omega_{\mu'_a} + \omega_{\mu'_b} &= \left[ 2 + \frac{(\mu'_a - \nu'_a) + (\mu'_b - \nu'_b)}{p/2} (1-s) \right] 2\pi f_1 \end{aligned}$$

Thus

$$\begin{aligned} p' &= \mu'_a - \mu'_b & f'_- &= \frac{(\mu'_a - \nu'_a) - (\mu'_b - \nu'_b)}{p/2} (1-s)f_1 \\ p' &= \mu'_a + \mu'_b & f'_+ &= \left[ 2 + \frac{(\mu'_a - \nu'_a) + (\mu'_b - \nu'_b)}{p/2} (1-s) \right] f_1 \end{aligned} \quad (59-7)$$

Inserting Eqs. 56-50 and 56-51

$$\begin{aligned} p' &= \mu'_a - \mu'_b & f'_- &= (k_{2a} - k_{2b})m_2(1-s)f_1 \\ p' &= \mu'_a + \mu'_b & f'_+ &= [2 + (k_{2a} + k_{2b})m_2(1-s)]f_1 \end{aligned} \quad (59-8)$$

for the wound rotor and

$$\begin{aligned} p' &= \mu'_a - \mu'_b & f'_- &= (k_{2a} - k_{2b}) \frac{Q_2}{p/2} (1-s)f_1 \\ p' &= \mu'_a - \mu'_b & f'_+ &= \left[ 2 + (k_{2a} + k_{2b}) \frac{Q_2}{p/2} (1-s) \right] f_1 \end{aligned} \quad (59-9)$$

for the squirrel-cage rotor.  $\mu'_a$ ,  $\mu'_b$ ,  $k_{2a}$ , and  $k_{2b}$  in Eqs. 59-8 and 59-9 can be positive as well as negative.

For the squirrel-cage rotor,  $k_2 = \pm 1$  yields the largest amplitude for the rotor flux harmonic. For this rotor, from Eq. 59-9 with  $k_{2a} = \pm 1$  and  $k_{2b} = \pm 1$

$$f'_- = 0 \quad f'_+ = \left[ 1 \pm \frac{Q_2}{p/2} (1-s) \right] 2f_1 \quad (59-10)$$

when  $k_{2a}$  and  $k_{2b}$  have the same sign and

$$f'_- = \frac{Q_2}{p/2} (1-s)2f_1 \quad f'_+ = 2f_1 \quad (59-11)$$

when  $k_{2a}$  and  $k_{2b}$  have different signs.

For a single rotor harmonic,  $\mu'_a = \mu'_b = \mu'$ ,  $k_{2a} = k_{2b} = k_2$  and from Eqs. 59-8 and 59-9

$$\begin{aligned} p' &= 2\mu' & f'_+ &= [1 + k_2 m_2 (1-s)]2f_1 \\ p' &= 2\mu' & f'_+ &= \left[ 1 + k_2 \frac{Q_2}{p/2} (1-s) \right] 2f_1 \end{aligned} \quad (59-12)$$

The quantity

$$\frac{Qn_s}{60} = \frac{Qf_1}{p/2} \quad (59-13)$$

is called *slot frequency*.

It is seen from Eqs. 59-10 to 59-12 that flux harmonics of the squirrel-cage rotor produce vibrations either of double line frequency or of approximately



double slot frequency. They are normally not disturbing with respect to magnetic noise.

(c) *Combinations of stator and rotor harmonics.* The disturbing magnetic noise in induction motors is produced by combinations of stator and rotor flux harmonics. For these combinations, in Eq. 59-4  $n' = \nu'_b$  and  $m' = \mu'_a$ .  $\mu'_a$  is produced by a stator harmonic  $\nu'_a$ . Eqs. 59-4, 56-13, and 56-33 yield

$$p' = \nu'_b - \mu'_a \quad f'_- = \frac{\mu'_a - \nu'_a}{p/2} (1-s)f_1 \quad (59-14)$$

$$p' = \nu'_b + \mu'_a \quad f'_+ = \left[ 2 + \frac{\mu'_a - \nu'_a}{p/2} (1-s) \right] f_1$$

Inserting the value of  $\mu'_a - \nu'_a$  from Eqs. 56-60 and 56-51,

$$p' = \nu'_b - \mu'_a \quad f'_- = k_{2a} m_2 (1-s) f_1 \quad (59-15)$$

$$p' = \nu'_b + \mu'_a \quad f'_+ = [2 + k_{2a} m_2 (1-s)] f_1$$

for the wound rotor and for the squirrel-cage rotor

$$p' = \nu'_b - \mu'_a \quad f'_- = k_{2a} \frac{Q_2}{p/2} (1-s) f_1 \quad (59-16)$$

$$p' = \nu'_b + \mu'_a \quad f'_+ = \left[ 2 + k_{2a} \frac{Q_2}{p/2} (1-s) \right] f_1$$

It is seen from the Eqs. 59-15 and 59-16 that the frequency of the vibration produced by a stator flux harmonic in combination with a rotor flux harmonic does not depend upon the order of the stator harmonic. It depends upon the value of  $k_{2a}$  and the number of rotor phases, if the rotor is a wound rotor, or upon the number of rotor slots, if the rotor is of the squirrel-cage type.

Several combinations of stator and rotor harmonic fluxes will be considered.

( $\alpha$ ) The rotor harmonic belongs to the first column of the harmonic chart (see Art. 57-7). In this case  $k_{2a} = 0$ ,  $\mu'_a = \nu'_a$  and from Eq. 59-14

$$\begin{aligned} p' &= \nu'_b - \mu'_a & f'_- &= 0 \\ p' &= \nu'_b + \mu'_a & f'_+ &= 2f_1 \end{aligned} \quad (59-17)$$

This is the same as for two stator harmonic fluxes.

( $\beta$ ) The rotor harmonic  $\mu'_a$  is a rotor slot harmonic of first order. In this case, since  $\mu'_{as1}$  is produced by  $\nu'_a = p/2$ , for the wound rotor from Eqs. 56-50 and 56-52

$$\mu'_{as1} = k_{2a} m_2 \frac{p}{2} + \frac{p}{2} = \pm Q_2 + \frac{p}{2} \quad \text{or} \quad k_{2a} m_2 = \frac{\mp Q_2}{p/2}$$

Inserting this into Eq. 59-15

$$p' = \nu'_b - \mu'_a \quad f'_- = \frac{Q_2}{p/2} (1-s) f_1 \quad (59-18)$$

$$p' = \nu'_b + \mu'_a \quad f'_+ = \left[ 2 \pm \frac{Q_2}{p/2} (1-s) \right] f_1$$

The same formulae apply to the squirrel-cage rotor: for the slot harmonics of this rotor  $k_{2a} = \mp 1$ . Eq. 59-16 yields with  $k_{2a} = \mp 1$  Eq. 59-18.

( $\gamma$ )  $\mu'_a$  is a rotor slot harmonic of first order,  $\nu'_b$  is a stator slot harmonic of first order. In this case, from Eqs. 56-43 and 56-52,

$$p'_{s1} = \nu'_{bs1} - \mu'_{as1} = \mp Q_1 \pm Q_2 \quad (59-19)$$

$$p'_{s1} = \nu'_{bs1} + \mu'_{as1} = \mp Q_1 \pm Q_2 + p$$

The smallest absolute values of  $p'_{s1}$  are

$$p'_{s1} = Q_1 - Q_2 \quad (59-20)$$

$$p'_{s1} = Q_1 - Q_2 \pm p$$

The frequencies in this case are the same as under ( $\beta$ ), because the frequencies are independent of the order of the stator harmonic.

The combination under ( $\gamma$ ) where the slot harmonics of stator and rotor are involved is the most dangerous with respect to magnetic noise. For this reason the value of  $p'_{s1}$  given by Eq. 59-20 must be as large as possible.

The frequencies given by Eq. 59-18 are those which appear most often as noise frequencies of induction motors. As can be seen from this equation, these frequencies are approximately slot frequency or approximately slot frequency  $\pm$  twice line frequency.

**59-2. The 2-pole force wave ( $p' = 1$ ).** It has been mentioned that  $p'$  must be as large as possible.  $p' = 1$  must be avoided. The condition under which  $p' = 1$  may occur will be determined for the case (c) considered above, i.e., for the case when the force wave is produced by a combination of a stator flux harmonic and a rotor flux harmonic. In order that  $p' = 1$ , one of the following equations must be satisfied

$$\nu'_b - \mu'_a = \pm 1$$

$$\nu'_b + \mu'_a = \pm 1$$

It follows from Eqs. 56-42, 56-50, and 56-51 that, for  $p' = 1$  the following equations must be satisfied

$$\pm 1 = (k_{1b} - k_{1a})m_1 \frac{p}{2} - k_{2a}m_2 \frac{p}{2} \quad (59-21)$$

$$\pm 1 = [(k_{1b} + k_{1a})m_1 + 2] \frac{p}{2} + k_{2a}m_2 \frac{p}{2}$$

for the wound rotor and

$$\begin{aligned}\pm 1 &= (k_{1b} - k_{1a})m_1 \frac{p}{2} - k_{2a}Q_2 \\ \pm 1 &= [(k_{1b} + k_{1a})m_1 + 2]p/2 + k_{2a}Q_2\end{aligned}\quad (59-22)$$

for the squirrel-cage rotor. For the normally used integral-slot, 2-layer,  $60^\circ$  phase-belt winding,  $k_{1b}$  and  $k_{1a}$  are even integers.  $k_{2a}$  can be even and odd. The first right-hand terms of Eqs. 59-21 and 59-22 are, therefore, even numbers. In order that the left sides of the equations be equal to  $\pm 1$ , the second right-hand terms must be odd numbers. With  $m_2=3$ , this occurs in the wound-rotor motor when  $k_{2a}(p/2)$  is an odd number. In the squirrel-cage rotor this occurs when  $Q_2$  is an odd number. It is advisable to make  $Q_2$  an even number. When  $Q_2$ , for manufacturing reasons, is made an odd number, care must be taken that the amplitude of the  $p'=1$  force wave is small.

By the same reasoning as that applied to the case of the combination of a stator flux harmonic and a rotor flux harmonic, it is found that two stator harmonics of the normally used integral-slot, 2-layer,  $60^\circ$  phase-belt winding cannot produce  $p'=1$ . Two rotor harmonic fluxes of the squirrel-cage rotor may produce  $p'=1$  when the  $Q_2$  is an odd number.

**59-3. Magnitudes of the force waves.**  $p'=1$  represents an unbalanced force (Fig. 59-1) which also produces stresses in the rotor. For all other values of  $p'$ , the forces are balanced.

(a)  $p'=1$  (2-pole force wave). Since the force on each surface element is directed radially, it is necessary, in order to find the resultant force, to determine the sum of the projections of all elementary forces on a diameter, i.e., to integrate the projections over the total armature surface. Eq. 59-1 yields for the amplitude of the force produced by a stator flux harmonic in combination with a rotor flux harmonic

$$F_r = 1.385 \times 10^{-8} \times 2l_s \int_0^{p\tau} b_{\nu_s} b_{\mu_s} \cos \frac{\pi}{(p/2)\tau} x_1 dx_1 \quad (59-23)$$

The factor 2 has to be used when a stator and rotor harmonic are involved (see explanation to Eq. 59-1). For the 2-pole force wave,  $2\pi$  corresponds to  $p\tau$ . Inserting into Eq. 59-23 Eqs. 56-13 (or 56-44), 56-33, 56-50), and 56-51, the integration yields

$$F_{r(p'=1)} = 1.385 \times 10^{-8} \times \frac{\pi}{2} D l_s B_{\nu_s} B_{\mu_s} \text{ lbs.} \quad (59-24)$$

The frequency of this force wave corresponds normally to that of Eq. 59-18, the more general form of which are Eqs. 59-15 and 59-16.

When  $p'=1$  is produced by two rotor harmonic fluxes,  $B_{\mu_s}$  has to be substituted in Eq. 59-24 for  $B_{\nu_s}$  and the frequency is given for the squirrel-cage rotor by Eqs. 59-10 and 59-11.

(b)  $p' = 0$ . This is a uniformly distributed pulsating force the amplitude of which, per inch circumference, is

$$F_{r(p'=0)} = 1.385 \times 10^{-8} l_s B_{\nu'} B_{\mu_a} \text{ lbs. per inch circumference} \quad (59-25)$$

when produced by a stator flux harmonic in combination with a rotor flux harmonic. The frequency is normally given by Eq. 59-18, or, more generally, by Eqs. 59-15 and 59-16.

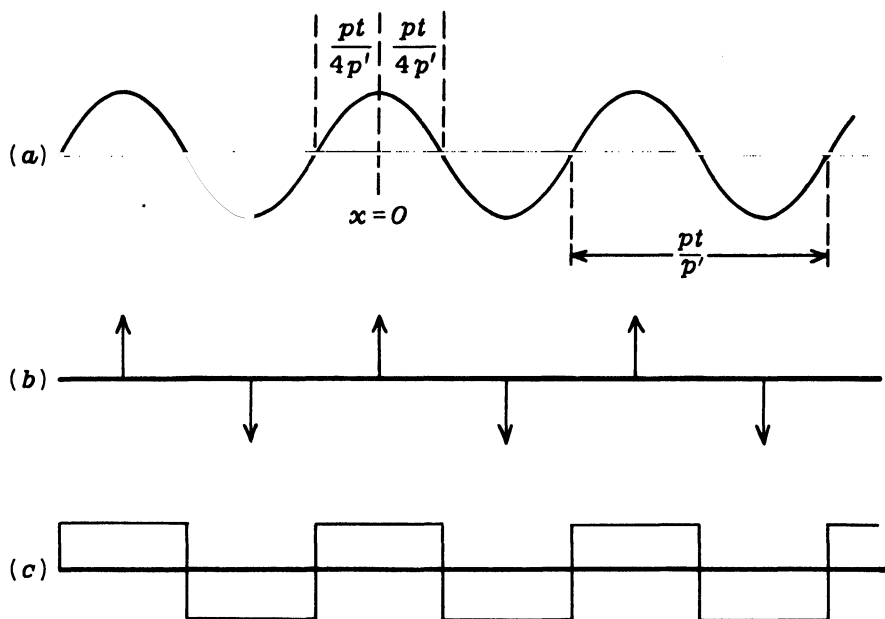


FIG. 59-2. Force wave with  $p' = 4$  as concentrated and as a uniformly distributed force.

(c)  $p' > 1$ . Fig. 59-2a shows a force wave with  $p' = 4$ . The resultant force can be considered either as a concentrated force, as shown in Fig. 59-2b, or as a uniformly distributed force, as shown in Fig. 59-2c, or as a sinusoidally distributed force. In the first case, the sum of the projections of the elementary forces for a force-pole has to be determined; in the second case, the average force over a force-pole has to be taken. For a combination of stator and rotor flux harmonics, the force in the first case is determined by the following equation.

$$F_{r(p'>1)} = 1.385 \times 10^{-8} \times 2l_s \int_{-p\tau/4p'}^{+p\tau/4p'} b_{\nu'} b_{\mu_a} \cos \frac{\pi}{(p/2)\tau} x_1 dx_1 \quad (59-26)$$

The integrand yields a pair of terms with the force order  $\nu_b' + \mu_a'$  and a pair of

terms with the force order  $\nu'_b - \mu'_a$  (see Eq. 59-4). With the same substitutions as for Eq. 59-23, the force per force pole, for each force order, becomes

$$F = 1.385 \times 10^{-8} B_{\nu'_b} B_{\mu'_a} l_e D \times \frac{1}{2} \left[ \frac{1}{p' - 1} \sin \frac{p' - 1}{p'} \frac{\pi}{2} + \frac{1}{p' + 1} \sin \frac{p' + 1}{p'} \frac{\pi}{2} \right] \quad \text{lbs per force pole} \quad (59-27)$$

For  $p' \geq 3$  the expression in the brackets is practically equal to  $2/p'$ .

For the uniform distribution, Fig. 59-2c, and for the sinusoidal distribution, the force per force pole is obtained by integrating Eq. 59-26 without the term  $\cos(\pi/\frac{1}{2}p\tau)x_1$  as

$$F_{r(p' > 1)} = 1.385 \times 10^{-8} \frac{1}{p'} D l_e B_{\nu'_b} B_{\mu'_a} \quad \text{lbs} \quad (59-27a)$$

The frequency of these forces is normally given by Eq. 59-18 or, more generally, by Eqs. 59-15 and 59-16.

For  $p' > 1$  produced by two stator harmonic fluxes,  $B_{\nu'_b}$  has to be substituted for  $B_{\mu'_a}$  in Eqs. 59-27 and 59-27a. The frequency is given by Eq. 59-5.

For  $p' > 1$  produced by a single stator harmonic flux,  $\frac{1}{2}B_{\nu'_b}$  has to be substituted for  $B_{\mu'_a}$  in Eqs. 59-27 and 59-27a and the frequency is given by Eq. 59-6.  $p'$  is then equal to  $2\nu'_b$ .

*The amplitudes  $B_{\nu'_b}$  and  $B_{\mu'_a}$ .* The amplitude  $B_{\nu'_b}$  is given by Eq. 56-45. The damping factor  $D_{\nu'}$  is given by Eq. 57-71. The absolute value of the damping factor is

$$D_{\nu'} = (1 - C_{\nu'} \cos \Theta)^2 + (C_{\nu'} \sin \Theta)^2 \quad (59-28)$$

with

$$C_{\nu'} = \frac{\sqrt{[(s_{\nu'} x_{m2\nu'})^2 (1 + \tau_{2\nu'})]^2 + (s_{\nu'} x_{m2\nu'} r_{2\nu'})^2}}{r_{2\nu'}^2 + [s_{\nu'} x_{m2\nu'} (1 + \tau_{2\nu'})]^2} \quad (59-29)$$

and

$$\tan \Theta = \frac{r_{a\nu'}}{s_{\nu'} x_{m2\nu'} (1 + \tau_{2\nu'})} \quad (59-30)$$

The disturbing noise of high frequency (Eq. 59-18) is normally caused by high order harmonics. If the skin effect is not too great, the terms with  $r_{2\nu'}$  can be neglected and

$$D_{\nu'} \approx 1 - \frac{1}{1 + \tau_{2\nu'}} \quad (59-31)$$

For harmonics of high order, the rotor slot and end-winding leakage reactances become small in comparison with the harmonic leakage reactance and

$$D_{\nu'} \approx 1 - \frac{1}{1 + \tau_{2h\nu'}} \quad (59-31a)$$

With Eqs. 58-34 in this case

$$D_r \approx 1 - \xi_{2v}^2 K_{kv}^2 \quad (59-32)$$

The amplitude of the rotor harmonic flux  $B_{\mu_r}$  is given for wound and squirrel-cage rotors by Eqs. 58-16 and 58-17. The approximate values for  $G$  are given by Eqs. 58-32 and 58-35.

**59-4. The sound intensity.** In the previous articles of this chapter, the electromagnetic aspects of the vibration and noise problem were considered. The problem is not only an electromagnetic one, but also a mechanical and acoustical one. The radial forces originate in the active parts of the machine, but the total machine participates in the vibration, and the natural frequency of the stator, which is normally the source of the magnetic noise, is determined by its active (core laminations) and inactive parts. Even a small traveling force wave may produce heavy magnetic noise if its frequency coincides with the natural frequency of the stator or parts of it. The size of the machine, the composition of the stator punchings (single piece or segment arrangement) and the mechanical construction of the stator are of great importance with respect to noise. A fabricated frame which behaves like a membrane with many natural frequencies is much more sensitive to the radial forces than a cast iron frame.

The investigation of the noise problem taking into account the mechanical construction of the stator is difficult and impractical for the designer, because even in the case of single piece punchings it leads to a considerable number of simultaneous differential equations which are tedious to solve (Ref. M 18). It is simpler for the designer to consider only the stator core and to use his own judgment, based on experience, with respect to the accuracy of his computations.

Two *approximate* methods can be used for the determination of the noise level of small machines with single piece punchings. One method considers the core as a *cylindrical radiator* (Refs. M14 to M16), the other as a *spherical radiator* (Refs. M17 and M18). An abstract of the last two references and an example computed by both methods will be given.

(a) *Cylindrical radiator.* The radial force  $F_r$  is given by Eq. 59-27a. With the notations

$h_c$  = height of the stator core behind the teeth

$D_m$  = stator core diameter in the middle of the core ( $= D_{\text{outs.}} - h_c$ )

$E' = 3 \times 10^7$  modulus of elasticity for steel

The deflection of a thin ring under a sinusoidal radially applied force is, in microns  $= 1 \times 10^{-6}$  inch,

$$d = \frac{F_r D_m^3 \times 10^6}{l_e 6E'h_c^3} \quad \text{for } p' = 2 \quad (59-33)$$

$$d = \frac{F_r}{l_e} \frac{9D_m^3 \times 10^6}{256E'h_c^3} \quad \text{for } p' = 3 \quad (59-34)$$

$$d = \frac{F_r}{l_e} \frac{D_m^3 \times 10^6}{75E'h_c^3} \quad \text{for } p' = 4 \quad (59-35)$$

For values of  $p' > 4$ , the formula for a freely supported beam can be applied

$$d = 0.75 \frac{F_r}{l_e} \frac{D_m^3 \times 10^6}{p'^3 E'h_c^3} \quad p' > 4 \quad (59-36)$$

$2p'$  is the number of nodes of core flexure.

The natural frequency of a thin steel ring is

$$f_n = \frac{36,700 p' (p'^2 - 1) h_c}{D_m^2 \sqrt{p'^2 + 1}} \quad \text{cps} \quad (59-37)$$

The natural frequency of a freely supported beam is

$$f_n = \frac{37,400 p'^2 h_c}{D_m^2} \quad \text{cps} \quad (59-38)$$

The sound intensity of a plane wave is

$$I_d = 7 + 20 \log_{10} (d \times f_r) \quad \text{decibels} \quad (59-39)$$

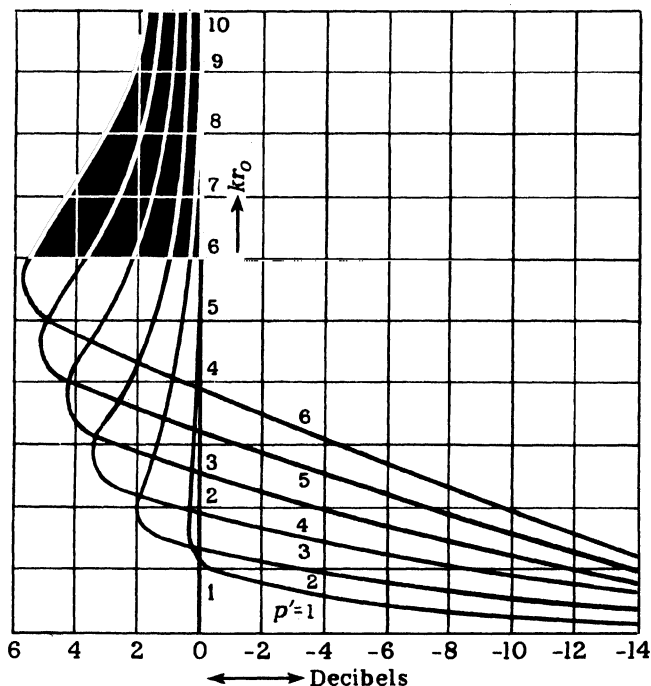


FIG. 59-3. Correction for an indefinitely long cylinder.

where  $d$  is the deflection in microns and  $f$ , the force frequency. The correction for an indefinitely long cylinder is given in Fig. 59-3.  $p'$  is used as a parameter. The "effective" radius of the cylinder

$$kr_0 = 0.00559f_r \times r_0 \quad (59-40)$$

is drawn as ordinate, where  $r_0$  is the cylinder radius  $r_0 = (D_{\text{outs.}}/2)$  in feet. The abscissa yields the correction factor which may be positive or negative.  $I_a$  plus the correction yields the sound intensity at the surface of the motor. The rate at which the sound falls off with distance is given in Fig. 59-4.  $p'$  is used as a parameter. The radius  $kr$  is drawn as abscissa; the ordinate shows decibels. The difference between the ordinates at  $kr_0$  and  $k(r_0 + D')$ , where  $D'$  is the distance from the motor surface, gives the number of decibels that should be subtracted from the value determined previously.

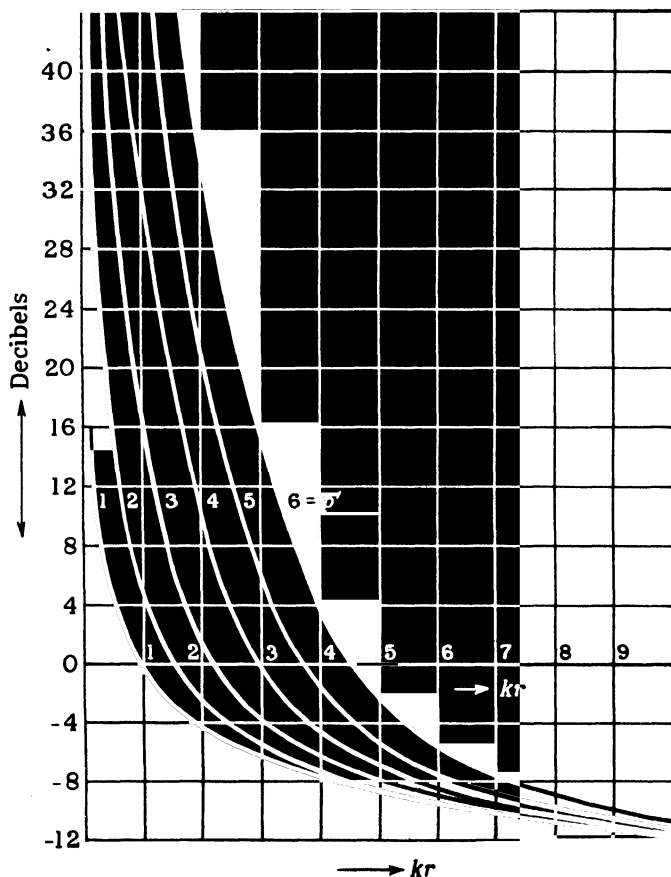


FIG. 59-4. Correction for distance from the motor surface.



(b) *Spherical radiator.* In this consideration, the amplitude of the radial force per square inch is used. This is obtained for  $p'=0$  by dividing Eq. 59-25 by  $l_e$  and for  $p'>1$  by multiplying Eq. 59-27a by  $(p'/Dl_e)$ . This yields for  $p'>1$

$$F_r = 1.385 \times 10^{-8} \times B_{\nu} B_{\mu_e} \text{ lbs./in.}^2 \quad (59-41)$$

The static deflection is

$$p'=0 \quad d_{st} = F_r \frac{D_m/2}{3 \times 10^7} \left( \frac{D_m/2}{h_c} \right) \text{ in.} \quad (59-42)$$

$$p'>1 \quad d_{st} = F_r \frac{D_m/2}{3 \times 10^7} \left( \frac{D_m/2}{h_c} \right)^3 \frac{12}{(p'^2-1)^2} \text{ in.} \quad (59-43)$$

When the natural frequency of the core is much larger than the forced frequency  $f_r$ , the static deflection can be used for the computation of the sound intensity. When the natural frequency of the core is of the same order as that of the forced frequency  $f_r$ , i.e., when the system is not far from resonance, the dynamic deflection has to be used. It is

$$d_{dyn} = d_{st} \xi_r = d_{st} \frac{1}{1 - (f_r/f_n)^2} \quad (59-44)$$

$\xi_r$  is the amplification factor.  $f_n$  is the natural frequency of the core. It is given by the equations

$$f_{n(p'=0)} = \frac{83,750}{D_m/2} \sqrt{\Delta} \frac{1}{2.54} \text{ cps} \quad (59-45)$$

$$\Delta = \frac{\text{Weight of core}}{\text{Weight of core} + \text{weight of teeth} + \text{weight of embedded copper}} \quad (59-46)$$

$$f_{n(p'>1)} = f_{n(p'=0)} \frac{1}{2\sqrt{3}} \frac{h_c}{D_m/2} \frac{p'(p'^2-1)}{\sqrt{p'^2+1}} \text{ cps} \quad (59-47)$$

The radiated wave length is

$$\lambda = \frac{34,300}{f_r \times 2.54} \text{ in.} \quad (59-48)$$

The correction factor for spherical sound radiation,  $C'_p$ , is given in Fig. 59-5 as a function of  $\pi D_{\text{outs.}}/\lambda$ .  $C'_p$  is the ratio of the radiated energy of a spherical radiator to that of a plane radiator.

With all factors involved, the sound intensity at the surface of the machine is for  $p'=0$

$$L_{(p'=0)} = 20 \log_{10} \left[ 165 \frac{(\pi D_{\text{outs.}}/\lambda)^2}{\sqrt{1 + (\pi D_{\text{outs.}}/\lambda)^2}} \xi_{r(p'=0)} \frac{D}{D_{\text{outs.}}} \frac{D_m/2}{h_c} F_{r(p'=0)} \right] \text{ phon} \quad (59-49)$$

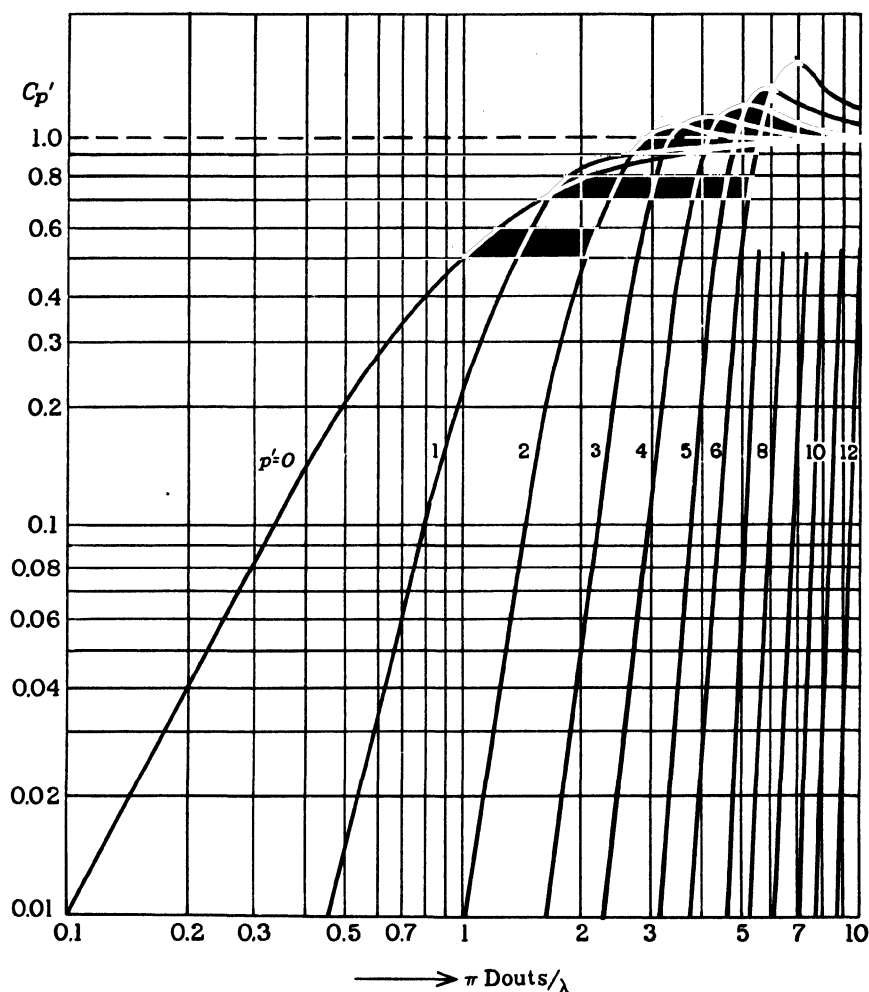


FIG. 59-5. Correction for spherical radiator.

and for  $p' > 1$

$$L_{(p' > 1)} = 20 \log_{10} \left[ 1900 \sqrt{C'_p} \xi_{r(p' > 1)} \frac{\pi D_{\text{outs.}}}{\lambda} \left( \frac{D_m/2}{h_c} \right)^3 \frac{F_{r(p' > 1)}}{(p'^2 - 1)^2} \right] \quad \text{phon} \quad (59-50)$$

For frequencies between 400 and 4000 c/s, which normally appear in electrical machines, the phon scale almost coincides with the decibel scale.

**Example.** As an example, the sound intensity of the following machine (Ref. M14) will be computed:

Squirrel-cage induction motor, 53.5 hp, 4 poles, 50 cycles.

$$D_{\text{outs.}} = 13.8 \text{ in.}$$

$$\Delta = 0.62$$

$$D = 9.05 \text{ in.}$$

$$Q_1 = 36$$

$$D_m = 12.43 \text{ in.}$$

Two rotors with  $Q_2 = 30$  and 44.

$$h_c = 1.36 \text{ in.}$$

The slot harmonics of first order of stator and rotor will be considered, because they are the most dangerous with respect to magnetic noise.

(a) *Cylindrical radiation.* The slot harmonics are (Eqs. 56-43 and 56-52)

$$\nu'_{s1} = -34 + 38$$

$$\mu'_{s1} = -28 + 32$$

The smallest value of  $p'$  is produced by

$$\nu'_b = -34 \quad \text{and} \quad \mu'_a = +32$$

$$p' = -34 + 32 = -2$$

This is a 4-pole force wave. For this wave

$$B_{\hat{r}} = 18,000 \quad B_{\hat{\mu}} = 17,200 \text{ lines/in.}^2$$

These values include the influence of the slot openings. From Eq. 59-27a

$$\begin{aligned} F_r/l_e &= 1.385 \times 10^{-8} \times \frac{1}{2} \times 0.95 \times 18,000 \times 17,200 \\ &= 19.4 \text{ lbs./per pole, per inch core length} \end{aligned}$$

From Eq. 59-33, the deflection

$$d = 19.4 \times 12.43^3 \times \frac{10^6}{6 \times 3.0 \times 10^7 \times 1.36^3} = 82.3 \text{ microns}$$

From Eq. 59-37, the natural frequency of the core

$$f_n = \frac{36,700 \times 2 \times 3 \times 1.36}{12.43^2 \sqrt{5}} = 867 \text{ c/s}$$

The frequency of the force wave, since  $k_{2a} = +1$  (Eq. 59-16)

$$f_+ = \left[ 2 + \frac{30}{2} (1 - s) \right] 50 = 825 = f_r$$

$s = 0.035$ . The closeness of  $f_r$  and  $f_n$  indicates a noisy motor. From Eq. 59-39, the sound intensity of a plane wave,

$$I_a = 7 + 20 \log_{10} (82.3 \times 825) = 103.6 \text{ db}$$

The "effective" radius of the cylinder (Eq. 59-40)

$$kr_0 = k(D_m/24) = 0.00559 \times 825 \times (13.8/24) = 2.65$$

The correction factor for cylindrical radiation is found from Fig. 59-3 equal to +2 db. Thus, the sound intensity of the core is  $103.6 + 2 = 105.6$ . The noise level was measured at a distance of 1.64 feet (=50 cm.) from the machine. This yields an effective radius

$$kr = 0.00559 \times 825(13.8/24 + 1.64) = 10.2$$

Fig. 59-4 yields for  $kr_0 = 2.65$  the value -6 db and for  $kr = 10.2$  the value -12 db. The correction factor for distance is  $-12 - (-6) = -6$ . Thus, the computed sound intensity at the distance of 1.64 feet is  $105.6 - 6 = 100$  db. The tested value is 97 to 110 db.

The same motor was built and tested with  $Q_2 = 44$ . The slot harmonics of first order are with  $Q_2 = 44$

$$\nu'_{s1} = -34 \quad +38$$

$$\mu'_{s1} = -42 \quad +46$$

The smallest value of  $p'$  is produced by

$$\nu'_b = +38 \quad \text{and} \quad \mu'_a = -42$$

$$p' = +38 - 42 = -4$$

This is an 8-pole force wave. Since  $\nu'_b = +38$  is also a slot harmonic,

$$B_{\nu'_b} \approx \frac{34}{38} 18,000 = 16,100$$

Considering Eq. 57-112,  $I_{2\nu'}$  is inversely proportional to  $Q_2$ , and therefore,  $B_{\mu'_a}$  decreases directly with  $\mu'_a$

$$B_{\mu'_a} = \frac{32}{42} 17,200 = 13,100$$

$$F_{r/1_s} = 1.385 \times 10^{-8} \times \frac{1}{4} \times 9.05 \times 16,100 \times 13,100 = 6.6$$

From Eq. 59-35

$$d = 6.6 \times 12.43^3 \frac{10^6}{75 \times 3 \times 10^7 \times 1.36^3} = 2.24$$

$$f_n = \frac{36,700 \times 4 \times 15 \times 1.36}{12.43^2 \sqrt{17}} = 4700$$

The frequency of the force wave, since  $k_{2a} = -1$  (Eq. 59-16)

$$f_+ = \left[ 2 - \frac{44}{2} \times 0.965 \right] 50 = 960 = f_r$$

$$I_a = 7 + 20 \log_{10}(2.24 \times 960) = 73$$

$$kr_0 = 0.00559 \times 960 \frac{13.8}{24} = 3.08$$

Correction for cylindrical radiation from Fig. 59-3 is +3 db. The sound intensity at the motor surface is  $73 + 3 = 76$  db. The test was made at a distance of 1.64 feet from the motor

$$kr = 0.00559 \times 960 \left( \frac{13.8}{24} + 1.64 \right) = 11.9$$

From Fig. 59-4, the correction factor for distance is

$$-12 - (-1) = -11$$

Thus, the computed sound intensity at the distance of 1.64 feet is  $76 - 11 = 65$ . The tested value is 75 to 78 db.

(b) *Spherical radiation.* Again the slot harmonics will be considered. For the slot combination 36/30

$$p' = -2 \quad B_{\nu_s} = 18,000 \quad B_{\mu_s} = 17,200$$

From Eq. 59-41

$$F_r = 1.385 + 10^{-8} \times 18,000 \times 17,200 = 4.27 \text{ lb./in.}^2$$

The static deflection is (Eq. 59-43)

$$d_{st} = 4.27 \frac{12.43/2}{3 \times 10^7} \left( \frac{12.43/2}{1.36} \right)^3 \frac{12}{9} = 114 \text{ microns}$$

The natural frequency of the core is (Eqs. 59-45 and 59-47)

$$f_{n(p'=0)} = \frac{83,750}{12.43/2} \times \sqrt{0.62} \frac{1}{2.54} = 4180$$

$$f_{n(p'=2)} = 4180 \frac{1}{2\sqrt{3}} \frac{1.36}{12.43/2} \frac{2 \times 3}{\sqrt{5}} = 708$$

The amplification factor is (Eq. 59-44)

$$\xi_{r(p'=2)} = \frac{1}{1 - (825/708)^2} = 2.78$$

The forced frequency is the same as under (a) for  $p' = 2$ . The radiated wave length is (Eq. 59-48)

$$\lambda = \frac{34,300}{825 \times 2.54} = 16.35 \text{ in.}$$

The quantity  $\pi \times D_{\text{outs}} \lambda$  is  $\pi \times 13.8/16.35 = 2.65$ . Fig. 59-5 yields for the correction factor for spherical radiation  $C'_{\nu_s} = 0.85$ . From Eq. 59-50, for the sound intensity at the surface of the motor

$$L = 20 \log_{10} \left[ 1900 \sqrt{0.85} \times 2.78 \times 2.65 \left( \frac{12.43/2}{1.36} \right)^3 \frac{4.27}{9} \right] = 115.5 \text{ phon}$$

Applying the same correction for distance as under (a) for  $p' = 2$ , the calculated sound intensity at the distance of 1.64 feet from the motor is  $118 - 6 = 112$  phon. The tested value is 97 to 110 db.

For the slot combination 36/44,  $B_{r_s}$ ,  $B_{\mu_s}$  and  $f_r$  are the same as for this slot combination under (a)

$$B_{r_s} = 16,100 \quad B_{\mu_s} = 13,100 \quad f_r = 960 \quad p' = 4$$

$$F_r = 1.385 \times 10^{-8} \times 16,100 \times 13,100 = 2.92 \text{ lb./in.}^2$$

$$f_{n(p'=0)} = 4180$$

$$f_{n(p'=4)} = 4180 \frac{1}{2\sqrt{3}} \frac{1.36}{12.43/2} \frac{4 \times 15}{\sqrt{17}} = 3840$$

$$\xi_{r(p'=4)} = \frac{1}{1 - (960/3840)^2} = 1.065$$

$$\lambda = \frac{34,300}{960 \times 2.54} = 14.1 \quad \frac{\pi \times 13.8}{14.1} = 3.08$$

From Fig. 59-5  $C'_p = 0.14$  and

$$L = 20 \log_{10} \left[ 1900 \sqrt{0.14} \times 1.065 \times 3.08 \times \left( \frac{12.43/2}{1.36} \right)^3 \frac{2.92}{225} \right] = 69 \text{ phon.}$$

Applying the same correction factor for distance as under (a) for  $p' = 4$ , there results  $69 - 11 = 58$  against the tested value of 75 to 78 phon.

It can be seen from these examples that the magnitude of the radial force is not the main factor with respect to the noise intensity. An error of 10 to 15 per cent in the determination of the magnitude of the force will have little influence on the sound intensity. Of greater importance than the magnitude of the force are the number of force pole pairs ( $p'$ ) and the height of the core ( $h_c$ ).

A large ratio  $Q_2/Q_1$  reduces the magnitude of the flux harmonics of the rotor, i.e., the radial forces, and increases  $p'$ , but increases the additional iron losses and increases the parasitic torques.

Only the harmonic combinations and the force waves which are most dangerous with respect to magnetic noise were considered in the example. There is always in the machine a large number of traveling force waves which interfere with each other. Experience shows that, in small motors skewing reduces the noise, since it reduces the rotor currents of higher frequency. Of similar importance is a proper coil span of the stator winding.

In wound rotor motors, magnetic noise also may appear at no-load, due to a combination of the main wave and the slot-opening harmonics. In squirrel-cage motors the noise appears at load.

## Chapter 60

### TRANSIENT AND SUBTRANSIENT REACTANCES SUDDEN SHORT CIRCUIT OF A SYNCHRONOUS GENERATOR

The steady-state operation of a synchronous machine is determined, completely by its field current, the resistance and leakage reactance of the stator winding, and the synchronous reactance (or synchronous reactances in the case of the salient-pole machine). The synchronous reactance includes the armature reaction due to the load current of the machine. In the consideration of the steady-state operation of the synchronous machine the *rotor* constants of the machine, i.e., its leakage reactance and resistance, are not involved. This is true not only with respect to the damper winding, if there is any, and to the eddy-current circuits in the solid iron of a turbo-rotor or in the solid poles of a salient-pole machine, but also with respect to the field winding itself.

The situation becomes different when the synchronous machine is operating under *transient* conditions. Here the constants of the field winding, the damper winding, and eddy-current circuits are of great importance.

To make this clear, the short-circuit operation of a generator under steady-state conditions and under transient conditions will be considered, both neglecting saturation.

Consider an unexcited generator the armature of which is short-circuited. If excitation is applied, the armature current will be determined solely by

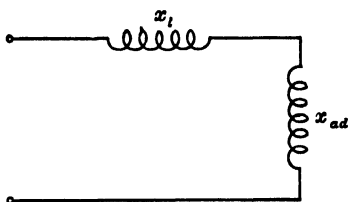


FIG. 60-1. Equivalent circuit of the synchronous machine under steady-state conditions. (Stator resistance neglected.)

the synchronous reactance  $x_d$  in the direct axis (see Art. 33-1), i.e., by the leakage reactance of the armature winding  $x_l$  and by the reactance of armature reaction in the direct axis  $x_{ad}$ . The equivalent circuit corresponding to this condition of operation is given by Fig. 60-1. The direct axis is the axis of the main flux. Writing  $x_{ad} = 2\pi f L_{ad} = 2\pi f L_m$ , where  $L_m$  is the coefficient of self-inductance of the main flux in the direct axis,  $I_a L_m$  is the main flux produced by the

armature winding, and  $I_a x_l / 2\pi f$  is the leakage flux produced by the armature winding.

**60-1. Transient currents with resistances of both windings neglected.** Consider the elementary generator (Fig. 60-2), with cylindrical rotor, the field winding and armature winding of which each consist of a

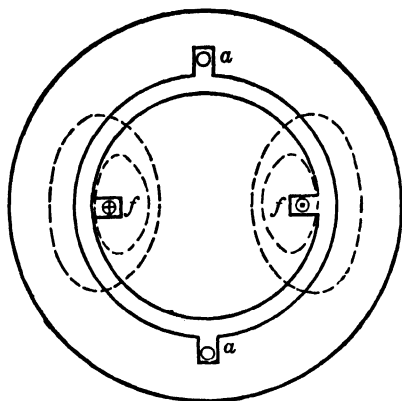


FIG. 60-2. Elementary generator.

single coil, coil  $ff$  and coil  $aa$ , respectively. The stator winding is open, and the rotor winding is excited by a d-c current of the magnitude  $I_f$ . The rotor rotates with constant speed. At the time  $t=0$ , when the axes of both windings are perpendicular to each other (Fig. 60-2), the stator winding suddenly is short-circuited.

The assumption  $r=0$  for the two windings means that the emf induced in each winding by the sum of all its flux interlinkages is zero,

$$e = -\frac{d}{dt}(\sum n_x \Phi_x) = 0, \quad (60-1)$$

This follows from Kirchhoff's mesh law. (For the field winding, the impressed voltage is zero for zero resistance.) Eq. 60-1 states: *the sum of all flux interlinkages  $\sum n_x \Phi_x$  is constant for each winding.* (See Ref. N1.) This statement will be applied, in order to get an idea about the currents in both windings shortly after the short-circuit occurred.

The total flux interlinked with the field winding at  $t=0$  consists of *two parts*, one  $L_m I_f$ , going through the path of the main flux, the other  $L_l I_f$ , going through the leakage path of the rotor (Fig. 60-2). The total flux interlinked with the field winding at  $t=0$  thus is

$$(L_m + L_l) I_f = L_m (1 + \tau_f) I_f \quad (60-2)$$

where

$$\tau_f = \frac{L_l}{L_m}.$$

$\tau_f$  is the leakage coefficient of the field winding. The total flux interlinked with the armature at  $t=0$  is zero. The flux interlinkage  $L_m (1 + \tau_f)$  must be sustained by the field winding, while the zero flux interlinkage of the armature must be sustained by the armature winding.

During the time  $t$  the rotor moves through an angle  $\alpha = \omega t$  ( $\alpha$  is the angle between the axis of the field winding and the plane of the armature winding). This produces a current  $i_a$  in the armature winding and also forces a current



$i_f$  to flow in the field winding in order to sustain there the flux interlinkage  $L_m(1 + \tau_f)I_f$ . Thus for the flux interlinkages of the armature winding

$$i_a L_m(1 + \tau_a) + (i_f + I_f)L_m \sin \alpha = 0, \quad \tau_a = \frac{x_l}{\omega L_m}, \quad (60-3)$$

and for the flux interlinkages of the field winding

$$I_f L_m(1 + \tau_f) + i_f L_m(1 + \tau_f) + i_a L_m \sin \alpha = I_f L_m(1 + \tau_f). \quad (60-4)$$

From Eqs. (60-3) and (60-4):

$$i_a = I_f \frac{(1 + \tau_f) \sin \alpha}{\sin^2 \alpha - (1 + \tau_a)(1 + \tau_f)} \quad (60-5)$$

$$i_f = -I_f \frac{\sin^2 \alpha}{\sin^2 \alpha - (1 + \tau_a)(1 + \tau_f)}. \quad (60-6)$$

It follows from Eqs. (60-5) and (60-6) that the transient currents  $i_a$  and  $i_f$  are determined by the angle  $\alpha$  as well as by the leakage coefficients of both windings, i.e., by the leakage fluxes of both windings. The armature reaction flux  $L_m I_a$  which determines the steady-state operation of the short-circuited generator does not appear in the equations for the transient currents of the suddenly short-circuited generator. It should be noted that while the armature current  $i_a$  is an alternating current, the transient field current  $i_f$  is a direct (*unidirectional*) current supporting the field current  $I_f$  to sustain the initial flux interlinkage of the field winding.

$i_a$  and  $i_f$  become maximum for  $\alpha = \pi/2$ , i.e., a quarter-period after the short-circuit occurred. They are

$$i_{a \max} = -I_f \frac{1 + \tau_f}{\tau_a + (1 + \tau_a)\tau_f}, \quad (60-7)$$

$$i_{f \max} = I_f \frac{1}{\tau_a + (1 + \tau_a)\tau_f}. \quad (60-8)$$

The two currents have different signs and are approximately equal.

Multiplying numerator and denominator of Eq. (60-7) by  $\omega L_m$  and noting that  $\tau_a \omega L_m = x_l$  and  $\tau_f \omega L_m = x_f$ , where  $x_f$  is the leakage reactance of the field winding there follows

$$i_{a \max} = -I_f \omega L_m \frac{1 + \tau_f}{x_l + (1 + \tau_a)x_f}. \quad (60-9)$$

$I_f \omega L_m$  is the amplitude of the terminal voltage (induced emf) of the generator before the short-circuit occurred, i.e.,

$$i_{a \max} = -E_{\max} \frac{1 + \tau_f}{x_l + (1 + \tau_a)x_f}. \quad (60-10)$$

This equation shows that the maximum transient armature current is

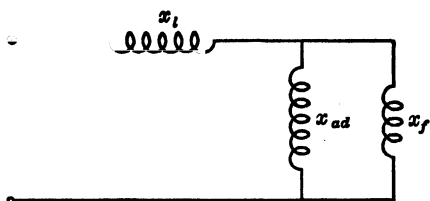


FIG. 60-3. Equivalent circuit for the transient reactance in the direct axis.

determined by the equivalent circuit of Fig. 60-3. The reactance that corresponds to this circuit is the *direct-axis transient reactance*  $x'_d$ .

In the preceding derivations only the field winding of the rotor has been considered. If there is a damper winding in the poles of the salient-pole machine or if eddy-current circuits are possible the axis of which coincides with the direct axis, these circuits are interlinked at the time  $t=0$  with the main flux produced by the field winding and they also will tend to sustain this flux, i.e., they support the field winding. They have to be considered in parallel with the field winding, and the equivalent circuit for this case is given by Fig. 60-4.  $x_{Dd}$  is the leakage reactance of the damper winding or of the eddy-current circuits or of both together in the direct axis. The reactance that corresponds to the circuit, Fig. 60-4 is the *direct-axis subtransient reactance*  $x''_d$ . It is smaller than the direct-axis transient reactance  $x'_d$  and therefore the presence of a damper winding or of eddy-current paths increases the maximum values of the transient currents  $i_a$  and  $i_f$ .

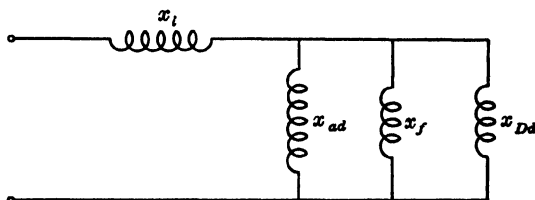


FIG. 60-4. Equivalent circuit for the subtransient reactance in the direct axis.

The direct-axis subtransient reactance which corresponds to the equivalent circuit Fig. 60-4 is

$$x''_d = x_i + x_{Dd} \frac{\tau_f}{\tau_{Dd} + \tau_f(1 + \tau_{Dd})} \quad (60-11)$$

where  $\tau_{Dd} = x_{Dd}/x_{ad}$ . This equation can also be derived by a consideration similar to that which has led to the transient reactance Eq. (60-10).

**60-2. Transient currents with resistances not neglected.** The assumption that the resistances of the windings are equal to zero means that the transient currents will flow in the windings indefinitely without changing their amplitudes as given by Eqs. (60-7) and (60-8). Practically, however, this is not the case. The amplitudes decrease with the time  $t$ , and this is due to the resistances of the windings which gradually consume the magnetic energy accumulated in magnetic field at the time  $t=0$ . The *rate of decrease*

of the consecutive peaks is determined by the *time constants of the windings*. The damper winding and the eddy-current circuits have much larger ratios of resistance to leakage reactance, i.e., much smaller time constants, than the field winding. Their influence on the transients therefore will be much shorter than that of the field winding. As a matter of fact, the damper winding and eddy-current circuits influence the transient currents only during the *first few cycles*. The field winding determines the decrease of the amplitudes for a much longer time. The change of the amplitudes during the short-circuit period is such that the amplitudes are determined at first by the subtransient reactance  $x''_d$  (Fig. 60-4), then by the transient reactance  $x'_d$  (Fig. 60-3), and finally by the synchronous reactance  $x_d = x_l + x_{ad}$  (Fig. 60-1), i.e., the transient armature current ends with the steady-state short-circuit current while the transient field current ends with the value zero. During the short-circuit period *the reactance of the machine changes* from the subtransient reactance  $x''_d$  to the synchronous reactance  $x_d$ .

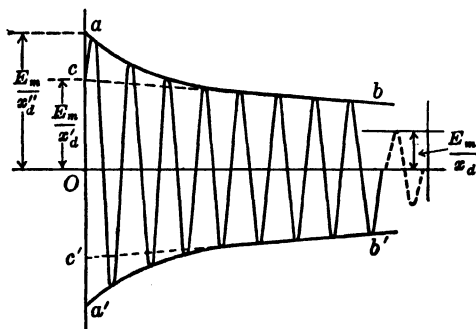


FIG. 60-5. Oscillogram of the armature current of a generator short-circuited at the instant when the steady-state current would pass through zero.

Fig. 60-5 shows the oscillogram of the armature current for the case when the sudden short circuit occurs at the time instant given by Fig. 60-2, i.e., at the time instant when the flux interlinkage of the armature winding is zero and the emf induced in the armature winding is maximum. The current wave is symmetrical with the time axis. When the envelope  $ab$ ,  $a'b'$  and also the envelope  $cb$ ,  $c'b'$  ignoring the first few cycles are drawn,

$$Oa = Oa' = \frac{E_{\max}}{x''_d}, \quad x''_d = \frac{E_{\max}}{Oa},$$

and

$$Oc = Oc' = \frac{E_{\max}}{x'_d}, \quad x'_d = \frac{E_{\max}}{Oc}$$

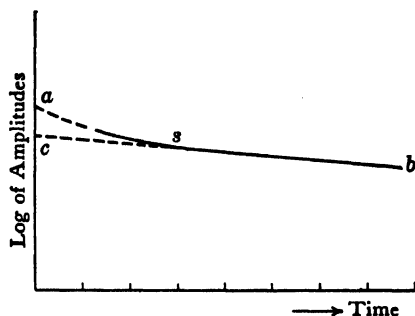


FIG. 60-6. Determination of the transient reactance in the direct axis from the oscillogram Fig. 60-5.

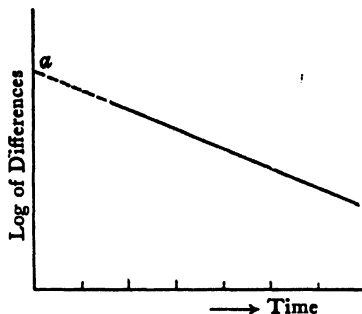


FIG. 60-7. Determination of the subtransient reactance in the direct axis from the oscillogram Fig. 60-5.

The following consideration makes it possible to determine the points *a* and *c* with greater accuracy. The current in the circuit, Fig. 60-4, may be considered to consist of two superimposed transient currents, one due to the circuit Fig. 60-3 and the other caused by the presence of the branch  $x_{Dd}$ . Both currents decay at different rates but both decay logarithmically. Therefore, if the logarithms of the amplitudes are plotted on semi-log paper as curve *asb* (Fig. 60-6), the part *sb* of this curve which is determined by the circuit Fig. 60-3, i.e., by the transient reactance alone, will be a straight line. The intercept of this straight line with the axis of ordinates locates the point *c*. The differences between the curve *as* and the straight line *sc* are due to the branch  $x_{Dd}$ . The logarithms of these differences plotted on semi-log paper again will yield a straight line (Fig. 60-7) whose intercept with the axis of ordinates locates the point *a*.

**60-3. Maximum transient currents.** Fig. 60-5 represents the transient armature current  $i_a$  for the case when the short circuit occurs at the instant of time represented by Fig. 60-2. The transient current  $i_a$  has another shape when the short circuit occurs at any other instant of time. In Fig. 60-2 at  $t=0$  the armature coil is not interlinked with the rotor flux. Now consider the other extreme position of the rotor when at  $t=0$  the armature coil is interlinked with the total main flux of the rotor. This is the position in which the axes of both windings coincide. It will be assumed that the rotor has only a field winding. The condition that the flux of each winding has to remain unchanged yields the following relation for the armature winding, at the time  $t = \alpha/\omega$ :

$$i_a L_m (1 + \tau_a) + (I_f + i_f) L_m \cos \alpha = I_f L_m, \quad (60-12)$$

and for the field winding at the same instant of time:

$$I_f L_m (1 + \tau_f) + i_f L_m (1 + \tau_f) + i_a L_m \cos \alpha = I_f L_m (1 + \tau_f). \quad (60-13)$$

$\alpha$  is the angle between the axes of the 2 windings. Eqs. (60-12) and (60-13) yield:

$$i_a = -I_f \frac{(1 - \cos \alpha)(1 + \tau_f)}{\cos^2 \alpha - (1 + \tau_a)(1 + \tau_f)}, \quad (60-14)$$

$$i_f = I_f \frac{\cos \alpha - \cos^2 \alpha}{\cos^2 \alpha - (1 + \tau_a)(1 + \tau_f)}. \quad (60-15)$$

The transient armature current consists of two parts. The second part is an alternating current which has the *same magnitude as before*. (Note that here the angle  $\alpha=0$  is shifted  $90^\circ$  with respect to the angle  $\alpha=0$  in Fig. 60-2.) The first part is a *unidirectional* current. Accordingly the transient field current also consists of two parts. The second part is a direct current of the same magnitude as before. This current, as before, counteracts the a-c armature current in order to sustain the initial flux interlinked with the field winding. The first part of the transient field current is an alternating current due to the direct current in the armature. The latter current produces a flux which is *fixed* with respect to the armature. Since the field winding rotates with synchronous speed with respect to the armature, this flux induces an alternating current of fundamental frequency in the field winding. This rotor current produces an alternating field fixed with respect to the rotor, which can be considered to consist of two rotating fields traveling at synchronous speed with respect to the rotor (see Art. 26-3). One of these rotating fields is at standstill with respect to the armature and counteracts the unidirectional component of the armature current. The other rotating field has double synchronous speed with respect to the armature and is balanced by a second harmonic current in the armature winding.

The transient currents  $i_a$  and  $i_f$  [Eqs. (60-14) and (60-15)] become maximum for  $\alpha = \pi$ , i.e., half a period after the short circuit occurred:

$$i_{a \max} = 2I_f \frac{1 + \tau_f}{\tau_a + (1 + \tau_a)\tau_f}, \quad (60-16)$$

$$i_{f \max} = 2I_f \frac{1}{\tau_a + (1 + \tau_a)\tau_f}. \quad (60-17)$$

These values are twice as large as in the first case where the short circuit occurred at the moment when the steady-state armature current would pass through zero. In the case just considered the voltage induced in the armature winding at  $t=0$  is zero and the steady-state current would be maximum, since  $r_a=0$  and the circuit is purely inductive. This is similar to the phenomena which occur in other a-c circuits under transient conditions. For example, when an alternating voltage is applied suddenly to an inductance and a resistance in series, the magnitude of the transient current depends upon the instant at which the voltage is applied. If it is applied at the instant when the steady-state current would be zero, there will be no unidirectional

transient current and the alternating current assumes its steady-state values immediately. If the voltage is applied at the instant when the steady-state current would have its maximum, a unidirectional current appears, increasing the peak value of the current to twice the value of the first case, if the resistance of the circuit is small.

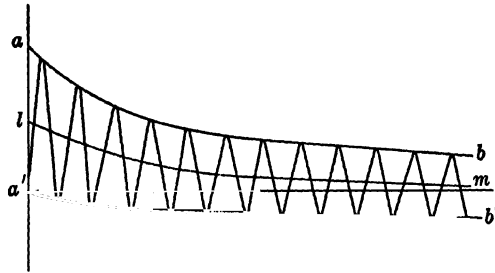


FIG. 60-8. Oscillogram of the armature current of a generator short-circuited at the instant when the steady-state current would pass through its maximum.

Fig. 60-8 shows an oscillogram of the armature current of a generator short-circuited at the instant when the steady state current would pass through its maximum. Due to the d-c component the current wave is unsymmetrical with respect to the time axis. In order to determine the subtransient and transient reactances from this oscillogram, draw the envelope of the wave  $ab, a'b'$  and also a line  $lm$  midway between the two sides of the envelope. The distances between the line  $lm$  and the time axis give the d-c components of the armature current. Redraw the envelope  $ab, a'b'$  with its axis horizontal, i.e., eliminating the d-c component, as shown in Fig. 60-9, and also draw the envelop  $cb, c'b'$ , ignoring the first few cycles. The reactances can be determined as before in Fig. 60-5 from the points  $a$  and  $c$ . They will be approximate values.

Consider the *main flux* interlinked with the rotor winding at the time  $t' = \pi/\omega$  after the short circuit occurred, i.e., at the instant when the arma-

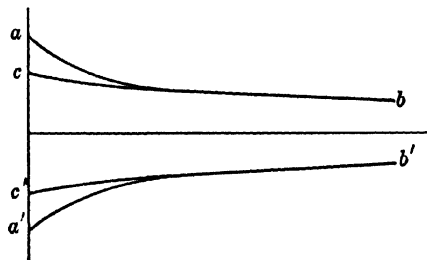


FIG. 60-9. Determination of transient and subtransient reactances in the direct axis from the oscillogram Fig. 60-8.

ture and rotor windings have their maximum currents given by Eqs. (60-16) and (60-17). Then

$$\Phi_m = L_m(I_f + i_{f\max}) - L_m i_{a\max}. \quad (60-18)$$

Inserting Eqs. (60-16) and (60-17) into Eq. (60-18), there results

$$\Phi_m = \frac{L_m I_f}{\tau_a + (1 + \tau_a)\tau_f} \tau_a \tau_f \approx 0. \quad (60-19)$$

A very small main flux exists at the instant considered. Since the total flux interlinked with the rotor winding is the same as at the time  $t=0$ , when the short circuit occurs, this means that the main flux is pushed into the leakage paths. This explains the high transient currents during a sudden short circuit: in order to sustain the initial flux in the *leakage paths* with their high magnetic reluctance high currents are necessary. In the case considered under 60-1 where the maximum transient currents are  $\frac{1}{2}$  of the values given by the Eqs. (60-16) and (16-17), about  $\frac{1}{2}$  of the main flux is pushed into the leakage paths at the instant when the maximum currents given by Eqs. (60-7) and (60-8) occur. The rotor and armature windings move with respect to each other and both have to sustain their fluxes at the initial values. For certain relative positions of both windings, one winding needs a large main flux and the other a small main flux; both windings may even need fluxes of opposite direction. In these positions the windings are forced to sustain the fluxes in the leakage paths and this leads to very high transient currents.

#### 60-4. Transient and subtransient reactance in the quadrature axis.

In the foregoing article a sudden short circuit at the terminals of the generator was considered. In this case the armature circuit is almost purely inductive and the axis of armature reaction lies along the field axis, i.e., along the direct axis (Art. 33-1). If the sudden short circuit occurs at a distance from the generator so that there is a considerable resistance in the circuit, the axis of armature reaction is shifted with respect to the direct axis. In this case both axes have to be treated in a way similar to that for steady state operation (Art. 35-1) and different constants have to be applied to each axis. Corresponding to the transient and subtransient reactances of the direct axis,  $x'_d$  and  $x''_d$ , a transient and subtransient reactance of the quadrature axis,  $x'_q$  and  $x''_q$ , have to be introduced. It is evident that the transient reactance in the quadrature axis is given by the circuit of Fig. 60-10, since there is no field winding in the quadrature axis, i.e.,  $x'_q = x_q$ . If the salient-pole machine has a damper winding the reactance of which, with respect to the quadrature axis, is  $x_{Dq}$ , then the subtransient reactance in the quadrature axis is given by the circuit in Fig. 60-11. The same circuit applies to the solid rotor if the reactance of the eddy-current paths is substituted for  $x_{Dq}$ .

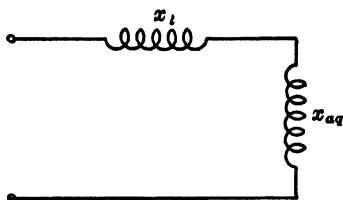


FIG. 60-10. Equivalent circuit for the transient reactance in the quadrature axis.

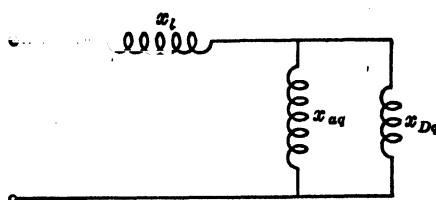


FIG. 60-11. Equivalent circuit for the subtransient reactance in the quadrature axis.

**60-5. Determination of the subtransient reactances from a locked test.** If the rotor is locked, the field winding short-circuited, and voltage applied to 2 terminals of the Y-connected stator, there are 2 positions of the rotor with respect to the stator which will yield the reactances  $x''_d$  and  $x''_q$ , respectively. The first position is that at which the mmf of the excited stator phases lies in the pole (direct) axis, i.e., the position at which the induced field current is a maximum. The second position, which yields  $x''_q$ , is shifted 90 electrical degrees with respect to the first position. In the second position the induced field current is zero. In both cases the subtransient reactance is equal to  $\frac{1}{2}$  of the ratio of the applied voltage to the armature current. The reactances obtained are unsaturated reactances.

Approximate values of the various reactances of the synchronous machine expressed in p-u are given in the table following.

	<i>Salient-Pole Generators with dampers and continuous end-rings</i>		<i>Turbo-Generators</i>
	High Speed	Low Speed	
$x_l$	0.10 to 0.15	0.15 to 0.25	0.06 to 0.08
$x_d$	1.00 to 1.25 (non-satur.)		1.0 to 1.2
$x_q$	0.65 to 0.80		1.0 to 1.2
$x'_d$	0.35 to 0.40		0.15 to 0.25
$x''_d$	0.20 to 0.30		0.09 to 0.14
$x''_q$	0.20 to 0.30		0.09 to 0.14



## Chapter 61

### PULLING INTO STEP OF SYNCHRONOUS MOTORS

**60-1. Equation of motion of the synchronous motor pulling into step.** After the synchronous motor has been brought up to speed by means of its rotor windings, it runs with a slip  $s_L$  which corresponds to the shaft-load torque  $T_L$  (Fig. 61-1). By applying the d-c excitation the motor must pull into step,

i.e., reach its synchronous speed and then continue to run as a synchronous machine.

The d-c excitation does not change the main flux of the machine materially, since this flux is determined by the terminal voltage impressed on the stator. The d-c excitation produces stator currents which flow through the lines with a frequency  $f_1(1 - s_L)$ . The stator mmf corresponding to these currents opposes the d-c mmf, leaving only a small residual flux corresponding to the leakage reactance and

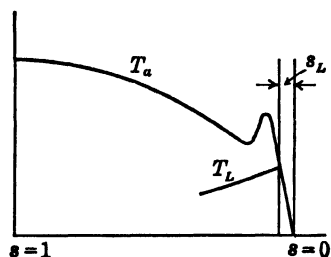


FIG. 61-1. Determination of the slip  $s_L$  from which the motor has to pull into step.

ohmic resistance drops in the stator winding. Thus, after the application of the d-c excitation, it is necessary to consider two different torques:

- (a) the asynchronous torque produced by the rotating flux and the a-c currents in both rotor windings.
- (b) the synchronous torque produced by the rotating flux and the d-c current in the field winding.

While the asynchronous torque is almost independent of the position of the poles relative to the rotating flux; the synchronous torque depends to a great degree on this position; it changes in magnitude, depending upon the position of the poles with respect to the rotating flux, between a positive and a negative maximum. In order for the motor to pull into step, it is of great importance whether the *synchronous torque is positive or negative* when the d-c excitation is applied.

In order to understand clearly the interaction of the asynchronous and synchronous torques, the assumption will be made that the rotating flux is at standstill, i.e., produced by stationary poles, and the torque produced by

the d-c currents will be considered for the rotor operating at an angular velocity of  $s_L\omega_s$ . This angular velocity corresponds to the slip  $s_L$ . The torque produced by the direct current is approximately proportional to the sine of the angle  $\alpha$  (Fig. 61-2) which is the angle between the positive normal to the plane of the field winding  $F$  and the positive direction of the rotating flux ( $NS$ ). Thus, the torque is zero when  $\alpha$  is  $0^\circ$  or  $180^\circ$  and a maximum when  $\alpha$  is  $90^\circ$  or  $270^\circ$ .

If  $T_{S\max}$  denotes the maximum value of the synchronous torque when the machine is operating at synchronous speed, then for any angle  $\alpha$ , approximately,

$$T_S = T_{S\max} \sin \alpha. \quad (61-1)$$

A *positive* synchronous torque is defined as one which opposes the rotation of the rotor, thereby attempting to diminish the speed (slip) of the rotor and thus trying to bring the rotor nearer to synchronous speed. A negative torque is one which attempts to increase the speed (slip) of the rotor and thus forces it farther away from synchronous speed.

It can be seen from Fig. 61-2 that the synchronous torque is positive between  $\alpha = 0$  and  $180^\circ$  and negative between  $\alpha = 180^\circ$  and  $360^\circ$ .

It is expedient to apply the d-c excitation at an instant of time *when the synchronous torque is positive* ( $\alpha < 180^\circ$ ), i.e., when the synchronous torque reduces the slip. If the d-c excitation is applied at an instant of time when the synchronous torque is negative ( $180^\circ < \alpha < 360^\circ$ ), the slip is increased and it may happen, when the excitation is insufficient, that the positive half wave of the synchronous torque which follows the negative half wave will be unable to bring the rotor up to its synchronous speed. *The conditions for pulling into step are most favorable if the d-c excitation is applied when  $\alpha = 0^\circ$* : under this condition, the *entire positive half wave* of the synchronous torque is available for decreasing the slip. The least favorable condition occurs when the d-c excitation is applied at  $\alpha = 180^\circ$ .

The question now arises as to how large the d-c excitation must be in order that the motor pull into step when it is applied at the most favorable or unfavorable pole positions. The answer to this question is found in the analytical investigation of the phenomena of pulling into step.

During the transition from steady-state asynchronous (slip =  $s_L$ ) to steady-state synchronous condition (slip = 0) the sum of both machine torques, the asynchronous torque  $T_a$  and the synchronous torque  $T_S$ , must be equal at any instant of time to the sum of the external torques, the load torque  $T_L$  and the torque of the rotating mass  $T_M$ .

$$T_a + T_S = T_L + T_M. \quad (61-2)$$

The counter-torque of the load  $T_L$  will be considered constant during the

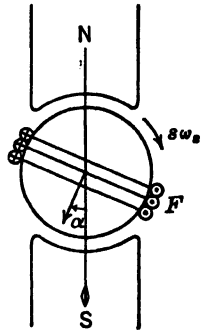


FIG. 61-2. Schematic representation of a 2-pole motor while pulling into step.

period of pulling into step. Since a proportionality exists between slip and torque for small values of slip, then for any slip  $s$

$$T_a = \frac{T_L}{s_L} s. \quad (61-3)$$

The mechanical angular velocity of the rotor at the slip  $s$  is equal to  $\omega_r = (1-s)[\omega\tau/(p/2)]$ . If the moment of inertia of the rotating mass is designated by  $J$  then the torque of the rotating mass is given by the expression

$$T_M = J \frac{d\omega_r}{dt} = -J \frac{\omega_s}{p/2} \frac{ds}{dt}. \quad (61-4)$$

Then, according to Eq. (61-2),

$$\frac{T_L}{s_L} s + T_{S\max} \sin \alpha = T_L - J \frac{\omega_s}{p/2} \frac{ds}{dt}. \quad (61-5)$$

Furthermore, the relationship exists (see Fig. 61-2)

$$s\omega_s = \frac{d\alpha}{dt}. \quad (61-6)$$

Hence

$$\frac{J}{p/2} \frac{d^2\alpha}{dt^2} + \frac{T_L}{s_L \omega_s} \frac{d\alpha}{dt} + T_{S\max} \sin \alpha = T_L. \quad (61-7)$$

The solution of this equation is not simple, for it leads to elliptic functions. In order to get a clear insight of the problem, an approximate solution satisfies.

**61-2. Solution of the equation of motion for  $\alpha=0$  (most favorable pole position).** A. Fraenkel (Ref. O1) solved the equation of motion (61-7) for the most favorable pole position  $\alpha=0$  by means of a step-by-step method of integration. Figs. 61-3, 61-4, and 61-5 refer to a 550-hp 12-pole 50-cycle motor. The load torque  $T_L$  during the period of pulling into step is equal to the rated torque  $T_n$ . Furthermore,  $s_L=3\%$  and the  $WR^2$  of the rotating mass is  $42.8 \times 10^2$  lb.-ft.<sup>2</sup> Fig. (61-3) shows the variation of the slip

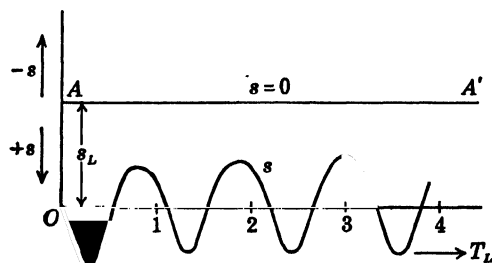


FIG. 61-3. Variation of the slip when the d-c excitation is applied at the most unfavorable rotor position.

when the d-c excitation is applied at  $\alpha = 180^\circ$ . Fig. 61-4 shows this same variation for  $\alpha = 0^\circ$ . The unit of time along the axis of abscissa is taken equal to the period of the slip frequency, corresponding to the slip  $s_L$ . The field current is the same in both cases and corresponds to a synchronous pull-out torque  $T_{s\max} = 1.5 T_n$ .

As Fig. 61-3 shows, the field current selected does not allow the motor to pull into step when it is applied at  $\alpha = 180^\circ$ . Immediately after the field current is applied the slip *increases* due to the retarding synchronous torque and synchronous speed ( $s = 0$ ) cannot be reached; the machine oscillates about a mean value of slip ( $s_L = 3\%$  in this case) and the poles slip by the rotating field. This causes a disturbing low beat frequency in the line current which is due to the superposition of the current which the machine takes from the line as an induction motor and the current produced by the d-c excitation.

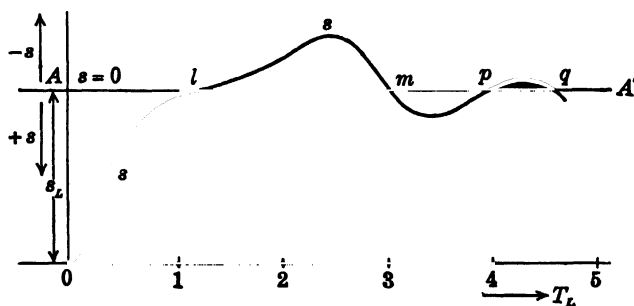


FIG. 61-4. Variation of the slip when the d-c excitation is applied at the most favorable rotor position.

The conditions are entirely different when the d-c current is applied in the favorable pole position,  $\alpha = 0^\circ$  (Fig. 61-4). Immediately after applying the excitation the slip *decreases* due to the accelerating synchronous torque, and the synchronous speed is reached after approximately 1 period of the slip frequency. Between  $l$  and  $m$  the slip is negative, i.e., in Fig. 61-2, the rotor rotates in a direction opposite to that between  $A$  and  $l$ . Between  $m$  and  $p$  the direction of rotation is the same as the original, between  $p$  and  $q$  it is changed again. The rotor reaches synchronous speed after several oscillations, *remaining under the same pole* of the rotating field. No disturbing low-frequency beat appears in the line in this case.

Fig. 61-5 shows the variation of the asynchronous and synchronous torques corresponding to Fig. 61-4. Curve I shows the synchronous torque. Corresponding to excitation being applied at  $\alpha = 0^\circ$  and the fact that the rotor remains under the same pole of the rotating field, only the positive half wave of the synchronous torque curve has to be considered. Curve II shows the asynchronous torque. This curve is identical with the slip curve of Fig. 61-4 since slip and asynchronous torque are proportional to each other

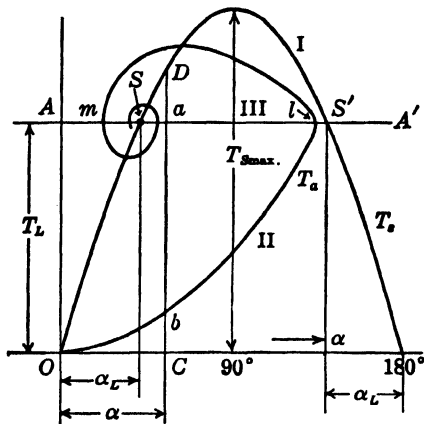


FIG. 61-5. Variation of the synchronous and asynchronous torques corresponding to Fig. 61-4.

$T_{S\max}$  which will enable the machine to pull into step, when the exciting current is applied at the most favorable pole position  $\alpha = 0^\circ$ .

During the transition from the stationary asynchronous speed ( $s = s_L$ ) to the synchronous speed ( $s = 0$ ) the asynchronous torque decreases and therefore a part of the synchronous torque has to be delivered to the load. For any angle  $\alpha$  (Fig. 61-5),  $T_a = ab$  represents the asynchronous torque,  $T_s = CD$  represents the synchronous torque, and  $Ca$  the load torque. At this angle  $\alpha$  the torque  $bC = T_L - T_a = Ca - ab$  is the part of the synchronous torque delivered to the load. The remaining part of the synchronous torque  $bD = CD - bC$  serves to accelerate the rotating mass. This applies to any value of  $\alpha$ , i.e., the distance along the ordinate between the curves I and II represents the accelerating and retarding torques of the rotating mass, and the area between any two ordinates and these curves represents a definite amount of work.

At the moment of applying the field current the slip is  $s_L$  and  $\alpha = 0$ . When synchronous speed ( $s = 0$ ) is reached at point  $l$  the entire load torque must be delivered by the synchronous torque. If  $\alpha_L$  (Fig. 61-5) is the angle corresponding to the load torque, then when synchronous speed is reached at point  $l$ ,  $\alpha_l = Al$  must be *not larger* than  $(\pi - \alpha_L)$  or else the pole structure will slip by to the next pole of the rotating field. When  $Al < AS' = (\pi - \alpha_L)$ , the synchronous torque at  $s = 0$  is larger than the load torque and the slip will become negative as shown in Figs. 61-4 and 61-5. When the curve of asynchronous torques II intersects the curve of synchronous torques I at a point below  $S'$ , the motor will slip by the next pole. When  $Al = \pi - \alpha_L$ , i.e., the point  $l$  coincides with the point  $S'$ , the motor will pull into step, but will be unstable; a decrease of the load or an increase of the excitation will accelerate the motor and bring it to the stable point  $S$ ; on the other hand, an increase

(Eq. 61-3); however, it has a different shape than in Fig. 61-4 because it is not drawn as a function of time but rather as a function of the angle  $\alpha$ . The asynchronous torque therefore is represented by the distance between the curve II and the straight line  $AA'$ . The negative asynchronous torques of Fig. 61-5 correspond to the negative slips of Fig. 61-4 between  $l$  and  $m$  and  $p$  and  $q$ . The scale for the asynchronous torques is given by the distance  $OA$  (Fig. 61-4) which corresponds to the slip  $s_L$  as well as to the load torque  $T_L$ .

With the aid of Fig. 61-5, it is possible to determine the lowest value of field current or of synchronous torque

of the load or a decrease of the excitation will pull the motor out of step.

First the amount of work required to accelerate the rotating mass between the limits  $s=s_L$  and  $s=0$  will be determined, and second the area between the curves I and II (Fig. 61-5) for the limits  $\alpha=0$  and  $\alpha=(\pi-\alpha_L)$ . This area represents the same amount of work. Both expressions for the work then yield the solution of the problem. It follows from Eqs. (61-4) and (61-6) that

$$T_M d\alpha = -J \frac{\omega_s ds}{p/2 dt} s \omega_s dt = -J \frac{\omega_s^2}{p/2} s ds. \quad (61-8)$$

This expression when integrated between  $s=s_L$  and  $s=0$  yields the work for the acceleration of the rotating mass as

$$W_{acc} = \frac{1}{2} J \frac{\omega_s^2}{p/2} s_L^2.$$

In Fig. 61-5 the same work is represented by the area between the curves I and II and the limits  $\alpha=0$  and  $\alpha=\alpha_L$ . Let

$$\frac{T_{Smax}}{T_n} = C, \quad \frac{T_{Smax}}{T_L} = K. \quad (61-9)$$

$C$  is the synchronous overload capacity of the motor. It has been found that for values of  $k$  larger than 1.2 the lower part of curve II can be taken as a parabola which passes through the point  $S'$  in Fig. 61-5. The area between the sine curve and the parabola between the limits  $\alpha=0$  and  $\alpha=\pi-\alpha_L$  is then equal to the expression

$$W_{acc} = T_{Smax} (1 + \cos \alpha_L) - \frac{T_L}{3} (\pi - \alpha_L).$$

Since  $T_L = T_{Smax} \sin \alpha_L$ , then  $\sin \alpha_L = T_L / T_{Smax} = 1/K$  and  $\cos \alpha_L = \sqrt{K^2 - 1}/K$ . Introducing these relations in the last equation for  $W_{acc}$

$$W_{acc} = T_L \left[ K + \sqrt{K^2 - 1} - \frac{1}{3} \left( \pi - \sin^{-1} \frac{1}{K} \right) \right] = T_L f(K)$$

where

$$f(K) = \left[ K + \sqrt{K^2 - 1} - \frac{1}{3} \left( \pi - \sin^{-1} \frac{1}{K} \right) \right]. \quad (61-10)$$

Since the uppermost limit  $(\pi - \alpha_L)$  was used in determining the area in Fig. 61-5, the following equation must be satisfied:

$$T_L f(K) \geq \frac{1}{2} \frac{J}{p/2} \omega_s^2 s_L^2. \quad (61-11)$$

Fig. 61-6 shows the relation between  $f(K)$  and  $K = T_{Smax}/T_L$  in which for values of  $K \geq 1.2$  the approximate Eq. (61-10) is used, while for values of  $K < 1.2$  a more accurate calculation has been made.

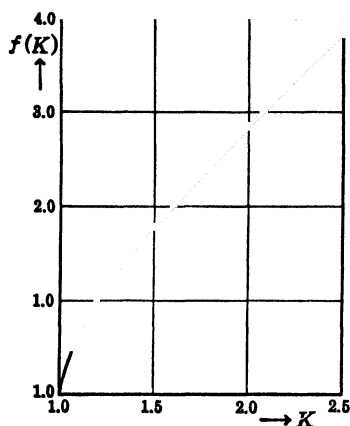


FIG. 61-6. Determination of  $f(K)$  for calculation of the slip  $s_L$  according to Eq. (61-12).

With the aid of Eq. (61-11) and Fig. 61-6, it is possible for given values of  $T_L$ ,  $s_L$ , and  $J$  to determine the magnitude of  $K$  and thus, the synchronous pull-out torque  $T_{Smax} = KT_L$ ; therefore the field current necessary for the machine to pull into step at the most favorable pole position  $\alpha = 0$  is also determined.

$s_L$  is the slip corresponding to the load torque (Fig. 61-1). It can be seen from Eq. (61-11) that the synchronous pull-out torque  $T_{Smax} = CT_n$  necessary for pulling into step is smaller, the smaller the value of  $s_L$ . The magnitude of  $s_L$  for a given value of  $T_L$  depends essentially upon the design of the damper winding and the ratio of the leakage reactance and resistance of the field winding.

By inserting a proper resistance in the field winding, it is possible to raise the speed-torque curve at small slips and to reduce  $s_L$ . A similar result is achieved by means of a double-cage damper winding instead of a single-cage.

Equation (61-11) now can be solved for  $s_L$ . Introducing  $\omega_s = 2\pi f_1$  and  $WR^2$  for  $J$ .

$$s_L \leq \frac{830}{n_s} \sqrt{\frac{f(K)}{K}} \sqrt{\frac{CP_n}{WR^2 \times f_1}} \quad (61-12)$$

In this equation  $P_n$  is in kw and  $WR^2$  in lb.-ft.<sup>2</sup>

Equation (61-12) prescribes the magnitude of the slip which must correspond to the load torque  $T_L$  in the asynchronous speed-torque curve (Fig. 61-1) when the synchronous overload capacity  $T_{Smax}/T_n = C$  and  $WR^2$  of the rotating mass are given. If the asynchronous speed-torque curve is given and a certain slip  $s_L$  corresponds to the load torque  $T_L$  in this curve, then the machine will pull into step if this value of  $s_L$  is equal to or smaller than the value of  $s_L$  given by Eq. (61-12). If it is larger than the value of  $s_L$  given by Eq. (61-12) the machine will not pull into step.

Equations (61-11) and (61-12) apply to the case when the d-c excitation is applied in the most favorable position of the rotor ( $\alpha = 0$ ). For small slip frequencies (up to 2 cps, corresponding to a slip of 3% at  $f_1 = 60$  cycles) the most favorable pole position can be determined easily with the aid of a polarizing or center-scale ammeter inserted in the field circuit. If the excitation is applied by hand, the field switch must be closed at the instant when the slip current in the field circuit goes through zero in the same direction in which the direct current has to flow. Since the d-c field current does not rise instantly and since switching also introduces a time delay, it is necessary to

close the switch earlier by approximately  $\frac{1}{4}$  of a period of the slip current. If the slip frequency exceeds 2 cps, hand switching is not reliable. Usually automatic angle switching is applied.

**61-3. Solution of the equation of motion for  $\alpha \neq 0$ .** Various authors (Ref. O2) have investigated the torque  $T_{S\max}$  and the slip  $s_L$  which are necessary in order to pull the machine into step when the d-c excitation is applied to a rotor position where  $\alpha = 0$ . The work of H. E. Edgerton and F. J. Zak will be described briefly in the following:

With the aid of the substitution

$$t = t' \sqrt{\frac{J}{p/2 T_{S\max}}} \quad (61-13)$$

Eq. (61-7) becomes

$$\frac{d^2\alpha}{(dt')^2} + K_D \frac{d\alpha}{dt'} + \sin \alpha = \frac{T_L}{T_{S\max}} \quad (61-14)$$

where

$$K_D = \frac{T_L}{s_L \omega_s \sqrt{(J/\frac{1}{2}p) T_{S\max}}} \quad (61-15)$$

If Eq. (61-14) is written in the form of a double integral, it can be solved with the aid of the intergraph.

For a fixed value of  $K_D$  and variable values of  $T_L/T_{S\max}$  as well as of the angle of switching  $\alpha_{(t=0)} = \alpha_0$ , Fig. 61-7 shows the relation between  $\alpha_0$  and  $T_L/T_{S\max}$ . The cross-hatched area corresponds to those pairs of  $\alpha_0$  and

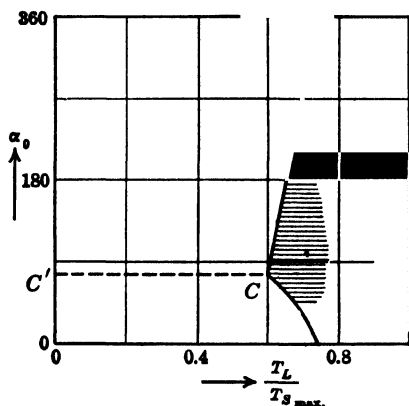


FIG. 61-7. Determination of the torque ratio  $T_L/T_{S\max}$  at which the motor pulls into step at the most unfavorable rotor angle for a given value of  $K_d$ .

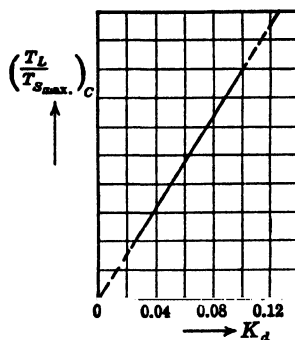


FIG. 61-8. Torque ratio  $T_L/T_{S\max}$  at which the motor pulls into step at the most unfavorable rotor angle as a function of  $K_d$ .



$T_L/T_{s\max}$  for which the machine will not pull into step. At the torque ratio  $T_L/T_{s\max} = C'C$  the motor pulls into step for all switching angles  $\alpha_0$ .

Fig. 61-7 applies to a fixed value of  $K_D$ . If Fig. 61-7 is evaluated for various values of  $K_D$  and the magnitude of  $C'C = (T_L/T_{s\max})$  is plotted as a function of  $K_D$ , the straight line of Fig. 61-8 will be obtained. From this figure the following relation results:

$$\left(\frac{T_L}{T_{s\max}}\right)_C \leq 1.057 K_D = 1.057 \frac{T_L}{s_L \omega_s \sqrt{(J/\frac{1}{2}p)} T_{s\max}}. \quad (61-16)$$

This is the condition which must be satisfied, if the machine is to pull into step when the excitation is applied at the *most unfavorable* rotor angle. If the power is given in kw and  $WR^2$  in lb.-ft.<sup>2</sup>, the slip will be:

$$s_L = \frac{620}{n_s} \sqrt{\frac{CP_n}{WR^2 \times f_1}}. \quad (61-17)$$

As has been explained in the foregoing discussion of Eq. (61-12), Eq. (61-17) determines the slip which must correspond to the load torque  $T_L$  in the asynchronous speed-torque curve (Fig. 61-1), if the overload capacity  $T_{s\max}/T_n = C$  and the  $WR^2$  of the rotating mass are given. If in the curve in Fig. 61-1 the slip  $s_L$  corresponding to  $T_L$  is larger than the value of  $s_L$  given by Eq. (61-17), the machine does not pull into step. In this case either the resistance in the field circuit has to be changed, or, if this does not suffice, then the dimensions of the damper winding must be changed, or a double-cage damper used.

Comparing Eq. (61-12) with Eq. (61-17), it is seen that when the excitation is applied in the most favorable rotor position ( $\alpha = 0$ ) the slip  $s_L$  may be  $1.33 \sqrt{f(K)/K}$  times as large as the slip  $s_L$  when the excitation is applied in the most unfavorable rotor position  $\alpha = 180^\circ$ . For a motor with a synchronous pull-out torque  $T_{s\max}$  equal to 1.5 times the rated torque  $T_n$  ( $C = 1.5$ ) which has to pull into step at 50% of rated torque ( $T_L = 0.5T_n$ ,  $K = T_{s\max}/T_L = 3$ ) the ratio of both slips is 1.7 to 1. From this it can be seen that any automatic device which makes it possible to apply the d-c excitation in the most favorable rotor position  $\alpha = 0$  (angle switching) is of great advantage in the synchronous motor operation.

The equation used for the synchronous torque (Eq. 61-1) is

$$T_s = T_{s\max} \sin \alpha.$$

As was explained in Art. 36-1, this relationship applies when the reluctance is constant around the periphery of the armature, as is the case for machines with cylindrical rotors, when the saturation is low, and when the stator resistance is neglected. The stator resistance reduces the synchronous torque. The variation of the reluctance increases the synchronous torque since the reluctance in the quadrature axis usually is larger than in the direct axis (reluctance torque, see Art. 36-1). For this reason, for salient-pole motors a

somewhat larger value of  $s_L$  is permissible than that obtained from Eqs. (61-12) and (61-17).

According to Eq. (61-9),

$$CT_n = T_{Smax}.$$

Therefore (see Art. 36-1 and 36-5)

$$CP_n = P_{m,dev,max} \times 10^{-3} = m \frac{VE_f}{x_d} 10^{-3} \text{ kw} \quad (61-18)$$

$E_f$  is the emf induced in the stator winding by the flux of the field current applied to the rotor for pulling it into step. This usually is the field current which corresponds to the rated KVA of the stator, i.e., to  $(KVA)_n = (746 \times \text{hp} / \eta \cos \varphi) 10^{-3} = m V I_n \times 10^{-3}$ . Expressing the quantities of Eq. (61-18) in p-u (see Art. 33-1, Eq. 33-3)

$$m = 1, \quad V = 1, \quad \frac{1}{x_d} = SCR, \quad E_{f(p.u.)} = \frac{E_f}{V}.$$

Hence

$$CP_n = \frac{E_f}{V} SCR \times (KVA)_n \text{ kw} \quad (61-19)$$

Thus, for  $CP_n$  in Eq. (61-17) can be introduced

$$CP_n = \frac{E_f}{V} SCR \frac{\text{hp} \times 746}{\eta \cos \varphi} 10^{-3} \text{ kw.} \quad (61-20)$$

## Chapter 62

### DESIGN PRINCIPLES OF AN ELECTRIC MACHINE—SPECIFIC TANGENTIAL FORCE

---



---

**62-1. Magnitude of the tangential force.** It has been pointed out in Art. 1-2d, that the source of torque and power of the electric machine is the *tangential* force produced by the main flux on the current carrying armature conductors. The active material of the electrical machine, i.e., the core iron and copper, is utilized better the higher the specific tangential force (lb./in.<sup>2</sup>) on the armature surface. Following will be given some approximate data on this specific tangential force which are based on experience.

If  $T$  is the torque of the machine in lb./ft., the total tangential force is

$$F = \frac{T \times 12}{R} = \frac{T \times 12}{D/2} \quad \text{lb.} \quad (62-1)$$

and the specific tangential force

$$\sigma = \frac{12T}{\frac{1}{2}D\pi D l_e} \quad \text{lb./in.}^2 \quad (62-2)$$

where  $l_e$  is the effective core length (see Art. 50-2). On the other hand

$$P \cos \varphi = \frac{Tn}{7.04} 10^{-3} \quad (62-3)$$

where  $P$  is the apparent power in kva. Therefore,

$$\sigma = \frac{24}{\pi D^2 l_e} \frac{7.04 \times 10^2 \times \cos \varphi \times P}{n} = 54 \times 10^3 \times \cos \varphi \left[ \frac{P}{D^2 l_e n} \right] \quad \text{lb./in.}^2 \quad (62-4)$$

Since the tangential force depends upon the flux and the ampere-conductors, the expression in the bracket also must depend upon these quantities. There is

$$P = mEI \times 10^{-3}, \quad (62-5)$$

$$E = 4.44 f N k_{ap} \Phi 10^{-3}, \quad (62-6)$$

$$\Phi = \frac{2}{\pi} \tau l_e B, \quad f = \frac{pn}{120}, \quad \tau = \frac{\pi D}{p}. \quad (62-7)$$

Further, the ampere-conductors per inch circumference,

$$A = \frac{2mNI}{\pi D}. \quad (62-8)$$

Inserting Eqs. (62-6), (62-7), and (62-8) into Eq. (62-5) there results

$$P = \frac{1}{8.6} D^2 l_e n k_{ap} A B \times 10^{-11}. \quad (62-9)$$

or

$$\left[ \frac{P}{D^2 l_e n} \right] = \frac{1}{8.6} k_{ap} A B \times 10^{-11}. \quad (62-10)$$

Thus, from Eqs. (62-10) and (62-4)

$$\frac{\sigma \times 10^{-3}}{54 \times \cos \varphi} = \frac{1}{8.6} k_{ap} A B \times 10^{-11}. \quad (62-11)$$

Although  $A$  and  $B$  increase with the output of the machine, the quantity on the right side of Eq. (62-11) and with it the specific tangential force varies within relatively narrow limits compared to the range in power output. The value of  $\sigma$  (of  $A$  and  $B$ ) is limited by the heating, i.e., by the permissible temperature rise of the insulating materials, and by the performance of the machine. High values of  $A$  and  $B$  increase the copper and iron losses, thus increasing the heating and decreasing the efficiency. In induction motors a large  $B$  is undesirable also from the standpoint of the power factor. In small machines the space necessary for insulation is relatively larger than in large machines. This makes it necessary to reduce the copper area, i.e.,  $A$ . Since the teeth become tapered in small machines, the gap induction  $B$  also must be reduced, in order to avoid high tooth saturation at the root of the tooth. The pole pitch also has an influence on the value of  $\sigma$ , because the machine with the larger pole pitch has better cooling than the machine with smaller pole pitch, due to the larger extension of the end winding. Also the voltage is of importance: the higher the voltage the more space is necessary for the insulation and the less space is left for the copper.

**62-2. Output constant.** Due to the fact that the specific tangential force varies between relatively narrow limits, the quantity represented by Eqs. (62-10) and (62-11) is called *output constant* and denoted by  $C$ . In Figs. 62-1 to 62-3 this quantity, i.e.

$$C = \frac{P}{D^2 l_e n}, \quad (P \text{ in kva}), \quad (62-12)$$

is given for d-c machines (generators and motors), 3-phase induction motors and 3-phase salient-pole synchronous generators (see Ref. A5 to 12).

In Fig. 62-1 for the d-c machines, kw/rpm are plotted as abscissae and  $D^2L$  as ordinates.  $L$  is here the total length of the armature core. In Figs. 62-2 and 62-3 for 3-phase induction motors and salient-pole synchronous machines respectively the pole pitch is plotted as abscissae and  $C \times 10^6$  as ordinates. Figs. 62-4 and 62-5 are auxiliary curves to Figs. 62-2 and 62-3 which give the ratio between the effective core length  $l_e$  and pole pitch. This ratio cannot be chosen arbitrarily because it is of importance for the cooling of the machine.

Having the value of the output constant  $C$ , it is possible to determine the  $D^2l_e$  of a machine when  $P$  and  $n$  are given or the power  $P$  of a machine when  $D$ ,  $l_e$ , and  $n$  are given. For the induction motor  $P$  is the input of the stator in kva. The voltage for Figs. 62-2 and 62-3 is assumed to be 220 volts for the smaller machines and up to 2300 volts for the larger machines. For Fig. 62-3 it is assumed further that the rotor is wound with round or rectangular wire and not with copper strips placed on edge.

It must be pointed out that the Figs. 61-1 to 62-3 give conservative approximate values.

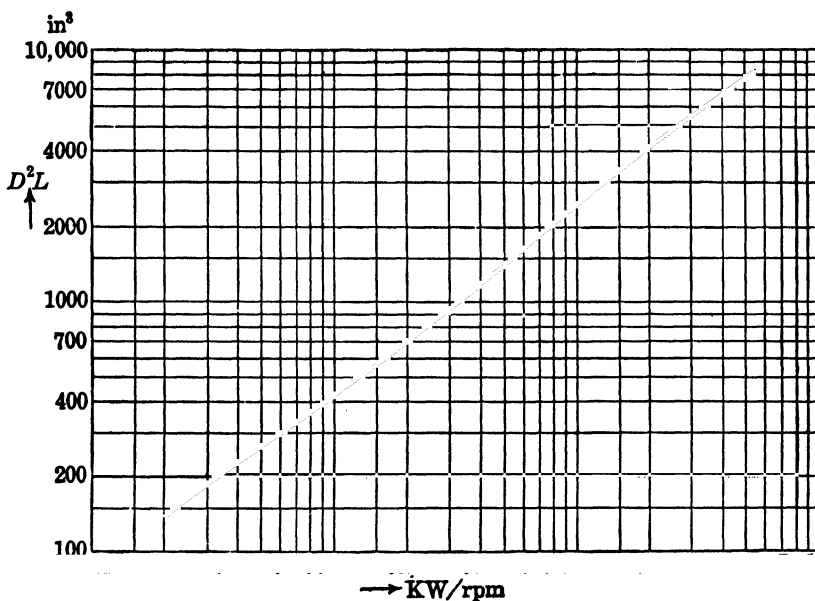


FIG. 62-1.  $D^2L$  as a function of kw/rpm for d-c machines.

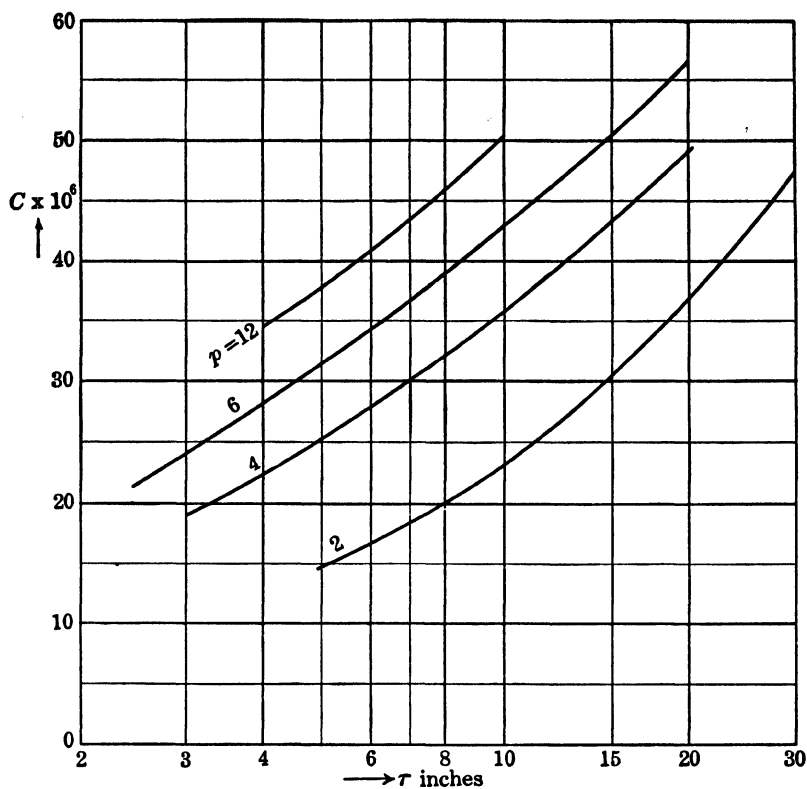


FIG. 62-2. Output constant of induction motors as a function of pole pitch.

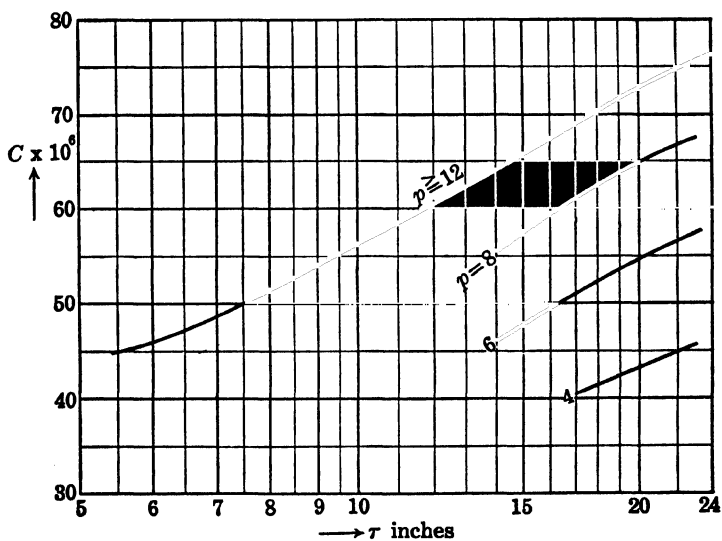


FIG. 62-3. Output constant of salient-pole synchronous machines as a function of pole pitch.

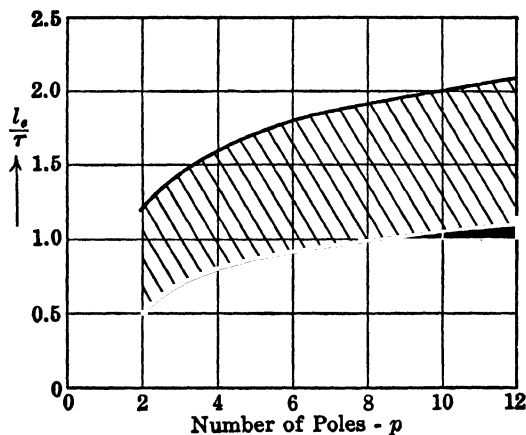


FIG. 62-4. Ratio of effective core length to pole pitch as a function of the number of poles (to Fig. 62-2).

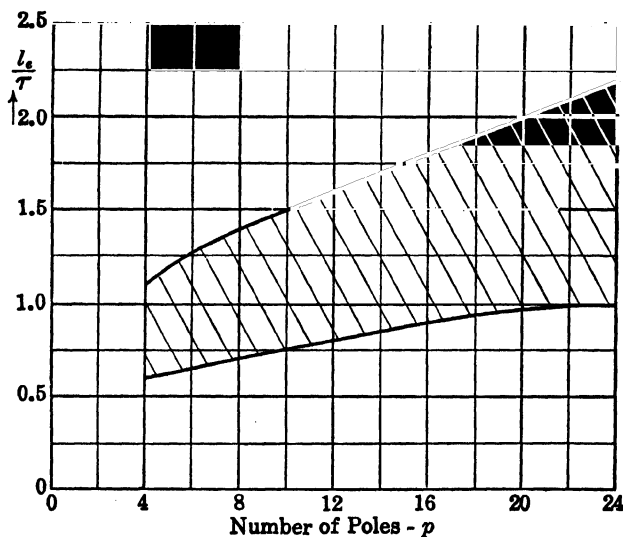


FIG. 62-5. Ratio of effective core length to pole pitch as a function of the number of poles (to Fig. 62-3).

**62-3. Range of tangential force.** It follows from Fig. 62-1 and Eqs. (62-10) and (62-11) that for the range of d-c machines given by Fig. 62-1 the specific tangential force varies between 0.8 and 3.5 lb./in.<sup>2</sup> These values may be as low as 0.4 lb./in.<sup>2</sup> in very small machines and as large as 5.0 lb./in.<sup>2</sup> in large machines.

For the range of the 3-phase induction motors represented by Fig. 62-2 the specific tangential force varies approximately between 0.7 and 2.8

lb./in.<sup>2</sup> In small single-phase motors  $\sigma$  is as low as 0.3 lb./in.<sup>2</sup>, and in large induction motors it may reach the value 4.0 lb./in.<sup>2</sup>

In Fig. 62-3, which refers to medium-size and larger salient-pole machines,  $\sigma$  varies approximately from 1.7 to 3.2 lb./in.<sup>2</sup> For large machines it may reach 5.0 lb./in.<sup>2</sup>



## Chapter 63

### TANGENTIAL FORCES AND POWER FLOW IN ELECTRICAL MACHINES

**63-1. The tangential forces.** In Chaps. 52 and 58 the tangential forces on the armature and the torques were derived on the basis of Biot-Savart's law (Art. 1-2d)

$$F = \text{const} \times BII$$

where  $I$  is the current of a conductor lying *within* the  $B$ -flux. Accordingly, it was assumed for the derivations of both chapters that the armature conductors lie *directly within the gap flux*. In reality this is not the case. The armature conductors are placed in slots, i.e., they are moved away from the gap and, therefore, lie in a flux the density of which is much smaller than that in the gap. If the tangential force of the machine were calculated with the *actual* value of  $B$  in which the conductors lie, a much smaller force would be obtained than that measured by tests.

In Art. 1-2d the electromagnetic power of a machine was derived from Biot-Savart's law. Vice versa, Biot-Savart's law can be derived from the electromagnetic field energy. This law and the derivations made in Chaps. 52 and 58 are correct and are in agreement with tests. Thus, Biot-Savart's law, applied under the assumption that the conductors lie within the gap flux and that the forces are exerted on the conductors themselves, yields accurate results, but in reality the forces are not exerted upon the conductors. It follows from this, that there must be *another kind of mutual influence* between the  $B$ -flux in the gap and the conductors carrying the current  $I$ , i.e., the two elements of Biot-Savart's law, which accounts for the tangential force of the electrical machine. This other combination effect of  $B$  and  $I$  can be found by applying Faraday-Maxwell's conception of the stresses in the magnetic field. This yields the result that the tangential forces are exerted upon the iron.

**63-2. The power flow.** Poynting Vector. Here also the Faraday-Maxwell conception of the electric and magnetic fields yields another explanation for the power flow in electrical machines than that obtained from the concept that the energy flows through conductors.

Each atom of a substance is made up of its nucleus and the associated electrons in the proper atomic shells. In a conductor the electrons are free, i.e., they are loosely associated with their nuclei and are therefore free to be accelerated in the direction opposite to the electric field intensity. In an insulator the electrons are bound. If an insulator is subject to an electric field, the orbits of the electrons in the various atomic shells will be distorted with respect to the position of the nucleus. The average position of the electrons will be shifted toward the region of higher electric potential. In Maxwell's terminology a "displacement"  $D$  of the electrons takes place which is proportional to the field intensity  $\vec{E}$

$$\vec{D} = \epsilon \vec{E} \quad (63-1)$$

where  $\epsilon$  is the dielectric constant. The work corresponding to an elementary displacement is

$$dW = E dD = \epsilon E dE \quad (63-2)$$

The work which corresponds to any finite displacement is

$$W = \epsilon \int_0^D E dE = \frac{1}{2} \epsilon E^2 = \frac{1}{2} ED \quad (63-3)$$

This work is accumulated as potential energy of the field, per unit volume. The total field energy in a volume  $\tau$  is

$$F_E = \frac{1}{2} \int_{\tau} \epsilon E^2 d\tau = \frac{1}{2} \int_{\tau} ED d\tau \quad (63-4)$$

Corresponding to Eq. (63-4), the potential energy of the magnetic field in a non-ferromagnetic medium is

$$F_M = \frac{1}{2} \int_{\tau} \mu H^2 d\tau = \frac{1}{2} \int_{\tau} HB d\tau \quad (63-5)$$

Consider a certain region (a *closed* surface). The increase of the total energy in this region with time is

$$\text{Increase of energy} = \frac{\partial}{\partial t} (F_E + F_M) + Q \quad (63-6)$$

where  $Q$  is Joule heat which appears in the considered region, when there are conductors.

The principle of conservation of energy requires that there should be a *stream of energy through the surface into the region* equal to the increase of energy given by Eq. (63-6). Conversely, a stream of energy through the surface *out of the region* must appear, if the energy of the region decreases. This stream of energy in and out of the *closed* surface is represented by *Poynting vector*. Eq. 63-6 must be written as

$$\frac{\partial}{\partial t} (F_E + F_M) + Q = \int_S N_n dS \quad (63-7)$$

where  $N_n$  is the component of Poynting's vector perpendicular to the surface element  $dS$ .

In order to get an idea about the physical meaning of the Poynting vector, the power flow in a polyphase induction motor running with rated load will

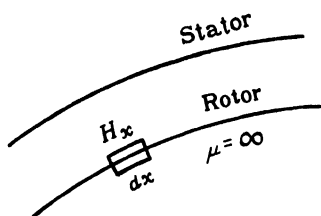


FIG. 63-1. Application of Ampere's Law to a closed loop at the surface of the rotor of a polyphase induction motor.

be considered. Fig. 63-1 shows a part of the periphery of stator and rotor. The conductors are perpendicular to the plane of the figure. According to Biot-Savart's law (Eq. 1-29), the total force is

$$F = \int B l_e A dx \quad (63-8)$$

where  $B$  is the density of the rotating flux in the gap and  $A$  indicates the ampere-conductors per unit length of the circumference of the rotor.  $B$  and

$A$  ( $E$  and  $I$ , Fig. 17-5) are assumed to be in time phase, as is almost the case in the induction motor running with rated load. The power transferred is

$$P = F \times v = \int B v l_e A dx \quad (63-9)$$

where  $v$  is the velocity of the rotating flux.

Consider Eq. 1-12. According to Faraday-Maxwell's concept of electric and magnetic fields, an emf can be induced not only in conductors but in insulators as well. Consider a loop in the gap the plane of which is parallel to the stator and rotor surface. Writing Eq. 1-12 in the form

$$-\frac{\partial \varphi}{\partial t} = \int_l E dl = B l v \quad (63-10)$$

the electric field intensity in the gap is

$$E = B v \quad (63-11)$$

Applying Ampere's law to a closed loop of the length  $dx$  at the rotor surface (Fig. 63-1) and assuming that, for the rotor iron,  $\mu = \infty$ , there results  $H dx = A dx$ , because, for the part of the loop which runs through the iron  $H = 0$ . The total transferred power thus becomes (see Eqs. 63-7 and 63-9)

$$P = \int_s E H dS = \int_s N_n dS \quad (63-12)$$

where  $dS = l_e dx$  is a surface element of the rotor.

It is seen from the latter equation that the magnitude of Poynting vector is determined by the magnitudes of the electric and magnetic field intensities.  $E$  and  $H$  are vectors. In order to find the magnitude of Poynting vector and

its position with respect to  $\dot{E}$  and  $\dot{H}$ , the directions of  $\dot{E}$  and  $\dot{H}$  for the example under consideration will be determined.

It must be noticed that outside the gap  $H=0$  since  $\mu$  of the iron has been assumed infinitely large. Thus,  $E$ ,  $H$ ,  $P$  and Poynting vector must be determined only for the gap. The direction of  $E$  is obtained from Eq. 63-11 and the right-hand rule (Art. 1-2a):  $v$  is tangential to the rotor surface,  $B$  is radial, and  $E$  is, therefore, axial and perpendicular to the plane of Fig. 63-1. The direction of  $H$  is determined by Ampere's law. Since the current flow is axial,  $H$  must be tangential to the rotor surface (see Fig. 63-1). Thus,  $E$  and  $H$  are *perpendicular* to each other in the example under consideration. This yields the maximum value of power flow, i.e., the maximum value of Poynting vector. In general, the magnitude of Poynting vector is

$$\dot{N} = EH \sin(\dot{E}\dot{H}) \quad (63-13a)$$

According to Eq. (63-12) the power flow is radial. Since  $E$  is axial and  $H$  tangential, Poynting vector is perpendicular to  $B$  and  $H$ . In vector notation

$$\dot{N} = \dot{E} \times \dot{H} \quad (63-13b)$$

*This equation applies not only to the specific case considered but is general.* It determines the magnitude and the direction of Poynting vector. It should be noticed that Poynting theorem holds true only for a *closed* surface.

The induction motor was considered under rated load, i.e., it was assumed that  $B$  and  $A$  are in time phase. If the induction motor runs with a considerable slip,  $B$  and  $A$  are displaced in time phase and the instantaneous values of  $B$  and  $A$  must be introduced in Eqs. 63-8 and 63-9 (see Art. 1-2d), i.e., the time phase displacement between  $B$  and  $A$  must be taken into account. The same applies to  $E$  and  $H$  in Eqs. 63-12, 63-13a, and 63-13b.

Fig. 63-2 shows the relative position of the  $E$  and  $H$  distributions around the armature of a squirrel-cage rotor. Since the magnitude of the power flow depends upon the surface integral of the products of  $E$  and  $H$  around the armature, it is seen that, for the same amplitudes of  $\dot{E}$  and  $\dot{H}$ , the magnitude of the power flow is smaller when  $E$  and  $H$  ( $B$  and  $A$ ) are out of phase than when they are in phase. The same applies to the wound rotor motor.

When the induction motor runs at no-load (mechanical losses neglected), the waves of  $E$  and  $H$  (the waves of  $B$  and  $A$ , the waves of  $E$  and  $I$ -magnetizing) are shifted with respect to each other  $90^\circ$  and the surface integral, Eq. 63-12, yields the value 0; indicating that there is no power flow, as could be expected for no-load.

The concept of power flow corresponding to Poynting vector will be applied to several examples.

(a) *D-c power transferred through a line.* Fig. 63-3 shows an idealized two-conductor transmission line: the conductors are flat bars. There is no magnetic or electric field outside the conductors, but there is an electric field

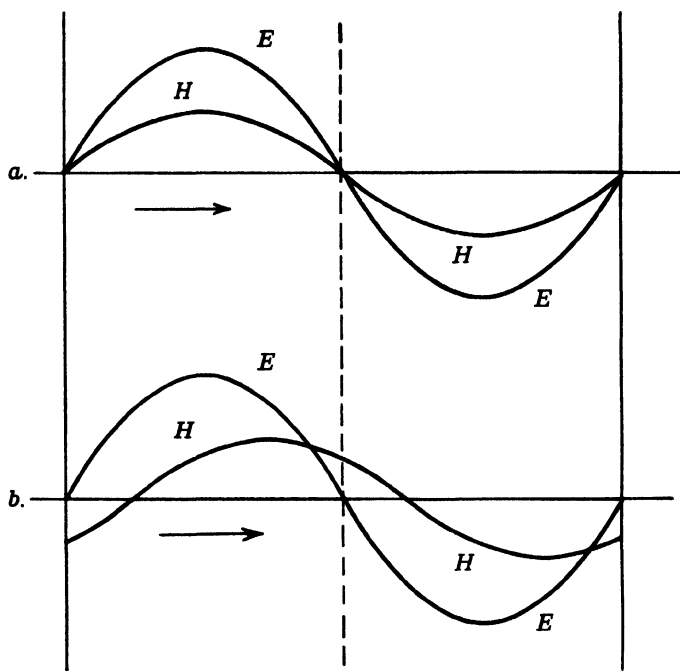


FIG. 63-2. (a) Relative position of the  $E$  and  $H$  distributions at rated slip.  
(b) Relative position of the  $E$  and  $H$  distributions at a large slip.

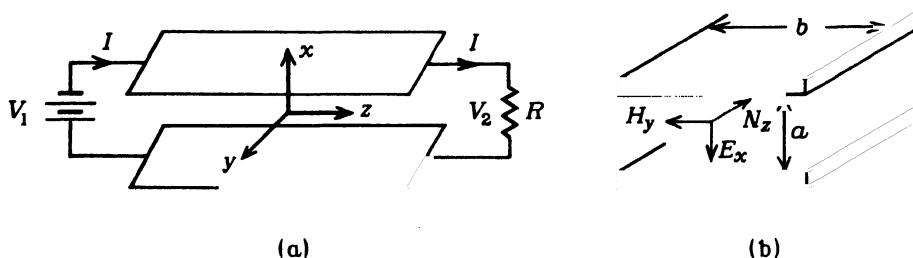


FIG. 63-3. Explanation of the power flow in an idealized 2-conductor transmission line.

inside the conductors and an electric and a magnetic field between the conductors.

It will be assumed at first that the line is lossless, i.e., that the resistivity ( $\zeta$ ) of the conductors is zero. In this case  $V_1 - V_2 = 0$  and, according to Eq. 1-12, the electric field intensity within the conductors is zero. It follows further from Eq. 1-12, that the electric field intensity between the conductors is (Fig. 63-3b)

$$\vec{E} = E_x = \frac{V}{a} \quad (63-14)$$

where  $V = V_1 = V_2$ . The magnetic field intensity in the space between the conductors is

$$\dot{H} = H_y = \frac{I}{b} \quad (63-15)$$

The power flow in the space between the conductors is then according to Poynting vector of energy flow

$$P_z = \int_S \frac{V I}{a b} dS = VI \quad (63-16)$$

since  $dS = a \times b$  and the angle between  $E_x$  and  $H_y$  is 90 degrees.

If the line is not lossless, the electric field intensity within the conductors is (Eq. 1-12)

$$\dot{E} = E_z = \frac{V_1 - V_2}{2l} \quad (63-17)$$

where  $2l$  is the length of the two conductors. The magnetic field intensity on the surface of the conductors is the same as before for the lossless line

$$\dot{H} = H_y = \frac{I}{b} \quad (63-18)$$

Eqs. 63-17 and 63-18 result in a power flow, i.e., a component of Poynting vector, in the  $x$ -axis of the magnitude

$$P_x = \int_S \frac{V_1 - V_2}{2l} \frac{I}{b} dS = \frac{V_1 - V_2}{2} I \quad (63-19)$$

since  $S = lb$  and the angle between  $E_z$  and  $H_y$  is 90 degrees. Eq. 63-19 is the power entering from the space between the conductors into one conductor. The power entering both conductors is twice as large.

Eqs. 63-16 and 63-19 which were derived from the energy of the magnetic and electric fields yield the same results as those obtained from the concept that the energy flow occurs through the conductors. The meaning of Eqs. 63-19 and 63-16 is that there is a power flow from the electromagnetic field between the conductors into the conductors equal to the Joule heat in the conductors and that the power supplied to the load is affected by a power flow from the electromagnetic field between the conductors toward the load. The conductors serve as guides for this power flow.

(b) *Single-phase transformer.* It is assumed that, in the iron,  $\mu = \infty$ . This means that inside the iron  $H = 0$  and the iron cannot carry any energy. The electric field is given by Eq. 1-12 and exists in the air as well as in the iron. When the secondary winding is open, the assumption  $\mu = \infty$  for the iron means that the magnetizing current (primary current) is zero. Since both currents are zero,  $\oint H_l dl = 0$  for any line of force, i.e.,  $H$  is zero in the iron as

well as in the air, and there is no power flow in the transformer. However, when the secondary is closed through a resistive load, the secondary current will produce a magnetic field corresponding to  $\oint H_1 dl = NI_2$ . With  $\mu = \infty$  in the iron, this field appears only in the air.

The establishment of the  $H$  field permits a power flow in the air (not in the iron). The direction of  $H$  is shown in Fig. 63-4. The electric field is perpendicular to the plane of the figure and power flows from the primary to the secondary.

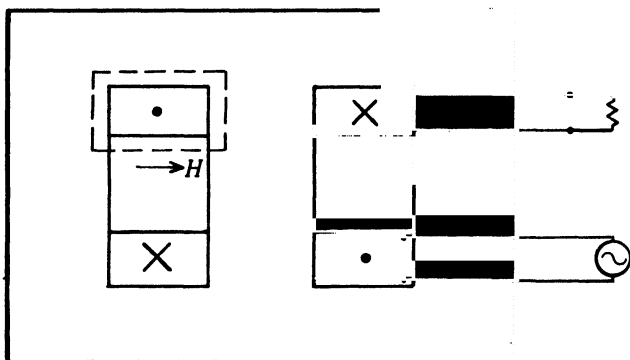


FIG. 63-4. Explanation of the power flow in a single-phase transformer.

The  $H$  field is the driving force for the leakage flux, hence a transformer must have leakage. In order to reduce the leakage reactance, the  $B$  associated with  $H$  must be reduced and this can be achieved by increasing the reluctance of the leakage path.

A resistive load has been assumed in the secondary of the transformer making  $E$  and  $H$  in time phase. If the secondary load is inductive or capacitive,  $E$  and  $H$  are not in time phase and the average power can be determined by taking the time average of the instantaneous power over one cycle. Considering  $E$  and  $H$  as phasors, this leads to the integration over space of the product of the magnitudes of  $E$  and  $H$  times the cosine of the time angle between them.

(c) *Synchronous motor.* Assume that the polyphase induction motor considered previously has a wound rotor excited by a d-c current, i.e., runs as a synchronous motor. Exactly the same considerations apply as to the induction motor. From the point of view of Poynting vector, nothing has been changed by the exciting of the rotor.

(d) *Rotary converter* (Fig. 63-5). This is also a synchronous motor, but the poles are at standstill and the supply is connected to the rotor. Since the exciting field is constant in time and space,  $E = Bv = 0$ , i.e., the electric field in the air gap is zero and there is no power transfer through the air gap.

The difference between the synchronous motor fed through the stator and that fed through the rotor is that in the former the electric power is supplied to the stator and the mechanical output is produced by the rotor, while in the latter both the electrical input and the mechanical output are connected with the rotor.

(e) *D-c motor*. The same considerations apply as to the rotary converter and there is no power flow across the gap. Power supplied to the rotor electrically is removed mechanically.

(f) *Generators*. The same considerations apply as to the motors.

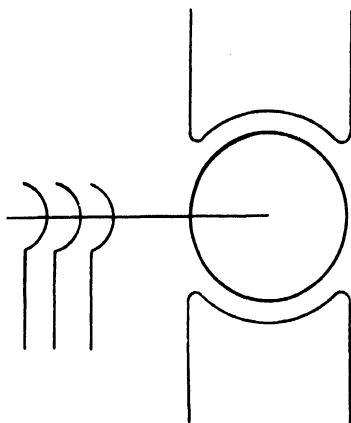


FIG. 63-5. Explanation of the power flow in a rotary converter.



## REFERENCES

### TEXTBOOKS

1. *Transformer Engineering*. L. F. Blume. 2nd ed., Wiley, 1951.
2. *Magnetic Circuits and Transformers*. M.I.T. Electrical Engineering Staff. Wiley, 1943.
3. *Principles of Alternating Current Machinery*. R. R. Lawrence and H. E. Richards. 4th ed., McGraw-Hill, 1953.
4. *Fundamentals of A-C Machines*. A. P. T. Sah. McGraw-Hill, 1940.
5. *Theory of Alternating Current Machinery*. A. S. Langsdorf. Wiley, 1955.
6. *General Theory of Electrical Machines*. B. Adkins. Wiley, 1957.
7. *Alternating Current Machines*. A. F. Puchstein, T. C. Lloyd, and A. G. Conrad. 3d ed., Wiley, 1954.
8. *Synchronous Machines*. C. Concordia. Wiley, 1951.
9. *Nature of Polyphase Induction Machines*. P. L. Alger. Wiley, 1951.
10. *Electric Machinery*. A. E. Fitzgerald and Charles Kingsley, Jr. McGraw-Hill, 1952.
11. *Electric Energy Conversion*. Y. H. Ku. Ronald Press, 1959.
12. *Alternating Current Machinery*. L. V. Bewley. Macmillan, 1949.
13. *Winding Alternating-Current Machines*. M. Liwischitz-Garik and C. Gentilini. Van Nostrand, 1950.
14. *Electromechanical Energy Conversion*. D. C. White and H. H. Woodson. Wiley, 1949.
15. *Performance and Design of Alternating Current Machinery*. M. G. Say and E. M. Pink. Pitman & Sons, 1936.
16. *The Induction Motor and Other Alternating Current Motors*. B. A. Behrend. McGraw-Hill, 1921.
17. *Alternating Current Motors*. A. S. McAllister. 3rd ed., McGraw-Hill, 1909.
18. *Electric Machines, Vol. II: A-C Machines*. M. Liwischitz-Garik and C. C. Whipple. Van Nostrand, 1946.
19. *Magnetic Control of Electric Motors*. P. B. Harwood. 2d ed., Wiley, 1949.
20. *Electric Motors in Industry*. D. R. Shoults and C. J. Rife. Wiley, 1942.
21. *Controllers for Electric Motors*. James and Markel. McGraw-Hill, 1952.

### ARTICLES

22. Field Harmonics in Induction Motors. M. Liwischitz. *Trans. AIEE*, 61:797 (1942).
23. Differential Leakage with Respect to the Fundamental Wave and to the Harmonics. M. Liwischitz. *Trans. AIEE*, 63:1139 (1944).
24. Distribution Factors and Pitch Factors of the Harmonics of a Fractional-Slot Winding. M. Liwischitz. *Trans. AIEE*, 62:664 (1943).
25. Y-Synchronizing Torque of the Synchronous Machine. *Siemens Z.*, 12:15 (1933).
26. The Mathematical Treatment of the MMF Armature Windings. B. Hague. *J. Inst. Elec. Engrs.*, 55:489 (1917).
27. Harmonics Due to Slot Openings. C. A. M. Weber and F. W. Lee. *JAIEE*, 43:687 (1924).
28. MMF of Polyphase Windings. Q. Graham. *JAIEE*, 46:19 (1927).

29. Dead Points in Squirrel Cage Motors. Q. Graham. *Trans. AIEE*, 59:637 (1940).
30. Quiet Induction Motors. L. E. Hilderbrand. *JAIEE*, 49:848 (1930).
31. Cause and Elimination of Noise in Small Motors. *Elec. Eng.* 56:1359 (1937).
32. Single-Phase Motor Torque Pulsation. P. L. Alger and A. L. Kimball. *Trans. AIEE*, 43:(1924).
33. Split Winding Starting of Three-Phase Motors. P. L. Alger, H. C. Ward, Jr., and F. H. Wright. *Trans. AIEE*, 71:867 (1952).
34. Speed-Torque Calculations for Induction Motors with Part Windings. P. L. Alger, Y. H. Ku, and C. H. T. Pan. *Trans. AIEE*, 73:151 (1954).
35. Speed Control of Induction Motors Using Saturable Reactors. P. L. Alger and Y. H. Ku. *Trans. AIEE*, 75:1335 (1956).
36. Single-Phase Motor Theory—A Correlation of the Cross-Field and the Revolving Field Concepts. C. T. Button. *Trans. AIEE*, 60:505 (1941).
37. A Physical Conception of Single-Phase Motor Operation. R. Beach. *Elec. Eng.* 63:254 (1944).
38. On the Equivalence of the Two Theories of the Single-Phase Induction Motor. V. Karapetoff.
39. A Contribution to the Theory of the Deep-Bar Induction Motor. J. F. H. Douglas. *Trans. AIEE*, 71:862 (1952).
40. Torques of Induction Motors During Starting. H. Möller. *Arch. Elektrotech.*, 24:401 (1930).
41. Starting of Induction Motors with Squirrel Cage Rotor. F. Kade. *Elektrotech. Z.*, 52:1135 (1931).
42. Three Rules for the Choice of Slot-Combination of Squirrel Cage Motors. H. Sequenz. *Elektrotech. Z.*, 55:269 (1934).
43. Torque Components Due to Space Harmonics in Induction Motors. K. L. Hansen. *Proc. AIEE*, 41:928 (1922).
44. Parasitic Torques in Induction Motors. M. Kronld. *Bull. Oerlikon*, 24:654 (1931); also 25:665 (1931).
45. Influence of the Slot Harmonics on the Torque-Speed Curve of the Induction Motor. B. P. Aparoff. *Publ. Natl. Research Inst. (Moscow)*, 1:47 (1924).
46. Performance Calculation of Induction Motors. C. G. Veinott. *Trans. AIEE*, 51:743 (1932).
47. Segregation Losses in Single-Phase Induction Motors. C. G. Veinott. *Trans. AIEE*, 54:1302 (1935).
48. Starting Windings for Single-Phase Induction Motors. C. G. Veinott. *Trans. AIEE*, 63:288 (1944).
49. Analysis of Unsymmetrical Machines. W. V. Lyon and C. Kingsley. *Elec. Eng.* (1936).
50. Symmetrical Components as Applied to the Single-Phase Induction Motor. F. W. Suhr. *Trans. AIEE*, 64:651 (1945).
51. Fundamental Theory of the Capacitor Motor. H. C. Specht. *Trans. AIEE*, 48:607 (1929).
52. The Revolving Field Theory of the Capacitor Motor. W. J. Morrill. *Trans. AIEE*, 48:614 (1929).
53. Performance Calculation of Capacitor Motors. P. H. Trickey. *Trans. AIEE*, 60:73 (1941).
54. An Analysis of the Shaded Pole Motor. P. H. Trickey. *Trans. AIEE*, 45:1431 (1947).
55. Performance Calculations of the Shaded Pole Motor. P. H. Trickey. *Trans. AIEE*, 66:1438 (1947).

56. The Hysteresis Motor. H. C. Rotors. *Trans. AIEE*, 66:1419 (1947).
57. Theory of Hysteresis-Motor Torque. B. T. Teare, Jr. *Trans. AIEE*, 59:907 (1940).
58. Selsyn Instruments for Position Systems. T. M. Linville and J. S. Woodward. *Trans. AIEE*, 53:953 (1934).
59. Induction Motors as Selsyn Drives. L. M. Novacki. *Trans. AIEE*, 53:1721 (1934).
60. Selsyn Design and Application. T. C. Johnson. *Trans. AIEE*, 64:703 (1945).
61. Damping and Synchronizing Torques of Power Selsyns. C. Concordia and G. Kron. *Trans. AIEE*, 64:366 (1945).
62. Synchronous Machines: Part I. An Extension of Blondel's Two-Reaction Theory; Part II. Steady State Power Angle. C. A. Doherty and C. A. Nickle. *Trans. AIEE*, 45:912 (1926).
63. Two-Reaction Theory of Synchronous Machines: Part I. R. H. Park. *Trans. AIEE*, 48:716 (1929); Part II. *Ibid.*, 52:352 (1933).
64. Two-Reaction Theory of Synchronous Machines. S. B. Crary. *Trans. AIEE*, 56:27 (1939).
65. The Calculation of the Armature Reaction of Synchronous Machines. P. L. Alger. *Trans. AIEE*, 47:493 (1928).
66. A Basic Analysis of Synchronous Machines. W. A. Lewis. *Trans. AIEE*, 77:436 (1958).
67. Calculation of Synchronous Machine Constants. L. A. Kilgore. *Trans. AIEE*, 50:1201 (1931).
68. Determination of Synchronous Machine Constants. S. H. Wright. *Trans. AIEE*, 50:1313 (1931).
69. Synchronous Machine Reactance Measurements. B. L. Robertson. *Gen. Elec. Rev.*, 35:126 (1932).
70. The Reactances of Synchronous Machines. R. H. Park and B. L. Robertson. *Trans. AIEE*, 47:514 (1928).
71. Fundamental Concepts of Synchronous Machine Reactances. B. R. Prentice. *Trans. AIEE*, Suppl. 1937, p. 1.
72. The Quadrature Synchronous Reactance of Salient-Pole Synchronous Machines. R. V. Shepherd and C. E. Kilbourne. *Trans. AIEE*, 62:684 (1943).
73. The Pulling into Step of a Synchronous Induction Motor. H. E. Edgerton and F. J. Zak. *J. Inst. Elec. Engrs. (London)*, 68:1205 (1930).
74. Synchronous-Motor Pulling-into-Step Phenomena. H. W. Edgerton, G. S. Brown, K. J. Germeshausen, and R. W. Hamilton. *Trans. AIEE*, 52:342 (1933).
75. Starting Performance of Synchronous Motors. H. V. Putnam. *Trans. AIEE*, 46:39 (1927).

## ANSWERS TO PROBLEMS

### Chapter 1

1. 0.096—2. 41.67 fpm—3. 225 rpm—4. 0.0015 vols—5. 292 turns—6. 22.6 V, 14.4 V—7. 200,000 maxwells, 3.33 V, 7.5 V—8. 2.8 V, 1.4 V—9. 7.07 V—10. 2040 rpm—11. 320,000 maxwells, 2 V, 1.6 V, 0.0 V, 2.52 V—12.  $3.2 \times 10^6$ , 3.2 mh—13.  $12.8 \times 10^6$ , 12.8 mh—14. 0.283 h, 0.488 h—15. 2450 V—16. 5250 V—17. 5.0 h, 40 joules, 80 v—18. 30 h—19.  $60 \times 10^8$ ,  $240 \times 10^8$ , 85.7 h—20. 362 V—21. 1280 at—22. 2260 at—23. 680, -300—24. 4.0, 7.2, 12.3, 20.0, 24.0 amps—25. 135, 85,000 lines/sq in.—26. 100 kilolines/sq in., 315,000 maxwells—27. 46,000 maxwells, 13,100 lines/sq in.—28. 9350 gauss, 60,300 lines/sq in.—29. 0.213 amp—30. 0.685 lb, 0.441 lb ft—31. 2.98 lb ft—32. 2.11 lb ft—33. 1.49 lb ft—34. 9420 lines/sq in.

### Chapter 3

1.  $W = 79.5$ ,  $\text{pf} = 0.476$ , lines = 94,000—2. 73,200 lines/sq in., 1.30 amp (assuming 0.0015" airgaps)—3. 544 turns—4. 1098.5 V, 109.85 V,  $5.15 \times 10^6$  maxwells—5. 109.8 V, 109.8 V, 109.8—6.  $\text{pf} = 0.290$ , 2299 V, 0.0870 amp, 0.287 amp—7. 1350 turns, 110 turns, 240 sq in.—9. 0.214 amp, 1.22 amp, 1.24 amp,  $\text{pf} = 0.172$ —10. 0.418 amp, 2.44 amp, 2.48 amp,  $\text{pf} = 0.172$ —11. 0.836 amp, 4.88 amp, 4.96 amp,  $\text{pf} = 0.172$

### Chapter 5

1. 41.4 amp, 0.996, 0.895 amp,  $\text{eff} = 0.950$ —2. 6.48 amp,  $\text{pf} = 0.995$ , 0.255 amp,  $\text{eff} = 0.982$ —3. 44.5 amp,  $\text{pf} = 0.866$ , 0.92 amp,  $\text{eff} = 0.984$ —4. 14.85 amp,  $\text{pf} = 0.77$ , 0.389 amp,  $\text{eff} = 0.989$

### Chapter 8

1.  $r_1 = 6.80$ ,  $r_2' = 3.73$ ,  $X_1 = X_2' = 11.15$ , 16,  $r_m = 77.6$ ,  $X_m = 2440$  ohms—2.  $r_1 = 9.55$ ,  $r_2' = 5.35$ ,  $X_1 = X_2' = 32.8$ ,  $r_m = 8600$ ,  $X = 32,400$  ohms—3.  $r_1 = 0.191$ ,  $r_2' = 0.105$ ,  $x_1 = x_2' = 1.24$ ,  $r_m = 112.4$ ,  $x_m = 885$  ohms—4. 0.0227, 0.972, 0.0454, 0.965, 0.968, 0.975, 0.975, 0.960, 0.970, 0.970—5. 0.0123, 0.978, 0.0387, 0.973, 0.955, 0.973, 0.978, 0.944, 0.966, 0.971—6. 0.00955, 0.987, 0.0451, 0.983, 0.976, 0.985, 0.988, 0.970, 0.981, 0.983—7. 0.0745, 0.0775, -0.00142—8. 0.0148, 0.0444, -0.0211—9. 0.00722, 0.0241, -0.0127—10. 0.0109, 0.0382, -0.0212—11. 0.0105, 0.0212, -0.0044, 0.980, 0.975, 0.975—12. 0.962—13. 0.986—14. 0.167, 0.0359, -0.00940, 0.975, 0.968, 0.968, 0.947, 0.965, 0.970, 0.966

### Chapter 10

1. (a) 7620/220 volts, 437/15,000 amp, 3333 kva,  $a = 34.6$ ; (b) 7620/127 volts, 437/26,200 amp, 3333 kva,  $a = 60$ ; (c) 13,200/127 volts, 252/26,200 amp, 3333 kva,  $2 = 104$ ; (d) 13,200/220 volts, 252/15,100 amp, 3333 kva,  $a = 60$ —2.  $N_1 = 34.1$ ,  $N_2 = 29.6$ —3. (a) 6600 volts, 15.1 amp; (b) 120 volts, 832 amp; (c) 55—4. Primary 6350 volts, 30.8 amp; Secondary 1100 volts, 179 amp—5. Primary 11,000 volts, 17.8 amp; Secondary 635 volts, 309 amp—6. Primary 11,000 volts, 17.8 amp; Secondary 1100 volts, 179 amp—8. (a) 947 amp; (b) 17.2 amp,  $I$  in line = 29.8 amp; (c) 0.998

lagging current—9. 2660/440 volts, 2.62/158 amp, 69 kva,  $a = 60.5$ —10. (a) 33.3 kva, 28.8 kw; (b) 33.3 kva, 28.8 kva; (c) 71.0 kva, 68.8 kw—11. Main:  $a = 10.46$ , Pri. 204 kva, Sec. 204 kva; Teaser:  $a = 12.1$ , Pri. 176 kva, Sec. 204 kva—12. Main: 150 kw, Teaser: 150 kw—13. Main: 1100/220 volts, 29.2/126 amp; Teaser: 952/220 volts, 29.2/126 amp—14. (A) 75 kw, 0.866 pf; (B) 75 kw, 0.866 pf—15. (A) 100 kw, 1.0 pf; (B) 50 kw, 0.50 pf—16. Main:  $a = 5$ , 1100/220 volts, 524/2620 amp; Teaser:  $a = 5$ , 952/191 volts, 524/2620 amp—17. 115 volts,  $120^\circ$ —18. Main: Pri. 26.9 kva, Sec. 23.3 kva; Teaser: Pri. 23.3 kva, Sec. 23.3 kva—19. 79.6 kw—20. 58.4 kw—21. For 625 volt converter: Pri. 11,500 volts, 25.1 amp, 166.7 kva,  $a = 26$ ; Sec. 442 volts, 377 amp, 166.7 kva—22. Pri. 11,500 volts, 25.1 amp, 166.7 kva,  $a = 30.1$ ; Sec. 382 volts, 218 amp, 166.7 kva—23. Pri. 11,500 volts, 25.1 amp, 166.7 kva,  $a = 52$ ; Sec. 221 volts, 377 amp, 166.7 kva

### Chapter 11

1. (a) I. 0.025, 0.01, 0.0229 in pu, 121, 48.4, 111 in ohms; II. 0.035, 0.008, 0.0341 in pu, 33.9, 7.74, 33.0 in ohms; (b) I. 0.980, 0.976, 0.976; II. 0.985, 0.980, 0.980; (c) I. 0.0103, 0.0218,  $-0.00545$ ; II. 0.00858, 0.0271,  $-0.0136$ —2. I. 250 amp, 109 kw, 0.989, 0; II. 890 amp, 391 kw, 0.999, 0—3. I. 250 amp, 96.2 kw, 0.876, 0; II. 890 amp, 303.8 kw, 0.775, 0—4. I. 290 amp, 1646 kw, 0.860, 0; II. 241 amp, 1330 kw, 0.837, 0—5. I. 54.5 amp, 121 kw, 0.964, 1.31 amp; II. 221.5 amp, 448 kw, 0.878, 1.31 amp—6. I. 56.4 amp, 124.5 kw, 0.958, 0; II. 219.5 amp, 444.5 kw, 0.880, 0—7. Losses in 5 =  $1.02 \times$  Losses in 6

### Chapter 12

1. (a) 12/11; (b) 183.3, 200, 16.7 amp; (c) 40.3 kw; (d) 3.67 kw—2. 60 kva, 54.5, 45.5, 9.1 amp, 50 kva, 10 kva(?)—7. 2 autotransformers: (a) 208/230 center-tapped; (b) 180/230 volt—8. 3 autotransformers: Pri. 133 volt, Sec. taps +150 volts, -150 volts

### Chapter 14

1.  $2.56 \times 10^8$  maxwells, 1995 volts—2. 16 volts,  $f = 1.11$ , 15.4 volts—3. (a) 306 volts; (b) 296 volts; (c) 283 volts—4. 10,860 volts

### Chapter 17

1. 0.867, 1.0, 2.0, 3.33 cps—2. (a)  $s = 0.022$ ; (b)  $72^\circ$ —3. (a) 720 rpm; (b) 16 rpm; (c) 720 rpm; (d) 0—4. (a)  $k_p = 0.966$ ,  $k_d = 0.958$ ; (b) 673,000 maxwells—5. 2.14—6. 0.865 volt—7. (a)  $k_p = 0.940$ ,  $k_d = 0.960$ ; (b) 512,000 maxwells—8. 2.12—9. 0.0228 volt

### Chapter 19

1.  $I_{st} = 166$  amp,  $T_{st} = 11.8$  lb ft,  $I_1 = 21.2$  amp, pf = 0.81,  $\eta = 0.88$ ,  $T_{dev} = 38.1$  lb ft,  $T_{del} = 11.7$  lb ft—2.  $I_{st} = 241$  amp,  $T_{st} = 78.2$  lb ft,  $I_1 = 32.7$  amp, pf = 0.85,  $\eta = 0.87$ ,  $T_{dev} = 39.7$  lb ft,  $T_{del} = 37.5$  lb ft—3.  $I_{st} = 144$  amp,  $T_{st} = 120$  lb ft,  $I_1 = 22.4$  amp, pf = 0.77,  $\eta = 0.90$ ,  $T_{dev} = 74.5$  lb ft,  $T_{del} = 71.5$  lb ft

### Chapter 22

1. 10.1, 9.40, 8.85, 7.52, 5.53, 3.50, 1.40 (pu) amp, pf = 0.616, 0.632, 0.668, 0.707, 0.791, 0.867, 0.785—2.  $T$  in lb ft = 26.7, 28.2, 30.5, 31.2, 29.9, 23.1, 8.95—3. amp in pu = 11.5, 10.8, 9.80, 8.55, 6.35, 4.05, 1.65, pf = 0.534, 0.633, 0.666, 0.538, 0.839, 0.867, 0.784—

4. amp in pu = 8.58, 8.00, 7.53, 6.40, 4.67, 2.96, 1.21, pf = 0.618, 0.634, 0.670, 0.707, 0.790, 0.869, 0.786—5.  $T$  in lb ft = 35.6, 37.5, 37.3, 40.7, 41.3, 31.6, 12.0—6.  $T$  in lb ft = 19.5, 20.3, 22.1, 22.7, 21.6, 16.6, 6.5—8.  $I_1$  (inrush) = 28.1 amp,  $T_{dev} = 30.4$ —9.  $I_1 = 4.15$  amp, pf = 0.797,  $T_{dev} = 8.66$  lb ft,  $P_{out} = 2.79$  hp, eff = 0.828—10. Sat. factor = 1.04,  $S_{po} = 0.324$ ,  $T_{po} = 31.0$  lb ft—11. (a) 1.25, (b) 2.42 ohms, (c) 64 per cent—12.  $r_1 = 0.103$ ,  $r_2' = 0.143$ ,  $x_1 = 0.710$ ,  $x_2' = 0.710$ ,  $r_m = 0.547$ ,  $x_m = 30.2$  at reduced voltage, i.e., unsaturated values for  $x_1 = x_2'$ ,  $r_1 = 0.103$ ,  $r_2' = 0.143$ ,  $x_1 = 0.54 = x_2'$ ,  $r_m = 0.547$ ,  $x_m = 30.2$  at full voltage, i.e., saturated values of  $x_1 = x_2'$ —13. HP output = 56.7, eff = 0.937,  $I_1 = 127$  amp,  $I_{dev} = 0.747$  in pu—14.  $I_1 = 1195$  amp,  $I_{dev} = 0.985$  in pu—15.  $I_1$  in pu = 7.96, 7.78, 7.57, 6.65, 5.46, 4.27, 0.847, pf = 0.212, 0.243, 0.284, 0.334, 0.485, 0.707, 0.895—16.  $T_{dev}$  in pu = 0.985, 1.18, 1.49, 1.71, 2.29, 2.81, 0.747—17.  $I_1$  in pu = 9.16, 8.95, 8.62, 7.56, 6.25, 4.92, 0.97, pf = 0.218, 0.242, 0.282, 0.333, 0.483, 0.722, 0.893—18.  $I_1$  in pu = 6.77, 6.65, 6.40, 5.65, 4.68, 3.96, 0.800, pf = 0.221, 0.243, 0.284, 0.333, 0.502, 0.691, 0.924—19.  $T_{dev}$  in pu = 1.32, 1.56, 1.93, 2.23, 3.01, 3.73, 0.970—20.  $T_{dev}$  in pu = 0.712, 0.855, 1.05, 1.22, 1.67, 2.39, 0.687—21.  $S_{po} = 0.102$ ,  $T_{po} = 2.81$  in pu—22. (a) 0.90 ohm per phase; (b) 0.46 ohm per phase—23. Saturated values: for  $x_1 = x_2'$  at full voltage,  $r_1 = 1.20$ ,  $r_2' = 0.72$ ,  $x_1 = 2.31$ ,  $x_2' = 2.40$ ,  $r_m = 2.04$ ,  $x_m = 41.2$  ohms per phase; Unsaturated values:  $r_1 = 1.20$ ,  $r_2' = 1.01$ ,  $x_1 = 1.80 = x_2'$ ,  $r_m = 2.04$ ,  $x_m = 41.2$ —24. HP output = 4.87, eff = 0.836, amp  $I_1 = 1.36$  in pu,  $T_{dev} = 30.6$  lb ft—25.  $I_1 = 8.33$  amp in pu,  $I_{st} = 63.0$  lb ft—26.  $I_1$  in pu = 8.33, 8.10, 7.74, 6.75, 5.29, 3.72, 1.36, pf = 0.515, 0.533, 0.564, 0.582, 0.674, 0.800, 0.762—27.  $T_{dev}$  in lb ft = 63.0, 66.0, 74.0, 76.5, 83.8, 30.6—28.  $S_{po} = 0.157$ ,  $T_{po} = 84.0$ —29.  $I_1$  in pu = 9.63, 9.34, 8.90, 7.75, 6.08, 4.28, 1.575, pf = 0.516, 0.533, 0.563, 0.584, 0.672, 0.80, 0.758—30.  $I_1$  in pu = 7.06, 6.88, 6.56, 5.72, 4.50, 3.16, 1.16, pf = 0.521, 0.535, 0.559, 0.585, 0.675, 0.800, 0.759—31.  $T_{dev}$  in lb ft = 81.9, 88.4, 89.6, 102, 112, 106, 41—32.  $T_{dev} = 43.9, 48.2, 53.8, 55.7, 56.5, 58.4, 22.1$  lb ft

## Chapter 23

1. 20.8 ohms per phase—2. 3.12 ohms per phase—3. 63.9 lb ft or 1.46 in pu—4.  $I_1 = 5.66$  pu,  $T_{dev} = 0.695$  pu or 30.4 lb ft, no—5. 15.9 ohms per phase, 15.1 amp or 1.023 pu, for squirrel-cage motor is 5–10 amp in pu—6. Voltage ratio = 3.2,  $T_{st} = 0.238$  pu, or 130 lb ft—7. 9.66 ohms per phase, 72 kw—8.  $T_{st} = 0.238$  pu—9. 5.22 ohms per phase—10.  $T_{st} = 0.238$  pu—11. (a) 0.314; (b) 0.94 ohm per phase—12.  $T_{st}$  auto =  $16 \times T_{st}$  with resistor—13.  $I_2' = 66.6$  amp, 0.956, 750 lb ft—14. 795 volts—15. Approximately 246 volts, 450 kva

## Chapter 24

3. 87.25°—4. 99.4°, 93.4°—5. 110.8°, 116.3°, 121.8°—6. 350 max, 110 min

## Chapter 27

1.  $I_1 = 3.1$  amp, pf = 0.574,  $T_{dev} = 13.6$  oz ft,  $T_L = 12.2$  oz ft, eff = 0.577—2.  $I_1 = 8.12, 7.45, 6.63, 4.47, 3.85, 3.20$  amp, pf = 0.795, 0.805, 0.810, 0.768, 0.716, 0.595—3.  $T = 32.9, 34.2, 33.5, 25.7, 20.5, 13.8$  oz ft—5.  $r_1 = 1.71$ ,  $r_m = 1.61$ ,  $r_2' = 1.22$ ,  $x_1 = 1.90$ ,  $x_m = 28.0$ ,  $x_2' = 0.95$  ohms—6.  $I_1 = 4.86$  amp, pf = 0.70,  $T_{dev} = 18.0$  oz ft,  $T_{del} = 16.02$  oz ft, eff = 0.642—7.  $I_1 = 14.8, 13.6, 12.1, 7.84, 4.85$  amp, pf = 0.820, 0.835, 0.849, 0.840, 0.812, 0.700—8.  $T_{dev}$  oz ft = 41.1, 42.6, 43.0, 33.4, 28.0, 18.0—9.  $r_m = 2.77$  ohms—10.  $I_1 = 2.54$  amp, pf = 0.70,  $T_{dev} = 9.32$  oz ft,  $T_{del} = 8.1$  oz ft, eff = 0.62—11. 7.25, 6.67, 5.97, 3.96, 3.32, 2.54 amps, ft = 0.795, 0.811, 0.827, 0.826, 0.798, 0.70—12.  $T_{dev} =$  oz ft = 18.6, 19.4, 19.9, 16.3, 13.6, 9.32—13.  $r_1 = 2.44$ ,  $r_m = 1.505$ ,  $r_2' = 1.796$  ohms,

$x_1 = 2.57$ ,  $x_m = 36.2$ ,  $x_2' = 1.285$  ohms—14.  $I_1 = 3.55$  amps, pf = 0.675,  $T_{dev} = 12.7$  oz ft,  $T_{del} = 11.62$  oz ft, eff = 0.661—15. amps = 10.35, 9.40, 8.34, 5.43, 4.56, 3.55, pf = 0.830, 0.844, 0.855, 0.827, 0.786, 0.675—16.  $T_{dev} =$  oz ft = 29.4, 29.8, 29.9, 22.7, 19.0, 12.7

## Chapter 29

1.	HP	slip	torque lb ft	power factor	efficiency
	8.9	0.0906	68.4	0.882	0.790
	4.25	0.0533	31.4	0.788	0.779
	0.667	0.0227	4.78	0.287	0.470

2. (a) 4130 watts; (b) 4000 watts; (c) 4320 watts; (d) 0.864; (e) 0.0315; (f) 16.15 lb ft—3. (a) 4975 watts; (b) 4788 watts; (c) 5220 watts; (d) 0.857; (e) 0.0376; (f) 19.5 lb ft—4. eff = 0.895, pf = 0.843—5. eff = 0.892, pf = 0.895, eff = 0.898, pf = 0.910—6. 449 hp, eff = 0.928, pf = 0.880—7. 343 hp, 0.930 eff, pf = 0.864; 555 hp, eff = 0.921, pf = 0.872

## Chapter 33

2. (a) 5.50 ohms or 0.191 pu; (b) 35 amp; (c)  $x_d = 31.3$  ohms, = 1.08 pu—3. 0.163, 0.263, -0.084—4. saturated SCR = 1.06, unsaturated = 0.92—5. (a)  $x_e = 1.21$  ohms, 0.15 pu; (b) 194 amp; (c)  $x_d = 11.1$  ohms, 1.37 pu—6. 0.31, 0.02—7. unsaturated = 0.73—8. (a) 0.404 ohms, 0.15 pu; (b) 371 amps; (c) 3.68 ohms, 1.37 pu—9. 0.22, 0.31, 0.02

## Chapter 35

1. 0.083, -0.181—2.  $x_d = 1.25$ ,  $x_{ad} = 1.06$ ,  $x_{aq} = 0.61$ ,  $x_q = 0.79$  pu—3. (a) 7175; (b) sat. SCR = 0.89, unsaturated = 0.80; (c) 0.122 at unity pf—4.  $x_e = 0.861$  ohm, 0.235 pu,  $M_a = 3.2$  amp—5. 0.252, 0.0236, 0.410—6.  $x_d = 1.14$ ,  $x_q = 0.944$  pu—7.  $x_{ad} = 0.655$  pu or 7.48 ohms,  $x_{aq} = 0.380$  pu = 4.35 ohms, SCR = 1.12, 178 amp—8.  $BC = 1910$  volts,  $CC' = 3030$  volts,  $\psi = 56.7^\circ$ ,  $\delta = 19.8^\circ$ ,  $M_a C_q = 68$  amps,  $C_q = 0.504$ ,  $C_d = 0.869$ —9. 0.142, 0.261, -0.178—10. 0.153, 0.272, -0.160—11. 0.259 ohm, 0.271 pu, 77 amp—12. 0.125, 0.312, -0.0334—13. SCR = 0.89,  $x_d = 1.12$  pu,  $x_q = 0.78$  pu—14. 2.02 ohms, 0.262 pu, 57 amps—15. 0.175, 0.317, 0.0625—16. SCR = 0.90,  $x_d = 1.11$  pu,  $x_q = 0.71$  pu

## Chapter 37

1.  $47.6^\circ$ ,  $45^\circ$ ,  $42.7^\circ$ ,  $40.8^\circ$ , 1000 kw—2. (a) 90.6, 88.9, 87.9, 87.5 amp; (b) 0.965, 0.984, 0.995, 0.999 lag,  $\delta = 40.4^\circ$ ,  $V = 8630$  volts—3. 3320 volts—4.  $62.2^\circ$ ,  $58.1^\circ$ ,  $54.5^\circ$ ,  $51.6^\circ$ ; 1200 kw,  $21.7^\circ$ ,  $20.8^\circ$ ,  $19.8^\circ$ ,  $19^\circ$ ; 500 kw—5. (a) 115.3, 111.6, 108.8, 197 amp; (b) 0.910, 0.940, 0.965, 0.981 lag; (a) 44.4, 45.5, 47.4, 49.7 amp; (b) 0.985, 0.961, 0.923, 0.880 lead—6. 1168 kw—7. (a) 23,100 kva; (b) 20,000 kw; (c) 11,550 kvar; (d) 10,650 V; (e)  $21.8^\circ$ ; (f)  $51.8^\circ$ —8. (a) 0.561 lag; (b) 1564 amp; (c) 7460 v; (d)  $16.3^\circ$ ; (e)  $72.2^\circ$ ; (f) 35,600 kva; (g) 29,400 kvar lag; (a) 0.952 lead; (b) 921 amp; (d)  $31.8^\circ$ ; (e)  $14^\circ$ ; (f) 20,950 kva; (g) 6,400 kvar lead—9. (a) 25,550 kw; (b) 29,550 kva; (c) 14,800 kvar; (d) 1292 amp; (e) 0.866 pf; (f) 11,660 v; (g)  $25.5^\circ$

## Chapter 41

1. eff = 0.955, 1650 amp per sq in.—2.  $I_f = 133.6$  amp, eff = 0.964—3.  $I_f = 113.7$  amp, eff = 0.960—4.  $I_f = 96.4$  amp, eff = 0.950

*Chapter 43*

1. (a) 442; (b) 221; (c) 383 v

*Chapter 45*

1. 136 v, 0—2. 0, 84.8 v—3. 14.95 lb ft—4. 3200 total turns

*Chapter 46*

1. 4110—2. (a) 88.3; (b) 77.4—3. (a) 132.7; (b) 144—4. 0.95 lb ft—5. 4.93, 150,000—  
6. 338,000 maxwells—7. 48 v

*Chapter 48*

1. 55 per cent, 24 and 33 cps—2. Approximately 55 per cent—3. Yes. Approximately 217 per cent





## INDEX

- A-C Windings**, 92; EMF induced in them, 1, 101; MMF produced by them, 106  
alternating field, 106  
differential leakage, 124  
distribution factor, 101  
effect of harmonics in the emf, 104  
angle between two adjacent slots, 101  
distribution and pitch factor, 101, 103  
number of recurrent groups and parallels, 93  
rules for laying out, 474  
slot star, 471  
field curve—no load, 3  
harmonic leakage, 124, 512, 518  
harmonics, 104  
order of stator mmf and field harmonics, 195, 482  
stator slot harmonics, 482  
speed of stator harmonics, 197  
order of rotor mmf and field harmonics, 485  
rotor slot harmonics, 485  
speed of rotor harmonics, 487  
mmf of a single phase winding, 106  
mmf of fractional pitch winding, 111  
mmf of polyphase winding, 108  
no-load field curve, 3  
pitch factor, 103  
rotating field, 108  
time and space harmonics, 323
- Alternating-current commutator motor**  
commutation, 358  
compensating winding, 357  
d-c armature in an alternating field, 353  
emf of rotation, 354  
polyphase motor, 374  
repulsion motor, 368  
repulsion motor at start, 368, 372  
repulsion motor running, 369  
repulsion motor, position of brushes, 372
- Alternating-current commutator motor, repulsion motor voltage diagram**, 370  
rotor emfs, 369  
series motor, 362  
characteristics, 365  
voltage diagram, 362  
winding arrangement, 362  
short-circuited winding element, commutation, 363  
single-phase motor, 353  
three-phase shunt motor, 374  
power factor correction, 377  
torque, 376  
voltage diagram, series motor, 362
- Motor application**, 379  
application of various types, 385  
characteristics of loads, 379  
class A motors, 386  
class B motors, 390  
costs, 382  
definitions, 404, 422  
frame size, 382  
gear motor, 384  
general purpose induction motor, 382, 386  
high slip motor, 390  
low starting current motors, 390  
NEMA classification of induction motors, 386  
normal starting torque—low starting current, 390  
relation of cost and weight to horsepower and speed, 383  
speed—torque characteristics, 385  
curve of induction motor, 385  
synchronous motor—characteristics and applications, 394  
wound rotor induction motor applications, 391
- Polyphase induction motor**, 114  
auto-transformer starting, 184  
basic torque relations, 141

- Polyphase induction motor, calculation of**  
 performance, 145  
 characteristics, 143, 173  
 circle diagram, 155, 446  
 constants of the motor, 163  
 dead points, 198  
 design principles, 578  
 developed power, 141  
 differential Selsyns, 202  
 double cage rotors, 169  
 effect of voltage and frequency variation, 175  
 efficiency, 174  
 electric power of the rotor, 141  
 emf in rotor and stator, 130  
 equivalent circuit, 137, 140  
 equivalent leakage reactance, 166  
 equivalent resistance, 166  
 examples and problems, 145, 148  
 fundamental vector diagram, 136  
 harmonics, 195  
   order of stator mmf and field harmonics, 195, 482-490  
   rotor slot harmonics, 246  
 induction generator, 157  
 induction voltage regulator, 211  
 influence of saturation, 170  
 influence of skewing, 199, 494, 539  
 input power line, 156  
 leakage reactance, 166, 500-523  
 locked rotor test, 164  
 locking torque, 199  
 mechanical power line, 156  
 mmf waves, 108  
 motor at standstill, 123  
 noise, 200, 540-549  
 no-load tests, 163  
 operation as a brake, 150  
 operation as a generator, 151  
 operation as a stationary transformer, 123, 440  
 parasitic radial forces, vibration and noise, 540-553  
 parasitic tangential forces and torques, 195-199, 529  
   asynchronous torques, 198, 533  
   locking torques (dead points), 198  
   synchronous torques, 198, 535  
 per unit calculation, 166  
 phasor diagram, 136
- Polyphase induction motor, position indicators, 210**  
 power, developed, 141, 156  
 power balance, 145  
 power of the rotating field, 141  
 primary and secondary currents, 129, 131, 442  
 pull-out torque, 143  
 reduction factors, current and voltage, 129  
 regulating sets, 189-192  
 saturation, influence of, 170  
 secondary current, 442  
 secondary resistance, effect of, 188  
 self synchronizers, 202  
 Selsyns, 202  
 single-phase Selsyns, 202  
 skin effect, 169  
 slip, 130  
 slip line, 446  
 special speed regulation sets, 188  
 special induction motors, 201-215  
 speed control of wound rotor, 188  
 speed-torque curve—influence of harmonics on, 195-199  
 squirrel cage as a polyphase winding, 132  
 standstill, 123  
 starting current, 183  
 starting induction motor with slip ring rotor, 186  
 starting squirrel cage motor, 183  
 starting torque, 183-193  
 synchronous speed, 126  
 tangential force (specific), 578  
 torque, 142  
 torque line, 158  
 torque—Selsyns, 202  
 vibration, 540-550  
 voltage equations, 135  
 voltage regulators, 211  
 wye-delta starting, 185
- Rotary converter, 341-352**  
 commutation, 350  
 comparison with d-c machine, 347  
 copper losses, 345  
 current ratio, 344  
 current wave shapes, 345  
 parallel operation, 351  
 starting, 351

Rotary converter, voltage ratio, 344  
voltage regulation, 350

**Single-phase induction motor, 216**  
calculation of characteristics, 231  
capacitor motor, 463-466  
capacitor start motor, 239  
circle diagram, 226  
equivalent circuit, 223  
examples and problems, 231  
iron losses, 244  
normal slip, 231  
pull-out slip, 231  
reactor start motor, 239  
reduction factors, 222  
repulsion start induction motor, 242  
resistance and reactance, influence of on  
speed torque curve, 231  
resistance and reactance from no-load  
and locked rotor tests, 228  
resistance start motor, 239  
rotor currents, 224  
shaded-pole motor, 243  
speed-torque curve, 221  
split-phase motor, 239  
starting single-phase motor, 238  
starting torque, 239  
stator current, 222  
two-rotating field theory, 219, 227  
voltage equations, 222

**Starting A-C motors and motor protection, 379-423**  
approximate full load currents, 387  
auto starter, 410  
controllers for wound rotor motor, 411  
definitions, 404, 422  
effect of heating on insulation, 419  
line starters, 407  
magnetic line starter, 408  
manual line starter, 407  
motor protection, 418  
reduced voltage starting, 409

**Starting A-C motors, resistor type starter, 411**  
reversing line starter, 409  
starting characteristics of various starters, 409  
starters for fractional HP motors, 414

**Starting A-C motors, starting synchronous motors, 415, 568**  
thermal protection, 418  
type of starter to be used, 416

**Synchronous machines,**  
angle-switching, 318, 568  
armature mmf in direct axis, 266, 269  
armature mmf in quadrature axis, 266, 269  
armature reaction, 266  
armature-reaction reactances, 266  
circle diagram of synchronous motor, 310-315  
circulating current, 305  
damper winding, 258  
design principles, 578  
forced oscillations, 326  
hunting of synchronous machine, 326-332  
leakage reactance, 499-528  
main flux reactance, 266  
natural frequency of oscillation, 331  
no-load characteristic, 264  
over-exciting of synchronous motors, 315  
overload capacity of synchronous motors, 316  
parallel operation, 303-308  
per unit quantities, 56, 166, 278  
Potier triangle, 274, 275  
pulling into step of synchronous motor, 568  
equation of motion, 568  
solution of equation of motion for most favorable rotor angle, 570  
solution for most unfavorable rotor angle, 575  
reactances of the salient pole machine, 285, 288  
regulation curves, 292  
salient-pole generator, 292

**Synchronous machines, salient-pole generator, voltage diagram, 288**  
short-circuit characteristic, 276  
short-circuit ratio, 276  
short-circuit, sudden of synchronous generator, 559-567  
subtransient reactance, 559  
determination from a locked test, 563

- Synchronous machines, synchronizing, 301**  
     synchronous motor—circle diagram,  
         310-315  
         starting, 318  
         V-curves, 315  
         voltage diagram, 268  
     synchronous reactance, 269  
     synchronous reactance of salient-pole  
         machine, 290  
     torque and power of synchronous ma-  
         chine, 300-301  
     tangential force (specific), 584  
     transient reactance, Chap. 60  
     two-reaction theory, 283  
     voltage diagram of salient-pole machine,  
         288  
     voltage and mmf diagram, nonsalient-  
         pole machine, 268  
     voltage regulation by empirical method,  
         278  
     zero power factor characteristic, 274
- Transformers, 20-91**  
     AIEE regulation, 52  
     auto-transformer, 84  
     circulating current, 79  
     constant current transformer, 88  
     construction, 20  
     cooling, 26  
     core type, 20  
     current transformers, 86  
     delta-delta, 67  
     delta-wye, 68  
     diametrical, 73  
     distributed shell type, 22  
     double delta, 74  
     double-wye, 73  
     eddy currents, 63  
     efficiency, 56  
     emf—induced in windings, 32  
     equivalent circuit, 42  
     flux, main, 28  
     flux, leakage, 28  
     harmonics, 61  
     hysteresis, 62
- Transformers, instrument transformers,**  
     85  
     Kapp diagram, 50  
     leakage, 29  
     leakage flux, 28  
     leakage voltage, 29  
     load diagram, 34  
     magnetizing current, 30  
     main flux, 28  
     main flux conductance, 30  
     main flux impedance, 30  
     main flux reactance, 30  
     main flux susceptance, 30  
     mmf, diagram of, 34  
     mutual inductance, 38  
     no-load current, 28  
     no-load test, 54  
     no-load voltage diagram, 30  
     open delta, 69  
     parallel operation, 77  
     per-unit calculation, 56  
     phase transformation, 71  
     polarity, 64  
     potential transformer, 87  
     ratio of transformation, 31  
     reactance, leakage, 29  
     reduction factors, 36  
     reduction to primary, 35  
     Scott connection, 71  
     shell type, 20  
     short-circuit test, 55  
     six-phase star, 73  
     skin effect, 55  
     spiral core type, 23  
     T-connection, 70  
     three-phase transformer, 47  
     transformation ratio, 31  
     voltage diagram, load, 41  
     voltage diagram, no-load, 29  
     voltage regulation, 50  
     wave shape of no-load current, 61  
     windings, 23  
     wye-delta, 69  
     wye-wye, 67



